UNIVERSITY OF HULL

Paper microfluidic sensors towards on-site environmental analysis of soil nutrients

being a thesis submitted in fulfilment of the

requirements for the degree of

Doctor of

Chemistry

in the University of Hull

by

Samira AL Hinai

October 2023

Acknowledgements

I would like first to express my sincere gratitude to Sultan Qaboos University for funding the whole scholarship and supporting me financially.

I would like to express my deepest appreciation to my supervisor Prof. Nicole Pamme and Prof. Mark Lorch for their supervision, unlimited support, and continuous guidance.

I would like also to thank, Samantha Richard for being part of my work and development journey. Thanks to all the technician staff and colleagues at the University of Hull.

Thanks also to the external examiner (Prof. Helen Bridle) and internal examiner (Prof. Will Mayes) for being part of my viva examination.

Publications and Conferences

Samantha Richardson, <u>Samira Al-Hanai</u>, Mila Sari, Bongkot Ngamsom, Will M. Mayes, Mark Lorch, Nicole Pamme, "Paper microfluidic for environmental analysis", CAMS conference, 17th Sep 2020.

Samantha Richardson, <u>Samira AlHinai</u>, Jesse Gitaka, Will M. Mayes, Mark Lorch, and Nicole Pamme, "Towards on-site monitoring of soil nutrients via cafetiere-based extraction and paper-based analysis", MicroTAS 2020, poster presentation, 4th – 8th Oct.

Samantha Richardson, <u>Samira AlHinai</u>, Jesse Gitaka3, Will M. Maye, Mark Lorch, and Nicole Pamme, "Monitoring soil nutrients using a simple cafetiere-based extraction with paper-based readout.", EGU2021 conference, 19th-30 April.

<u>Samira AL Hinai</u>, Samantha Richardson, Mark Lorch, Nicole Pamme, "Development of a paper microfluidic device towards in situ detection of nitrate in soil", ARF2021 conference, 15th and 16th June.

<u>Samira AL Hinai</u>, Samantha Richardson, Mark Lorch, Nicole Pamme, "Workflow for on-site extraction and analysis of nitrate in soil", MicroTAS2021 conference, 10th-14th October 2021

<u>Samira AL Hinai</u>, Samantha Richardson, Mark Lorch, Nicole Pamme, "Development of a paper microfluidic device towards in situ detection of manganese in soil", ARF2022 conference, 13th-14th June 2022.

<u>Samira AL Hinai</u>, Samantha Richardson, Mark Lorch, Nicole Pamme, "Portable, rapid detection system to measure soil nutrients via a simple to operate cafetière-based extraction and paper-based sensor readout", SDG2022 conference, 6th-7th July 2022.

Abstract

The increase in the world population leads to an increase in the need for production of crops. To optimise crop production fertilizer application needs to be managed by the farmer, consequently, regular information about the chemistry of the soil is required. There is a strong need for regular and in-field methods for the analysis of different essential nutrients in the soil which are in macro (e.g., nitrate) and micro (e.g., manganese) levels. Of the recently available lab techniques (e.g., IEC[1], ICP-MS[2]) and commercial techniques[3] (e.g., strips and palintest) some are not quantitative, some are expensive, some are time-consuming, and some combine all these disadvantages. Consequently, they are not practical, especially for low- and middle-income countries where agriculture is the main source of economy.

Here a simple (user-friendly) and low-cost workflow for routine monitoring of nitrate and manganese in soil samples, which is based on phone colourimetric paper-based sensor and cafetière extraction and meets on situ detection requirements, was developed.

Novel cafetière extraction was suggested for the first time for on-site extraction of soil nutrients. Cafetière consisted of plunger and meshes which provide the required mixing and filtration respectively. Initially nitrate determination workflow in soil was developed and tested with volunteers. The workflow requires 13 minutes total time for nitrate determination, 5 minutes extraction by cafetière (DIW solvent, 90% extraction efficiency) and 8 minutes detection by a phone-based colourimetric paper-based sensor. The PAD (paper-based analytical device) was able to detect as low as 27.10±2.64 mg kg^{-1} and 34.35±2.77 mg kg^{-1} of nitrate when a scanner and phone were used for the detection respectively. The developed PAD was small, portable, fast, easy to use, disposable, safe, low cost, robust (to interference and pH change), reliable and can be used in the field in a resource-limited setting. 97% of volunteers found the workflow easy and were able independently to perform the workflow for nitrate determination by following a simple instruction sheet.

Similarly, a workflow for manganese determination was developed in the lab to fit the field requirement. The workflow consists of two steps: 4 min cafetière extraction (NaCl solvent, 10% extraction efficiency) and 7 min detection (colourimetric paper-based sensor) with a total time of 11 minutes. The PAD was able to detect (LoD) 4.14±0.30 mg kg^{-1} and 5.12±1.88 mg kg^{-1} of manganese when a scanner and phone were used for the detection respectively. The developed PAD was inexpensive, easy to handle (based on dipping sample introduction) and with less toxic

The workflow showed promising results in detecting nutrients in the soil without the aid of an expert. This workflow will enable farmers in low-income countries to determine soil nutrient

content using non-expensive, simple, and easily available methods and hence get enough information about the recommended fertilizer application. Consequently, this may improve the crop and hence the economy in these countries. In the future, the workflow needs to be supported with an app that enables the lay people to determine the result of the analysis by themselves and share it with researchers.

Contents

List of Figures

List of Tables

Abbreviations

PAD   Paper-based analytical device.

IEC   Ion exchange chromatography

NED   N-(1-naphthyl)-ethylenediamine dihydrochloride

PVC   Polyvinylchloride

ICP-OES   Inductively coupled plasma optical emission spectroscopy.

TDS   Total dissolved salt

ICP-MS   Inductively coupled plasma mass spectrometry.

TMAH   Tetramethylammonium hydroxide

EDTA   Ethylenediamine tetra acetic acid

HPLC   High-performance liquid chromatography

PAN   l-(2-pyridylazo)-2-naphthol

PAR   4-(2-pyrldylazo) resorcinol

CL   Chemiluminescence

ECL   Electrochemiluminescence

CRM   Certified reference material

PDDA   Polydiallydimethylammonium chloride

LoD   Limit of detection

LoQ   Limit of quantitation

ANOVA Analysis of variance

Chapter 1 Introduction and literature review

1.1 Introduction

Plant growth depends on several components like Water, solar energy, CO_2 and soil nutrients which contribute directly to the growth of plants. The physical, chemical, and biological characteristics of soil do influence its productivity [4]. Some of these properties are acidity, texture, depth, water content and organic matter content of soil. For instance, the increase in the density of soil leads to the reduction of some plant growth since it is difficult for the plant root to penetrate deep in the dense soil [5]. Management and treatment of soil are very important factors to consider since they significantly affect the quality of the soil and consequently the growth of plants [6,7]. The addition of fertilizers and organic matter are methods which are used for soil treatment [6].

Nitrogen, phosphorous and potassium represent major nutrients which are required in macro amount [8]. Fe, Cu, Mn, Mo, Ni, B and Zn are elements which are consumed in mic amount by plants [8]. The problem of toxicity and the deficiency of nutrients may also result because of the variation in nutrient concentration. Plant growth generally responds to the increase and decrease in the level of specific nutrients. A very small concentration of nutrients leads to small plant production [9]. Once a suitable amount of nutrients is available the production is optimum, and a very high amount of nutrients can cause finally toxicity in plants [9]. The yield growth is controlled using fertilizer [10]. The use of fertilizers should be managed in an efficient way which causes no toxicity or deficiency in nutrients. Understanding the land, considering the natural resources, and increasing farmer knowledge about soil nutrients are all factors that contribute to the efficient use of fertilizer [11]. The most effective use of fertilizers has been impractical and challenging because intensive laboratory testing would be required where sampling and soil analysis should be done for ten to thousand acres of land, and this is expensive and time-consuming [12]. The recent approach ignores the variation of nutrients at different positions of the land. Nutrients vary geographically and over the year [13,14]. Consequently, overuse or deficiency in fertilizer components may occur. Overuse of fertilizer is associated with many problems. Contamination of surface and groundwater may occur [15]. Leaching of sulfur, nitrogen and phosphorus to rivers and lakes causes the growth of algae which tends to consume the oxygen and cause oxygen deficiency [16]. Also, the acid rain problem may increase by escaping sulphur and nitrogen gases [17].

Therefore, more attention should be given to soil issues. Knowing regular information about the soil nutrient contents is crucial for farmers [18]. The regular on-site monitoring system is strongly required. There should be an *in situ* analytical system to produce quantitative information about

nutrient content in soil for farmers at any time during the year. In addition, regular information can be used as a research tool to support a better understanding of how nutrients change within regions and over time and in different climate conditions. The traditional analytical system for nutrient determination is based on several sampling steps and complicated instrumentation [2,19-23]. In addition, there are field methods for soil nutrient determination, however, they require a lot of steps and an expert person to do the work. Also, some are still expensive, especially for poor countries [24-26].

Consequently, paper microfluidic systems have been proposed as cheap and easy-to-use alternatives for such complicated and time-consuming methods. The flow in the paper requires no external power due to the capillary action [27]. Furthermore, paper has hydrophilic cellulose [28]. Consequently, this helps in the flow of hydrophilic reagents within the paper. It is possible to store the reagent within the fibre of the paper while they are in their active form [29] and hence the reaction can happen within the paper. Simultaneous detection [29] can be performed within the paper due to the hydrophobic barrier that can be formed within the paper. Filtration of the sample before detection is also possible due to the porosity of the paper [27]. Compared to conventional methods [30] the volume of used reagent in paper is less and hence cost is reduced. In addition, the paper is inexpensive since they are used in small sizes. Paper devices are portable, easily accessible, and disposable [30,31] due to their small size and low cost. A combination of paper devices and smartphones was widely used for onsite determination by lay people without the need for an expert [32-35]. It was widely used for analyte determination in water and biological samples. Real in-field determination of phosphate in water in rivers across the UK was studied by a paper-based sensor which depended on colourimetric phone detection that was connected to an app for connection between researcher and volunteers [35]. These studies still do not discuss the use of phones when user and location change. In addition, as far as we know there is no paper sensor attached to the phone readout was tested for soil sample determination in the field with either volunteers or farmers themselves.

In this work, a simple paper microfluidic system was used for the determination of nutrients (nitrate and manganese) in soil. This study focuses on nitrate since it is important for plant growth and required in large amounts. In contrast, manganese which is required in a small amount was studied for comparison of the same system with two different nutrients and the purpose of novelty since less study on paper devices was on manganese. The method was specially designed for point-of-need analysis where anyone can perform the detection within a few minutes. The method was based on two steps, first the extraction of components from soil by simple method like use of coffee maker and second, the use of filter paper to design and fabricate a device which can detect the analytes calorimetrically. Simplicity and time of analysis

were two points which were significantly considered since finally, the aim was to release the device to lay people (*e.g.*, farmers) use. Simple novel cafetière extraction for in-field soil nutrients was introduced. In addition, there should be communication between the farmer in the field and the analytical scientist in the lab. The lack of this communication is the main reason for the mismanagement and misuse of fertilizer and soil. Therefore, a mobile phone will be used as a detection method that can be used in the future as a means to share information between lay people (e.g., farmers) and analytical chemists.

1.2   Traditional method for soil nutrient determination

1.2.1   Conventional methods for nitrogen detection in soil

1.2.1.1   Nitrogen in plant and soil

Nitrogen is an important component in nature for biological and non-biological processes. It present in soil in organic and inorganic forms. The most common inorganic forms are nitrate, nitrite, and ammonium [36]. Nitrogen uptake by plants as inorganic form nitrate, nitrite, and ammonium, However, the main source of nitrogen for plants is nitrate, which is why fertilizer with nitrate is applied to agriculture soil [37-40]. Nitrogen is an essential soil element for plant growth. Nitrogen transfers within plant through a process called the xylem process where the nitrogen moves from the roots to the leaves [41]. Nitrogen is needed in the metabolism and photosynthesis process [42,43]. It is a component of protein and chlorophyll [42,43]. It is involved in the catalysation processes within the plant. It is responsible for the dark green colour of the leaves. It also helps in root and leaf growth. The reduction of nitrogen in the plant causes spots in the leaves and chlorosis which is the change of the leaves from green to yellow. Consequently, this leads to poor crop yield.

The efficiency of nitrogen uptake in the plant is influenced by several factors, soil characteristics and climate are the two most important factors [44,45]. Soil behaviour includes soil pH, structure, texture, organic matter content, moisture, and oxidation-reduction within the soil. The best pH for nitrogen in the soil to be uptaken by plants is 6.5 to 7 [46]. In addition, looking at the texture of soil, sandy and coarse soil cannot hold nitrogen as well compared to clay and loamy soil [47]. Soil with good moisture levels has more available nitrogen compared to dry soil where nitrogen is exposed to volatilization [48]. The oxidation-reduction reaction of nitrogen in the soil also influences its availability since it can be converted from usable to non-useable form [49]. The organic matter like manure enhances the soil fertility [50].

There are several sources of soil nitrogen like organic sources, atmospheric fixation, biological fixation, and industrial fixation. Organic sources like manures [50]. Atmospheric fixation [51,52] when N_2 is converted into NO_2 which reacts then with oxygen to form NO_3. On the other hand, biological fixation [51,53] is with the aid of microorganisms where N_2 is converted to NH_4 by certain bacteria and then by another type of bacteria NH_4 is converted to NO_2 and NO_3. For the industrial fixation of nitrogen is well-known by the Haber process where ammonia is produced from nitrogen and hydrogen gas at high temperatures [54]. Nitrogen in fertilizer can be of several forms like urea, ammonium sulphate, ammonium nitrate, diammonium phosphate and monoammonium phosphate [55].

Farmers usually use fertilizer for agriculture to enhance the nitrogen (nitrate) and other nutrient content in the soil. The balanced supplement of nitrogen to soil is vital since a low amount can restrict or inhibit the growth of the plant and a large amount may cause environmental problems [56]. The excess amount of nitrate can leach into the groundwater and cause contamination [57]. Rivers also are affected by excessive nitrate, a high amount of nitrate in rivers leads to eutrophication which is the dense growth of plants and algae and hence the aquatic life is negatively affected [57]. Consequently, the drinking water can be contaminated too. The reaction of nitrite with amine in the body produces a carcinogenic compound [58]. The indirect effect of nitrate may further extend to climate change. More nitrate means more production of nitrous oxide which causes the ozone layer depletion [57]. Therefore, many different analytical techniques are recently used for the analysis of nitrate and nitrite in soil as well as in water. Spectroscopic methods, electrochemical methods and biosensors are some of the most used methods.

1.2.1.2 Nitrite and nitrate determination
1.2.1.2.1 Spectroscopic methods
Colourimetric method UV-Vis (based on reducing agent).

UV-Vis is a common, easy and widely used spectrophotometric method for several purposes. It is based on measuring the absorbance of visible light and near ultraviolet. In this technique, light passes through the sample which contains the analyte of interest. The sample absorbs some of the light and some of it is transmitted. The relationship between the light passed into? the sample and light transmitted out of the sample are used to determine the absorbance of light. The absorbance is directly proportional to the amount of analyte in the sample.

Figure 1.1 Steps for detection of analyte by UV-Vis spectrophotometer.

The use of Griess assay is the most common assay for nitrate and nitrite detection [59]. For the Griess reagent initially, 1-naphylamine was previously used [59] and due to its toxicity, it was replaced with N-(1-naphthyl)-ethylenediamine dihydrochloride (NED) [60]. In this assay, nitrite reacts with an aromatic compound like sulphanilamide in acidic media to produce a diazonium salt which then reacts with another aromatic compound like N-(1-naphthyl)-ethylenediamine dihydrochloride (NED) which leads to the production of azo dye with intense pink-red colour (**Equation 1.1**) [61]. The more the intensity of the colour, the more the absorbance and hence the high concentration of nitrite.

Sulphanilamide   eq. 1.1
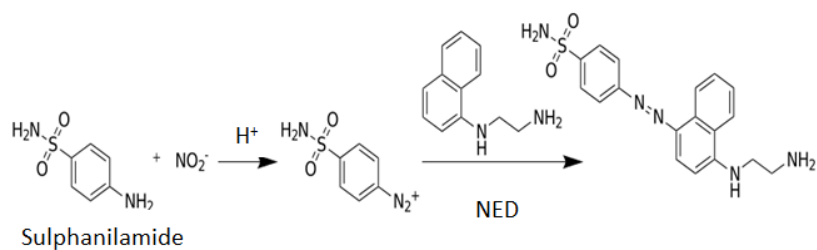
Nitrite is detected directly using the Griess assay whereas nitrate needs to be reduced first using a reducing agent. There are different methods of reduction in the literature where cadmium, vanadium and zinc were used to reduce nitrate to nitrite before performing Griess assay [62-64]. The most common method is the use of a coperized cadmium column for the reduction of nitrate in soil (equation 1.2) [64]. Though this method is very toxic, it provides around 100% reduction of nitrate (**Equation 1.2**). The use of a cadmium column was able to provide a 0.2 to 15 ppm detection range of nitrate in the soil in a fast analysis where 40-100 samples can be analysed per column [65]. However, other than cadmium is toxic the provided linear range is limited and cannot be expanded since linearity will be lost after a specific range due to the use of a spectrophotometer. The column preparation required a lot of complex effort. Therefore, this technique can be used in the laboratory with a lot of care, and it is not efficient to be used in the field. Zinc is also used for reduction in nitrate detection since it provides a less toxic environment compared to cadmium [62,63]. **Equation 1.3** shows the reduction of nitrate to nitrite by zinc. Zinc was used to reduce nitrate in a water sample, and it gave a 0.93 mg/L limit of detection [62]. Vanadium reagent is also used to reduce nitrate to nitrite in soil samples. The reduction took 2 hours at 60 °C. This method results in a 0.01 mg L^{-1} limit of detection [66]. Vanadium use is toxic and time-consuming. Zinc is a promising reducing agent since it also can do the reduction in low time as 12 minutes [67] and it is not toxic like cadmium and vanadium. This study will focus on using zinc as a reducing agent for nitrate detection.

$$Cd + NO_3^- + 2H^+ \rightarrow Cd^{2+} + NO_2^- + H_2O \qquad\qquad \text{eq. 1.2}$$

$$Zn + NO_3^- + 2H^+ \rightarrow Zn^{2+} + NO_2^- + H_2O \qquad\qquad \text{eq. 1.3}$$
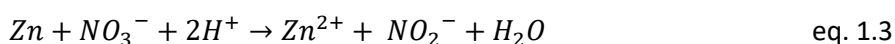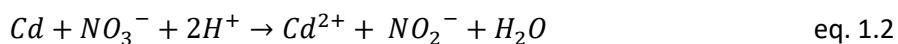
Near-infrared reflectance spectroscopy (NIRS).

Near-infrared spectroscopy is like UV-VIS where a light source and detector are required. NIRS is based on the vibration of the bond between two atoms to produce energy with the aid of light of a specific frequency. The result from NIRS is a spectrum that shows the intensity of the collected light as a function of wavelength. The reflectance was applied to various portable sensors where total nitrogen in the soil was determined [68]. Before the use of the sensor, the soil needed to be treated first by dying, sieving, and grounding hence avoiding the destruction of sensor [69]. However, there was also a soil penetration probe which was made of fibre optic cable and can transmit and collect light when it is in contact with soil [70,71]. The method is portable, commercially available, with a wide detection range for nitrate, requires sometimes no sample preparation and is fast. The full spectrum required 0.1 s to be produced [71,72]. However, the method requires an expert to handle, and expensive instruments are required. In addition, care for the fibre probes is required.

Mid-infrared Fourier transformation attenuated total reflectance spectroscopy.

Mid-infrared has the same principle as near infrared but instead, the radiation is not directed directly into the sample. It is directed first into the crystal which is in contact with the sample. The light then passes through the crystal then to the sample and finally to the spectrophotometer for spectrum determination. The spectrum can be produced within 3-5 seconds. Even though it is fast, and is considered a field-promising method, however, this technique sometimes still requires some sample preparation, and the dry soil is difficult to use [73,74]. It also requires the use of fibre like ATR ZnSe crystal and silver halide fibres [75]. Linke et al were able to detect nitrate in the 0-140 ppm range using this method [76]. Nitrate band detection in 1350-1370 cm^{-1} was interrupted by another band in 1450 cm^{-1} and hence the method was not with high accuracy [76]. This interference happened especially with samples with complex mixtures. Another study tried to solve this problem by adding some calculations and equations to remove the interference effect [77].

Chemiluminescence (CL).

In chemiluminescence, the detection is based on the emission of light because of chemical reaction [78]. This method is widely used for the determination of nitrate and nitrite [79-81] due to its simplicity and wide linear range. The absence of light in this method improves its background signal and consequently improves the limit of detection. There is gas CL where detection happens by reduction of nitrate/nitrate to NO and then reaction with Ozon [82]. The method was initially applied for the determination of nitrite in seawater and blood samples [83,84]. It was also

improved for interference removal [85]. It was combined with a flow injection system to improve the separation and the limit of detection [85,86]. However, the method requires the use of high temperature and inert gas. Also, a small amount of oxygen can cause interference and affect the result. There is also luminol CL for nitrate/nitrite determination [87,88], where luminol is oxidized to a 3-aminophthalate anion which then emits energy during relaxation [89]. An example is the detection of nitrite by reaction with ferrocyanide and the production of ferricyanide which react with the luminol [88]. Microflow injection which is attached to the chip was used [88]. Even though the Cl method has lots of advantages it still has drawbacks. Environmental conditions can affect the intensity of emissions. The method has poor stability and reproducibility [88].

Fluorometry.

It is based on the fluorescence of light from the sample. This happened after applying light to the sample and exciting its electrons which then emit light during relaxation [78]. Fluorometry is used widely for nitrate and nitrite determination [90-93]. An example of this oxidation of nitrite by Ce (IV) to produce Ce (III) [94]. This method may be influenced by interference of other redox components. In another fluorometric determination of diazonium salt which is produced by reaction of nitrite with 2-amino-4-chloro-1-hydroxybenzene-6-sulphonic acid or 4-aminofluorescein [95].

1.2.1.2.2 Electrochemical method

Ion selective electrode

Ion-selective electrode is a good and efficient alternative to the tedious and complicated laboratory methods [96,97]. The work of the electrode is based on the production of voltage which increases with the increase of the nitrate ion or concentration in the solution [98]. The electrode is coated with membrane for example polyvinylchloride (PVC) which allows specifically nitrate to pass through [98]. The movement of nitrate ions in the membrane is based on osmosis. The ions move through the membrane until equilibrium is reached. Consequently, the potential difference result between electrodes and the number of ions is proportional to this difference [98]. The use of ion-selective electrodes for nitrate analysis in soil is intensively studied since the ion-selective electrode is a promising method for in situ or field use [12,99-101]. These studies aimed to improve the accuracy, selectivity, efficiency, and limit of detection of the method. The accuracy of the method in some research reached 95% where the analysis was done using soil extract in deionized water [102]. A stable value was determined within 6 seconds [102] [103]. ISE is cheap, fast, accurate and provides good sensitivity for nitrate. Ion selective electrodes are easy to use and require less sample preparation, therefore, it was widely used for field or in situ analysis [98]. However, the main problem is the lifetime of the electrode after in contact with soil

since Interaction might occur between soil and electrode. In addition, the electrode needs to be washed after each run. The analytical technique of ion-selective electrodes also suffer from interference. Slurry from soil can significantly interfere with the result, consequently, a centrifuge is used to reduce the problem [98]. Anions like chloride, bromide and nitrite may also cause interferences [104]. Therefore, selectivity, sensitivity and robustness may be affected.

1.2.1.2.3   Biosensors

Nitrate biosensors are a kind of sensors which contain biological membranes which are permeable to nitrate. Nitrate interacts with the enzyme (nitrate reductase) which reduces nitrate to N_2O transducer. The N_2O then is detected. The main advantage of biosensors is that they can be used to detect nitrate in different types of samples such as soil, food, sea, and wastewater [105-107]. In addition, the sensor provided a wider linear range and low limit of detection (0.014 ppm) for nitrate [108]. The detection time is also short 15-60 seconds [108]. However, the method suffers from problems due to its instability and care needs to be taken to ensure selectivity.

1.2.1.2.4   Separation based method.

Ion chromatography

Ion chromatography is a separation technique where the separation of ions is based on their affinity and attraction to the ion exchanger which is a stationary phase [19]. There are two types of ions exchangers, cationic and anionic ion exchangers which are used to separate cations and anions respectively [19]. Nitrate and nitrite are widely determined by ion chromatography in analytical laboratory [20-22,109-114]. For example, nitrate in soil samples were analysed by ion chromatography which was able to reach 0.05 ppm limit of detection [22,104]. The separation of nitrate from other possible interferences in the column contributed to enhancing the sensitivity. In addition, deionized water was used for the extraction of nitrate from soil and plant and hence the study produced a good limit of detection [22,104]. In the chemistry laboratory, several tools are available to perform the extraction with the help of different kinds of solvents [115,116]. One of the favourable solvents for nitrate extraction is KCl [117] since it ensures efficient extraction of nitrate from the soil. However, the use of chloride leads to interference since chloride produces a huge peak which hinders the peak of nitrate during separation in the chromatogram [118]. In general, organic matter and solvent used for extraction are two important factors to consider when ion chromatography is used for nitrate analysis in soil since they may cause interference. Even though Ion chromatography is a fast, sensitive, and reliable method, it is a laboratory-based technique with sophisticated instrumentation and cannot be used in the field.

Capillary electrophoresis

Capillary electrophoresis is a separation technique which can be performed in several different modes [119]. It has a different concept than ion, gas and high-performance liquid chromatography techniques. GC (gas chromatography) and HPLC (high-performance chromatography) separation techniques are based on the affinity of the analyte to the stationary phase in the column. In comparison, the separation in capillary electrophoresis is based on the applied electrical field. The ions are separated according to their charge-to-size ratio [119]. When high voltage is applied anions move toward the positive electrode and cations move toward the negative electrode, consequently ions are separate based on their speed. Capillary electrophoresis is a fast simultaneous separation method which is applied for different matrices [120]. It is used for the determination of nitrite and nitrate where a UV detector can be used at a wavelength of 214 nm [120]. Several studies were published for the determination of nitrate and nitrate by capillary electrophoresis using different detection methods [121,122]. Although it is a good separation technique and many steps have been done to improve the limit of detection and sensitivity this technique still requires several separation and preparation steps to avoid interference and any adsorption which might occur in the wall of the capillary [123,124]. In addition, several solution preparations were required. **Table 1.1** summarises the method for nitrate determination and its advantages and limitations.

Table 1.1 LOD, sample preparation, advantages and limitations for methods used for nitrate determination.

Method	LOD/ sample	Sample preparation	Advantages	Limitation	Reference
UV-Vis Cd reduction	N/A Soil	- Extraction of components from soil by KCl - Use of centrifuge for soil separation from extract	100% reduction of nitrate	- The cadmium column required a lot of preparation and treatment. - Cd is toxic and carcinogenic. - Small detection range - Can be carried only in the lab by an expert	[64]
UV-Vis Zn reduction	0.01 mg/l Soil	- Extraction by solvent (water, KCl) - Use of centrifuge	- Zn is not toxic	- Reduction is not as perfect as reduction by cadmium. - The experiment is carried out in the lab by an expert	[62]
NIRS	0.05 µg/L Water	- Drying, sieving, and grounding are required if a soil probe is not used	- Portable for in-site detection - Wider detection range - Fast (spectrum produced within a second) - No or little sample preparation	- The experiment should be performed by an expert person	[125]

Method	LOD/ sample	Sample preparation	Advantages	Limitation	Reference
MIR	1.55 mg/L Soil	- A thin film of sample is used. - The sample is homogenized	- Fast requires 3-5 seconds. - No sample preparation is required	- A thin film of sample is used. - Expensive due to the use of optical mirrors.	[76]
Ion selective electrode	0.5 mg/L Soil	Extraction and removal of soil suspension is required	- Very specific for nitrate detection - Fast (6 seconds for each analysis) - 95% accuracy	- Lifetime of electrode - Interference from slurry, Cl ion, Br ion - Can be used in the field but by an expert person. - expensive	[99]
biosensors	0.014 mg/L Soil	Sometimes no sample preparation is required	- Wider linear range - Fast (15-60 seconds)	- Instability of the biosensor and care needs to be taken to ensure selectivity. - expensive	[108]
Ion chromatography	0.05 mg/L Soil	sample must be extracted first by solvent and centrifuged to remove the soil particles	- separation reduces the interference and enhances the sensitivity. - simultaneous detection	- a lot of instrumentation is required. - column choice and treatment - for lab work only but not for the field - expensive	[104]
Capillary electrophoresis	0.14 mg/L Soil	sample must be extracted first by solvent and centrifuged to remove the soil particles or suspension	- For simultaneous detection - Different samples can be analyzed	- Several steps are required to avoid interference. - Adsorption in the wall of the capillary may occur. - Not field instrument	[106]

Method	LOD/ sample	Sample preparation	Advantages	Limitation	Reference
				- expensive	

1.2.2 Conventional method for manganese determination

1.2.2.1 Manganese in plant and soil

Some plant nutrients are required from the soil in micro levels like zinc, iron, copper, and others. One of the essential micronutrients is manganese. Manganese is necessary for plant growth in a healthy way. It is needed for the biosynthesis of lipids, lignin, and carbohydrates in the plant [126]. Manganese has several forms, Manganese with oxidation states +2, +3, +4, +5, +6 and +7 [126]. The most available forms are manganese with oxidation states +2 and +3 [126]. However, Mn^{+2} is more soluble in soil compared to other oxidation state manganese [126]. In addition, it is the most common form which is uptaken by plants. pH of the soil significantly affected the availability of manganese at pH lower than 5.5 Mn^{+2} is the most common form of manganese [127]. However, at neutral pH or high pH Mn^{+3}, Mn^{+4} and Mn-oxides are the most common [126]. Microorganisms also affect Mn solubility in the soil since they can oxidise or reduce manganese [128,129]. The level of manganese in soil below which fertilizer should be applied is 10 mg kg^{-1} and around 10-30 mg kg^{-1} is the optimum level [130,131]. Very low levels can cause deficiency and very high levels can cause toxicity. Manganese deficiency can happen in the alkaline soil. Also, it may occur due to high concentrations of other minerals which can replace manganese absorption like iron, calcium, phosphorous and magnesium [126,127]. Manganese deficiency results in chlorosis (yellow leaves) due to the less chlorophyll since the photosynthesis is affected [126,127]. Tissue necrosis results from manganese deficiency [126,127]. Toxicity of manganese occurs in acidic soil [127]. It leads also to chlorosis tissue neurosis and brown spots on the plant [127].

1.2.2.2 Manganese determination

1.2.2.2.1 Atomic absorption spectroscopy

Atomic absorption spectroscopy is a technique which is based on atomization of the analyte by applying energy. The electron in the atom when it is exposed to the energy of a specific wavelength becomes exited and moves from a lower energy level to a higher energy level [78]. After that electron moves to a lower energy level and emits light or energy. Each atom or element emits a specific energy or wavelength which helps to distinguish it. The wavelength intensity is directly related to the concentration of the metal and hence quantification can be

determined [78]. There are two popular sample introductions systems either by flame or furnace. Flame atomic absorption spectroscopy is used to analyse elements like potassium, calcium, zinc, iron, and others [78]. The sample is introduced as spray which is evaporated and atomized in the flame. Hallow cathode lame is used as a source of light which is directed into the flame to excite the electron and the monochromator is used to collect light with a specific wavelength [78]. Graphite furnace atomic absorption spectroscopy is used to analyse elements in ppb levels like nickel, cadmium, manganese, and others. Sample this time is introduced to furnace [78]. There are several research for the detection of manganese by atomic absorption spectroscopy in different types of samples like food, biological, water and others [132-134]. Digestion of the sample is required before introduction to the instrument [134]. Sometimes extraction also from the water sample is needed [135]. manganese was extracted by cloud point extraction after forming a complex with a specific compound (1-(2-thiazolylazo)-2-naphthol (TAN)) [135]. This method was able to detect 0.28 ppb of manganese. This step aimed to preconcentrate manganese before introduction into the instrument and hence improve the sensitivity. Extraction under high temperature and pressure and ultrasound extraction were also used as preconcentration methods [136,137]. This method for manganese detection requires instrumentation and it can be performed in the lab only, it is impossible to drag it to the field, in addition, a lot of sample treatment and preparation are required.

1.2.2.2.2   inductively coupled plasma-(OES/MS)

Inductively coupled plasma optical emission spectroscopy (ICP-OES) is based on the measuring of energy of the ion or the atom after excitation and the detection can be as low as ppb and ppt level. The sample after digestion is introduced into the spray chamber and it is carried with argon gas to the torch at a high temperature where the sample is atomised and ionized. The ionized sample produces energy which is detected by the detector. The produced energy is proportional to the quantity of the analyte and hence the analyte can be quantified. ICP-OES is used for samples with high total dissolved salt (TDS) since it has a high tolerance level to the TDS compared to ICP-MS. Inductively coupled plasma mass spectroscopy is based on measuring the mass of the atom by mass spectrometry. It can detect up to ppt level which is more sensitive than ICP-OES. ICP-MS is efficient when it comes to isotope studies since it measures the mass per charge of specific ionized ions. Manganese was analysed by ICP-MS and ICP-OES in different samples like blood, food, water, and others [23,138-141]. When blood sample was used it was treated first in different ways, one of these ways is by treatment with tetramethylammonium hydroxide (TMAH), Ethylenediamine, tetra acetic acid (EDTA) and Triton X-100 [23]. In addition, some incubation is required to make it ready to be analysed by ICP-MS [23]. Also, ICP-MS was coupled with HPLC to increase the sensitivity and reduce the sample preparation for manganese

detection [132]. Using ICP-MS and ICP-OES is very sensitive and can detect manganese to trace level with less effect of interference. However, this requires a lot of instrument operation. An expert person should care for and handle the device. In addition, a lot of sample preparation and treatment with acid and digestion is required.

1.2.2.2.3 Colorimetric detection

The colorimetric method is based on the colour change which can be measured using a UV-Vis spectrophotometer where absorbance at a specific wavelength can be determined. The Persulphate method was used as a colourimetric detection method for manganese. In this method, sample pre-treatment is required [142]. The treated sample was mixed with the $(NH_4)_2S_2O_8$, boiled and stand for 1 min[142]. the absorbance was determined at 525 wavelength [142]. This method has an LOD of around 42 µg L^{-1} [142]. Another method is formaldoxime (FAD) which was prepared by a combination of formalin solution and hydroxylammonium hydrochloride [143]. This produces a complex with manganese which can be detected at 528 nm wavelength [143]. In addition, it tends to cause interference by iron [143]. Porphyrin [T(4CP) P] method is also another colorimetric method which was more sensitive compared to the Persulphate method. This method is based on forming a complex between cadmium and the detection compound where the manganese complex is more stable and hence the exchange of cadmium by manganese occurs [144]. The detection is at 458 nm wavelength [144]. The reaction is fast within 5 minutes [144]. The detection limit of manganese was 0.84 µg L^{-1} [144]. However, in this method, the toxic cadmium was used. In addition, gold and silver nanoparticles were used for the colourimetric detection of manganese [145,146]. In general, the nanoparticles tend to coagulate in the presence of manganese [145,146]. However, this method suffers from interference since another component in the sample may cause this coagulation. Another method for colourimetric detection of manganese is the PAN method (equation 1.4). This required the formation of a complex between l-(2-pyridylazo)-2-naphthol (PAN) and manganese [147]. However, this can happen at high pH. The use of a buffer was critical. In addition, l-(2-pyridylazo)-2-naphthol (PAN) did not dissolve easily in water organic solvent needs to be used and many people in literature adopted the use of the non-ionic surfactants like Triton X-100 instead of the organic solvent [147]. This method suffered from interference like Iron, cadmium, zinc, cobalt, and nickel. These were masked by a masking agent (cyanide) [147]. PAR method is another method for the colourimetric detection of manganese (**equation 1.5**). 4-(2-pyrldylazo) resorcinol (PAR) reacts with manganese to form a complex which is stable in basic conditions[148]. Several buffers for pH control were tried and

borate was the most effective to produce a stable complex [148]. This method also interfered with other metals like cobalt (II), nickel (II), and zinc (II) and hence masking agents were also required [148-150]. The colourimetric method is cheap and easy to work with. Therefore, this study focuses on the use of PAR and PAN (equation) methods for manganese detection since they are more applicable in paper devices and their toxic reagent can be replaced with other reagents. **Table 1.2** summarizes the methods for manganese detection, their advantages, and limitations.

eq. 1.4

eq. 1.5
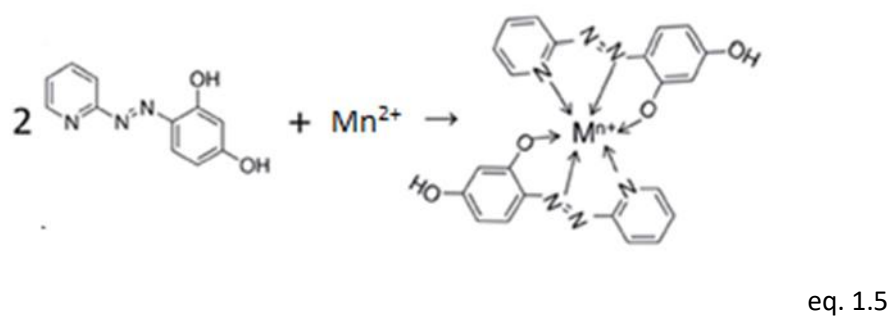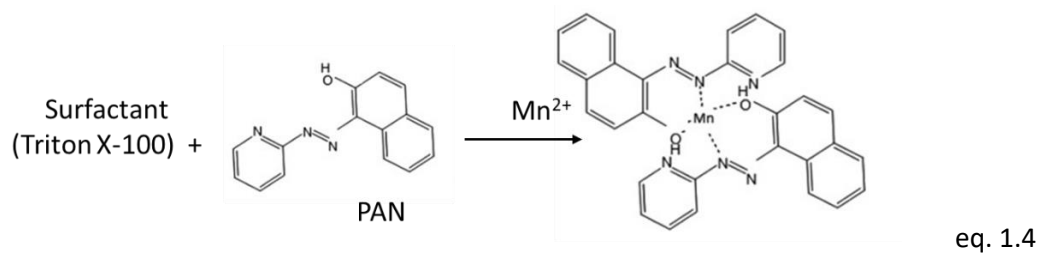
Table 1.2 Manganese detection limit in different type of sample using different methods.

Type of sample	method	LOD	advantages	Limitations	reference
Water (river, sea, tap)	Atomic absorption spectroscopy	0.28 µg L^{-1}	- sensitive to ppb level - widely used in the lab	- require instrumentation. - can be performed in the lab only. - impossible to drag it to the field. - a lot of sample treatment and preparation are required.	[135]
plant	Atomic absorption spectroscopy	2 µg L^{-1}			[132]
seawater	Atomic absorption spectroscopy	0.2pg L^{-1}			[151]
Food and water	Atomic absorption spectroscopy	2.9 µg L^{-1}			[152]
SOIL	Atomic absorption spectroscopy	0.52 µg L^{-1}			[153]
blood	ICP-MS	0.09 µg L^{-1}	- Sensitive detection can be up to ppb level. - High Selectively	- requires a lot of instrument operation. - An expert person should care for and handle the device. - a lot of sample preparation and treatment with	[23]
Plant (wheat flour)	ICP-MS	3.6 µg L^{-1}			[138]

Type of sample	method	LOD	advantages	Limitations	reference
				acid and digestion is required.	
Soil	ICP-MS	-			[154]
water	ICP-OES	0.11 and 21 µg L^{-1}.	- high tolerance level to the total dissolved salt TDS compared to ICP-MS	- An expert person should care for and handle the device.	[139]
coffee	ICP-OES	0.015 µg g^{-1}			[140]
Vegetable Samples	ICP-OES	0.50 µg L^{-1}		- sample preparation is still required.	[141]
water	Colorimetric (Persulphate)	42 µg L^{-1}	- Sensitive detection can be up to ppb.	- pre-treatment of the sample is required	[149,150]
water	Colorimetric (Porphyrin [T(4CP)P])	0.84 µg L^{-1}	- Sensitive detection can be up to ppb. - The manganese complex is stable. - reaction is fast within 5 minutes.	- Toxic Cadmium is used	[144]

Type of sample	method	LOD	advantages	Limitations	reference
water	Colorimetric (PAN)	-	- Easy to use and cheap	- pH sensitive. The use of a buffer was critical. - interference like Iron, cadmium, zinc, cobalt and nickel - toxic masking agent required (cyanide)	155
water	Colorimetric (PAR)	-	- Easy to use and cheap	- pH sensitive control - Toxic borate was used. - interfered with other metals like cobalt (II), nickel (II), and zinc (II)	148
Soil	Colorimetric: Bis(2-hydroxy-1-naphthaldehyde) Orthophenylenediamine	$1\ \mu g\ L^{-1}$	Easy to use and cheap	- interference like Iron, cadmium, zinc, cobalt and nickel - pH sensitive	156

1.3 Commercially available test for soil nutrient determination
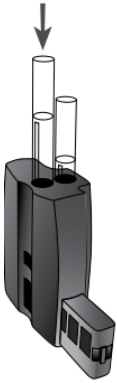
There are several available commercial methods for soil nutrients determination. These methods were developed by many suppliers for field use or fast determination of the nutrients.

They were aimed to determine the nutrients in the available range in the environment. Some of these methods were quantitative based on giving a number and some were semi-quantitative based on estimation of the quantity of nutrients. This estimation is based on a comparison with available standards by eyes. **Table 1.3** shows some examples of the existing and most available commercial kits for soil nutrients determination, the name of the kit, supplier, website photo of kit, price, method of detection and disadvantages were mentioned. Keep in mind that there are other similar kits (either for the same supplier mentioned here or for suppliers which are not mentioned here) which are not mentioned in **Table 1.3**. These mentioned kits have several advantages including simplicity, determination of several nutrients and good environment detection range. However, in the table we focus on the disadvantages and limitations which encourage researchers to develop new methods or to add improvement to existing ideas to fit the needs of the field use and the needs of low-income countries where such kits are difficult to provide. Most of the methods require the use of chemicals either for extraction or for the detection of the nutrients. Also, yes some kits can be used to analyse several nutrients; however, they are still expensive to be afforded by low-income people. In addition, some of the methods which are not expensive are not quantitative, and the detection is based on the eyes of the user. This increases the possibility of an error in the estimation of the nutrient content. The method which is based on the use of a meter and chemicals requires the user to buy the chemicals and battery of the meter from time to time. This is a difficult option in low-income countries. Therefore, there is a need for a portable method that combines several characteristics that make it usable in the field. The method should be cost-effective, quantitative, simple to use and affordable to farmer.
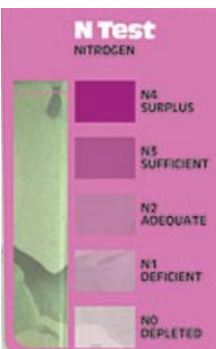
Table 1.3 Some commercially available kits for soil nutrients determination. The name of the kit, supplier, website photo of the kit, price, method of detection and disadvantages were mentioned.

Kit name and supplier	Website and photo	price	Method of detection	Disadvantages
Gardening naturally, Soil Testing Kit 32 Tests	https://www.gardening-naturally.com/soil-testing-kit-32-tests	£19.99	Colorimetric detection by eyes	Not quantitative

Kit name and supplier	Website and photo	price	Method of detection	Disadvantages
Lamotte, Nitrate-Nitrogen Test Kit	https://lamotte.com/nitrate-nitrogen-test-kit-3615-01			Use of chemicals (reagents for calibration)/ quantity of chemicals can go to 10 mL
Lamotte	https://lamotte.com/model-sth-7-soil-testing-outfit		Colourimetric by eyes	Use of chemicals, use of filter paper for filtration, Several steps, Not quantitative

Kit name and supplier	Website and photo	price	Method of detection	Disadvantages
Nutrient analyzer, CleanGrow	https://www.ionselectiveelectrode.com/products/cleangrow-multi-ion-nutrient-analyzer-kit	£1500	electrodes	Expensive, chemicals for calibration, a sensor that works with battery
AccuGrow, Soil Test Strips	https://www.environmental-expert.com/products/accugrow-soil-test-strips-247946		Colourimetric by eyes	Not quantitative
SoilDoc Kit, Columbia University, Agriculture and Food Security Centre	https://www.ifama.org/resources/files/2014-Conference/W1TTSoilDoc.pdf		electrodes	The use of chemicals requires multistep, complicated without practice
Rapitest® Digital, Soil Test Kit	https://www.carolina.com/environmental-science-meters/rapitest-digital-soil-test-kit/665413.pr	£37.14	Digital electronic meter with indicator	Use of chemicals

Kit name and supplier	Website and photo	price	Method of detection	Disadvantages
Soil Test Kit, EARTHEASY	https://eartheasy.com/soil-test-kit/	£14.65	Colourimetric by eyes	Chemicals in the form of capsules, not quantitative
Haofy, Soil Test Kit	https://www.amazon.co.uk/Haofy-Solution-Nitrogen-Potassium-Gardening/dp/B0BS44K83B	£12	Colourimetric by eyes	Chemicals use, not quantitative
Soil Test Kits, environmental expert	https://aicagroinstruments.com/products/soil-test-kits-2/		Colourimetric by eyes	Chemicals use, not quantitative, multistep are required

Kit name and supplier	Website and photo	price	Method of detection	Disadvant ages
Nagarjuna - Portable Soil Testing Kits	https://www.environmental-expert.com/products/nagarjuna-portable-soil-testing-kits-817196		Colourim etric by eyes	Chemicals use, not quantitativ e
PALINTEST SKW500 Complete Soil Managem ent Kit portable soil test	https://www.lab-shop.com/environmental-testing-c95/portable-laboratories-c96/palintest-skw500-complete-soil-management-kit-portable-soil-test-laboratory-p54	£1,8 81	Colourim etric with meter reader	Chemicals used, complicat ed, very expensive
LAQUA Twin Nitrate Meter	https://www.specmeters.com/nutrient-management/nutrient-meters/nitrate/laqua-twin-nitrate-meter/		Meter with electronic sensor	Chemicals used as calibration standards

Kit name and supplier	Website and photo	price	Method of detection	Disadvantages
	25			

1.4 Paper-based microfluidic device.

In general, the two common types of microfluidic devices are chips (silicon, glass and polymers) and papers [157]. Each of them has its characteristics including its advantages and disadvantages. The use of chips is widely common for soil analysis for nutrients, explosives and organisms in soil [158-169]. However, the use of chips is still complicated and requires a compartment for chemicals, needs pump and sometimes extraction of nutrients from soil before detection. This dissertation focuses on a paper microfluidic device and its environmental application [170]. Compared to conventional techniques or polymer, glass and silicon chip paper in microfluidic systems offer several merits. No external power for sample flow is required for paper. Capillary action within the paper is available. The capillary action is clearer at micro-scale level [27] and hence no pumps are needed [28]. In addition, paper devices are portable, easily accessible, and disposable [30,31] due to their small size and low cost.

1.4.1 Cellulose characteristic and type of paper

Paper consists of cellulose fibre as in **Figure 1.2** with monomers (n is the degree of polymerization which is based on extraction and manufacture [28,171]). Glucose molecules in cellulose have hydroxyl groups that help to bond molecules together by covalent bonds. Cellulose is stiff and rigid [28,171] due to its long chain and also due to the intra-molecular bonds between the monomers. Cellulose has partial positive and negative charge within the cellulose helps to give it its hydrophilic character and hence it can be attracted to water in solution. Cellulose is not soluble in organic solvent [28] and that makes it a good surface for chemical reactions. In addition, cellulose causes no harm or adverse effect on living system [172] (it is Biocompatible). Digestion of cellulose by grass-eating animals is possible (it is biodegradable). Cellulose can be obtained from mainly wood and cotton [173]. Annually 1.5×10^2 tons of cellulose are synthesized [172].
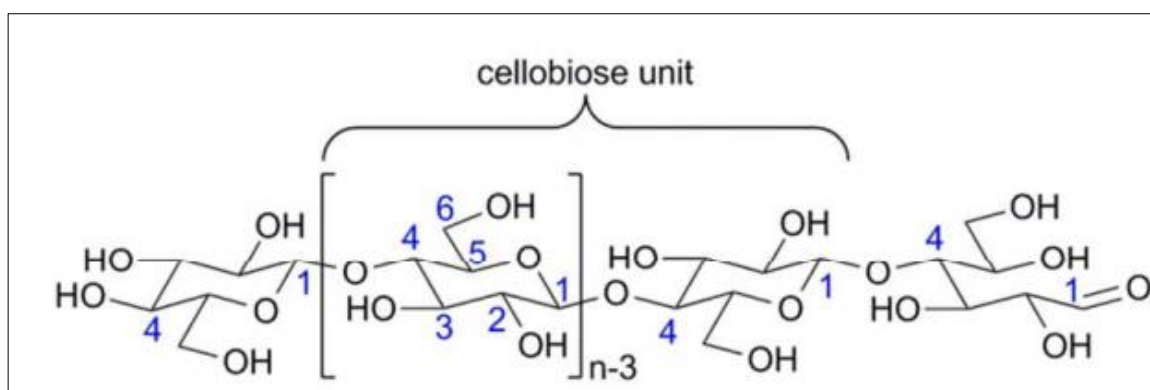
Figure 1.2 Cellulose molecular structure [28].

Filter Paper is used in laboratories. Mainly people use Whatman number 1 filter paper because of its medium retention and flow rate [174]. Whatman number 1 filter paper has an 11 µm pore size. There is also Whatman number 4 filter paper with a larger pores size which is 20-55 µm. As a result, the Whatman number 4 filter paper has a higher flow rate [174]. A high flow rate reduces the swelling of cellulose by the solvent. There is also another type of paper which is called nitrocellulose which is more useful for immunoassay since it is more compatible with proteins compared to the normal filter paper [175]. Nitrocellulose has a 0.45 µm pore size which results in more stable flow along the paper [174]. The nitrocellulose paper was tested for biomolecule analysis and its ability to deposit enzymes[176,177]. In addition, the wax barrier was created on the nitrocellulose paper [176,177]. It was observed that this paper provides uniform flow for the liquid. However, it experienced slow wax penetration compared to the normal filter paper. Mainly Whatman number 1 filter paper will be used in this work since it has uniform wicking, and can be treated easily with wax.

1.4.2   Fabrication of paper devices

Hydrophobic barriers are made within the hydrophilic paper. Or cutting is used instead of barriers. There are several methods [178] used for this purpose, basic methods are mentioned here.

Photolithograph

Martinez et al. [179] introduced a photolithograph. The device was made with the aid of photoresist material as in **Figure 1.3** [179]. The paper was immersed in a material called photoresist. The required shape was patterned by a mask. UV light is directed to the mask with the paper. After removing the mask, the channels were created [179]. Glucose and protein [179] were analysed by a device made by this method. Several studies came as a result of this work [180]. The method is with good resolution; however, it requires lots of steps and expensive equipment and reagents. In addition, it still suffers from drawbacks like the possibility of photoresist damage when the device is bent or folded.
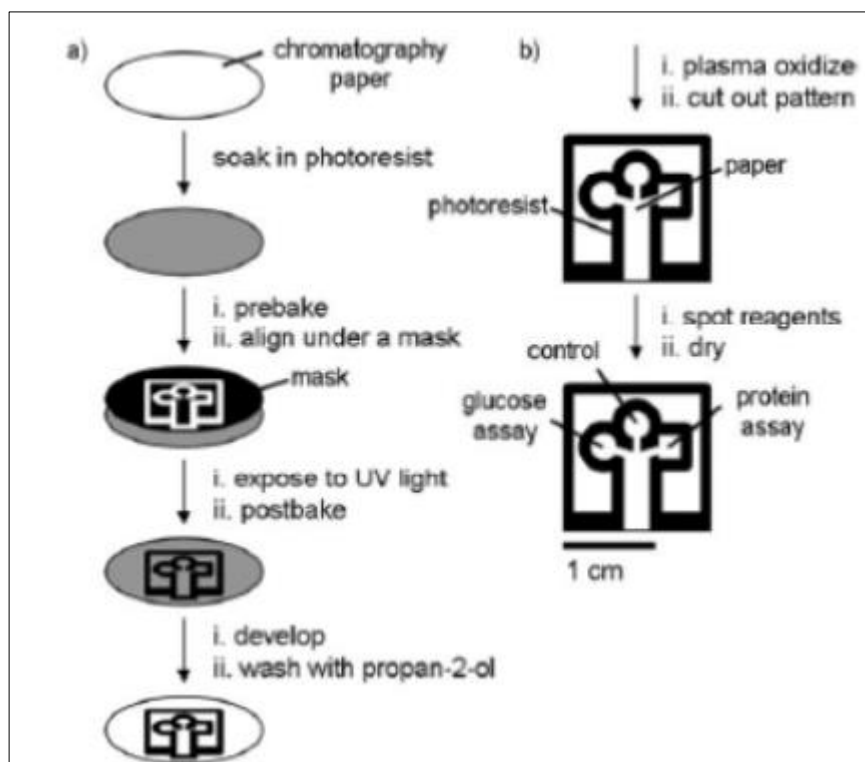
Figure 1.3 Photolithography technique for paper fabrication. It was used in 2007 by Martinez et al. The paper was immersed in a material called photoresist. The required shape was patterned by a mask. UV light is directed to the mask with the paper. After removing the mask, the channels were created [179].

Wax screen printing

In this method, the wax is rubbed off on the paper by using a screen. After that, the wax is melted on a hot plate and hence the paper absorbs the wax as in **Figure 1.4** [181]. This method is simple and requires no sophisticated instrumentation. Also, it is environmentally friendly since no solutions or chemicals were used [181]. However, it required a special screen for each pattern, and it still provides a low-resolution device due to the limited minimum width of the channel and the hydrophobic barrier [181]. Wax screen printing was widely used for the detection and analysis of several components like heavy metal, nitrite and glucose [182,183].
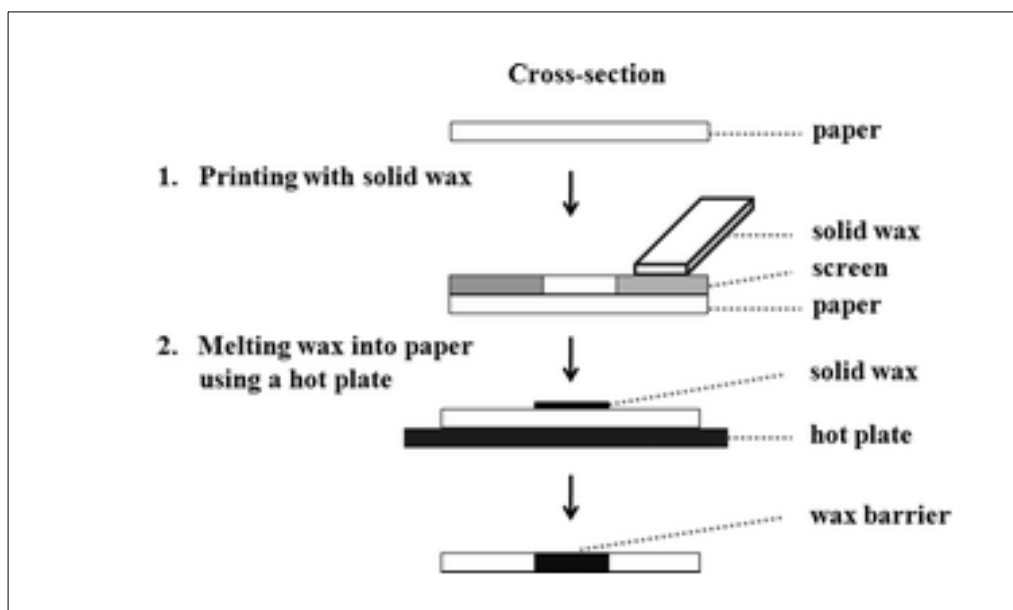
Figure 1.4 Screen wax printing for paper fabrication. This method requires two steps, printing the wax and melting it. [181]

Inkjet printing and etching

In this method, the ink (e.g., KD, methylsilsesquioxane, UV curable acrylates) is printed into the paper to form? the hydrophobic area within paper [184,185]. In inkjet etching the paper is dipped into polystyrene solution to make it hydrophobic. Then the chemical ink is printed on the paper by the inkjet printing device as in **Figure 1.5** [29]. This method was used by Koji et al. to determine the protein, glucose, and PH for urine sample [29]. Alkyl ketene dimer can be used as a cheaper alternative [186]. However, it requires heating which may cause damage to the paper itself [186]. The method is efficient to fit the purpose of the printing device; however, modification of the printer is required, and this reduces its lifetime [184,185].
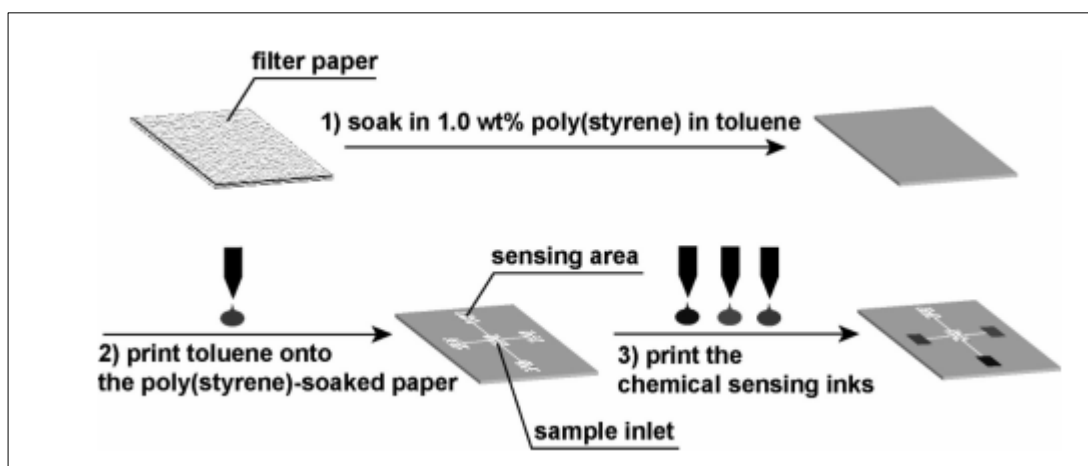
Figure 1.5 Steps for inkjet printing. Paper was dipped into a polystyrene solution and then toluene was printed onto that paper. Finally, chemicals are printed on the paper by the same inkjet printing device [29].

Plasma treatment

In this technique metal masks were used. The filter paper was sandwiched between the masks [187]. The mask has a specific pattern according to the design needed for experiment [187]. Then the sandwiched paper was treated under the plasma [187]. This created hydrophilic and hydrophobic areas within the paper.

laser toner printing

The toner was printed on paper and then heated at 200 degrees for 60 minutes in hot plate [188]. polyesters and styrene acrylates were examined and used as pattering agents [188,189]; this method requires high temperature which may change the characteristics of paper.

flexographic printing

In this method (**Figure 1.6**) the paper was added to the roll and the ink was added into the ink tank it moved then to the roll into the printing plate which had a specific shape to be printed into the paper [190]. Polystyrene and xylene were examples of ink used [190]. This method is good for mass production; however, it is expensive since it requires simultaneous cleaning, and needs different plates for printing.
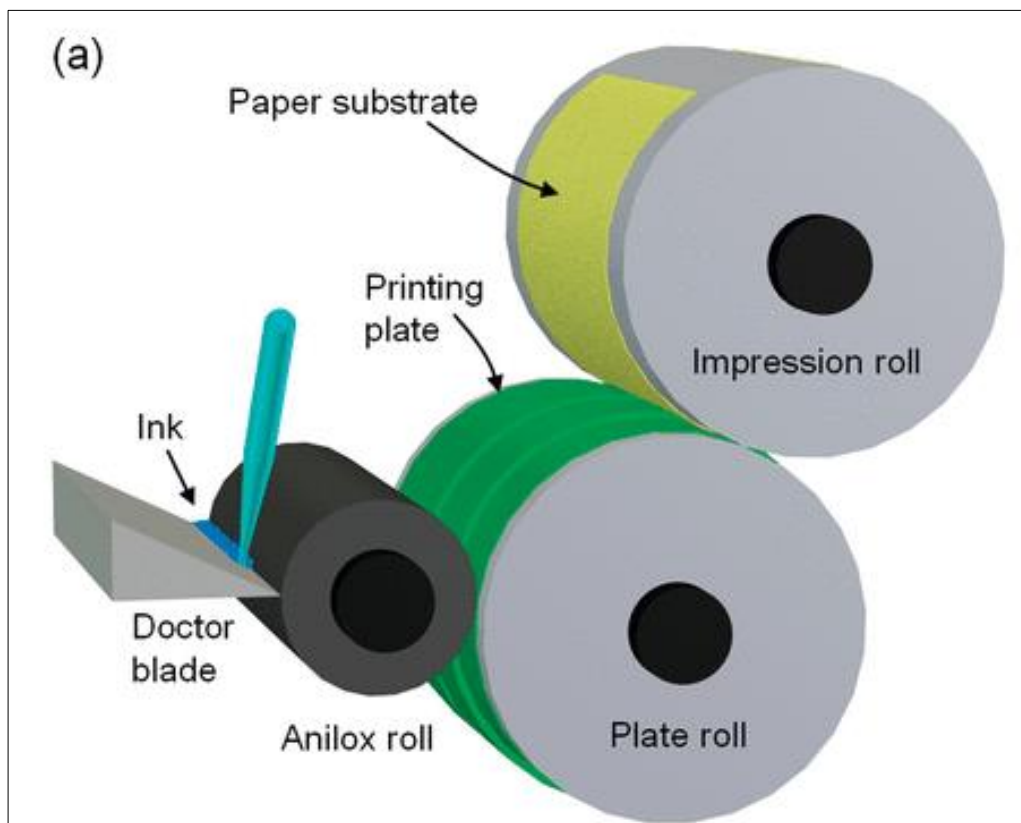
Figure 1.6 Flexographic printing paper was added to the impression roll and the ink was added into the ink tank and it moves then to the roll in the printing plate which has a specific shape to be printed into the paper [190]

Laser cutting

laser or blade are ways to cut the paper. However, laser cutting gives more precision [191]. In this method, the laser is used to define the channel or the pattern of the device. Edges control solution flow in the device. CO_2 laser cutting was used by Mahmud et al. to make the device [191]. Adhesive and foil layers were used to support the paper after cutting [191]. Another strategy for laser cutting was done by Nie et al. [192]. The device inlet and outlet were kept open and hence the device and substrate remain together [192]. Laser cutting is expensive; however, it is more precise and accurate than the blade.

Direct wax printing

Wax pens, inkjet printers and direct wax printers [177,193] are ways of wax printing. Different designs c can be printed on paper by direct wax printing. Wax is first added to the paper by the printer. Then the wax was heated to melt within the paper and create a barrier, The heating was done by hot plate or by laminator. The produced device is flexible and can be folded and hence 3D device can be made[194]. **Figure 1.7** shows the three main steps for direct wax printing. There are also several other existing paper fabrication techniques as mentioned below, however, in this study, mainly direct wax printing will be used since it is simple, easy to use and flexible to design different patterns of devices.
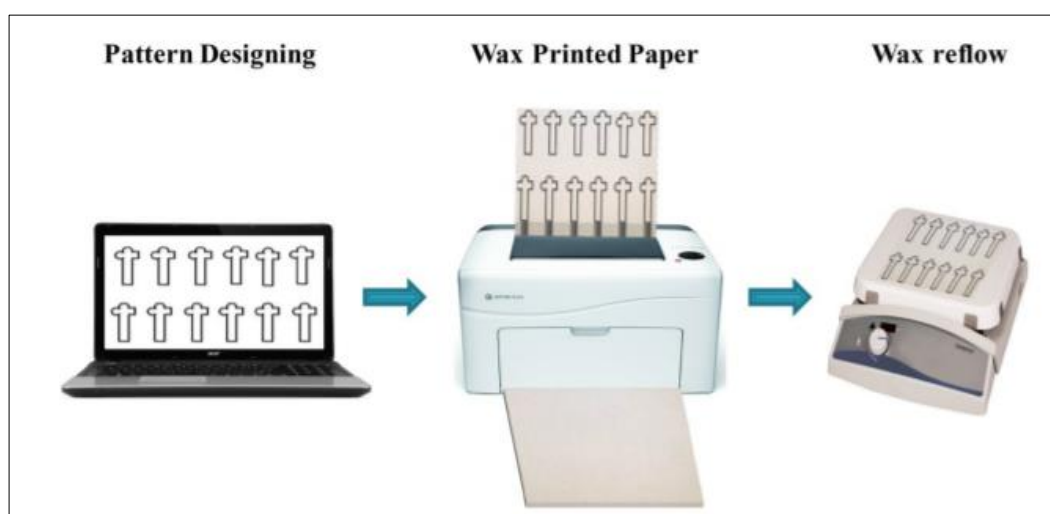
Figure 1.7 Direct wax printing by wax printer. First, the device was designed. Second, the wax was printed by the wax printer. Third, the wax was heated on a hot plate to penetrate the paper [195].

other methods

PDMS (polydimethyl siloxane) printing [196] methods are simple and not expensive, but it requires steps, and it is not applicable for mass production. In addition, it has low resolution.

wax dipping [197], Stamping [198,199], corona treatment [200] and spraying [201] are also some of the fabrication methods. These methods are simple and low in cost. However, it requires a specific stamp/ mold to be made for each pattern consequently it is not applicable for large production of devices.

The drawing [202] method is based on drawing by pen, and it requires no heating after the ink addition. It is not a consistent method since it is based on hand drawing.

1.4.3 Detection methods on paper device

Electrochemical detection

Electrochemical detection on paper was widely used for environmental and biomedical analysis [203-205]. The electrochemical process usually requires the use of electrodes. Three electrodes are required, reference, counter and working electrode [174]. Silver, gold, and platinum are widely used as electrodes since they provide high conductivity [206]. However, these electrodes had activity also toward the water and their potential range is narrow [207]. Another type of electrode which cheap is Carbone which has a wider potential range in comparison [207,208]. To create a paper device with electrochemical detection the electrode must be fabricated on the device. Ink is widely used to produce electrodes on paper-based microfluidic device [174]. Other than pencil/pen drawing [208-210], which is not precise several other methods were used for adding/implanting the electrode on the surface of paper like inkjet printing [211], and screen printing [212]. In addition, a potentiostate or reader is needed to perform the volumetric experiment. Examples of field readers were glucometer [213] and field-based potentiostat (smartphone connected to electronic point) [214]. The first paper-based microfluidic device with electrochemical detection was reported by Dungchai et al. [215]. The first electrodes were fabricated on the paper by screen printing method. This device was used for the determination of glucose, acetate, and uric acid [215]. Oxidase enzyme reaction was used for the detection where H_2O_2 was produced and hence H_2O_2 was detected electrochemically by electrodes [215]. A Good result was obtained from this study, as a result, this opened the horizon toward less expensive and portable devices. In another study more commercial reader was used other than potentiostate [216]. Nie et al. used a glucometer for electrochemical detection on a paper-based

microfluidic device [216]. The device provided rapid quantitative analysis [216]. It was used to detect glucose, alcohol and other components related to human health [216]. Electrochemical detection is efficient and can be used to create portable devices, however, a lot of effort has to be made to fit the electrode on paper. In addition, the device needs to be attached to some kind of detector. Failure of electrodes can happen and the electrode itself may be expensive. Therefore, more work is needed to be done especially if the aim is to use it out of the lab (in the field) or to be used by people.

Chemiluminescent (CL) and electro chemiluminescent (ECL) detection

This detection method is the detection of the light result due to a chemical reaction [174]. No source of light is required for this method, and it has low noise in the background, consequently a wide linear range and good sensitivity result [217,218]. Chemiluminescent detection on paper microfluidic devices started with Yu et al. who designed a device which is rapid and sensitive for glucose and uric acid analysis [219]. In this study, the oxidase enzyme reaction produces H_2O_2 which then interacts with Rhodamine in the detection zone in the paper device [219]. This interaction produces a light/ signal in the form of the peak which is proportional to the amount of analyte [219]. The most widely used luminophore is Luminol due to its high quantum yield. It was used widely on paper devices for the determination of heavy metals [220], pesticides [221,222], pathogenic bacteria [223], and disease biomarkers [224].

Electrochemiluminescence is the detection of the light which results from an electrochemical reaction. Electrochemiluminescence provides more sensitivity and hence it represents a good alternative to other detection methods [174]. Gao et al developed a 3D origami paper-based microfluidic device for the detection of carcinogen antigen where Ag was used as a working electrode which grows in cellulose paper and provides a good mean for electron transfer [225]. High sensitivity and low detection limit were obtained from this method [225].

Smartphone was connected to CL and ECL on PAD detection in fields [226-229]. However, still complex reagents are required for both CL and ECL. In addition, ECL requires more complex instrumentation. Both CL and ECL detection methods require the use of detectors and an expert person has to do such measurement. Consequently, it is not easy to be used for regular field tests.

Colorimetric detection

Colorimetric detection for enzymatic and chemical reaction detection is widely used in paper-based microfluidics devices. This detection method is based on the change of colour after the reaction. There are two types of readout for colorimetric detection on PAD, the readout that requires an instrument and the readout that requires no instrument.

The colour changes on the PAD with readout does not require an instrument. By this method, qualitative or semi-quantitative data can be determined. The detection by this method can be based on the change in colour in a specific position (**Figure 1.8 A**), distance change (**Figure 1.8 B**) and radius change (**Figure 1.8 C**). Change of colour in a specific position is based on eye observation. This way can give yes or no and hence can tell whether the analyte exists or not. The result varies sometimes from person to person if eyes are used and hence the result is not accurate. The device was developed and based on eye detection and the change of the colour tells if glucose and protein exist or not [230]. Distance-based detection is another widely used non-instrument colorimetric detection method [231-237]. It is based on the change of the colour due to the reaction of the analyte with the detection reagent across a specific distance. Once the reagent finishes the colour change stops. The distance of the colour change can be then measured by a ruler or attached scale. The length of distance travelled is related to the amount of the analyte in the sample. The distance-based method is a simple and in-field method since no detector is required. However, this method is difficult to control since the pretreatment of the sample or incubation or even control of the liquid flow is difficult. This problem was solved using a valve which provides rooms within the device to allow the pretreatment of the sample or incubation before detection by distance based in another room. An example of valve use is the detection of potassium iodate and glucose [238] where these analytes needed first to react with specific reagents in the leading zone and then the wax valve was opened by toluene (manually added) [238]. Then the analyte is detected by the distance travelled in the detection zone. Radius detection is another non-instrumental colourimetric detection method. It is like distance-based detection. However, the radius or diameter is the one which is measured here like in **Figure 1.8 C** where it is used for detection of Cu2+, Fe2+, Fe3+, and Zn2+ heavy metals [239].

The second type of readout is the one that requires the use of the instrument. In this method scanner is commonly used for this purpose in lab [240-243]. In addition, some were portable scanners for field use [240,243]. The scanner is an accurate method since it is not exposed to external light effects. The phone was also used for detection purposes.

Image J and Adobe Photoshop are some software that helps to get more quantitative results for analysis. Martinez et al. used Adobe Photoshop software [244]. The photo of the device was analysed by software and hence he got more quantitative results for his study [244]. The

concentration of the analyte is directly related to the pixel intensity from the software [244]. There are several studies where phones and scanners are used for picture taking and that use these types of software to get more quantitative results [245,246]. However, unlike scanners phone is exposed to external light effects when the image is taken. This problem was solved in several ways, the use of box or chamber [247,248], algorithm [249-251], transmittance reader [252], back Al reflector, V-shape optical pipe and QR code-PAD. Box or chamber [247,248] (**Figure 1.9 A**) was used to avoid the variation in the surrounding light and to fix the distance between the phone and the PAD. This method improves the reproducibility, however, the light scattering from the phone still influences the result. Algorithm [249-251] was also used during image analysis for background correction by analysing the image in different spaces (in green, red and blue channels) and taking the average of them. In the transmittance reader (**Figure 1.9 B**) [252] the density of light within the paper was measured. This method improved the limit of detection when it was used for ascorbic acid detection [253]. In the back Al reflector (**Figure 1.9 A**) [254] the diffusion of the light was controlled to reduce the non-reproducibility of the result. QR code-PAD (**Figure 1.9 C, d**) [255] is a code that produces a pattern based on the existing colour. An example is the detection of copper which changes the code intensity based on the intensity of colour produced for copper production [256]. The combination of smartphone and colourimetric detection provides easier-to-use and portable devices. However, the use of phones still suffer from variation due to the variation in lighting. Therefore, this study is trying to develop a method for colourimetric detection of analytes in the field with the aid of a smartphone.
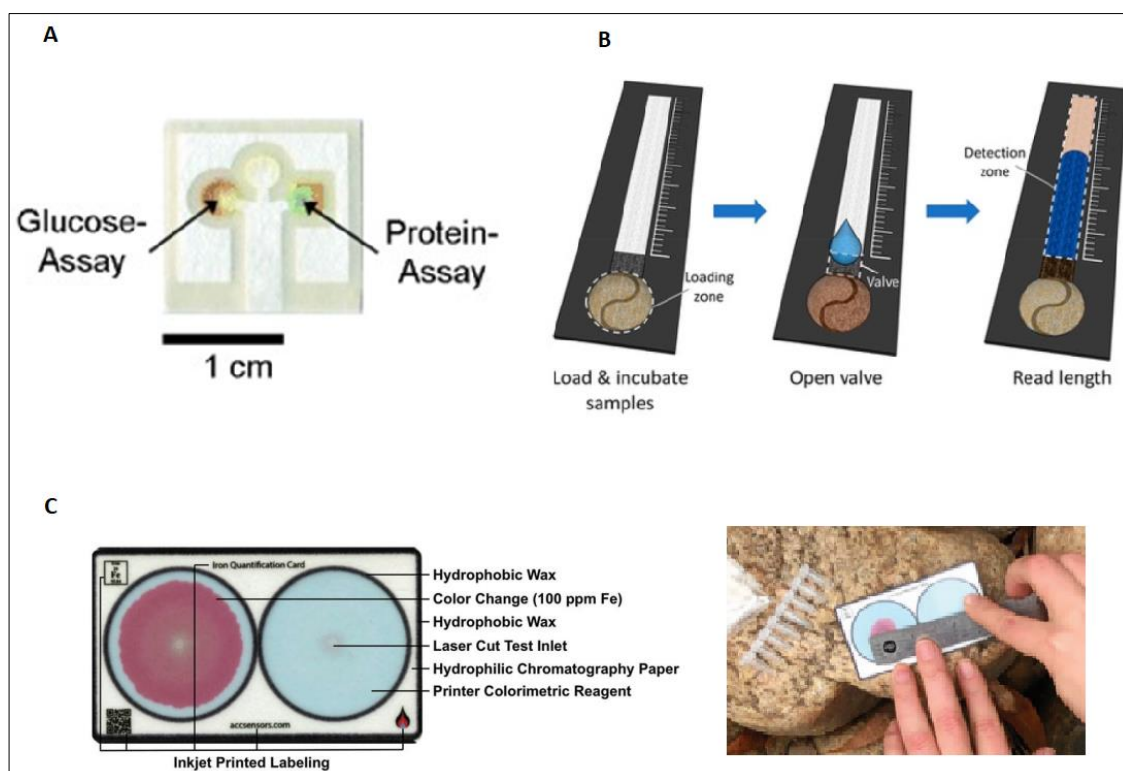
Figure 1.8 Colorimetric readout method that does not require an instrument. A method based on the change in colour in a specific position (A) [230], distance change (B) [238] and radius change (C) [239].
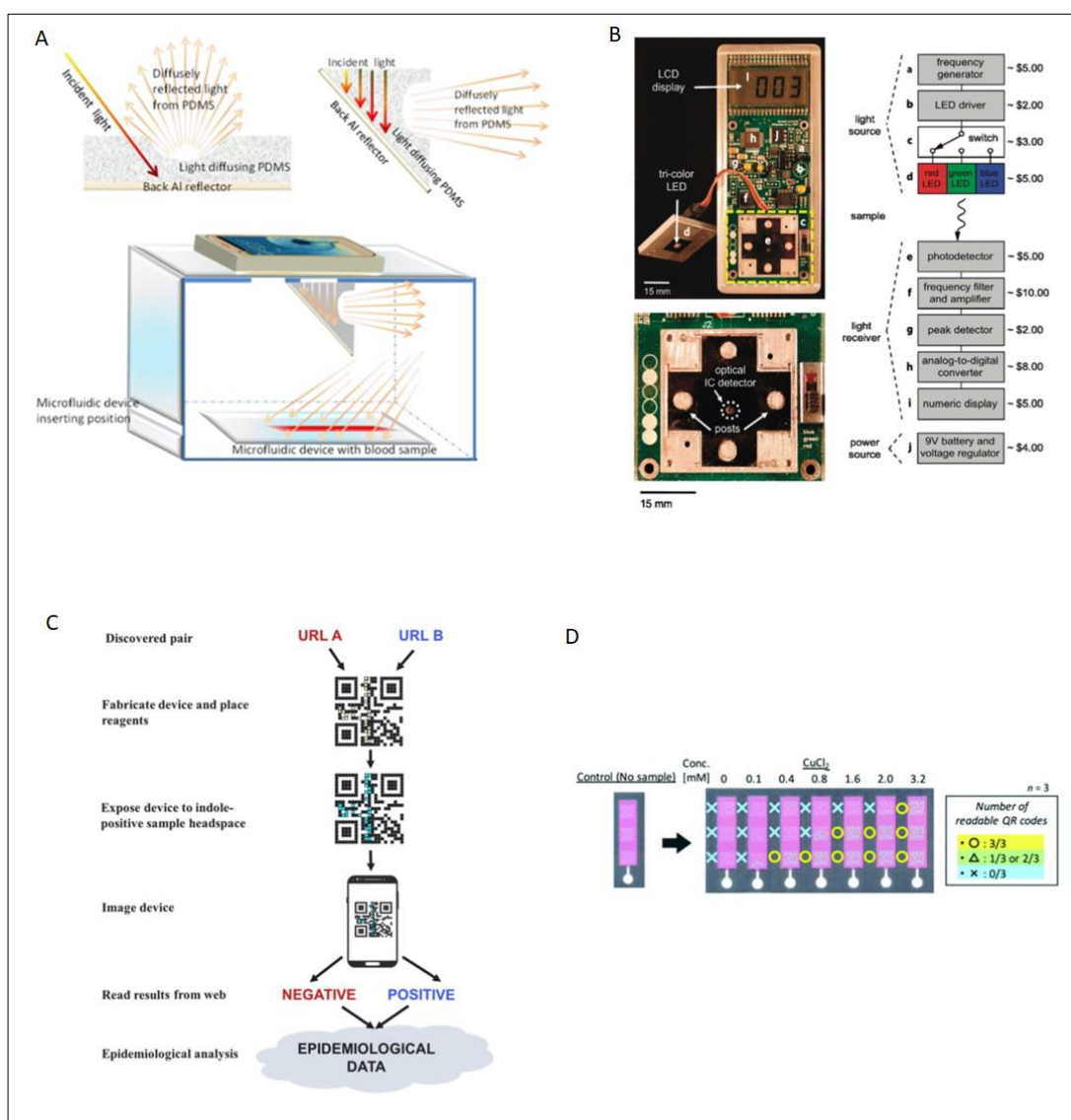
Figure 1.9 Method supported colourimetric readout method that does require instrument/ phone use(A)box or chamber (back Al reflector) [254], (B) transmittance reader [252], (C, D)QR code-PAD [255,256].

1.5 Paper-based microfluidic device applications.

1.5.1 Paper-based sensor for environmental application.

Paper-based microfluidic device has several uses in health diagnostic [257], food quality control [258] and environmental monitoring [259,260]. This study focuses on the environmental application. The environmental sample can be water from rivers, soil, and air particulates. There is a need for accurate, low-cost, easy methods for regular monitoring of environmental pollutants due to their increase. In-field detection is required due to several conditions the sample may be exposed to in the field. In addition, transportation is time-consuming, and the sample may lose

some of its characteristics during transportation. Therefore, on-site detection of nutrients and pollutants in water, air, and soil are important.

A sensor for detection of iron, copper and nickel simultaneously was the first paper device for heavy metals. This was done for air samples where the detection limit for metals ranges from 1 to 1.5 µg L^{-1} [261]. Copper is an important component to detect in the environment since it can leak from different sources [262]. Li et al. were able to develop a device to detect only copper in water [30]. TiO$_2$ nanoparticle was used to catalyse the process and was used as a colourimetric reaction for copper detection [30].

leakage of mercury can cause diseases [263]. Chen et al. group detected mercury II in river water colourimetric detection on paper device [264]. The detection limit for mercury II was 50 nM [264]. In addition, mercury II can be detected using the electrochemiluminescence detection method. Zhang et al. detected lead II and mercury II in lake water and human sample [265]. ECL carbon nanocrystal with silica nanoparticle and Ru(bpy)33- with AuNP were used to generate the ECL signal for lead II and mercury II respectively [265]. 10 pM and 0.2 nM were the detection limits for lead II and mercury II respectively [265]. Gold determination is also important since it has its economic value. Apilux et al. developed an electrochemical/colourimetric paper base device for gold and iron determination where the limit of detection for gold was 1 ppm [266]. Iron was detected with gold to remove the interference since iron interferes with gold [266]. Chromium (VI) is also another heavy metal which represents a threat to health and the environment since it is carcinogenic and not biodegradable [267]. Chromium was detected calorimetrically on paper by using gold nanoparticles leaching [268]. It was detected on paper to a limit of detection of 0.280 µM [268]. Toxic Lead (II) has a lot of application consequently it is widely used in water and food [269]. It was detected on paper by reaction with Rhodizonate [270]. It was also absorbed initially on filter paper by Zirconium silicate which coated on paper. Lead was detected as low as 10 µg L^{-1} [270].

Phosphate also if it is above a specific limit, is considered a contaminant in water. It was detected on paper with the aid of ascorbic acid and molybdenum blue reaction which were added into two different layers of the device which is with a detection limit of 0.05 mg L^{-1} P [271]. Another toxic organic compound which contaminates water is p-nitrophenol. It can cause headaches, fever and respiratory problems [272]. Santhiago et al detected this component on a paper device with the aid of electrochemical detection [273] with the aid of an expensive Graphite electrode. The limit of detection of p-nitrophenol was 1 µM [273].

These were examples of some components detected in water by paper-based sensors. This study focuses on paper-based sensors for soil sample analysis. Pollutants and nutrients in the

soil were studied by paper sensors. Trinitrotoluene TNT is an explosive material in soil. PAD was used to analyse TNT in soil using silver nanoparticles which was combined with Roman spectroscopy and 1.4 ppm of TNT was detected [274]. Chlorate is also another existing pollutant in soil which was detected electrochemically with the aid of a paper device (**Figure 1.10 A)** which was embedded into catalyst [275]. Carbon electrode was used [275]. After the addition of the soil sample to the paper the paper is added to the electrode which shows a response. 0.083 mg mL^{-1} of chlorate was the limit of detection. [275] Tetrabromobisphenol A (TBBPA) extract from soil was separated on a paper device (**Figure 1.10 B**) and detected by spray ionization mass spectrometry technique [276]. The soil sample was pretreated with methanol for the extraction purpose. a LOD of the device was 0.039 µg L^{-1} [276]. Phosphate is a soil nutrient which is required by plants in large amounts. Phosphate in soil extract was detected calorimetrically using acidic molybdate and ascorbic acid reagents [277]. The sample is pipetted into the sample entrance and then reacts with ascorbic acid in the first layer [277]. Finally, the colour is produced within 15 minutes after the reaction with molybdate (**Figure 1.10 C)** [277]. The soil sample was pretreated (extraction, centrifugation) before addition into the device [277]. There are not many studies on soil nutrient determination by PAD. In addition, there is no full extraction detection system which is simple for onsite detection of soil nutrients. This study focuses on developing a workflow system with an extraction method and simple paper-based detection.
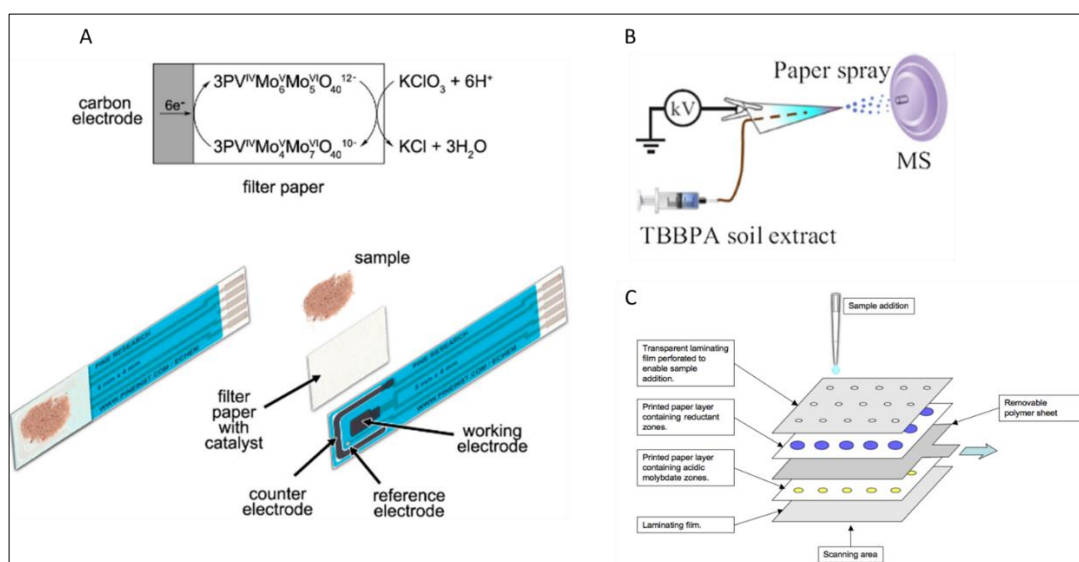
Figure 1.10 Examples of the paper-based sensor for soil sample analysis (A) chlorate analysis [275], (B) TBBPA analysis [276], (C) phosphate analysis [277]

1.5.2 Paper-based sensor and field accessibility.

One important point in this study is to evaluate the usability of the PAD in the field. There are many applications for paper-based sensors as mentioned above. Paper-based sensors were claimed to be for field/point of need use due to their simplicity in the lab. This is the aim of

microfluidic sense to move the analysis from the lab to the field. Several criteria must be available in the PAD, ASSURED criteria which are defined by the World Health Organization [278]. ASSURED refers to (A) affordable, (S) sensitive, (S) specific, (U) user-friendly, (R), (E) equipment-free, (D)delivered [278]. These criteria are not only applied to health sensors they can also applied to other in-field environmental sensors. The developed sensor/ workflow either lab or for the field should be robust, sensitive, and specific enough to target the analyte. user-friendly, (R), (E) equipment-free, and (D)delivered are more important factors for commercial PAD for end users in the field [279]. Consequently, the end user and the environment where the PAD is used should be well-defined. The device producer should consider the environment where the device is used. The availability of any auxiliaries with the PAD for the sample collection or the readout and readout interpretation is important since not all facilities are available in all environments, especially if it is in low- and middle-income countries. Therefore, communication with stockholders may be useful while developing the device.

In general, the more the steps of the workflow the more difficult to do the work by the end-user and the fewer the steps of the work the easier the work is to be performed by the end user. For field/ PON devices there are five processes [279] to be performed by the end user sample collection, sample processing, device operation, detection, and readout/interpretation. Sample collection by end users in the field is an important factor since proper collection is needed. The sample may be water, soil, food, or even medical samples like blood or sweat. In addition, the end user must be comfortable with the collection especially if the sample is blood. The volume of sample collected is important especially if the amount affects the result. Following sample collection is sample processing which should be easy enough for the end user. The more the steps in the sample the more the possibilities of errors. Consequently, the reproducibility of the method is affected especially if the workflow is performed by different people. Sometimes sample pretreatment is required like extraction, preconcentration [239], amplification [280], and separation [281]. Device operation simplicity is also important for end users. Complicated devices are hard to use by non-experts. Sometimes additional steps which should be done by the user like folding the device [282], cutting the device [283], sliding paper [284], adding solution, and pressing [285] as in **Figure 1.11**. All of these additional steps may vary from user to user and hence the reproducibility may be affected. The final step in the analysis is the readout and its interpretation. Some used methods for field detection which can be done by users are based on colourimetric readout (eye/ phone) [245,246], distance-based (eyes) [231-237] and they are the most common. Distance-based is mainly based on the yeses of the user and hence it may vary from reader to reader, especially in low concentration where the developed colour is not clear—colourimetric and by eyes or smartphone. The use of the eye as it said is not a reliable method. Phone can

provide a more quantitative method. However, the way of photo taking can vary from person to person due to the variation in the lightening of the surrounding environment or the side of photo taking. To fit the field, these problems in using a phone were solved by chart colour [286], reference mark [287] and side-by-side image [288] and use of the box. In this study, another method was introduced for field phone readout using a set of external standards. In such a way, the standards (calibration line) are run at the same conditions as a sample.

There are some good PAD samples which were improved to fit the field/point of care use as in **Figure 1.12**. **Figure 1.12** shows two different PADs for two different analyses ((A) water test [239], (B) drug quality test) and below each the improvement which was added to move them from lab to field [279]. A distance-based method was used to measure the detection of three analytes zinc, iron and copper [239]. The distance of the developed colour is measured from the centre of the circle. Previously scale was not available. As an improvement to fit the field use a scale which can make it easy for the user to read the distance instead of the use of a ruler. Even though the device operation was simplified this process still requires sample preconcentration out of before the detection. In **Figure 1.12 B** the PAD was developed for testing of falsified amoxicillin in drug [289]. There is no sample preparation. The powder drug was added to the PAD immediately and then immersed in water. After the colour development, the PAD was compared to standard [289]. This test is still based on eyes, and it tells only if it is a falsified drug or not. The addition of a Mark in the device to indicate where the sample should be added is one crucial point [279]. To decrease the gap between the lab test and field test. The simplicity of the work must be considered, simple things that might be too easy to apply or follow for researchers are not the same for lay people. Other than simplicity stability, reproducibility, analytical performance, and production is necessary to assign tests as field test methods that can be commercial. To do this other than the researcher people should test the developed device/workflow. Communication with the stockholder or end-user is important. In this study, a simple workflow will be developed to fit the field requirement. The developed work will be also tested with a group of volunteers. Finally, the workflow will be improved based on volunteers' feedback.
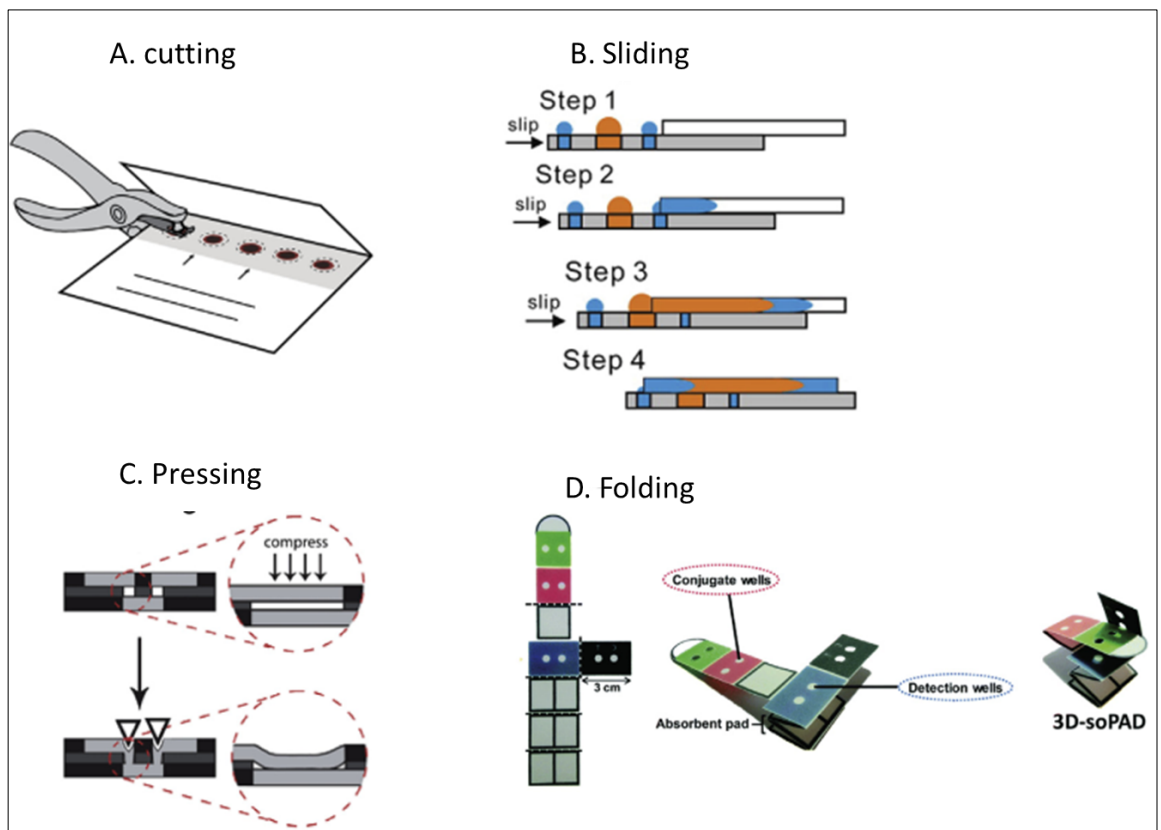
Figure 1.11 Additional step [279] which should be done by the user like (A) cutting the device [283], (B) sliding paper [284], and (C) pressing [285] and (D) folding [282].
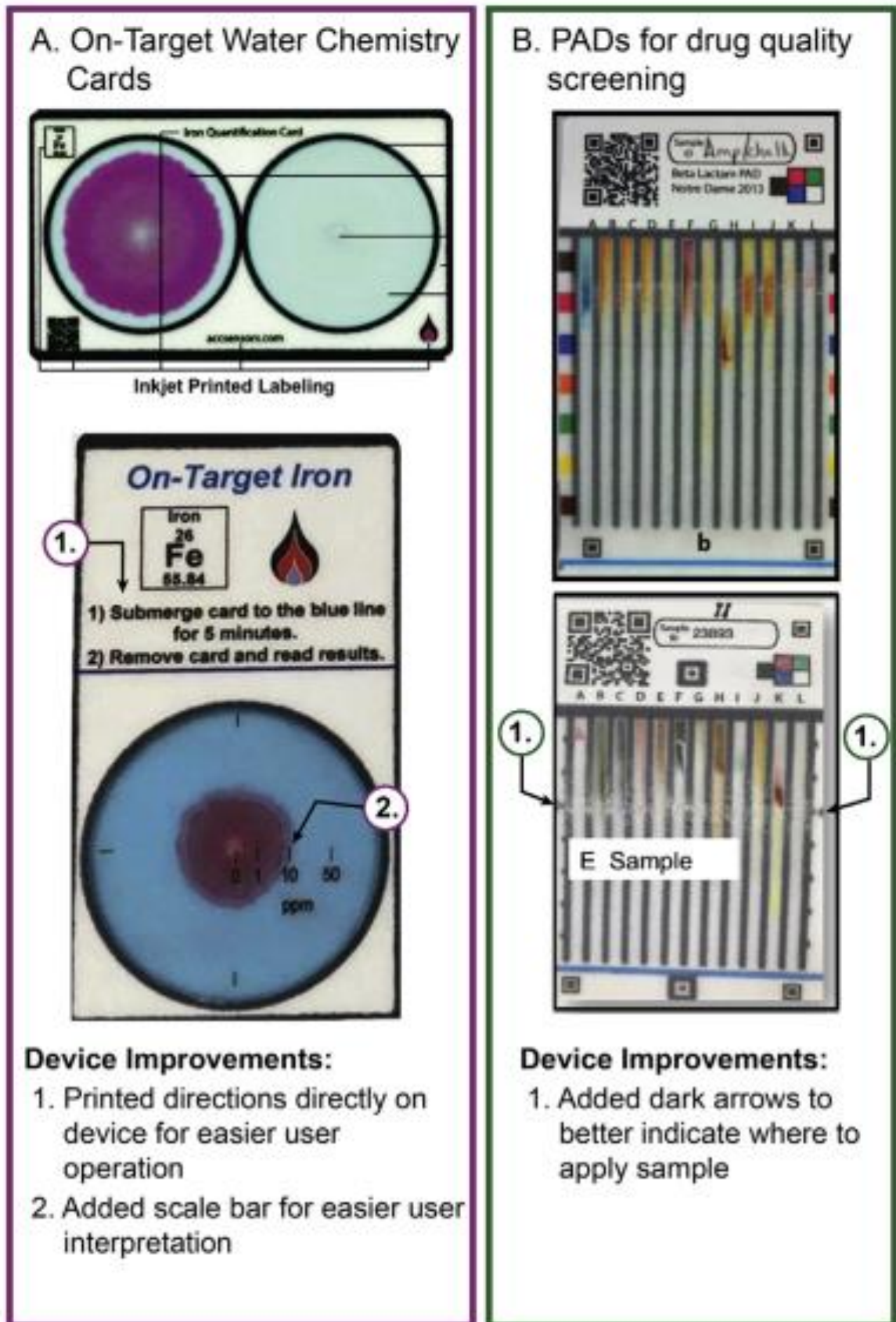
Figure 1.12 Two different PADS for two different analyses [279] ((A) water test [239], (B) drug quality test [289]) and below each the improvement which was added to move them from lab to field.

1.5.3 paper-based microfluidic device for colourimetric nitrite and nitrate determination.

There are several available studies which use paper-based microfluidic devices for nitrate and nitrite determination. Jayawardane et al. used a 3D paper device which is fabricated by the inkjet printer and consists of two sheets. In one sheet the detection zone and the transport channel and in the second sheet the reduction zone as in **Figure 1.13 A** [290]. Griess reagent was used in the detection zone for colour development and zinc was used in the reduction zone for the reduction of nitrate to nitrite [290]. This device was used to detect the total nitrate and nitrite in a water sample. Nitrate alone can be detected by subtraction of the nitrite signal from the total signal [290]. The detection of nitrite can be done without the use of a reducing agent since Griess immediately develops colour among interaction with nitrite [290]. Using the developed device, the amount of zinc, sample contact time with zinc, sample volume, amount of Griess reagent and colour development time were optimized. The resulting device was able to determine nitrate and nitrate in 50-1000 µM and 10-150 µM calibration ranges respectively [290]. 19 µM and 1.0 µM were the detection limits of nitrate and nitrite respectively [290].

In another study Teepoo et al used screen printing to fabricate a 2D paper device for the detection of nitrate and nitrite in food sample [291]. The device consists of six detection zones, 3 reduction zones and one sample zone. Those zones are connected by channels as in **Figure 1.13 B** [291]. Similarly, to the previous study, Griess reagent and zinc were used for detection and reduction respectively. The linear ranges for the device were 10-50 mg L^{-1} and 2-10 mg L^{-1} for nitrate and nitrite determination respectively [291]. In another similar study by Ratnarathorn et al. where flow within the channel is required nitrate and nitrite (**Figure 1.13 C**) were detected together with a limit of detection of 0.4 mg L^{-1} [292]. Similarly, Thongkam et al. used Griess reagent and channel device for nitrite and nitrate determination in food (**Figure 1.13 D**) and got a limit of detection of sample 0.1 and 0.4 mg L^{-1} for nitrite and nitrate respectively [293]. The only difference with the Thongkam et al. group was that vanadium (III) chloride was used as a reducing agent for nitrate instead of zinc [293]. vanadium (III) chloride is a solution and hence this makes it easy to deal with in the lab. However, it requires more time for reduction compared to zinc and this is not practical for field experiments [294].

In all studies by Jayawardane et al, Teepoo et al and Ratnarathorn et al. and Thongkam et al., the device needs training to use since they required flow in channels and slides of paper or layer during the reaction.

Charbaji et al. group was able to develop another device for nitrate and nitrite determination which is based also on Griess reagent detection [295]. This device required also folding the device

by the user while doing the analysis **(Figure 1.13 E**). In this study, the addition of zinc was performed using Zinculose [295]. Zinculose is a zinc particle impeded into the fibre to make sure that the zinc within the fibre instead of being on the top of the paper when the zinc was pipetted like in previous studies which were mentioned in an earlier paragraph in this section [295]. However, this method is labour-intensive where extra steps of preparation are required.

Ferreira et al. on the other hand used the weighing method to add the same amount of zinc in each disc of the reduction zone of the device [296]. However, this method was not practical since it is time-consuming and if the disc does not contain the right amount of zinc it needs to be disposed of and a new one needs to be prepared again. However, this device with circles and is much easier to use compared to other mentioned devices in the above paragraphs in this section. However, the device is still based on pipetting sample addition which is not practical in the field [296]. This study was able to detect 0.05 µM and 0.08 mM of nitrite and nitrate in the saliva sample.

Other than zinc E.coli cells was also used by Kelly et al. to detect nitrate in water by immobilization of the E.coli cell in paper [297]. Griess reagent was used for detection after the reduction [297]. The designed strip has been stable for more than one year [297]. Keeping in mind that the Griess reagent was not stored in the paper device and only E.coil cell was tested for stability [297]. The detection range for nitrate was 1-10 ppm which is within the highest acceptable level of nitrate in drinking water [297]. However, the method is still not a field method since the strip needs to be dipped and then folded after a specific time. This increases the work for the user and then increases the possibility of error. Ferreira et al used an enzymatic solution for the reduction purpose of nitrate to nitrite which is then detected by Griess reagent [298]. However, the PAD was stable only for 24 hours at room temperature [298].

There are other studies for nitrite determination compared to nitrate determination. Some of these studies are summarized in **Table 1.4**. This shows that most of the PADs relied on mixed Griess reagent components in one spot either in channel devices or non-channel devices. In addition, the PADs consisted of one layer only. Therefore, this study focuses on improving the sensitivity of Nitrite PAD by separating Griess reagent components and making it ready for soil sample analysis by layer addition.

In general, **Table 1.5** summarizes nitrate PADs available in the literature as far as we know. Jayawardare et al. and Charbaji et al. devices [290,295] require a slide of the layer by the user between the detection and reduction zone. Teepoo et al., Thongkam et al. and Ratnarathorn et al. devices [291-293] require the flow of the sample within channels. Also, published PADs were based on pipetting for sample addition which is not practical in the field. The previous studies did not discuss the effect of the dark colour of zinc if the zones of reagent are aligned above

each other and some of them solved this problem by having the zinc zone separated from the detection colour zone and this was not the case in our developed PAD. Most of the published work relayed on pipetting the zinc solution into the specific zones [290-292], however, most of these PADs had separated areas for the reduction zone which was not aligned above the detection zone, and this made it possible to add zinc with its dark colour without influencing the intensity of colour. In another study another layer was added to the PAD [295], the layer was called Zinculose and it is embedded zinc particles in the cotton layer. This was practical to keep the zinc embedded within the reduction area of the device. However, this still required a lot of work and preparation of the material which then will be added to the PAD. In addition, still the same problem exists, and it is unknown how much zinc is there. In Ferreira et al. work each well in the PAD was added to the zinc solution and this was followed by weighing of the well before and after the zinc addition [296] and this is not practical. This study focuses on improving the zinc addition into the PAD. Also, as far as we know most of the studies for nitrate detection on paper were performed for water and food samples but not soil. The previous devices are not ready for soil sample analysis. Therefore, this study will focus mainly on soil sample analysis. The PAD also will be simplified to fit the field analysis.
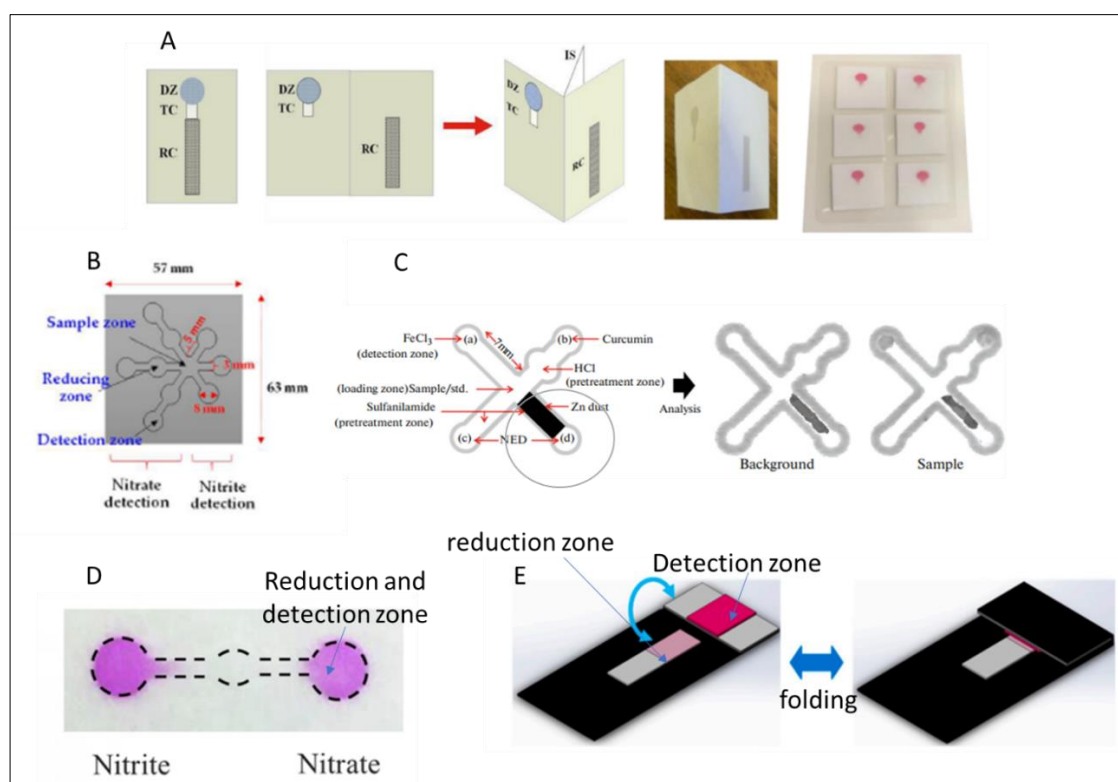
Figure 1.13 (A)3D paper device which is fabricated by the inkjet printer and consists of two sheets. In one sheet the detection zone (DZ) and the transport channel (TC) and in the second sheet the reduction channel (RC) [290]. (B)The 2D device consists of 6 detection zones (8 mm), 3 reduction zones (8 mm) and one sample zone (8 mm). Those zones are connected by channels (3×5 mm). (C) Channel device for simultaneous detection of nitrate and nitrite. Nitrate reduction and detection in the same zone. (D) device

required folding by the user while doing the analysis. The addition of zinc in the reduction zone was as a Zinculose layer.

Table 1.4 Comparison between different PADs studies for nitrite detection

Sample/ device shape	Number of layers	method	Components of detection reagent	Linear range (mg L⁻¹)	LoD (mg L⁻¹)	Reaction time (min)	Sample introduction	Reference
Water channels	1	Griess reagent	Mixed In one layer	4-85	0.52	15	Pipetting	[299]
Water channels	1	Tetrazine base	Mixed In one layer	0.23-23	0.0598	5	Pipetting	[300]
Saliva channels	1	Griess reagent	Mixed In one layer	0.92-7.36	0.345	5	Pipetting	[301]
Saliva channels	1	Griess reagent	Mixed In one layer	0-4.6	0.258	10	Pipetting	[302]
Water circles	1	Griess reagent	Mixed In one layer	0.1-10	0.1	15	Pipetting	[303]
Waster squares	1	Basic Fuchsine	Mixed In one layer	0.05-9.2	-	30	Immersing	[304]
Water Channels	1	Griess reagent	Mixed In one layer	0.23–2.26	0.03	12	Pipetting	[305]
water	1	Griess reagent	Mixed In one layer	3.5-115	-	2	Pipetting	[306]
Food channels	1		Mixed In one layer	0.5-40	0.1	5	Pipetting	[293]

Sample/ device shape	Number of layers	method	Components of detection reagent	Linear range (mg L⁻¹)	LoD (mg L⁻¹)	Reaction time (min)	Sample introduction	Reference
Saliva channels	1	Griess reagent	Mixed In one layer	0.46-46	0.46	15	Pipetting	[307]
Food squares	1	Griess reagent	Mixed In one layer	1-100	1	5	Pipetting	[308]
Food circles	1	Griess reagent	Mixed In one layer	1-250	1.1	15	Pipetting	[309]

Table 1.5 Comparison between different PADs studies for nitrate detection

sample	Linear range (mg L^{-1})	LOD (mg L^{-1})	Reaction time (min)	Zinc addition	Reduction efficiency %	Sample introduction	reference
water	3.1-62	1.18	5	Pipetting	20	pipetting	[290]
food	10-50	3.60	12	Pipetting	-	pipetting	[291]
water	0-50	0.53	10	External layer (Zinculose)	27	pipetting	[295]
saliva	200-1200	4.96	-	External layer of zinc (weighed before and after)	-	pipetting	[296]
food	0.5-40	0.4	10	-	-	pipetting	[293]
food	0.4-20	0.4	10	Pipetting	-	pipetting	[292]
urine	8.68-62	2.8	20	-	-	pipetting	[298]
water	1-10	0.87	15	Pipetting	-	pipetting	[310]
water	0-40	3.35	60	-	27	dipping	[311]

1.5.4 paper-based microfluidic device for colourimetric manganese determination.

Paper microfluidic was used for the detection and determination of several heavy metals [312]. Manganese detection was one of these metals. Most of the paper devices for manganese detection were used for water sample analysis. Henry et al. group used the wax printer to create a device with channels **Figure 114 A** to detect manganese with cobalt simultaneously by colourimetric detection [313]. For the manganese determination mixture of PAR reagent, pH 9.3 borate buffer and polydiallydimethylammonium chloride (PDDA) polymer were used as detection reagent [313]. The detection reagent was yellow in colour, and it formed a dark orange colour when it formed a complex with manganese. The PAR reagent was able to form a coloured compound with several metals as in **Figure 114 B**. Triethylenetetramine hydrate (trien) and dimercaptosuccinic acid (DMSA) were used as masking reagents for manganese detection [313]. Cu, Zn, Cd, and Pb are fully masked by trien whereas Ni is partially masked by trien [313]. Trien is a very toxic masking reagent.

In another study, manganese was detected by PAN reagent in the paper device (**Figure 114 D**) without the use of the wax since the use of PAR requires the use of organic solvent which can interact with the wax [314]. PAN reagent also tends to react with other metals other than manganese like Zn, Cu, Pb and Ni [314]. Cyanide was used as a masking agent for these metals [314]. 0.11 mg L^{-1} was the limit of detection. Cyanide is also considered a very toxic reagent.

Most of the methods which were mentioned for manganese by paper device are using open lab devices and most of them for water sample analysis. As far as we know there are no studies for manganese detection in soil by paper device. In this study, the manganese PAD is improved and designed for manganese detection in the field. Consequently, toxic compounds like cyanide and borate will be replaced with safer options.
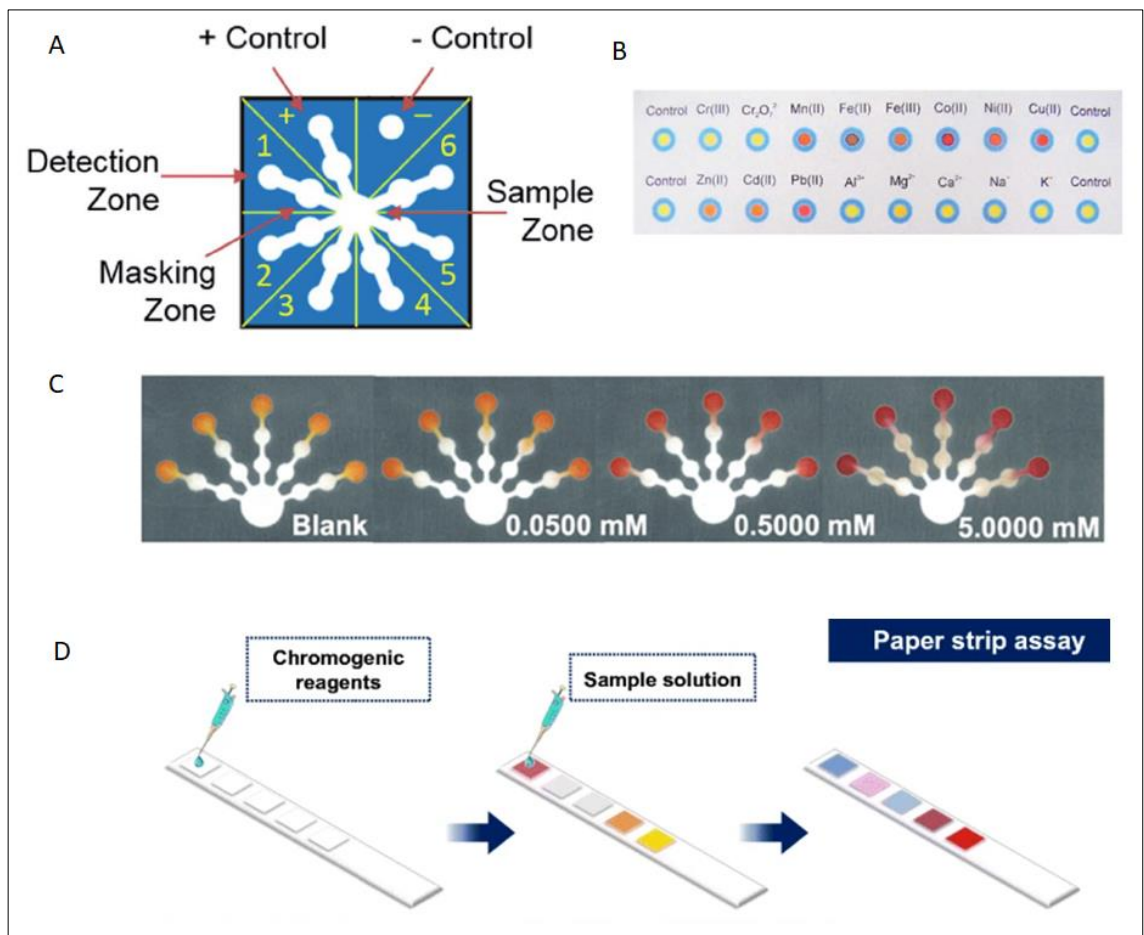
Figure 114 (A) show the channel device for manganese, masking device with 8 arms [313]. (B) PAR reagent reaction with some alkali, alkaline earth, and transition metal [313]. (C) Another device with 5 arms for detection of different concentration of manganese by PAR [315]. (D)Manganese PAD with PAN detection reagent in the paper device consisted with squares made by cutter without the use of the wax since the use of PAR requires the use of an organic solvent which can interact with the wax [314].

1.6   Hypothesis and aims.

There is a need for a simple, cheap, and quantitative method for the on-situ determination of soil nutrients. Paper-based sensors represent a good alternative which is if it is developed to be easy, safe (user friendly), suitable for field requirements and attached to a simple extraction system can be an efficient method which is cheap and easily accessible, especially for low-income countries. Therefore, the first aim of the study is to design and develop a simple and easy-to-use device which requires as minimum as possible steps for the analyte determination. The device can be finally moved from the top of the bench to the field for lay people use.

The second aim is to develop and improve colourimetry nitrite PAD (for determination of nitrite in soil at its environmental level) by separating the components of the detection reagent and adding multiple layers that provide soil filtration. Once established, it will be used for determining the existence of nitrite or not in soil. And it will be further used to develop another PAD (nitrate PAD). Phone-based colourimetry PAD for nitrate detection in soil samples will be developed and this is by introducing a new method of reducing agent addition into the developed PAD to avoid the dark colour of zinc that finally can contribute to the measured intensity.

The third aim is to attach the PAD detection system of nitrate into a simple, fast and novel cafetière extraction system which is based on the use of an accessible axillary in the field like the use of mineral water as solvent and spoon as a soil collection method. Once developed, the whole workflow (extraction attached to phone-based colourimetric PAD detection) will be validated using IEC (ion exchange chromatography) and CRM (certified reference material).

The fourth aim is to test the developed workflow for nitrate determination with a group of volunteers to assess its robustness and its simplicity and use the volunteers' outcome and feedback (quantitative and qualitative) to improve the system. The use of the phone as a detection method and the instruction sheet will be the two main studied factors.

The fifth aim is to apply a similar workflow based on paper sensors and cafetière extraction in micronutrient determination (manganese). Manganese PAD will be developed and improved to be easier and safer to use by lay people. This is by replacing the toxic reagent with non-toxic options that provide similar sensitivity and by adopting a simple dipping sample introduction system that reduces steps and reduces the possibility of errors. In addition, the Initial step for cafetière extraction of manganese toward using safer and easily available extraction solvent will be investigated.

This study hypothesises that a simple, safe, and reliable workflow which is based on phone colourimetry paper-based sensor and cafetière extraction and fits on situ detection requirements will be established for routine monitoring of nitrate and manganese in soil samples.

Figure 1.15 The overall workflow which consisted of three steps, cafetière extraction, transfer and PAD detection.

Chapter 2 Experimental

2.1 Chemicals and reagents

Milli-Q water (Mili-RO 12 plus Milli-Q station, Millipore, resistivity 18.2 MΩ cm) and deionized water (DIW) were obtained from the University of Hull laboratories. The reagents used in the experiment reported are summarised in **Table** 2.1.

Table 2.1 Reagents purchased and used in this work.

Chemical	Concentration	Supplier
Sulphanilamide	50 mM	SLS (Scientific Laboratory Supplies), UK
Citric acid	300 mM	Sigma Aldrich, UK
N-(1-naphthyl)-ethylenediamine dihydrochloride (NED)	6 mM	Sigma Aldrich, UK
Sodium nitrite	10 mM NO_2^-	Sigma Aldrich, UK
Potassium nitrate	10 mM NO_3^-	SLS, UK
Zinc powder ($\leqslant$ 10 μm)	50 mg mL^{-1}	SLS, UK
Sodium chloride	20 g L^{-1} Na$^+$	Fischer, UK
Potassium chloride	20 g L^{-1} K$^+$	Sigma Aldrich, UK
Sodium dihydrogen phosphate monohydrate	10 g L^{-1} PO$_4^{3-}$	Sigma Aldrich, UK
Sodium acetate	10 g L^{-1} CH$_3$COO$^-$	Fisher Scientific, UK

Chemical	Concentration	Supplier
Manganese sulfate monohydrate	37 g L^{-1} Mn^{2+}	Sigma Aldrich, UK
Potassium carbonate	38 g L^{-1} CO$_3^{2-}$	Sigma Aldrich, UK
Potassium phthalate	50 g L^{-1} phthalate	Sigma Aldrich, UK
Iron (II) chloride tetrahydrate	1 g L^{-1} Fe^{2+}	Across, UK
Calcium sulphate dihydrate	20 g L^{-1} Ca^{2+}	Sigma Aldrich, UK
Zinc sulphate heptahydrate	5 g L^{-1} Zn^{2+}	Alfa Aesar, UK
Sodium sulfate	50 g L^{-1} SO$_4^{2-}$	Fisher Scientific, UK
Copper (II) sulfate pentahydrate	20 g L^{-1} Cu^{2+}	Sigma Aldrich, UK
4-(2-pyridylazo) resorcinol (PAR)	6 mM	Sigma Aldrich, UK
polyDiallydimethylammonium chloride (PDDA)	2 %	Aldrich Chemistry
manganese (II) chloride	10 mM	Sigma Aldrich, UK
Sodium tetraborate decahydrate (Na$_2$B$_4$O$_7$.10H$_2$O)	0.125 mM	Sigma Aldrich, UK
Glycine	0.999 M	Sigma Aldrich, UK
Sodium carbonate	1.7mM	Sigma Aldrich, UK

Chemical	Concentration	Supplier
sodium bicarbonate	1.8 mM	Sigma Aldrich, UK
PAN(1-(2-pyridylazo)-2-naphthol)	3.8 mM	Sigma Aldrich, UK
Surfactant (Triton X-100)	8%	Sigma Aldrich, UK
Cobalt (II) chloride hexahydrate	1 mg L^{-1} Co^{2+}	Alfa aesar, UK
Ethanol	30%	Sigma Aldrich, UK
Sodium hydroxide (OH)	1 %	Sigma Aldrich, UK
Sodium thiosulfate	1 M	Sigma Aldrich, UK
DMSA (Dimercaptosuccinic acid)	0.4 M	Sigma Aldrich, UK
DFO (Deferoxamine)	0.05 M	Sigma Aldrich, UK
tri-Sodium citrate dihydrate (citrate)	0.5 M	Fischer, UK
EDTA	0.05 M	Sigma Aldrich, UK
EGTA(Ethyleneglycol bis(2aminoethylether)N,N,N',N'-tetraacetic acid)	0.05 M	Sigma Aldrich, UK

Unless otherwise stated all solutions were prepared in in deionized water (DIW). Griess reagent was prepared by mixing 50 mM sulphanilamide, 300 mM citric acid and 6 mM N-(1-naphthyl)-ethylenediamine dihydrochloride (NED). Separated Griess components solutions were also prepared. Griess solution 1 was 6 mM NED, and Griess solution 2 was a mixture of 50 mM sulphanilamide and 300 mM citric acid in DIW. Sodium nitrite was used to prepare 10 mM stock standard in DIW. Standards of nitrite ranging from 0-150 µM were prepared from sodium nitrite (10 mM). Zinc powder suspension ($\leqslant$ 10 µm) was used as a reducing agent and 50 mg mL^{-1} of it was prepared in DIW. Potassium nitrate was used to prepare a 10 mM nitrate stock solution in DIW. Nitrate standards (0-1000 µM) were prepared from the nitrate stock solutions. Sodium ion (20 g L^{-1}) was prepared by dissolving sodium chloride in DIW. Potassium ion (20 g L^{-1}) was

prepared by dissolving potassium chloride in DIW. Phosphate (10 g L^{-1}) ion was prepared by dissolving sodium dihydrogen phosphate monohydrate in DIW. Acetate ion (10 g L^{-1}) was prepared by dissolving sodium acetate in DIW. Manganese ion (37 g L^{-1}) was prepared by dissolving manganese sulfate heptahydrate in DIW. Carbonate ion (38 g L^{-1}) was prepared by dissolving potassium carbonate in DIW. Phthalate ion (50 g L^{-1}) was prepared by dissolving potassium phthalate in DIW. Iron (II) ion (1 g L^{-1}) was prepared by dissolving iron (II) chloride tetrahydrate in DIW. Calcium ion (20 g L^{-1}) was prepared by dissolving Calcium sulphate dihydrate in DIW. Zinc ion (5 g L^{-1}) was prepared by dissolving zinc sulfate heptahydrate in DIW. Sulfate ion (50 g L^{-1}) was prepared by dissolving sodium sulphate in DIW. Copper ion (20 g L^{-1}) was prepared by dissolving 7 copper (II) sulfate pentahydrate in DIW.

Manganese (II) ion (10 mM) was prepared by dissolving manganese (II) chloride in Milli-Q water. PAR solution was prepared from 6mM 4-(2-pyridylazo) resorcinol (PAR) and 2% of polyDiallydimethylammonium chloride (PDDA) (glycine buffer pH 9.9). pH 9.9 Borate buffer was prepared by dissolving boric acid in Milli-Q water. Carbonate buffer was prepared from 1.7 mM sodium carbonate and 1.8 mM sodium bicarbonate in Milli-Q water. PAN solution was prepared by prepared from 3.8 mM 1-(2-pyridylazo)-2-naphthol (PAN) and 8% of surfactant (Triton X-100) in carbonate buffer pH 8.

DMSA (Dimercaptosuccinic acid) (0.4 M) was prepared in Milli-Q water. DFO (Deferoxamine) (0.04 M) was prepared in Milli-Q water. Thiosulfate ion (1 M) was prepared by dissolving sodium thiosulfate in Milli-Q water. EDTA (0.05 M) was prepared in Milli-Q water. EGTA (0.05 M) was prepared in Milli-Q water. Citrate (0.5 M) ion was prepared by dissolving tri-Sodium citrate dihydrate in Milli-Q water. CaCl$_2$ (0.01 M) was prepared in Milli-Q water. KCl (0.01 M) was prepared in Milli-Q water. NaCl (0.01 M) was prepared in Milli-Q water.

The following reactions were studied:

Nitrite detection

Detection of nitrite via reaction with Griess reagent is shown in equation 2.1. Nitrite reacted with sulphanilamide in acidic media (citric acid) to produce diazonium salt which then reacted with N-(1-naphthyl)-ethylenediamine dihydrochloride (NED) to produce pink-red dye.

Nitrate detection

Detection of nitrate via reduction first by reaction with zinc to produce nitrite is shown in equation 2.2, followed by the detection of nitrite as described above and in equation 2.1.

eq. 2.1

$$Zn + 2NO_3^- + 4H^+ \rightarrow Zn^{2+} + 2NO_2^- + 2H_2O \qquad \text{eq. 2.2}$$
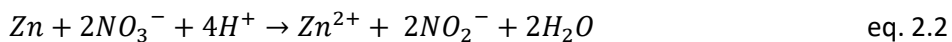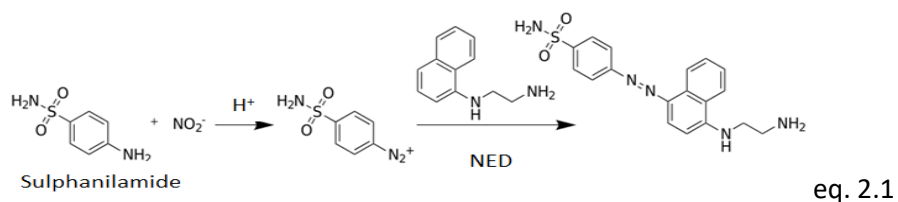
Manganese detection

Detection of manganese via collation with 4-(2-pyridylazo) resorcinol (PAR) to produce a red-orange complex at pH 9.9 is shown in equation 2.3.

eq. 2.3
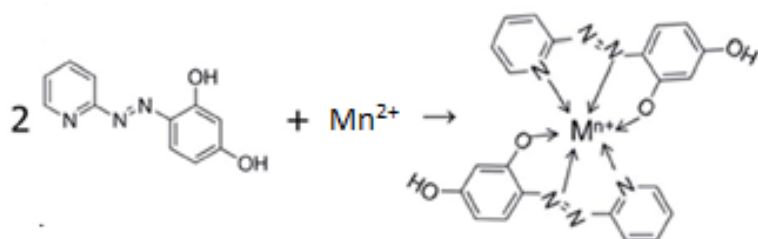
Detection of manganese via reaction with 1-(2-pyridylazo)-2- naphthol (PAN), and in the presence of surfactant (triton-100) to produce a red-orange complex at pH 8 is shown in equation 2.4.

eq. 2.4
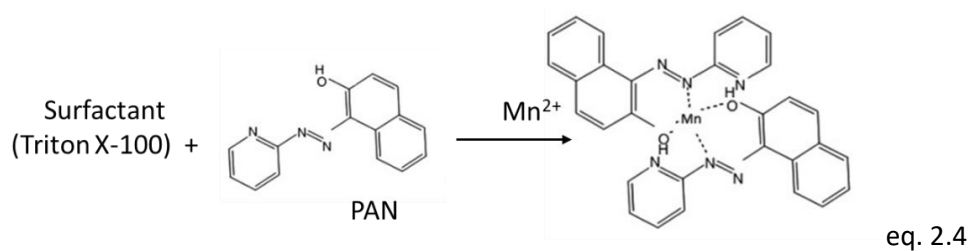
2.2 Statistical analysis

LoD and LoQ calculations

LoD and LoQ were calculated [316] as in equations 2.5 and 2.6 respectively using signal from blank and the equation of the straight line of the calibration curve. The blank signal in equations 2.5 and 2.6 can be replaced with the intercept.

$$LoD = \frac{(blank\ signal + 3SD) - intercept\ of\ stright\ line}{slope\ of\ stright\ line} \qquad \text{eq. 2.5}$$

$$LoQ = \frac{(blank\ signal + 3SD) - intercept\ of\ stright\ line}{slope\ of\ stright\ line} \qquad \text{eq. 2.6}$$

Statistic

Most of the data are described as mean ± standard deviation. A number of repeats are mentioned with each experiment as n.

T-test (two-tailed t-test) [316] was used to compare two sets of data. The test was performed automatically in using the excel. T value was used to determine the difference between the data. If $t_{state} < t_{critical\ two\text{-}tail}$ / $t_{state} > -t_{critical\ two\text{-}tail}$ then the difference between the data is not significant The opposite means that data are significantly different. The P value is 0.05.

ANONA (analysis of variance) test [316] was used to compare more than two groups of data. The test was performed automatically in using the excel. F value was used to determine the difference between the data. If $F < F_{critical}$ then the difference between the data is not significant. The data are significantly different when $F > F_{critical}$. The P value is 0.05.

2.3 Paper device fabrication

The PADs were fabricated using a wax printer or a circular hole punch.

2.3.1 Wax printing

Paper-based microfluidic devices for nitrite, nitrate and manganese detection were designed in AutoCAD 2019 software (AUTODESK, US). A solid wax printer (Xerox 8570) was used to pattern the hydrophilic filter paper with hydrophobic barriers. Before printing, the Whatman filter paper grade 1 (11 µm pore size) was cut to the size of A4 paper as this was the size the printer could handle. After printing, the paper was heated with a laminator (Fellow Saturn 3I A4) to 125 °C. Nitrate and nitrite paper devices (green wax) were heated 3 times while the manganese device (black wax) was heated 10 times. The heating is based on the colour of the wax; black wax needs more heating to penetrate the paper. Aluminium foil was used to cover the paper while heating to avoid transfer of the wax onto the laminator. During heating, the wax melts and diffuses

horizontally and vertically within the paper. The vertical movement leads to the formation of the three-dimensional wax barriers. The horizontal movement leads to an increase in the width of the design. Wax printing was adopted in this experiment since it is a cheap method, easy to use and several designs with various shapes can be printed easily in a short time. This method is commonly used in paper microfluidic science [317]. **Figure** 2.1 shows the three steps for device fabrication by wax printing, designing, printing, and heating.
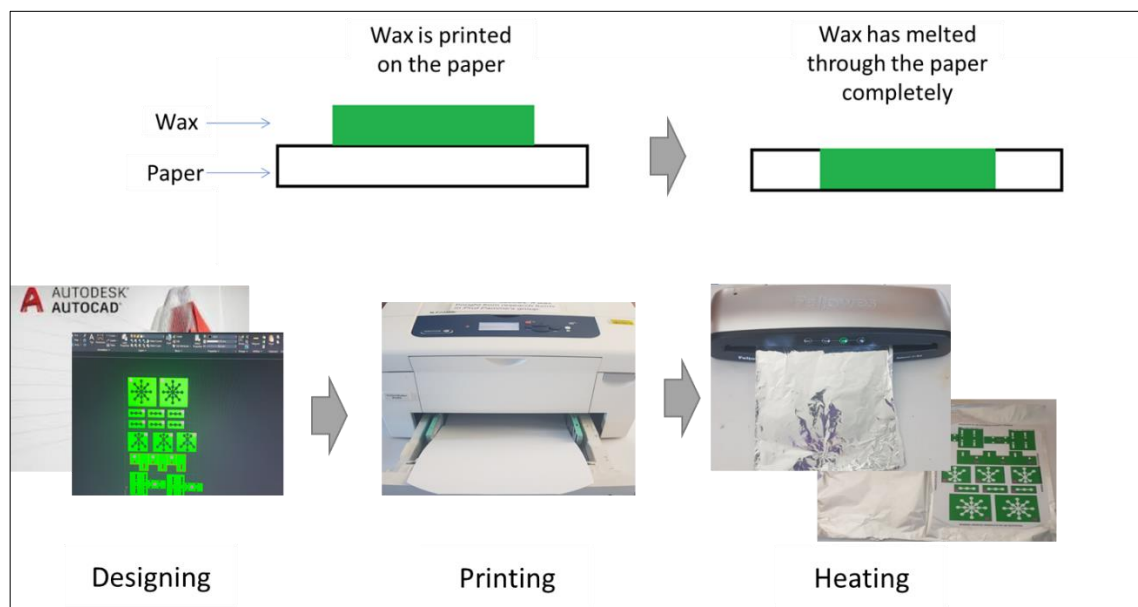
Figure 2.1 Paper device fabrication by wax printing. Step 1: the design of the device by AutoCAD. Step 2: Print the device in a filter paper. Step 3: Heating of the wax by lamination 3 times at 125 °C using a Fellow Saturn (3I A4) laminator.

2.3.2 Hole punch

A hole punching cutter (1.5 cm diameter) was used to make the second manganese PAD without the use of the wax barrier. In **Figure** 2.2 the punch (1.5 cm diameter) was used to cut three circles in Whatman filter paper. These were treated with reagents and used directly as detection PADs.
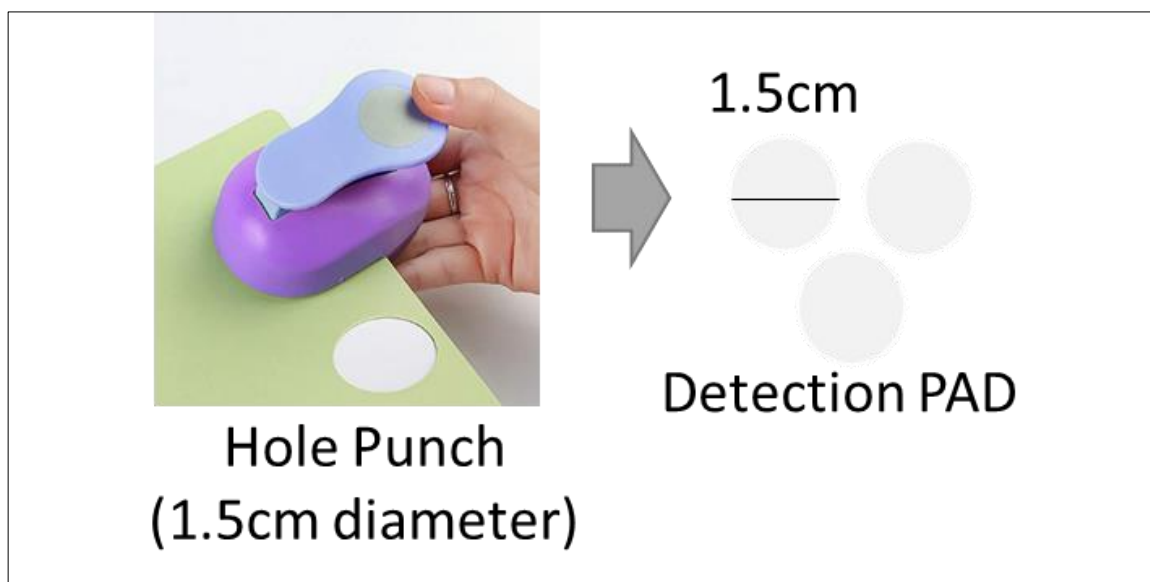
Figure 2.2 circle punch (1.5 cm diameter) which was used to cut three circles (in Whatman filter paper 1) which were then used directly as detection PADs after treating with reagents.

2.4 Sample introduction system

The sample/standard in this work was added or introduced to the paper device either by pipetting or by dipping.

2.4.1 Pipetting of sample

A micropipette was used to add a specific amount of the sample directly into the sample introduction zones on the paper devices. After that, the sample was allowed to react with the reagent in the modified paper for a specific time based on the experiment. A photo was then taken using a smartphone camera (Samsung, Vietnam) or flatbed scanner (Canon LiDE 220).

2.4.2 Dipping of sample

Dipping of the device into the sample was carried out in a Petri dish which was filled with the required sample (**Figure** 2.3). The device was dipped into the sample for a specific time then a photo was taken using a smartphone camera or flatbed scanner.
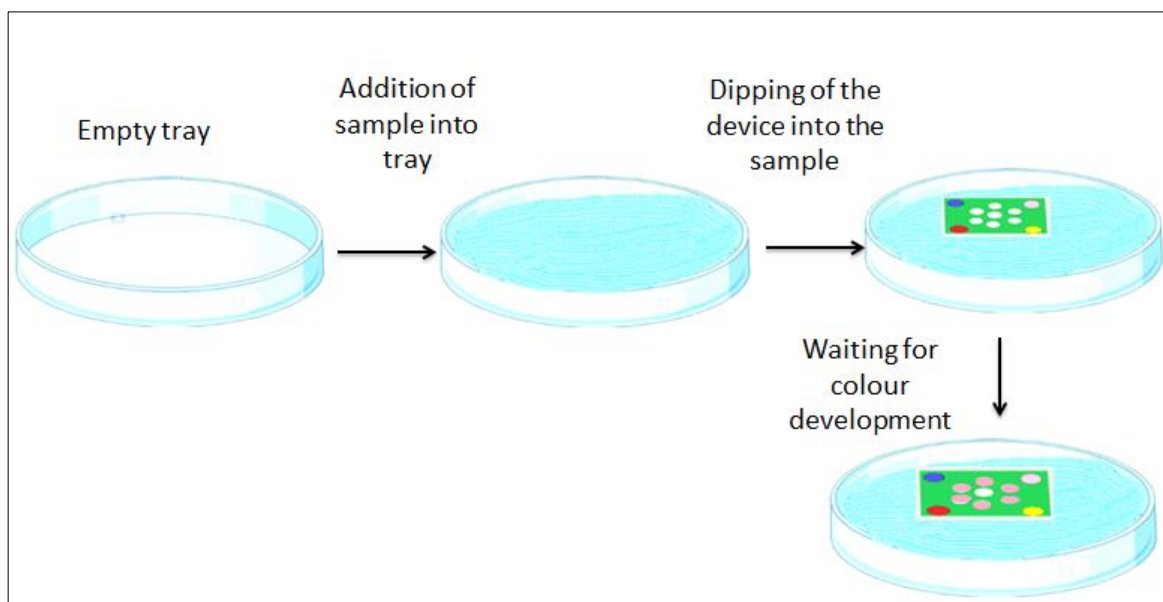
Figure 2.3 Sample introduction by dipping. The sample (nitrite or nitrate or manganese solution) first was added into a tray. The device then was dipped into the sample for a specific time based on the experiment.

2.5   Image analysis

Image-J software was employed to analyse the photo which was taken using a flatbed scanner (Canon LiDE 220), a Samsung Galaxy S8 phone (Samsung, Vietnam) or an Apple iPhone 11 [291,318]. The software was able to convert the qualitative data (colour) taken by the camera into quantitative data (numbers) by measuring the intensity of the colour in the detection zone. After opening the image in the software, the image was inverted and then converted into an RGB stack image type with separate, red, green, and blue channels. The intensity of the colour for each spot was determined using the three channels and the channel which gives the highest intensity was chosen as the optimum channel for further analysis. The overall steps for Image-J analysis are shown in **Figure** 2.4.
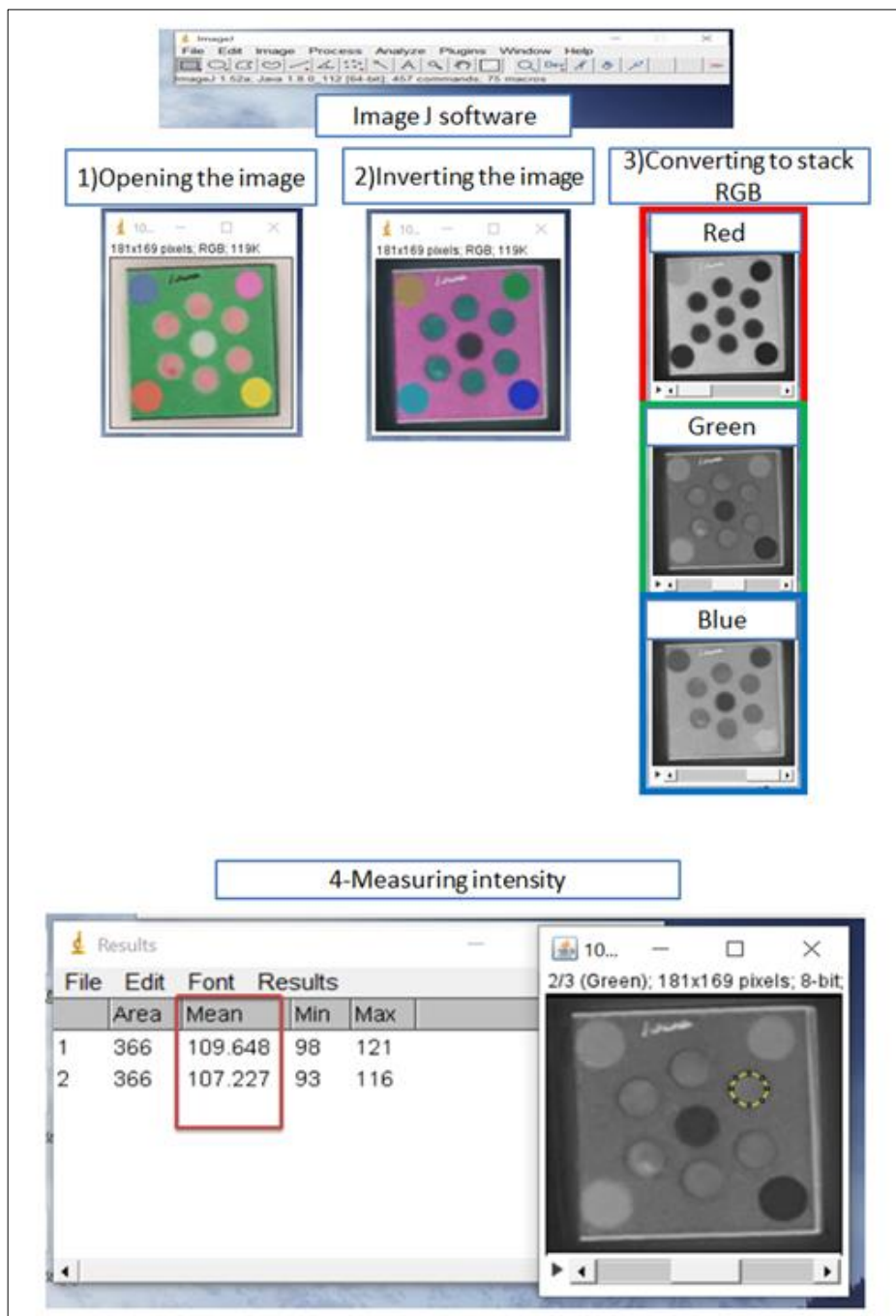
Figure 2.4 Image-J software which was used for image analysis. The image was taken using a flatbed scanner or Samsung phone and then was analysed by this software. Step 1: The file was opened. Step 2: the image was inverted by going to edit → invert. Step 3: The image type was chosen to be RGB stack by going to image → type → RGB stack and the channel was chosen. Step 4: The colour intensity is determined by going to analyse → measure. The mean represents the colour intensity. The mean intensity (pixel intensity) of each spot is in the read box. This method is not accurate; therefore, whole numbers were used for the analysis.

63

Intensity determination

Two methods were used and compared to calculate the relative intensity of the colours of the PAD detection zones. **Figure** 2.5 shows the circular spots for intensity calculation in the image which was analysed by Image-J software. The red circle shows how the area around the zone was taken for the intensity which was determined.

For uniformity of the method used especially with phone images standard deviation and surface plot were used. Standard deviation (of distributed colour) and surface plot were also determined for each spot to determine the uniformity of the colour within the detection zone. The standard deviation from each spot should not be more than 5%. The surface plot should be uniform square. If the square is not uniform, then the colour distribution within the circle is not uniform. **Figure** 2.6 shows an example of the Standard deviation (analyse->measure) and surface plot (analyse -> surface plot) for the zone in red.

Method 1 took the mean value (intensity) of each spot the same from the software as the intensity. It was called mean value by the software since for each spot the software was taken the mean of the distributed colour from the same spot. Then the average mean of all spots (pixel intensities) for each device was taken (n=6). The surrounded light effect was not considered in method 1. Therefore, some errors might be associated with method 1.

Method 1 equation:

$$intensity = intensity\ from\ standard\ or\ sample\ \ eq.\ 2.7$$

In method 2 the internal standard was used to reduce the errors. The pixel intensity from spots was divided by pixel intensity from the internal standard as in equation 2.8. The average of that was taken for the detection spots (n=6).

Method 2 equation:

$$Relative\ intensity\ = \frac{intensity\ from\ standard\ or\ sample}{intensity\ from\ internal\ standard}\ \ eq.\ 2.8$$
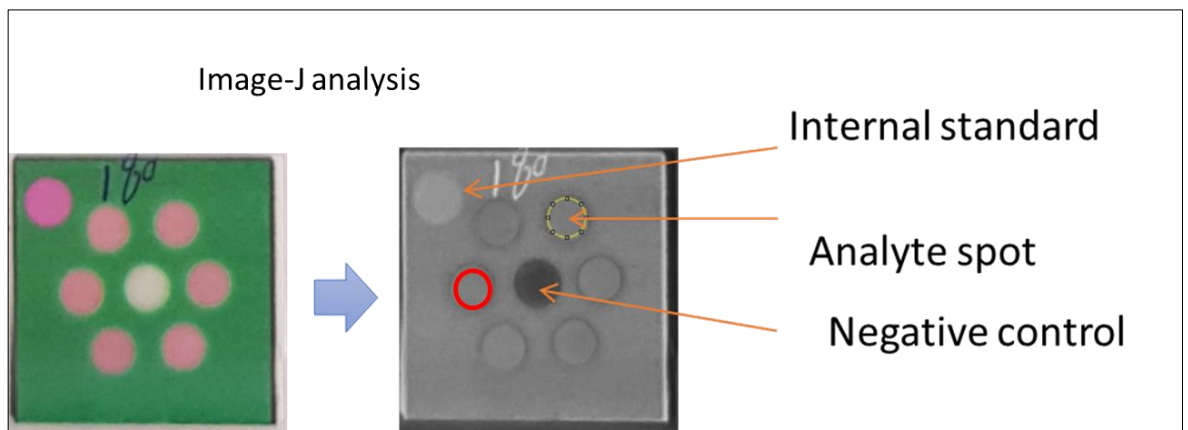
Figure 2.5 Photo analysed by Image-J software. It shows the crucial spots which were used in the analysis and calculation, internal standard, analyte and negative control. This device was produced from 1000 µM nitrate analysis. The device with n=6.
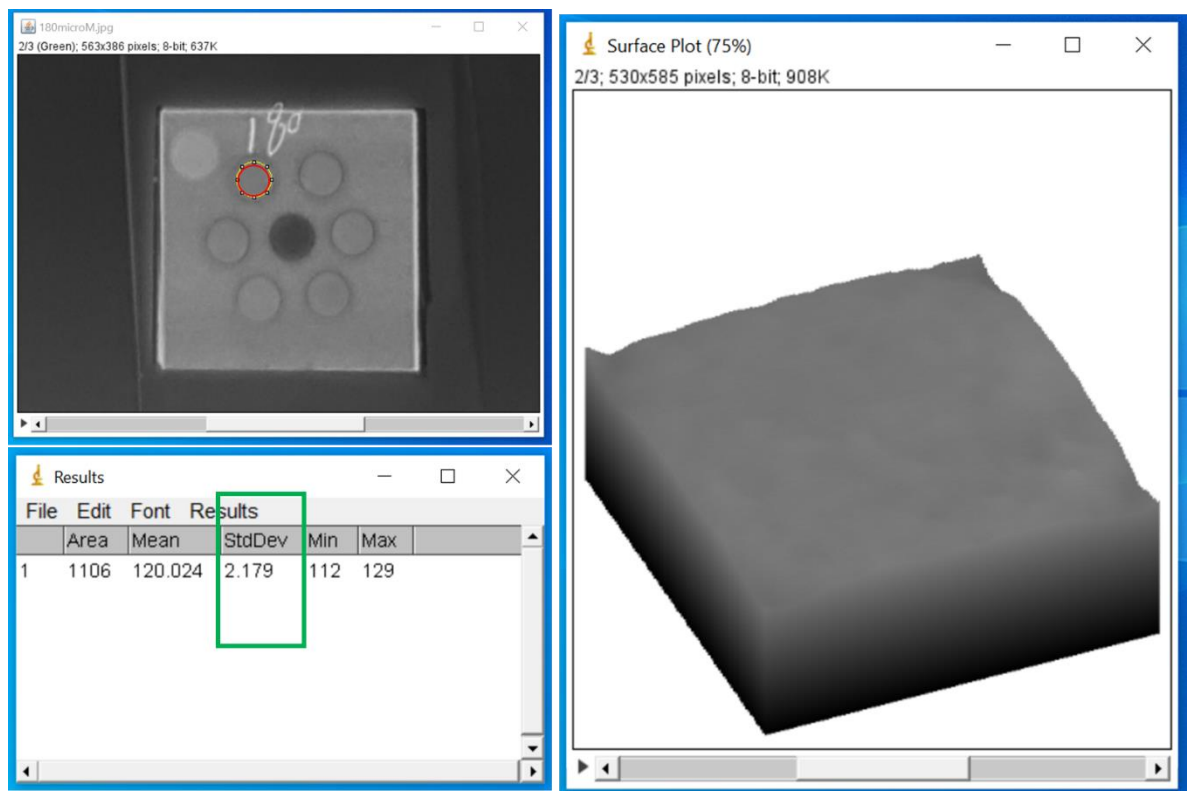
Figure 2.6 Example of the Standard deviation (Edit→ invert, image → type → RGB stack (green), analyse → measure) and surface plot (Edit→ invert, image → type → RGB stack (green), analyse → surface plot) for the zone in red by image-J.

Chapter 3 Nitrite determination

3.1   Introduction

Nitrogen is essential for plant growth. It is an important part of proteins, nucleic acids, phosphatides, alkaloids, vitamins, enzymes, and hormones [42,43]. Nitrogen is needed also in photosynthesis in plants. It is also an important chlorophyll component since chlorophyll itself is needed in photosynthesis [43]. Nitrogen is uptake by plants as inorganic form nitrate, nitrite, and ammonium, However, the main source of nitrogen for plant is nitrate, which is why fertilizer with nitrate is applied to agricultural soil [37-40]. Nitrogen is needed to produce most of the world's crops. For healthy growth of plants more than 100 million tonnes per a year of nitrogen is applied to soil as fertilizer [319]. The issue happens when there is a shortage in the nitrogen supplement or there is excess in nitrogen in such a way it causes pollution and toxicity [56]. Therefore, monitoring of nitrogen is needed.

Nitrate and nitrite are usually detected together or simultaneously using several methods like electrochemistry [320-322], spectrophotometry [323-325] and chromatography [326,327]. These methods mostly are sensitive and quantitative lab-based methods. Paper-based sensor is a used alternative which reduces the complexity, the price, and the use of chemicals and at the same time maintains the sensitivity and the quantification [328]. Paper-based sensors are commonly used for small ions analysis in water like nitrate [329,330], nitrite [306,308,309], phosphate [331] and other heavy metals [332-339]. There are also some studies on soil sample analysis [340-347]. Most were used for explosive analysis in soil and none were used for nitrite and nitrate analysis. These sensors were laboratory-based methods and mostly based on the pretreatment of the soil sample before detection. In addition, there are some commercial field sensors which are complicated, expensive, and not quantitative [3,348]. Therefore, paper-based sensors combined with the use of mobile phones for recording measurements may be a simple, inexpensive option. If the workflow is simple then lightly trained users may benefit, for example, farmers in low- and middle-income countries could use the method to monitor soil nutrients.

A common colourimetric method for the detection of nitrates is Griess reagent [61,349-351]. In a Griess assay nitrite reacts with an aromatic compound (sulphanilamide) in an acidic media to produce a diazonium salt which then reacts with another aromatic compound (N-(1-naphthyl)-ethylenediamine dihydrochloride (NED)), this leads to the production of azo dye with intense pink-red colour (equation 2.1). However, this method requires nitrate to first be reduced to nitrite and then detected as nitrite. Hence nitrate and nitrite are indistinguishable using this method. Nitrite in soil usually exists in very small amounts, hence using nitrite PAD as an initial way toward nitrate PAD development is a reasonable approach. This section focuses on the

development of PAD for nitrite determination, based on the Griess reagent. There are several paper-based sensors for nitrite determination in literature [303-306,308,309,352]. However, as far as we know none of this sensor is ready for soil sample analysis. In addition, most of them are not possible for field use.

This chapter describes the development of PADs based on Griess reagents. The chapter covers a comparison of several PAD designs, an assessment for their simplicity and ease of handling. The chapter describes the optimization of reagent component concentrations and the separation of reagents into two layers to improve the sensitivity (to the required environmental level) and reduce the auto-colour development. The measurement of colourimetric changes using a phone is assessed considering the effect of surrounding light. The robustness of the PAD was assessed by the determination of interference effect and effect of pH change on results. In addition, soil samples were analysed by the PADs and the method was validated by UV-Vis and IEC.

3.2 Experimental

3.2.1 UV-VIS Spectrophotometric analysis of nitrite

UV-VIS Spectrophotometer (mini-1240, SHIMADZU) was used for colourimetric determination of nitrite[353,354]. 10 mL of nitrite standard was mixed with 1 mL of Griess reagent. The absorbance of the solution was measured at 540 nm. The time of the reaction was 14 minutes. the calibration line was determined at the range of 0-60 μM. The Griess reagent consists of 6 mM of NED, 50 mM sulphanilamide and 300 mM citric acid. The optimized parameters are shown in **Table** 3.1.

Table 3.1 Optimizes parameters for nitrite determination by Griess reagent and UV-Vis. 20 μM of nitrite was used for the optimization.

Parameter	Optimized range
Time of reaction	0-20 minutes
NED concentration	0-12 mM
Sulphanilamide concentration	0-60 mM
Calibration range	0-250 μM

3.2.2 Ion exchange chromatography for analysis of nitrite

Ion exchange chromatography instrument (Dionex-ICS-2000) with Dionex IonPac^{TM} AS16 (RFIC^{TM}, 2 × 250mm) separator column, Dionex ASRS 300 (2 mm) suppressor column and DS6 heated conductivity cell were used as conventional method for nitrite determination. More details about columns and conditions are in **Appendix A**. Optimization was carried out using the parameters in **Table** 3.2. 15 mM KOH was used as eluent at 0.3 ml min^{-1} flow rate. A mixture of nitrate and nitrite standard (600 μM) was used for the analysis to avoid any interference from nitrate. 30-1000 μM mixture standard of nitrite and nitrate was run to determine the calibration line for nitrite. The analysis was performed over 6 minutes, the nitrite peak was eluted at 4.1 minutes.

Table 3.2 Optimized parameter for nitrite detection. 600 µM of nitrite was used for optimization.

Parameter	Value (optimized range)
Flow rate	0.30ml/min (0.2-0.6 ml/min)
KOH concentration	15 mM (15-45 mM)
Volume pump	20 µL
Pump pressure	1000-4000 psi
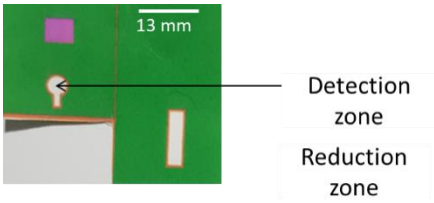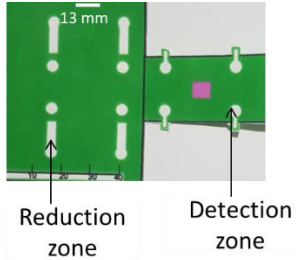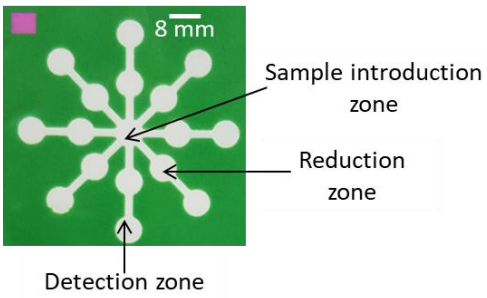
Resolution equation [78]
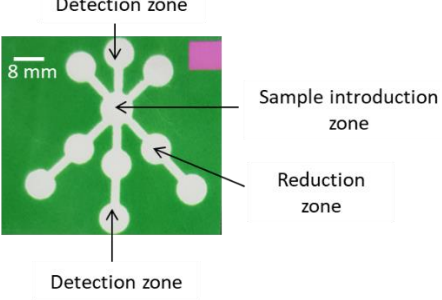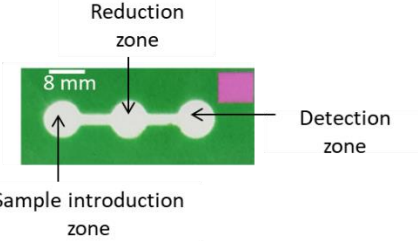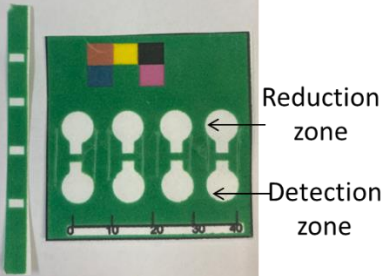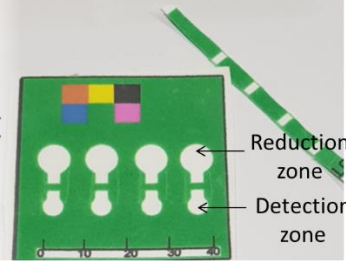
$$Resolution = \frac{\text{peak2 retention time} - \text{peak1 retention time}}{\text{peak2 width} + \text{peak 1 width}}$$ equation 3.1
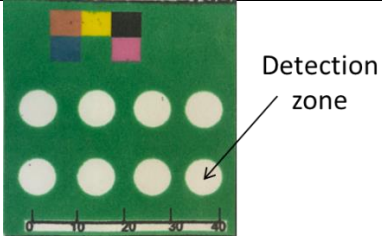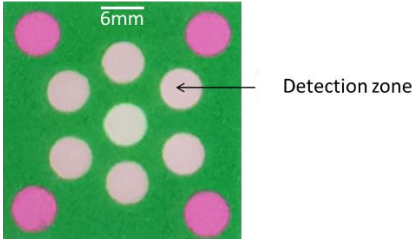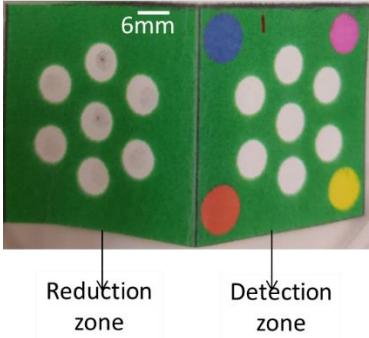
3.2.3 Designed device.

Paper devices were fabricated using the method described in **Section 2.3.1**. Green wax was used since it represents a good contrast to the pink colour generated by the Griess reaction. The wax background was important to avoid the leakage which may occur due to the movement of the PAD and imperfect alignment when two layers were used. Mainly all devices contained a sample introduction zone, detection zone and reduction zone. **Table** 3.3 summarises the dimensions of these zones if available. Most devices contained detection and reduction zones for future purpose of detection of nitrate too.

Table 3.3 Summary of device (1 to 11) dimensions, sample zone, detection zone and reduction zone.

Device	Sample entrance	Detection zones number/size	Reduction zones number/size
1	Reduction zone	1/ 5 mm	1/ 4×13mm
2	Reduction zone	4/ 5 mm	4/ 4×13.5 mm
3	8 mm	8/ 8 mm	8/ 8 mm
4	9 mm	6/ 8 mm	6/ 8 mm

Device	Sample entrance	Detection zones number/size	Reduction zones number/size
5	8mm	1/ 8 mm	1/ 8 mm
6	Reduction zone	4/ 9 mm	4/ 9 mm
7	Reduction zone	4/ 6 mm	4/ 9 mm
8	Detection zone	8/ 9 mm	none

Device	Sample entrance	Detection zones number/size	Reduction zones number/size
Detection zone			
9 6mm Detection zone	Detection zone	6/ 6 mm	None
10 6mm Reduction zone Detection zone	Reduction zone	6/ 6 mm	6/ 6 mm
11 6 mm Reduction zone (3) Detection zone (2) Detection zone (1)	Reduction zone	6/ 6 mm (Two layers)	6/ 6 mm

Device 1 (two layers, 3D device)

Device 1 consisted of two zones in two different layers, the detection and reduction zones (**Figure** 3.1). The reduction (4×13mm) zone was designed to host the reducing agent. The detection zone (5mm diameter) was designed finally to detect the analyte based on the intensity of colour developed. The purpose of the two layers was to separate the reduction process from the detection process. The reduction would occur first, then the detection after folding the two layers. The device also consisted of a transfer channel (2×2.7 mm) which was necessary to transfer the solution from the reduction zone to the detection zone. The device has one detection zone. In addition, internal standards (coloured squares) were used to account for lighting variation. The aim future of this device was to detect both nitrite and nitrate. The idea of the design was similar to Jayawardane. M et al. idea[290].
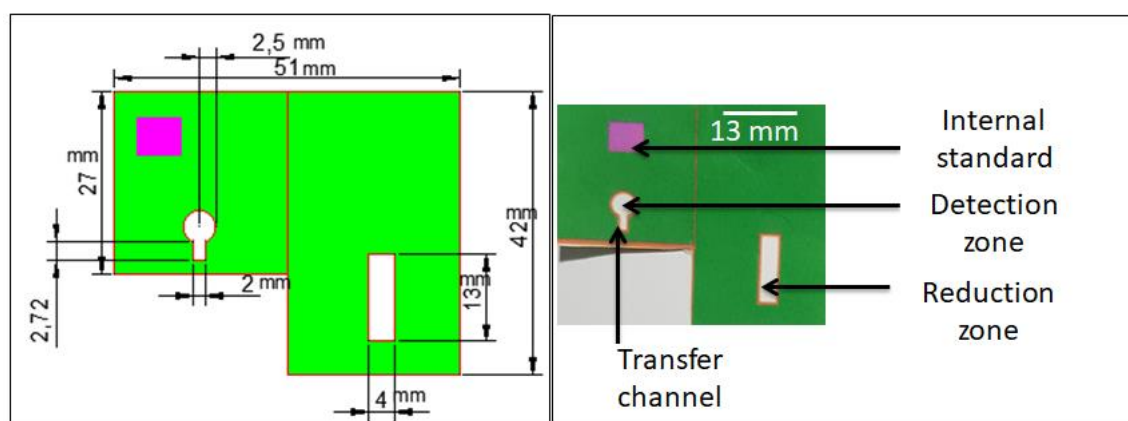
Figure 3.1 Paper device 1. The device consisted of two zones detection and reduction zone. The reduction zone is a 4×13 mm channel. The detection zone consisted of the detection area (circle with a diameter of 5mm) and transfer 2×2.7 mm channel. The coloured square was used as an internal standard. N=1.

Device 2 (two layers 3D device Modified from device 1)

Device 2 was slightly modified from Device 1, with small variations in the dimensions as shown in **Figure** 3.2. The device consisted of two detection and reduction zones. The reduction zone was a channel with one curved end (4×13.5 mm). The detection zone consisted of the detection area (a circle with a diameter of 5mm) and transfer channel (2×3.7 mm). Device 2 had four detection zones. The design features four circles in the reduction zone which matched with the circles in the detection zone after folding the device. These prevent the loss of the analyte into the wax. This device aimed to detect both nitrite and nitrate.
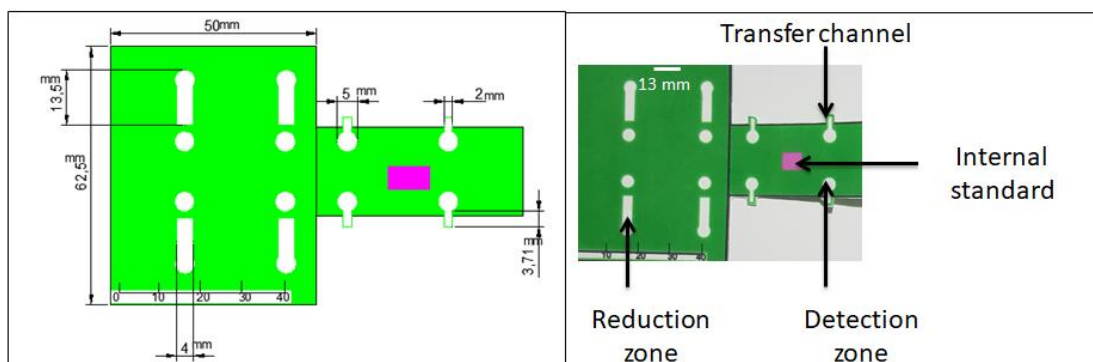
Figure 3.2 Paper device 2 was a modified design from design1. Design 2 was designed with several detection zones allowing for repeat measurements within one device (n=4). The device consisted of two zones detection and reduction zone. The reduction zone is a channel with one curved end (4×13.5 mm). The detection zone consisted of the detection area (circle with a diameter of 5mm) and transfer channel (2×3.7 mm). There were also 4 circles (5 mm) in the reduction zones which were designed to avoid losing the sample from the detection zone after folding the device.

Device 3 (a 2D device with circular zones and channels)

Device 3 (**Figure** 3.3) consisted of one sample introduction zone, 8 detection zones and 8 reduction zones. All circles with 8 mm in diameter. The sample zone, reduction zones and detection zones were connected by channels (3×4.9 mm). This design aimed to reduce the errors which may occur from using two-layer device. The device aimed to detect nitrite and nitrate simultaneously.
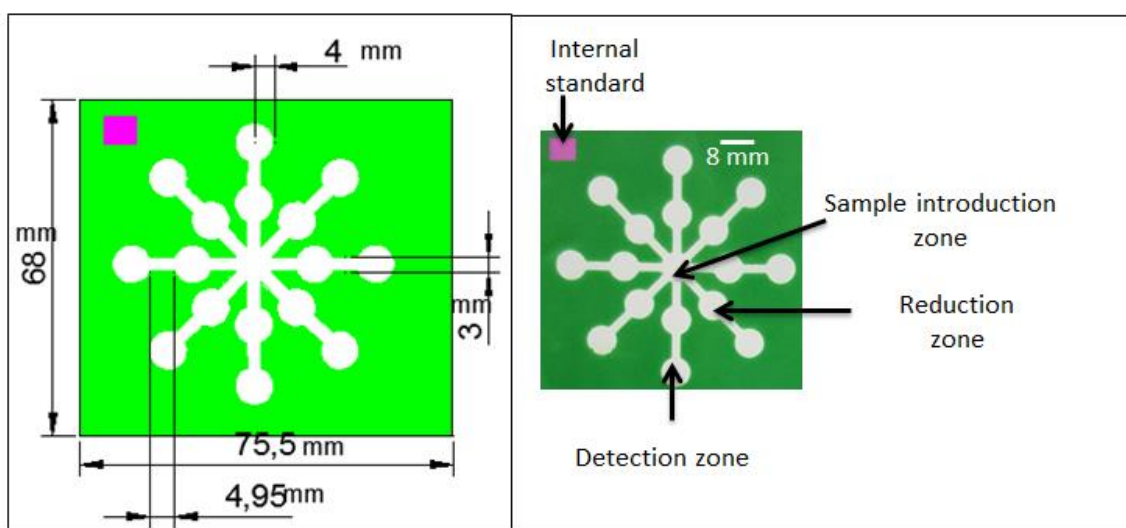
Figure 3.3 Paper device 3 which was modified from design 3. This design consisted of one sample introduction zone, 8 detection zones and 8 reduction zones. All circles with 8 mm diameter. The sample zone, reduction zones and detection zones were connected by channels (3×4.9 mm). N=8.

Device 4 (2D device modified from device 3)

Device 4 consisted of sample introduction (9 mm), reduction (8mm) and detection (8mm) zones in the same plane as in **Figure** 3.4. The top three detection zones were designed to detect nitrite and the three zones in the bottom were designed to detect nitrate. This design aimed to detect nitrate and nitrite simultaneously. This design aimed to reduce or avoid the non-uniform flow of the solution into the channels. This design was based on a similar device described by Teepo et al [291].
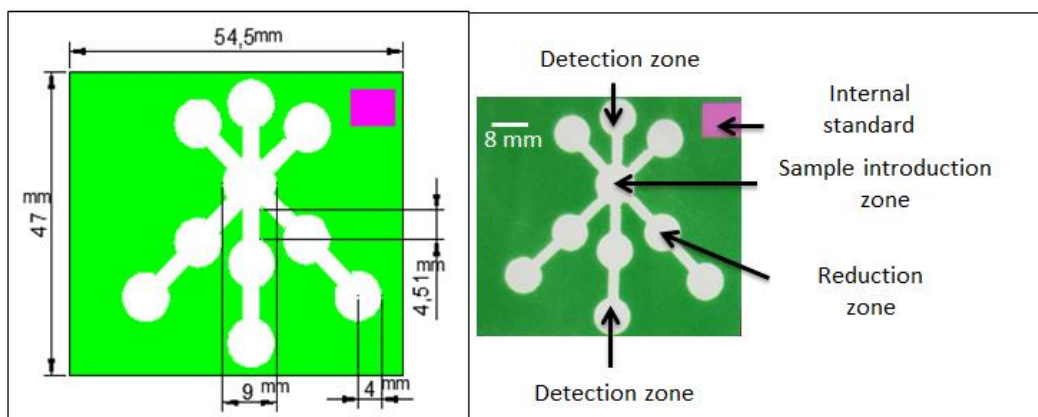
Figure 3.4 Paper device 4 (2D) consisted of 1 sample introduction zone (9mm diameter), 6 detection zones (8mm diameter) and 3 reduction zones (8 mm diameter) in the same plane. The three top detection zones were designed for detection of nitrite (n=3) and the bottom three were designed for nitrate detection (n=3).

Device 5 (2D simple device)

Device 5 (**Figure** 3.5) consisted of one channel with a single sample introduction, reduction, and detection zone (all with 8 mm diameter). The zones were connected with channels (3×5 mm).
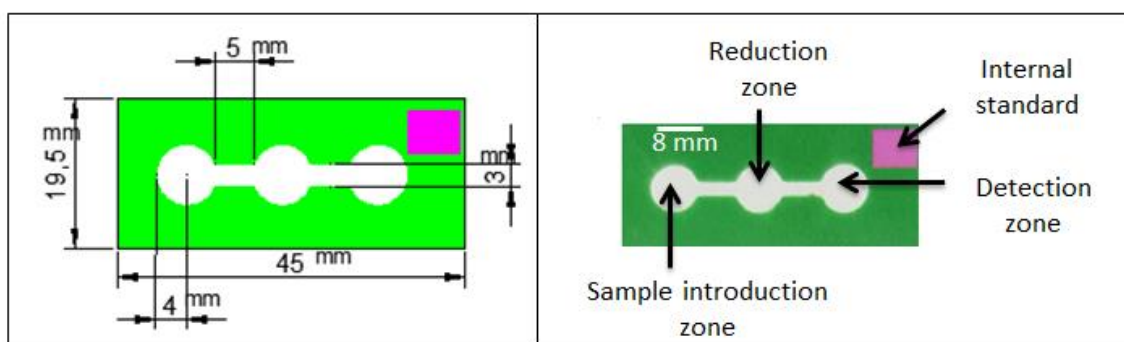
Figure 3.5 Paper device 5 (45×19.5 mm) consisted of one sample introduction zone, one reduction zone and one detection zone. All the circles with 8 mm diameters. The zones were connected with channels (3×5 mm). The pink square was the internal standard. The device was designed for one repeat only (n=1).

Device 6

Device 6 included a valve. The valve was introduced to the device instead of the central circle in device 5. The valve was designed to control the sample flow when several separated channels are presented in the device. Design 6 (**Figure** 3.6) consisted of a valve and 4 sample introduction zones (10 mm) and 4 detection zones (10mm).
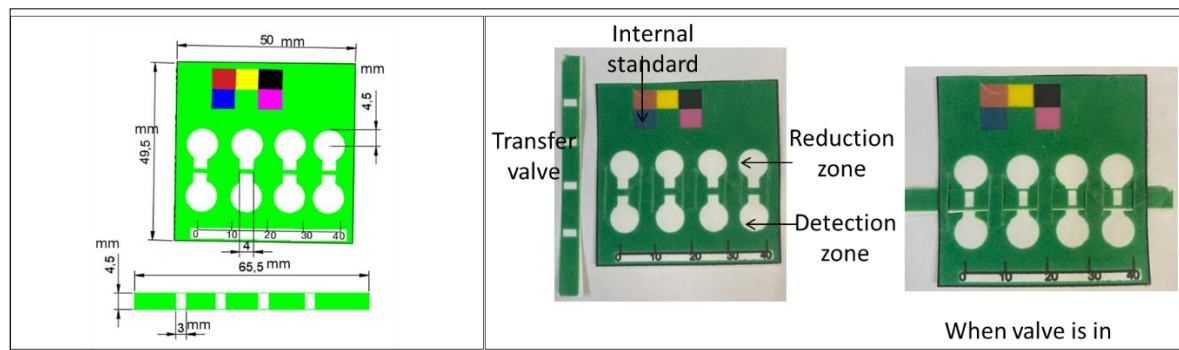
Figure 3.6 Paper device 6 (50 × 50 mm) consisted of 4 sample introduction zones (9 mm), and 4 detection zone (9 mm). All the circles with 10 mm diameters. The zones were connected with a valve. The pink square was the internal standard. The device was designed for 4 repeats (n=4).

Device 7

Device 7 (**Figure** 3.7) is a minor modification of device 6. The only difference is the diameter of the detection zone which was reduced to 6 mm from 10 mm.
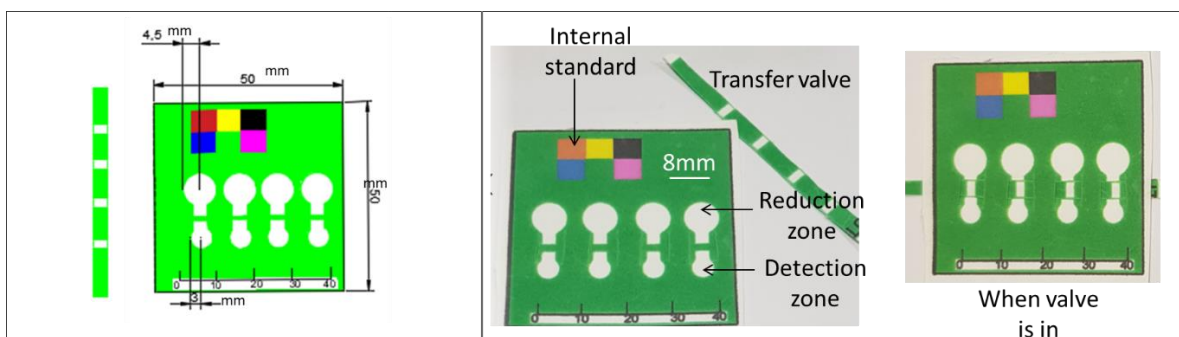
Figure 3.7 Paper device 7 (50 × 50 mm) consisted of 4 sample introduction zones (9 mm), and 4 detection zones (6 mm). The zones were connected with a valve. The pink square was the internal standard. The device was designed for 4 repeats (n=4).

Device 8

Device 8 (**Figure** 3.8) consists of 8 circular detection zones (10 mm).
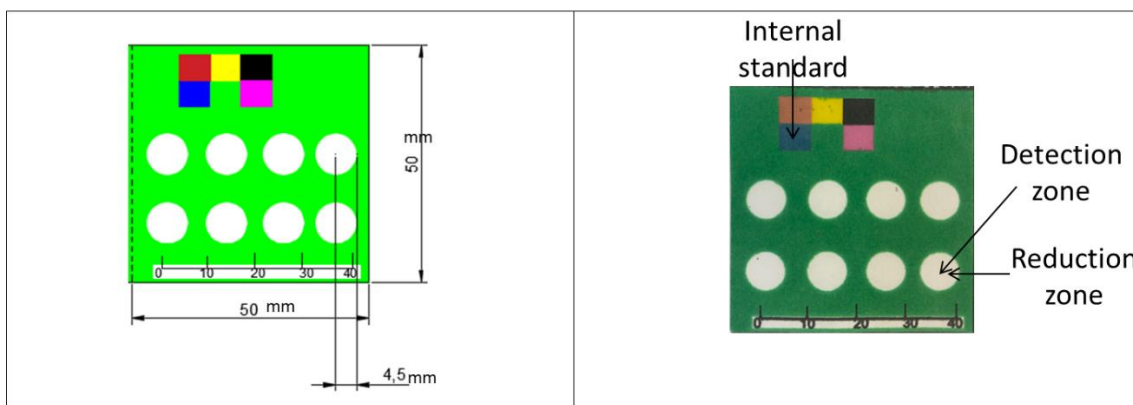
Figure 3.8 Paper device 8 (50 × 50 mm) consisted of 4 detection zones (9 mm). The zones were connected with a valve. The pink square was the internal standard. The device was designed for 8 repeats (n=8). The purpose of the device was to detect nitrite.

Device 9

The designed device (**Figure** 3.9) consisted of 7 detection zone circles (6 mm) and 4 pink circles in the corners. The pink circles were used as internal colour standards. The circle in the very centre is a negative control. The six surrounding circles were used for the detection of the analyte. This device was used to detect nitrite only.
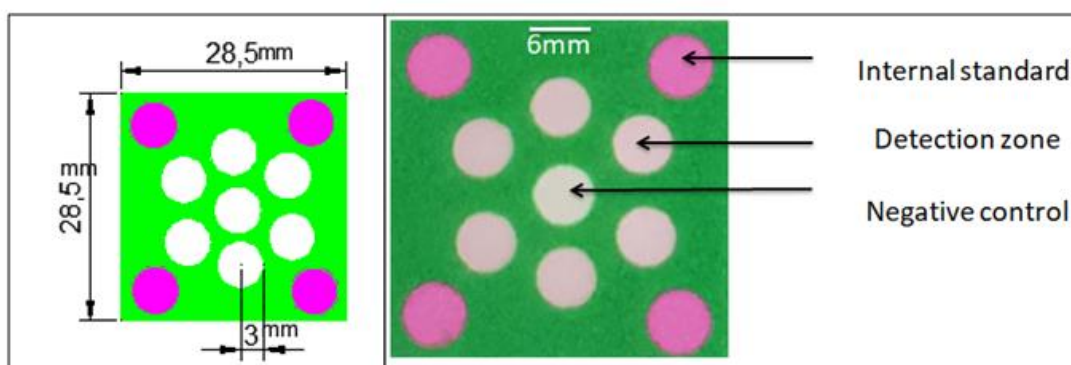
Figure 3.9 Paper device 9 (28.5×28.5 mm) with 6 detection circles, 1 negative control circle, 4 internal standard circles and a green wax background. The device was used for nitrite (n=6) analysis only.

Device 10

This device (**Figure** 3.10) consisted of separate reduction and detection zones, which come into contact with each other when the device is folded, thus forming a 3-dimensional device. The dimensions and the number of circles of the two zones same as in device 9. Different colours for internal standards were utilised for comparison. The reduction zone had no internal standard.

77
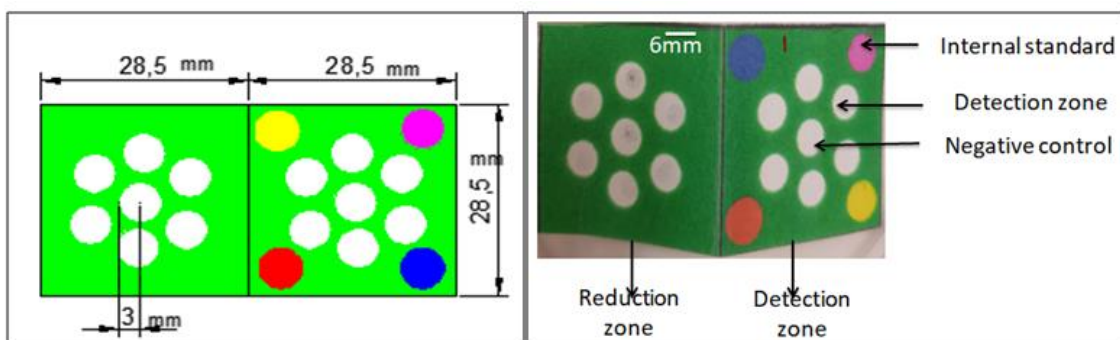
Figure 3.10 Paper device10 (57×28.5 mm) with two zones, reduction and detection zones. Each zone had 7 circles which had 6 mm diameter. The detection zone consisted of 4 internal standards, yellow, pink, red and blue. The device was adopted for the detection of nitrite and nitrate (n=6).

Device 11

Device 11 (**Figure** 3.11) was a modified form of device 10. It had similar dimensions for detection and reduction zones. However, device 11 had two detection zones compared to device 10 which had one detection zone. The device was folded to a form three-dimension device. Once the device was folded the three zones should match each other.
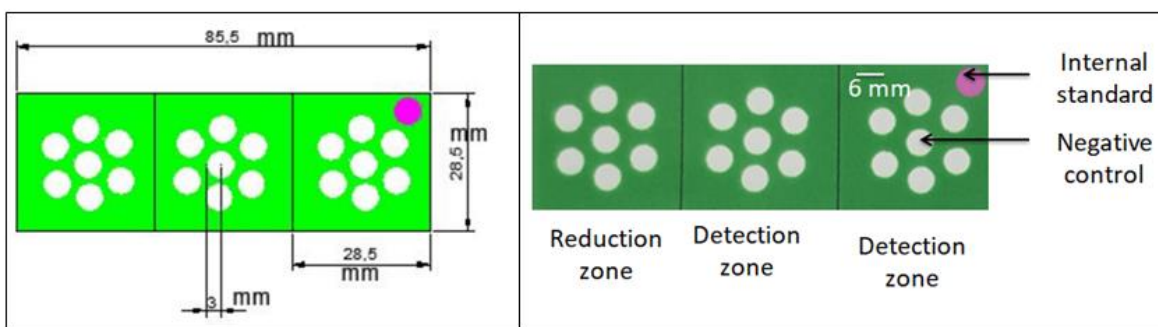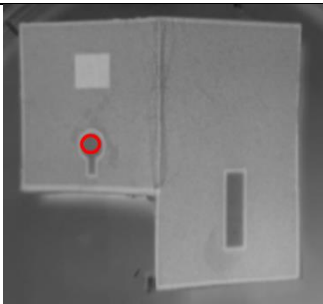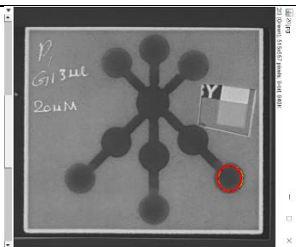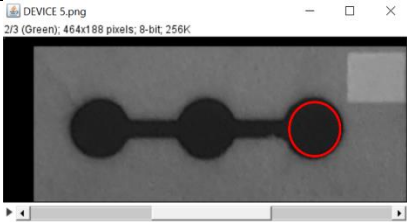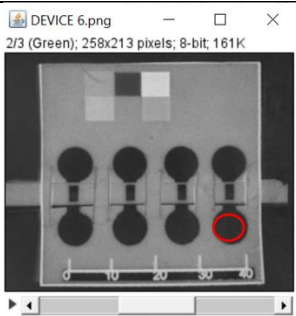
Figure 3.11 Paper device 11 (85.5×28.5 mm) with three zones, 1 reduction and 2 detection zones. Each zone had 7 circles which had 6 mm diameter. The detection zone consisted of pink internal standard. The device was adopted for the detection of nitrite and nitrate in the future (n=6).
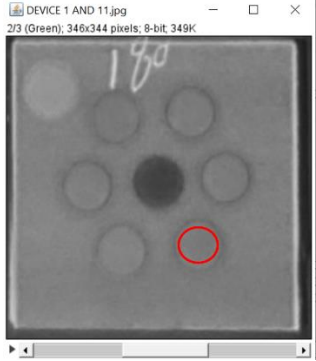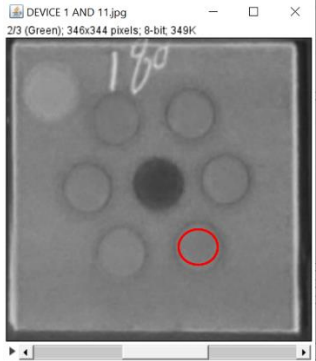
3.2.4 Device modification

The devices in general were modified similarly. A specific amount of detection reagent (Griess reagent) was added to the detection zone, and it was allowed to dry for a specific time after that the device was folded or laminated or kept without lamination. Then analyte was pipetted (specific amount) or it was added by dipping. The reaction was then allowed for colour development (specific time). A phone/ scanner was used for image capture. Finally, the image was analysed by image-J. **Table** 3.4 summarizes the amount of reagent added to zones, time of drying, amount of analyte added, reaction time, image capture and analysis of the image by image-J. Details of the modification of each device were mentioned later.

Table 3.4 Summarises the amount of reagent added to zones, time of drying, amount of analyte added, reaction time, image capture and analysis of image by image-J.

device	Amount of reagent in the detection zone	Drying time of detection zone	Amount of reagent in the reduction zone	Amount of analyte	Reaction time	Image analysis around all detection zones (in red)
1	1 µL	10 min	0 µL	20 µL	14 min	
2	-		-	-		-
3	-		-	-		-
4	µL	10 min	0 µL	100 µL	14 min	
5	3 µL	10 min	0 µL	50 µL	14 min	
6	5 µL	10 min	0 µL	30 µL	14 min	

device	Amount of reagent in the detection zone	Drying time of detection zone	Amount of reagent in the reduction zone	Amount of analyte	Reaction time	Image analysis around all detection zones (in red)
7	3 µL	10 min	0 µL	30 µL	14 min	
8	5 µL	10 min	0 µL	10 µL	14 min	
9	1.5 µL	10 min	0 µL	6 µL	5 min	

device	Amount of reagent in the detection zone	Drying time of detection zone	Amount of reagent in the reduction zone	Amount of analyte	Reaction time	Image analysis around all detection zones (in red)
10	1.5 µL	10 min	0 µL	dipping	5 min	
11	1.5 µL in each layer	10 min	0 µL	dipping	5 min	

Device 1 and 2 modifications.

Paper device 1 was modified for nitrite detection in a similar way as described in the literature with some variations (**Figure** 3.12)[290]. 1 µL of Griess reagent was added to the detection zone and it was allowed to dry for 10 minutes at room temperature (around 20 ^{0}C). 20 µL of analyte (nitrite standard, 100 µM) was added to the detection zone and allowed to stand for 75 seconds. The device was then folded from the centre to allow the analyte to move from the reduction to the detection zone with the help of a transfer channel. The photo for the detection zone was taken after 14 minutes of colour development. Device 2 was modified the same way as Device 1. However, device 2 had several reaction zones in one device.
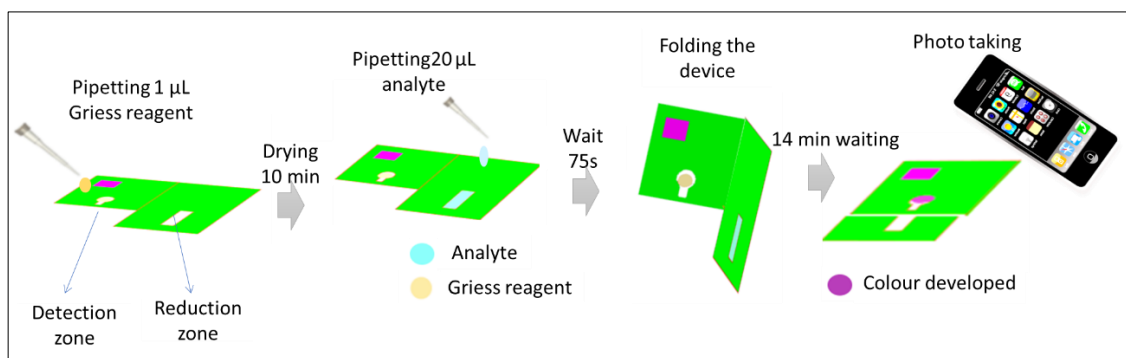
Figure 3.12 Modification of paper device 1. 1 μL Griess reagent was added to the detection zone and then allowed to dry for 10 minutes. 20 μL of nitrite was pipetted into the reduction zone and it was allowed to stand for 75 seconds. After that, the device was folded from the centre. 14 minutes was the time for colour development. Finally, a photo was taken using a Samsung Galaxy S8 phone and analysed by ImageJ software (method 2). n=3.

Device 3 and 4 modifications

The aim of designing devices 3 and 4 was to simultaneously detect nitrite and nitrate. The designs consisted of channels; therefore, it was important first to test the efficiency of the flow of the solution within the device. The flow was demonstrated using coloured red food dye (**Figure** 3.13). Red food dye (Allura Red AC) (8-200 μL) was pipetted into the sample introduction zone and a photo was taken each second for 20 seconds. The flow of the dye was then observed. If the dye moves equally to all channels, it means the flow is efficient. If the flow is uneven, then the device is unsuitable for analyte detection. Both devices 3 and 4 were tested for fluid flow. Device 4 was used for nitrite detection since it shows uniform flow. 3 μL of Griess reagent was added to the detection zones and it was allowed to dry for 10 minutes. The device was then ready to be used. 100 μL of analyte (nitrite standard, 100 μM) was added to the sample introduction zone and allowed to stand for 14 min. **Figure** 3.14 shows the modification of device 4.
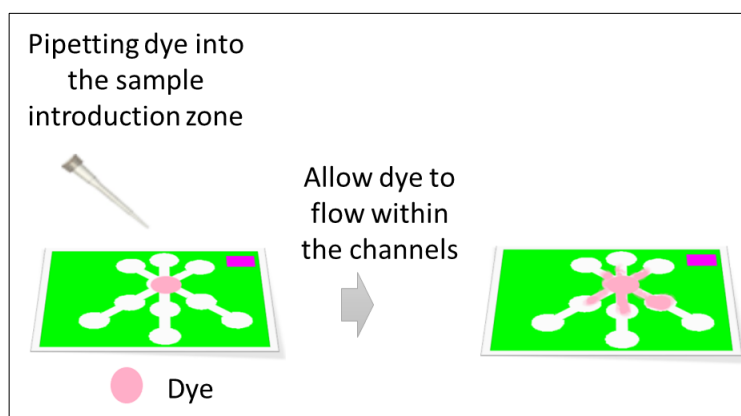
Figure 3.13 Flow test for paper device 4. Red dye (100 μL) was pipetted into the sample introduction zone. The dye was allowed to flow within the channels. A photo was taken each second for 60 seconds. The ability of the device to achieve uniform flow was studied.
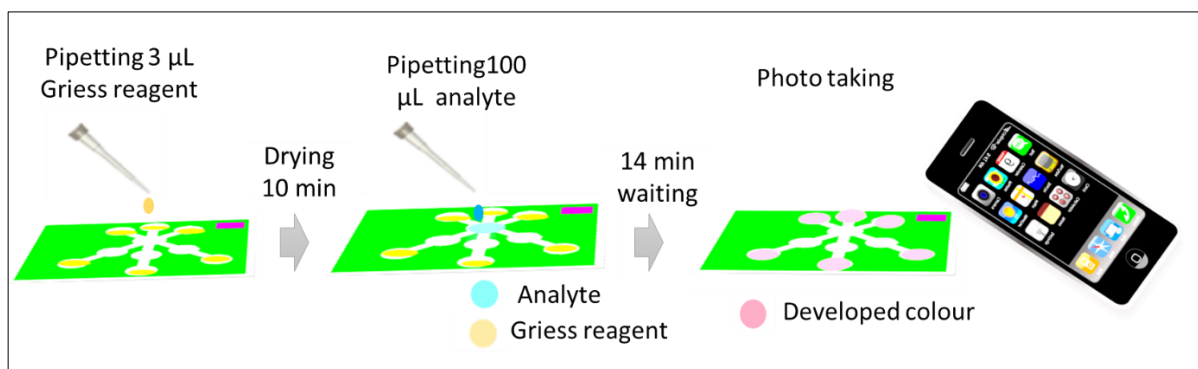
Figure 3.14 Modification of paper device 4. 3 µL of Griess reagent was initially pipetted to the detection zone. It was allowed to dry for 10 minutes. Then 100 µL of analyte (nitrite) was pipetted into the sample introduction zone and was allowed to flow to the detection zone for 14 minutes. Finally, a photo was taken for Image-J software ANALYSIS (method 2 in **Section 2.5**).

Device 5 modification

Paper device 5 is a simplified version of designs 3 and 4 since Device 5 has one channel and hence has one direction flow. 3 µL of Griess reagent was added into the detection zone. Then it was allowed to dry for 10 min. 50 µL of the standard was added then to the sample introduction zone. After 14 minutes a photo was taken for Image-J analysis. The paper device 5 modification is **in Figure** 3.15.
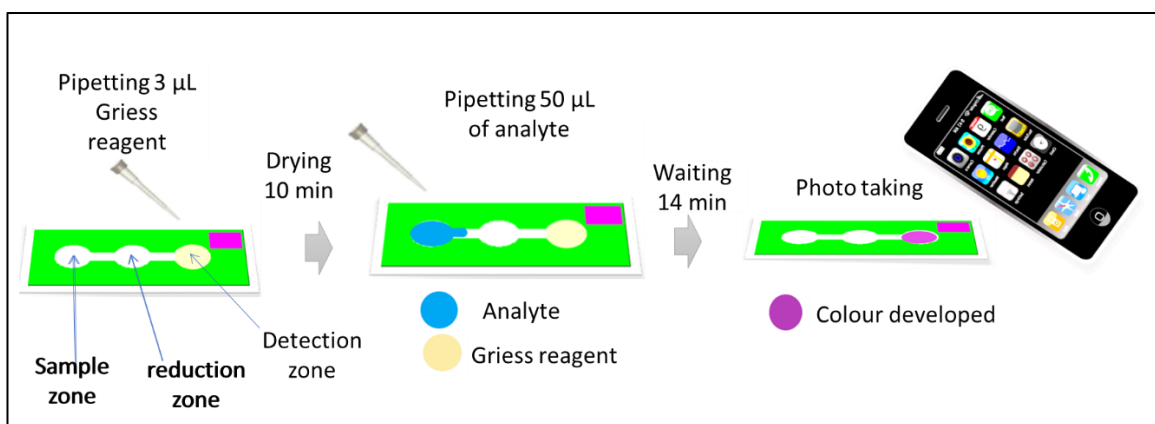
Figure 3.15 Modification of paper device 5. 3 µL of Griess reagent was initially pipetted to the detection zone. It was allowed to dry for 10 minutes. Then 50 µL of analyte was pipetted into the sample introduction zone and was allowed to flow to the detection zone for 14 minutes. Finally, a photo was taken by phone (Samsung Galaxy S8) for Image-J software (method 2 in **Section 2.5**) analysis.

Device 6 modification

Device 6 was modified **(Figure** 3.16) by adding the detection reagent (5µL Griess reagent) in the detection zones and allowed to dry for 10 minutes. The analyte (30 µL nitrite solution) was added into the sample introduction zone and allowed to flow by opening the valve. Colour development was allowed for 14 minutes. The phone was used for picture taking which was

then analysed by image-J. N=3. Device 6 with valve provided one channel device with several repeats while the channels are still separated (sample flow only in one direction).
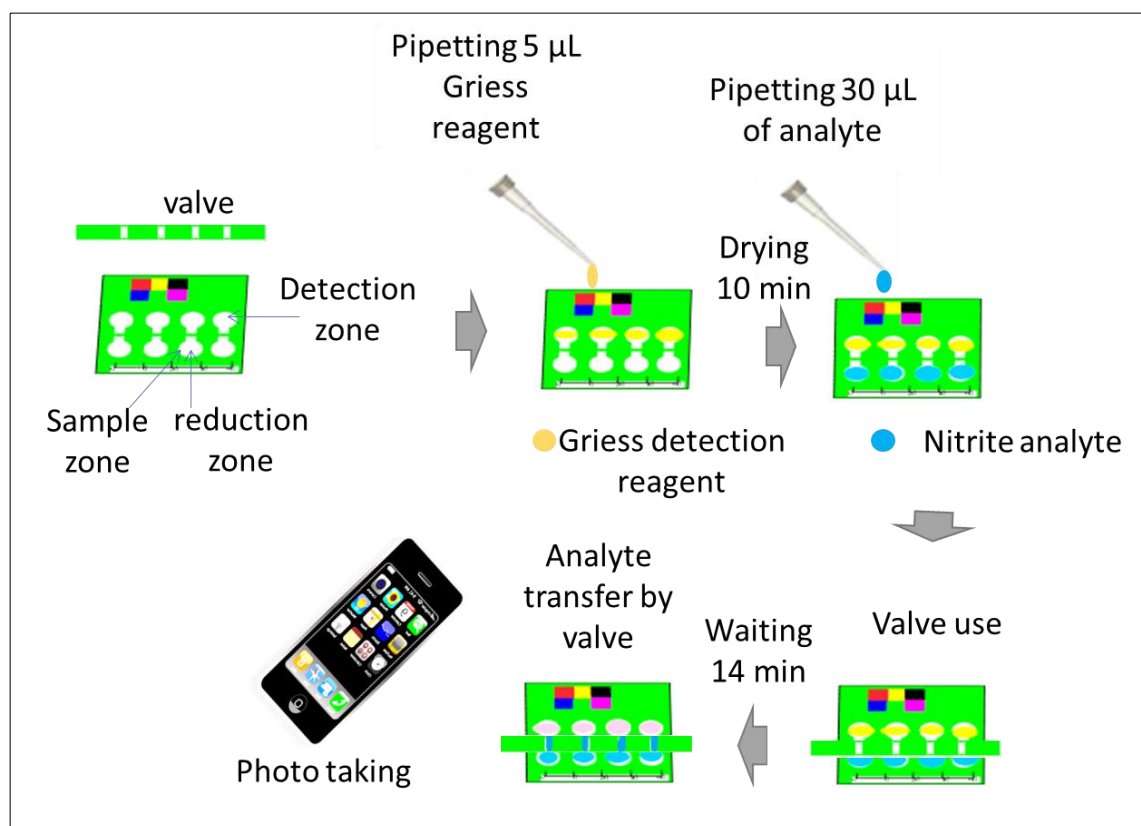
Figure 3.16 Modification of paper device6. detection reagent (5µL Griess reagent) in the detection zones and allowed to dry for 20 minutes. The analyte (30 µL nitrite solution) was added into the sample introduction zone and allowed to flow by opening the valve and developing colour for 14 minutes. A phone (Samsung Galaxy S8) was used for picture taking which was then analysed by image-J (method 2 in **Section 2.5**). N=3.

Device 7 modification

Device 7 was also a device with a valve, and it is an improved form of device 6. The only difference is the diameter of the detection zone which was reduced to 6 mm instead of 10 mm. Device 7 allows the solution to move to a smaller area and hence enough solution is transferred to fill the detection area. Device 7 was modified (**Figure** 3.17) by adding the detection reagent (3 µL Griess reagent) in the detection zones and allowed to dry for 10 minutes. The analyte (30 µL nitrite solution) was added into the sample introduction zone and allowed to flow by opening the valve and the colour was allowed to develop for 14 minutes. scanner was used for picture taking which was then analysed by image-J. N=3.
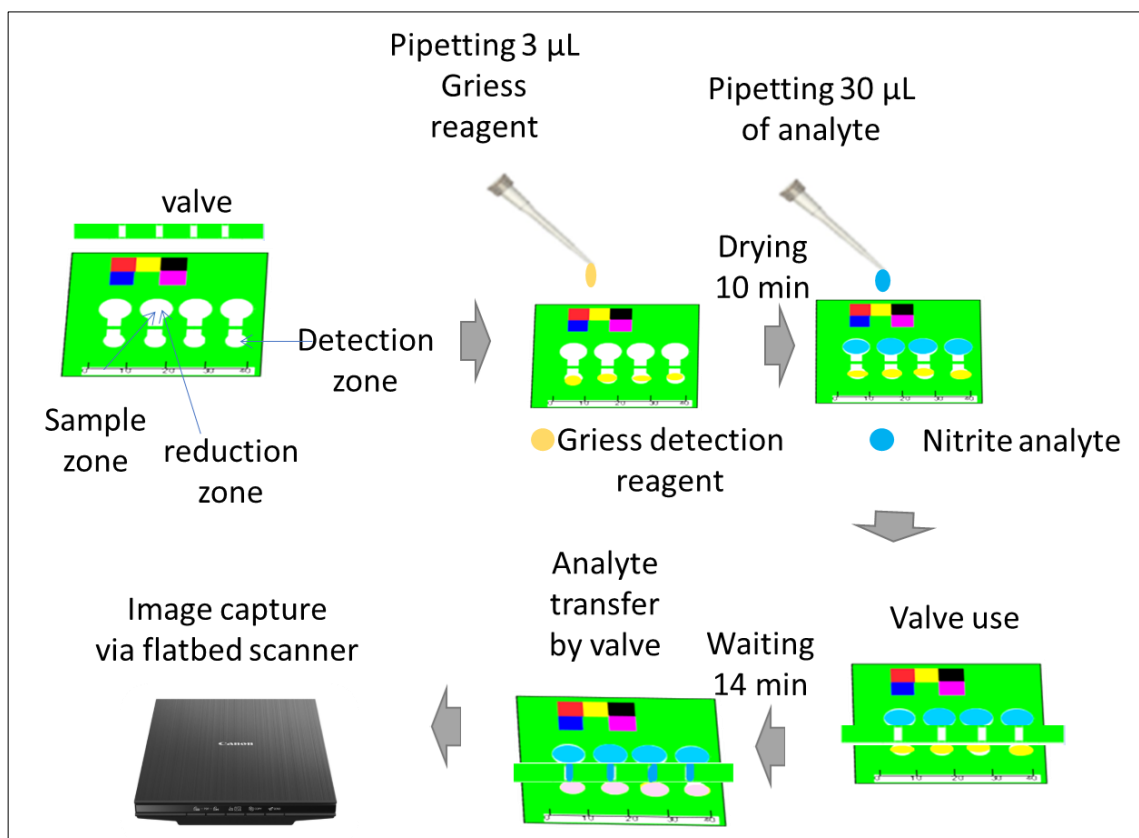
Figure 3.17 Modification of paper device 7. 3 µL Griess reagent) in the detection zones and allowed to dry for 10 minutes. The analyte (30 µL nitrite solution) was added into the sample introduction zone and allowed to flow by opening the valve and developing colour for 14 minutes. scanner was used for picture taking which was then analysed by image-J (method 2 in **Section 2.5**). N=3.

Design 8 modification

Device 8 was modified (**Figure** 3.18) by adding the detection reagent (5 µL Griess reagent) in the detection zones and allowed to dry for 10 minutes. The analyte (10 µL nitrite solution) was added into the sample introduction zone and allowed to flow by opening the valve and developing colour for 14 minutes. The phone was used for picture taking which was then analysed by image-J. N=6.
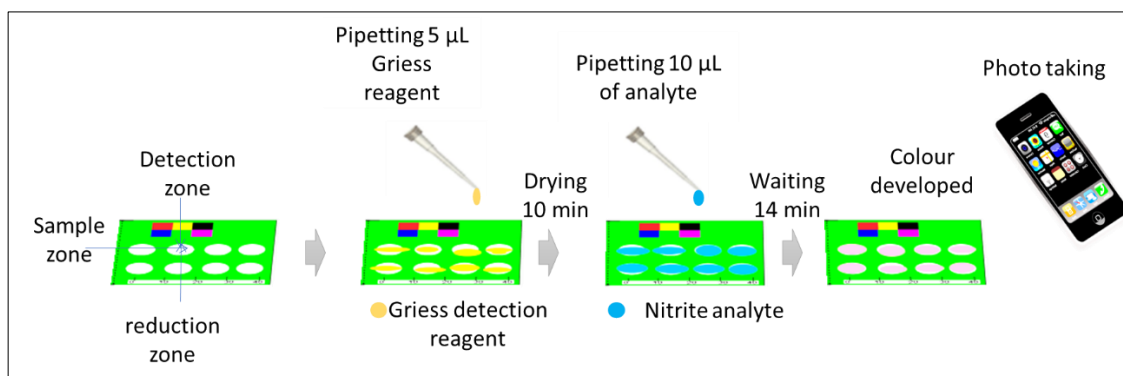
Figure 3.18 Device 8 was modified by adding the detection reagent (5 µL Griess reagent) in the detection zones and allowed to dry for 10 minutes. The analyte (10 µL nitrite solution) was added into the sample introduction zone and allowed to flow by opening the valve and developing colour for 14 minutes. A phone (Samsung Galaxy S8) was used for picture taking which was then analysed by image-J (method 2 in **Section 2.5**). N=6.

Device 9 Modification

 Paper device 9 modification is clarified in **Figure** 3.19. 1.5 µL Griess reagent was initially added to the 6 detection circles. The central circle is the negative control, and no chemicals were added there. The device was allowed to dry for 10 minutes. 6 µL Nitrite standard was then added to the same 6 circles and the central circle. The reaction was allowed to develop for 5 minutes. After that, a photo was taken for analysis by Image-J software.
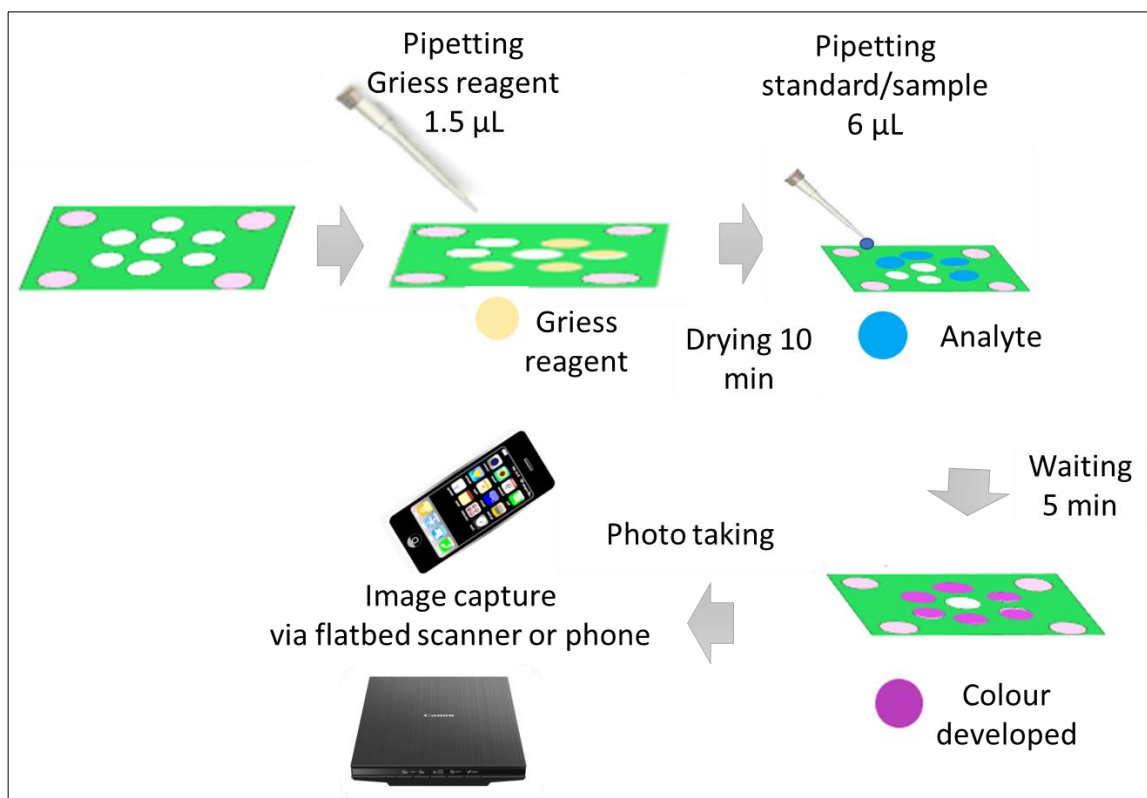
Figure 3.19 Device 9 modification. 1.5 µL Griess reagent was added to the 6 detection circles. The device was dried for 10 minutes. 6 µL nitrite standard was added to the 6 detection circles and the central circle (negative control). The reaction was allowed to develop for 5 minutes. A phone (Samsung Galaxy S8) or scanner were used for image capture.

Device 10 modification

Device 10 has two zones, the detection and reduction zone as in **Figure** 3.20. 1.5 µL of Griess reagent was pipetted into the circles in the detection zones. The device was allowed to dry for 10 minutes. After 10 minutes the device was folded. The circles in the detection zone should match the circles in the reduction zone after folding. The folded device was laminated at 80 °C. Small slits were made in the back side of the device (reduction zone) by a scalpel. The device was dipped into a tray with standard/sample for 5 minutes. A photo was taken after 5 min of reaction, and it was analysed by Image-J software (method 2). Several internal standards (pink, yellow, blue and red) were used and compared during the analysis.
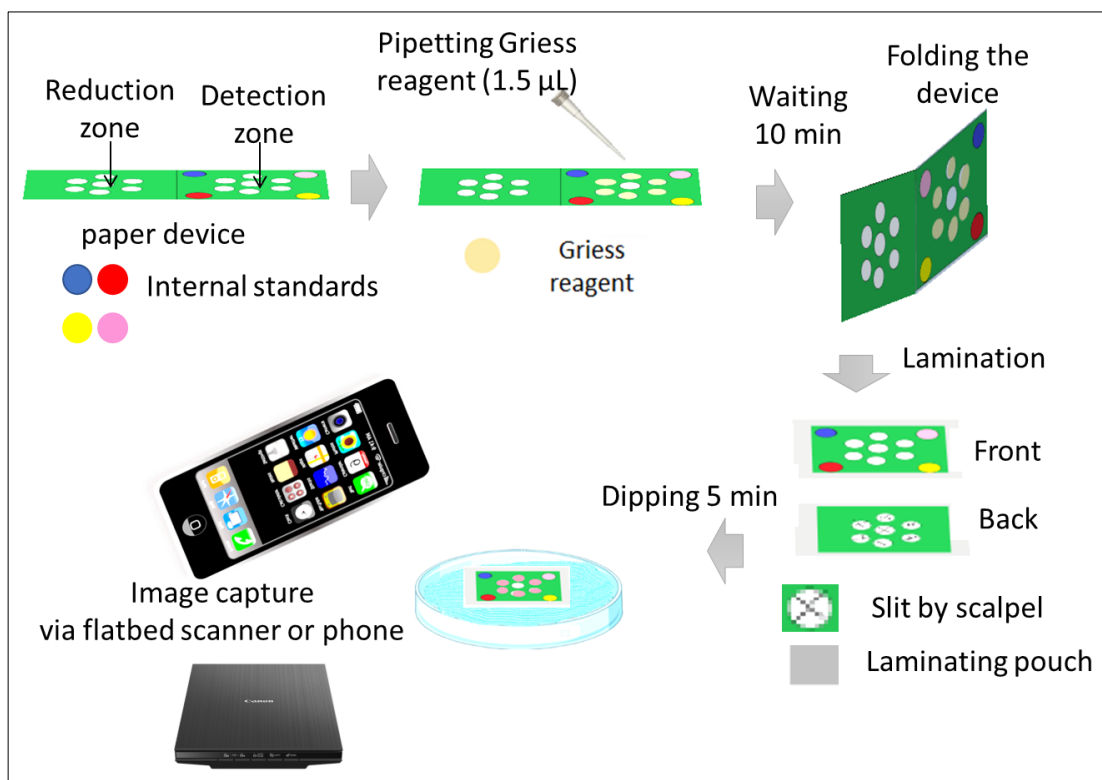
Figure 3.20 Modification of paper device 10. (1) 1.5 µL Griess reagent was added to the detection zone (all circles except the negative control). (2) The device was allowed to dry for 5 minutes. (3) A fold from the centre of the device was made. (4) The folded device was laminated in a laminating punch three times by a laminator at 80 °C. (5) Slits were made in all circles using a scalpel. (6) The device was dipped in standard/sample (nitrite) for 5 minutes. (7) A photo was taken by a scanner or phone camera (Samsung Galaxy S8), and it was analysed by Image-J software (method 2 in **Section 2.5**).

Device 11 modification

Device 11 has three zones, two detections and one reduction zone as in **Figure** 3.21. In this section, the detection zone was only modified. 1.5 µL of solution 1 (6 mM NED) was pipetted into the circles in the detection zone 1. 1.5 µL of solution 2 (50 mM sulphanilamide and 300 mM citric acid) was pipetted into the circles in the detection zone 2. The device was allowed to dry for 10 minutes. After 10 minutes the device was folded. The folded device was laminated at 80 °C. A small slit was made in the back side of the device (reduction zone) by a scalpel. The device was dipped into a tray with standard/sample for 5 minutes. A photo was taken after 5 min of reaction, and it was analysed by Image-J software (method 2).
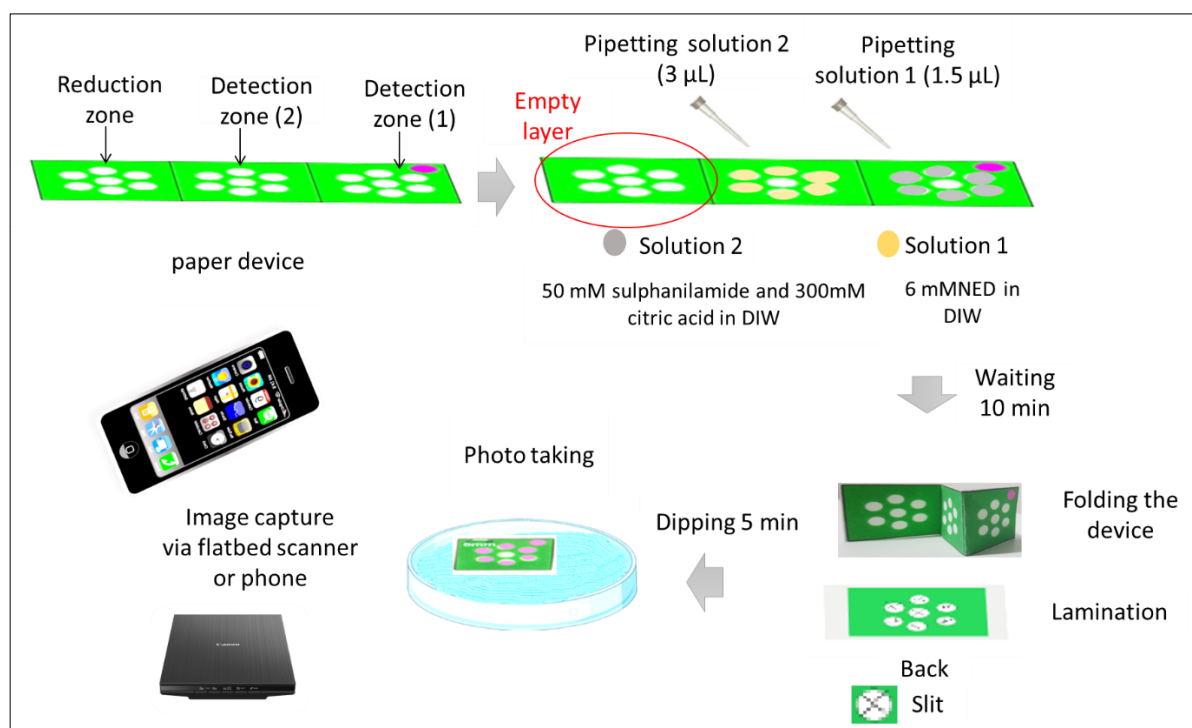
Figure 3.21 Modification of paper device 11. (1) 1.5 µL of solution 1 (6 mM NED) was pipetted into the circles in the detection zone 1. 1.5 µL of solution 2 (50 mM sulphanilamide and 300 mM citric acid) was pipetted into the circles in the detection zone 2. In all circles except the negative control. (2) The device was allowed to dry for 10 minutes. (3) A fold from the centre of the device was made. (4) The folded device was laminated in laminating punch three times by a laminator at 80 °C. (5) Slits were made in all circles using a scalpel. (6) The device was dipped in standard/sample (nitrite) for 5 minutes. (7) A photo was taken by phone camera (Samsung Galaxy S8) or scanner, and it was analysed by Image-J software (method 2 in **Section 2.5**).

3.2.5 Choice of the device design

The work described in this thesis aimed to create analytical devices that are useable by people such as citizen scientists or farmers, without the need for significant training. As such it was necessary to design devices that are simple and easy to use. As with any analytical device any measurements need to be accurate and reproducible. To achieve these goals several paper device designs were tested.

3.2.6 Optimization of PAD

Device 9 was optimized with the suitable amount of Griess reagent, amount of standard, reaction time and concentration of Griess components. 60 and 100 µM nitrite standards were used most of the time in the optimization. The device was treated in a similar way as in **Figure 3.19**. Initially different amount of Griess reagent was added to the device while other parameters remained constant. Once the optimum quantity of Griess reagent was determined and then the second parameter was optimized. The time of reaction was optimized by taking measurements every minute for 14 minutes. The time at which the signal remains constant was determined. Two methods in Image-J analysis were tested to determine the signal (colour

89

intensity) and the best method was chosen. Three channels (red, green, and blue) in Image-J software were used and the channel with the best result was chosen too. Four internal standards were used. The signals from the four internal standards were determined and compared. All parameters were optimized one by one as their order in **Table** 3.5.

Table 3.5 Time of colour development, amount of Griess reagent, amount of standard, concentration of sulphanilamide, citric acid concentration and concentration of NED were the optimized parameters with different studied ranges.60 and/or 100 µM nitrite standards were used during optimization.

Optimized parameter	Studied range
Time for colour development	0-10 minutes
Amount of Griess reagent	0.5-2 µL
Amount of standard	4-8 µM
Concentration of sulphanilamide	20-60 mM
Concentration of NED	4-12 mM
Citric acid concentration	200-450 mM

Lamination effect

Device 9 (**Figure** 3.19) was not laminated and a pipette was used to introduce sample/ standard to the device. It was compared to device 10 (**Figure** 3.20) which was laminated, and sample/standard was introduced to the device by dipping it into a sample or standard solution. This effect was studied at 0, 60 and 100 µM nitrite standard concentrations. The device was changed from device 9 to device 10 for lamination purposes to avoid the scratch of the detection layer when the scalpel was used to make sample entrance. In the next section device 10 was changed to device 11 to separate Griess reagent into two layers of the device.

Separated Griess reagent components.

The Griess reagent was separated into two solutions as in **Figure** 3.21. These two solutions were added to different detection zones in device 11. The separation of components aimed to improve the intensity of the colour resulting from the reaction. The intensity from device 10 with non-separated Griess components (treated as in **Figure** 3.20) was compared to the signal

from device 11 with separated Griess components (treated as in **Figure** 3.21). 0, 60 and 120 μM nitrite standards were used in the comparison.

Stability of the devices (separated and non-separated Griess reagents)

Device 10 and device 11 were tested for their stability over 4 days. The two devices were prepared as mentioned in **Figure** 3.20 and **Figure** 3.21. Then they were stored in the freezer. Each day a photo was taken of the two devices without any reaction with nitrite. After the photo was taken, the devices were returned to the freezer and the next day photos were taken again for the same device and so on for 4 days. The stability of devices 10 and 11 were compared then by comparing the intensities from each alone in the 4 days.

3.2.7 Calibration curve: Scanner and phone

Paper device 11 (Figure 3.11) was used to obtain the calibration curve. The optimum conditions were used, and the device was modified as in **Figure** 3.21. 0-150 μM standard solutions were run. The limit of detection and limit of quantitation were calculated using **Equation 2.5** and **Equation 2.6**. The calibration line was determined using a scanner and phone.

3.2.8 Interference studies

Sodium, potassium, chloride, phosphate, acetate, manganese, sulfate, carbonate, iron (II), calcium, zinc and copper (II) ions were studied for their interference with nitrite detection using the reagents mentioned in **Table** 2.1. The interference was determined by analysis of 60 μM of nitrite alone and then analysis a mixture of the interference with 60 μM of nitrite as in **Figure** 3.22. The concentration of the interference was varied until the lower concentration that caused interference was found. Device 11 and images taken with a scanner were used for the detection.
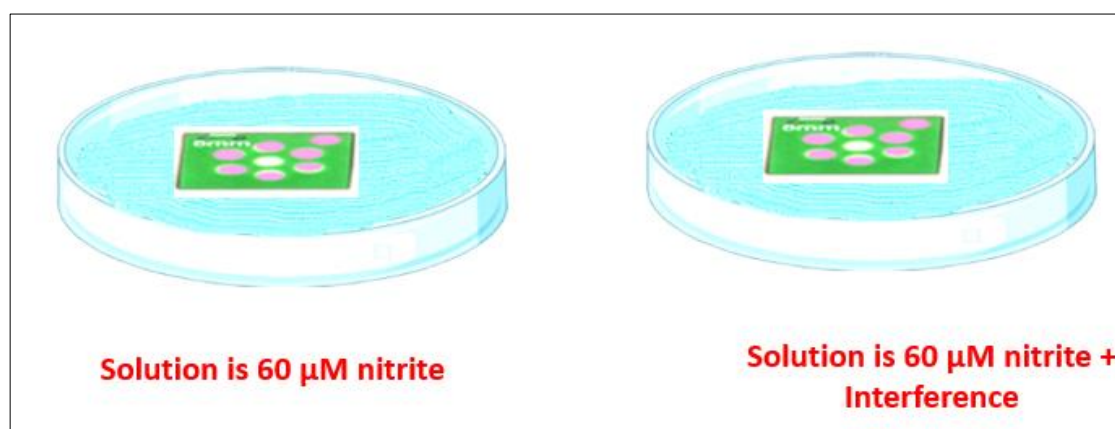
Figure 3.22 Interference studies for nitrite detection. The nitrite was detected alone as in the left of the figure using device 11. The nitrite and specific concentration of interference were detected together as in the right side of the figure. A scanner was used for the detection. 60 μM of nitrite was used in the analysis.

3.2.9 pH effect studies

Device 11 was used for pH studies. Calibration lines for nitrite (0-90 µM) were determined at different pH 5, 6, 7 and 8. The standards were prepared in 25 mL DIW. The pH of standards was adjusted by 1% NaOH and 1% HCl. A 3510 pH meter (JENWAY) was used to measure the pH.

3.2.10 Soil sample treatment

Information about the soil sample

Three types of commercial compost were utilized in this study; John Innes No 1 (young plants compost), John Innes No 2 (potting on compost) and John Innes No 3 (mature plants compost), all were from wetland store via Westland store, Amazon. Soil samples were also studied including commercial topsoil samples with no nutrient additions (topsoil 1) from Westland store, Amazon and topsoil samples from Arable farmland (topsoil 2), Hull Yorkshire world, Hull (Rooting zone, 0-15cm depth usually).

Nitrite extraction

8 g of soil was mixed with 100 mL of deionized water and allowed to be mixed for 2 minutes in cafetière, the extracted was then allowed to settle for 3 minutes (these parameters were chosen to fit the nitrate extraction in Chapter 4). The extracted solution was then analysed by PAD for nitrite detection. The same samples were extracted for nitrite by the addition of 8 grams of soil with 100 mL of DIW in a shaker for 1 hour (these parameters were chosen to fit the nitrate extraction in Chapter 4). The extract passed through a 0.25 µm filter and was then analysed with the IEC and UV-Vis.

3.3 Result and Discussion

3.4 Conventional method for nitrite determination

3.4.1 UV-Vis

Colourimetric detection of nitrite by Griess reagent is widely used due to its simplicity [355]. It requires less instrumentation and is quick compared to other analytical techniques based on electrochemical and biological processes [355-357]. Griess reagent reacts with nitrite to produce a pink/red colour (**Equation 2.1** in the experimental section). When carried out in solution this colour change can be easily detected using UV-Vis spectroscopy. The more intense the colour the higher the concentration of analyte. Studying the analysis of nitrite by UV-Vis spectrophotometer is necessary in this study since it is important to base the initial experiments of paper devices on the result from UV-Vis analysis. In the coming sections, the optimization of several parameters for nitrite detection by Griess reagent is described.

Reaction Time optimization

Characterisation of reaction times is necessary to determine when the endpoint measurement should be taken. **Figure** 3.23 shows reaction kinetics, which shows the absorbance from 20 µM nitrite standard after reaction with Griess reagent each minute for 20 minutes. A range of 0-20 min time was studied based on previous studies which take 10 to 20 minutes as the reaction time [351,358,359] and hence there was no need to go to a longer time. The absorbance was measured at the maximum absorption wavelength of 540 nm as shown in **Figure** 3.24. Initially, the absorbance increases with time since the reaction was not complete yet. Between 14 and 20 minutes the signal became stable (t_{stat}=2.375, t_{crit}=2.776, P= 0.078, at α=0.05, n=3 for two-tailed test between points at 14 and 20 min) and reached around 98% of maximum at this range. As a result, 14 minutes was chosen as the optimum time for complete reaction between nitrite and Griess reagent**.**
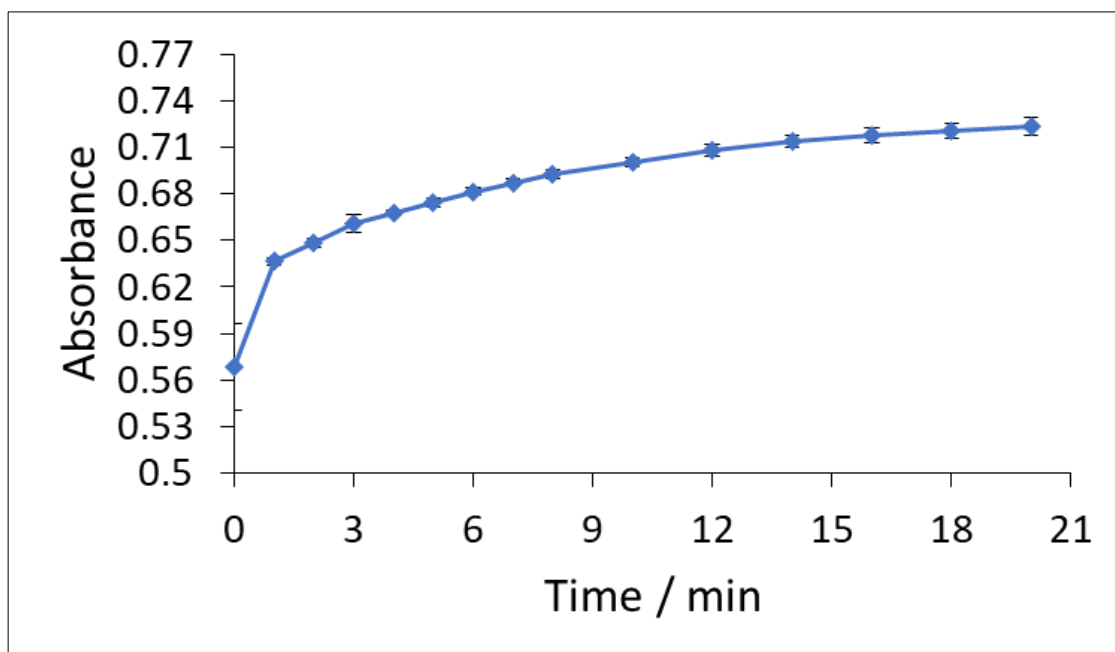
Figure 3.23 Absorbance at 540nm versus time (min). Result from UV-Vis spectrophotometer. 20 µM nitrite standard (10 mL standard+ 1 mL Griess reagent) was used. 14 min was chosen as the optimum time for the colour development. 10, 330 and 50 mM of NED, citric acid and sulphanilamide were used respectively in the Griess reagent.
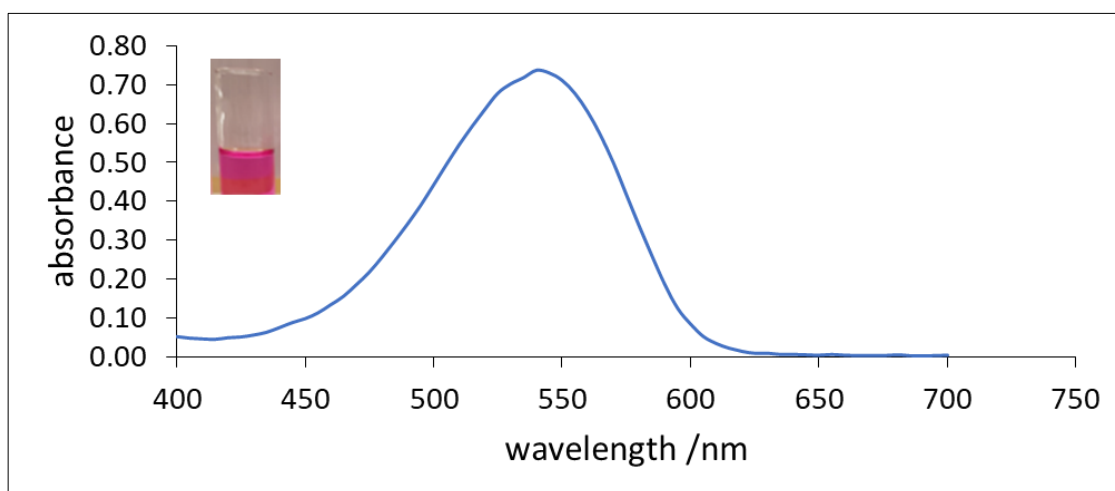
Figure 3.24 Absorbance versus wavelength (nm). This spectrum from 20µM nitrite standard (10mL standard + 1 mL Griess reagent). The spectrum was taken after 14 minutes of colour development. The maximum absorbance was at 540 nm. 10, 330 and 50 mM of NED, citric acid and sulphanilamide were used respectively in the Griess reagent.

NED concentration optimization

NED, citric acid and sulphanilamide are used in Griess reagents. Each of them has its role. NED was important in forming the coloured pink compound. NED concentration was optimized as in **Figure** 3.25 which shows the absorbance versus the concentration of NED. As the concentration of the NED increases the absorbance increases until it reaches a maximum at around 4-6 mM (t_{stat}=-1.061, t_{crit}=2.776. P= 0.35, at α=0.05, n=3 for two-tailed test), then the absorbance

decreases with further increase in the concentration of NED. These decreases may be due to the excess amount of the NED causing a reversal of the reaction and a reduction in the formation of the coloured compound. Also, NED may tend to compete with sulphanilamide for nitrite. 6 mM was chosen to be the optimum.
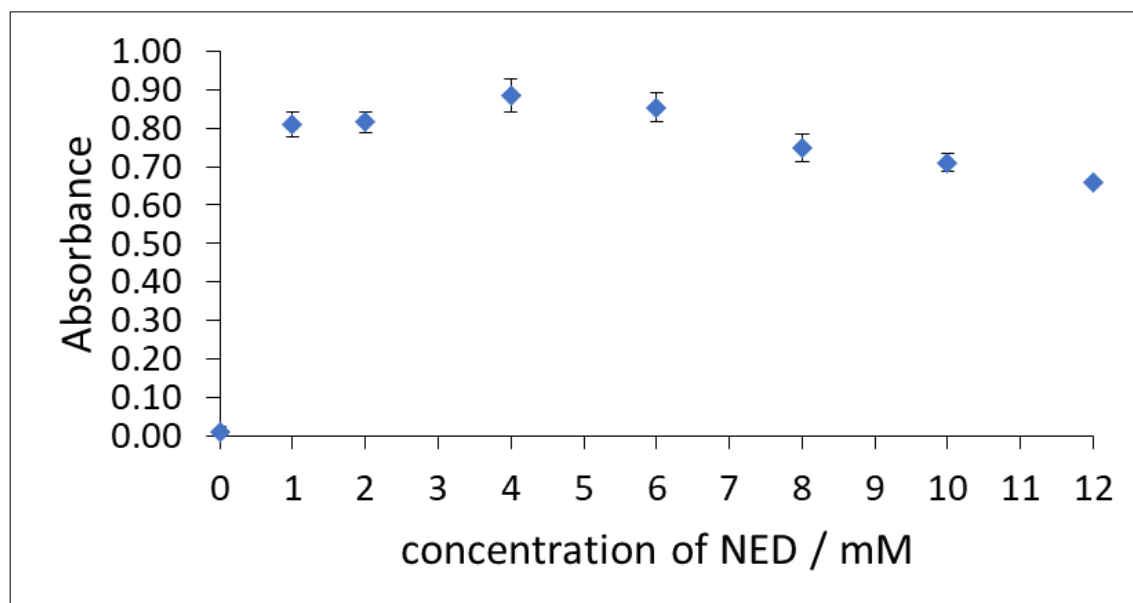
Figure 3.25 Absorbance versus the concentration of NED (mM). 20µM nitrite standard (10mL standard+1 mL Griess reagent) was used. The spectra were taken after 14 minutes of colour development. The maximum absorbance was at 540 nm. 330 and 50 mM of citric acid and sulphanilamide were used respectively in the Griess reagent. 6 mM was chosen to be the optimum.

Sulphanilamide concentration optimization

Sulphanilamide reacts with nitrite to form intermediate compounds as in **Equation 2.1**. This intermediate reacts with NED to form the coloured pink compound. Sulphanilamide concentration was optimized also as in **Figure** 3.26 which shows the absorbance versus the concentration of sulphanilamide. At low concentrations, there was not enough sulphanilamide and hence the absorbance was low. 50 mM of sulphanilamide was chosen as optimum since it shows the highest absorbance. More than 50 mM of sulphanilamide started to decrease the absorbance maybe due to the reverse reaction.
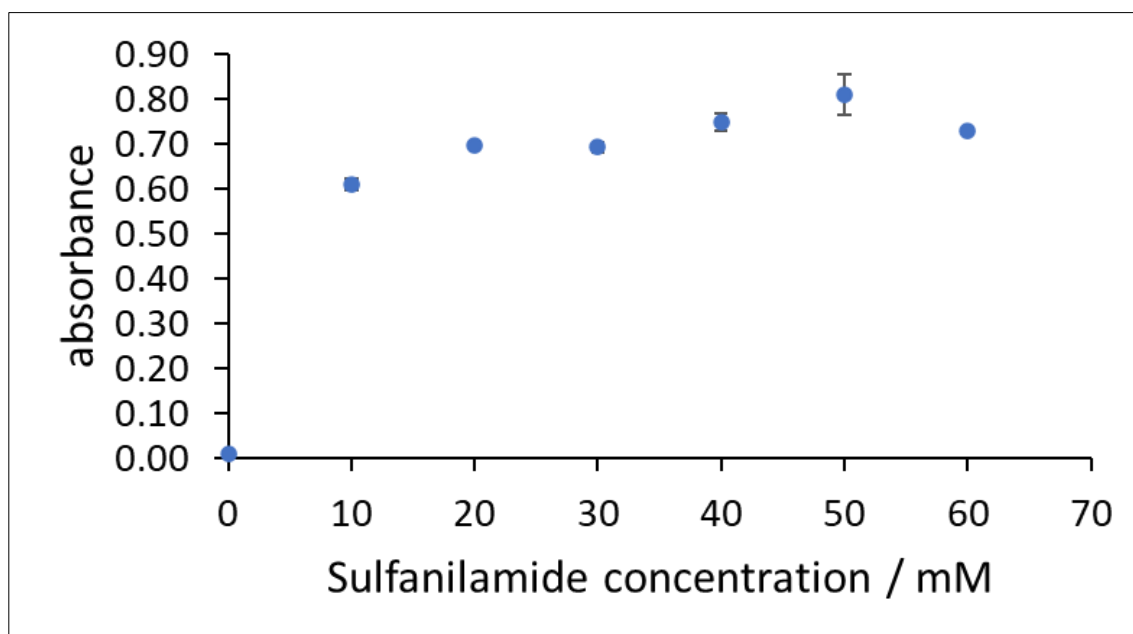
Figure 3.26 Absorbance versus the concentration of sulphanilamide (mM). 20μM nitrite standard (10mL standard+1 mL Griess reagent) was used. The spectrum was taken after 14 minutes of colour development. The maximum absorbance was at 540 nm. 330 and 6 mM of citric acid and NED were used respectively in the Griess reagent. 50 mM of sulphanilamide was chosen as the optimum.

Calibration line

A calibration curve was produced to allow for quantification of nitrite in a sample. The calibration was plotted based on the optimum concentrations of the Griess reagent components; 6, 330 and 50 mM of NED, citric acid and sulphanilamide respectively. **Figure** 3.27 shows the calibration line for nitrite from the UV-Vis spectrophotometer. The linear range was from 0 to 60 μM. Within this range, R^2 is 0.99 which indicates a good fit of the data points to a straight line. This method showed a small relative standard deviation which was not more than 5%. The limit of detection and quantification were 0.053 and 0.179 μM respectively (around 0.030 and 0.103 mg kg^{-1} respectively if 8 grams of soil and 100 mL of solvent is used) (**Table** 3.6). LoD and LoQ were calculated as methods in **Equation 2.5 and 2.6** in the experimental section. These values are similar to those reported in the literature where spectrophotometric methods were used for nitrite detection in various samples [360-364]. In addition, the LoD and LoQ are both lower than the maximum allowed level of contamination of nitrite in drinking water (21.7 μM /1mg L^{-1}) [365] according to the US Environmental Protection Agency. When UV-Vis is compared to the level of nitrite in soil, it shows also lower results for LoD and LoQ. The level of nitrite in soil rarely exceed 164 mg kg^{-1} and most of the time is lower than 0.3 mg Kg^{-1} [366,367]. The reproducibility of the method was determined by repeating the calibration curve. The new calibration line fits the previous line and hence this indicates the reproducibility of the method.
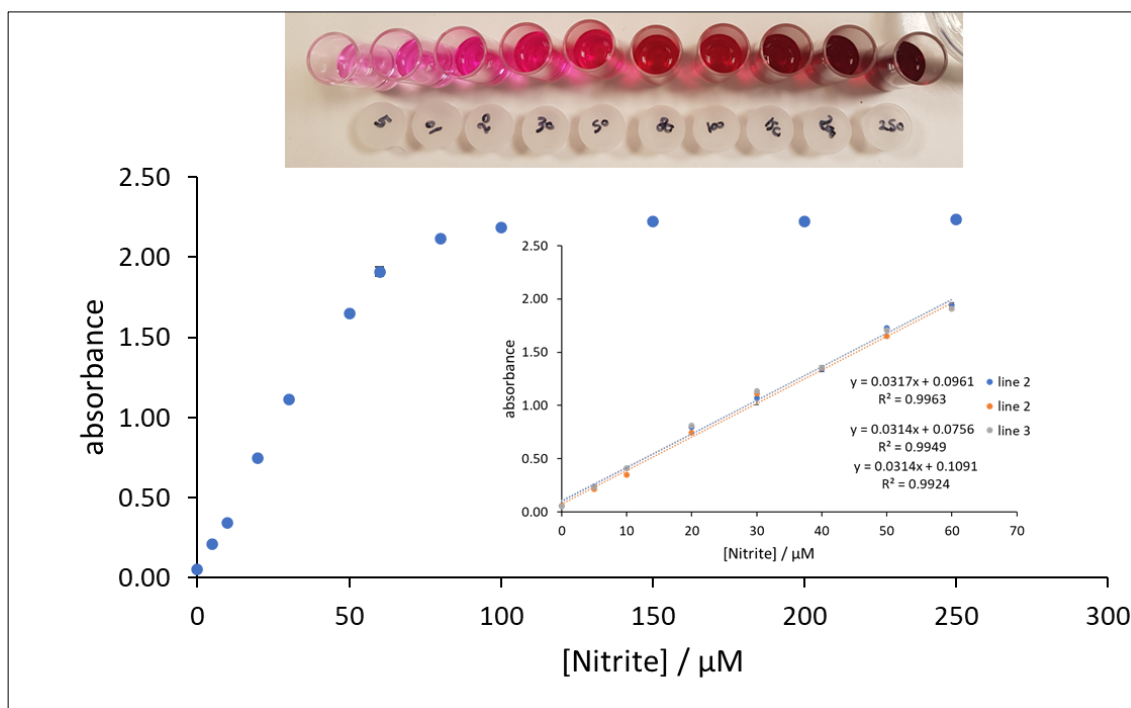
Figure 3.27 Absorbance at 540nm versus concentration (µM). For each standard: 10 mL of it was mixed with 1 mL of Griess reagent. Griess reagent consisted of NED, sulphanilamide and citric acid with concentrations of 6 mM, 50 mM and 330mM.

Table 3.6 limit of detection (LoD) and limit of quantitation (LoQ) for nitrite detected by UV-Vis spectrophotometer. LoD and LoQ were calculated using **Equations 2.5 and 2.6**.

	line1	*line2*	*line 3*	*Average* ± SD
LOD (µM)	*0.050*	*0.054*	0.055	0.053 ± 0.003
LOQ (µM)	*0.174*	*0.180*	0.184	0.179 ± 0.005

3.4.2　Ion Exchange Chromatography (IEC)

3.4.2.1　IEC optimization

Ion exchange chromatography is a well-known method for ion separation and quantification. For ion exchange chromatography there are several factors to optimise the work of the instrument. However, this work focuses on optimisation of the flow rate and the concentration of the eluent. There are several possible eluents which were used for the ion exchange column. The one which was used in this work is potassium hydroxide since it is efficient for anion separation according to some Dionex studies for anion separation [20,112,368].

Flow rate optimization

The flow rate of the eluent was studied since it significantly influences the time of elution and peak separation. The flow rate of the eluent was first optimized using a mixture of 600 μM nitrate and nitrite standards. The soil sample John Innes 1 (prepared as in **section 3.2.10** by mixing 8 g of soil with 100 mL of deionized water in a shaker for 1 h, the extract was then filtered for injection to IEC which was run as in **section 3.2.2**) was also monitored during each optimization to observe the movement of other peaks (other than nitrate and nitrite) in soil to ensure good separation and avoid overlap. Therefore, there were three repeats of the standard and one soil sample run during the optimization as in **Figure** 3.28 which shows the peak height (μS) versus the retention time (min). The chromatogram is for the soil sample (John Innes 1) and a mixture of nitrate/nitrite standard. Nitrite peak eluted with a retention time of 5.6 min and nitrate peak eluted with a retention time of 6.6 min. The soil sample has 4 peaks. Peak 3 of the soil sample corresponded to nitrate when compared to standards. A nitrite peak was not observed in the soil sample. There are other peaks in the soil peaks 1 and 2 which may be chloride, bromide, or fluoride according to literature [20,112,368]. The last peak is peak 4 which may correspond to phosphate or sulfate, based on previous literature [112,368].
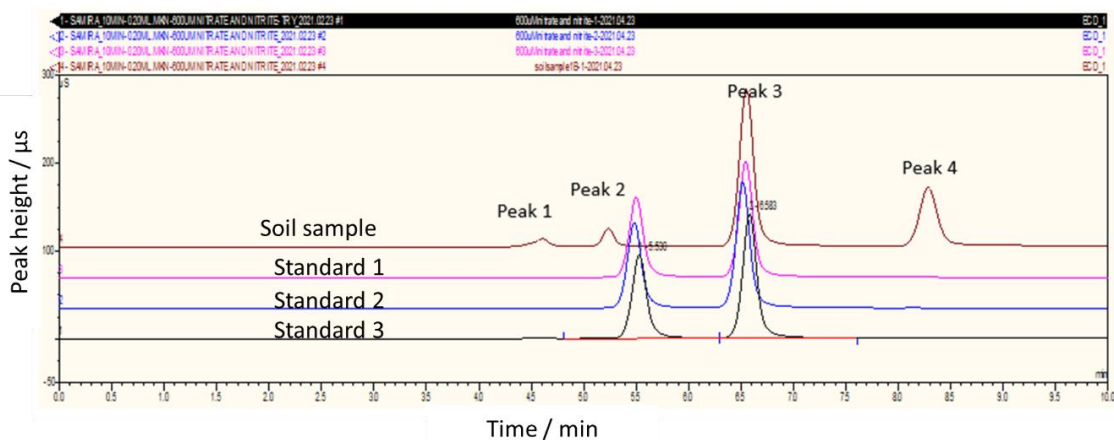
Figure 3.28 Peak height (μS) versus retention time (min). 600 μM nitrate and nitrite standards and soil sample John Innes 1 were used in the analysis. This analysis with 20mM KOH and 0.38 mL min⁻¹ flow rate. IEC was run with conditions as in section 3.2.2.

The flow rate of eluent was varied from 0.25 mL min⁻¹ to 0.60 mL min⁻¹. **Figure** 3.29 shows the retention time versus the flow rate for nitrate and nitrite peaks. As the flow rate increases the nitrate and nitrite peaks eluted earlier. This is because the anions have less time to interact with the column's stationary phase. The lowest flow rate in the optimization was 0.25 mL min⁻¹, any slower than this leads to an increase in the retention time to more than 6 minutes. We need to reduce the time to avoid the long-time work of the instrument as long as good separation was provided for the study purpose. **Figure** 3.30 shows the area of the peak versus the flow rate in

mL min^{-1}, the area increased with the decrease in the flow rate since more time is given for the ion to interact with the stationary phase and hence good separation results and a good quantity of ion is eluted. The highest area was at 0.25 mL min^{-1}. The resolution was calculated (using equation 3.1) as in **Figure** 3.31 which shows the chromatogram when two peaks were separated. Resolution describes the separation of the two peaks. The higher the resolution the better the separation and the less the overlap between peaks. The width of the peaks and retention time were used to calculate the resolution. Resolution at different flow rates were studied as in **Figure** 3.32. There was no clear trend. This means the flow rate does not significantly affect the resolution or separation of peaks. Therefore, based on the results from Figure 3.29 to **Figure** 3.32, 0.30 mL min^{-1} was chosen as the optimum flow rate since it gave a good peak area and good separation in a show elution time, of under 6 minutes.
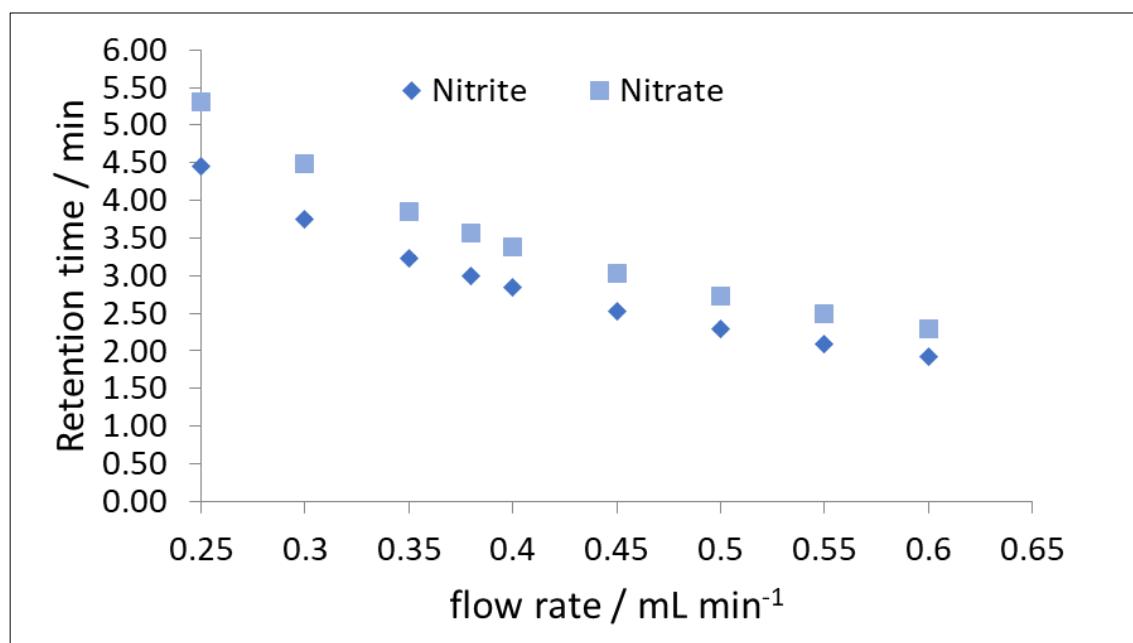
Figure 3.29 Retention time (min) versus the flow rate (mL min^{-1}). 600 µM nitrate and nitrite standards were used in the analysis. This analysis was done with 20mM KOH eluent. IEC was run with conditions as in section 3.2.2, unless it is an optimized parameter.
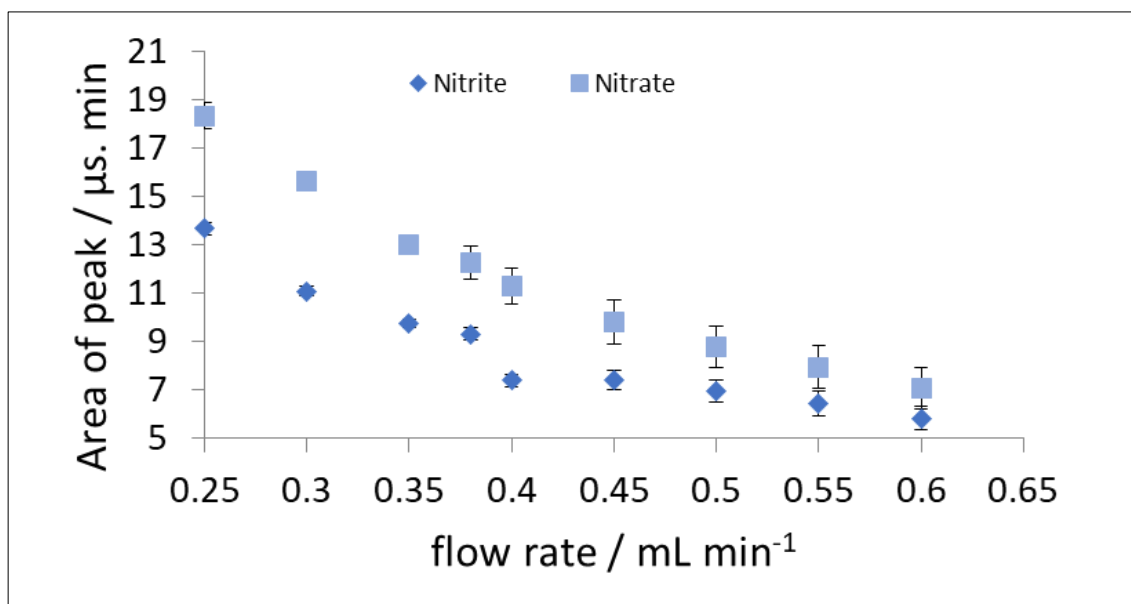
Figure 3.30 Peak area (µS*min) versus flow rate (mL min^{-1}). 600 µM nitrate and nitrite standards were used in the analysis. This analysis was done with 20 mM KOH eluent. IEC was run with conditions as in section 3.2.2, unless it is an optimized parameter.
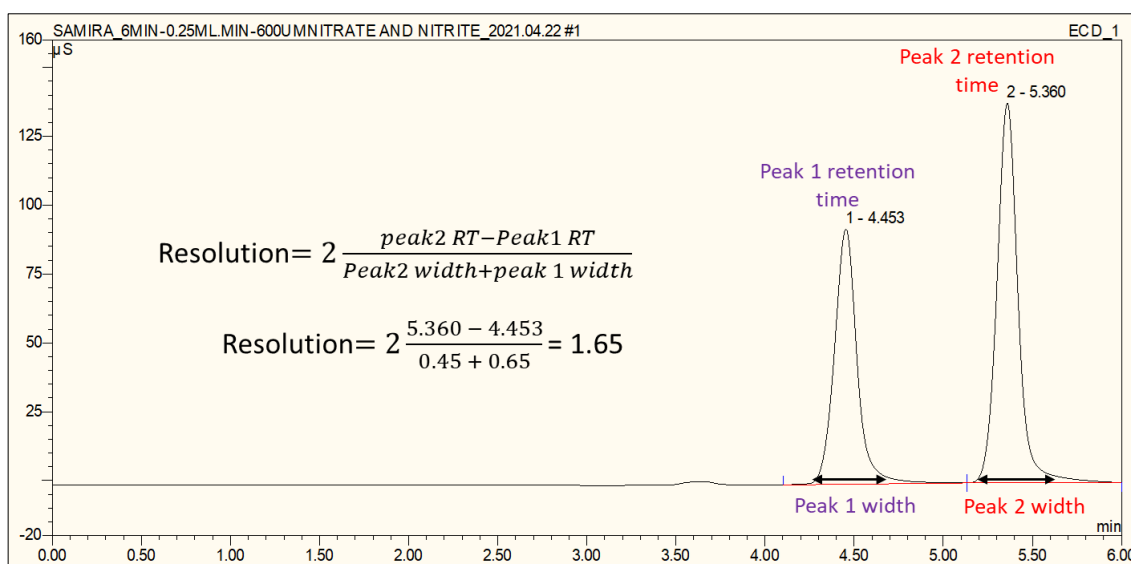
Figure 3.31 Example of resolution calculation for nitrate (RT 5.360) and nitrite (RT 4.453) peaks. 600 µM nitrate and nitrite standards were used in the analysis. This analysis was done with 30 mM KOH eluent and 0.25 mL min^{-1} flow rate. IEC was run with conditions as in section 3.2.2, unless it is an optimized parameter.
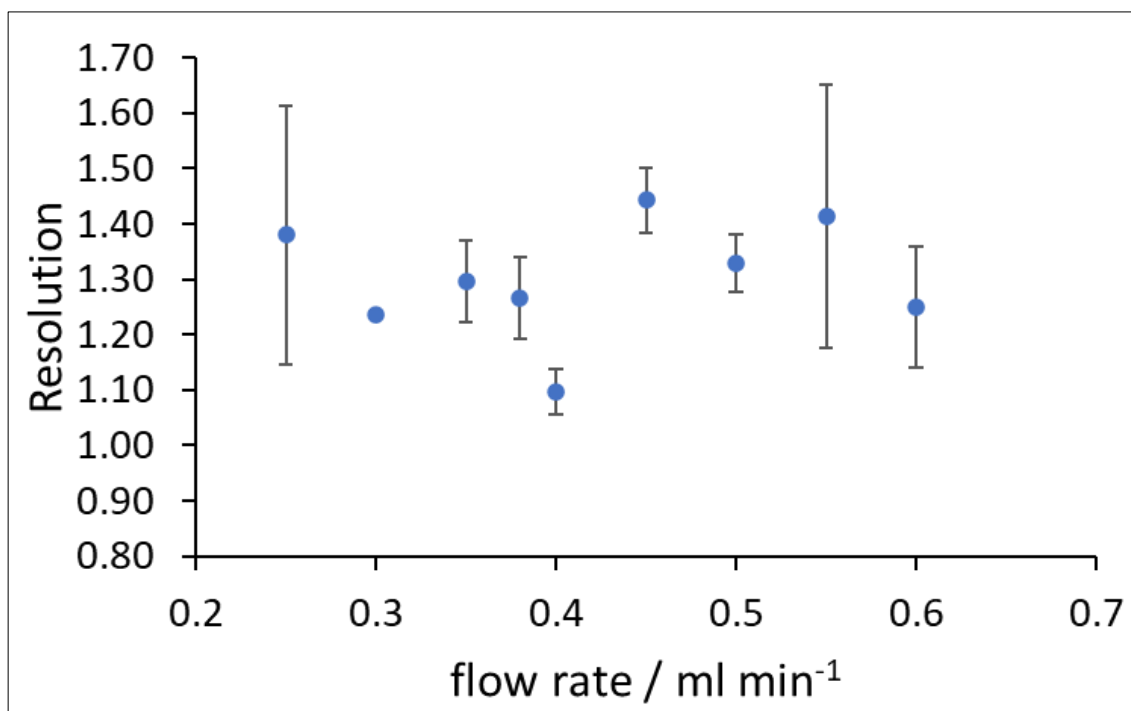
Figure 3.32 Resolution versus the flow rate (mL min⁻¹). 600 µM nitrite and nitrate standards were used in the analysis. This analysis was done with 20mM KOH eluent. IEC was run with conditions as in section 3.2.2, unless it is an optimized parameter.

Eluent concentration optimization

Another factor that affects the ion separation in the column is the concentration of the eluent. The concentration of eluent KOH (ranging from 15 to 45 mM) was optimised using mixture of standards (600 µM nitrate and 600 µM nitrite standard) and a soil sample extract (John Innes 1 extracted as in **section 3.2.10**). **Figure** 3.33 shows the retention time in minutes versus potassium hydroxide concentration (mM). Increasing the concentration of the eluent KOH leads to decreases in the difference between the retention times of nitrate, nitrite and the peaks from the soil extract. At concentrations above 30 mM KOH, individual peaks begin to merge (**Figure** 3.34), particularly the peaks from the soil extract. Separation worked with concentrations as low as 5mM, however, the best separation that satisfied the purpose of the study was reached at 15 mM eluent concentration.

Peak 2 (**Figure** 3.28), in the soil extract, appeared close to the nitrite peak which may cause interference. Therefore, this peak was monitored in the soil extract and the peak was compared to a standard nitrite peak. **Figure** 3.35 shows the retention time for the two peaks versus the concentration of eluent. As the concentration increased the difference in the retention time decreased, therefore, 15 mM is the concentration with the best separation. **Figure** 3.36 shows the area of the peak for nitrate and nitrite versus the concentration of eluent. It was observed that the area remained almost constant with the increase of the concentration of eluent which

means that the quantity eluted remained the same regardless of the eluent concentration. Finally, to ensure that the best separation was at 15 mM the resolution of the peaks was calculated at different eluent concentrations (**Figure** 3.37). The resolution was stable from 15 to 25 mM, then it started to decrease. Therefore, based on Figure 3.33- Figure 3.37, 15 mM was chosen as the optimum eluent concentration.
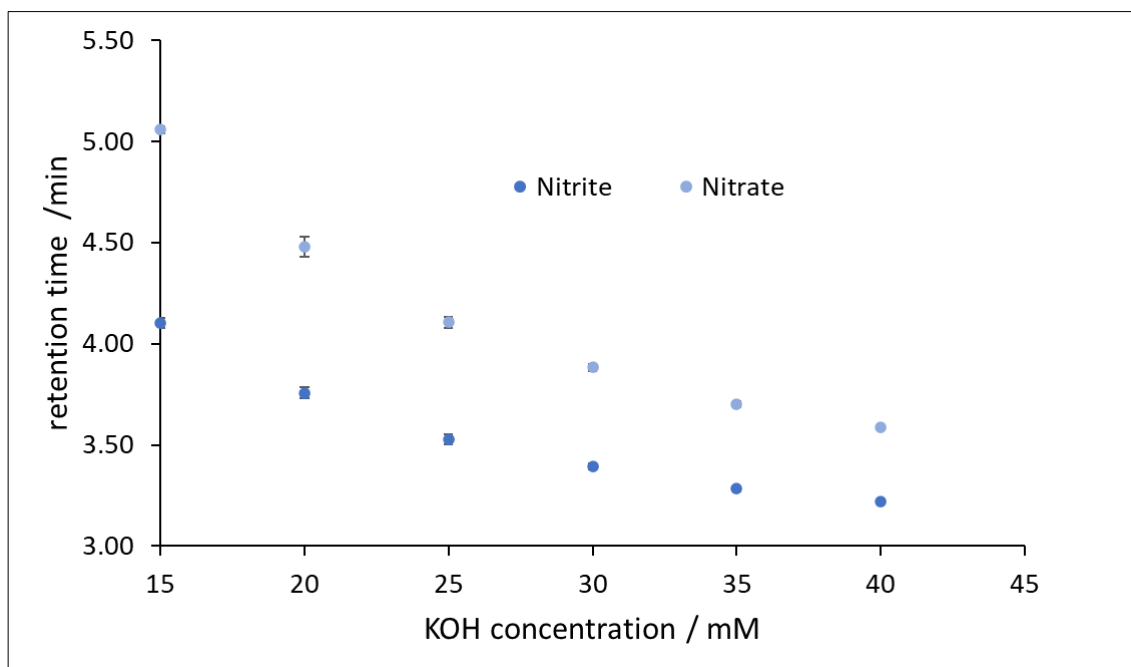
Figure 3.33 Retention time (minutes) versus KOH concentration (mM). 600 µM nitrate and nitrite standards were used in the analysis. This analysis was done with a 0.30 mL min^{-1} flow rate.
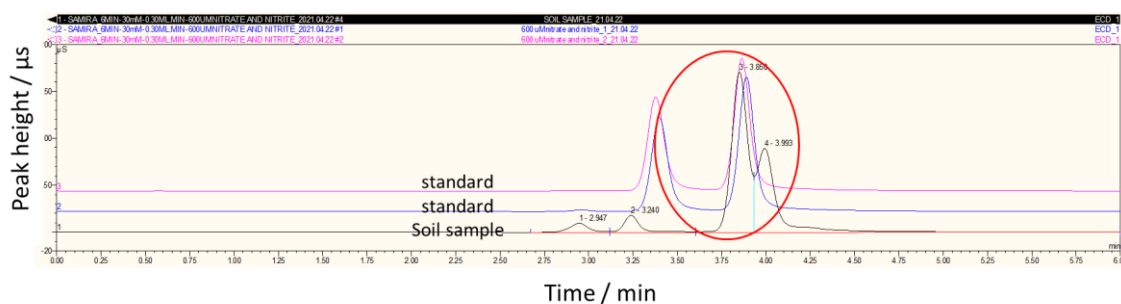
Figure 3.34 Peak height versus retention time(min). A mixture of standard (600 µM nitrate and 600 µM nitrite standard) and a soil sample extract (John Innes 1 extracted as in **section 3.2.10**) were used in the analysis. This analysis was done with 0.30 mL min^{-1} flow rate and 30 mM KOH eluent concentration.
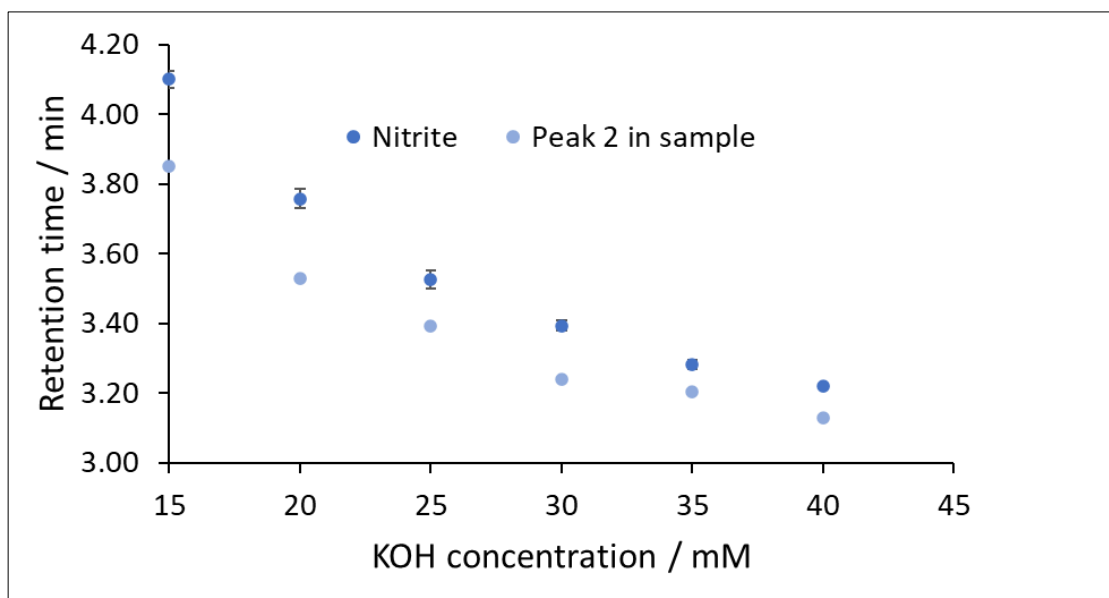
Figure 3.35 Retention time (minutes) versus KOH concentration (mM). 600 µM nitrite standards and a soil sample extract (John Innes 1 extracted as in **section 3.2.10**) were used in the analysis. This analysis was done with a 0.30 mL min⁻¹ flow rate.
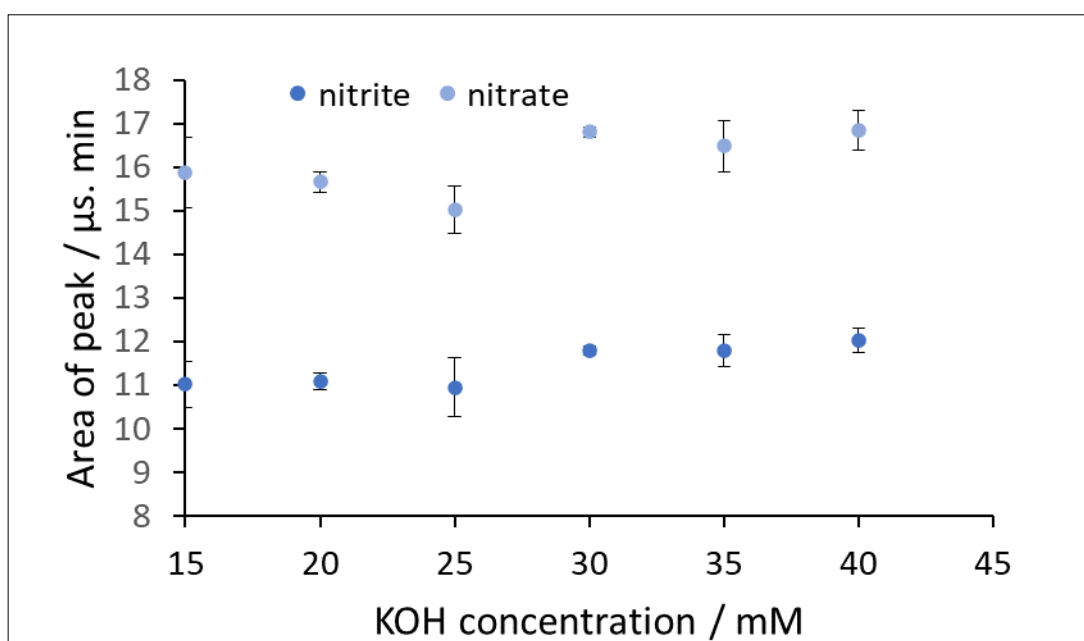
Figure 3.36 Peak area(µS*min) versus KOH concentration (mM). a mixture of standard (600 µM nitrate and 600 µM nitrite standard) were used in the analysis. This analysis was done with a 0.30 mL min⁻¹ flow rate.
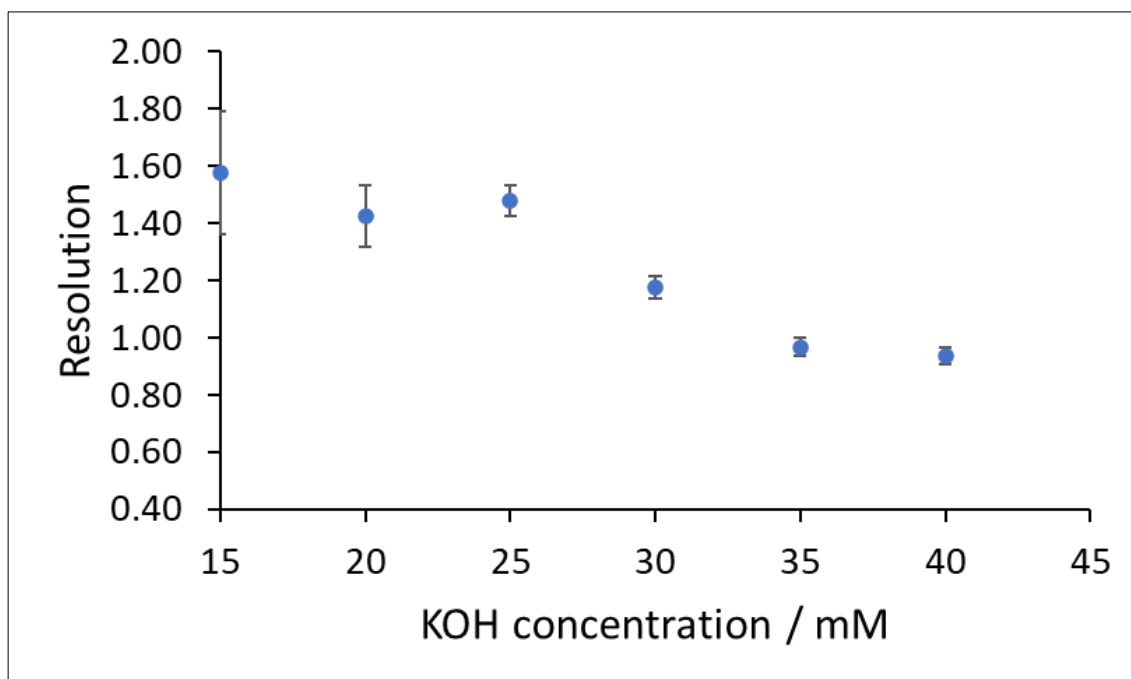
Figure 3.37 Resolution versus KOH (mM). A mixture of standard (600 µM nitrate and 600 µM nitrite standard) were used in the analysis. Resolution of nitrate and nitrite peaks were calculated as in Figure 3.31. This analysis was done with a 0.30 flow rate (mL min^{-1}).

3.4.2.2 Calibration line for IEC method

The optimum conditions (0.30 mL min^{-1} flow rate and 15 mM KOH eluent concentration) were used to create a calibration curve (from 0-10000 µM of nitrate) for nitrite to determine the limit of detection of the method and its reproducibility. The R^2 is 0.99 which indicates a good fit of the data to a straight line. The reproducibility was determined by running the calibration curve three times on three different days. The resulting calibration curve is shown in **Figure** 3.38. The LoD is 5.17±0.47 µM (around 2.97 mg kg^{-1} if 8 grams of soil and 100 mL of solvent are used) and the LoQ is 17.45±1.55 µM as summarized in **Table** 3.7. LoD and LoQ were calculated as methods in **Equation 2.5 and 2.6** in the experimental section. This limit is higher than some of the results reported in literature [113,114,369-372]. This may be due to the old column in the instrument. Nevertheless, the limit of detection and quantitation is lower than the maximum toxic level of nitrite in water (21.7 µM /1mg L^{-1}) according to US Environmental Protection Agency [365]. LoD and LoQ were also compared to the level of nitrite in soil. The level of nitrite in soil rarely exceeds 164 mg kg^{-1} and most of the time nitrite level is lower than 0.3 mg Kg^{-1} [366,367]. The LoD and LoQ from IEC are higher than the lower level of nitrite in soil. However, they are still lower than the highest possible limit of nitrite in soil. In the future, the soil that has low nitrite levels can be treated by the UV-Vis since it can deal with low-range nitrite concentrations as mentioned in the previous **section 3.4.1**. IEC will be used for soil with high nitrite levels and to determine the existence of any possible interference in the sample which are not visible by UV-Vis. In addition, the IEC method is also needed in chapter 4 for nitrate analysis.
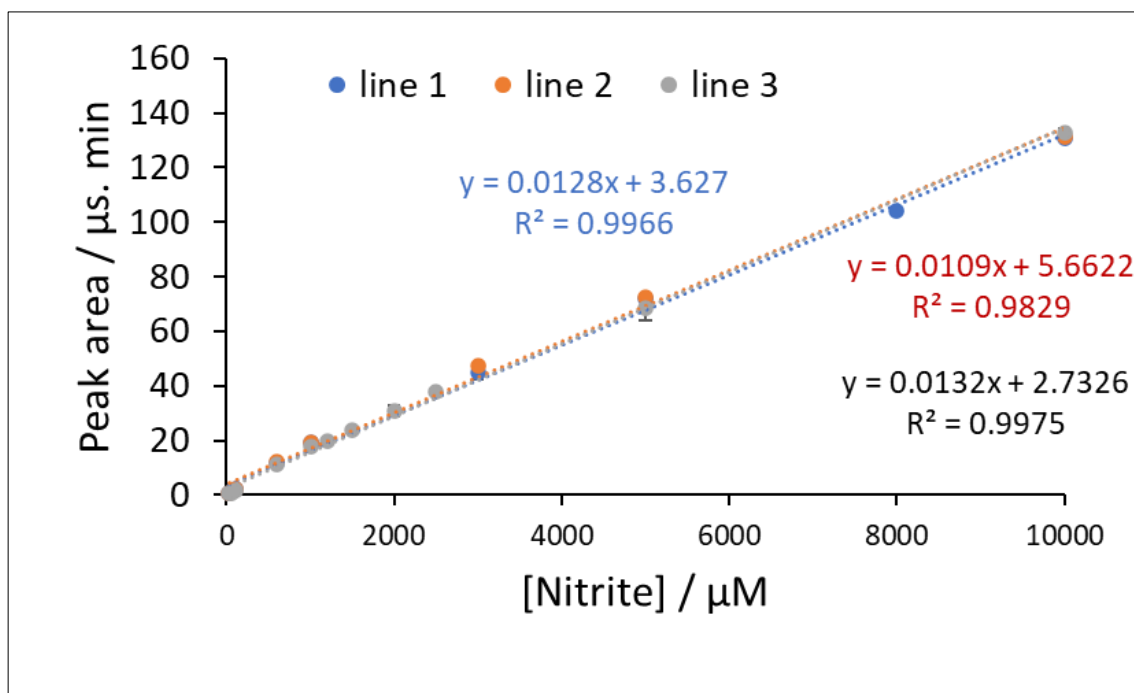
Figure 3.38 The peak area(µS*min) versus the concentration of nitrite(µM).15 to 1000 µM of nitrite were used.

Table 3.7 LOD and LOQ For three nitrite calibration lines in Figure 3.38. LoD and LoQ were calculated as in **Equation 2.5 and 2.6** in the experimental.

	line 1	line2	Line 3	average
LOD(µM)	4.68	5.22	5.61	5.17±0.47
LOQ(µM)	15.62	17.41	18.71	17.25±1.55

3.5   Paper microfluidic device for nitrite determination

3.5.1   Image-J software

There were two areas in the PADs the hydrophobic and hydrophilic area. Hydrophilic area allowed the aqueous solution to pass through. The hydrophobic area did not allow the absorbance of aqueous solution. This characteristic of the paper helped to restrict the movement of the reagents and to control the reaction and detection. Green wax was used as a hydrophobic area in this device. Green was chosen because it is the complementary colour to the pink-red colour in the colour wheel [373]. The developed colour for nitrite determination was observed and detected by taking photos which were then analysed by Image-J software (**Section 2.5**). The more intense the colour the more the nitrite.

Choice of channel in image-J

Cameras on smartphones and scanners were used as devices to record the colours of the PADs. Photographs were analysed using Image-J software. Image-J software helps to convert the qualitative data (intensity of colour developed from the reaction) into quantitative data (numbers) as in **Figure** 2.4. Stack RGB image type was chosen during the analysis. This image type consisted of three channels, green, red and blue. The intensity of the colour was determined using the three channels as in **Figure** 3.39 which shows the average pixel intensity from the detection zone in the PAD from analysis of 0, 90, 120 and 150 µM of nitrite solutions in the three channels of Image-J. The intensity of the red channel is low, and the values produced from different concentrations are not appreciably different. The green channel, however, showed higher intensity. When compared to red and blue channels the green channel gave the highest average pixel intensity with more uniform colour intensity. The intensities increase with increasing concentration. **Figure** 3.40 shows clearly how the colour from the green channel is more uniform and clearer compared to the blue and red channels. Therefore, the green channel was chosen as the optimum channel for this study. Device 10 was used for this study as an example of intensity determination, for the rest of the devices studied in the coming sections the intensity was always taken from the colour developed in the detection zone.
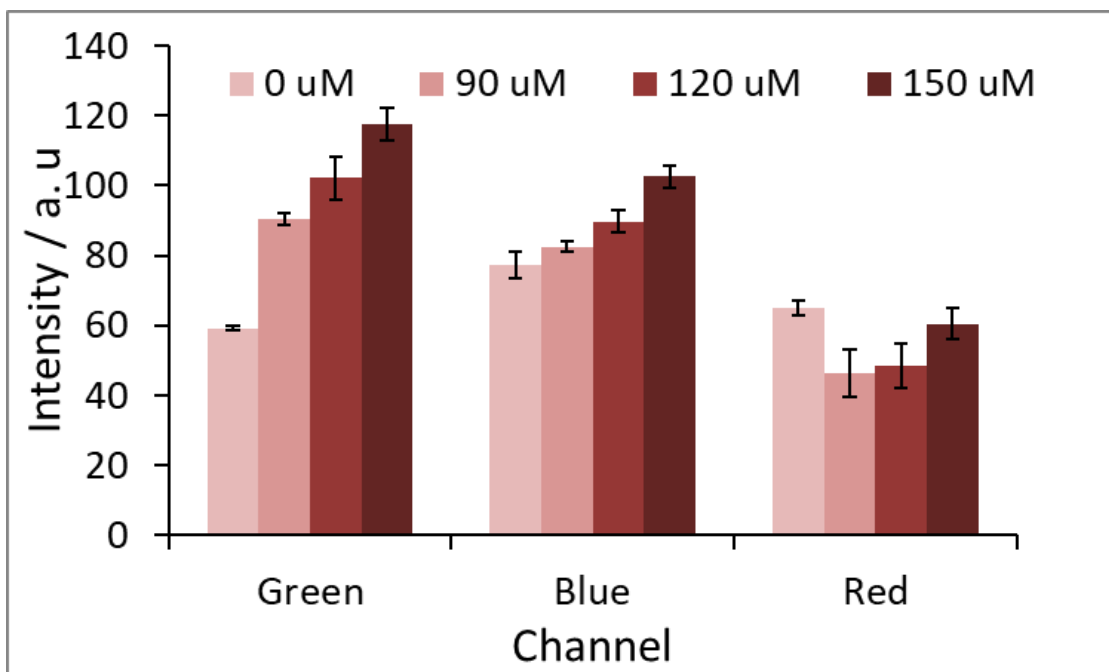
Figure 3.39 Average pixel intensity for PAD analysis of nitrite solution (0, 90, 120 and 150 µM) versus the colour of the channel (Green, blue and Red), n = 6.
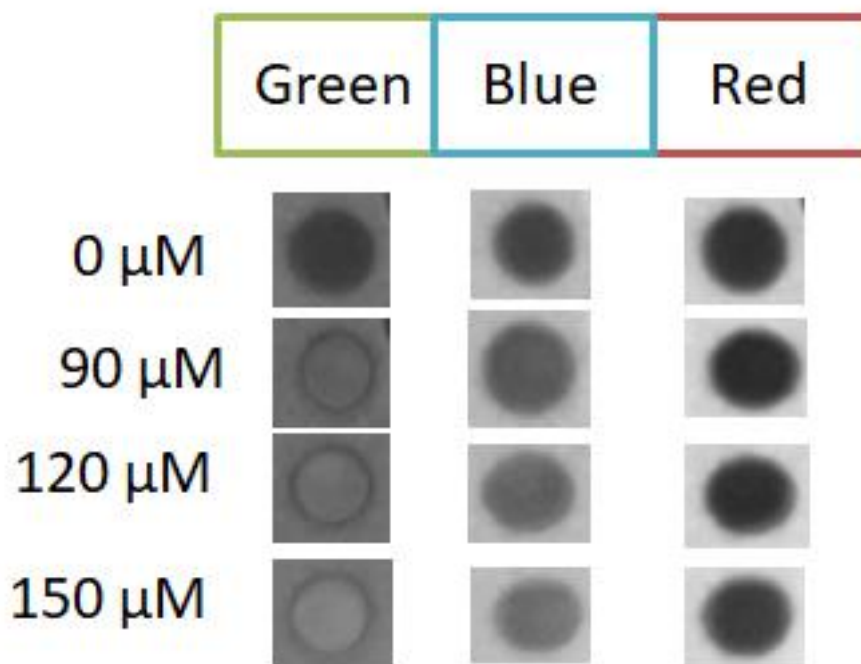
Figure 3.40 Result from image-J software when green, red and blue channels were used. The result from PAD analysis of 0, 90, 120 and 150 µM nitrite standards.

Calculation

The intensity of the detected colour was determined using two methods and the best method was chosen. The pixel intensity was taken immediately from the software in method 1 (**Equation 2.7**) and the average of all points was finally determined for each standard or sample. This method is still affected by errors due to the lighting variation of the surrounding environment. Method 2 (**Equation 2.8**) was more efficient than method 1 because this kind of error was considered. Consequently, method 2 was adopted in this work. The calculation of the intensities using the two methods is shown below. This calculation is for one point in the device. The average of all points in the device was then determined.

Example of calculation

Pixel intensity for 90 µM nitrite standard: 92, 92, 87, 91, 91, 90

Negative control pixel intensity: 52

Internal standard pixel intensity: 148
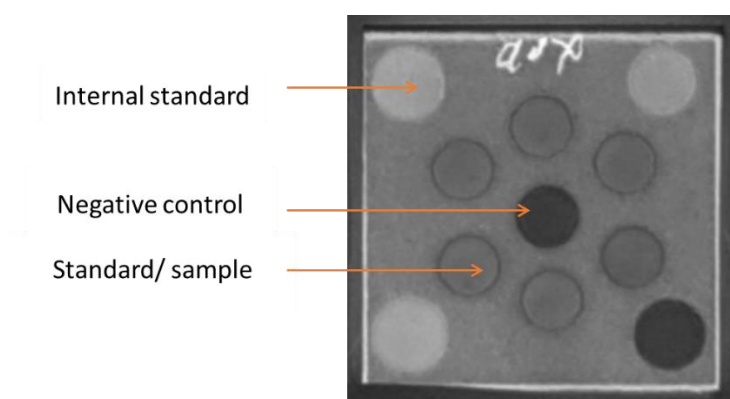
Figure 3.41 Photo analysed by Image-J software. It illustrates the position of internal standard, negative control and standard/ sample which were used as intensities for calculation in methods 1 and 2. This photo was taken from the analysis of 90 µM of nitrite.

Method 1

$$Pixel\ intensity = intensity\ from\ standard\ or\ sample\ \ eq.\ 2.7$$

$$Pixel\ intensity = 92$$

Method 2

$$Relative\ intensity\ 2 = \frac{pixel\ intensity\ from\ standard\ or\ sample}{pixel\ intensity\ from\ internal\ standard}\ \ eq.\ 2.8$$

$$Relative\ intensity\ 2 = \frac{92}{148} = 0.622$$

3.5.2 The choice of the paper device

The shape of devices and how easy they are to use are very important points to consider since the target users will be lay people, such as citizen scientists or farmers. Several designs for devices were tested. PADs with detection and reduction zones were developed in this chapter. The device which will be chosen finally will be used with both reduction and detection zones for nitrate detection in Chapter 4.

3D device designs were tested (see **Figure** 3.1 and **Figure** 3.2). These devices consisted of two layers, one for the detection and the second for reduction. Device 1 (**Figure** 3.1) consisted of two zones in two different layers, the detection (4×13mm) and reduction (5mm diameter) zones. Also, it consisted of a transfer channel (2×2.7 mm) which was necessary to transfer the solution from the reduction zone to the detection zone. Device 1 required the analyte to first be reduced in the reduction zone for a specific time and then transferred by a special channel into the detection zone as in **Figure** 3.42 A. However, this design was not easy to use since it required several steps which may be too complicated for a non-expert. In addition, the device showed poor reproducibility as in **Figure** 3.43 due to poor transfer of the solution from the reduction zone to the detection zone; some of the solution was lost during the folding of the device and the absorption of the solution by the paper differed from one device to the next. **Figure** 3.43 shows the reproducibility of device 1 tested with a nitrite standard. Data shown in the red bars result from the standard being pipetted directly into the reduction zone and then transferred to the detection zone by folding the device, as shown in **Figure** 3.42 **A**. The blue bars resulted from the standard being pipetted into the detection zone as in **Figure** 3.42 **B**. It was clear that avoiding the two layers resulted in a more reproducible result. Device 2 (**Figure** 3.2) was an improved form from design 1 to improve the reproducibility. Device 2 is the same as device 1 but with four reaction zones within a single device. However, it was observed that preparing the device was difficult the solutions frequently slipped between the paper when the PAD was folded.
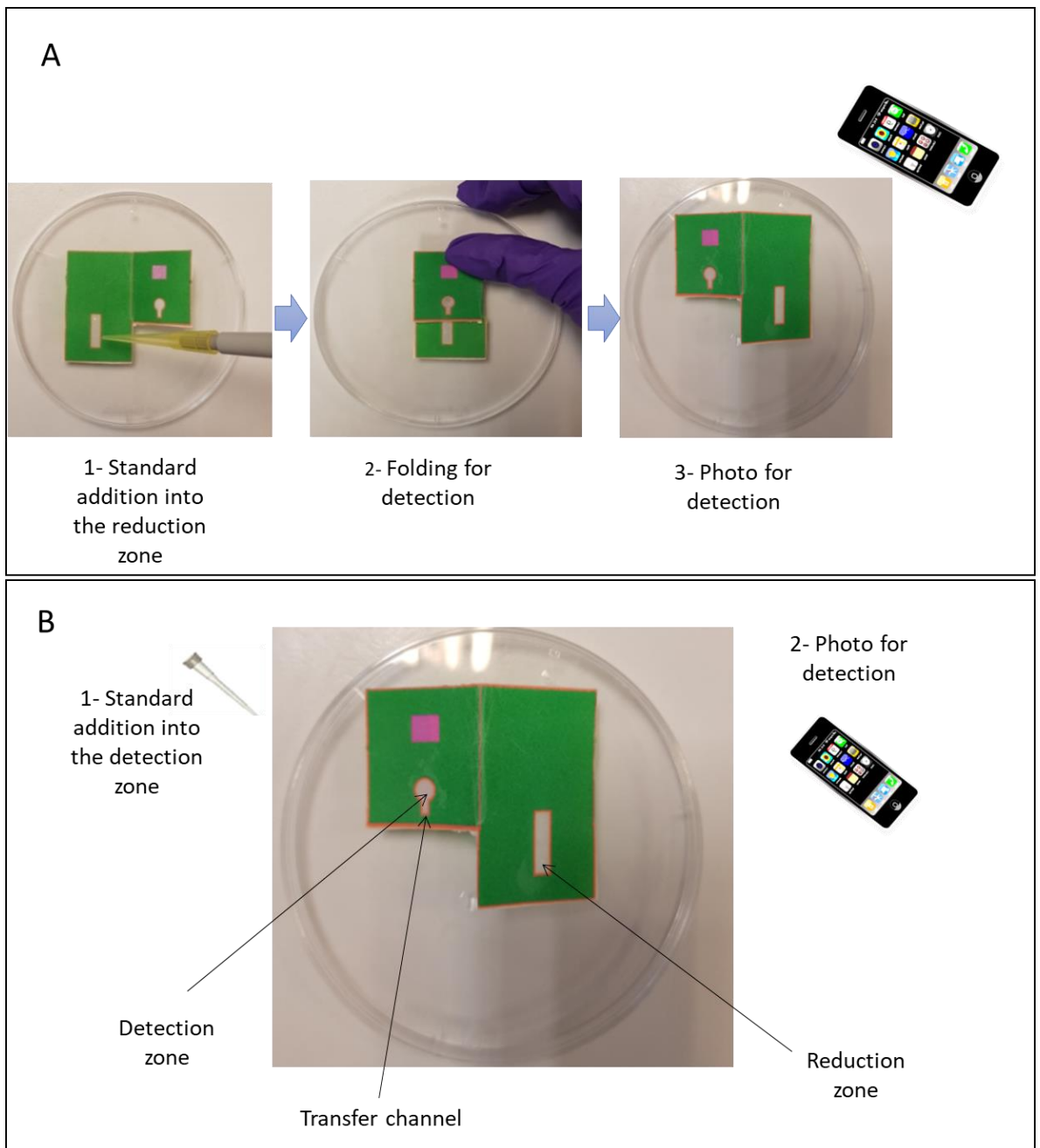
Figure 3.42 (A) Standard was pipetted into the reduction zone and then transferred to the detection zone by folding. 0, 50 and 90 µM of nitrite were detected by Griess assay. 1 µM of Griess was used in the detection zone and 20 µL of nitrite was added to the reduction zone and allowed to stand for around 1 minute. The device was folded then for detection. (B) Standard was pipetted immediately into the detection zone. Figure 3.1 shows details about the device.
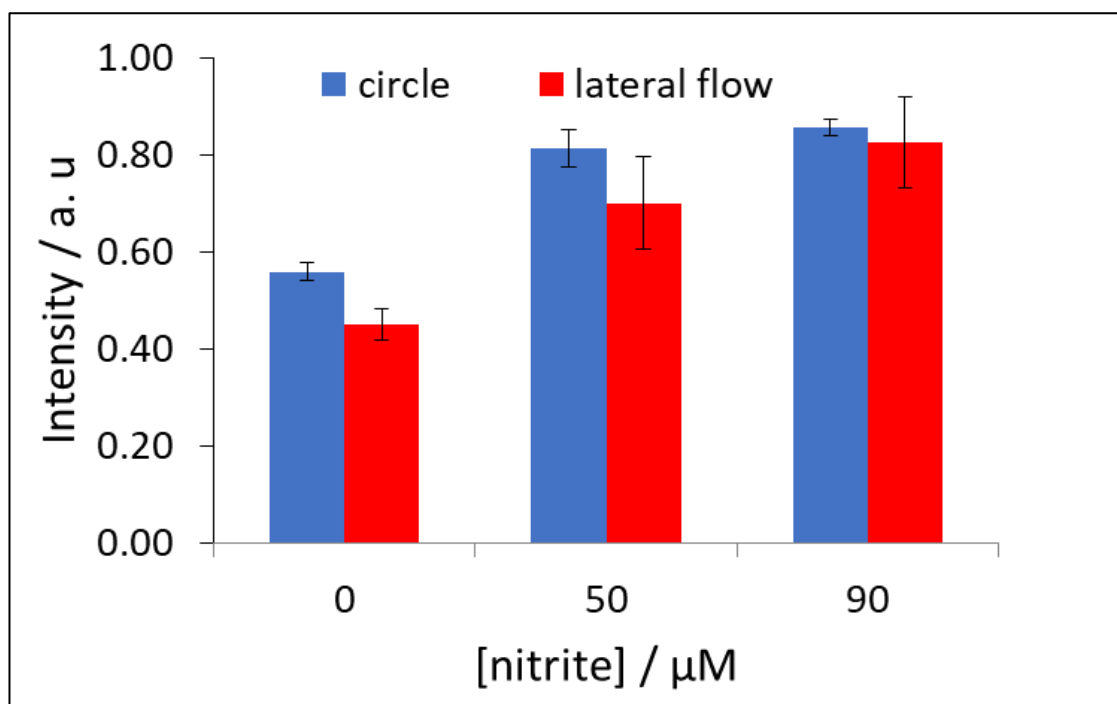
Figure 3.43 Intensity versus concentration of nitrite (μM). The result from device 1. The red bars resulted when the sample was pipetted into the reduction zone and then transferred to the detection zone by folding. The blue bars resulted when the standard was pipetted immediately into the detection zone. The relative standard deviation for the blue bars is ⩽ 5%. The relative standard deviation for red bars is⩾ 10%, n = 3. The intensity was measured by method 2 in **Section 2.5**.

To reduce the complexity of the devices 2D devices were tested. Device 3 (**Figure** 3.3) consisted of one sample introduction zone, 8 detection zones and 8 reduction zones. All circles were 8 mm in diameter. The sample zone, reduction zones and detection zones were connected by channels (3×4.9 mm). It was first necessary to make sure that the flow of the solution from the sample introduction zone to the detection zones was uniform and equal in all channels. The design was tested with a food dye. The dye was introduced to the sample introduction zone and was allowed to flow within the device. **Figure** 3.44 shows the flow of the dye starting from the solution introduction. It was clear that the flow was not uniform, and the dye reached the detection zone of some channels quicker than others. For these reasons, the design was adjusted to reduce the number of detection zones and replications of the reduction zones similar to the Teppo et al. design, as in **Figure** 3.4 (device 4). The size of the sample introduction zone was increased compared to the size of the detection and reduction zones to avoid the accumulation of samples in the introduction zone. This design had three channels, without reduction zones, for nitrite detection. And three channels with reduction zones for the detection of nitrate. The flow of the solution in the device was tested again using the food dye (**Figure** 3.45). The flow within this design was much more uniform, the dye reached completely all the detection zones in 1 min after the addition of 100 μL of dye.
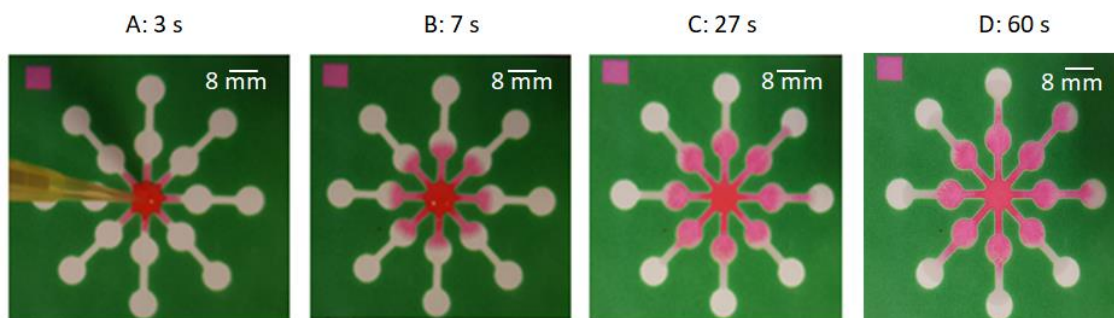
Figure 3.44 Device 3 when 100 µL red food dye was pipetted into the sample introduction zone (A). A photo was taken for 60 seconds. These are 4 of the photos taken from left to right (A, B, C and D) at different times within the 60 seconds.
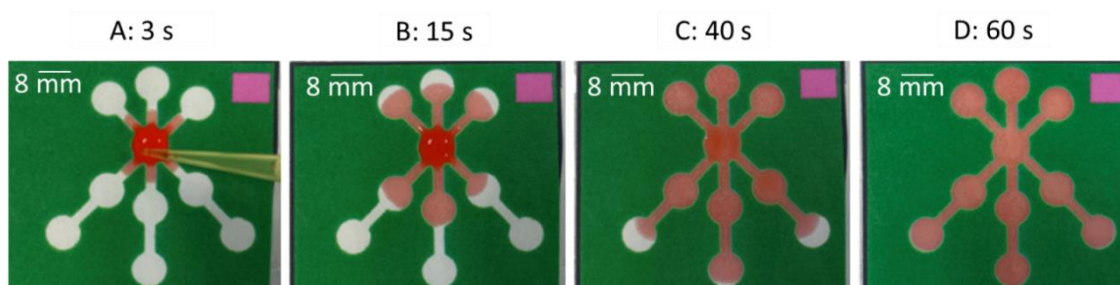
Figure 3.45 Device 4 when 100 µL red food dye was pipetted into the sample introduction zone (A). A photo was taken for 60 seconds. These are 4 of the photos taken from left to right (A, B, C and D) at different times within the 60 seconds.

Device 4 was used for nitrite detection (as in **Figure** 3.14). The detection solution (Griess reagent) was added into the detection zone and allowed to dry for 10 minutes. The analyte (nitrite ion) was then added into the sample introduction zone and allowed to flow and react for 14 minutes. Several concentrations of nitrite were tested. **Figure** 3.46 shows the colour intensity increasing with nitrite concentration. The variation in intensity and the standard deviation indicated the devices suffer from a lack of reproducibility.
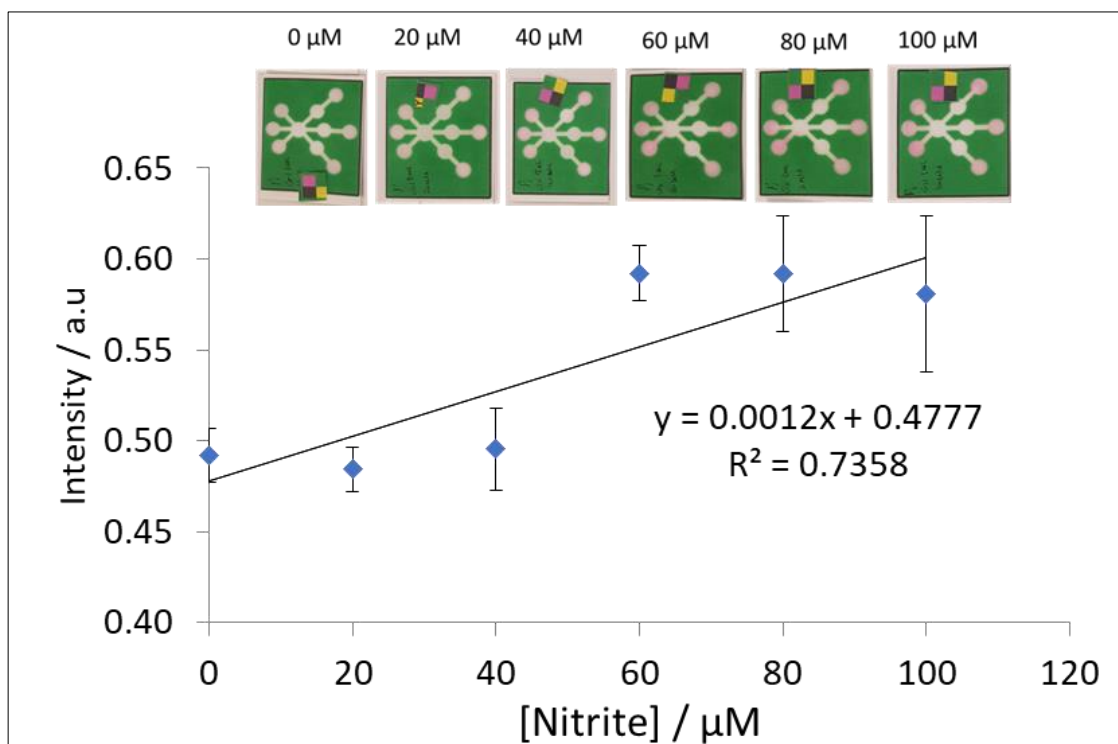
Figure 3.46 Intensity versus nitrite concentration (µM). Device 4 was used, and the device was modified (Figure 3.14). N=6.

Device 4 was re-designed to reduce the complexity of the system and increase its reproducibility. Design 5 (**Figure** 3.5) consisted of one channel, one sample introduction zone (8 mm diameter), one reduction zone (8 mm diameter) and one detection zone (8 mm diameter). The device was modified (**Figure** 3.15) by adding the detection solution (Griess reagent) into the detection zone and allowing it to dry for 10 minutes. The analyte, nitrite solution was then added to the sample introduction zone and allowed to flow and develop colour for 14 minutes. The device was run three times for each concentration. **Figure** 3.47 shows the intensity of the developed colour versus the concentration of nitrite. Device 5 controlled the flow of the solution much better than Device 4 since the flow of the introduced solution was in one direction. And consequently, it produced a better calibration curve. Device 4 and device 5 have R^2s of 0.7358 and 0.9013 respectively.
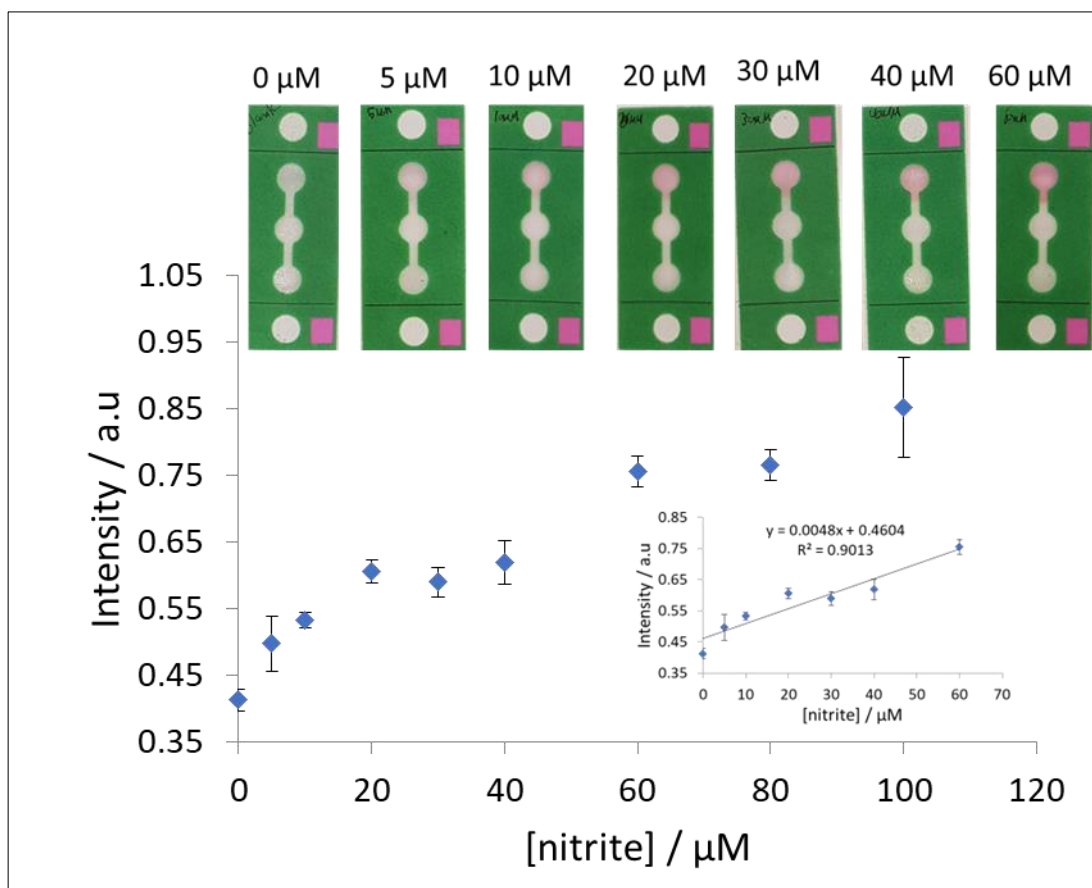
Figure 3.47 Intensity versus nitrite concentration (μM). Device 5 was used, and the device was modified (Figure 3.15. N=3.

Device 4 requires practice to be able to handle, device 5 is much easier to work with since it has only one detection zone and one direction for the flow of the solution, unlike device 4. The problem now with device 5 is that has just one reaction zone. Therefore, one channel device with several reaction zones, allowing for reproduced measurements within one device was needed. To enable this a valve was introduced to the device instead of the central circle in device 5 and hence the valve allowed the flow in one direction. Device 6 (**Figure** 3.6) includes a valve, 4 sample introduction zones and 4 detection zones. Sample introduction zones and detection zones are both 10 mm in diameter. **Figure** 3.48 shows the intensity from device 6 versus the concentration of nitrite after treatment of the PAD as in **Figure** 3.16. The relative standard deviation is still higher than 5% and the linearity is not perfect; R^2 =0.944. This is maybe due to the equal size of the detection and sample introduction zone because not enough analyte moved from the sample introduction zone to the detection zone to fill the detection zone with analyte within the 14 minutes and some of it was lost due to evaporation or within the valve movement. Therefore, the detection zone diameter was reduced to 6mm as in **Figure** 3.7, device 7 allowed the solution to move to a smaller area and hence enough solution was transferred. The same experiment that was applied in design 6 was applied also in device 7 (**Figure** 3.17) and the results are in **Figure** 3.49. The variation was still similar and hence the problem was not with

the size of the detection zone. The use of valves based on researcher observations requires more practice to get a reproducible result. The last option which is the easiest is the use of circles only with no channels as in device 8 (**Figure** 3.8**)**. The PAD was modified for nitrite detection **(Figure 3.18)** in a similar way by adding the detection reagent into the circle and allowing it to dry. This time the analyte was added directly to the detection zone circle. **Figure** 3.50 shows the calibration line with much better linearity (R^2 0.964) and less standard deviation from the first run because the problem of flow control was avoided. In addition, dealing with device 8 will be much easier for non-experts compared to any other complicated device.

Complicated designs are common in the literature, and in the lab and after of few practices, it is easy for a researcher to use any of these designs or those described here. However, this work aims to design a device that can be used with little or no practice by a citizen scientist or other interested lay person. Consequently, Design 8 with circular zones will be further studied and discussed in the following sections. **Table** 3.8 summarizes the comparison between the device 1, 4, 5, 6, 7 and 8. It compares devices in terms of the simplicity of to handle, the way the sample was introduced to the PAD and data on the calibration curve. The collected data shows that device 8 was the easiest to use. In addition, the sample introduction was simple, as the whole device could be dipped into a test solution. Also, device 8 produced a high-quality calibration range and good R^2.
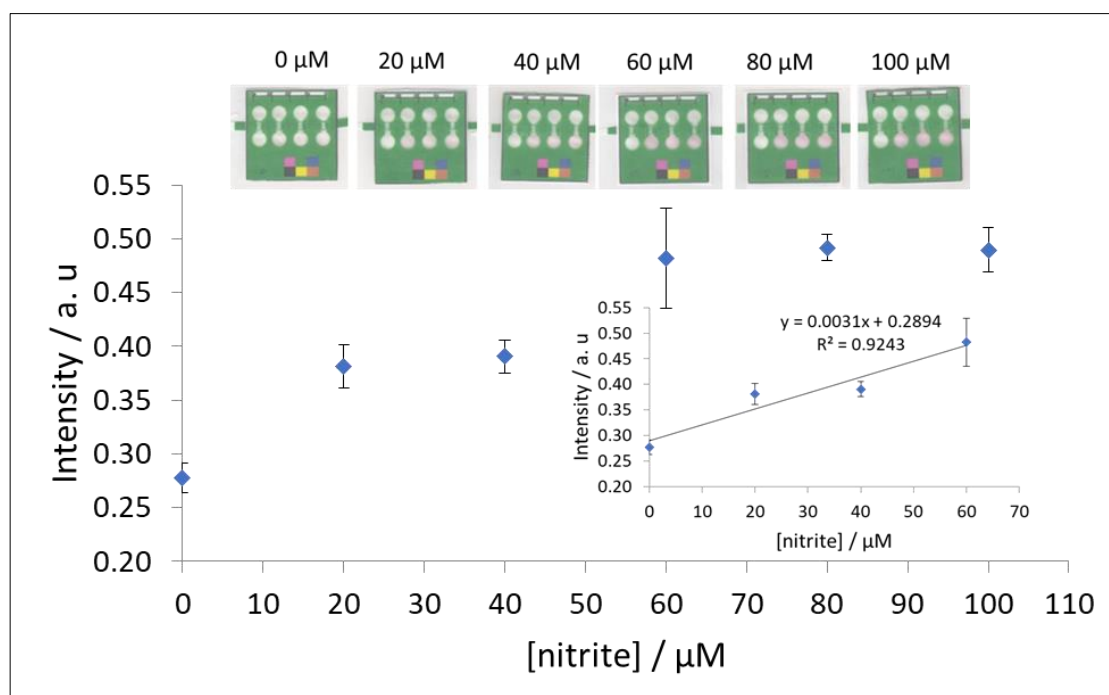
Figure 3.48 Intensity versus nitrite concentration (µM). Device 6 was used, and the device was modified (Figure 3.16. N=3.
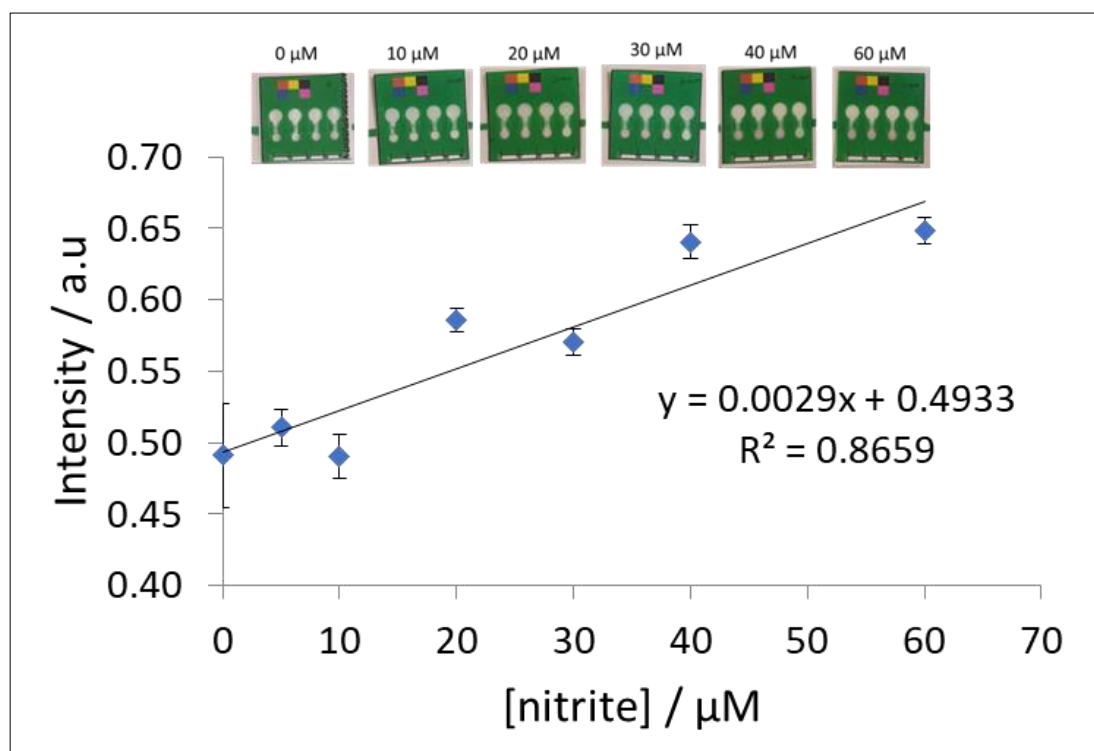
Figure 3.49 Intensity versus nitrite concentration (µM). Design 7 was used, and the device was modified (Figure 3.17). N=3.
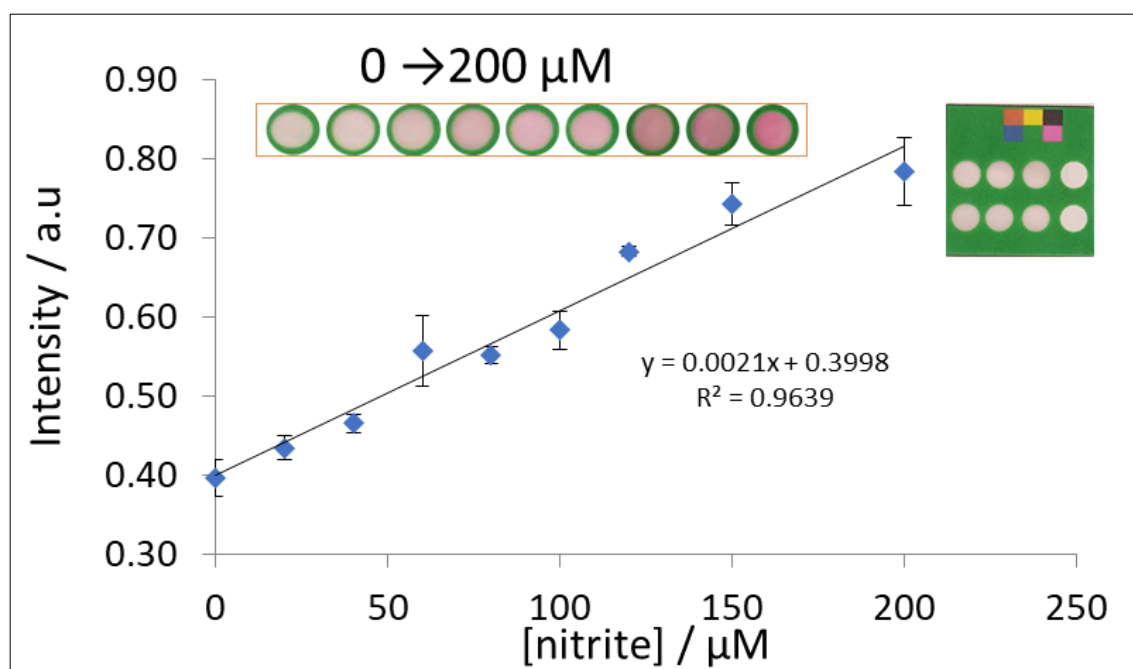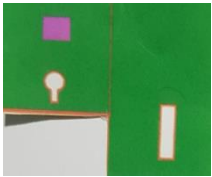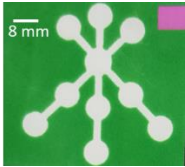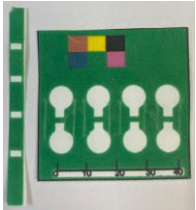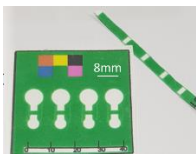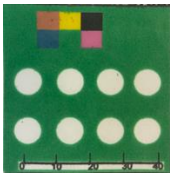
Figure 3.50 Intensity versus nitrite concentration. Design 8 was used, and the device was modified (Figure 3.18). N=6.

Table 3.8 Comparison between devices 1, 4, 5, 6, 7 and 8 in terms of the simplicity to handle, way of sample introduction and calibration line from one time run.

Device	How easy to use the PAD (based on observation)	Possible Sample introduction	Calibration range (µM)	Slope of calibration(µM^{-1})	R^2 of calibration
Device 1	Needs training, folding of layers is required	Pipetting,	-	-	-
Device 4	Complicated, and needs training, if the solution is not pipetted exactly in the centre, it may not reach all detection zones	Pipetting, can be dipped but after lamination solution does not move smoothly within the channel	0-100	0.0012	0.7358

Device	How easy to use the PAD (based on observation)	Possible Sample introduction	Calibration range (µM)	Slope of calibration($µM^{-1}$)	R^2 of calibration
Device 5	Easy, but with only one repeat	pipetting, can be dipped but after lamination solution does not move smoothly within the channel	0-60	0.0048	0.9013
Device 6	Needs training, valve needs to be handled carefully to avoid solution loss	Pipetting only	0-60	0.0031	0.9243
Device 7	Needs training, valve needs to be handled carefully to avoid solution loss	Pipetting only	0-60	0.0029	0.8659

Device	How easy to use the PAD (based on observation)	Possible Sample introduction	Calibration range (µM)	Slope of calibration(µM⁻¹)	R² of calibration
Device 8	Easy to use and handle from first use	Pipetting and dipping after lamination, liquid goes directly to the zone	0-200	0.0021	0.9639

3.5.3 Lightening and internal standard effect

The designed paper microfluidic device 9 (**Figure** 3.9) consisted of circles with 6 mm diameter and hence very small amount of reagent was required compared to a reaction in a test tube. Device 9 was modified as in **Figure** 3.19. After the reaction between the standard and Griess reagent, a photo was taken for the device to determine the colour intensity or the signal. This photo was then analysed by Image-J software which produces the intensity of light as a quantitative number as mentioned in the previous section. The photo was taken by a scanner or phone. When the phone is used the surrounding light and the way the photo was taken may have a significant effect on the intensity from time to time or from day to day. In addition, the intensity of light within the same photo may have an effect too. For example, a good-quality photograph can be seen in **Figure** 3.51 the intensity of light across the device is constant. Therefore, the intensity measurement taken from each circle on the device can be trusted since it was not affected by variations in lighting. **Figure** 3.52 shows a poor-quality photograph, the signal across the device varies dramatically. This means the measurement from that photograph cannot be used.
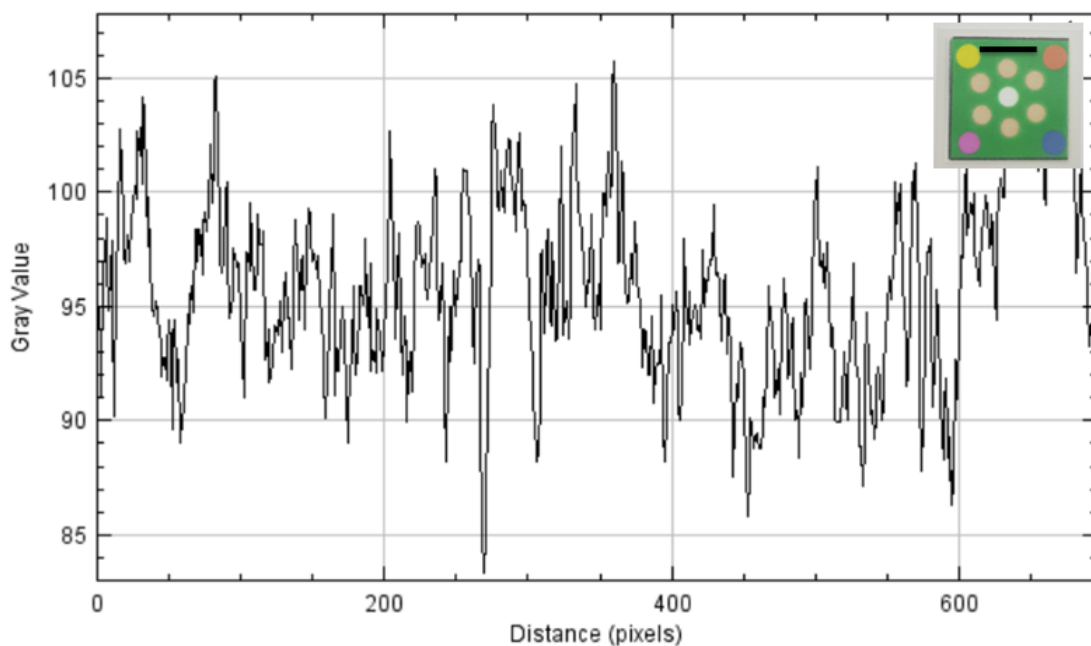
Figure 3.51 Gray value (intensity) versus distance (pixels) along the device photo which was taken by Samsung phone in laboratory lightening. This intensity graph resulted from the distance along the black line. The signal or the intensity of light was the same all over the device.
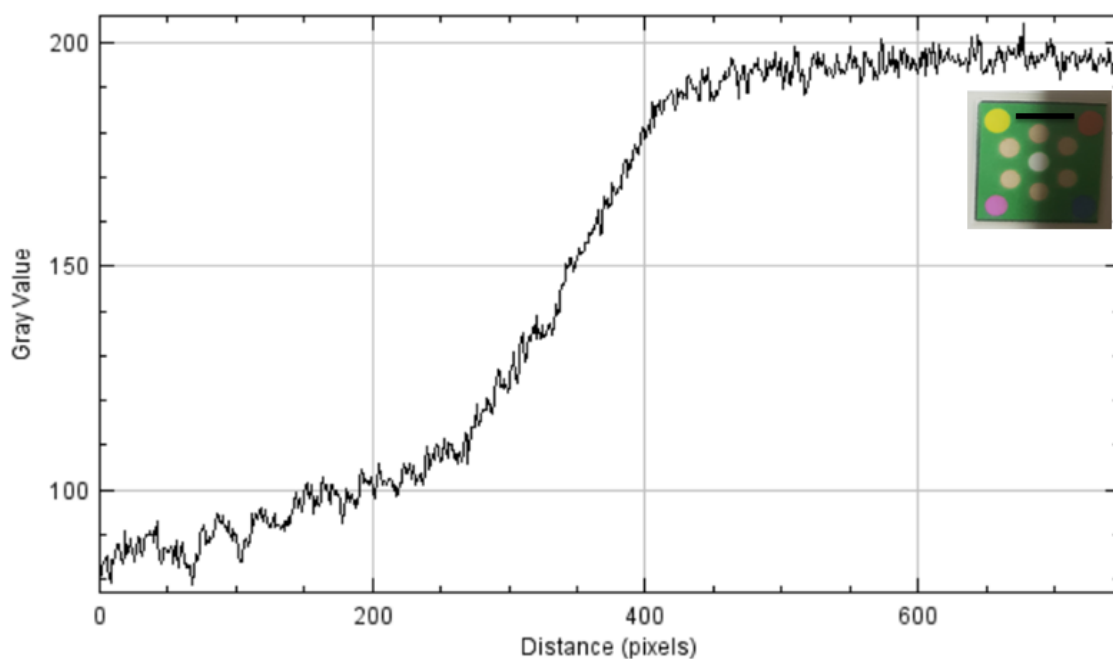
Figure 3.52 Gray value (intensity) versus distance (pixels) along the device photo which was taken by Samsung phone in laboratory lightening. This intensity graph resulted from the distance along the black line. The signal or the intensity of light was different from left to right of the device.

An internal standard was also used to compensate for the lighting variation effect. In normal analytical analysis which was performed in bulk aqueous solutions an internal standard is usually used. The internal standard is a substance which has similar properties as the analyte, and it should not interfere with the analyte detection. In this experiment, colour was used as an

internal standard to account for the variation of lighting that can affect the colour detected. The internal standard circle is affected by the lighting in the same way as the detected pink colour. Several colours are possible to be used as internal standard. Pink, yellow, red and blue were used as in **Figure** 3.53. Yellow internal standard caused shorter linear ranges than other internal standards but also it gave higher slop. However, it was not shown as an internal standard since the developed detection colour is pink and hence the two colours may not be influenced in the same way by the surrounding light. Pink, blue and red internal standards showed in general similar intensities. The colour developed in the analysis was pink, therefore, pink was chosen as the internal standard. The internal standard can remove the errors which happened due to light within the photo itself.
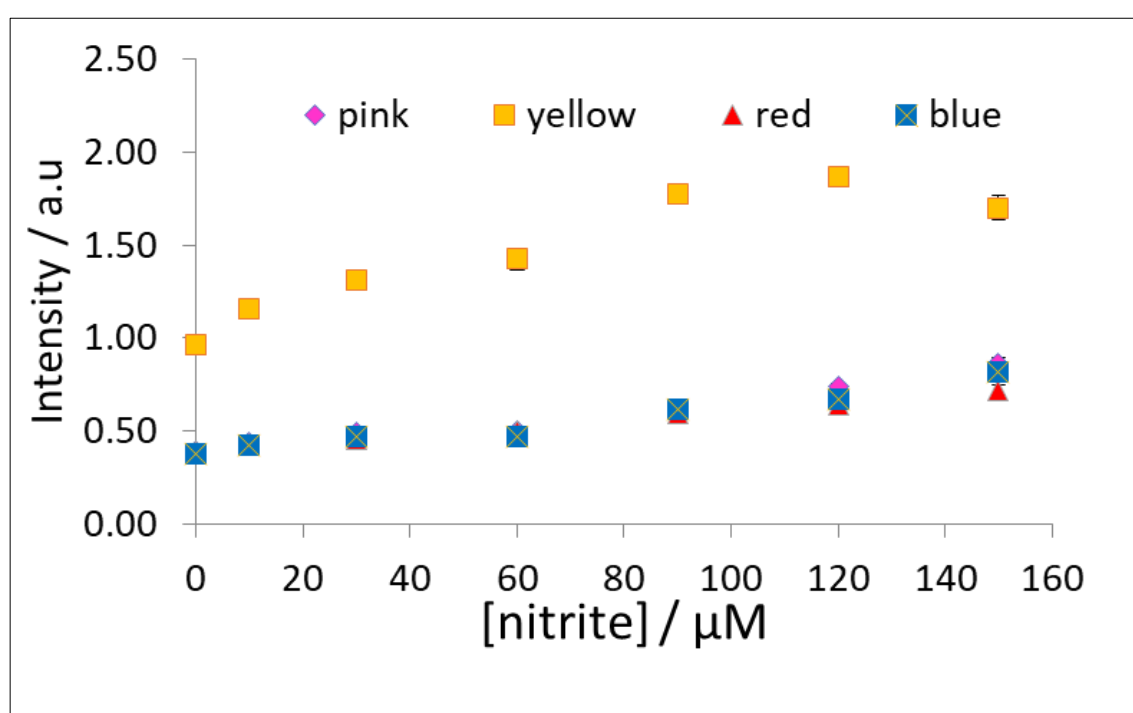
Figure 3.53 Intensity versus nitrite concentration (µM) when pink. Yellow, red and blue internal standards were used. The relative standard deviation was less than 5% for each point and n=6. Device 9 (Figure 3.9) was used for this experiment (modified as in Figure 3.19), colour development was allowed for 14 minutes, and Phone was used for photo capture and analysed by image-J (The intensity was measured by method 2 in **Section 2.5**).

3.5.4 Optimization of time and amount of reagent

The paper microfluidic device was optimized for the amount of standard, reaction time and Griess reagent amount as in **Figure** 3.54, **Figure** 3.55 and **Figure** 3.56 respectively. As the amount of standard increased the signal increased too (**Figure** 3.54) which is logical since more amount of nitrite was needed to react with the Griess reagent on the paper. After 6 µL of standard, the signal started to be constant which means Griess reagent reacted completely with the standard.

Therefore, 6 µL was chosen as the optimum standard/sample volume. The maximum volume of standard which was tried in this experiment was 8 µL since more than this volume required more time to dry and it was a lot for a 6 mm circle.
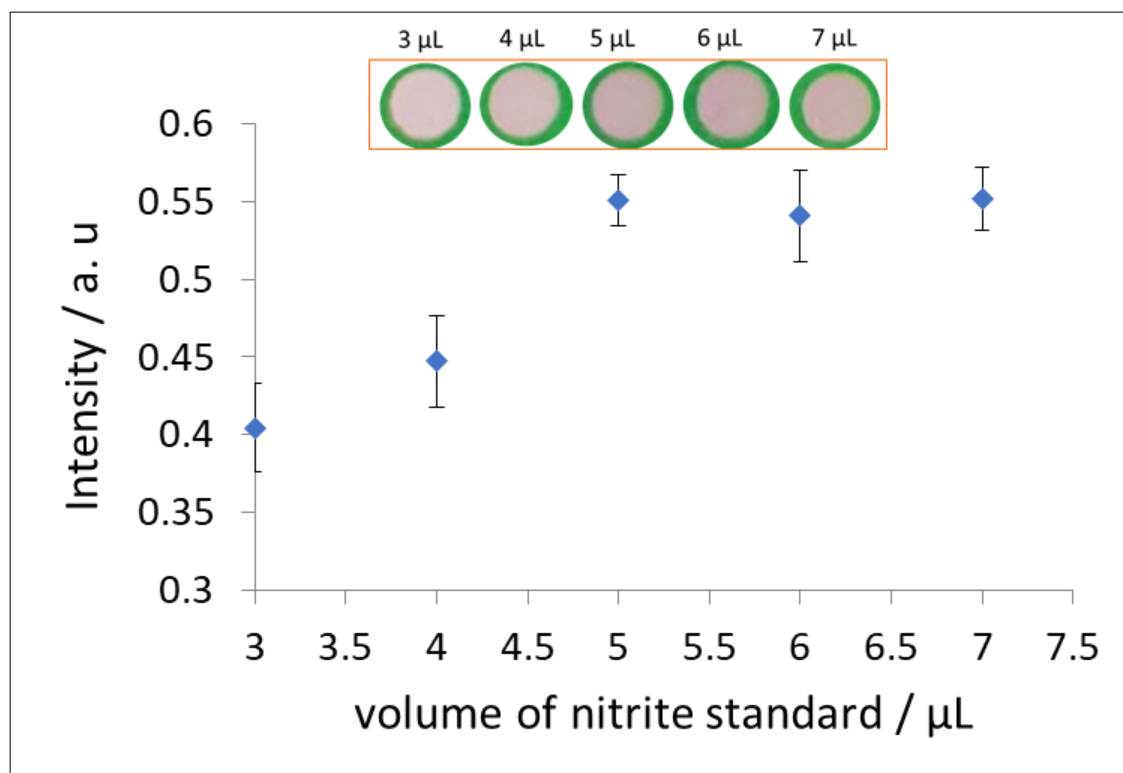
Figure 3.54 Intensity versus standard volume (µL). 1 µL Griess reagent was deposited into device 9 (modified as in Figure 3.19) and allowed to dry for 10 min. The Griess reagent components concentrations were 50mM SA, 10mM NED and 330 mM citric acid. 60 µM nitrite standard was added (volume of analyte was varied) to the modified device and the Colour development time was 14 min. pink colour was used as an internal standard and the photo was taken by phone and analysed by image-J (The intensity was measured by method 2 in **Section 2.5**). The optimum standard volume was 6 µL. n=6.

Once nitrite reacted with Griess reagent the colour started to develop, and the time of colour development or time of reaction represents a key point to get accurate and precise results on paper microfluidic device. Therefore, a UV-Vis spectrophotometer was used to determine the optimum time for the colour development as in **section 3.4.1**. The time was determined to be 14 minutes and it was used initially as a reaction time in a paper device. The colour development on the paper itself was also measured with time (**Figure** 3.55). The signal raised gradually with time since still there is an analyte to react with the detection reagent. After 4 minutes it became stable, and the analyte reacted completely with the detection reagent. 5 minutes seemed to be the optimum time to capture the photo for analysis.
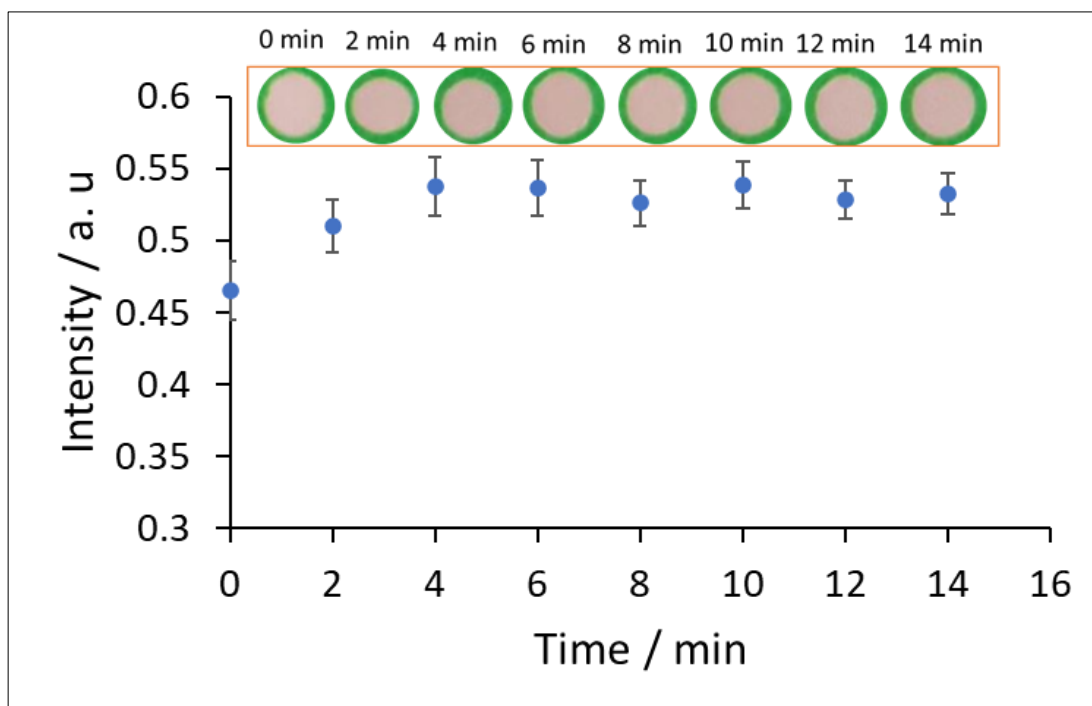
Figure 3.55 Intensity versus time (minutes). 1 µL Griess reagent was pipetted into the detection zone in device 9. It was allowed to Dry 10 min. The Griess reagent components concentrations were 50mM SA, 10mM NED and 330 mM citric acid. 6 µL of 60 µM nitrite standard was added to the detection zone. Pink colour was used as internal standard, and the phone was used for photo taking. A photo was taken for 14 minutes each 2 minutes. The photo was analysed by image-J (The intensity was measured by method 2 in **Section 2.5**). The optimum time for colour development was 5 minutes. (n=6).

The amount of the Griess reagent in the detection zone has also an effect on the sensitivity of the device. The amount of Griess reagent was optimized in the 0-2.5 µL range (**Figure** 3.56)**.** High volume is considered a lot for a 6 mm diameter circle, and it took a longer time to dry. A very small volume was not enough for a complete reaction. The signal increased with increasing the amount of Griess reagent until it became approximately constant after the addition of 1 µL of the detection reagent. 1.5 µL is the optimum volume of Griess reagent. **Table** 3.9 summarizes all the optimized parameters and their optimum values.
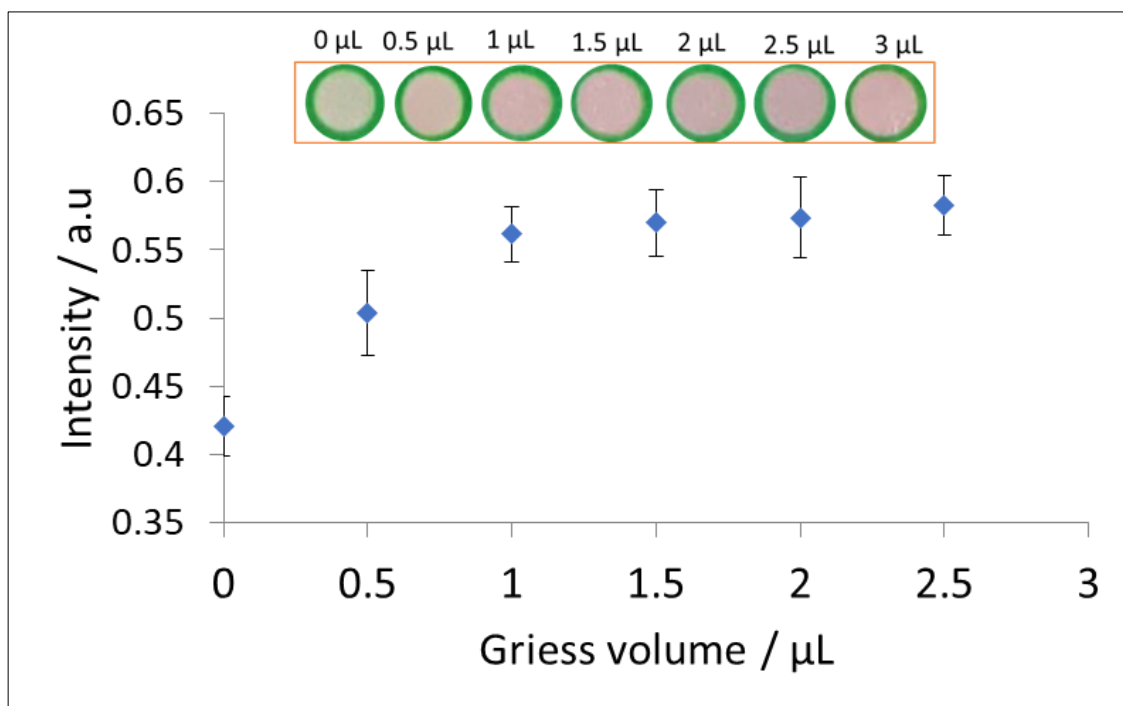
Figure 3.56 Intensity versus Griess reagent volume (µL). 60 µM standard was used. Griess reagent (volume varied) was added to the detection zone in device 9, and it was allowed to dry for 10 min. The Griess reagent components concentrations were 50mM SA, 10mM NED and 330 mM citric acid. Pink colour was used as internal standard, and the phone was used for photo taking. The photo was taken after 5 minutes. The photo was analysed by image-J (The intensity was measured by method 2 in **Section 2.5**). The optimum Griess volume is 1.5 µL. (n=6).

Table 3.9 The optimum value for Standard/sample volume, Reaction time and Griess reagent volume. 60 µM nitrite standard and device design 9 were used during optimization.

Optimized parameter	Optimum value
Standard/sample volume	6 µL
Reaction time	5 minutes
Griess reagent volume	1.5 µL

3.5.5 Optimization of Griess reagent component

Griess reagent consisted of three components, acid (citric acid), sulphanilamide and NED. Each component had its use in the reaction, for example, the acid was important to catalyse the intermediate reaction which resulted in formation of diazonium salt. In this reaction, nitrite standard (60 μM or 100 μM) reacted with sulphanilamide to produce diazonium salt (intermediate) which then reacted with NED to produce azo dye with pink- red colour. The three components of Griess reagent were optimized in the paper device and the optimum concentration of each was determined. NED, sulphanilamide and citric acid were optimized as in **Figure** 3.57, **Figure** 3.58 and **Figure** 3.59 respectively. The three components were mixed to make Griess reagent (1.5 μL) which was then added into the PAD (device 9) and allowed to dry. The dry PAD was then ready for nitrite analysis by adding nitrite (6 μL) to the device. Finally, the colour change was observed. In **Figure** 3.57 as the concentration of NED increased the colour intensity increased too until it reached a maximum at around 6 mM and then the intensity decreased. At small concentrations there was not enough amount of NED to react with the intermediate (diazonium salt) which was why the signal increased gradually with the increase in the concentration. On the other hand, the signal decreased at higher concentrations because NED may tend to compete with sulphanilamide for reaction with the nitrite. Overall, 6 mM of NED was the optimum concentration.
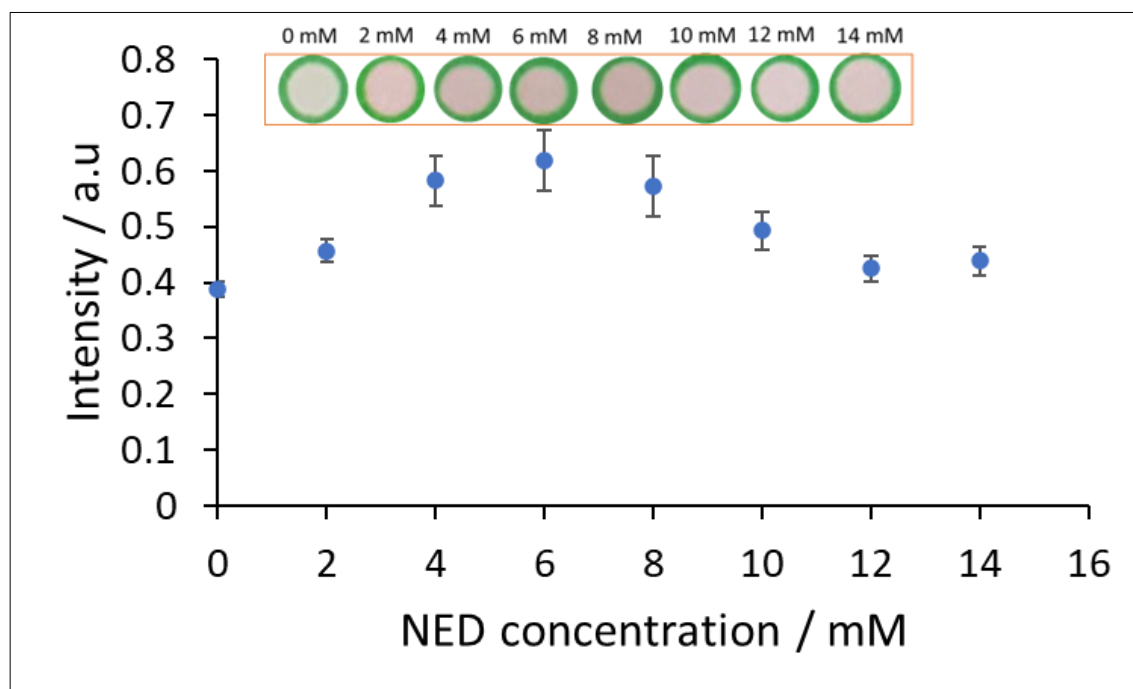
Figure 3.57 Intensity versus NED concentration (mM). 60 μM standard was used. 1.5 μL Griess reagent was added to the detection zone in device 9 (modified as in Figure 3.19), and it was allowed to dry for 10 min. The Griess reagent components concentrations were 50 mM SA, XX mM NED and 330 mM citric acid. The pink colour was used as the internal standard and phone was used for photo taking after 5 min of addition of 60 μM nitrite standard. The photo was analysed by image-J (The intensity was measured by method 2 in **Section 2.5**). The optimum concentration of NED was chosen to be 6 mM.

Sulphanilamide concentration was optimized too as in **Figure** 3.58 and for the purpose of validity, the concentration was optimized at two different concentrations of nitrite, 60 and 100 µM. The higher the concentration the more the signal or the intensity of the colour since more sulphanilamide was available to react with nitrite. In general, the intensity raised as the concentration increased until it reached maximum and then showed a small decline and this is maybe due to the back reaction which led to the dissociation of the diazonium intermediate. 50 mM of sulphanilamide was chosen to be the optimum concentration since both 60 and 100 µM of nitrite solutions gave the same result.
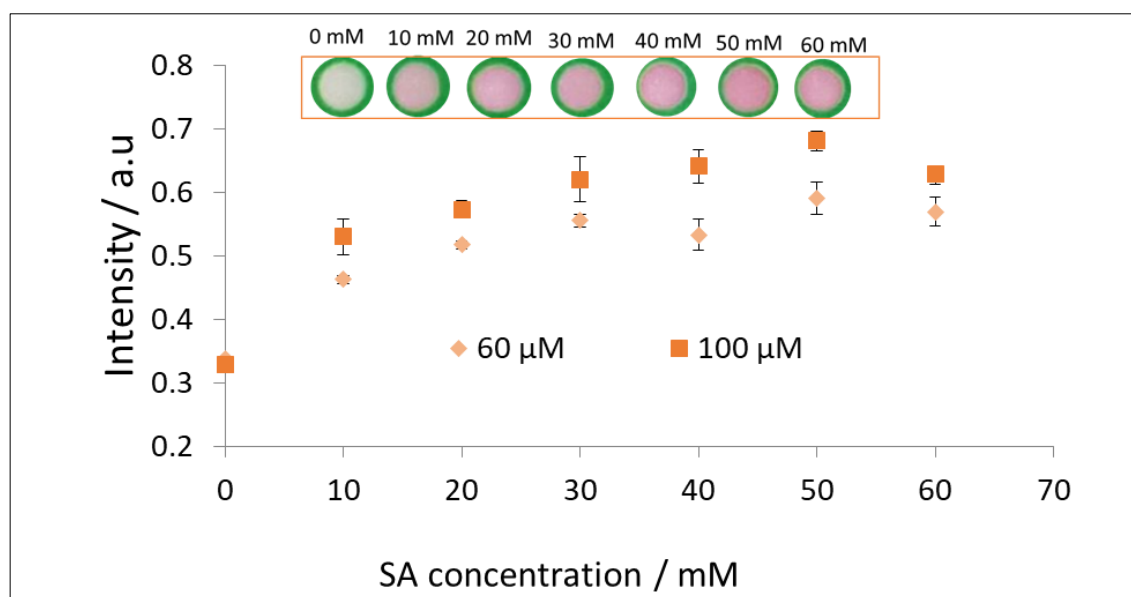
Figure 3.58 Intensity versus concentration of sulphanilamide SA (mM). 1.5 µL Griess reagent was added to the detection zone in device 9 (modified as in Figure 3.19), and it was allowed to dry for 10 min. The Griess reagent components concentrations were XX mM SA, 6 mM NED and 330 mM citric acid. The pink colour was used as the internal standard and phone was used for photo taking after 5 min of addition of 60 or 100 µM nitrite standard. The photo was analysed by image-J (The intensity was measured by method 2 in **Section 2.5**). The optimum concentration of sulphanilamide was chosen to be 50 mM.

The third component of the Griess reagent was citric acid which was used to catalyse the reaction. There are several acids which were used in the literature as components for Griess reagents like phosphoric acid and hydrochloric acid [374,375]. However, both are strong and aggressive acids and hence they were not used in this experiment. Citric acid was chosen as a non-aggressive option which was not reactive with a paper device. The pH had a significant effect on the reaction as is clear in **Figure** 3.59, at high pH (small concentration of acid) the signal was low since there was not enough acid to catalyse the reaction. Furthermore, a very high amount of acid can suppress the reaction. 300 mM was the optimum concentration of citric acid. The optimum values for Griess components are summarized in **Table** 3.10.
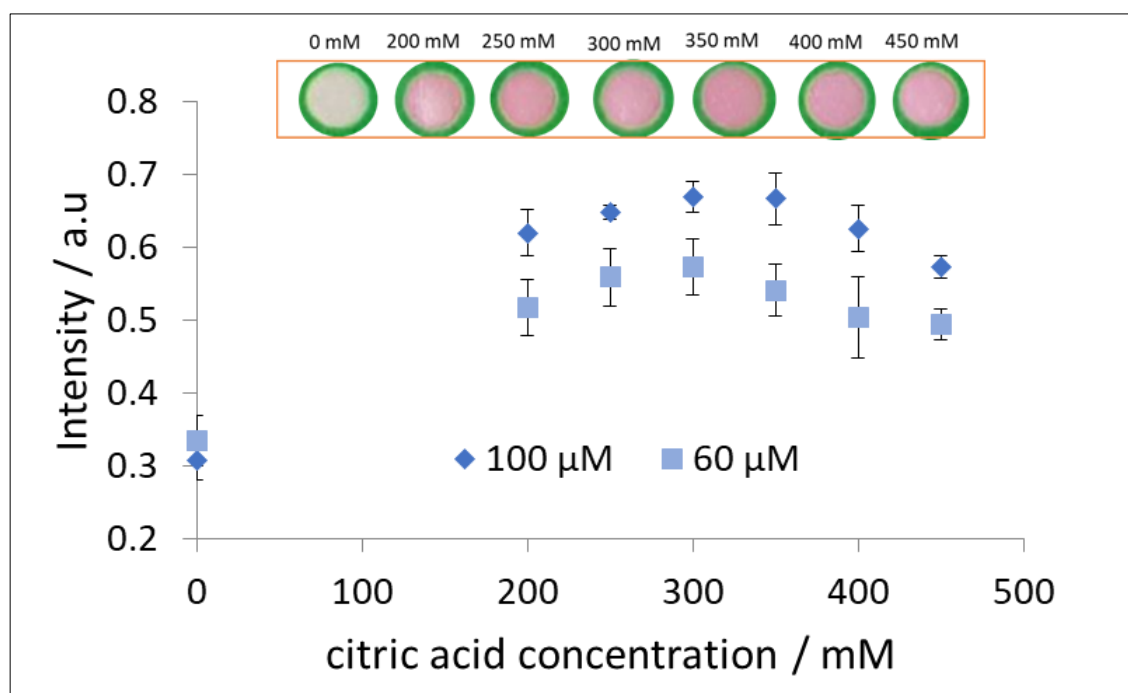
Figure 3.59 Intensity versus concentration of citric acid (mM). 1.5 µL Griess reagent was added to the detection zone in device 9 (modified as in Figure 3.19), and it was allowed to dry for 10 min. The Griess reagent components concentrations were 50 mM SA, 6 mM NED and XX mM citric acid. The pink colour was used as the internal standard and the phone was used for photo taking after 5 min of addition of 60 or 100 µM nitrite standard the photo was taken. The photo was analysed by image-J (The intensity was measured by method 2 in **Section 2.5**). The optimum concentration of citric acid was chosen to be 300 mM.

Table 3.10 The optimized components of Griess reagent (NED, sulphanilamide, and citric acid) and their optimum values. 60 and 100 µM of nitrite standard were used during optimization. The optimization was applied in device design 9 (n=6).

Optimized component	Optimum value
NED	6 mM
Sulphanilamide	50 mM
Citric acid	300 mM

3.5.6 Lamination and dipping for sample introduction.

Device 9 was previously used for optimization work where the device was not laminated, and the standard was added by pipette into the reaction zone. Then the idea of lamination came. Lamination of the device is needed since the device finally is used by non-experts. In addition, lamination should increase the lifetime of the device. Lamination protects the reagents in the device from interaction with air and hence from degradation. **Figure** 3.60 shows the two methods, with and without lamination. The device was prepared using conditions in **Table** 3.9

and **Table** 3.10. In the device which was not laminated (**Figure** 3.60 **A**), the nitrite solution (60 µM) was pipetted into the zones for the reaction to happen. However, the device which was laminated (**Figure** 3.60 **B**) was dipped into the nitrite solution (60 µM). The two methods were compared and the result is in **Figure** 3.61. The intensity was determined for three nitrite concentrations in both laminated and non-laminated devices. The two methods show similar results with a small increase in the intensity for a laminated device which means that the detection solution in the detection zone was not affected by the heat of lamination at 80 °C. At zero nitrite (blank) concentration, the non-laminated device showed a small increase in intensity than the laminated device. This is maybe due to the high chance of interaction between air and detection reagents in the non-laminated device.
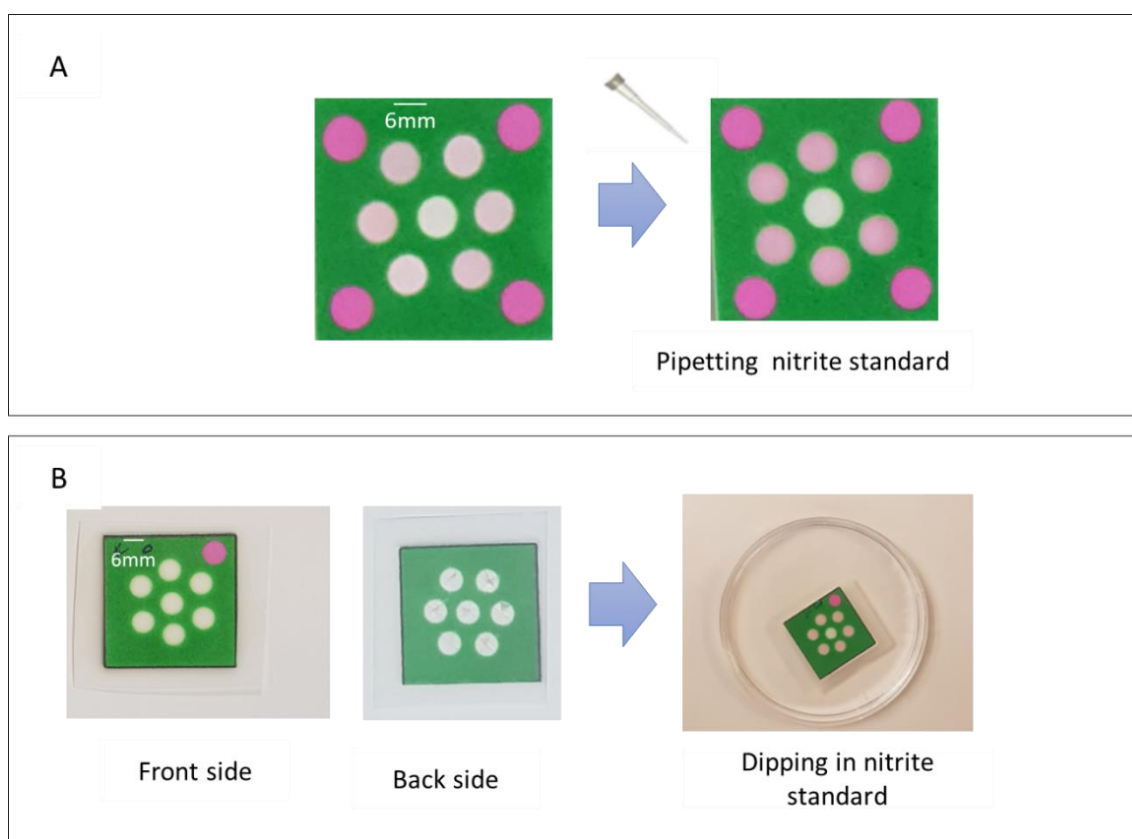
Figure 3.60 The detection of 60 µM nitrite ion in non-laminated and laminated devices. (A) non-laminated device 9 (modified as in Figure 3.19) where the nitrite standard was pipetted during detection. (B) laminated device 10 (modified as in Figure 3.20) where the device was dipped into the nitrite standard.
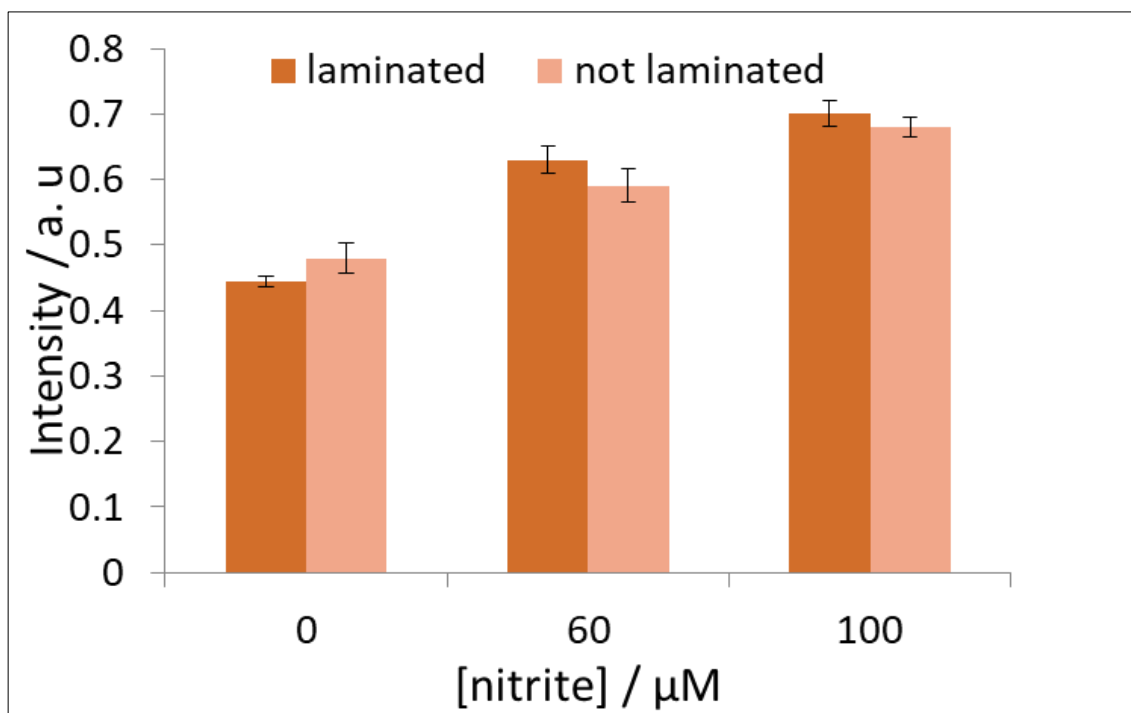
Figure 3.61 Intensity versus concentration of nitrite ion (µM) for laminated device 10 (modified as in Figure 3.20) and non-laminated device 9 (modified as in Figure 3.19).

3.5.7 Improving the device by separating of Griess component

The Griess reagent consists of three components as mentioned previously, NED, sulphanilamide and citric acid. The three components were working together to produce the pink-red colour for nitrite detection as in **Equation 2.1** in the experimental part. The previous experiments were performed when the three components were mixed in solution before the addition into the detection zone as in **Figure** 3.62 **A**. However, mixing the three components increases the chance and the possibility of the interaction between them especially in the presence of air. In addition, sulphanilamide should react first with nitrite. The two components NED and sulphanilamide may compete to react with nitrite when they are in the same solution. Therefore, the components of the Griess reagent were separated. Two solutions of Griess reagent were prepared as in **Figure** 3.62 **B**. The two solutions were added to two different zones in the device 11. In zone 1 NED solution was added. In zone 2 a mixture of sulphanilamide and citric acid was added. Zone 3 was left empty for nitrate detection purposes (chapter 4). The device was folded and laminated as normal and used for nitrite detection. The comparison between the two devices (devices 10 and 11) was clear as in **Figure** 3.63. The figure shows intensities for nitrite standards (0,60, 120 µM). There was no significant difference between devices with separated and non-separated Griess reagent components. Both devices showed similar intensities except for the blank which shows a reduction in the intensity when the Griess reagent component separated into two layers. This led in the reduction in the slope by around 40% (exactly 39.6%) and hence an increase in the sensitivity.

129
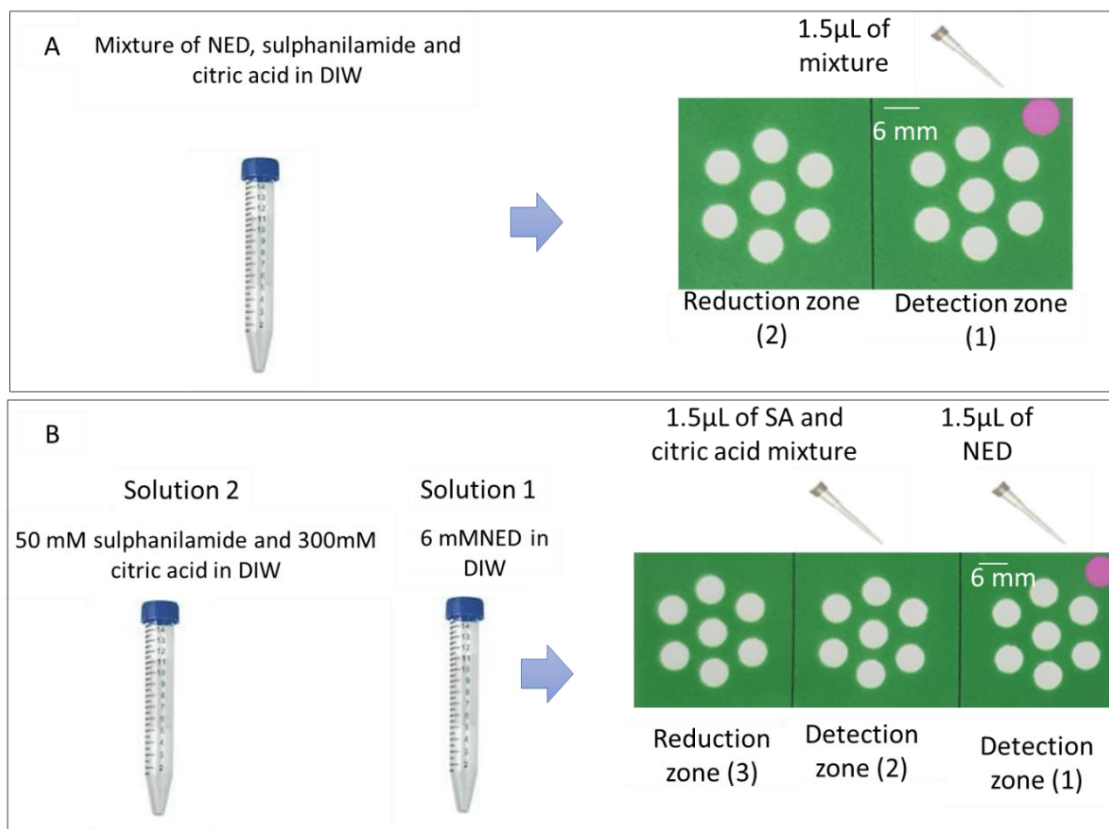
Figure 3.62 (A) Device 10 which was prepared from Griess reagent with mixed components (NED, sulphanilamide and citric acid). (B) Device 11 which was prepared from separated Griess components. NES solution and (sulphanilamide+ citric acid) solution. Conditions from Table 3.9 and Table 3.10 were followed. The devices were laminated and dipped in the solution. A scanner was used for detection.
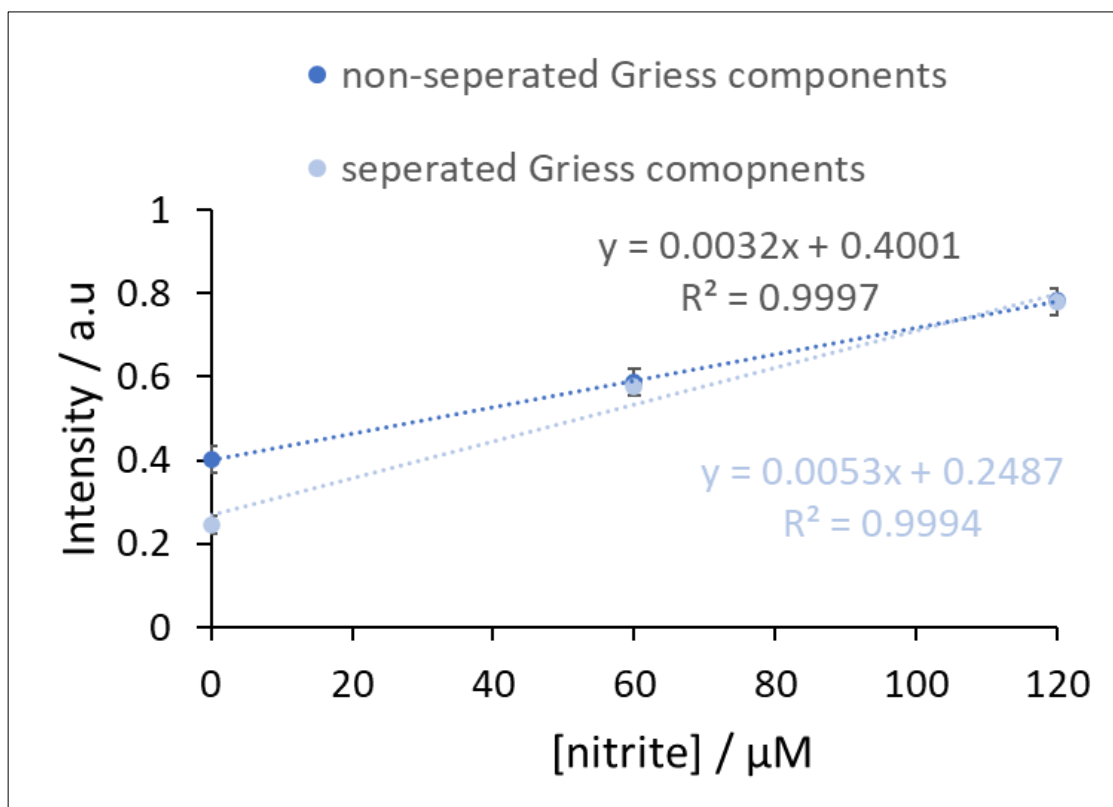
Figure 3.63 Intensity versus nitrite concentration (µM). The devices in Figure 3.63 were used. The two devices show similar results except for the blank. The scanner was used for photo taking and the photo was analysed by image-J (The intensity was measured by method 2 in **Section 2.5**).

The device with separated Griess components seemed to work well according to **Figure** 3.63. This was explained by studying the stability of the two devices according to **Figure** 3.64. The Griess components were added to the devices as in **Figure** 3.62 **A** and **B**. The devices then were laminated and left in the freezer for 4 days. Without any reaction, a photo was taken of the two laminated devices. It was noticed that the device with non-separated Griess components (device 10) produced higher signal than device with separated Griess components (device11) (**Figure** 3.64) and this explain the improve in the sensitivity which was described in **Figure** 3.63. The intensity decreased by around 70% when the Griess reagent components were separated. In addition, there was a small increase with days in the intensity of devices with non-separated Griess components compared to device with separated Griess components. Device 11 seemed to be more stable than device 10 for the 4 days. This is maybe because during device preparation the mixed components were more affected by air than when they were separated. Also, during storage, the mixed components had more chance to interaction with each other.
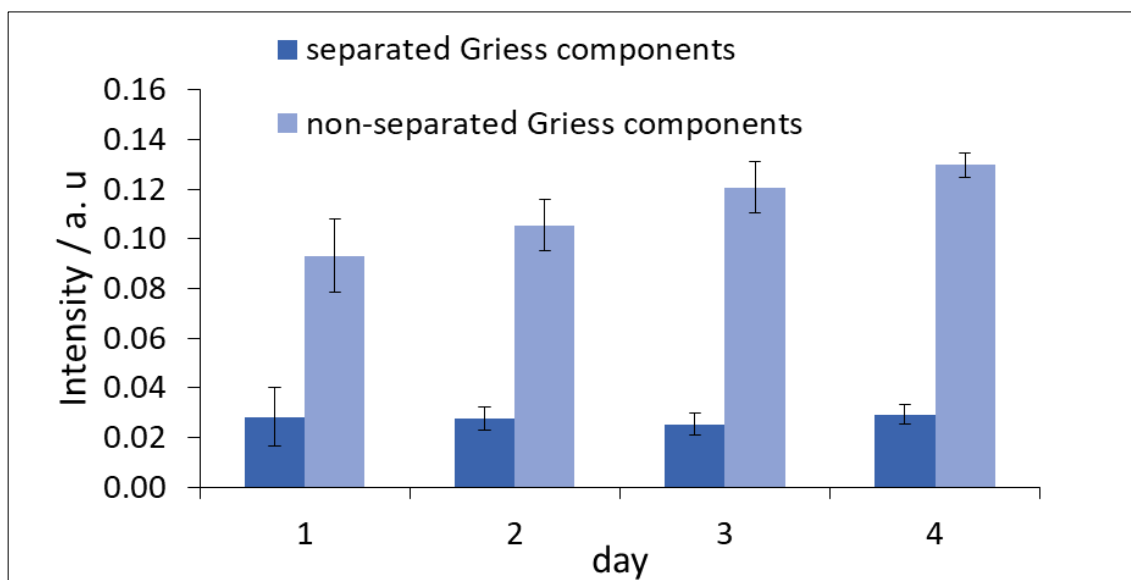
Figure 3.64 Intensity versus the day. This is the result from devices 10 (n=6) and 11 (n=6) with non-separated and separated Griess components respectively. Devices 10 and 11 were prepared as in Figure 3.20 and Figure 3.21 respectively but without any reaction with analyte nitrite the device was scanned each day. Device 11 seemed to be more stable.

3.5.8 Calibration by Scanner

A scanner was initially used to capture a photo for analysis. The use of a scanner was effective since it was not associated with the surrounding light effect. The calibration curve for nitrite was necessary to determine the concentration of analyte in the sample. It was plotted using device 11. Nitrite standard concentrations between 0-180 µM were tested. It was clear that linearity was lost after 90 µM of nitrite as seen in **Figure** 3.65. The reproducibility of the PADs was determined by taking measurements over three different months as in **Figure** 3.66. The three lines appear close, however, an ANOVA test of the three data sets indicated that F >F $_{critical}$, (e.g., at point 10 µM, F=6.34, $F_{Critical}$= 3.68, P= 0.010, ANOVA test). Therefore, it was concluded that the PADs are not quantitative, and it can be said that they are semi-quantitative data since approximate concentration can be determined (not- exact). The average LoD, R^2 and slope of the three lines are not more than 16%RSD (**Table** 3.11) and hence this indicates the agreement of the calibration lines. R^2 is around 0.9909±0.0065. Most of the points pass through the line and all of them with relative standard deviation of less than 5%. The limit of detection was around 0.67±0.11 µM as in **Table** 3.11.
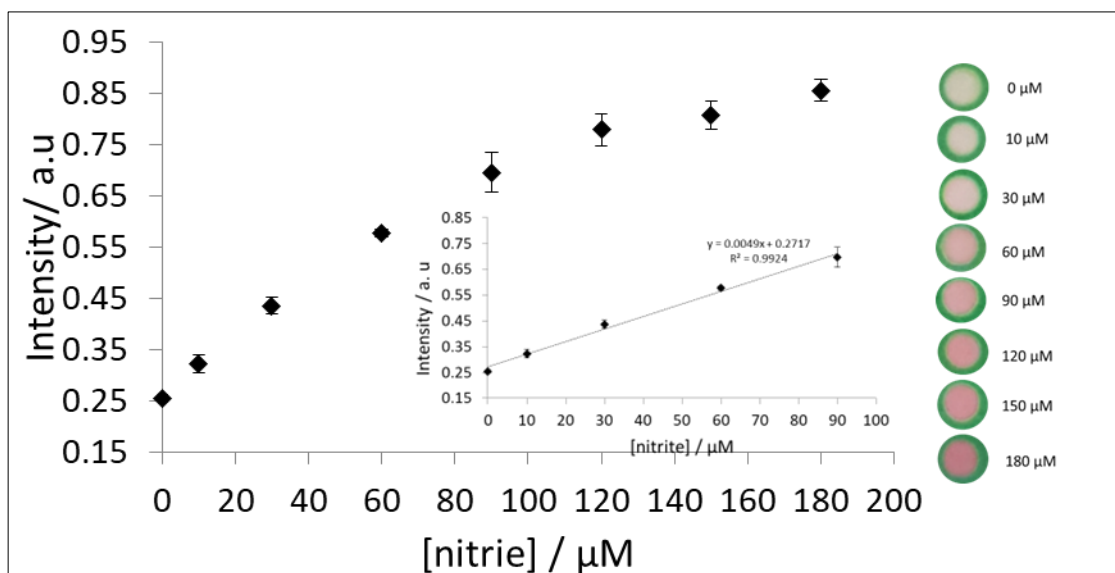
Figure 3.65 Intensity versus concentration of nitrite (µM). Laminated device design 11 was used (n=6). Dipping was applied. A scanner was used for detection. The line lost its linearity after 90 µM nitrite concentration. The photo was analysed by image-J (The intensity was measured by method 2 in **Section 2.5**).
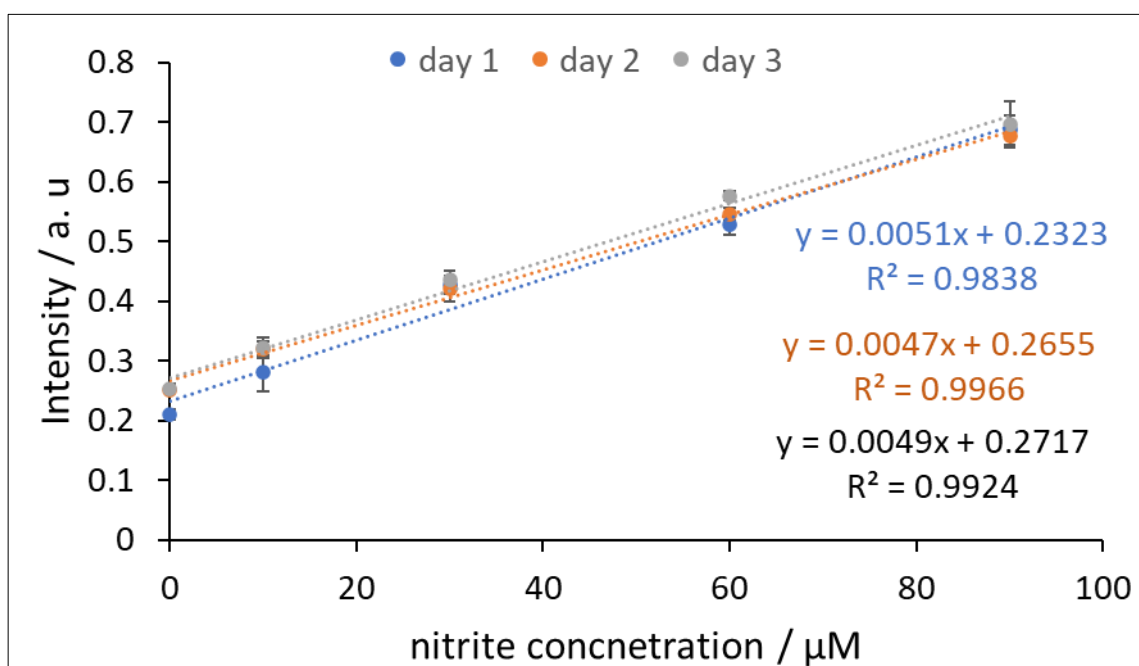
Figure 3.66 Intensity versus concentration of nitrite ion (µM). Laminated device design 11 was used (n=6). Dipping was applied. A scanner was used for detection. The photo was analysed by image-J (The intensity was measured by method 2 in **Section 2.5**). The three lines from three different days.

Table 3.11 LoD, slope and R^2 for nitrite detection by the PAD when a scanner was used as a detection method. LoD was calculated as in **Equation 2.5** in the experimental.

	Line 1	Line 2	Line 3	average	%RSD of average
LoD (µM)	0.67	0.78	0.56	0.67±0.11	16.34
slope	0.0051	0.0047	0.0049	0.0049±0.0002	4.08
R^2	0.9838	0.9966	0.9924	0.9909±0.0065	0.68

3.5.9 Calibration by phone

Since a scanner is not portable it is not practical in the field. Nowadays most people rely on smartphones in their daily life. The use of the smart phone was necessary to ensure an easily accessible method of detection which is accessible to most people. In this experiment, a phone camera was also used to capture a photo which was then analysed by Image-J software and the intensity of the PAD signal was calculated. Then calibration lines were determined (**Figure** 3.67). Most of the points pass through the straight line, R^2 0.9664±0.0188. The limit of detection was 0.81±0.06 µM (around LoD 0.466 mg kg^{-1} if 8 grams of soil and 100 mL of solvent is used). LoD from the phone experiment was comparable to the result from the scanner as described in the previous section. Using this method, the limit of detection and quantitation is lower than the maximum toxic level of nitrite in water (21.7 µM /1mg L^{-1} according to the US Environmental Protection Agency) [365]. However, when this is compared to the level of nitrite in soil, the LOD is also lower than the maximum level of nitrite in soil and close to the minimum level of nitrite in soil [366,367]. The level of nitrite in soil rarely exceeds 164 mg kg^{-1} and most of the time is lower than 0.3 mg Kg^{-1} [366,367]. **Figure** 3.67 also summarizes the reproducibility of the PAD when the phone was used. The three lines are close, however, when the ANOVA test was used to compare each three points in the three curves, F >F $_{critical}$. Therefore, it was concluded that the result which was generated from these curves is not quantitative and it can be said again that it is semi quantitative data since the average LoD and slope of the three lines not more than 13 %RSD as in **Table** 3.12.

.
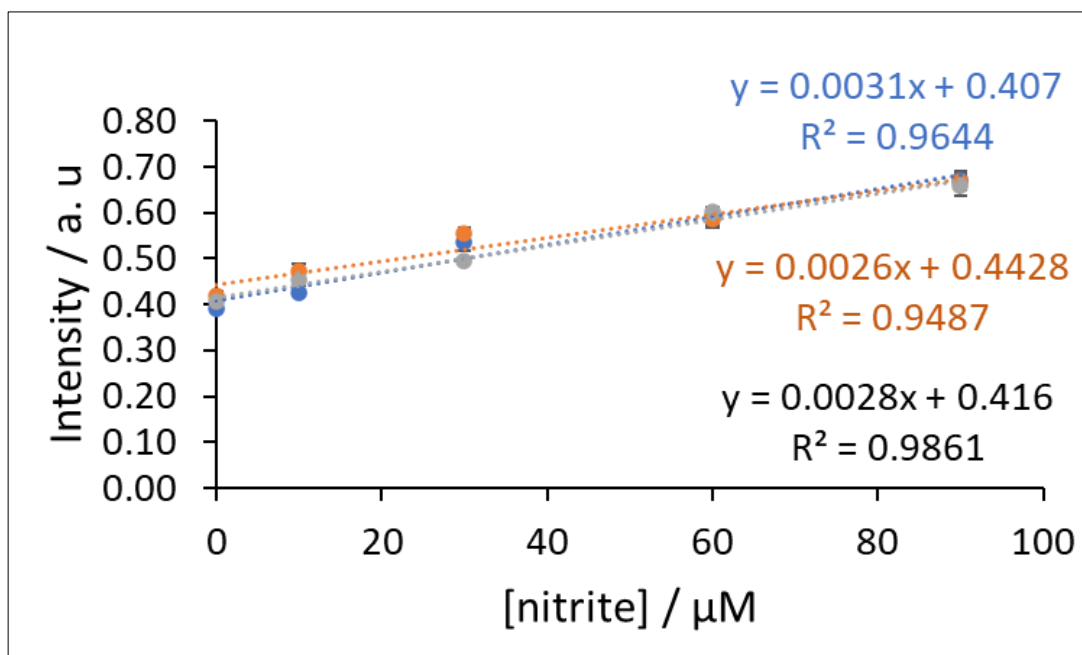
Figure 3.67 Intensity versus concentration of nitrite ion (μM). Laminated device 11 was used (n=6). Dipping was applied. A phone was used for detection. The photo was analysed by image-J (The intensity was measured by method 2 in **Section 2.5**).

Table 3.12 LoD, R2 and slope of curves in Figure 3.67. Laminated device 11 (n=6) was used for the analysis. LoD was calculated as in **Equation 2.5** experimental.

	Line 1	Line 2	Line 3	average	%SD of average
LOD (μM)	0.84	0.84	0.73	0.81±0.06	7.31
R2	0.9644	0.9487	0.9861	0.9664±0.0188	1.94
slope	0.0031	0.0026	0.0028	0.0028±0.0003	8.88

3.5.10 Interferences

Soil contains other cations and anions other than nitrate and nitrite. These components may have the ability to interfere with the detection of nitrite either by competing with nitrite to reach the Griess reagent first or by reaction of interference with nitrite itself to prohibit it from reaching the Griess reagent. Several possible interferences (Ca^{2+}, Na^+, K^+, Fe^{2+}, Cu^{2+}, Zn^{2+}, Mn^{2+}, CO_3^{-2}, PO_4^{-3}, Cl^-, SO_4^{-2}) for nitrite detection were studied as in **Figure** 3.22 (There are other interferences which may cause interference and are not studied in this work due to shortage of time). Nitrite 60 μM was used in the study. Each time a specific concentration of the interference was mixed with 60 μM of nitrite. The concentration of interference was increased and decrease until the highest concentration where no interference was reached, and that concentration was called the tolerance level of the interference. **Figure** 3.68 summarizes the tolerance level for all the interferences. The t-test was used to compare two means and to decide if they are equal or

not within the standard deviation, and the t-test shows no interference for all mentioned concentrations of interference ($t_{state} < t_{critical}$, two-tailed test). The tolerance level was compared to the level of these interferences in the environmental soil sample. In this study, the levels from different studies were used for comparison as in **Table** 3.13 which shows the level of each interference in some studies for soil samples. Most of the time iron, copper, zinc and manganese exist in environment soil at low levels; less than 5 mg L^{-1}. Hence, they are not going to interfere with this PAD when compared to their tolerance level. Also, the other cations and anions that may exist in soil such as sodium, potassium, calcium, chloride, sulphate, and phosphate, exist most of the time at levels lowers than their tolerance level.
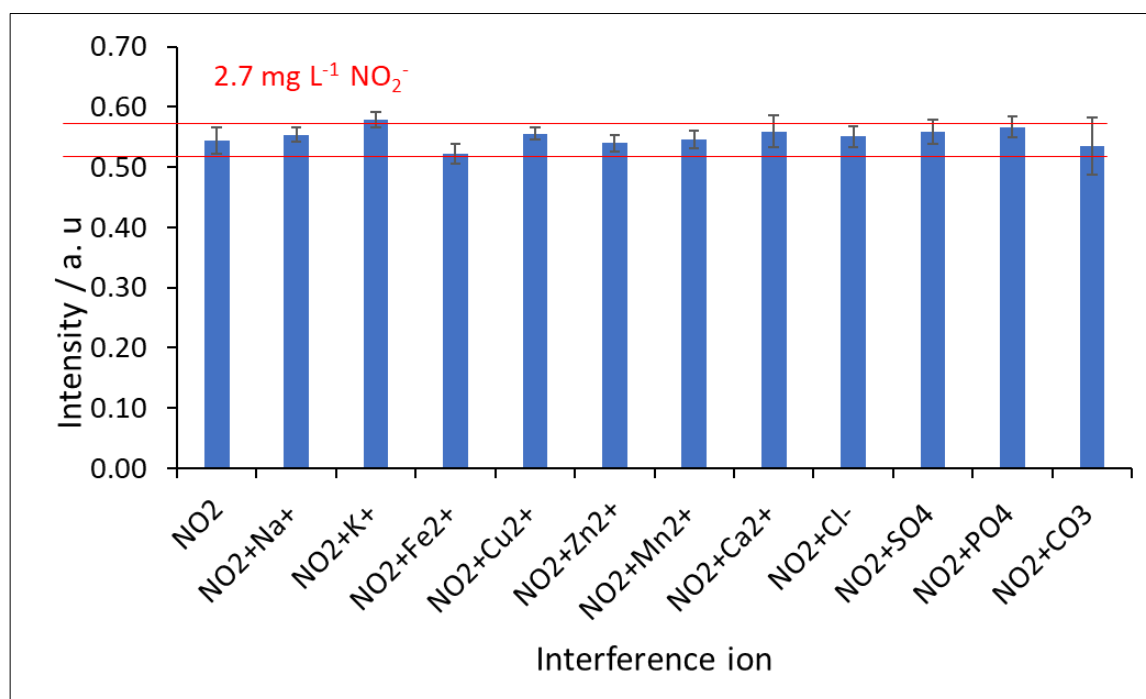
Figure 3.68 Intensity versus interference tolerance concentration in (mg L^{-1}). 60 µM/2.7 mg L^{-1} of nitrite was mixed with the interference [Ca^{2+} (0.5 g L^{-1}), Na^+ (5 g L^{-1}), K^+ (30 g L^{-1}), Fe^{2+} (0.2 g L^{-1}), Cu^{2+} (1 g L^{-1}), Zn^{2+} (0.2 g L^{-1}), Mn^{2+} (4 g L^1), CO_3^{-2} (0.1 g L^{-1}), PO_4^{-3} (5 g L^{-1}), Cl^- (3 g L^{-1}), SO_4^{-2} (10 g L^{-1})] in the same solution. Device 11 was used.

Table 3.13 The level of some of cations and anions in environmental soil samples based on some studies.

.

Ion	mg L^{-1}	Mass: Volume	Mg kg^{-1}	reference
Mn^{2+}	27.7	0.25:10	1108	[376]
	4.225	0.25:10	169	[376]
	1.888	0.004:2.5	1180	[377]
Fe^{2+}	1.51-4.89	25:250	15.1-48.9	[378]
	65.4	2:100	3270	[379]
	0.190	1:25	4.75	[380]
Cu^{2+}	0.201, 0.133	-	-	[381]
Zn^{2+}	0.128, 0.023	-	-	[381]
	0.0067-0.1175	2:20	0.067-1.175	[382]
PO$_4^{3-}$	0.148	2.5:50	2.96	[383]
	1.27-3.05	-	-	[384]
Ca^{2+}	7.54-110.15	20:80	30.16-440.6	[385]
	9.46-45.69	10:100	94.6-456.9	[386]
	9.7-18.8	10:200	194-376	[387]

Ion	mg L^{-1}	Mass: Volume	Mg kg^{-1}	reference
SO$_4^{2-}$	2.45-3.654	20:100	12.28-18.27	[388]
	0.2-1.6	5:25	1-8	[389]
K$^+$	22.8-182	20:100	114-910	[388]
	5.7-7	2.5:25	57-70	[390]
Mg	0.85-9.85	10:200	17-197	[387]
Na$^+$	1.9-2.52	10:200	38-50.4	[387]
	1.00-1.43	10:200	20-28.6	[387]
Cl$^-$	6-300	1:50	300-15000	[391]
	1.6	5:40	13	[392]
	7.8	5:40	62	[392]

3.5.11 pH effect

Griess reagent is pH sensitive. It works at a low pH much better compared to a high pH. Acetic acid was used as a component in the Griess reagent to keep the solution acidic. The pH of the deionized water is around 5.3. At this pH, the calibration line of nitrate was determined, and the other nitrite studies were performed. However, in this study, we are aiming to use soil samples where the pH may be higher than 5.3. Therefore, the effect of the pH on the calibration line was studied. Even though the pH of the soil can be from 3 to 10 [393], the studied pH range was from 5 to 8 because at around this range, most of the soil nutrients exist and it is the best range for plant growth [394] and most of the UK soil are in this range [395]. In addition, the soils that will be studied in this study are within this pH range. The calibration line was run using nitrite solutions of different pH, ranging from 5 to 8 as in **Figure** 3.69. This figure shows the intensity of the PAD versus the concentration of nitrite solution. ANOVA test was used to compare between different pH at the same concentration. The intensities were similar at different pH for 0, 10, 30, and 60 UM concentrations (e.g., at 10 µM of nitrate: F=1.681, $F_{Critical}$=3.098, P= 0.20, α 0.05, n=6). It was observed that the pH change does not affect the small concentration of nitrite from 0 to 60 µM. However, at higher concentrations of nitrite above and 60 µM, the result was affected. It is expected that soil samples treated to have very small amounts of nitrite and hence this variation at high concentration has no influence.
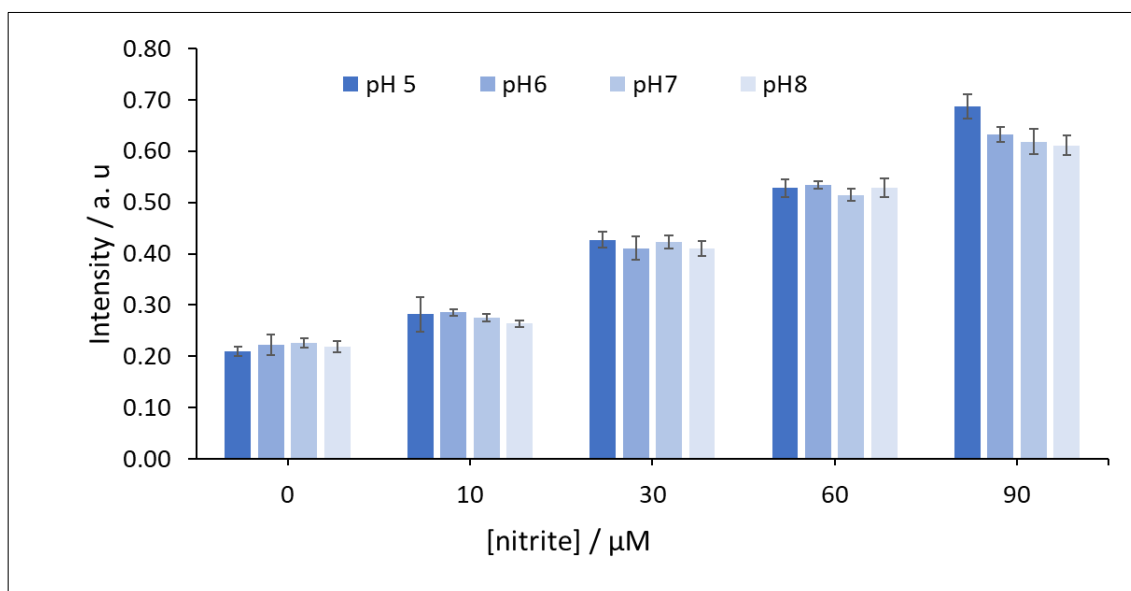
 Figure 3.69 Intensity versus nitrate concentration (µM) at different H. Device 11 was used and treated as in Figure 3.21.

3.6   Comparison between PAD, UV-Vis and IEC and literature

Nitrite was also analysed by UV-Vis spectrophotometer and IEC, the result was compared to the result from paper device**. Table** 3.14 shows a comparison between paper device, IEC and UV-Vis spectrophotometer results from this work. In general, UV-Vis gave a narrower detection range for nitrite than the paper device. Whereas IEC showed a wide detection range. The detection range of the paper device was 0-90 µM, whereas 0- 50 µM was the detection range of nitrite when the spectrophotometer was used. The limit of detections of nitrite using UV-Vis spectrophotometer, IEC and paper microfluidic scanner and phone were 0.053 ± 0.003, 5.17±0.47, 0.67±0.11 and 0.81±0.06 µM respectively. UV-Vis is more sensitive than the IEC and PAD, however, it can be exposed to more interference than IEC where all ions can be separated in the column before detection. Therefore, UV-Vis will be used for nitrite determination especially if the soil has a low level of nitrite. When the nitrite level is high, and more interferences are expected in the sample then IEC is used.

The developed PAD was also compared to the existing nitrite PAD in literature as in **Table** 3.15 which shows the sample analysis, device type, number of layers in the device, LOD, detection range, reaction time and sample introduction method for each nitrite PAD which already exist in literature. The developed method shows good sensitivity in terms of LOD compared to most other methods and this is mainly due to the step of separation of Griess reagent components as it was mentioned in **Figure** 3.64, this step reduced the auto colour development which may lead to the reduction in the sensitivity by around 40%. In other studies, Griess reagent components were all mixed in one zone/layer, consequently, they are more exposed to interact with each other. Moreover, other PADs are made from one layer of paper, and some are based on flow channels which is complicated for field use as studied in **section 3.5.2**. The developed PAD has three layers of paper. The sample moves through layers before reaching the detection zone. The number of layers makes the PAD ready for soil sample analysis since multi-layers work as filters for the extracted solution before it reaches the detection layer. Consequently, other PADs in literature are not ready for soil sample analysis in the field since the detection zone can be contaminated by the soil if it is not filtered before analysis. In this study also dipping system for sample introduction was adopted compared to most of other study which make it easier in the field to introduce the sample than if the sample is pipetted.

Table 3.14 LoD and linear range for scanner detection, phone detection, UV-Vis and IEC. Laminated device 11 (n=6) was used for the analysis

Detection method	LoD (µM)	linear range (µM)
Scanner PAD	0.67±0.11	0-90
phone PAD	0.81±0.06	0-90
UV-Vis	0.053 ± 0.003	0-50
IEC	5.17±0.47	30-1000

Table 3.15 Comparison between different PAD studies for nitrite detection.

Sample/ device shape	Number of layers	method	Components of detection reagent	Linear range (mg L^{-1})	LoD (mg L^{-1})	Reaction time (min)	Sample introduction	Reference
Water channels	1	Griess reagent	Mixed In one layer	4-85	0.52	15	pipetting	[299]
Water channels	1	Tetrazine base	Mixed In one layer	0.23-23	0.0598	5	pipetting	[300]
Saliva channels	1	Griess reagent	Mixed In one layer	0.92-7.36	0.345	5	pipetting	[301]
Saliva channels	1	Griess reagent	Mixed In one layer	0-4.6	0.258	10	pipetting	[302]
Water circles	1	Griess reagent	Mixed In one layer	0.1-10	0.1	15	pipetting	[303]

Sample/ device shape	Number of layers	method	Components of detection reagent	Linear range (mg L^{-1})	LoD (mg L^{-1})	Reaction time (min)	Sample introduction	Reference
Waster squares	1	Basic Fuchsine	Mixed In one layer	0.05-9.2	-	30	immersing	[304]
Water Channels	1	Griess reagent	Mixed In one layer	0.23–2.26	0.03	12	pipetting	[305]
water	1	Griess reagent	Mixed In one layer	3.5-115	-	2	pipetting	[306]
Food channels	1		Mixed In one layer	0.5-40	0.1	5	pipetting	[293]
Saliva channels	1	Griess reagent	Mixed In one layer	0.46-46	0.46	15	pipetting	[307]
Food squares	1	Griess reagent	Mixed In one layer	1-100	1	5	pipetting	[308]
Food circles	1	Griess reagent	Mixed In one layer	1-250	1.1	15	pipetting	[309]
Soil (scanner) circles	3	Griess reagent	Separated into two layers	0-4.1	0.031 (0.67 µM)	5	dipping	This work
Soil (phone) circles	3	Griess reagent	Separated into two layers	0-4.1	0.037 (0.81 µM)	5	dipping	This work

3.7 Nitrite in soil sample

Nitrite was determined in the soil sample using the developed PAD. The result from the PAD was validated by UV-Vis and IEC.5 soil samples were analysed, 3 were commercial compost samples (John Innes 1, 2 and 3) and two were real topsoil samples. The nitrite was initially extracted from the soil by mixing 8 grams of soil in 100 mL of water in a cafetière for 2 minutes and then allowed to settle for 3 minutes (these parameters were chosen to fit the nitrate extraction in Chapter 4). The extract was analysed by device 11 (modified as in **Figure** 3.21) which was dipped into the extracted solution for 5 min. the photo was taken then and analysed by image-J. The result for nitrite content is in **Figure** 3.70 which shows mg kg^{-1} of nitrite in the five soil samples from UV-Vis and PAD. The soil samples contain no nitrite or less than 1 mg kg^{-1} (0.080 mg L^{-1} / 1.7 µM) of nitrite. IEC was used also to double-check the existence of nitrite since this method is less exposed to interference. The result is in **Figure** 3.71 which shows the nitrite peak from standard and no equivalent nitrite peak from soil. This was expected since both PAD and UV-Vis showed also no or very small nitrite content for all soils. The IEC result for the rest of the soils is in **Appendix B**.
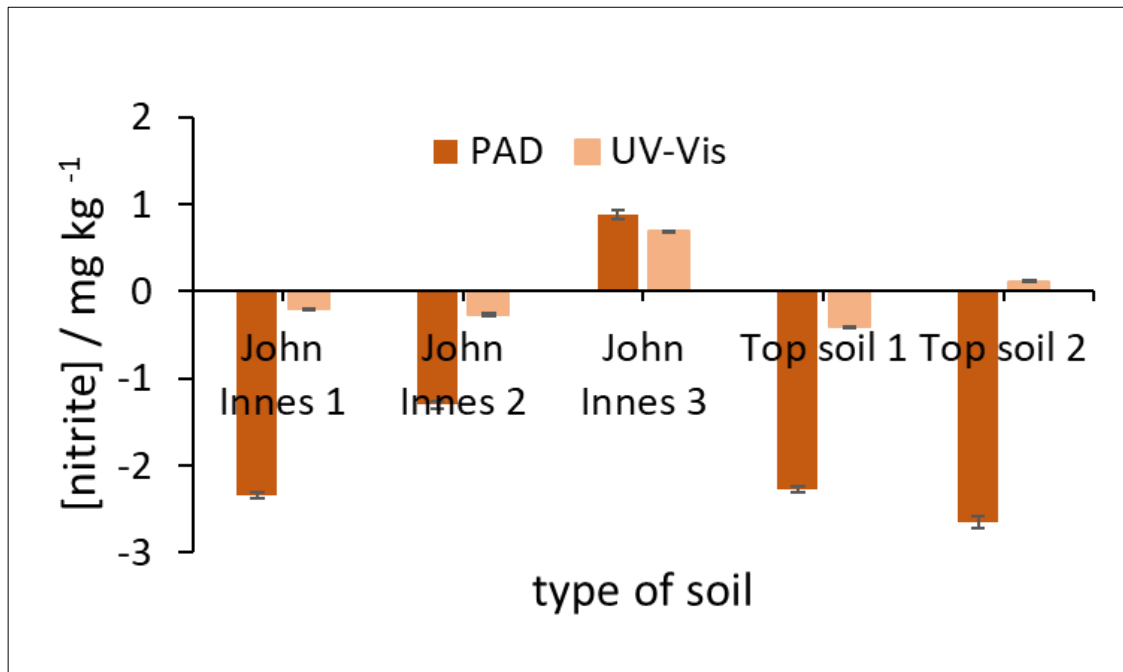
Figure 3.70 Nitrite content mg kg^{-1} versus the type of soil. 3 commercial composts samples (John Innes 1, 2 and 3) and two real topsoil samples were used. The nitrite was extracted from the soil by mixing 8 grams of soil in 100 mL of water in a cafetière for 2 minutes and then allowed to settle for 3 minutes and readout was taken by PAD. Then the 8 grams of the same sample were mixed in a shaker for 1 hour and the readout was taken by UV-Vis and IEC.
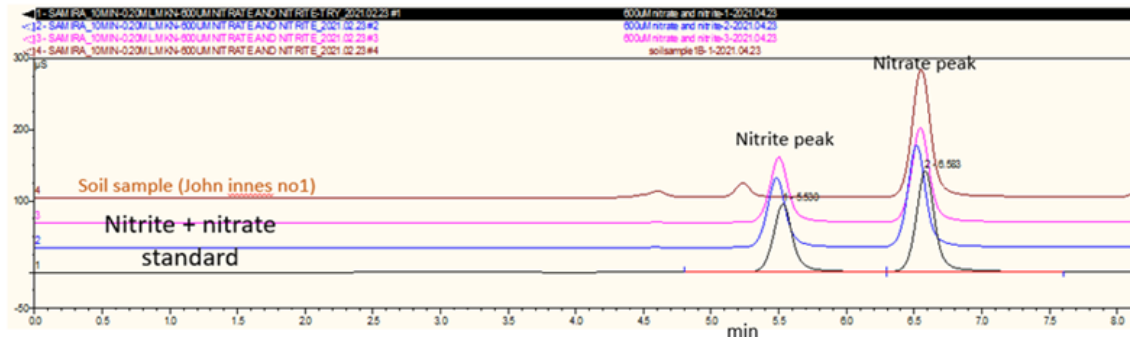
Figure 3.71 Peak height (µS) versus retention time (min). 600 µM nitrate and nitrite standards and soil Sample (John Innes 1) were used in the analysis (8 grams soil in 100 mL of DIW mixed in a shaker for 1 hour). This analysis with 20mM KOH and 0.38 mL min^{-1} flow rate. There is no peak for nitrite in the soil sample.

3.8 Discussion and Conclusion

Nitrate is one of the soil nutrients which is required for plants to grow healthily. It is applied in soil using fertilizer [37-40]. Fertilizer management is crucial, therefore, soil nutrients regular monitoring in the field is required. Griess reagent is commonly used for colorimetric detection [61,349-351]. However, nitrate must first be reduced to nitrite and then detected as nitrite and hence nitrate and nitrite by this reaction are detected together in soil. Therefore, this chapter aimed to develop PAD which is simple for lay people to use for *in situ* nitrite determination in soil. The simplicity and sensitivity of the PAD are two issues which were studied here.

The main challenge with develop field use device is the simplicity of the device while maintaining its sensitivity. Developing easy to use device means reduction in the steps which should be performed by user and reduction of steps within the device. In this study, a PAD with a circle (device 9) was chosen from several complicated designs either with flow channels or with valves (devices 1, 2, 3, 4, 5, 6, 7). The result was based on the first-time handling of each PAD. The aim was to find a design that can be used with little or no practice and hence be easy to use by non-experts. At the same time, the design should be sensitive enough to be useful in the field. The multiple steps of the reaction (detection and reduction) should happen in the PAD. This was why the study started with a complicated device that can provide several areas for the multiple reaction steps to achieve better sensitivity. However, handling such complicated devices was not as easy as expected from the first use. The devices were compared in terms of the simplicity to handle, the way the sample was introduced to the PAD and data on the calibration curve. The collected data showed that devices with circular reaction zones only and no valves or channels were easier to use with good calibration from first-time use.

The circular zones in the PAD helped for easy sample addition by dipping while the PAD was laminated. The solution enters immediately into the detection zone. This is significantly easier than other systems (**Table** 3.15) which require users to pipette a sample into a reaction zone or channels. Furthermore, the reaction time was studied, and it was found to be 5 minutes which is short for field use. The design ended up with a small PAD (28.5 mm × 28.5 mm) with three layers. The PAD is small, portable, easy to use, disposable, use-friendly, inexpensive (price ≤ £ 1, price of the device was calculated in **appendix H**) and can be used in resource-limited setting.

Other than the simplicity of the device its sensitivity for soil sample analysis is another challenge. Therefore, The PAD was optimized for the Griess reagent components (330 mM citric acid, 50 mM sulphanilamide and 6 mM NED) which are more stable if they were separated into two layers of the PAD. Most of the previous studies **(Table** 3.15) always mix all reagents in one layer. Separation of the Griess reagent reduces the auto-colour development by around 70% hence

the degradation of the reagents and their interaction when they are mixed. After this separation, the sensitivity of the PAD increased by around 40% (based on the slop of the calibration line). The LoDs of nitrite by the PAD were 0.39 ± 0.06 and 0.46 ± 0.03 mg kg^{-1} with the use of a scanner and phone respectively. The developed PAD was more sensitive and with lower LoD compared to most of the LoDs published previously (**Table** 3.15**)**. This makes the PAD usable for nitrite detection in soil since nitrite in soil exists in small or neglected concentrations, around 0.3 mg Kg^{-1} [366,367]. Moreover, the PAD was supported by three layers and hence this makes it ready for soil sample analysis compared to other PAD in literature since the layers provide the filtration for slurry (organic matter). Soil samples were analysed by PAD for nitrite content. The method was validated by UV-Vis and IEC. In general, the PAD, UV-Vis and IEC show no or less than 1 mg kg^{-1} nitrite content for all soil types.

In conclusion, three three-layer device which is easy to use by non-expert and can detect nitrite in soil within 5 minutes after dipping the PAD into the extracted solution was developed. This PAD will be used to develop nitrate PAD in Chapter 4.

Chapter 4 Nitrate determination

4.1 Introduction

As mentioned in Chapter 3 nitrate is one of the nutrients which is required by plants in large amounts and needs to be monitored regularly by farmers [396]. In conventional methods Filtration of the soil particles is required. The sample needs to be transported from the field to the specific laboratory. Then after some time, the result of the analysis is returned to the farmer. This process is expensive and time-consuming especially for farmers who mainly rely on their crops to gain their income especially farmers in low- and middle-income countries where agriculture is main source of income [418]. In the field qualitative nitrate strips are used [26]. However, the determination of nitrate is based on the visual observation which is usually not clear. There is also a portable UV-Vis detector (palintest) which can give quantitative data for nitrate in soil [419]. However, this method is expensive and still requires the use of toxic chemicals.

Therefore, in this study, we aim to develop a method for nitrate extraction and detection in the field by an easy method which is easy to handle by farmers for regular nitrate monitoring without the help of an expert. As mentioned in Chapter 3, a paper-based sensor represents a good alternative for nitrate detection since it can provide simplicity, low price and portability. There are some recently published paper-based sensors for nitrate detection [290-293,295,296,298,310,311], however, none of them is ready for soil sample analysis in the field. In addition, some of them are still complicated to be used by lay people. Furthermore, extraction of the nutrients from soil is required before detection. In the field, there were several available techniques like hand shaking followed by use of filter paper [420], syringe connected to filter extraction [421] and automatic extraction mounted with full extraction-detection unit [422]. However, most of these methods are complicated and still require the use of sophisticated devices and the use of filters, sieves, and chemicals. Therefore, a simple extraction method is required for farmer's daily use.

Here, a simple-to-use cafetière-based extraction method was combined with a colorimetric paper-based sensor with smartphone readout. Initially, the extraction of the nitrate by the cafetière was optimized for the best mass, volume, and extraction time and compared to the conventional extraction by shaker. Then, the PAD described in Chapter 3 was developed and used for nitrate analysis. This included the addition of a reduction step from nitrate to nitrite with zinc as a reducing agent. The reaction time was optimized, and a range of zinc introduction approaches were studied. The developed method was also studied for the effect of interference and pH change. Finally, the developed workflow with extraction and detection was applied to soil samples. IEC (ion exchange chromatography) and CRM (certified reference material) were used for the method validation.

4.2   Experimental

4.2.1   Ion exchange chromatography

Ion exchange chromatography instrument (Dionex-ICS-2000) with Dionex IonPac™ AS16 (RFIC™, 2 × 250mm) separator column, Dionex ASRS 300 (2 mm) suppressor column and DS6 heated conductivity cell were used as conventional method for nitrate determination. Optimization was done as in **Table** 4.1. 15 KOH was used as eluent at 0.3 ml min⁻¹ flow rate. A mixture of nitrate and nitrite was used for the analysis to avoid any interference from nitrite since they are eluted simultaneously. 30-1000 µM mixture standard of nitrite and nitrate was run to determine the calibration line for nitrate. The analysis was done in 6 minutes where nitrate peak was eluted at 5.1 minutes. other columns were used as in **Appendix A**.

Table 4.1 Optimized parameter for nitrite detection. 600 µM of nitrate was used for optimization.

parameter	Value (optimized range)
FLOW RATE	0.30mL min⁻¹ (0.2-0.6 30mL min⁻¹)
KOH concentration	15 mM (15-45 mM)
Volume pump	20 µL
Pump pressure	1000-4000 psi

4.2.2   Designed devices.

Device 10

This device (**Figure** 4.1) consisted of separate reduction and detection zones, which come into contact with each other when the device is folded, thus forming a 3-dimensional device. The dimensions and the number of circles of the two zones same as device 9. Different colours for internal standard were utilised for the purpose of comparison. The reduction zone had no internal standard.
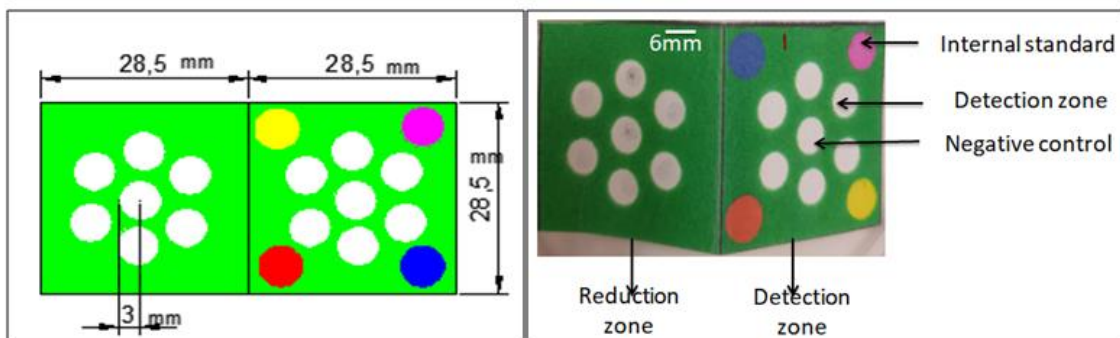
Figure 4.1 Paper device 10 (57×28.5 mm) with two zones, reduction and detection zones. Each zone had 7 circles which had 6 mm diameter. The detection zone consisted of 4 internal standards, yellow, pink, red and blue. The device was adopted for detection of nitrite and nitrate (n=6).

Device 11

Device 11 **(Figure** 4.2) was a modified form of device 10. It had similar dimensions for detection and reduction zones. However, device 11 had two detection zones compare to device 10 which had one detection zone. The device was folded to a form three-dimension device. Once the device was folded the three zones should match each other.
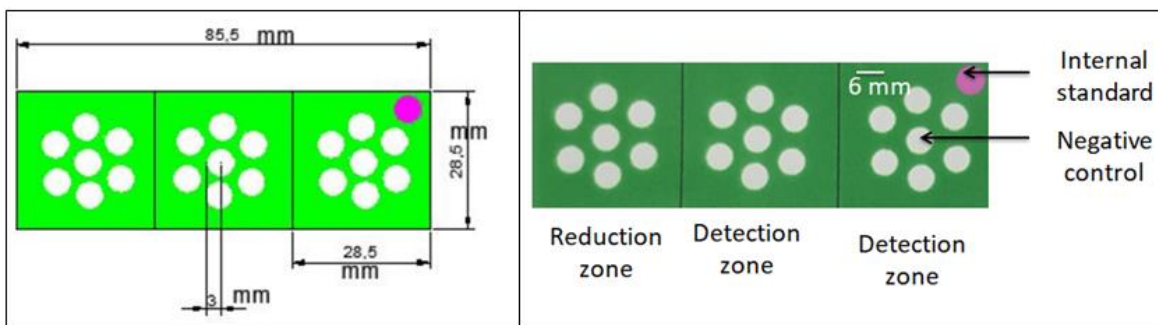
Figure 4.2 Paper device 11 (85.5×28.5 mm) with three zones, 1 reduction and 2 detection zones. Each zone had 7 circles which had 6 mm diameter. The device was adopted for detection of nitrite and nitrate in the future (n=6).

Device 12

Device 12 (**Figure** 4.3) was a modified form of device 11. It had similar dimensions for detection and reduction zones. However, device 12 had an empty zone in compared. The empty layer is located between the reduction zone and the detection zone to reduce any possible interaction between chemicals in the two zones.
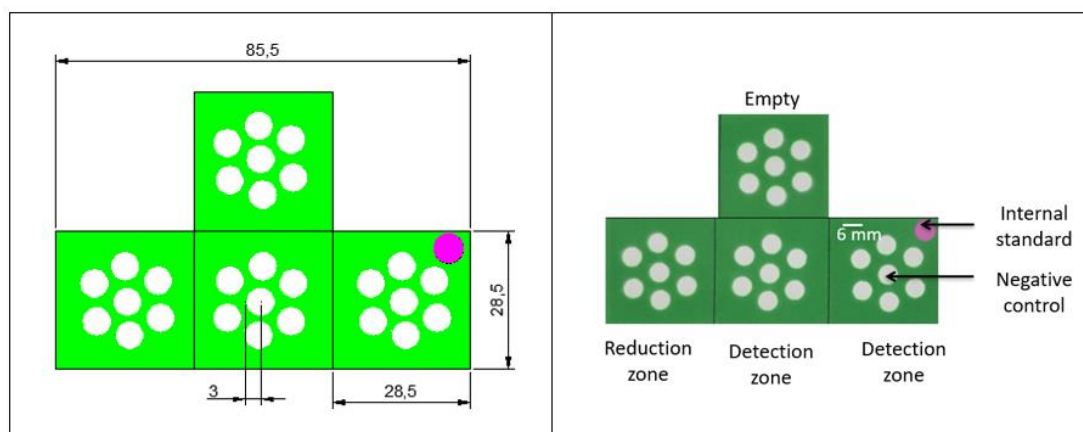
Figure 4.3 Paper device 12 (85.5×28.5 mm) with four zones, 1 reduction and 2 detection zones and 1 empty zone. Each zone had 7 circles which had 6 mm diameter. The device was adopted for detection of nitrate in the future (n=6).

4.2.3 Device modification

Device 10 modification

The paper device for nitrate detection (device 10) was modified the same way as device for nitrite detection. However, this time zinc was added to the reduction zone as in **Figure** 4.4**.** 50 mg mL^{-1} zinc solution was first homogenised in test tube by vortex for 30 seconds. Then 6 µL of the solution was added into all circles in the reduction zone. It was allowed to dry for 10-20 minutes at room temperature to ensure water evaporation. The device then was treated the same way as the device for nitrite detection (**Figure** 4.4). However, finally instead of dipping the device in nitrite solution the device was dipped in nitrate solution.
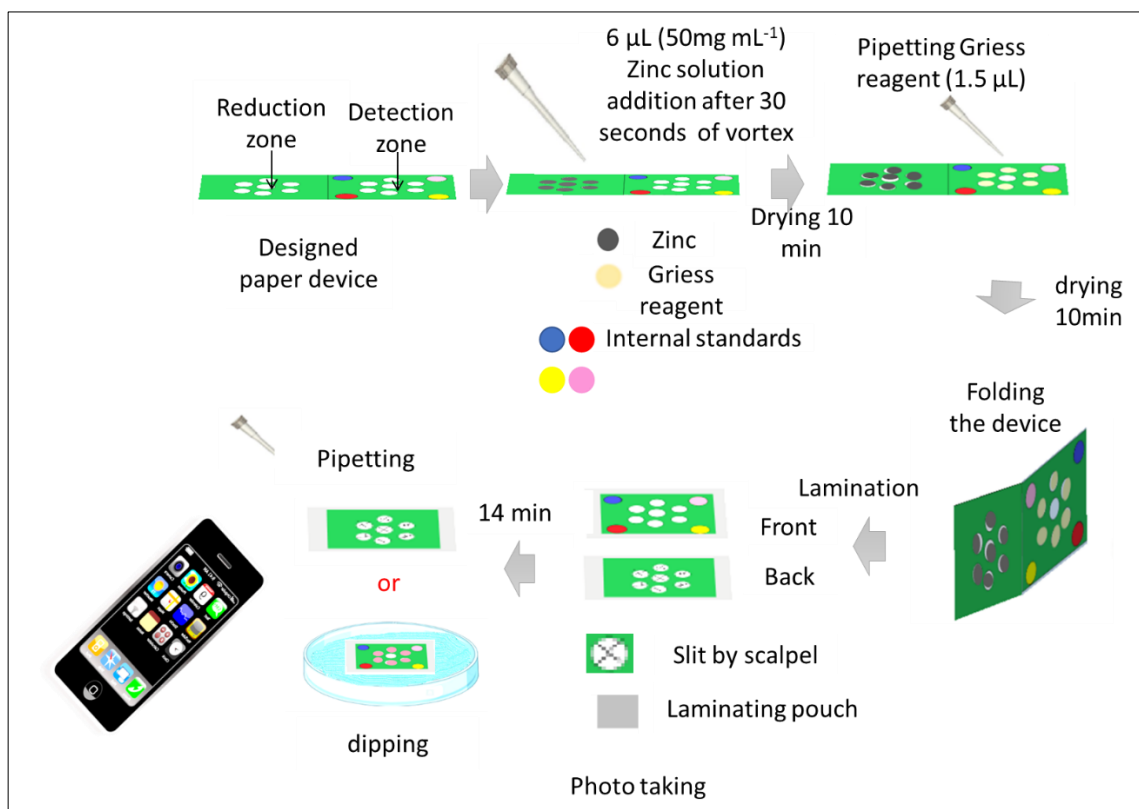
Figure 4.4 Paper device 10 modification for nitrate detection. Zinc solution was vortex for 30 seconds before addition into the detection zone. 6 µL of Zinc solution was pipetted to all circles in the reduction zone. It was then allowed to dry for 10-20 minutes. After drying 1.5 µL Griess reagent was added to the detection zone (all circles except the negative control). The device was allowed to dry for 10 minutes. A fold from the centre of the device was made. The folded device was laminated in laminating punch three times by laminator at 80 ^{0}C. Slits were made in all circles using scalpel. The device was dipped in standard/sample (nitrate) for 14 minutes or standard/sample was introduced by pipetting and followed by 14 min colour development. A photo was taken by phone camera (Samsung Galaxy S8), and it was analysed by Image-J (method 2) and pink colour was used as internal standard.

Design 11 and 12 modifications

Device 11 (**Figure** 4.5) and 12 (**Figure** 4.6) for nitrate detection were modified the same way. The difference between the two designs is that design 12 has empty layer and design 11 has no empty layer. The purpose of the empty layer is to separate reagents and reduce their interaction. The empty layer in design 12 separate the reduction zone and the detection zone 2. The device was modified by addition of zinc first in the reduction zone, zinc was added by immersing the reduction zone into solution of zinc (50mg mL^{-1}) which is under stirring (600 rpm) for 1 second. The device then was dried in the oven for 20 minutes at 40 ^{o}C. 1.5 µL of detection solutions 1 (6 mM NED) and 2 (50 mM sulphanilamide and 300 mM citric acid) was pipetted into detection zone 1 and 2 respectively. The device was then air dry under a box for 15 minutes. Box was used to provide dark environment and reduce degradation of chemicals due to light. After drying the device was fold and laminated. A slit was made in the back side of the device. The device was

ready to be dipped into the sample/solution for 14 minutes. Photo was finally taken by phone or scanner for image-J analysis.
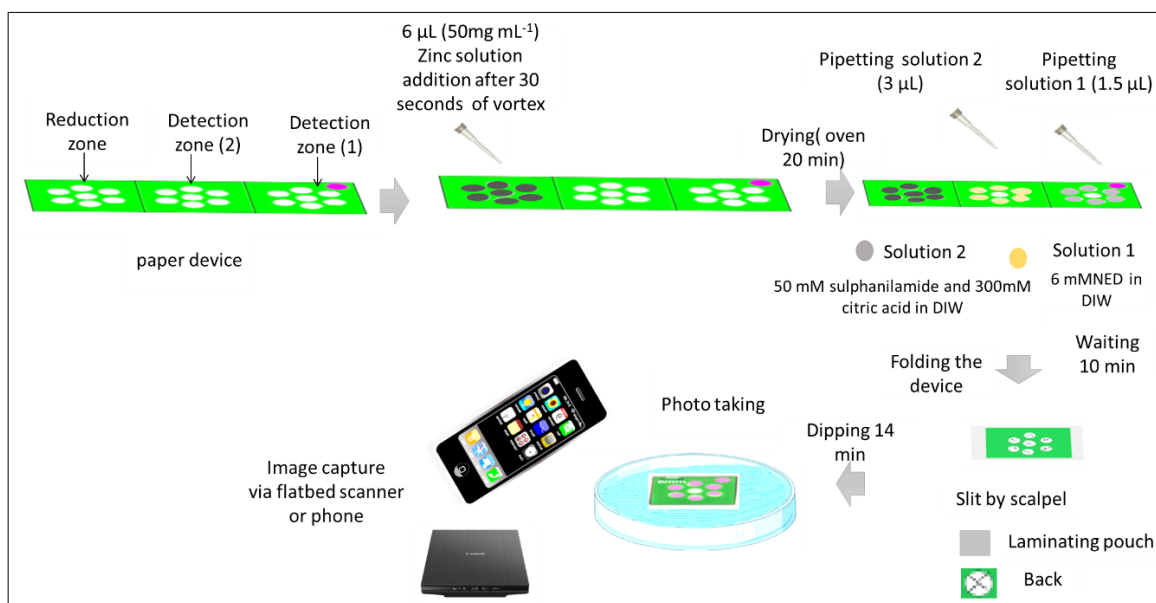
Figure 4.5 Paper device 11 modification for nitrate detection. Zinc solution was vortex for 30 seconds before addition into the detection zone. 6 µL of Zinc solution was pipetted to all circles in the reduction zone. It was then allowed to dry in oven for 20 minutes at 40 °C . After drying 1.5 µL Griess reagents was added to the detection zone 1 and 2 (all circles except the negative control). The device was allowed to dry for 15 minutes. The device was folded. The folded device was laminated in laminating punch by laminator at 80 °C. Slits were made in all circles using scalpel. The device was dipped in standard/sample (nitrate) for 14 minutes. A photo was taken by phone camera (Samsung Galaxy S8) or scanner, and it was analysed by Image-J (method 2) and pink colour was used as internal standard.
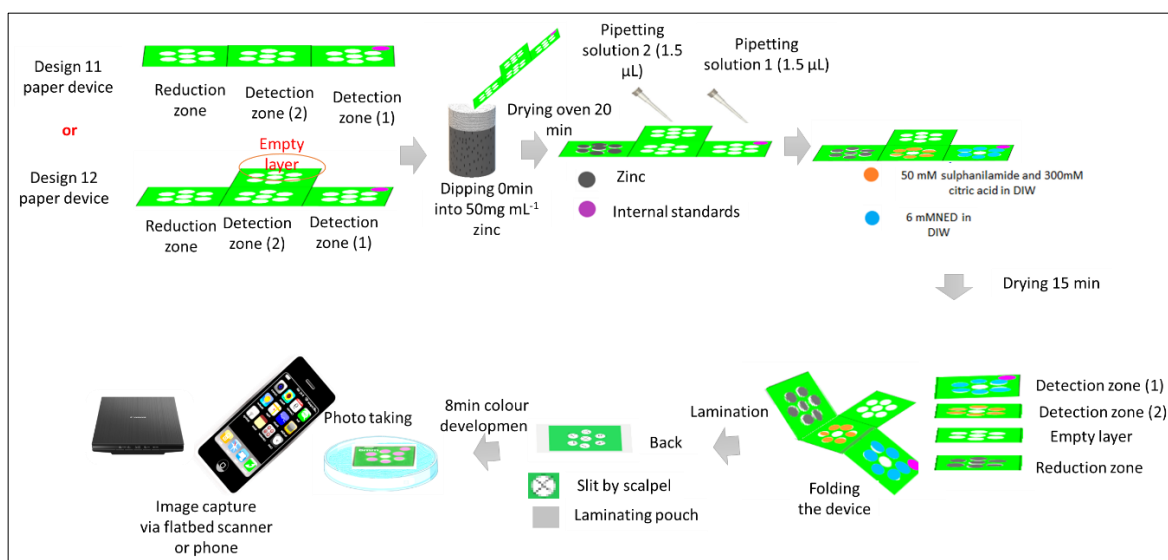
Figure 4.6 Paper device (11 and 12) modification for nitrate detection. The zinc solution was into the reduction zone by immersion. Zinc solution was added to all circles in the reduction zone. It was then allowed to dry in the oven for 20 minutes at 40 °C. After drying 1.5 µL Griess reagents were added to the detection zone 1 and 2 (all circles except the negative control). The device was allowed to dry for 15 minutes. The device was folded. The folded device was laminated in laminating punch by a laminator at 80 °C. Slits were made in all circles using a scalpel. The device was dipped in standard/sample (nitrate) for 8 minutes. A photo was taken by phone camera (Samsung Galaxy S8) or scanner, and it was analysed by Image-J (method 2) and pink colour was used as internal standard. vice modification

4.2.4 Reducing Agent Optimization

The major difference between nitrate and nitrite detection is the use of zinc solution as reducing agent. The device 10, 11 and 12 was optimized for the best amount of zinc suspensions which was added to the reduction zone (0-8 µL). The homogeneity of the zinc solution and its effect in the result was also investigated. Pipetting after hand shaking, pipetting after vortex, pipetting while stirring and immersing while stirring were used for zinc suspensions addition into paper device. The optimized parameters are summarized in **Table** 4.2.

Table 4.2 Optimized volume range and homogenization method for zinc suspensions added in the paper device (10, 11 and 12) where 500 and 1000 µM nitrate standard was used in the optimization.

Optimized parameter	Ranges/options
Amount of zinc solution	0-8 µL
Method of homogenization	Pipetting after Handshaking (1minute) Pipetting after vortex (30 seconds) pipetting while stirring immersing while stirring

4.2.5 Calibration curve

0-1000 µM of nitrate standards were used to run the calibration curve. Paper device 12 was modified as mentioned in **Figure** 4.6. Limit of detection, limit of quantitation. Phone and scanner were compared.

4.2.6 Interference studies

Sodium, Potassium, chloride, phosphate, Manganese (II), sulphate, carbonate, Iron (II), Calcium. Zinc, and Cupper (II) ions were studied for their interference for nitrate detection. The interference was determined by analysis of 600 µM of nitrate alone and then analysis of a mixture of the interferent with 600 µM of nitrate as in **Figure** 4.7. The concentration of the interference was lowered and raised until the lower concentration that caused interference was found. PAD design 12 and a scanner were used for the detection. The intensity from the two detections was compared. The change in the intensity indicates interference.
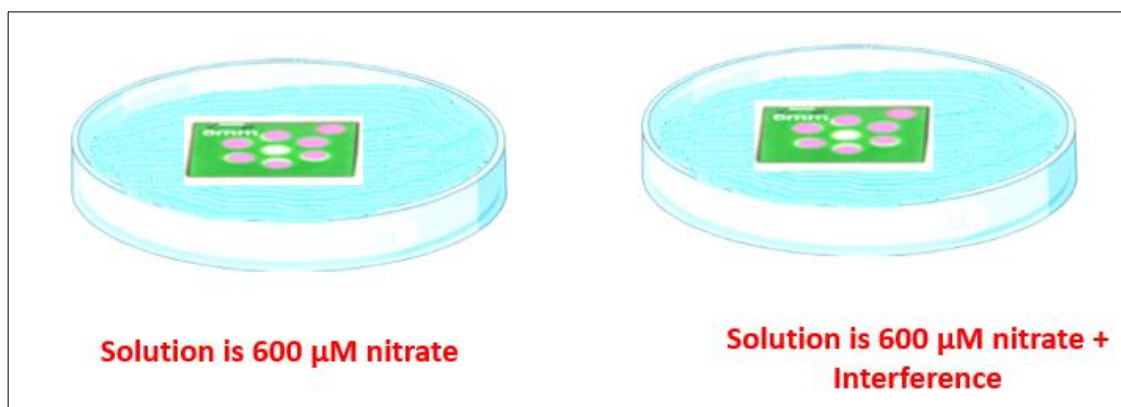
Figure 4.7 Interference studies for nitrate detection. The nitrate was detected alone as in right of figure using device 12. The nitrate and specific concentration of interference was detected together as in the right side of the figure. Scanner was used for the detection. Method 2 was used for the calculation. 600 µM of Nitrate was used in the analysis.

4.2.7   pH effect

Device 12 was used for pH studies. Calibration lines for Nitrate (0-800 µM) were determined at different pH, 4, 5,7 and 8, 10. The nitrate standards was prepared in 25 µL DIW. The pH was adjusted by 1% NaOH and 1% HCL. 3510 pH meter (JENWAY) was used to measure the pH.

4.2.8   Stability studies

The stability of device 12 which was modified as in **Figure** 4.6 Error! Reference source not found. was determined over time (54 days) at different storing conditions, out at room temperature (21 ^{0}C) in the light, out at room temperature (21 ^{0}C) in the dark, and in the freezer (-4 ^{0}C) in the dark. 0 and 600 µM of nitrate were used for the study.

4.2.9   Soil treatment

Soil samples

Three types of commercial compost were utilized in this study; John Innes No 1 (young plants compost), John Innes No 2 (potting on compost) and John Innes No 3 (mature plants compost), all were from wetland store via Westland store, amazon. Real soil samples were also studied including commercial topsoil samples with no nutrient addition (topsoil 1) from Westland store, amazon and topsoil samples from Arable farmland (topsoil 2), Hull Yorkshire, Hull (Rooting zone, 0-15cm depth). Soil CRM (Product no.: SQC013-30G) was purchased from Sigma Aldrich.

Devices for extraction

Cafetiere

Cafetiere (French Press Coffee Maker, 1 L, Bodum) was used to extract analyte (nitrate) from soil sample with the help of deionized water. The device consisted of a cup, spiral plate, filter plate, cross plate and plastic led which was attached to a piston. The device parts are in **Figure** 4.8. Piston was used to press the soil down the cup. Spiral plate filtered very large particles. Filter plate filtered smaller particles. The cross plate was used to hold the other two plates.
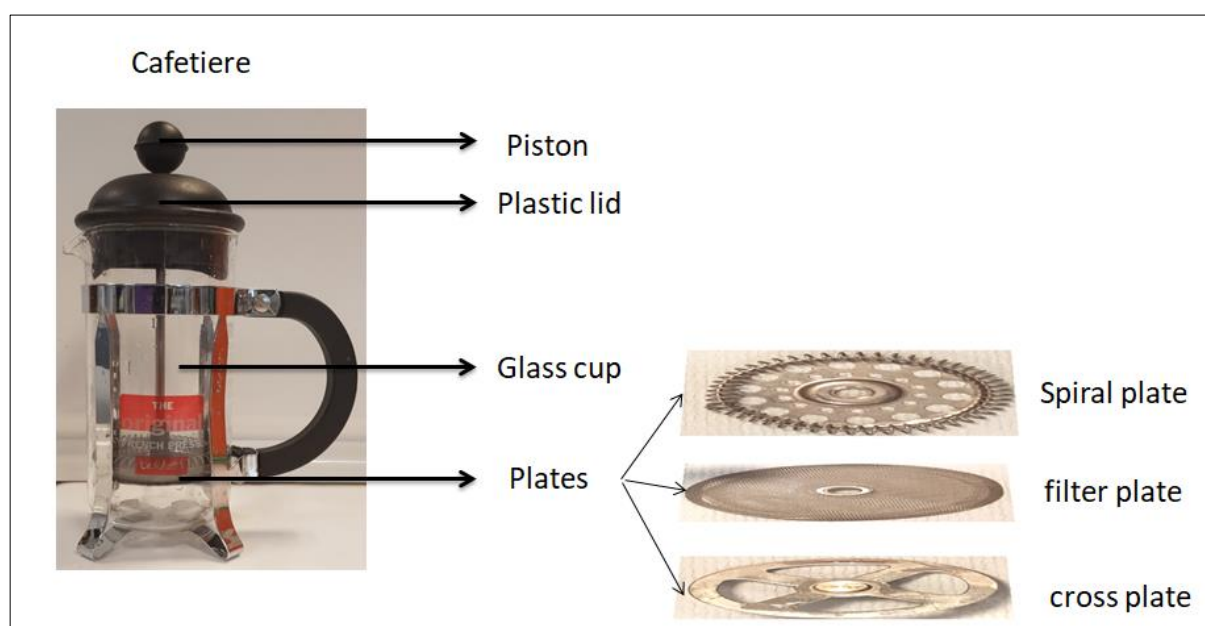
Figure 4.8 Cafetiere (volume, 1L) coffee maker parts. Is consisted of a glass cup, plastic lid which was connected to piston and 3 plates. The plates are spiral plate, filter plate and cross plate. Spiral plate filter very large particles. Filter plate filtered smaller particles. The cross plate was used to hold the other two plates.

AeroPress

AeroPress (black, 0.5 L. plastic, AeroPress brand) consisted of a piston and a plastic cup which was attached to filter where a filter paper (TKC81R24, AeroPress brand) can be used. **Figure** 4.9 shows the parts of the AeroPress.
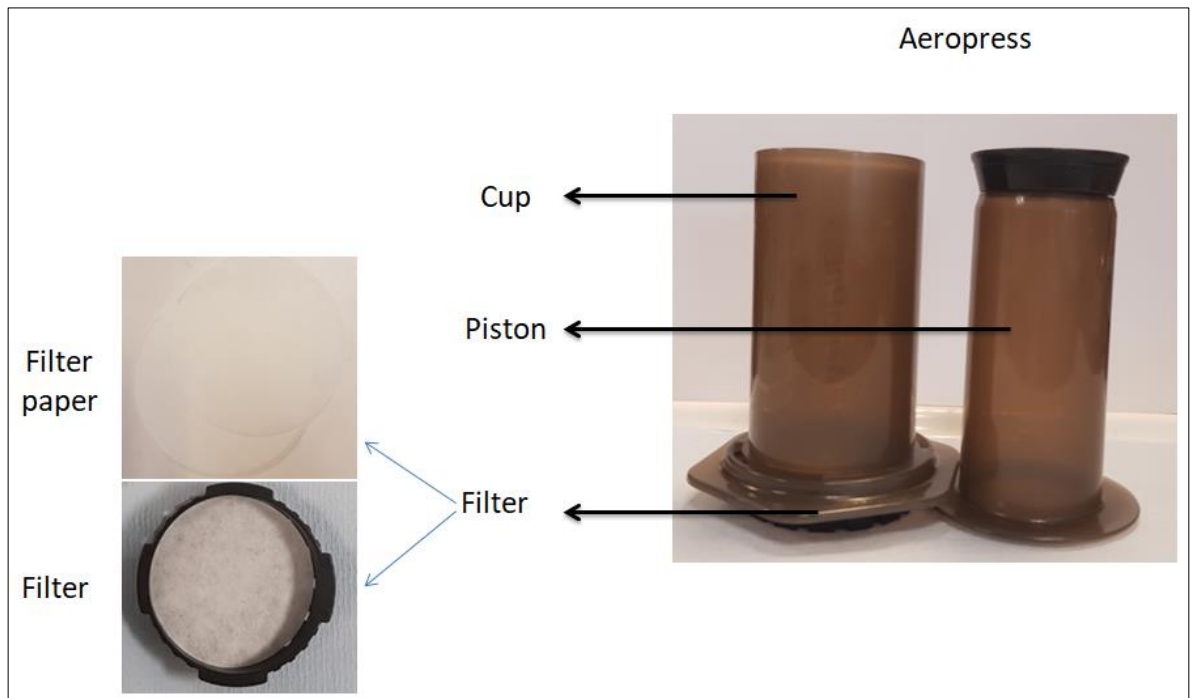
Figure 4.9 AeroPress parts. It consisted of a plastic cup to add the sample, piston which was used to press against the sample and filter. The filter can be attached to filter paper.

Paper cup

Paper cup (0.5 L) consisted of the cup itself and the plastic lid. The open in the plastic lid was covered with tape for the purpose of shaking. **Figure** 4.10 shows the paper device.
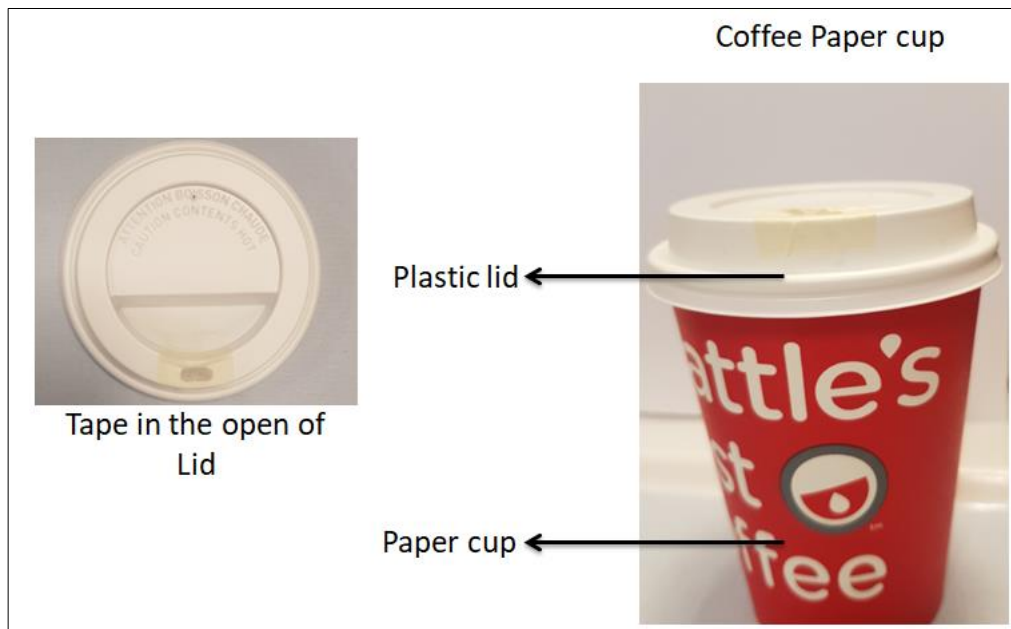
Figure 4.10 Coffee paper cup (0.5 L) with aplastic lid. Tape was used to cover the open of lid for the purpose of shaking.

The work of extraction devices

Cafetiere

Soil sample was added into the cafetiere cup (1 L). 100 mL deionized water (DIW) was then added into the sample. The cup was covered by the plastic lid. The plastic led was attached to the piston and the three plates (spiral, filter and cross). The piston then was pressed against the soil water mixture. The soil particles moved down in the cup and the water with analyte was expected to move up. The soil extract was then added to petri dish. The extract in tray was analysed by device 12. **Figure** 4.11 shows the process of extraction in cafetiere.
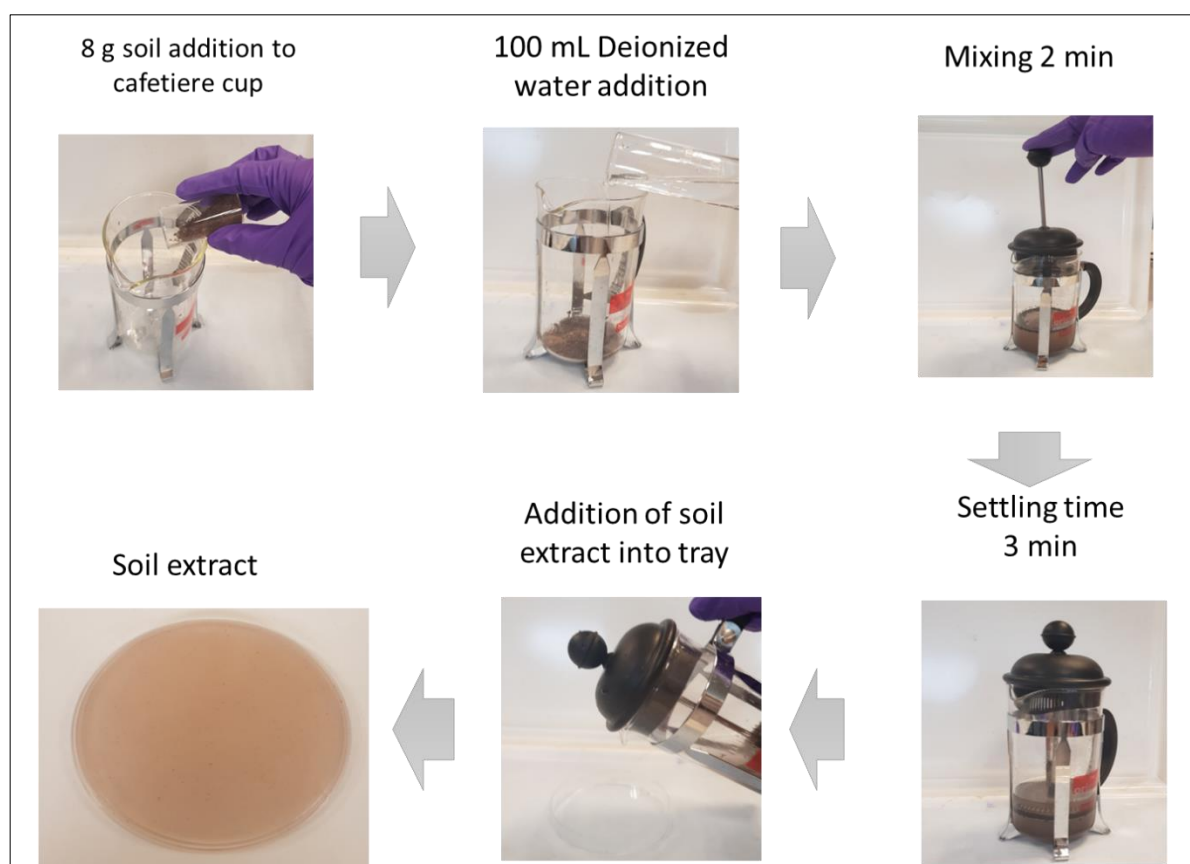
Figure 4.11 Steps for analyte extraction from soil by cafetiere. Soil sample was added into the cup. Deionized water was added to the soil. Piston (attached to plates and lid) was pressed against water & soil mixture. A time of 3 min was given for extraction. Then soil extract was transferred into a petri dish for detection of analyte. Device design 12 was used for analysis of soil extract.

AeroPress

8 g of the sample was added to the cup of AeroPress after fitting the filter and filter paper. 100 mL of deionized water was then added. The extraction was allowed for three minutes. During these three minutes drops of solution filled into the petri dish with time. The Piston was pressed once the three minutes was over. Parameters were chosen randomly based on the initial experiment to estimate the amount of nitrate, the most important, they are the same with the three extraction devices.

The final extract was analysed by device 12. **Figure** 4.12 shows the complete process of extraction.
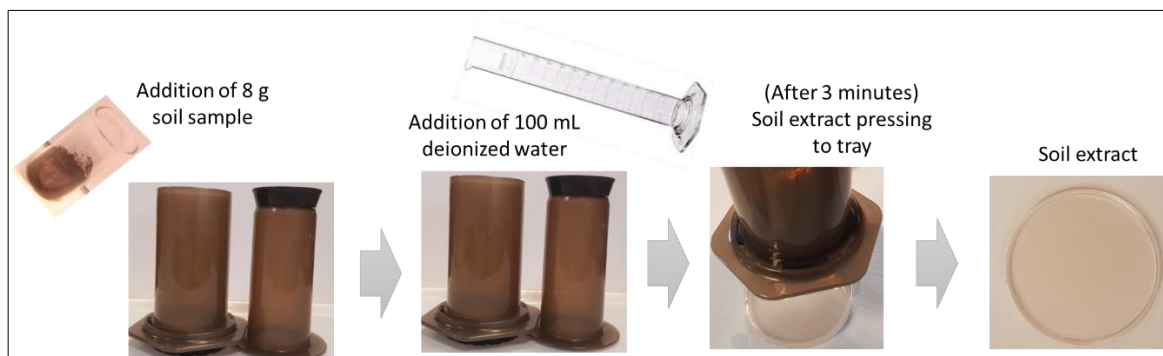
Figure 4.12 Extraction of nitrite from by AeroPress. 8 g of the sample was added to the cup of AeroPress. 100 mL deionized water was them added. The extraction was allowed for three minutes. Soil extract was added into try for analysis by device 12.

Paper cup

8 g of soil sample was added to the paper cup. 100 mL of Deionized water was added then. The cup was covered with a plastic lid. The opening of the plastic lid was covered by tape. The cup was shaken for 2 minutes, and it was allowed to stand for 3 minutes to separate soil particles from the water. The extract was then added to a petri dish for analysis by device 12. The extraction process is in **Figure** 4.13.
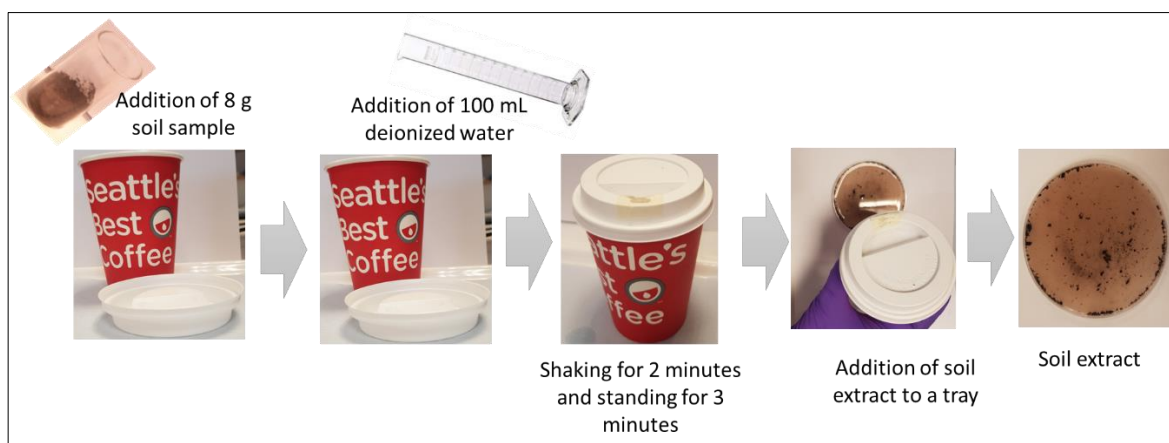
Figure 4.13 Paper cup device for nitrite extraction from soil. 8 g of soil sample was added to the paper cup. 100 mL of Deionized water was added then. The cup was covered with a plastic lid. The open of the plastic lid was covered by tape. The cup was shaken for 2 minutes, and it was allowed to stand for 3 minutes. The soil extract was analysed by device 12.

Test for the efficiency of extraction devices

8 g of sample was extracted with 100 mL of deionized water using the three methods of extraction. A blank device (device 12, the last chosen optimized device) without any modification was laminated and dipped into each of the extracts and deionized water. The resulting intensity of PAD from each extract was compared to the intensity of PAD dipped in deionized water.

Optimization of cafetiere extraction

The use of cafetiere as extraction method was optimized for the mass of soil, volume of solvent and the number or times of pushes. John Innes no1 soil was used for the optimization purpose. The starting volume was 100 mL with one push and 3 minutes of waiting (steps as in **Figure** 4.11). The mass of soil was optimized in the range of 3-9 g of soil. This was followed by optimization of the extraction solvent (DIW) 100-200 mL. The number of pushes was then optimized in the range 1-6 pushes. The time of pushes instead of number of pushes was optimized from 0-3 minutes. After the pushes there will be 3 minutes for the soil to settle to ensure good separation. The optimized parameter as in **Table** 4.3 .

Table 4.3 Cafetiere optimized parameter (mass, volume, push time)

Optimized parameter	Range
Mass	3-9 g
Volume of DIW	100-200 mL
Number of pushes	1-6 push
Time of push	0-3 minutes

Soil analysis with cafetiere extraction

8 g of soil was added to the cafetiere, and this was followed by the addition of 100 mL of DIW. The cafetiere was pushed up and down for 2 minutes. The soil was then allowed to settle for 3 minutes. 25 mL of the extracted solution was analysed by PAD (phone/scanner) and 10 mL was analysed by IEC after filtration with a 0.22µm filter. Also, a Spoon was used to measure the mass of soil instead of the use of balance since the spoon is much easier to use by people or in the

field. 4 spoons were equivalent to 8 grams. The tap water and mineral water were tested as a solvent instead of DIW. **Table** 4.4 summarizes some of the studied parameters.

Table 4.4 studied conditions for the Way of measuring the mass, type of solvent and detection method.

Parameter	The comparison
Way of measuring the mass	Spoon, balance
Type of solvent	DIW, tap water, mineral water
Detection method	IEC, PAD scanner, PAD phone

Soil analysis by conventional extraction

John Innes 1, 2 and 3 were analysed by conventional extraction [403,423]. 8 g of soil in 100 mL of DIW was Shaked in the shaker for 1 hour, the soil then was centrifuged at 4500 rpm. 25 mL of the extracted was analysed by the PAD and 10 mL of it was analysed by IEC (after filtration with 0.22μm filter).

Soil organic matter content

3 g of soil was weighed in a crucible which was pre-weighed. The soil was placed in the furnace at 300 C for 30 min. After ignition, the soil was allowed to cool in a desiccator for 5 minutes. the weight of the crucible and the soil were then determined. The % organic matter was then calculated as in equation 4.1.

$$\% organic\ matter = \frac{weight\ loss\ during\ ignition}{mass\ of\ soil} \times 100\% \quad \text{eq. 4.1}$$

4.2.10 Palintest Commercial kit for soil nitrate detection

The water was initially added to the sample container. The blue scoop was used to add one scoop of N powder. This is followed by adding two white scoops of soil. The mixture was mixed for 1 minute. The extract was filtered then. 10 mL of the extract was transferred to the test tube. 1 tablets of Nitricol N tablets were dissolved and crushed into the solution. The mixture was stood for 10 minutes for colour development. N test was then chosen in the photometer to determine N in mg L^{-1}.

4.3 Result and Discussion

4.4 Conventional method for nitrate detection

4.4.1 UV-Vis

Nitrate detection was based into two steps as in **Equation 2.1 and 2.2**. The first step is reduction of nitrate to nitrite by reducing agent (zinc was used in this study). The second step is the detection of nitrite by Griess reagent as in **Section 3.4.1**. The optimization of the detection step was done already in **Section 3.4.1**. The reduction step was optimized by changing the mass of reducing agent, pH of the solution and the method of zinc filtration after reduction as in **Appendix C**. However, the method was not promising.

Problem with detection of nitrate by UV-Vis

The zinc particles are too small ($\leq$10 µm) to be filtered and any remaining zinc may interact with the acid in the Griess reagent leading to reduction in the absorbance. The particles size was changed to bigger size; however, this reduces the efficiency of the reduction. In addition, the standard deviation is high and there are some variations from experiment to experiment or from day to day. Therefore, IEC was used instead for nitrate detection.

4.4.2 Ion exchange chromatography

4.4.2.1 Optimization

Optimization was the same as in **Section 3.4.2** for nitrite since they were optimized together.

4.4.2.2 Calibration line

The optimum conditions were used to run the calibration line for nitrate to determine the limit of detection of the method and its reproducibility. The calibration line was determined for several concentrations as in **Figure** 4.14. it was found to be in the range of 30-10000 µM nitrate. At around 10000 µM of nitrate the peak started to show a bit of bend and hence 10,000 µM of nitrate was the last point in the calibration line. The R^2 was around 0.99 and this indicated the fitness of the point to the line. The LoD was around 2.63±0.14 µM (0.163 mg L^{-1}) and LoQ was around 8.78±0.48 µM (0.544 mg L^{-1}). LoD and LoQ were calculated as in **Equation 2.5 and 2.6** respectively. The method was reproducible as in **Figure** 4.14 which shows the peak area versus the concentration of nitrate in µM for three calibration lines. **Table** 4.5 summarized LoD and LoQ for the three calibration lines with RSD less than 6%. The method was reproducible; however, it was calibrated with each run to avoid any variation which may happen in the calibration curve from day to day. The result was similar to some of the result in the literature [424] and lower than some [425]. However, the limit of detection of the optimized method meets the requirement since the aim is to detect nitrate in soil and the good level of nitrate in soil is mainly around 92.93 mg

kg^{-1} [348,426,427]. Below 44 mg kg^{-1} fertiliser is required to be applied [348,426,427], this value is higher than the LOD (2.63±0.14 µM (0.163 mg L^{-1})), if 8 g of soil and 100 mL of soil is used.
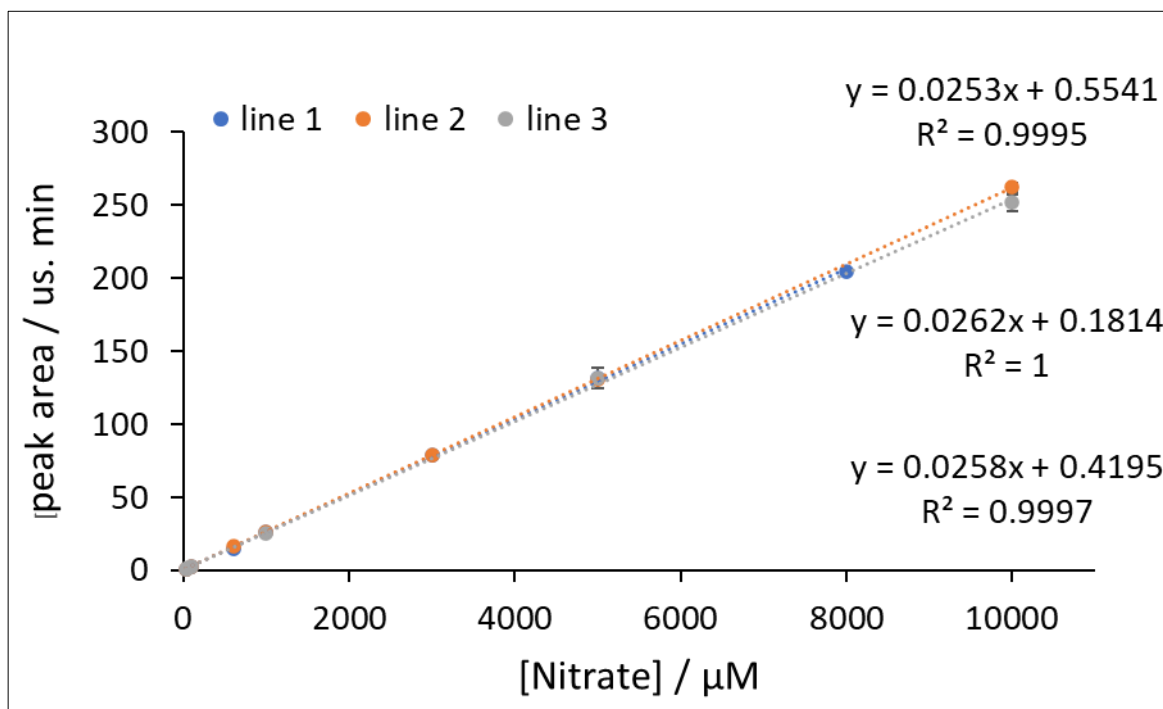
Figure 4.14 The peak area versus the concentration of nitrate in µM. The lines from IEC were run at three different days of the month.

Table 4.5 LoD, LoQ, R2 and slope for calibration lines of nitrate from IEC. LoD and LoQ were calculated as using **Equation 2.5 and 2.6**.

	line1	line 2	line 3	average	RSD (%)
LoD (µM)	2.50	2.61	2.79	2.63±0.14	5.51
LoQ (µM)	8.34	8.704	9.29	8.78±0.48	5.51
R^2	0.9995	1.0000	0.9997	0.9997±0.0003	0.03
slope	0.0253	0.0262	0.0258	0.025±0005	1.75

4.5   Paper microfluidic device for nitrate determination

The same device, which was used to analyse nitrite in chapter 3, it was also used to analysed nitrate. At this stage the reduction of nitrate to nitrite was needed. Zinc powder ($\leqslant$ 10 μm particles size) was used for this purpose. This size of zinc particle was used based on previous study [290]. The aim was to deposit these particles in the paper device in small amount, μL amount. The smaller the particle the higher the surface area and the more the interaction of the reagent with the surface. As result, reduction efficiency of nitrate to nitrite is expected to be significant and hence small zinc particles were used in this experiment.

4.5.1   Reduction time optimization

Reaction time control was necessary to direct the reaction, increase the sensitivity and ensure reproducibility. Therefore, the reduction time of nitrate was first studied. After the addition of the reagents into the device and without lamination the nitrate was added to the reduction zone. It was allowed to be reduced for a specific time. Then it was detected in the detection zone by folding the paper. The reduction time was controlled by opening and closing the folded paper according to the time needed. The colour then was allowed to develop to total time of 5 min since 5min was the optimum time for colour development according to **Table** 3.9. The steps for reduction time optimization as in **Figure** 4.15.
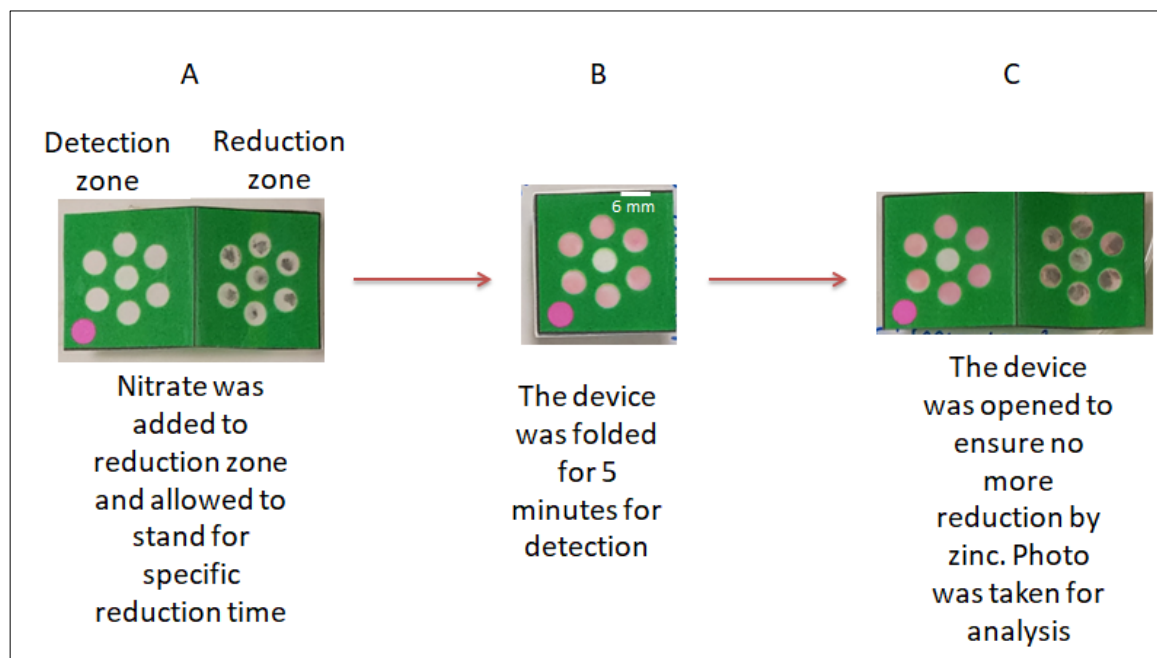
Figure 4.15 Steps for reduction time optimization in device 10. 1000 μM nitrate standard was used. 2 μL zinc (50 mg mL⁻¹) was added to the reduction zone. 1.5 μL of Griess reagent was added to the detection zone. After drying, the paper was folded and 7 μL of the standard was pipetted to the reduction zone. The reduction time was controlled by folding the paper according to the time needed. Then the colour was allowed to develop for total time of 5 minutes

The result of the reduction time study was as in **Figure** 4.16 and the optimum reduction time seems to be after 4 minutes. The result suffered from high relative standard deviation higher than 5% and fluctuation in the signal was observed. This was maybe because the folded device was opened to take the photo for the analysis and some of the colour was lost in the reduction zones (**Figure** 4.15 **C**) and hence this step was not same each time experiment was done. Therefore, the device 10 (modified as in **Figure** 4.4) was laminated and reduction and detection were performed together at the same time. In addition, the amount of zinc was increased from 2 μL to 4 μL to ensure good and clear reduction. The sample was introduced this time by dipping same as in the previous chapter 3. The result in **Figure** 4.17 shows significant decrease in the standard deviation. The intensity remains constant from 5 to 14minutes. Consequently, 5 minutes is the total optimum time for reduction and detection. However, to avoid any change in reaction time that might happen during optimization, 14 minute was used as reaction time since it is within the stable range.
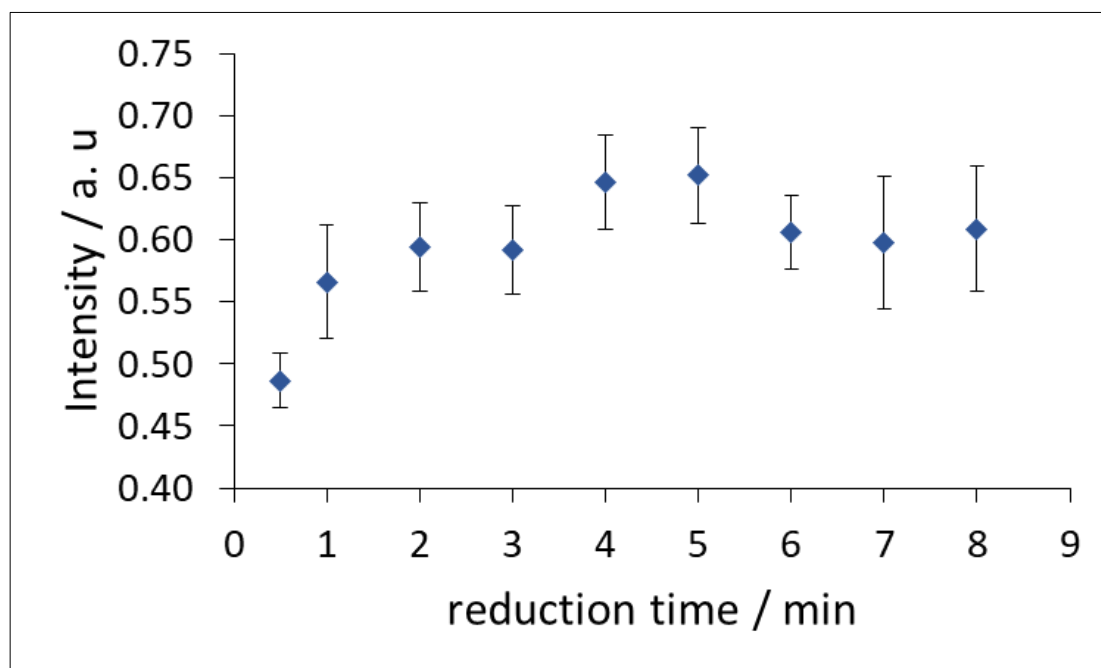
Figure 4.16 Intensity versus time of reduction (minutes). 1000 μM nitrate standard was used. 2 μL zinc (50 mg mL^{-1}) was added to the reduction zone. 1.5 μL of Griess reagent was added to the detection zone. After drying, the paper was folded and 7 μL of standard was pipetted to the reduction zone. The reduction time was controlled by folding the paper according to the time needed. Then the colour was allowed to develop to total time of 5 minutes. The optimum reduction time seems to be 4 minutes. device 10 was used in this study. Photo was taken using Samsung phon. The photo was analysed using Image-J software (method 2).
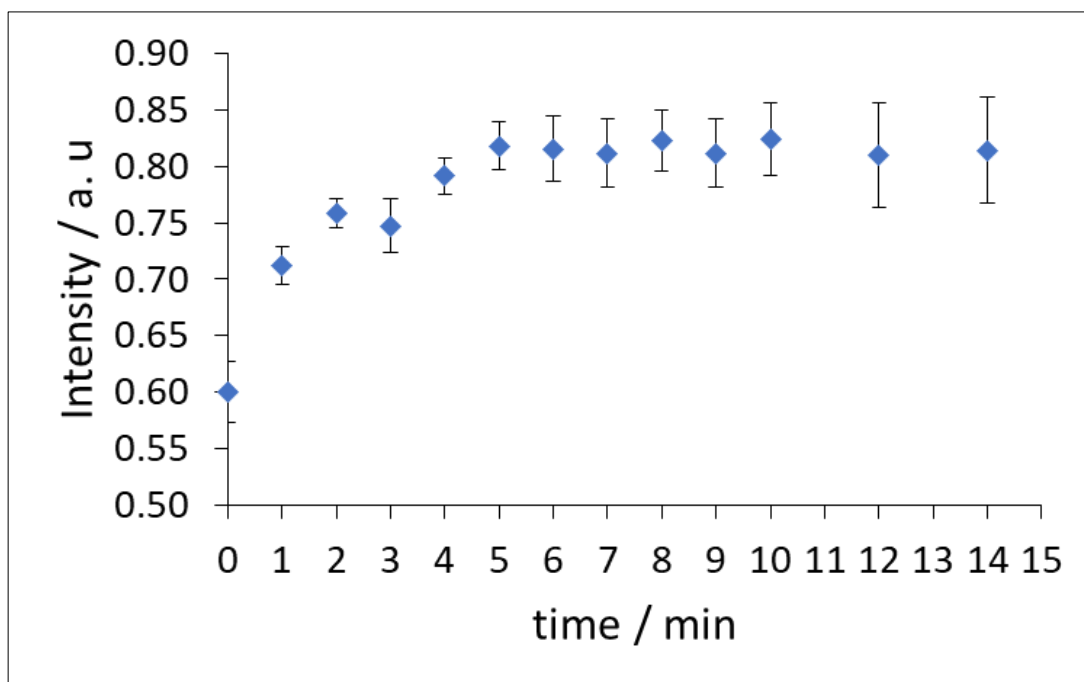
Figure 4.17 Intensity versus time (min). 1000 µM nitrate standard was used. The laminated device was dipped into the standard solution. The device has 1.5 µL Griess reagent in the detection zone and 4 µL Zinc suspensions (50 mg mL^{-1}) in the reduction zone. The Photo was taken each minute for 14 minutes. 5 minutes is the best time to get a stable signal. device 10 (modified as in **Figure** 4.4) was used in this study. Photo was taken using Samsung phon. The photo was analysed using Image-J software (method 2).

4.5.2   Reducing Agent Optimization

There are several reducing agent that was used on paper device for reduction of nitrate to nitrite like vanadium chloride [295,311], enzymatic reagent [298], and zinc [290-293,296,310],. This study focus in zinc reducing agent since it is fast and easy to work with compared to other options. Zinc addition to the PAD is challenging especially for our developed PAD since all the reaction zones above each other including the zine, where also the detection colour develops. Zinc has dark black colour which can participate in the intensity if it is too dark. Most of publish work relied on pipetting the zinc solution into the specific zone [290,291,293,298,310], however, some of these PADs [290,291,293] had separated area for the reduction zone which was not aligned above the detection zone and this make it possible to add zinc with its dark colour without influencing the intensity of colour in the detection zone. **Table** 4.6 summarize the PAD information about reduction area and reducing agent, reducing agent addition and the reduction efficiency. In another study another layer was added to the PAD [295], the layer was called Zinculose and it was embedded zinc particles in cotton layer. This was practical to keep the zinc embedded within the reduction area of the device and it provided 27% reduction efficiency. However, this is still required a lot of work and preparation of the material which then will be added to the PAD. In addition, still the same problem exist which is still it is unknown how much zinc is there. It is impossible to know how much zinc papricles were added into the paper since it was added as solution where it is unknown exactly how much it was transferred. In Ferreira et al. work each well in the PAD was added to zinc

solution and this followed by weighing of the well before and after the zinc addition [296]. This is not practical and require time. This method means that the well should be weighed until acceptable weight range is achieved. Here several approaches were studied for zinc addition into the PAD (addition by pipetting and addition by immersion), in addition to the PAD restructure based on the adopted method.

Table 4.6 PAD information about reduction area and reducing agent, reducing agent addition and the reduction efficiency.

sample	Reduction area	Reducing agent / its addition	Reduction efficiency %	reference
Water two layers	Separated from the detection area	Zinc/pipetting	20	[290]
Food channels	Separated from the detection area	Zinc/pipetting	-	[291]
Water two sides	Separated from the detection area	Zinc / External layer (Zinculose)	27	[295]
saliva	Aligned with the detection area	Zinc / External layer of zinc (weighed before and after)	-	[296]
food	Aligned with the detection area	Vanadium/pipetting	-	[293]
Food channels	Separated from the detection area	Zinc/pipetting	-	[292]
Urine circles	Aligned with the detection area	Enzymatic reagent/pipetting	-	[298]
Water circles	Aligned with the detection area	Zinc/pipetting	-	[310]
Water circles	Aligned with the detection area	Vanadium/pipetting	27	[311]

4.5.2.1 Zinc addition by pipetting after vortex and handshaking

The amount of zinc added to the reduction zone was crucial step to design an effective device. High amount of zinc may lead to over reduction of nitrite to less oxidation state like ammonium [428]. However, small amount of zinc is not enough for reduction of nitrate to nitrite. Optimum amount of zinc was determined by varying the amount of zinc which was added to the reduction zone as in **Figure** 4.18. Overall, as the amount of zinc increased the intensity increased until it reached maximum and then started to decrease again. The intensity was compared to the molar ratio. The optimum zinc volume was 2 μL with 0.0046 molar ratio (NO_3^-/Zn). The optimum molar ratio further low than the normal ratio which is 2 according to **Equation 2.2** and this mean more zinc was added in practical work compared than needed from calculation. This indicates that not all the zinc participated in the reduction and this what other literature showed too [290].
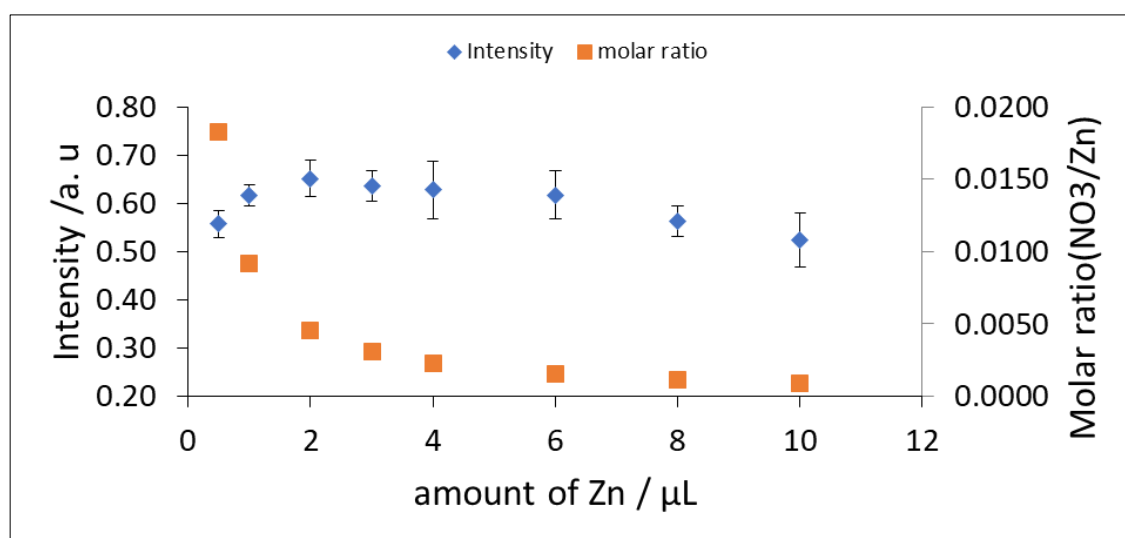
Figure 4.18 Intensity and molar ratio versus the amount of zinc (μL). 1000 μM nitrate was used. Two side paper device design 10 was used (modified as in **Figure** 4.4/ pipetting sample introduction). In one side 1.5 μL of the detection reagent was added (Griess reagent) (10 min drying) and in the second side specific volume of zinc was added (50 mg mL^{-1}) (10 min drying). Then 7 μL of nitrate standard was added to the reduction zone. 5min was taken for reduction and colour development. Finally, photo was taken using Samsung phon. The photo was analysed using Image-J software (method 2).

Therefore, the calibration curve for nitrate was plotted when the optimum zinc amount (2 μL) was used. **Figure** 4.19 shows the calibration curve for nitrate. It was clear that the linearity was missing, the curve seemed to be linear up to 400 μM of nitrate and this indicated that there was not enough amount of zinc to reduce nitrate at higher concentration higher than 400 μM. The reason for this inconvenient result maybe the homogeneity of zinc solution. Small zinc particles have the tendency to stack in the wall of container during the solution preparation and hence

not the right amount was added to PAD. Also, there is possibility for coagulation of the particles to happen. Consequently, the amount of zinc added to each device or even each circle was not the same. **Figure** 4.20 shows device when 6 µL of zinc was added to the reduction zones. The zinc deposition was not homogeneous and clearly the amount of zinc in the circles is different even though same amount of zinc was added.
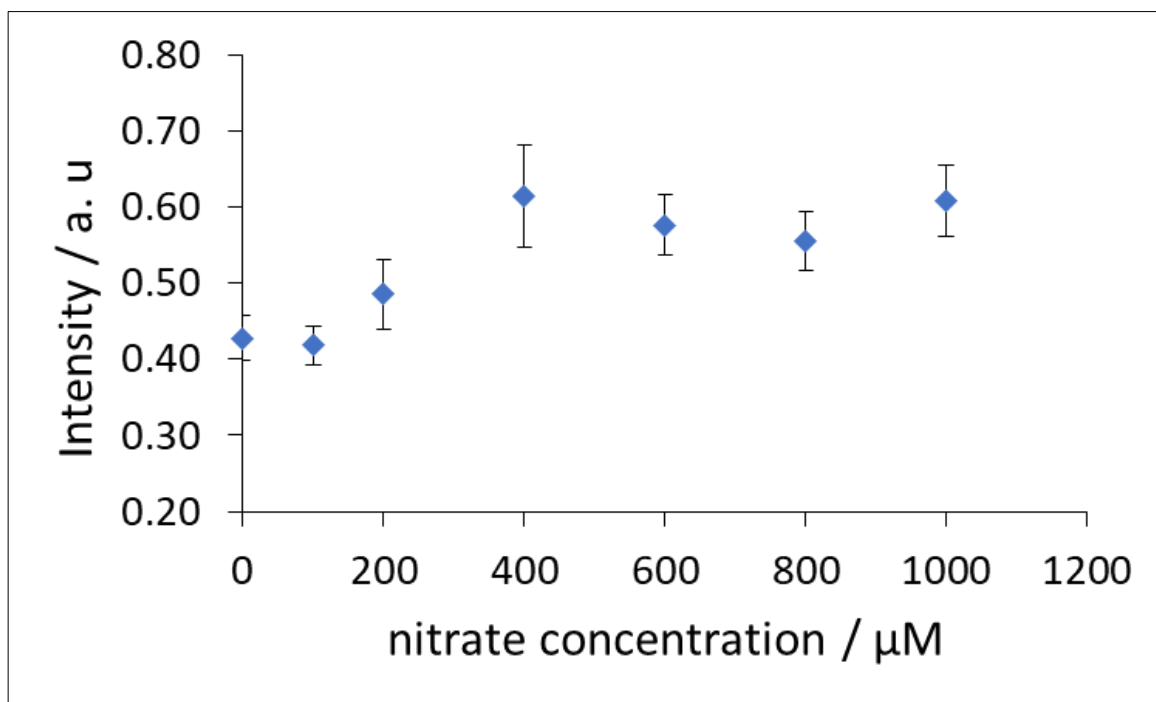
Figure 4.19 Intensity versus concentration of nitrate (µM). Device 10 was used in this study (modified as in **Figure** 4.4 / pipetting sample introduction). Photo was taken using Samsung phon. The photo was analysed using Image-J software (method 2).
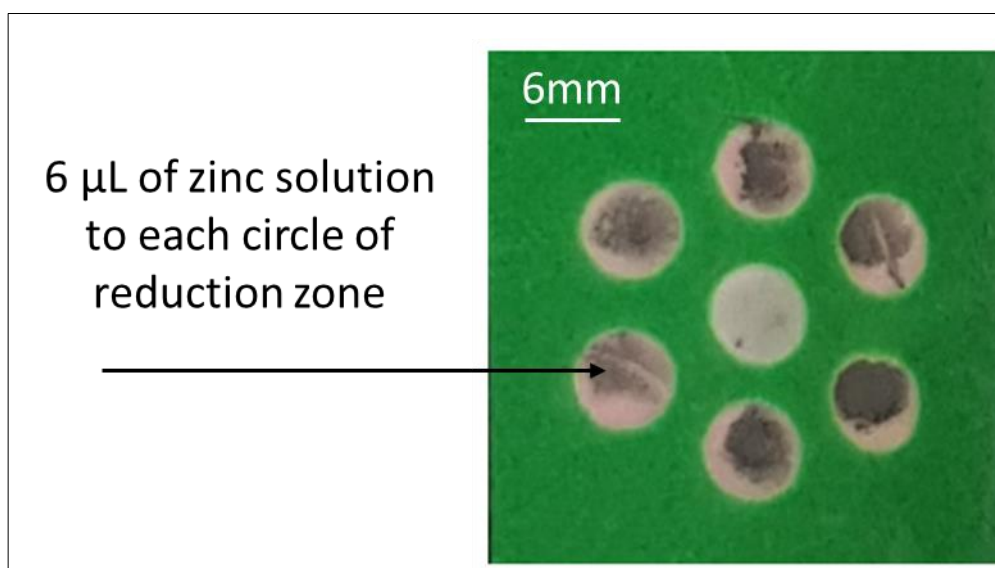
Figure 4.20 Circles in the reduction zone after the addition of 6 µL of zinc by pipette.

The homogeneity of zinc particles was improved by vigorous hand shaking and vortex. **Figure** 4.21 shows the optimization of the amount of zinc when the zinc solution was shaken by hand for 1 minutes. The trend was totally different than **Figure** 4.18. The intensity increased with the increase of zinc until it became constant and finally decreased at high amount of zinc. The gradual increase at the beginning may be because there was not enough zinc to react with analyte. The constant range means there was enough zinc to react with analyte. Finally, the decrease in the signal maybe because some of produced nitrite was also reduced to lower oxidation state. This result means (constant range of zinc) that the hand shaking has significant effect on the result since it reduced the coagulation of zinc particles and increased the homogeneity of the solution compared to **Figure** 4.18. The optimization was done twice to ensure the reproducibility. In addition, at this stage dipping system had introduced her for sample introduction instead of pipetting. The device was laminated, and this helped to keep the zinc particles within the device and reduce their removal from the device during sample addition. Dipping made the process of sample addition easy and ensure that the sample inter the wells at the same time since pipetting means adding the sample to wells well by well. This helped to reduce variation in result.
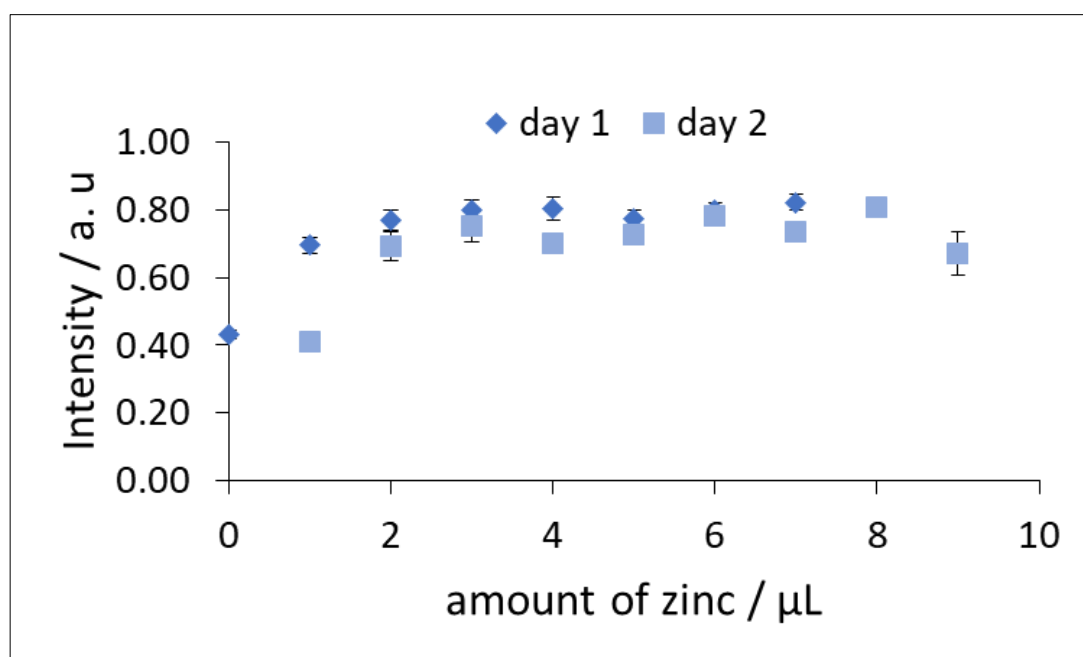
Figure 4.21 Intensity l versus amount of zinc (µL). 1000 µM nitrate standard was used. 1.5 µL Griess reagent was added to the detection zone (10 minutes drying). The zinc was added to the reduction zone after 1 minute of handshaking (10 minutes of drying). The laminated device was dipped in the solution and a photo was taken after 14 minutes. The experiment was performed on two different days to determine how stable was the result. The results from day one and two showed some variation. Device 10 was used in this study (modified as in **Figure** 4.4/ dipping sample introduction). The photo was taken using a Samsung phon. The photo was analysed using Image-J software (method 2)

Vortex was also used to improve the homogeneity of the solution and the result as in **Figure** 4.22. The zinc was added to the device after 30 seconds of vortex. The reproducibility of the result was checked by doing the experiment twice (**Figure** 4.22). **Figure** 4.23 shows photos which were a result from **Figure** 4.22. 4 µL and less of zinc gave less homogeneous colour due to the non-homogeneous distribution of the zinc in the reduction zone. Therefore, volume 4 µL and less of zinc solution was not used as optimum. Volume 5, 6 and 7 µL of zinc gave homogeneous colour in the detection zone because of homogeneous distribution of zinc in the reduction zone after the vortex. 6 µL was chosen to be the optimum volume because it was in between the two volumes where at more or less than these two volumes a variation in the signal may occur. Hand shaking and vortex showed similar trend and similar intensities, therefore for easy use vortex was used since it is easier. **Table** 4.7 summarize the optimum conditions for nitrate detection.
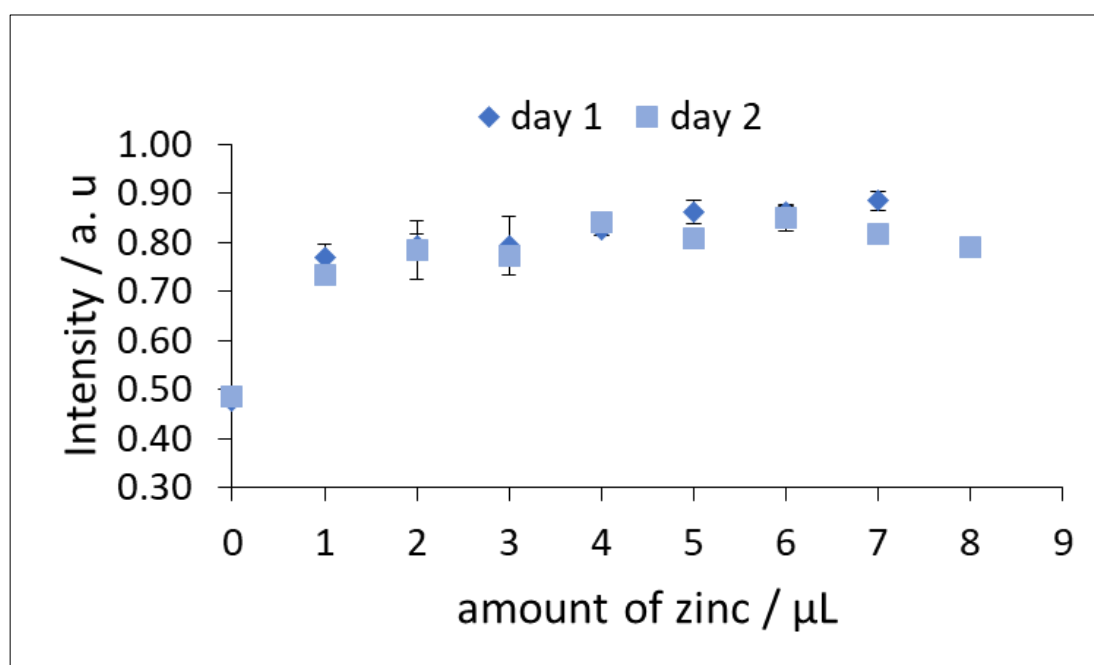
Figure 4.22 Intensity versus amount of zinc (µL). 1000 µM nitrate standard was used. 1.5 µL Griess reagent was added to the detection zone (10 minutes drying). The zinc was added to the reduction zone after 30s of vortex (10 minutes drying). The laminated device was immersed in the solution and photo was taken after 14 min. The experiment was performed in two different days to determine how stable was the result. Device 10 was used in this study (modified as **Figure** 4.4). Photo was taken using Samsung phon. The photo was analysed using Image-J software (method 2).
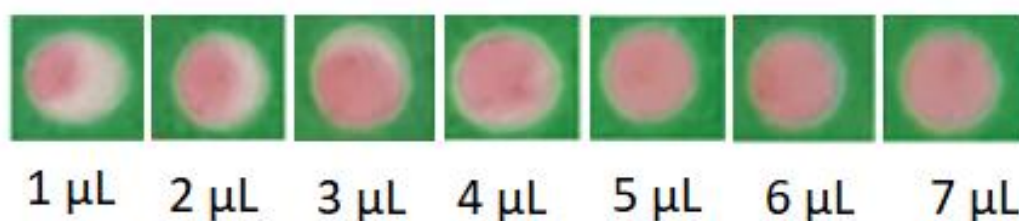
Figure 4.23 These photos are result from **Figure** 4.22. 4 µL and less gave less homogeneous colour due to the non-homogeneous distribution of the zinc in the reduction zone. Therefore, volume 4 µL and less was

not used as optimum volume. Volume 5, 6 and 7 μL of zinc gave homogeneous colour in the detection zone because of homogeneous distribution of zinc in the reduction zone. 6 μL was chosen to be the optimum volume.

Table 4.7 Optimum zinc amount, shaking method and reduction-detection time. 1000 μM nitrate was used during the optimization. Device 10 was used in this study. Photo was taken using Samsung phon. The photo was analysed using Image-J software (method 2).

Parameter	Optimum value
Zinc amount	6 μL
Shaking method	Vortex
Reduction and detection time	5 to 14 minutes

Change two layers to three layers device before further optimization of reduction agent.

The device which was finally used for nitrite detection consisted of three layers (device 11) where the detection reagents were separated to enhance the stability. Three three-layer device was also used for nitrate detection to reduce the dark colour effect (by increasing the number of layers) which was caused by zinc and enhance the stability by the separation of Griess reagent components (as mentioned in chapter 3, **Section 3.5.7**). The reduction zone was kept the same. The two devices with two and three layers for nitrate detection were compared in **Figure** 4.24. Device design 10 (modified as in **Figure** 4.4)and 11 (modified as in **Figure** 4.5) were used. The figure shows the intensity versus the type of the device used in the analysis. The signal stayed constant for the 1000 μM of nitrate. However, 0 μM of nitrate showed a lower signal when a three-layer device was used. The intensity from the blank was reduced by around 21 %. This can be explained as before for nitrite (chapter 3, **Section 3.5.7**) by the auto colour development when the detection reagents are all mixed. In addition, this reduction can be explained by the reduction in the black colour of zinc itself when the number of layers was increased. Reduction in the intensity of the blank may lead in the future to improve the steepness of the calibration line which means the increase in the slope and hence the improvement of the limit of detection of the method. Three layers device (design 11) will be used from now on for the analysis of nitrate.
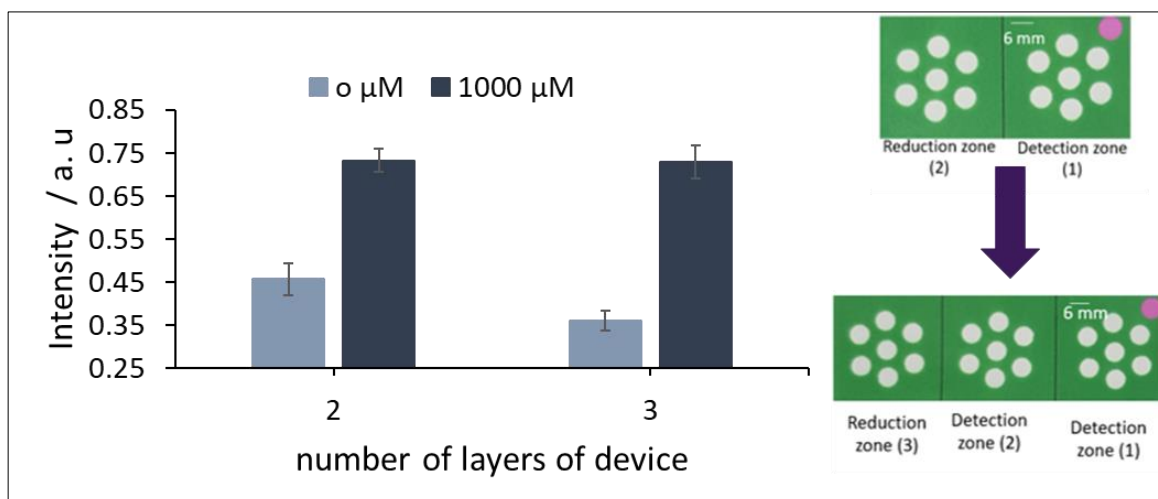
Figure 4.24 Intensity versus the number of layers in the device. 0 and 1000 µM of nitrate standards were used. Device design 10 (modified as **Figure** 4.4) and 11 (modified as in **Figure** 4.5) were used. The photo was analysed using Image-J software (method 2).

Drying condition of the reducing agent zine

The zinc suspension takes too long time to dry completerly when it is added to whatman paper. Previously it was dired for aroon 10-20 minurs, however, the paper was still wet and this can cause interaction between reagent after long time storing. Therfore, after addition of zinc suspenstion the device was dried at different temperature for 20 minutes to determine which temperature can give the best drying that does not destroy the paper or oxidized zinc itself. **Figure** 4.25 shows intensity versus temperature when three different concentration of nitrate were used in the study, 0, 600 and 1000 µM. The effect of temperature varation was not signifcant. Howevere, as the temperature increasre the intensity decrease especailly at 80 $^{\circ}$C temperature. This means that the zinc maybe oxidized due to the high temperature and hence very high temperature is not good option for drying. 40 $^{\circ}$C seems to be good option sinc the intensity was similar to the intensity when experiment was perform at room temperature.
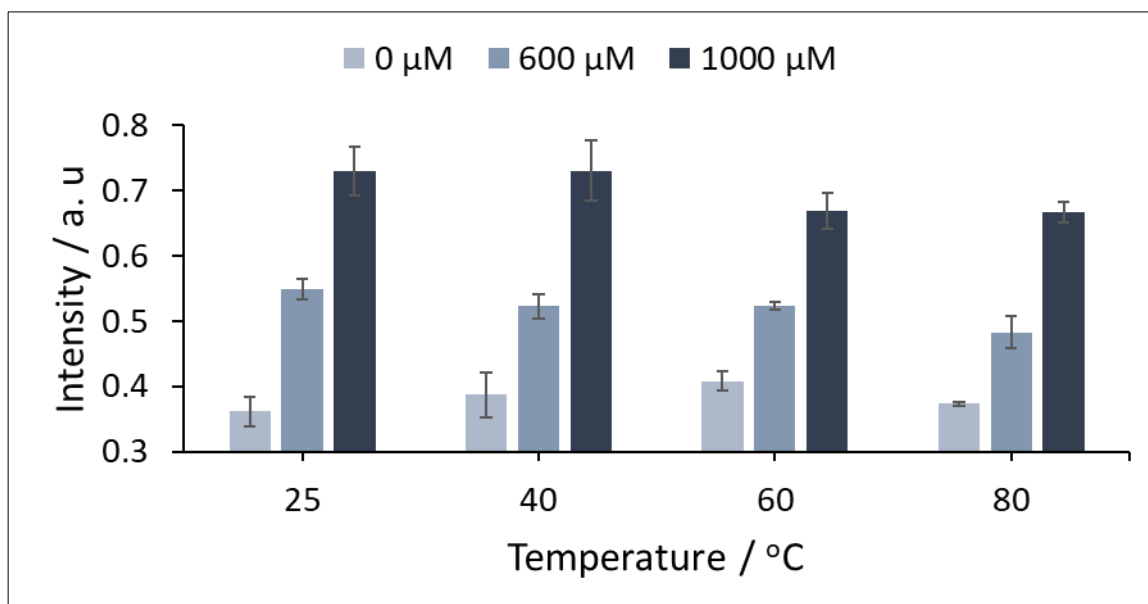
Figure 4.25 Intensity versus temperature ºC. 0, 600 and 1000 μM of nitrate standards were used. Device design 11 was used (modified as in **Figure** 4.5). Scanner was used for photo capture. The photo was analysed using Image-J software (method 2). 25, 40, 60 and 80 °C temperature were studied for zinc drying on the paper. 40 °C was choosen as optimum to avoid any oxidation for zinc at high temperature.

4.5.2.2   zinc addition by immersion

Pipetting was one method of adding zinc as it was mentioned previously as in **Figure** 4.21 and **Figure** 4.22. Solution was first vortexed and then 6 μL of the suspension was pipetted to the reduction zone. The problem with this method the accumulation of dark zinc in the PAD. If this dark colour is not constant, then this can affect the sensitivity and the confidentiality of the method. Two other methods for zinc addition were added, the pipetting while stirring and immersion while stirring. **Figure** 4.26 shows the intensity versus concentration of nitrate when different method of zinc addition was tested. For immersion method, the reduction layer of the device was immersed into the zinc suspension which is under stirring at 600 rpm as in **Figure** 4.27. stirring provide homogenous solution of zinc during the addition into the device. The immersion may destroy the device. Therefore, immersion was performed for different time as in **Figure** 4.28. 1, 30 and 60 seconds were tested. As the time increase as the device was destroyed more. 1 second of immersion was chosen to be the optimum time since it gave good intensity, and the device was not destroyed by the zinc. Adding zinc by this way offer advantages compare to pipetting the zinc, it reduced the dark colour of zinc accumulation in the device. The dark colour can affect finally the intensity of colour for nitrate detection especially for blank since it changes from time to time when zinc was added. **Figure** 4.29 showed PADs where zinc was added by pipetting and immersion. Immersion reduces the accumulation of zinc. The intensity of blank was reduced by around 22 %. In addition, immersion helped to deposit zinc in the two side of the device. The reproducibility of the immersion method was determined by doing 10 repeats for the same device with zinc immersing method as **Figure** 4.30. Even though

by immersion the amount of zinc added was unknown, the means of repeats were the same within the standard according to ANOVA test (F=1.21, $F_{ritical}$=2.07, P= 0.31, α=0.05, n=6).

Figure 4.26 Intensity versus nitrate concentration (µM). Zinc was added to the reduction zone by pipetting and immersion. Device 11 (modified as in **Figure** 4.5) was used. 600 and 1000 µM of nitrate standards were used for the analysis. Scanner was used for photo capture. The photo was analysed using Image-J software (method 2).
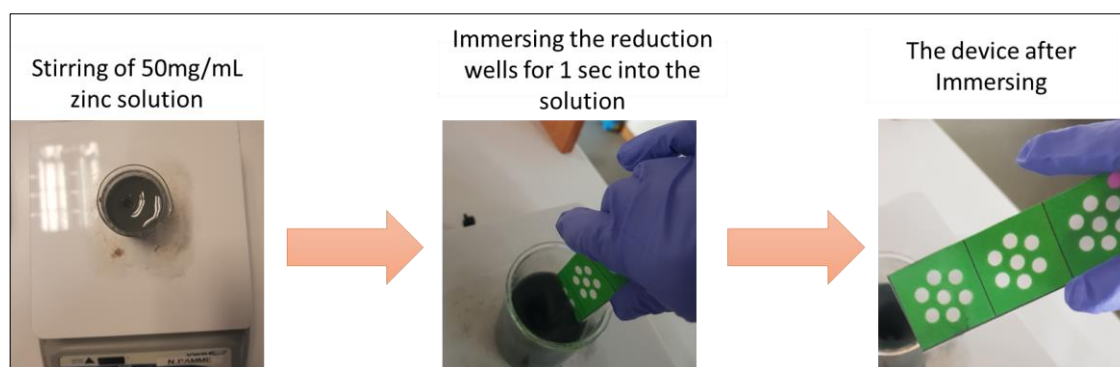
Figure 4.27 Step by step method for zinc addition into the reduction zone. Zinc was stirred 50 mg mL^{-1} of zinc was stirred in beaker. The reduction zone in the device was immersed into the stirred solution (under stirring at 600 rpm) for a second and removed immediately. The modification of device 11 (modified as in **Figure** 4.6).
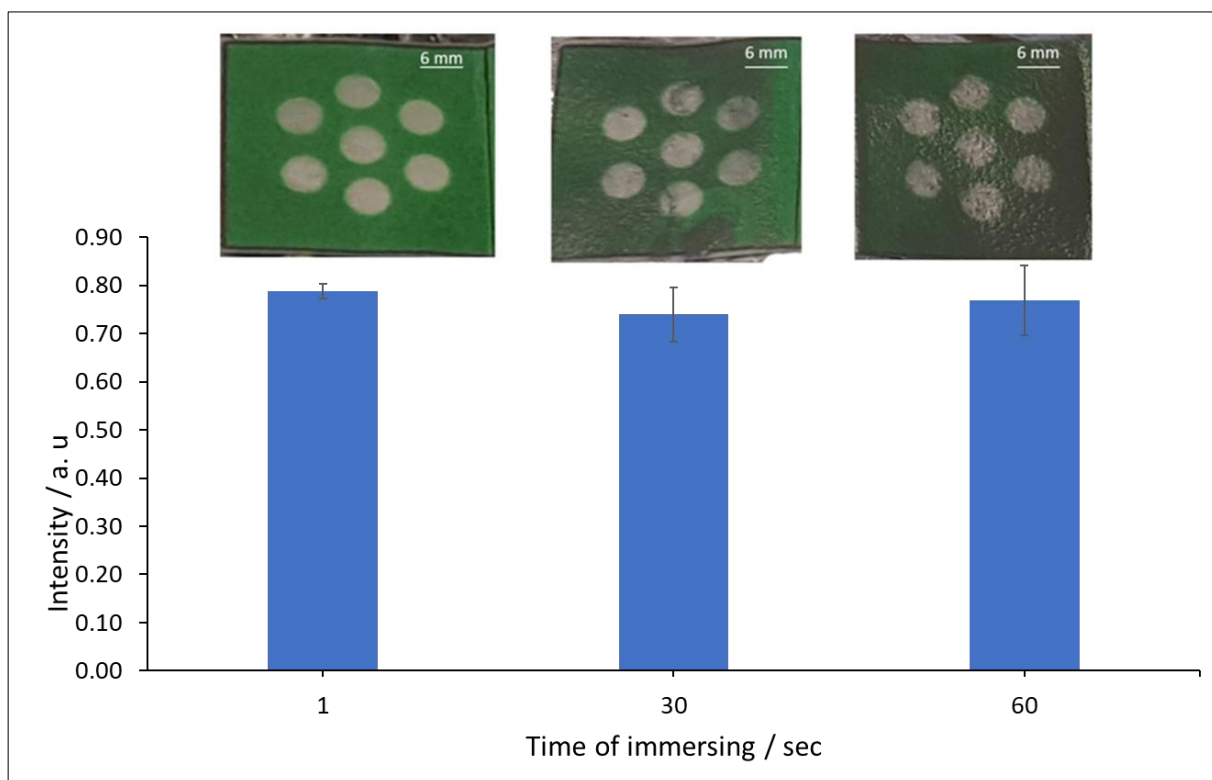
Figure 4.28 Intensity versus time of immersion (min). 1000 µM of nitrate standards were used for the analysis. Device 11 (modified as in **Figure** 4.6) was used. Scanner was used for photo capture. The photo was analysed using Image-J software (method 2).
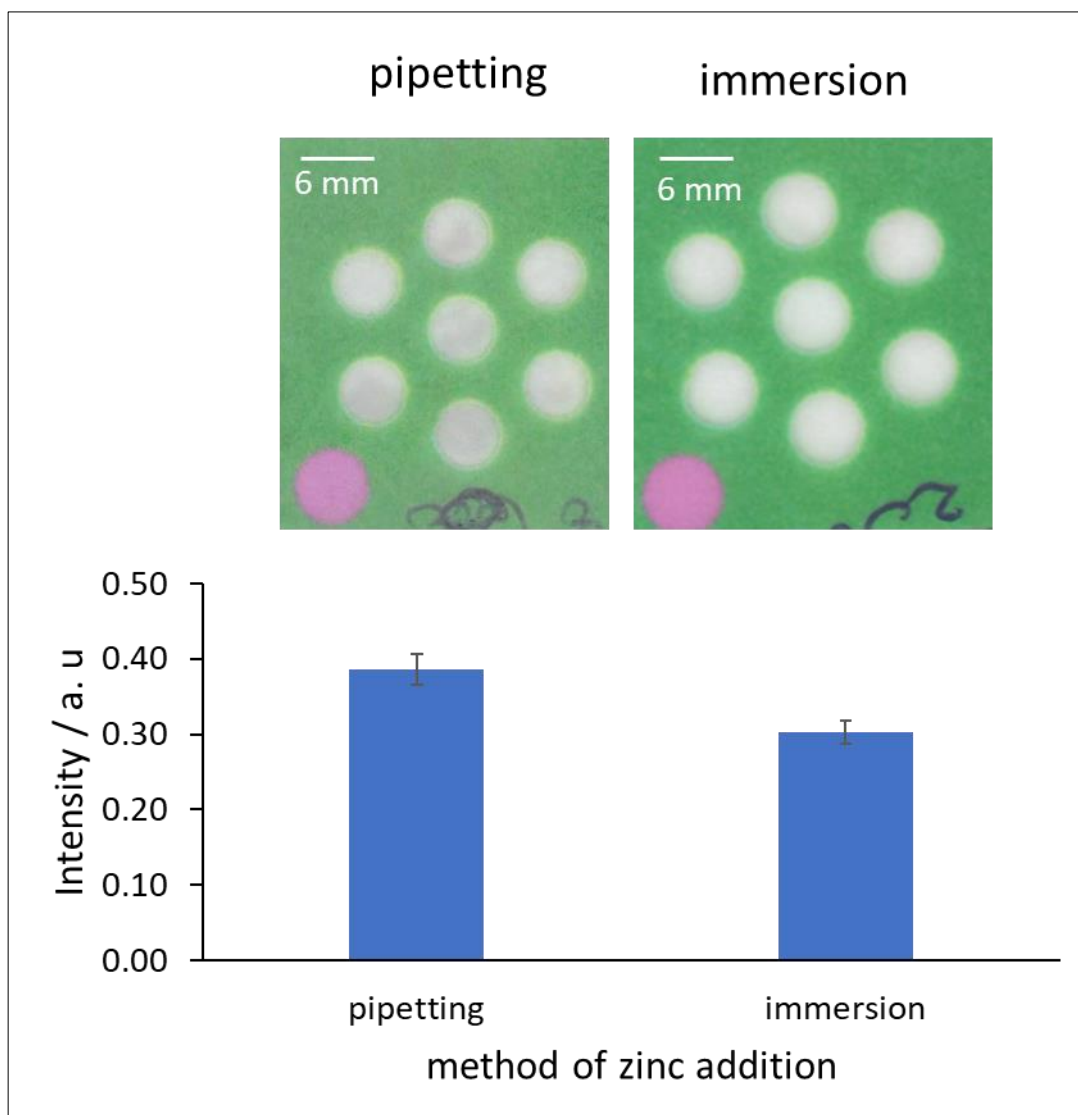
Figure 4.29 Intensity from blank versus the method of zinc addition. Pipetting and immersion were used to add zinc to the device. The variation in the dark colour leads to variation in the intensities. Intensity reduced by 21.50%.
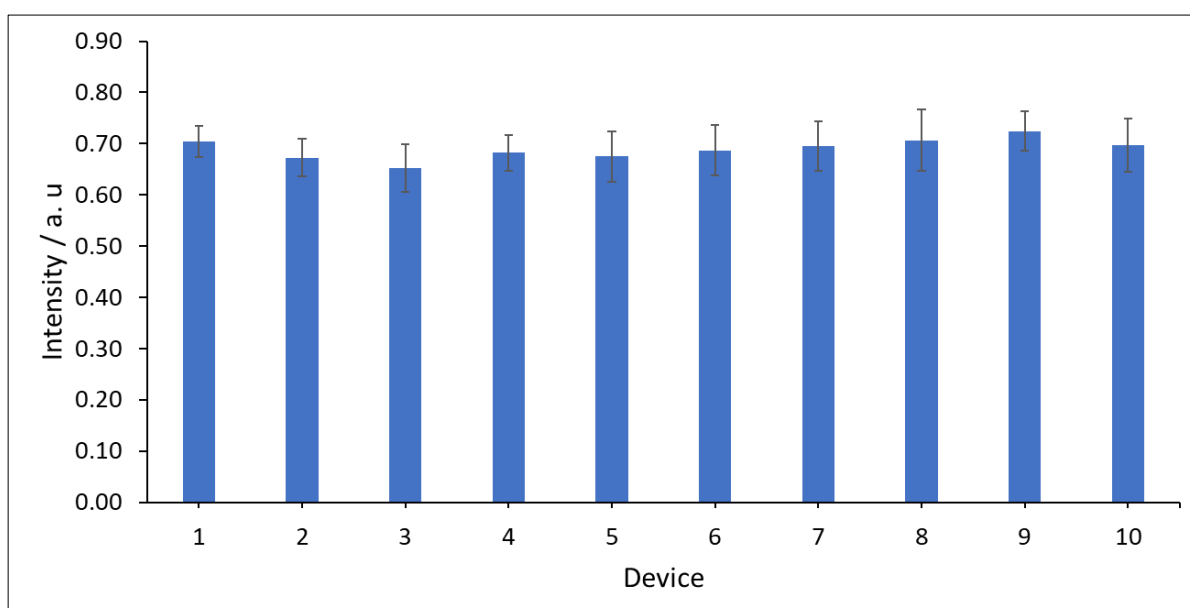
Figure 4.30 Intensity versus the number of devices. This experiment was done to determine immersion reproducibility. 600 µM of nitrate standards were used for the analysis. Device 12 was used. Scanner was used for photo capture. The photo was analysed using Image-J software (method 2). The means were the same within the standard according to ANOVA test ($F=1.21$, $F_{critical}=2.07$, $\alpha=0.05$, $n=6$).

4.5.3 Reaction time determination

After several optimization the time of reaction was determine as in **Figure** 4.31 which Shows intensity versus time for 0, 600 and 800 µM nitrate. Photo was taken each minute for 12 minutes. Scanner was used for the detection; therefore, the device was dipped into the solution for 30 second and then moved into the scanner to take a scan for the device with time over the 12 minutes and hence some variation in the intensity may happened compared to if the device is dipped for the whole 8 or 14 minutes. 8 minutes is the optimum time for nitrate detection. The intensity was stable from 8 to 12 minutes using ANOVA test ($F=1.56$, $F_{critical}=2.53$, $P= 0.20$, $\alpha=0.05$, $n=6$). The study did not go for longer time since our aim is not to test how long the colour can stay. The aim is to have stable result with short time work that works for lay people like farmer.
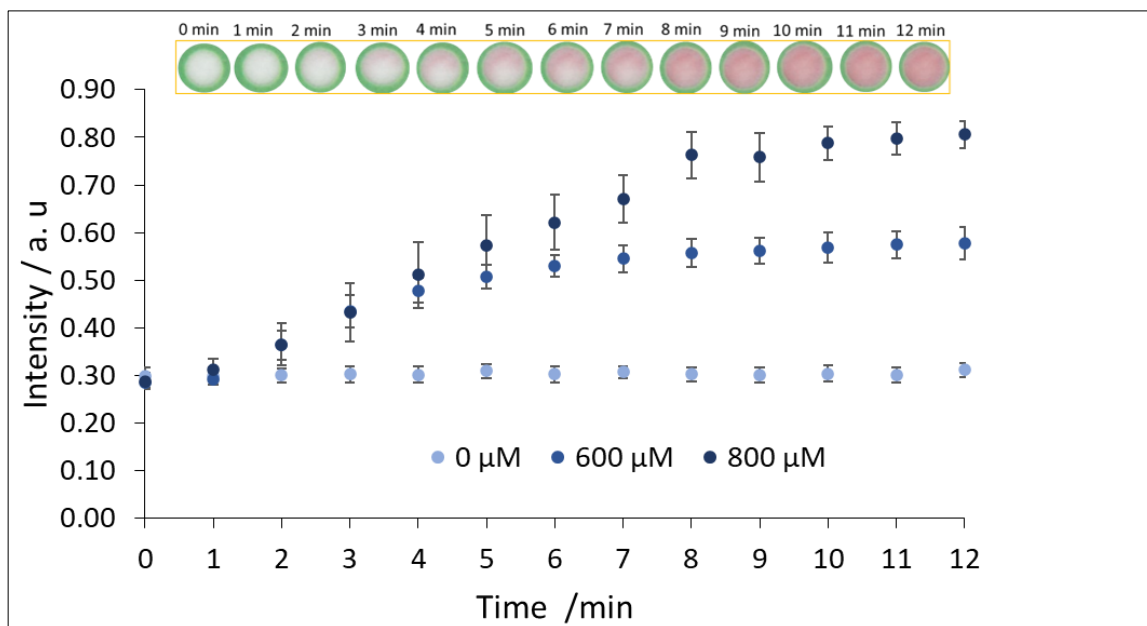
Figure 4.31 Intensity versus the time of detection of nitrate (minutes). 0, 600 and 800 µM were used as standards. Device design 11 was used (modified as in *Figure* 4.6). Scanner was used for photo capture. The photo was analysed using Image-J software (method 2). The optimum time for nitrate detection was 8 minutes.

4.5.4 Improvement of reaction by addition of an empty layer

Zinc can react with the acid to produce H_2 gas and zinc salt (e.g., $Zn+2HCl \rightarrow H_2+ZnCl_2$). In the detection zone one component of Griess reagent is citric acid. Once the layers overlapped and sample was added there was possibility of interaction between zinc and the acid. So, some of the zinc is not available to reduce the nitrate to nitrite since it is consumed by the acid in the detection zone. In addition, the acid was used for producing the pink colour and zinc leads to eliminate some of it. Therefore, if there is a barrier that can separate the detection zones and

reduction zone the efficiency of the device may be enhanced as suggested by Ferreira et al. [296]. Additional empty paper layer was added into the device. This layer is empty with no reagents, it was used to separate the detection and reduction layers. **Figure** 4.32 Shows intensity versus concentration of nitrate when two types of devices (design 11 and 12) were used with and without empty layers. The empty layer showed significant enhancement in the intensity of the standards. This happened due to the more available zinc for reduction step. Therefore, empty layer will be used for the device. The recent device consists of four layers.
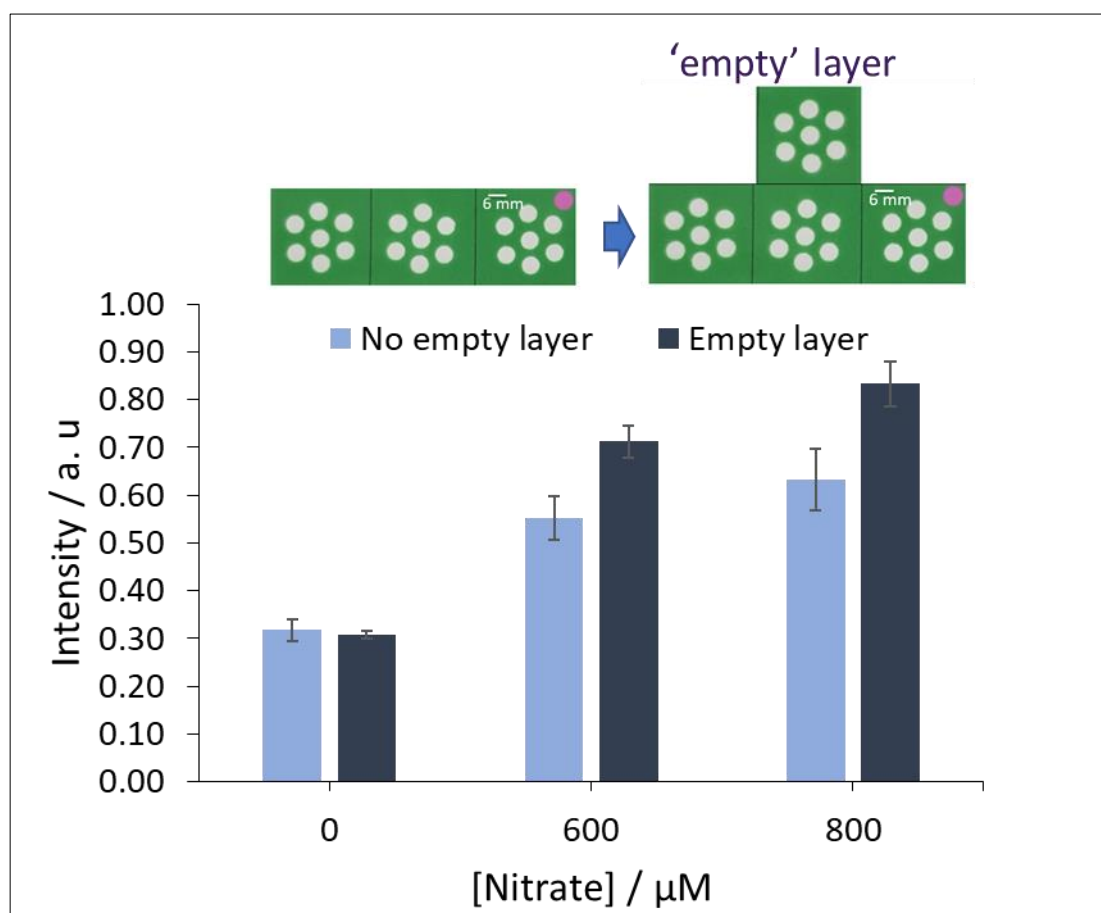
Figure 4.32 Intensity versus nitrate concentration (μM) when device 11 (with no empty layer) and device 12 (with empty layer) were used for nitrate detection. 0, 600 and 800 μM nitrate standards were used in this study. Scanner was used for photo capture. The photo was analysed using Image-J software (method 2).

4.5.5 Reduction efficiency

The reduction efficiency was determined by comparing the intensity from nitrate and nitrite detected by the same PAD. The intensity of the two analytes should be the same if the nitrate is reduced totally to nitrite according to **Equation 2.2** in the experimental. **Figure** 4.33 Shows the intensity from nitrate and nitrite. The intensity from the two PADs were different which means that nitrate was not reduced totally to nitrite. The reduction % was calculated by

comparing the two intensities from nitrite and nitrate and it was found to be 53.61 ±0.78%. This % was calculated using one same concentration for both nitrate and nitrite.
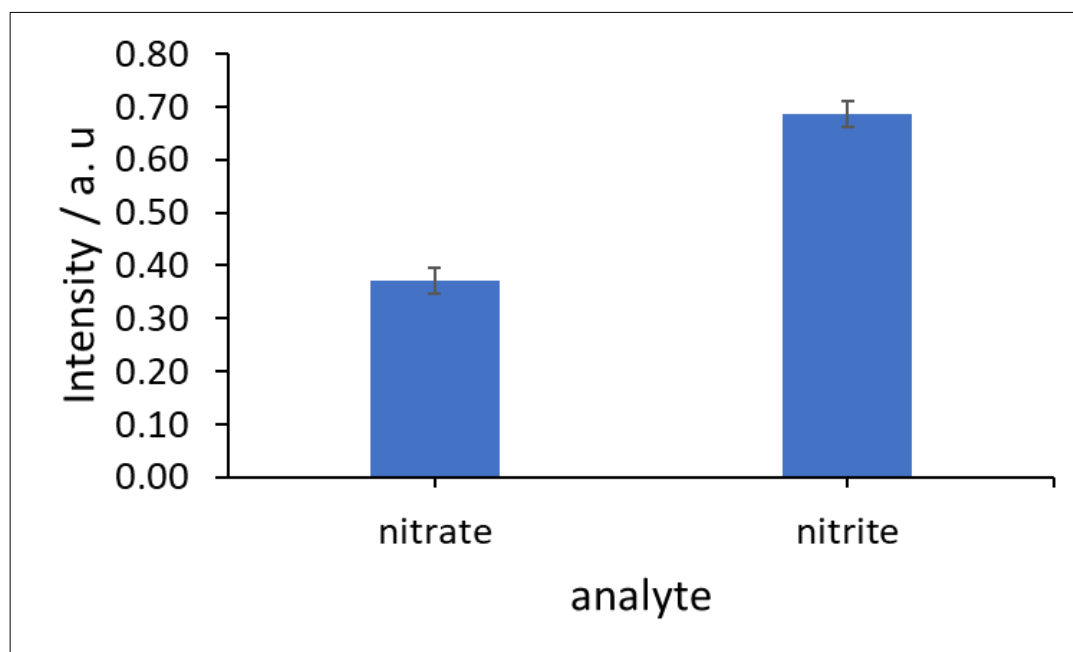
Figure 4.33 Intensity versus analyte type nitrate (90 µM) and nitrite (90 µM). Device 12 was in the analysis. A scanner was used for detection. The photo was analysed using Image-J software (method 2).

4.5.6   Calibration line with scanner

Calibration line was determined from 0 to 1000 µM and was found to be as in **Figure** 4.34. The detection range was found to be from 0 up to 800 µM. The calibration line shows good linearity with R^2 close to one and this indicates the fitness of the points to the straight line. The limit of detection and quantification was determined as in **Table** 4.8. The LoD and LoQ were 34.97±3.41µM (2.2 mg L^{-1}) and 121.61±9.02 µM (7.5 mg L^{-1}) respectively. LoD and LoQ were calculated as in **Equation 2.5 and 2.6** respectively. The limit of detection of the optimized method meets the requirement based on environmental level[348,426,427348,426,427]. The reproducibility of the calibration line was checked and determined in three different days and was found as in **Figure** 4.35. ANOVA test used to determine the difference between points in the calibration line and it showed that the means are equal within the standard deviation (e.g., at 200 µM (F= 0.16, $F_{critical}$=3.68, α=0.05, P= 0.088, n=6, ANOVA test)). However, since the LoQ was higher than the aimed level of nitrate in soil it can be said that the developed PAD is more semiquantitative rather than quantitative.
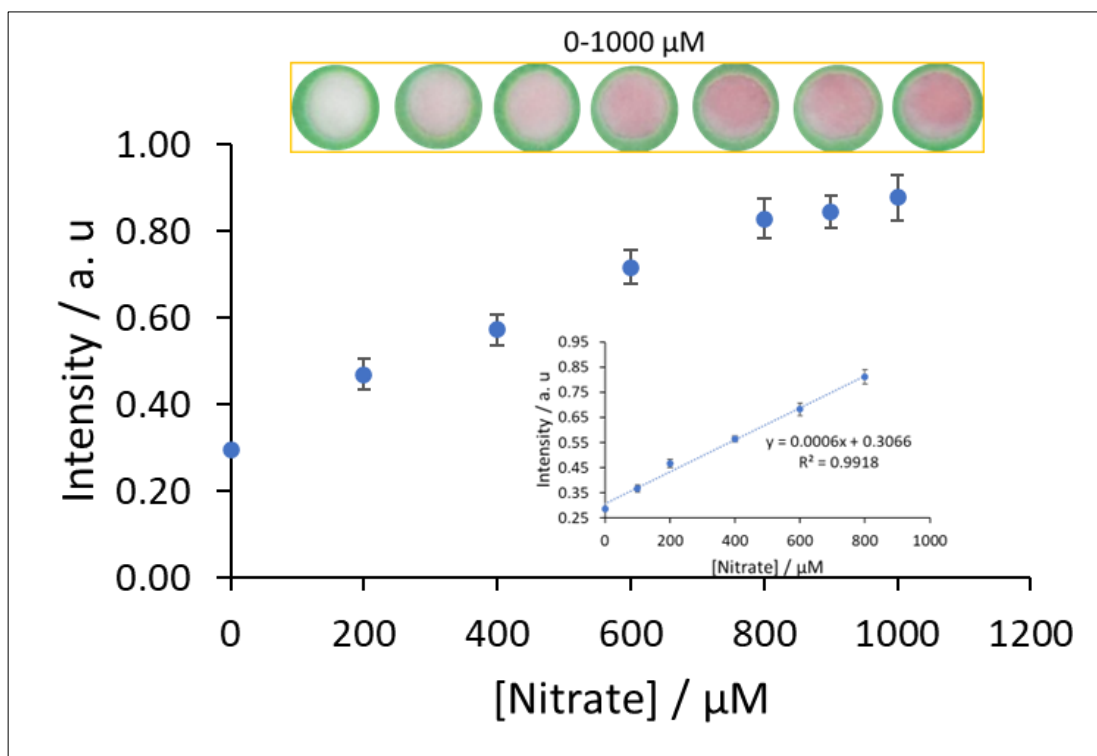
Figure 4.34 Intensity versus nitrate concentration (µM). Calibration line was determined from 0 to 1000 µM, device design 12 (modified as in **Figure** 4.6) and scanner was used for detection. The photo was analysed using Image-J software (method 2). The linear range was found to be from 0 up to 800 µM.

Table 4.8 LoD, LoQ, R2 and slope for nitrate calibration lines. device design 12 and scanner were used. The photo was analysed using Image-J software (method 2). LoD and LoQ were calculated using **Equation 2.5 and 2.6**.

	line 1	line 2	line 3	Average	% RSD OF AVERAGE
LOD (µM)	38.85	32.51	33.54	34.97±3.41	9.74
LOQ (µM)	129.51	123.53	111.79	121.61±9.02	7.41
R2	0.9939	0.9918	0.9953	0.9937±0.0018	0.18
slope	0.0007	0.0006	0.0006	0.0006	9.116057
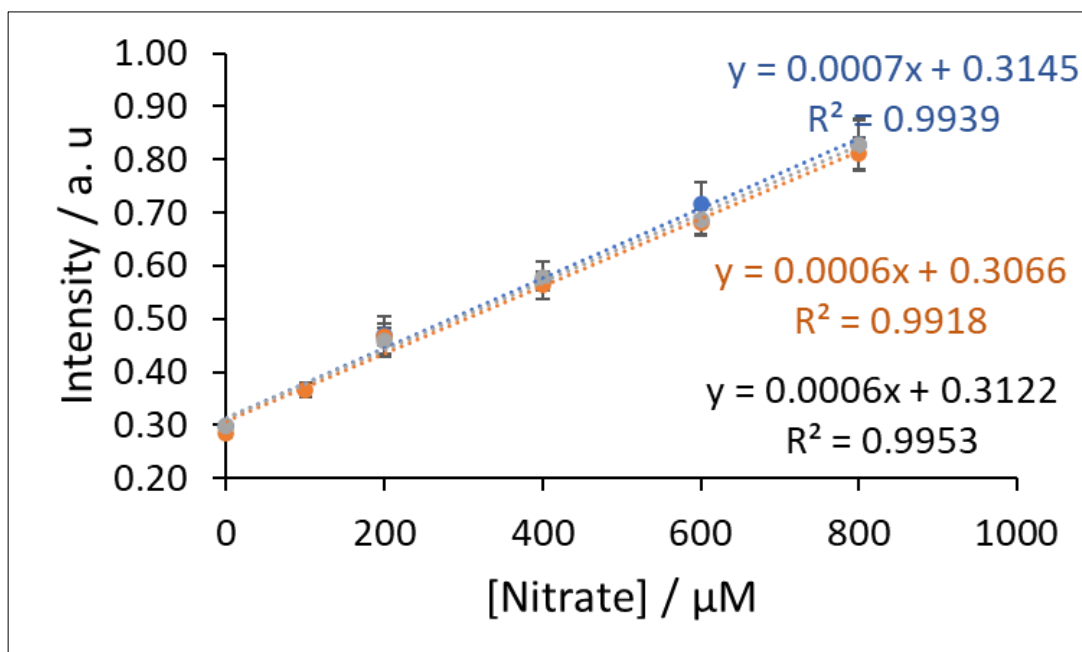
Figure 4.35 Intensity versus nitrate concentration (µM). device design 12(modified as in **Figure** 4.6) and the scanner was used for detection. The result was determined three times in three different days. The photo was analysed using Image-J software (method 2).

4.5.7   Phone versus scanner

Calibration line was run using phone and the result as in **Figure** 4.36 which show intensity versus nitrate concentration. The line shows good linearity with around 0.99 R^2. The method is reproducible when the calibration line was repeated in two different weeks. Points in the calibration lines were compared by t-test which shows that means are equal within standard deviation (e.g at 400 M, t_{stat}= 2.10, $t_{critical}$= 2.23, P= 0.062, α= 0.05. n=6, two tailed test). The result was compared to result from scanner as in **Figure** 4.37**.** At very low and very high concentration the difference was significant due to the reflection of light on the surface of the paper when the paper is white or too pink (e.g., at 800 µM, t_{stat}=4.41, $t_{critical}$=2.23, P= 0.0013, α= 0.05, n=6, two tailed test). This variation leads to small change in the limit of detection of the method. When phone was used the limits of detection and quantification were 44.32±3.58 µM (2.75mg L^{-1}) and 150.36±15.43 µM (9.32 mg L^{-1}) respectively. The limit of detection is still lower than the lower level of nitrate at which fertiliser needs to be applied. The use of phone was important since finally in the field phone will be used to collect the data from the lay people (e.g., farmer).
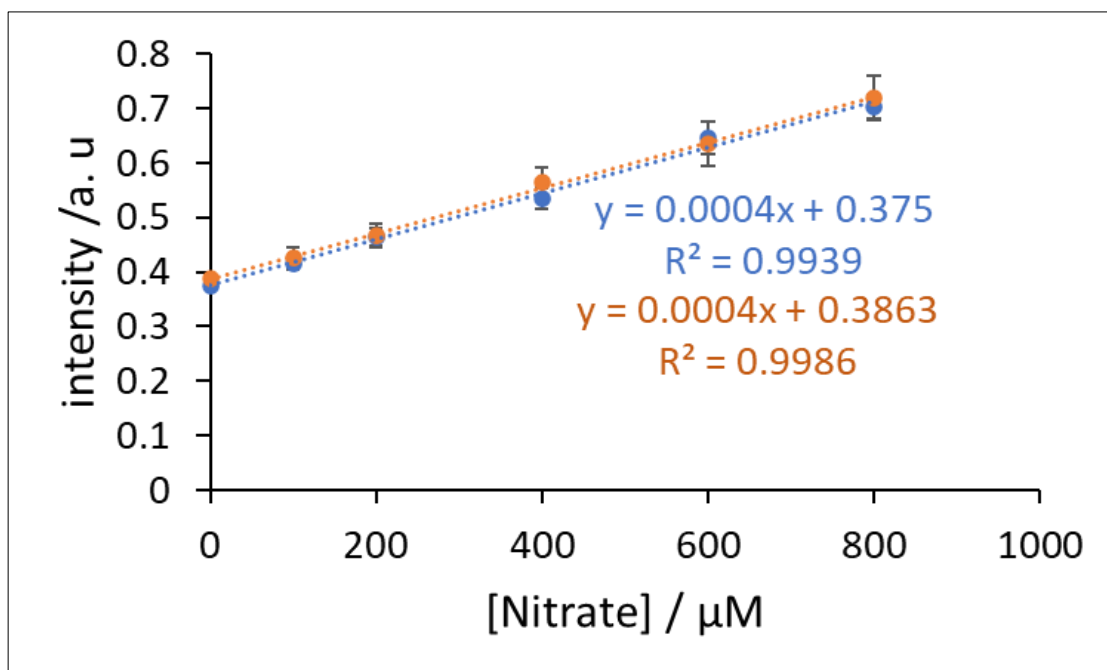
Figure 4.36 Intensity versus nitrate concentration (μM). device design 12 (modified as in Figure 4.6) and the phone was used for detection. The photo was analysed using Image-J software (method 2). The lines were from two different days.
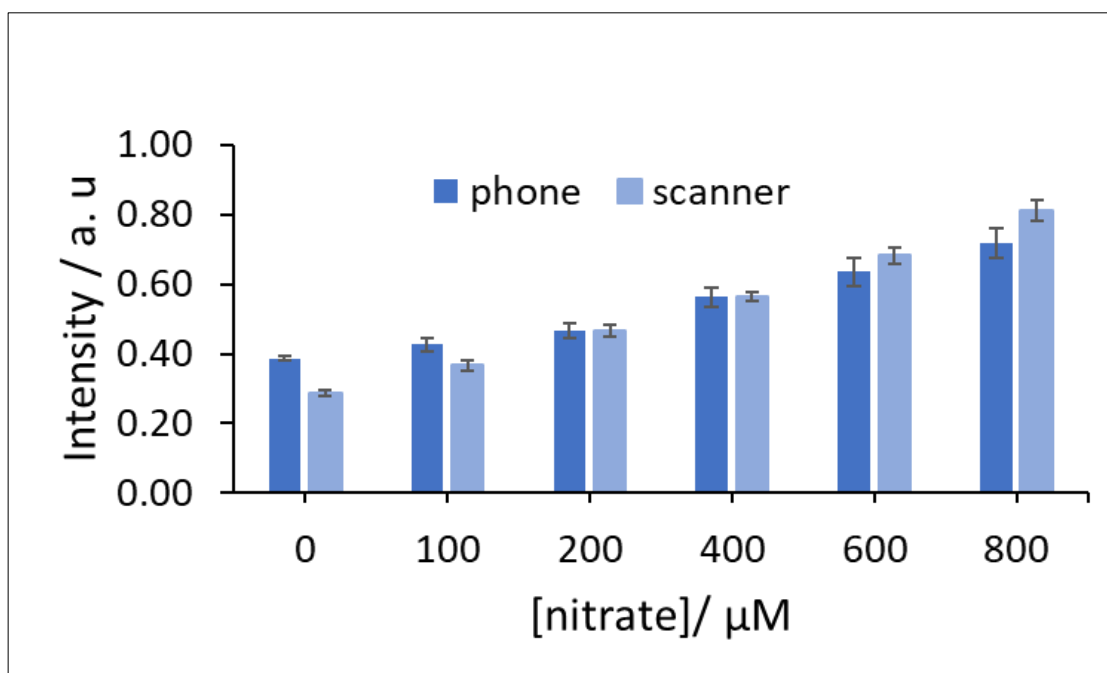
Figure 4.37 Intensity versus nitrate concentration (μM). device design 12 (modified as in **Figure** 4.6**)** was used for detection. Phone and scanner were compared. The photo was analysed using Image-J software (method 2). **.** At very low and very high concentration the difference was significant due to the reflection of light on the surface of the paper when the paper is white or too pink (e.g., at 800 μM, t_{stat}=4.41, $t_{critical}$=2.23, α= 0.05, n=6, two tailed test).

4.5.8   Interference studies

Interference for nitrate was studied based on the interference result for nitrite (**Section 3.5.10**).

The maximum tolerance concentration which caused no interference for nitrite was used as a

start to study the interference for nitrate. 600 µM of nitrate was mixed with the interference in the same solution. The PAD was dipped into the solution for 8 min and a scanner was used for the photo capture. Several interferences [Ca^{2+}, Na^+, K^+, Fe^{2+}, Cu^{2+}, Zn^{2+}, Mn^{2+}, CO_3^{-2}, PO_4^{-3}, Cl^-, SO_4^{-2}] were chosen for study based on their availability in water and soil. There are other interference which may interfere and were nit studied here due to the shortage of time. The result is in **Figure** 4.38 which shows the tolerance concentration for some anions and cations which may exist in soil and water. T-test was used to compare the means of intensities when interference exists and does not exist in the solution (e.g., Ca^{2+}, t_{stat}=0.19, $t_{critical}$=2.23, P= 0.86, α= 0.05, n=6, two-tailed test) and it shows that the two means are not significantly different for all interference in the specified concentrations. Copper and iron cause interference at a very low level around 1 mg L^{-1}. This is maybe because these two cations tend to inhibit nitrate from reaching the PAD. **Table** 4.9 shows the level of some of the possible interferences in soil based on some studies. The tolerance level is higher than the concentration of most interference in soil. Except for iron which sometimes shows higher level in soil than the tolerance level which is 1 mg L^{-1}. This information will be mentioned when the PAD is released to the user.
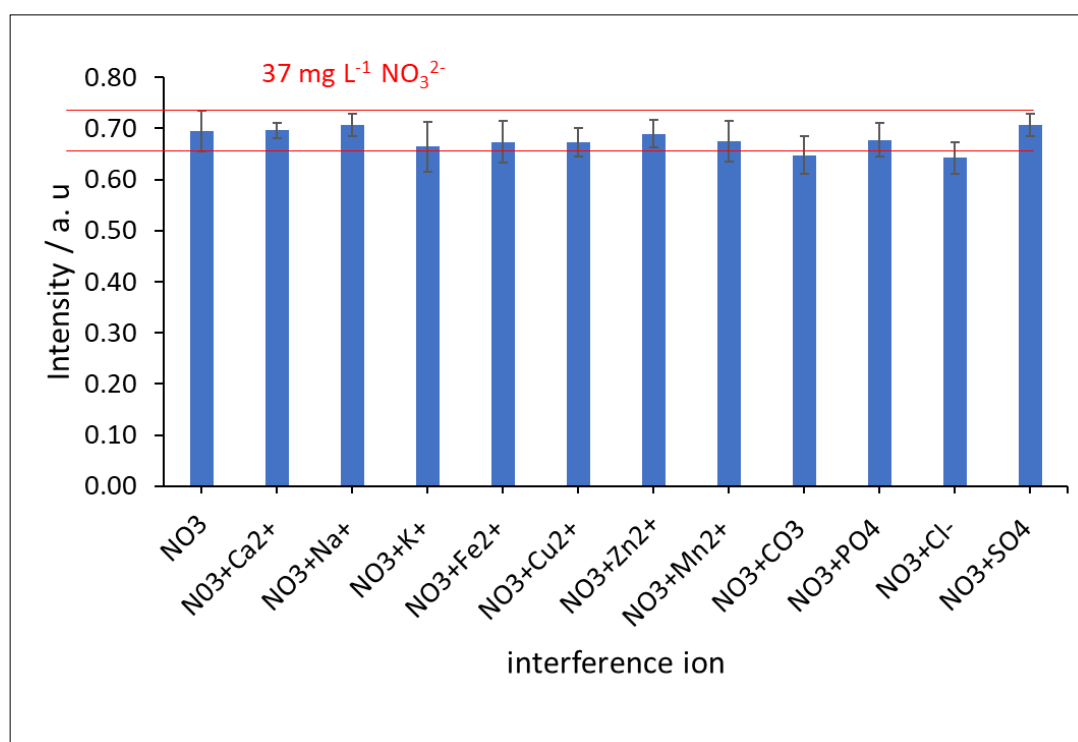
Figure 4.38 Intensity versus interference ion concentration mg L^{-1}. 600 µM/37 mg L^{-1} of nitrate was mixed with the interference [Ca^{2+} (0.5 g L^{-1}), Na^+ (5 g L^{-1}), K^+ (5 g L^{-1}), Fe^{2+} (1 mg L^{-1}), Cu^{2+} (1mg L^{-1}), Zn^{2+} (0.2 g L^{-1}), Mn^{2+} (2 g L^1), CO_3^{-2} (0.08 g L^{-1}), PO_4^{-3} (2 g L^{-1}), Cl^- (3 g L^{-1}), SO_4^{-2} (10 g L^{-1})] in the same solution. The PAD was dipped into the solution for 8 min and a scanner was used for the photo capture. device design 12 (modified as in **Figure** 4.6) was used for detection. The photo was analysed using Image-J software (method 2).

Table 4.9 The level of cations and anions in soil based on previous studies.

ion	mg L^{-1}	Mass: Volume	Mg kg^{-1}	reference
Mn^{2+}	27.7	0.25:10	1108	[376]
	4.225	0.25:10	169	[376]
	1.888	0.004:2.5	1180	[377]
Fe^{2+}	1.51-4.89	25:250	15.1-48.9	[378]
	65.4	2:100	3270	[379]
	0.190	1:25	4.75	[380]
Cu^{2+}	0.201, 0.133	-	-	[381]
Zn^{2+}	0.128, 0.023	-	-	[381]
	0.0067-0.1175	2:20	0.067-1.175	[382]
PO$_4^{3-}$	0.148	2.5:50	2.96	[383]
	1.27-3.05	-	-	[384]
Ca^{2+}	7.54-110.15	20:80	30.16-440.6	[385]
	9.46-45.69	10:100	94.6-456.9	[386]
	9.7-18.8	10:200	194-376	[387]

ion	mg L^{-1}	Mass: Volume	Mg kg^{-1}	reference
SO$_4$$^{2-}$	2.45-3.654	20:100	12.28-18.27	[388]
	0.2-1.6	5:25	1-8	[389]
K$^+$	22.8-182	20:100	114-910	[388]
	5.7-7	2.5:25	57-70	[390]
Mg	0.85-9.85	10:200	17-197	[387]
Na$^+$	1.9-2.52	10:200	38-50.4	[387]
	1.00-1.43	10:200	20-28.6	[387]
Cl$^-$	6-300	1:50	300-15000	[391]
	1.6	5:40	13	[392]
	7.8	5:40	62	[392]

4.5.9 pH effect on nitrate detection

There are two steps for nitrate determination and according to literature reduction step is more efficient in neutral and basic condition while the detection step is more efficient in acidic condition [349]. Therefore, pH effect on nitrate detection was determined in the range 4 to 10 as in **Figure** 4.39. ANOVA test was used to compared between intensities at different pH and at same studied concentration of nitrate. PH 5 to 10 show that means were the same for all pH in different nitrate studied concentrations (e.g., at 400 µM of nitrate, pH 5-10, F= 1.48, F$_{Critical}$=3.10, P= 0.25, α0.05, n=6, ANOVA). The effect of the PH was significant at pH lower than pH 5 especially at high concentration of nitrate. This is maybe due to the ability of the zinc to interact with H$^+$ to form H$_2$ and hence zinc was consumed. This means there was less zinc available for reduction of nitrate to nitrite and this is why the effect was more significant at high concentration. There was no significant difference in the result at pH range 5-10 and this where

around most of soil nutrients exists and within this range is the best range for plant growth [394] and a range within this range most of the UK soil[395].
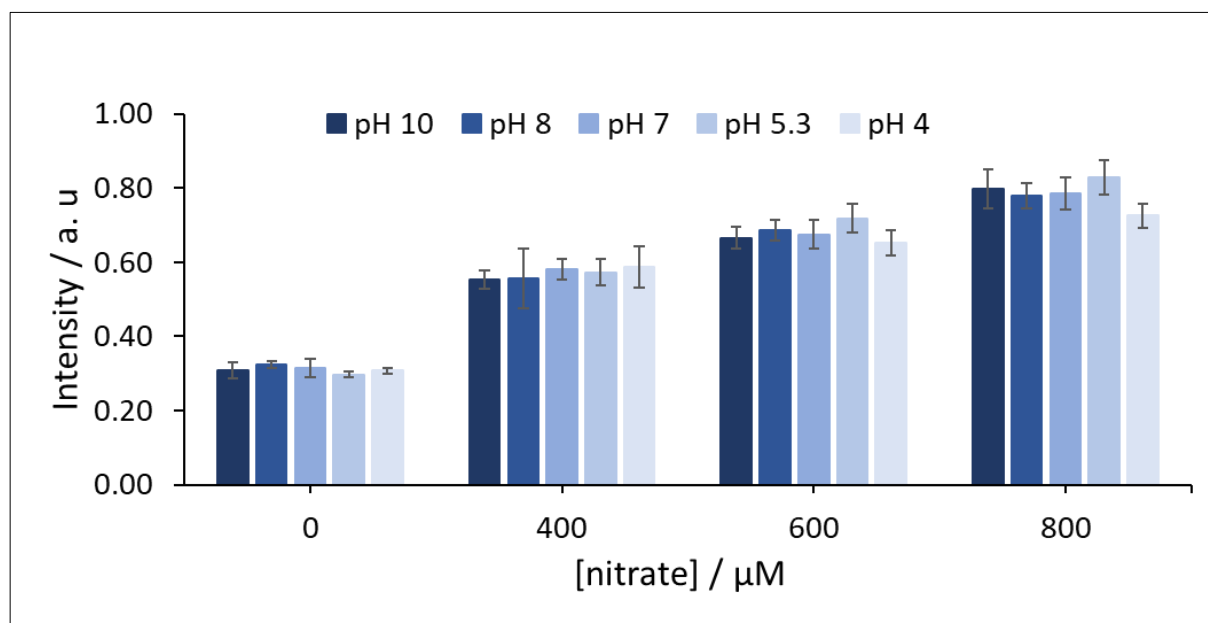
Figure 4.39 Intensity versus nitrate concentration (μM). PH effect on nitrate detection was done in the range of 4 to 10. device design 12 was used for detection. Phone and scanner were compared. The photo was analysed using Image-J software (method 2).

4.5.10 Stability studies

Stability of the device is another important factor to investigate since the device finally should be released to the use of lay people like farmer and hence farmer should know exactly how to store the device before use. For example, storage at room temperature may cause the degradation of the reagent stored within the paper device. The stability of device 12 which was modified as in **Figure** 4.6 was determined over time at different storing conditions, out at room temperature (21 ^{0}C) in the light, out in room temperature (21 ^{0}C) in the dark, and in the freezer (-4 ^{0}C) in dark. 0 (blank) and 600 μM of nitrate were used for the study. **Figure** 4.40 showed the intensity of the colour versus nitrate concentration for a device which was stored at room temperature under light effect. A decrease in the intensity of colour was observed over weeks for 600 μM nitrate standards, however, an increase was observed for the blank. This was expected since the light leaded to degradation of the reagent in the device and cause auto-colour development. The second week the device is still stable. The effect was significant in the third week. **Figure** 4.41 shows auto-colour development from device which was not reacted with anything. A photo was taken of the device over days for 26 days. clearly after day 3 the device automatically develops a colour due to the exposure to light. Therefore, the device was stable for only three days at room temperature (21 ^{0}C) in the light.
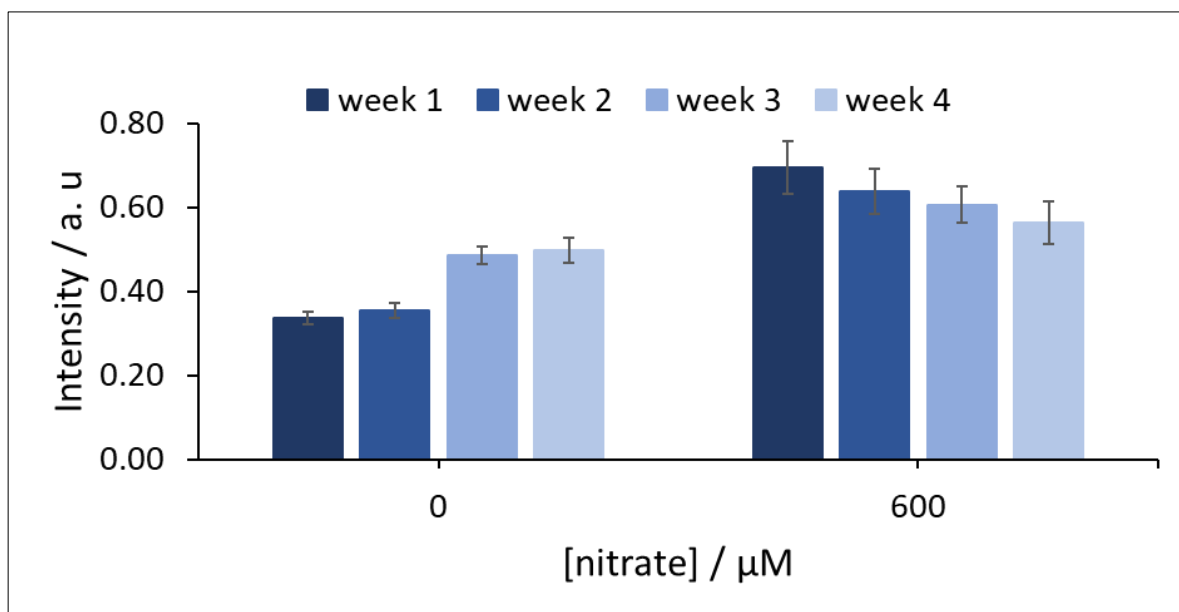
Figure 4.40 Intensity versus nitrate concentration (μM). 0 and 600 μM of nitrate were used for the study. Stability was studied at room temperature (21 ^{0}C) in the light. Device 12 was used.
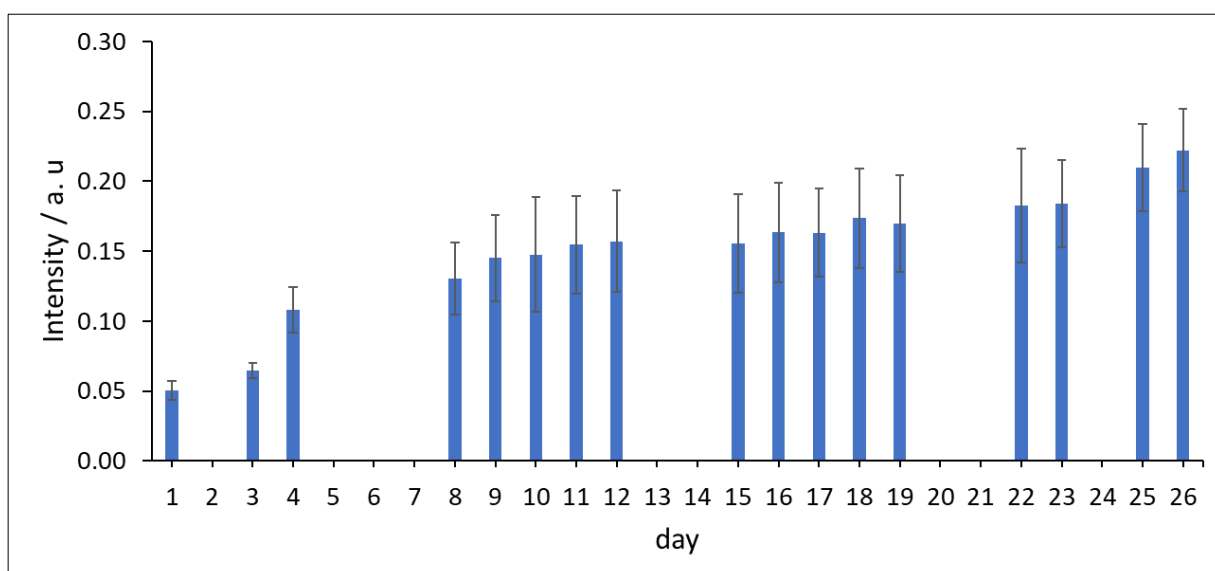
Figure 4.41 Intensity versus day. device with no reaction with standard or blank was used for the study (It is same device, it was kept in the room for 26 days and each day a photo was taken for the same device). Auto-colur development was measured. Stability was studied at room temperature (21 ^{0}C) in the light. Device 12 was used.

The second condition which was studied is stability at room temperature, but this time device stored in dark box away from light. The device was kept in drawer in a dark box. The intensity was then determined over time for 54 days around 8 weeks (2 months). **Figure** 4.42 shows the intensity versus nitrate concentration when device with no reaction, device reacted with blank, and device reacted with 600 μM of nitrate were used. AS it is clear there was no significant auto colour development up to day 17, mainly the intensity was below 0.1, whereas in light (as in

Figure 4.41) the auto-colour development intensity was above 0.1 from day 4. The blank signal was also constant with some variation up to day 17, after this blank start to show some increase in the intensity. T-test was used to compare intensity from day 1 and the day of at which stability studied (e.g., t_{stat}=1.92, $t_{critical}$=2.23, P= 0.08, α= 0.05, n=6, two tailed test). Even though the 600 µM nitrate standard showed significant change in the signal after day 40 (t_{stat}=-0.34, $t_{critical}$=2.23, P= 0.74, α= 0.05, n=6, two tailed test), the blank signal change earlier and hence the stability was based on the change in the blank signal. Therefore, the device was stable for 17 days (around 2 weeks) at room temperature (21 ^{0}C) in the dark.
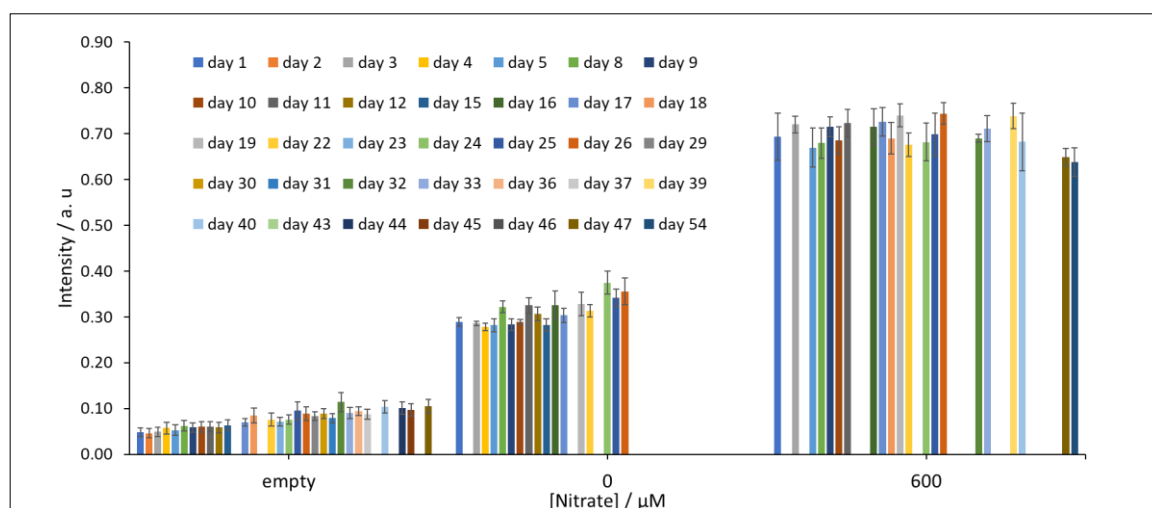
Figure 4.42 Intensity versus nitrate concentration (µM). 0 and 600 µM of nitrate were used for the study. Stability was studied at room temperature (21 ^{0}C) in the dark. Device 12 was used. Empty means a device with no reaction with the analyte.

The third condition to study the stability is at the freezer (-4 ^{0}C) in dark. The result as **in Figure** 4.43 which shows the intensity versus nitrate concentration when device with no reaction, device reacted with blank, and device reacted with 600 µM of nitrate were used. The empty and blank device shows stability up to 54 days (day 1 and day 54, t_{stat}=0.94, $t_{critical}$=2.23, P= 0.37, α= 0.05, n=6, two-tailed test), whereas the 600 µM nitrate device showed decrease in the intensity in day 54 (day 1 and day 54, t_{stat}=5.18, $t_{critical}$=2.23, P= 0.00041, α= 0.05, n=6, two-tailed test)and stay stable in day 53 (day 1 and day 53, t_{stat}=1.40, $t_{critical}$=2.23, P= 0.19, α= 0.05, n=6, two-tailed test). However, there are still some fluctuations during the days, this can be explained by the error (e.g., loss of reagent due to improper pipetting) that can occur when big batch of PADs are prepared in the same day. Based on these it was assumed that device in freezer was stable for around 53 days around 8 weeks.

In conclusion, the device was stable for only three days at room temperature (21 ^{0}C) in the light, for 17 days (around 2 weeks) at room temperature (21 ^{0}C) in the dark and for around 53 days around 8 weeks. This information should be mentioned with the PAD when is sold for user.
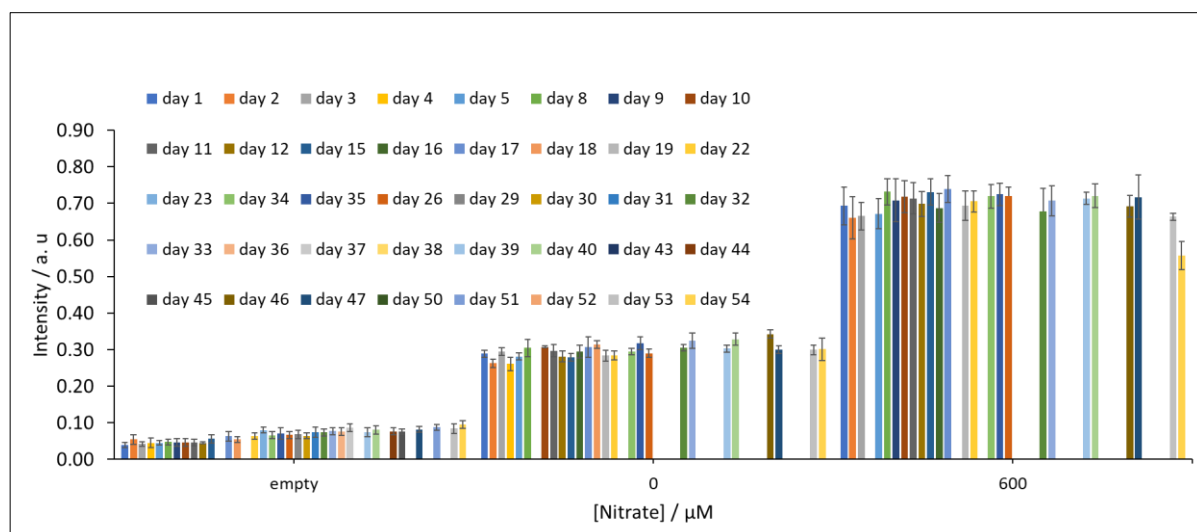
Figure 4.43 Intensity versus nitrate concentration (µM). 0 and 600 µM of nitrate were used for the study. Stability was studied at freezer temperature (-4 ^{0}C) in the dark. Device 12 was used. Empty means a device with no reaction with the analyte.

4.6 Comparison between PAD and IEC and literature

Paper device was compared to conventional method in term of LoD, LoQ and the detection range as in **Table** 4.10. Result from IEC was more sensitive than the PAD and it has wider detection range. However, the PAD detection is still applicable for detection of nitrate in soil when few grams of soil and mL of water are used for the extraction as mentioned in **section 4.5.6**. IEC method and the PAD both are going to be used for nitrate detection in soil.

The PAD from this work was compared to other studies as in **Table** 4.11. Some of the published PADs have higher LoD and some have lower. The reaction time for most of the PAD including the developed PAD in this study is between 5 to 20 minutes. None of the previous studies focus on the study of soil samples, most of them concentrate on the water and food samples. In addition, some of these devices were difficult to use and they are not ready to be used in the field. Jayawardare et al. and Charbaji et al. devices [290,295] require a slide of the layer by the user between the detection and reduction zone. Teepoo et al., Thongkam et al. and Ratnarathorn et al. devices [291-293] require the flow of the sample within channels. The developed PAD focuses on the deposition of reagents at multiple layers which can be aligned above each other to avoid the complexity of the device during use. Also, most published PADs were based on pipetting for sample addition whereas the developed design allowed dipping system for sample introduction and hence easier use in the field.

The addition of zinc as a reducing agent was also an issue of discussion. Zinc addition to the PAD is challenging especially for our developed PAD since all the reaction zones above each other

including the zine, where also the detection colour develops. Zinc has a dark black colour which can participate in the intensity if it is too dark. Most of publish work relayed on pipetting the zinc solution into the specific as summarized in **section 4.5.2**. In this study the zinc was added by immersion of a hole device into the solution while the solution was under stirring, consequently, avoiding the accumulation of the zinc in the PAD. Adding zinc in this way offers advantages compared to pipetting the zinc, it reduces the dark colour of zinc accumulation in the device. The dark colour can affect finally the intensity of colour for nitrate detection especially for blank since it changes from time to time when zinc is added. Immersion reduces the accumulation of zinc and hence the intensity of the blank was reduced by around 22 %. In addition, immersion helped to deposit zinc in the two sides of the device. Even though by immersion the amount of zinc added was unknown, the method is reproducible (**section 4.5.2.2**), practical, and simple.

Table 4.10 LoD, LoQ and detection range for nitrate detection from PAD and IEC.

	scanner (PAD)	**phone (PAD)**	**IEC**
LOD (μM)	34.97±3.41	44.32±3.58	2.33±0.63
LOQ (μM)	121.61±9.02	150.36±15.43	7.78±2.10
Range (μM)	0-800	0-800	30-1000

Table 4.11 Comparison between different PAD studies for nitrate detection.

sample	Linear range (mg L^{-1})	LOD (mg L^{-1})	Reaction time (min)	Zinc addition	Reduction efficiency %	Sample introduction	reference
water	3.1-62	1.18	5	Pipetting	20	pipetting	[290]
food	10-50	3.60	12	Pipetting	-	pipetting	[291]
water	0-50	0.53	10	External layer (Zinculose)	27	pipetting	[295]
saliva	200-1200	4.96	-	External layer of zinc (weighed before and after)	-	pipetting	[296]
food	0.5-40	0.4	10	-	-	pipetting	[293]
food	0.4-20	0.4	10	Pipetting	-	pipetting	[292]
urine	8.68-62	2.8	20	-	-	pipetting	[298]
water	1-10	0.87	15	Pipetting	-	pipetting	[310]
water	0-40	3.35	60	-	27	dipping	[311]
Soil (scanner)	0-50 (0-800 µM)	2.2 (34.97±3.41µM)	8	Dipping (while stirring solution)		dipping	This work

sample	Linear range (mg L^{-1})	LOD (mg L^{-1})	Reaction time (min)	Zinc addition	Reduction efficiency %	Sample introduction	reference
Soil (phone)	0-50 (0-800 µM)	2.7 (44.32±3.58 µM)	8	Dipping (while stirring solution)		dipping	This work

4.7 Soil sample treatment

Extraction was necessary to extract nitrate ion from soil. In chemistry laboratory several tools are available to perform the extraction with the help of different kind of solvent [115,116]. For example, mixing device can be used to mix the soil with solvent to ensure good extraction of analyte. Later, the soil can be separated from the extract either by centrifuge or filtration by vacuum. In the field this equipment is not easily available. Therefore, there is a strong need for simple extraction method which can be performed by non-chemist like farmers.

4.7.1 Device for extraction

Three devices were compared for their ability to extract nitrate ion analyte from soil samples. Cafetiere (shape of equipment in **Figure** 4.8 and modified as **Figure** 4.11), AeroPress (shape of equipment in **Figure** 4.9 and modified as in **Figure** 4.12) and paper cup (shape of equipment in **Figure** 4.10 and modified as in **Figure** 4.13) were compared in this section. The soil extract from the three devices was compared by using device 12 without any modification (blank device). No reagents were added to device 12. The device was laminated and dipped into the extracts. The result was as in **Figure** 4.44. The intensities from the blank device of cafetiere and AeroPress were close to the intensity from deionized water (F= 1.11, F$_{Critical}$=3.68, P=0.35, α=0.05, n=6, ANOVA test). This means the colour of sample was not significant. However, the paper cup showed very high intensity for the blank device. This was maybe because unlike cafetiere and AeroPress there was no filtration system in the paper cup device. AeroPress was more difficult to use compared to cafetiere since it requires applying pressure to get the solution out. In addition, using AeroPress mixing was not possible. Therefore, cafetiere was used in this study. Cafeteria was suggested as an easy option for analyte soil extraction. It consists of a cup, spiral plate, filter plate, cross plate and plastic led with piston as in **Figure** 4.8. The process of extraction was as in **Figure** 4.11. The soil was added to the cup and DIW was added as a solvent. The plates

were fitted into the led. The three plates are important for separating the soil particles from the extract. The piston then was pressed against the mixture of soil and water. Consequently, the soil particles move down, and the nitrite moves up from soil to water. After a specific time of extraction, some of the extract was poured into a tray. The soil extract was then analysed by the paper device.
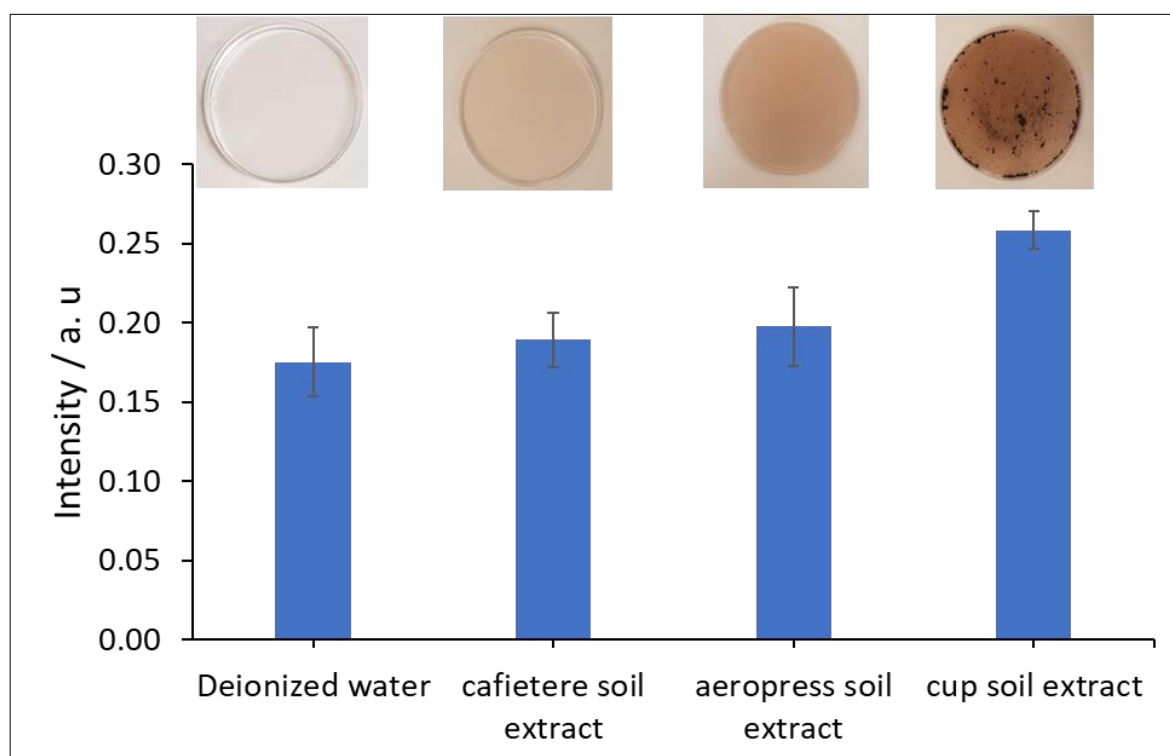
Figure 4.44 Intensity from a blank device 12 (n=6) which was used to analysed Deionized water, cafetiere soil extract (**Figure** 4.11), AeroPress soil extract (**Figure** 4.12) and paper cup soil extract (**Figure** 4.13). The extract from each device was shown above the bar. Scanner was used for detection and method 2 was used for intensity calculation. Repeats n=6 from one PAD.

4.7.2   Cafetière extraction optimization

Mass of soil

One important parameter to study is the amount of soil the farmer can use in the cafeteria. Too much soil can destroy the cafetiere and the small amount can be difficult to treat in the cafetiere. The mass of soil needs to be studied carefully. 3 to 9 grams of soil were studies and ion chromatography were used for the optimization since it is a known conventional method for nitrate detection. Specific gram of soil (3-9 g) was taken into the cafetiere with 100 mL of water and the piston was pushed down and the soil was allowed to settle down for three minutes. Then a 10 mL of the soil was filtered and analysed by IEC. **Figure** 4.45 shows the concentration of nitrate in soil in mg kg^{-1} versus the amount of soil in gram. The nitrate concentration should be the same since it is calculated per 1 kg of soil. However, at low mass like 3, 4 and 5 g the concentration is very hight with high standard deviation. This is maybe the small amount is not enough compared to the amount of water which is 100 mL at which the equilibrium between nitrate in soil and in water was not the same each time and that is why maybe the standard deviation was high. 6-9 g gave result with no significant difference according ANOVA TEST (F= 0.78, $F_{Critical}$=4.06, P=0.54, α=0.05, n=3, ANOVA test). After 7 g the standard deviation start to be low, and this is maybe because the amount of soil starts to be enough for the amount of water (solvent). Therefore, 8 g was chosen to be the optimum mass for the extraction.
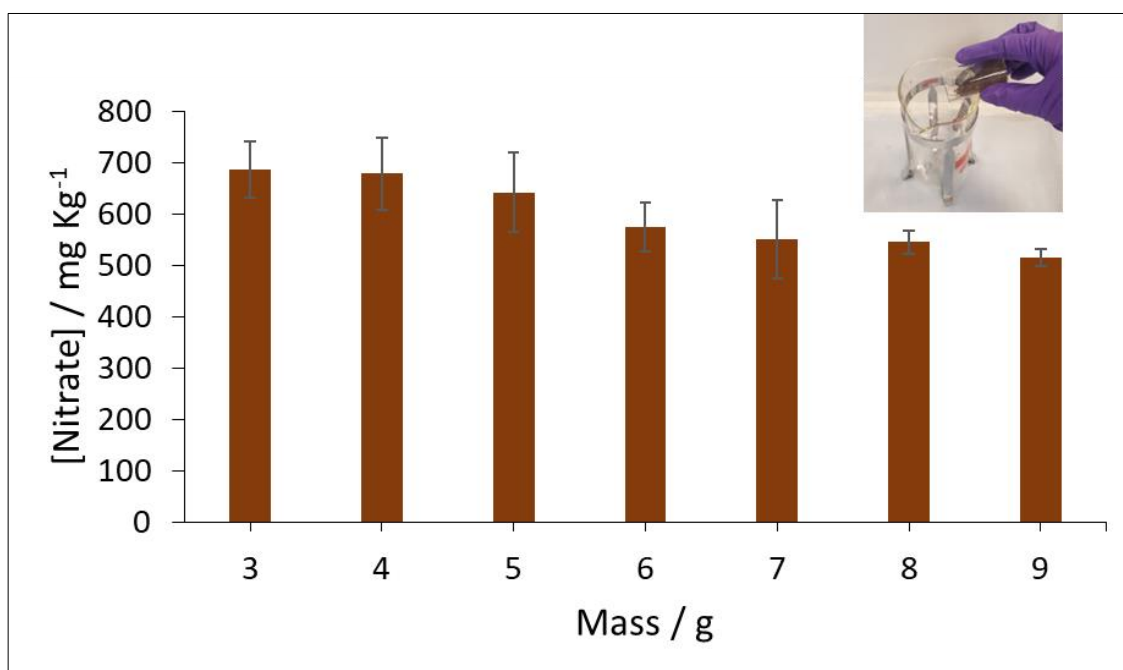
Figure 4.45 Nitrate concentration (mg kg^{-1}) versus the mass of soil (g). the extraction was done as in **Figure** 4.11. John Innes no1 was studied and detection of nitrate was done by IEC. Repeats n=3.

The volume of water solvent

Another parameter for the extraction is the volume of the solvent. There were several solvents which were used by researcher like calcium chloride, sodium carbonate and the most common is potassium chloride [429]. In this study deionised water was used since water is easier to be provided by the lay people (e.g., farmer) compared to other solvent. Volume from 100 to 200 mL of deionized water was used in this study. The cafetiere can occupied 500 mL of water and 60 mL as minimum since lower than 60 mL will be below the mesh level. The 8 g of soil was first added to the cafetiere, and volume of water was then added (100-200 mL), the piston was pushed down, and 3 minutes was allowed for soil settlement. **Figure** 4.46 result and it shows the concentration of nitrate in mg kg^{-1} of nitrate versus the volume of water in mL the concentration of nitrate sounds to be similar (with no significant difference) at different volume using ANOVA test result (F= 1.78, $F_{Critical}$=3.11, P=0.19, α=0.05, n=3, ANOVA test). Therefore, 100 mL of water was chosen as optimum volume for the extraction since very high volume can cause dilution of the of soil sample with very low concentration of nitrate.
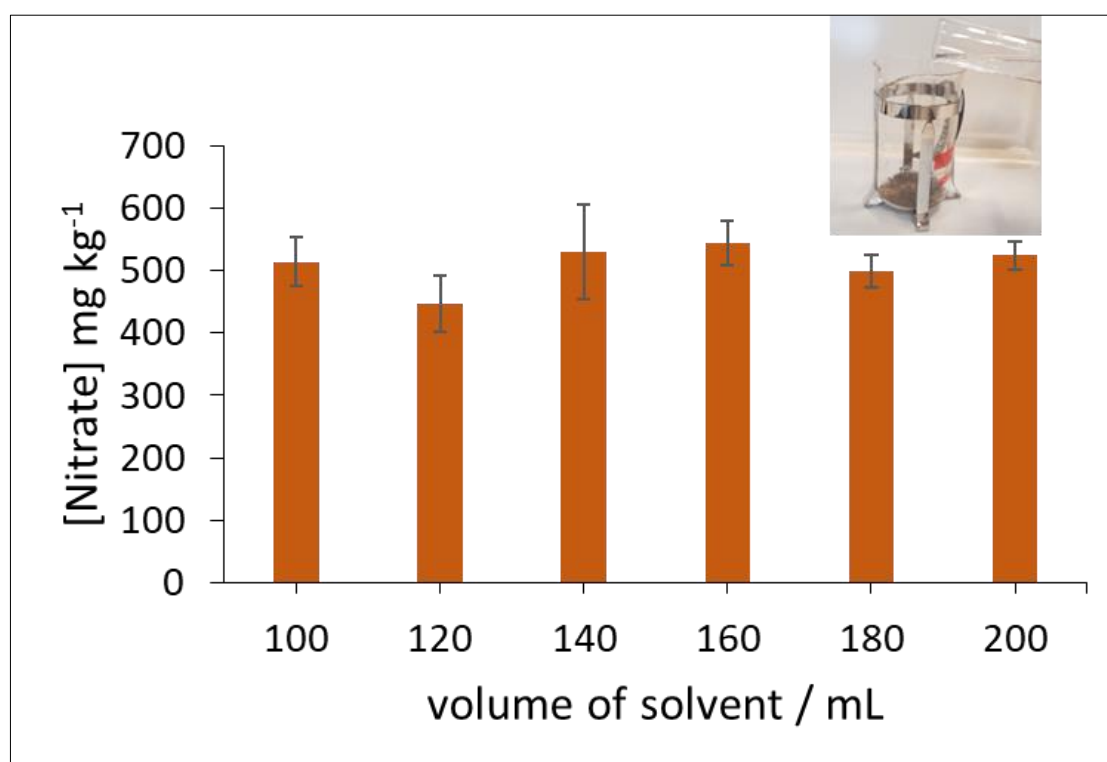
Figure 4.46 Nitrate concentration (mg kg^{-1}) versus the volume of deionized water (mL). the extraction was done as in **Figure** 4.11. John Innes no1 was studied and detection of nitrate was done by IEC. Repeats n=3.

Number and time of pushing.

Mixing of the soil and the solvent is a critical step to reach a good equilibrium for nitrate between soil and the solvent(water). In usual lab work a shaker was used to achieve this purpose. Here

the piston of the cafetiere was moved up and done to do the shaking. The soil (8g) was added to the cafetiere, and 100 mL of the water was then added, and the piston was pushed down for specific time (from 1 push up to 6 push). The result as in **Figure** 4.47 which shows the concentration of nitrate in mg kg^{-1} versus the number of pushes. As the number of pushes increased the concentration of nitrate increased, however, after two pushes the concentration start to be constant up to 6 pushes. 2 pushes seem to be the optimum number of pushes.
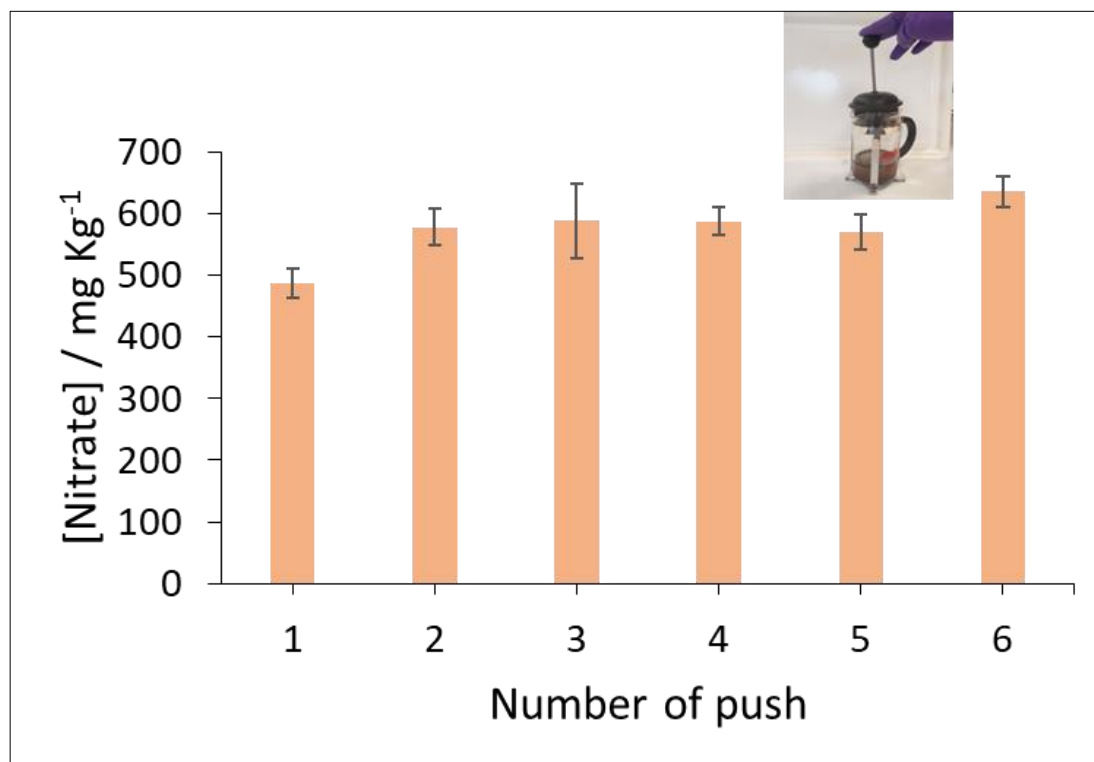
Figure 4.47 Nitrate concentration mg kg^{-1} versus the number of pushes. the extraction was done as in Figure 4.11. John Innes no1 was studied and detection of nitrate was done by IEC. Repeats n=3.

Other than the number of pushes the time of pushes was tried. The pushing was done continuously for specific time from 0 to 3 minutes where at zero minutes 2 push was done since it was the optimum as in **Figure** 4.47. **Figure** 4.48 shows nitrate concentration in mg kg^{-1} versus the time of pushes. The result stays same from 1 to 3 minutes (with no significant difference) according to ANOVA test (F= 4.13, $F_{Critical}$=5.13, P=0.074, α=0.05, n=3, ANOVA test). 1 minutes pushing time seems to be enough to reach a good equilibrium of nitrate between soil and water. However, 2 minutes was chosen as optimum to avoid any decrease in the signal that may result if the person who is doing the pushing is tired and slow down the pushing a bit. **Table** 4.12 summarized the optimized parameter for cafetiere extraction of nitrate from soil.
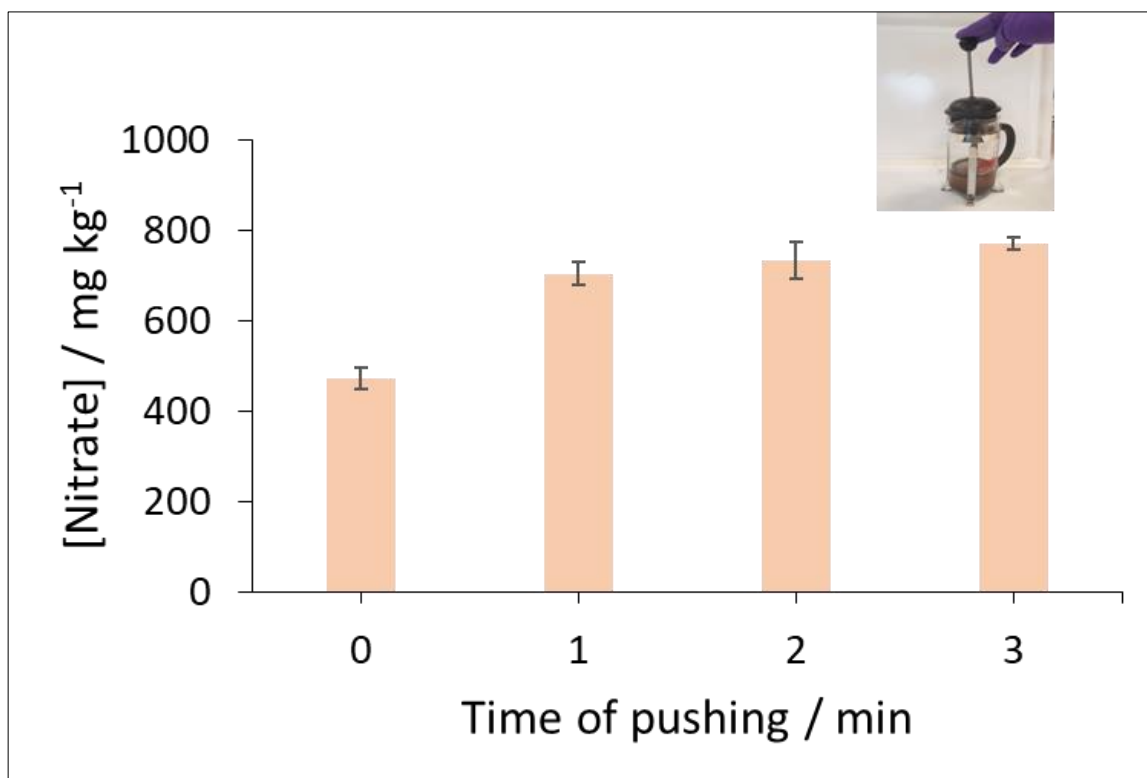
Figure 4.48 Nitrate concentration mg kg^{-1} versus the time of pushes(min). the extraction was done as in **Figure** 4.11. John Innes no1 was studied and detection of nitrate was done by IEC. Repeats n=3.

Table 4.12 summary of optimized parameter for cafetiere extraction of nitrate from soil.

Optimized parameter	Study range	Optimum
Mass of soil	3-9 g	8 g
Volume of water	100-200 mL	100 mL
Time of pushing	0-3 minutes	2 minutes

4.7.3 Efficiency of extraction

The cafetiere extraction cannot be trusted unless it is compared extraction which is usually perfumed in scientific laboratory. Shaker was used for this purpose. The extraction was done twice for soil samples, one by the cafetiere and the second by the shaker. Same mass of soil and volume of deionized water was used in both extractions to keep the same effect of the amount and quantities which are used. For cafetiere extraction the optimum condition was used. 100 mL of deionized water was added to 8 gram of soil in the cafetiere, and the piston was pushed up and done for 2 minutes and then the soil was allowed to settle for 3 minutes. For the conventional extraction 8 gram of soil and 100 mL of water were added into 250 mL bottle and

it allowed to be shaken in the shaker for 1 hour. Other conventional method in the literature are using other more efficient extraction solvent and some of them do the shaking for shorter time than 1 hour [115,116]. In this experiment 1 hour was chosen to ensure a good extract ion by water solvent. **Figure** 4.49 shows the result from ion exchange chromatography for soil one when the two extractions where performed. The two extractions gave similar result with no significant difference (t_{stat}=--0.17, $t_{critical}$=2.78, P=0.87, α= 0.05, n=3, two tailed test) for nitrate concentrations which is around 780 mg kg^{-1}, hence this indicates the efficiency of the cafetiere compare to the shaking device.

Another point which needs to be determine is the efficiency of the normal extraction itself. This was done by doing several conventional extractions for the same soil sample. After doing the first extraction the water was removed totally from the soil and the soil sample was dried in room overnight. Then the second extraction was done for the same dried sample by adding to it 100 mL of water. The result from the three extractions as in **Figure** 4.50. Around 90 % of nitrate in the soil was extracted by extraction 1 and the rest 10% was extracted in extraction 2. Therefore, the cafetiere was also able to extract around 90 % (93.49 ±2.06%) of the nitrate from soil since it gave the same result as mentioned previously in **Figure** 4.49. **Figure** 4.51 show the nitrate concentration in three types of soil when conventional and cafetiere extraction where used. The result from the two soil, John Innes1 (t_{stat}=--0.17, $t_{critical}$=2.78, P=0.87, α= 0.05, n=3, two tailed test) and John Innes 2 (t_{stat}=0.94, $t_{critical}$=2.78, P=0.40, α= 0.05, n=3, two tailed test) shows similarity for conventional and cafetiere extraction using t-test. This indicates good efficiency of the cafetiere extraction method. However, John Innes 3 shows 7 % difference between conventional and cafetière extraction and this is happened maybe due to error during the experiment like sample loss or different days of doing the experiment. However still 7% is not a huge difference.
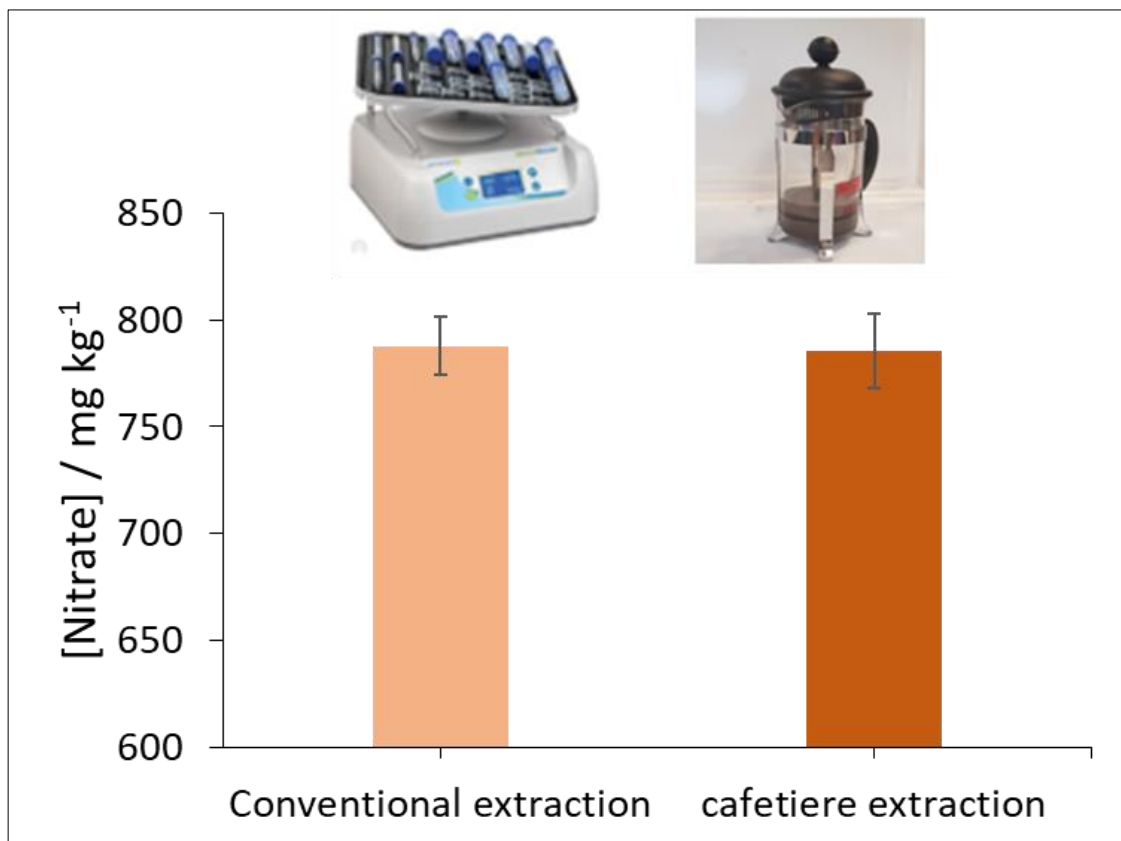
Figure 4.49 Nitrate concentration mg kg^{-1}versus the type of extraction. For cafetiere extraction: 8 gram of soil in the cafetiere and the piston was pushed up and done for 2 minutes and then the soil was allowed to settle for 3 minutes. For the conventional extraction: 8 grams of soil and 100 ml of water were added into 250 mL bottle, and it allowed to be shaken in the shaker for 1 hour. John Innes no1 was used. Detection was by IEC. Repeats n=3.
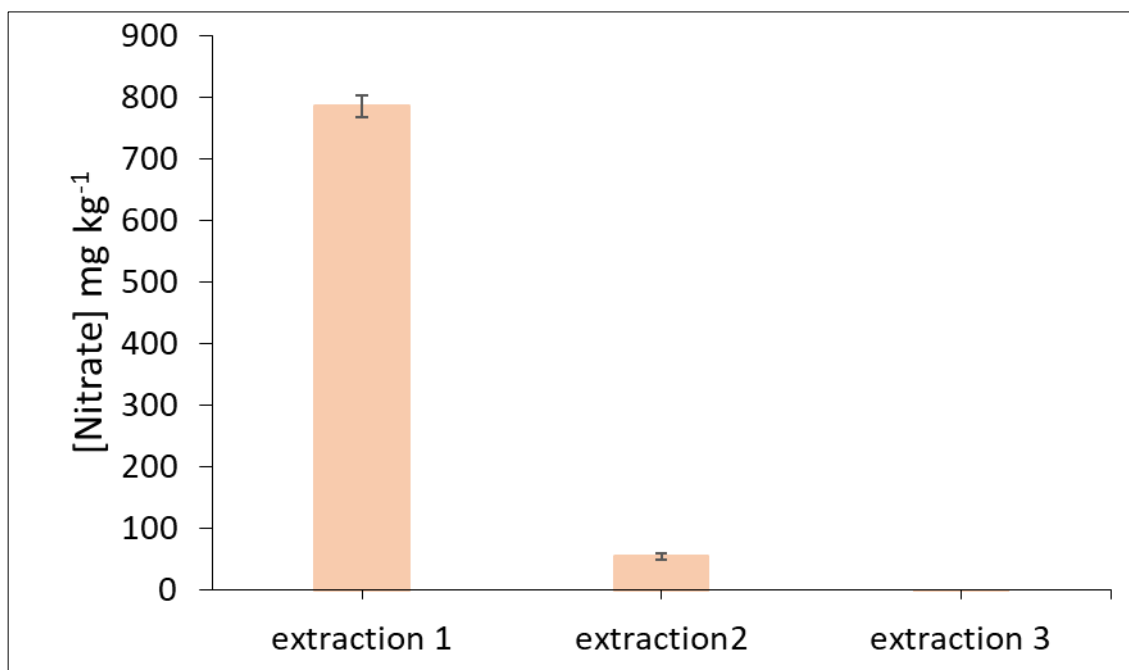
Figure 4.50 Nitrate concentration mg kg^{-1} versus the number of extractions. For the conventional extraction: 8 grams of soil and 100 ml of water were added into 250 mL bottle, and it allowed to be shaken in the shaker for 1 hour. Jhon Innes no1 was used. Detection was by IEC. Repeats n=3.
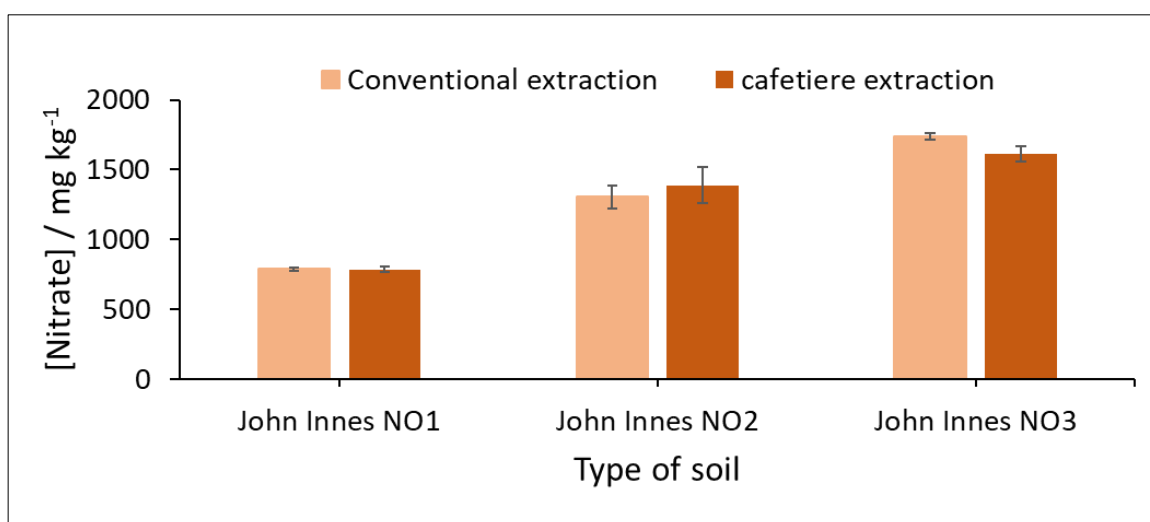
Figure 4.51 Nitrate concentration mg kg^{-1} versus the type of soil. For cafetiere extraction: 8 gram of soil in the cafetiere and the piston was pushed up and done for 2 minutes and then the soil was allowed to settle for 3 minutes. For the conventional extraction: 8 grams of soil and 100 ml of water were added into 250 mL bottle, and it allowed to be shaken in the shaker for 1 hour. John Innes no1, 2 and 3 were used. Detection was by IEC. Repeats n=3.

4.7.4 Efficiency of PAD detection

The optimization and the previous comparison in the previous sections were done by ion exchange chromatography. To determine the PAD efficiency nitrate detection by the PAD was compared to ion chromatography. Both the developed cafetiere extraction and μPAD detection were used to analysed soil sample as describe in **Figure 4.52** . After the extraction some of the extracted solution was analysed by PAD and some by IEC. IEC was used to validate the result

from the developed µPAD. The result was as in **Figure 4.52** where three compost soil samples (John Innes 1,2,3) and two real topsoils were analysed. µPAD agree with IEC with no significant difference using t-test (e.g. John Innes soil 1, t_{stat}=1.09, $t_{critical}$=2.78, P=0.34, α= 0.05, n=3, two tailed test). Compare to commercial compost the topsoil sample has less nitrate and this is expected since the real soil sample has no nutrients additives. Compost and real soil sample were tested for organic matter content as **Figure** 4.53 . Up to 25% organic matter did not cause coloration in the paper fibre as in **Figure** 4.54 Which compare a blank µPAD which was immersed for 8 minutes in DIW, extract of John Innes 1,2,3 and extract of top soil 1 , 2.
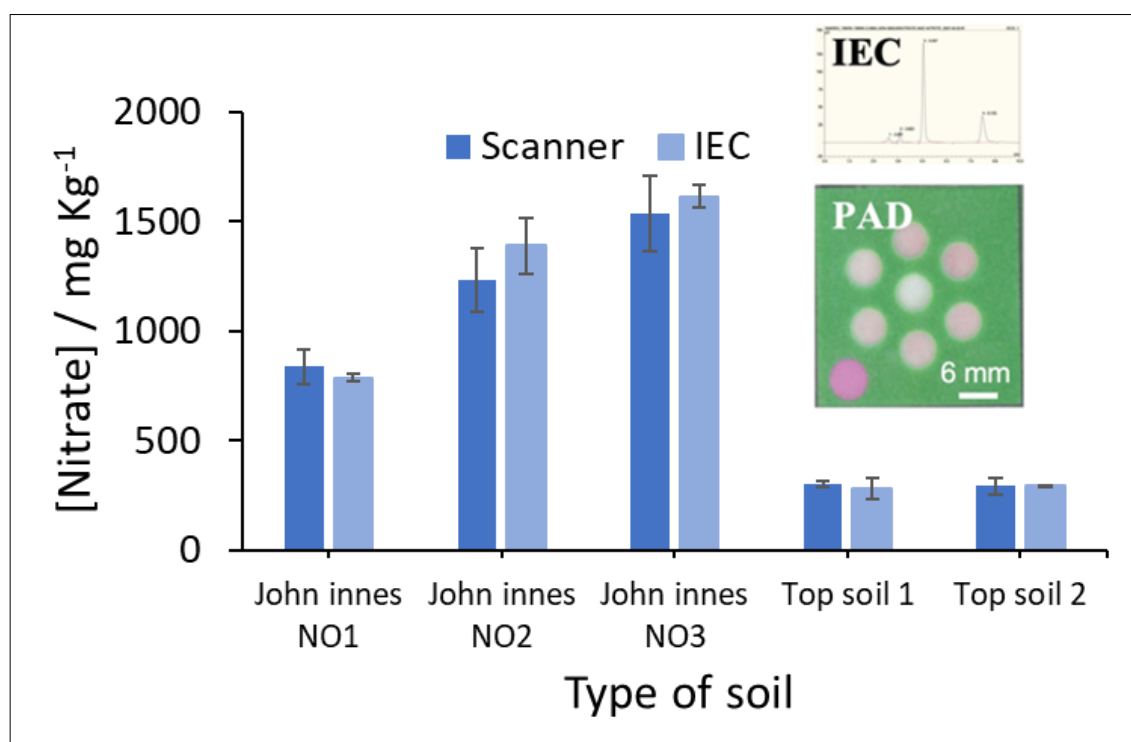
Figure 4.52 Nitrate concentration mg kg^{-1} versus the type of soil. For cafetiere extraction: 8 gram of soil in the cafetiere and the piston was pushed up and done for 2 minutes and then the soil was allowed to settle for 3 minutes. John Innes no1, 2 and 3 and to topsoil samples were used. Detection was by IEC and PAD. Repeats n=3 PAD.
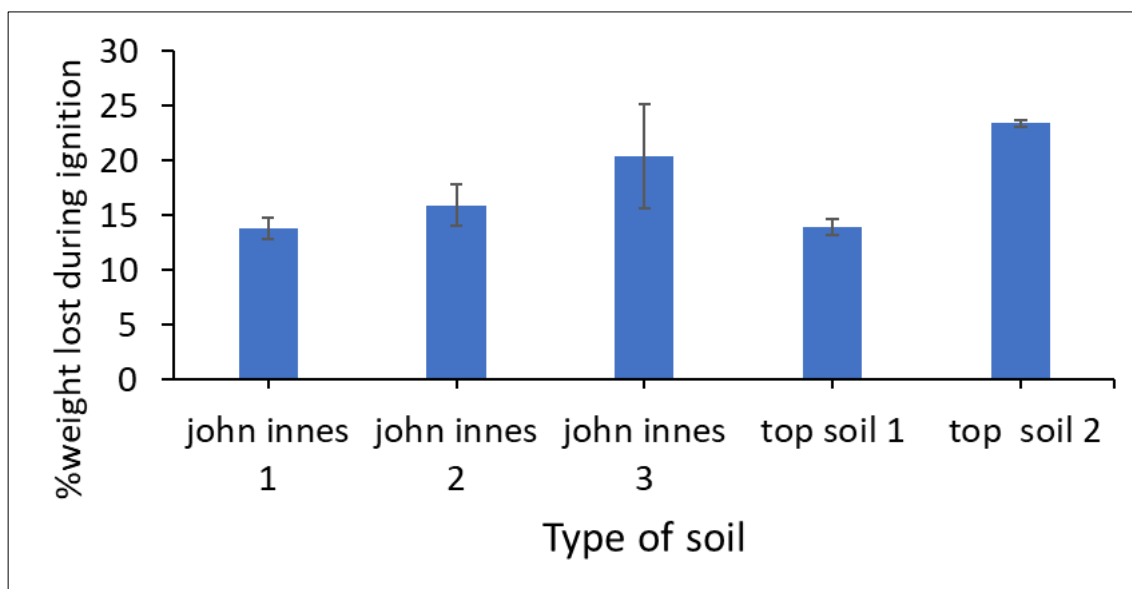
Figure 4.53 % of mass loss versus the type of soil. organic matter % in John Innes No 1,2,3 soil and topsoil 1, 2. % calculated as in equation 4.1. Repeats n=3.
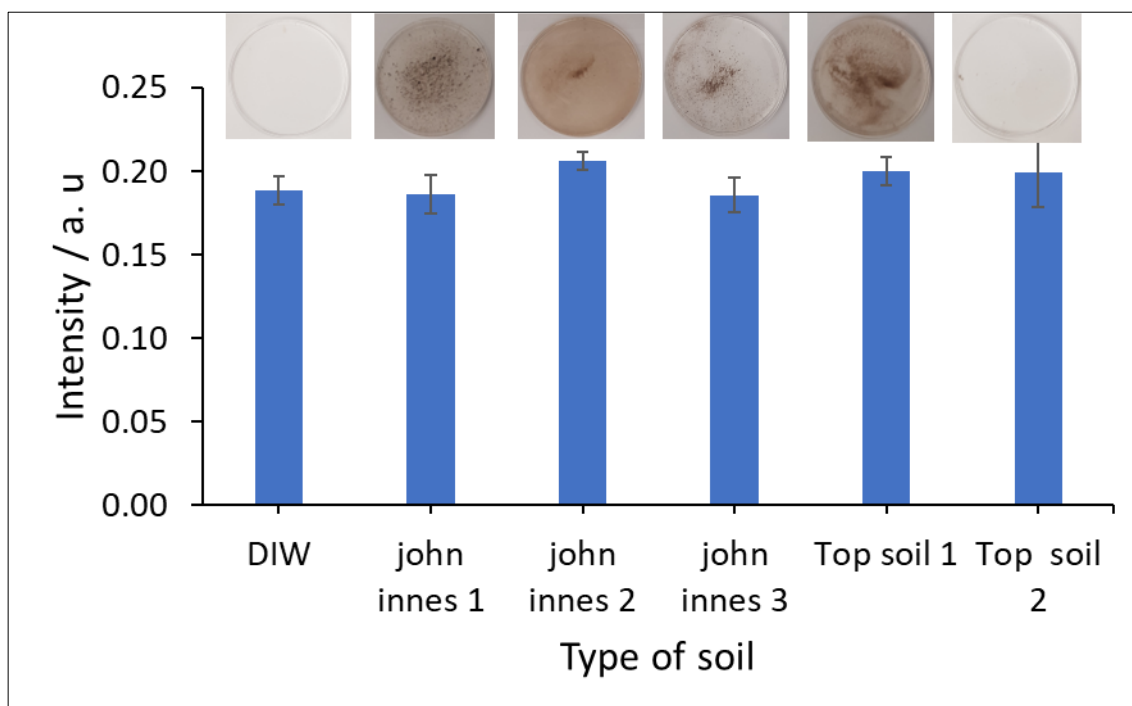
Figure 4.54 Intensity versus type of soil. Intensity from blank PAD 12 (with no reagents) after dipping for 8 min in DI water, John Innes No 1,2,3 soil and topsoil 1,2.

4.7.5   Spiking soil sample

The three types of soil were spiked with 310 mg kg^{-1} of nitrate. The spiking was done to determine the ability of the method to recover the added nitrate. The soil was allowed to dry over night after spiking. **Figure** 4.55 shows the nitrate concentration before and after removing the spike (310 mg kg^{-1}). The analysis readout was done by the PAD. **Figure** 4.56 compare the spiked soil (after removing the spike effect) and the soil which is not spiked. The result is not

significantly different using t test (e.g., John Innes soil 2, t_{stat}=1.39, $t_{critical}$=2.78, P=0.24, α= 0.05, n=3, two tailed test) and this make sense.
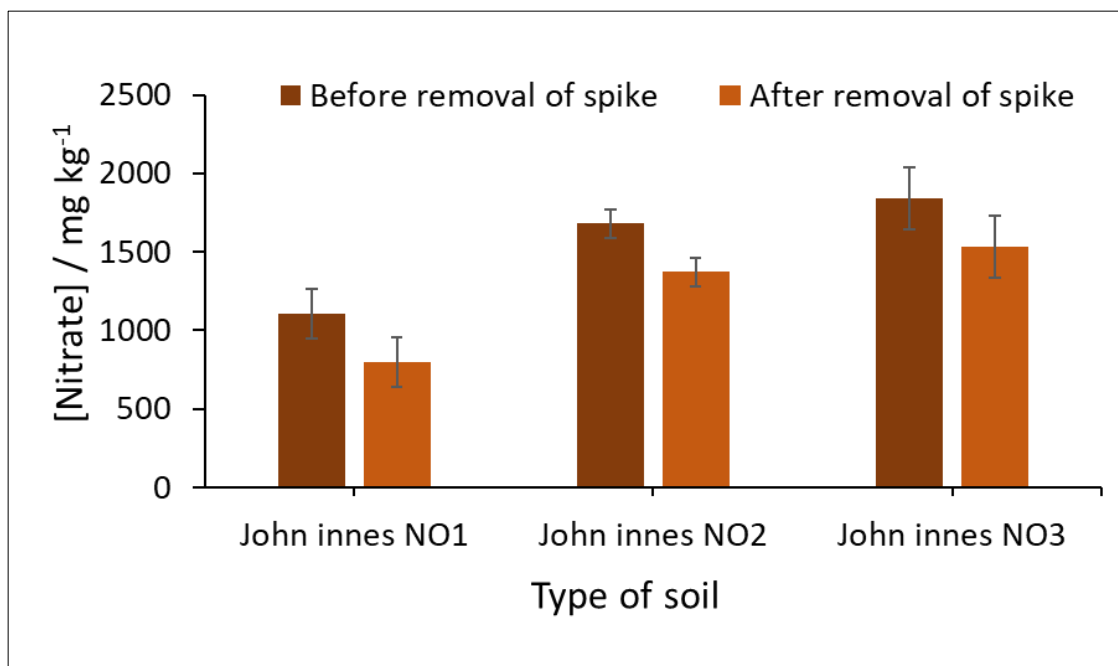
Figure 4.55 nitrate concentration mg kg^{-1} versus the type of soil. Result before and after spiking the soil sample. For cafetiere extraction: 8 gram of soil in the cafetiere and the piston was pushed up and done for 2 minutes and then the soil was allowed to settle for 3 minutes. Jhon Innes no1, 2 and 3 were used. Detection was by PAD. Repeats n=3.
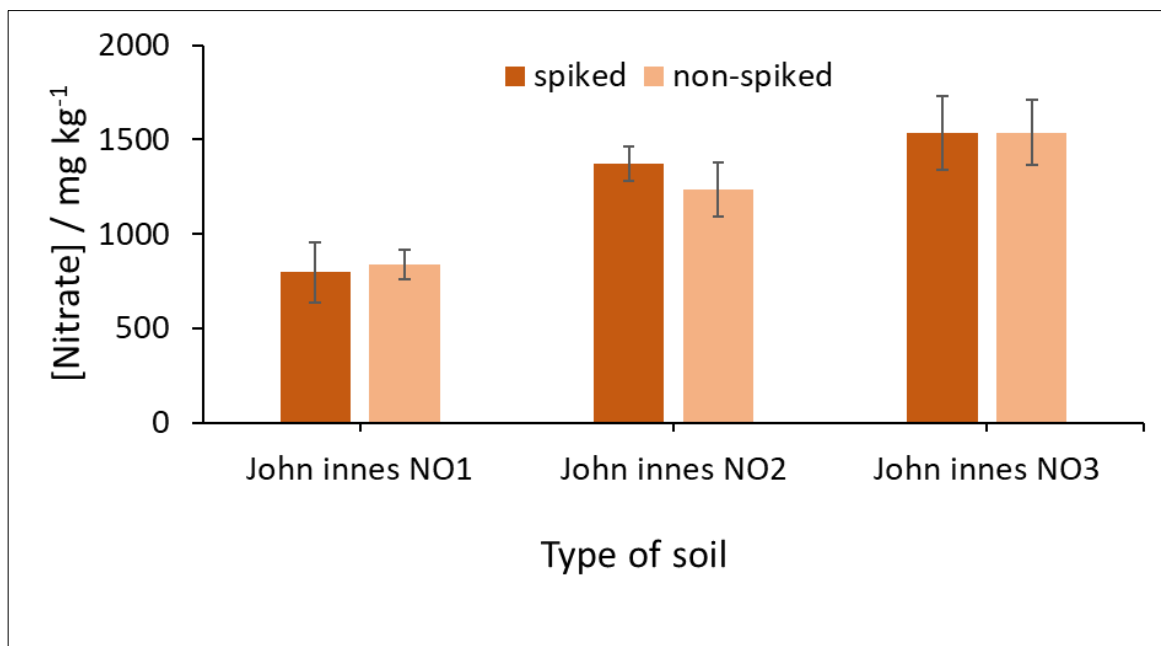
Figure 4.56 Nitrate concentration mg kg^{-1} versus the type of soil. Result of spiked (after removing the spike effect) and non-spiked soil sample. For cafetiere extraction: 8 gram of soil in the cafetiere and the piston was pushed up and done for 2 minutes and then the soil was allowed to settle for 3 minutes. Jhon Innes no1, 2 and 3 were used. Detection was by PAD. Repeats n=3.

4.7.6   Field accessibility

4.7.6.1   Spoon versus balance

The aim of this work is to design method which is easy to be used by the lay people (e.g., farmers) themselves. The use of cafetiere for extraction and the PAD for detection make this process easy. Cafetiere can be bought and used easily by farmer by only moving the piston and adding the soil and water to it. The PAD can be easily used by only dipping it into the solution. There is another thing which need to be improved yet the use of balance to measure the mass of soil since the farmer cannot provide balance in the field. Therefore, the use of spoon was suggested since other kits relay on scoops too. Instead of using the balance a specific number of spoons were used. The mass of soil which was used in this study is 8 g. 8 gram was equivalent to 4 spoons (2 mL spoon) of soil. Repeats were done to measure the soil by taking 4 spoons of soil three times each 30 minutes as in **Figure** 4.57. 30 minutes was taken between measurements to make sure that the result was not consistent only due to getting use to the way of taking soil. The result was compared using ANOVA test and showed no significant difference between tries. Therefore, John Innes no 1, 2 and 3 soil were analysed by the PAD and spoon instead of Balance. 4 spoons of soil in the cafetiere with 100 mL DIW and the piston was pushed up and done for 2 minutes and then the soil was allowed to settle for 3 minutes. The result as in **Figure** 4.58 which shows nitrate concentration versus the type of soil when balance and spoon were used to measure the mass of soil. The result from spoon and balance is similar and agree when t-test was used for comparison (e.g., John Innes soil 1, t_{stat}=-2.04, $t_{critical}$=2.78, α= 0.05, P=0.11, n=3, two tailed test). The spoon may vary from place to place in term of shape. The farmer will be advice first to use the balance and determine how many spoons is equivalent to 8 gram or the spoon can be provided for farmers.
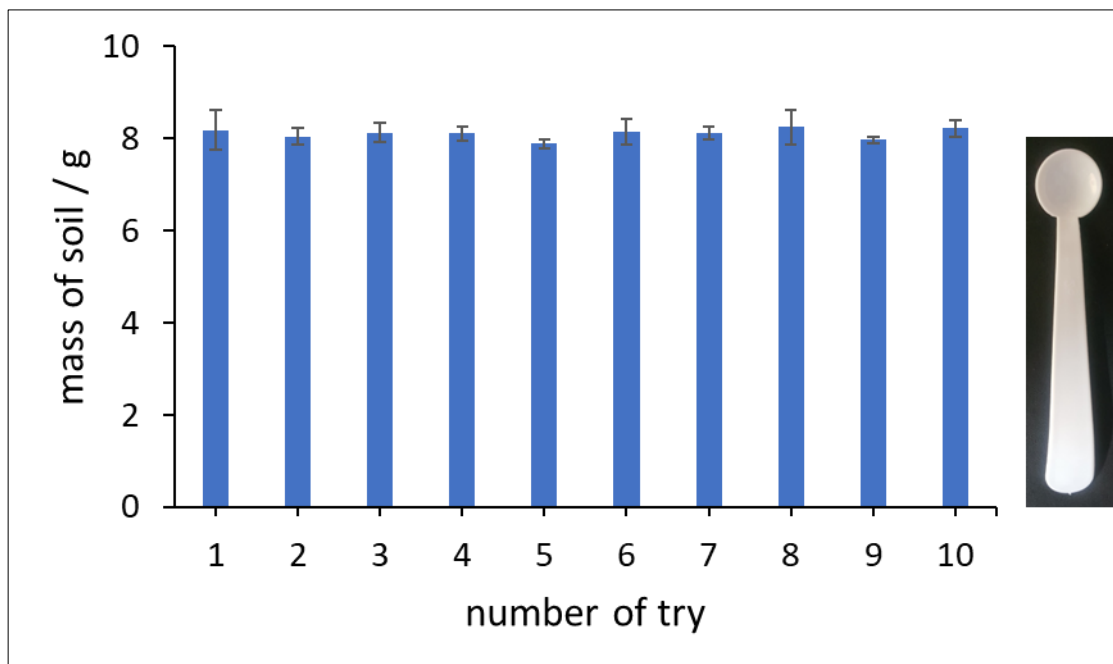
Figure 4.57 Mass of soil versus the number of repeats. measuring of 8 g mass of John Innes No 1 three times each 30 seconds using 4 spoons of soil and analytical balance, the average of masses (n=3) showed no significant difference.
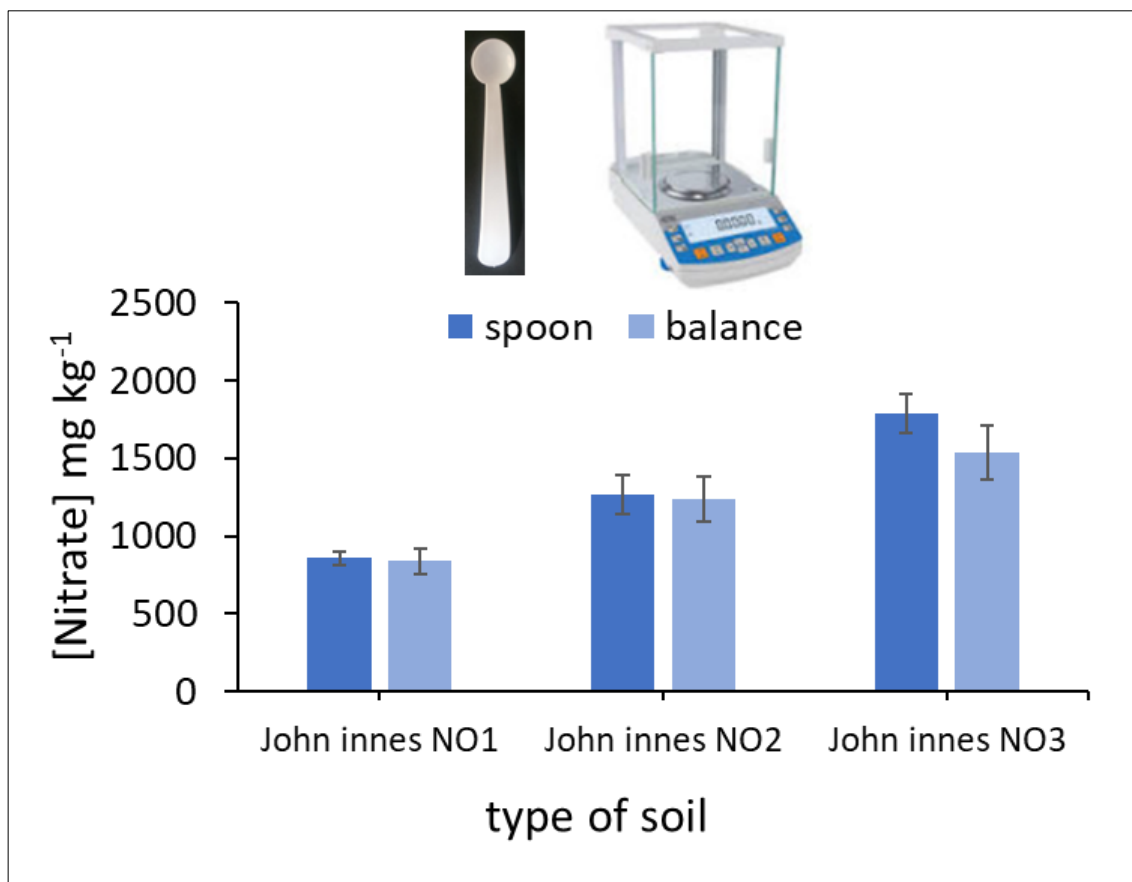
Figure 4.58 Nitrate concentration mg kg^{-1} versus the type of soil. For cafetiere extraction: 8 gram or 4 spoons of soil in the cafetiere with 100 mL DIW and the piston was pushed up and done for 2 minutes and then the soil was allowed to settle for 3 minutes. John Innes no1, 2 and 3 were used. Detection was by PAD. Repeats n=3.

4.7.6.2   Type of solvent

The solvent which was used for extraction is deionized water. However, in the field it is difficult to provide deionized water especially in the non-developed countries. Therefore, two other solvents were suggested to be studies, mineral and tap water. Mineral water is easy to be used since its nitrate content is already written in the bottle which is around 3.5 mg L^{-1}. This amount is very small, especially if the soil has high amount of nitrate. However, in case of small amount of nitrate the farmer can subtract the 3.5 mg L^{-1} from the concentration that they will get finally. However, the use of tap water is a bit complicated because of two reasons, the first reason is that the exact amount of nitrate in tap water is unknown, and the farmers must measure the nitrate content in tap water separately and then remove this effect from the soil which was extracted by tap water. The second reason is that tap water has a lot of interference that may interfere with the result. **Figure** 4.59 shows nitrate concentration in DIW, mineral and tap water when PAD and IEC were used for detection. Mineral water showed similar result from PAD and IEC which is the same as the result from the mineral water bottle around 3.5 mg L^{-1}. However, the tap water shows lower result from the PAD readout compared to IEC, this is maybe due to the interference from the tap water which leads to the reduction of the colour. The concentration from the PAD is around 20 % less than that from IEC. If this % is constant, then this can be solved by some calculation. **Figure** 4.60 shows concentration of nitrate from soil John Innes no 1 when tap and deionized water were used. This concentration is after removing the effect of Tap water. The tap water nitrate concentration was determined alone using separate PAD. The difference between the result from tap and DIW is around 18% reduction when tap water was used. This make sense since the reduction in intensity was around 20% from **Figure** 4.59. The problem with tap water is that this effect or reduction in signal will not be the same for all tap water, tap water from different area. **Figure** 4.61 show the result from the three soils when mineral and DIW were used. Soil John Innes no 2 shows some variation with significant difference between use of DIW and mineral water (e.g., John Innes soil 2, t_{stat}=-2.91, $t_{critical}$=2.78, P=0.044, α= 0.05, n=3, two tailed test) which was not expected. This was maybe due to the experimental error during sample preparation or due to doing experiments in different days since nutrients content in soil may change with time.
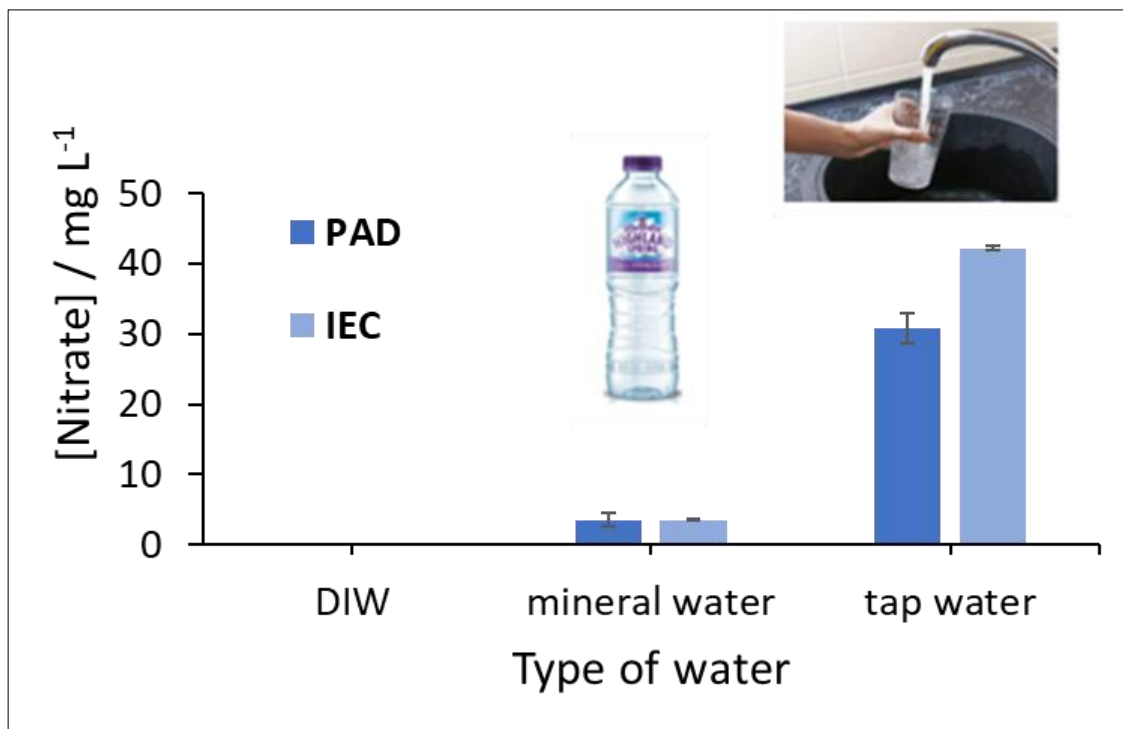
Figure 4.59 Nitrate concentration mg L^{-1} versus the type of water. DIW, Tap and mineral (HIGHLAND SPRING) water were analysed. Detection was by PAD and IEC. Repeats n=3.
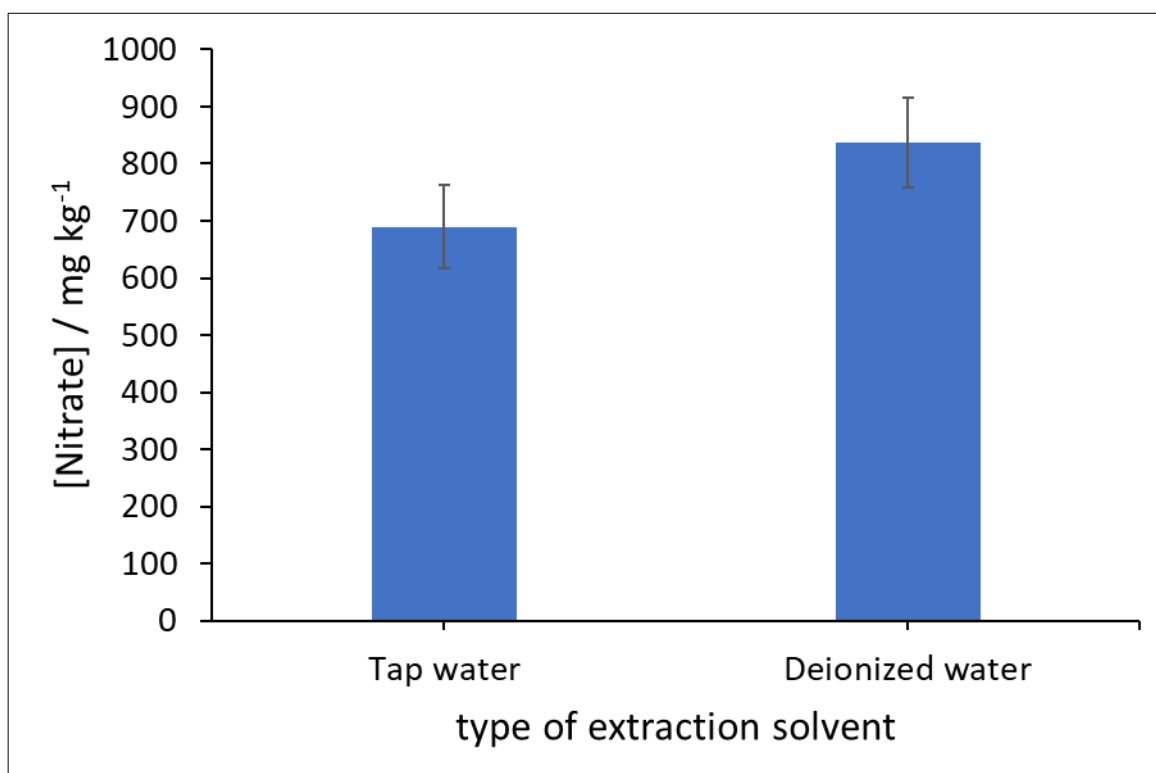
Figure 4.60 Nitrate concentration mg kg^{-1} versus the type of water. Tap water was used as extraction solvent. For cafetiere extraction: 8 gram of soil in the cafetiere with 100 mL of water and the piston was pushed up and done for 2 minutes and then the soil was allowed to settle for 3 minutes. John Innes no1 was used. Detection was by PAD. Repeats n=3.
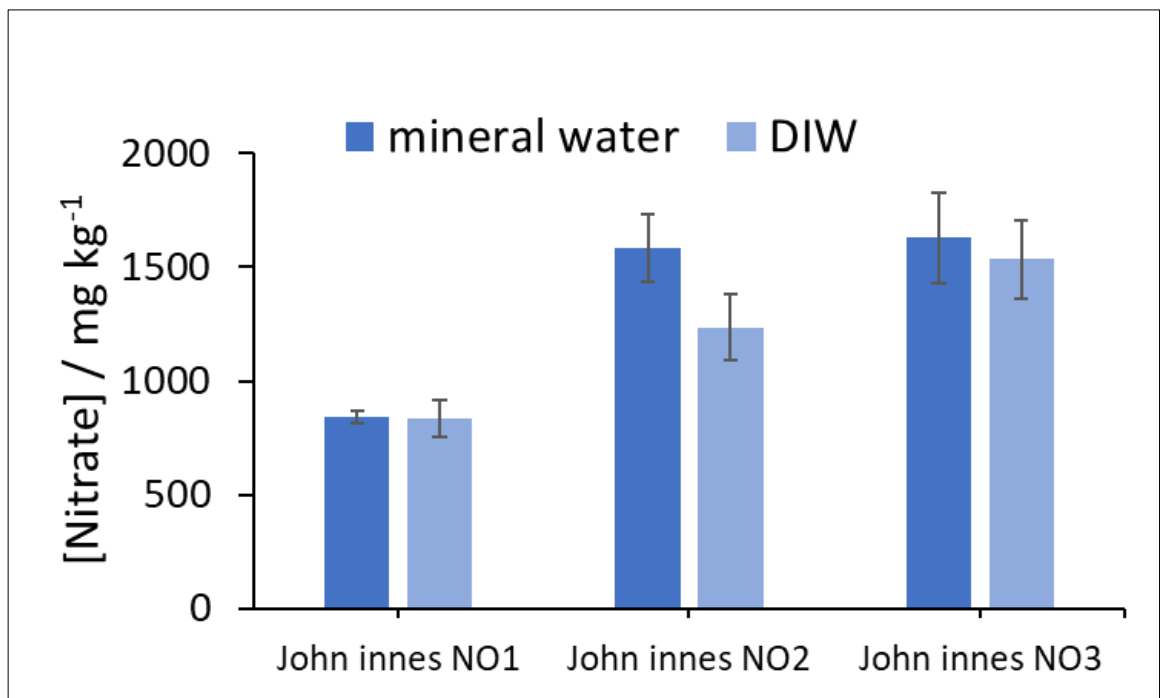
Figure 4.61 Nitrate concentration mg kg^{-1} versus the type of soil. Minera and DIW water were used as extraction solvent. For cafetiere extraction: 8 gram of soil in the cafetiere with 100 mL of water and the piston was pushed up and done for 2 minutes and then the soil was allowed to settle for 3 minutes. John Innes no1, 2 and 3 were used. Detection was by PAD. Repeats n=3.

4.7.6.3   Phone versus scanner

Another concern to make the process easier for the farmer is the use of portable device to do the detection. Smart phone is a good option to do this as mentioned previously. Therefore, the concentration from the five types of soil was also determine using photo from the phone instead of the use of scanner. The result is as in **Figure** 4.62 which shows the concentration of nitrate in the three soils by phone and scanner. The two methods show consistent result with no significant difference for all soil samples using t test (e.g., John Innes soil 1, t_{stat}=1.09, $t_{critical}$=2.78, P=0.34, α= 0.05, n=3, two tailed test). Therefore, phone is an efficient method for the detection. **Table** 4.13 summarized soil experiment for nitrate detection in soil.
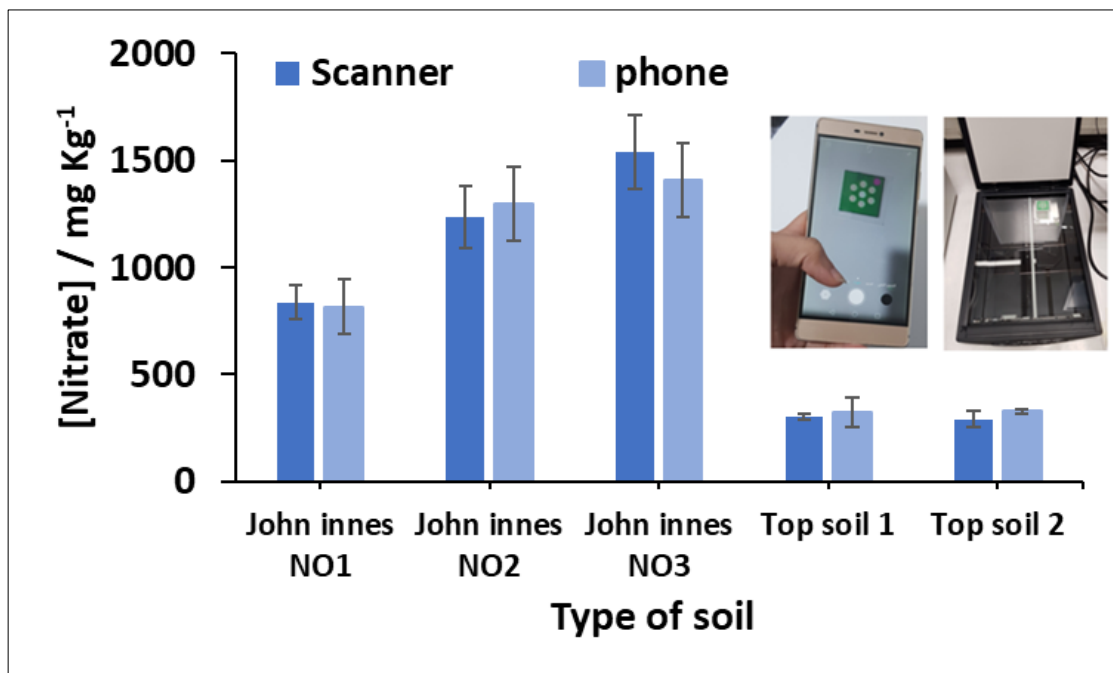
Figure 4.62 Nitrate concentration mg kg^{-1} versus the type of soil. Phone and scanner were compared for detection. 8 gram of soil in the cafetiere with 100 ml of water and the piston was pushed up and done for 2 minutes and then the soil was allowed to settle for 3 minutes. Jhon Innes no1, 2 and 3 and topsoil 1 and 2 were used. Detection was by PAD (phone and scanner). Repeats n=3.

Table 4.13 Summary of soil experiments for nitrate detection by PAD and IEC where two extraction method were compared (cafetiere and conventional extraction). Spoon and balance were compared for measuring the amount of soil. Soil was spiked to determine the recovery. DIW were compared with Mineral water. John Innes no1, 2 and 3 and topsoil 1 and 2 were used.

Detection method	IEC		PAD (SCANNER)		PAD(PHONE)
extraction method	Cafetière	Conventional	Cafetière	conventional	Cafetière
John Innes no 1	785.72±17.34	787.96±13.85	836.75±79.32	714.52±26.30	814.44±127.70
John Innes no 1 SPOON	706.56±77.42		855.83±39.16		
John Innes no 1 MINERAL WATER	894.91±19.66		842.36±28.64		
John Innes no 1 +SPIKE	1011.29±19.78		1107.01±158.89		
John Innes no 1-SPIKE	701.29±19.78		797.01±158.89		
John Innes no 2	1387.73±128.30	1304.49±84.06	1233.97±145.04	1420.36±47.06	1297.99±173.65
John Innes no 2 SPOON	1440.97±108.87		1265.71±126.64		
John Innes no 2 MINERAL	1421.78±11.77		1584.02±149.50		
SOIL2+ SPIKE	1825.92±87.16		1681.10±90.81		

Detection method	IEC		PAD (SCANNER)		PAD(PHONE)
John Innes no 2-SPIKE	1515.92±87.16		1371.10±90.81		
John Innes no 3	1613.70±53.50	1738.33±23.67	1535.13±172.19	1502.74±52.09	1406.31±171.53
John Innes no 3 SPOON	1848.28±117.81		1786.32±124.99		
John Innes no 3 MINERAL WATER	1826.62±27.44		1629.56±197.97		
John Innes no 3+ SPIKE	1621.24±158.53		1841.68±195.65		
John Innes no 3-SPIKE	1311.24±158.53		1531.68±195.65		
Topsoil 1 (spoon + mineral water)	279.60±45.53		301.39±15.01		329.07±11.33
Topsoil 2 (spoon + mineral water)	290.48±5.38		290.53±38.95		325.59±67.66

4.7.7　Validation of workflow by CRM

Certified reference material was used to double validate our method either for IEC or the PAD when the cafetière was used for the extraction. **Figure** 4.63 shows the nitrate content in CRM which was extracted by cafetiere and analysed by IEC and PAD (scanner). The two result was compared to the true value which was given by the sealer. The CRM contains approximately 200 mg kg^{-1} of nitrate. This finally helped to trust both our extraction by cafetière and detection by the developed PAD.
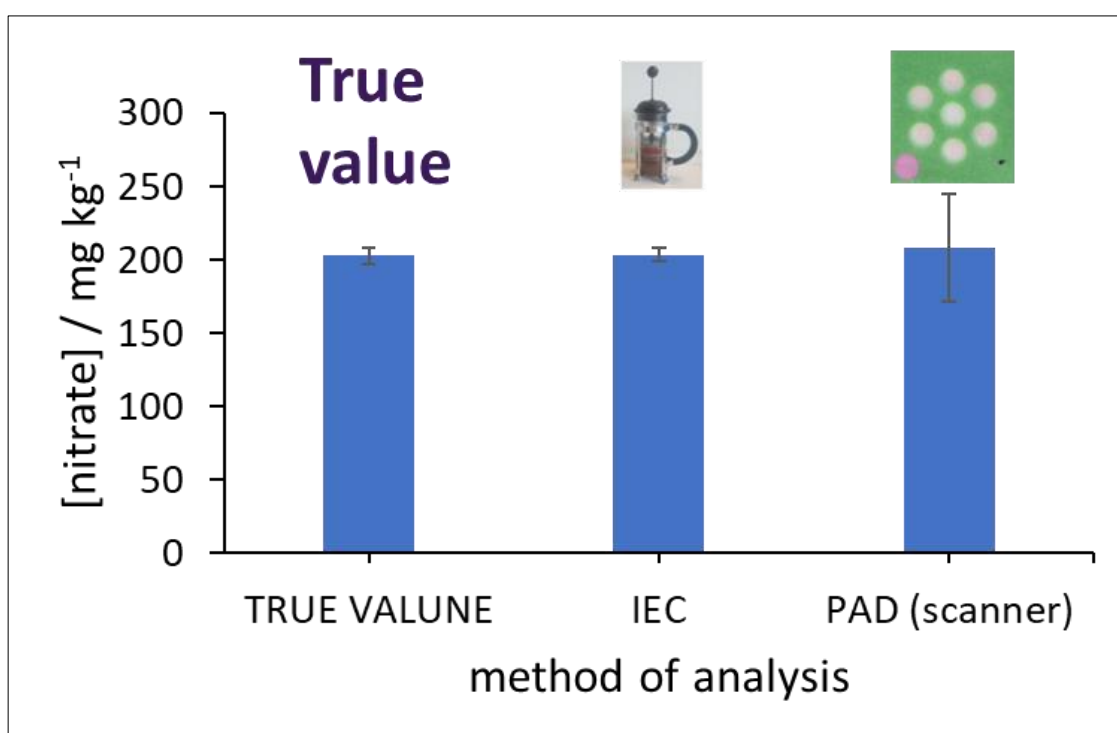
Figure 4.63 Nitrate content (mg kg^{-1}) versus the method of analysis. nitrate content in CRM which was extracted by cafetiere and analysed by IEC and PAD (scanner). Repeats n=3.

4.7.8　Comparison with field method (Palintest)

Palintest is one of the commercial tests which was used for soil nutrient determination included nitrate. The Palintest content as in **Figure** 4.64. The chemicals were bought separately. Some of the chemicals were toxic as mentioned by the seller. Filtration is required finally to separate the soil. The developed workflow was compared to the Palintest as in **Figure** 4.65 which shows the content of nitrate versus the type of soil when two analysis method was used (our workflow and the palintest). John Innes 1, 2, 3 and topsoil 1, 2 and CRM were studied by the two methods. The Palintest overestimate the nitrate by around 90% more for all samples. This may be due to the interferences that interfere during the extraction and detection. This also may be due to the

reading meter itself since it was not new and borrowed from different lab. Also, maybe a systematic error occurs due to doing any of the steps by the same wrong way since it was first time for researcher to use palintest. Since the effect was the same in the soil samples and CRM, we expect that there is something wrong with the method. Especially that our workflow agreed with the CRM as mentioned in **section 4.7.7**. This method is expensive [419] and difficult to provide by low-income countries. It also required multi steps to be performed by the user and this is why error happened. Multi step work means more possibility of error to occur.

Figure 4.64 Palintest is commercial tests which was used for soil nutrient determination included nitrate. chemicals were bought separately. Filtration was required.
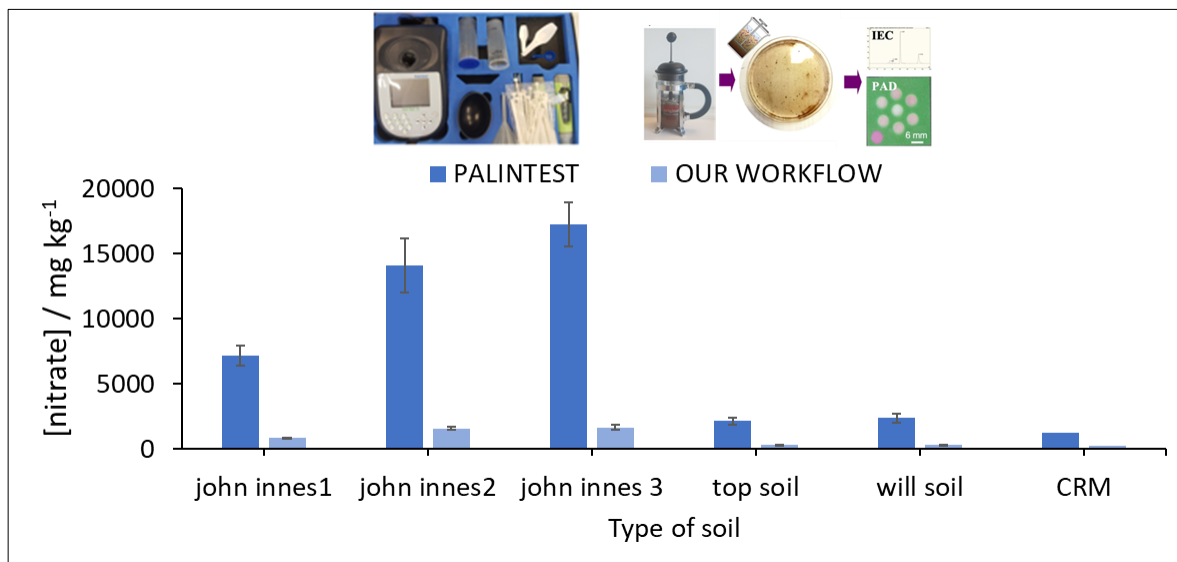
Figure 4.65 The content of nitrate (mg kg^{-1}) versus the type of soil when two analysis method was used (our workflow and the palintest). John Innes 1, 2, 3 and topsoil 1, 2 and CRM were studied by the two methods. Repeats n=3.

4.8   Discussion and Conclusion

Regular monitoring of nitrate in the field is required. The available in field methods are costly and needs time. We successfully developed simple workflow which was based on two steps, extraction by cafetière and detection by paper-based sensor which was based on phone readout.

Extraction of the soil nutrients in the field is challenging due to the difficulty of the availability of the equipment, the multi steps of extraction and the requirement of non-user-friendly reagent use to perform the extraction. In this study three devices (Cafetiere, AeroPress and paper cup) were compared for their simplicity in extraction and their ability to filter the soil slurry from the extracted solution. AeroPress was hard to use since it required applying pressure to filter the sample. Also mixing with was not possible. The paper cup contains no filtration system even though it was easy to use. In comparison cafetière was easy to use and extract shows same intensity to the DIW intensity. The cafetière was easiest to use since plunger provide method for mixing. In addition, the end of the plunger was attached to meshes which helped in the filtration. Using cafetière it was found that 8 g of soil, 100 mL of water solvent and 2-minute mixing in the cafetière provided good nitrate extraction with no significant difference when compared with shaker The extraction efficiency of cafetière was found to be around 90%. 90% of nitrate was extracted from the first extraction and 10% of nitrate was extracted in the second extraction.

Other than using easily available equipment (cafetière) other parameter was considered since balance and DIW are not available in the field. The extraction method was further improved to fit the field needs by the replacement of the weighing machine with the use of the spoon to add the soil sample. The use of 4 spoons of soil was equivalent to 8 g of soil. In field for long term use the farmer should be advised to check how many spoons are equivalent to 8 grams of soil since spoon may vary. In addition, mineral water was an alternative with no significant difference to DIW for nitrate extraction. Mineral water is easy to be provided from shop compared to the DIW, consequently, it can be easily provided in the field by lay people. In general, 5 minutes extraction step was developed and simplified for the field use. Compared to other field extraction methods Which required hand shaking followed by use of filter paper [420], syringe connected to filter extraction [421] and automatic extraction mounted with full extraction-detection unit [422], the developed extraction is simple, short, used existing equipment, require no chemicals and require no filtration. These features make it good alternative method that can be used in the field.

For the detection step the PAD from chapter three was developed for nitrate detection by adding a layer for deposition of zinc reducing agent. The developed PAD focus on deposition of

reagent at multi layers which can be aligned above each other to avoid the complexity of the device during use as mentioned in chapter 3. Zinc addition was challenging since pipetting zinc leads to accumulation of zinc and the development of dark colour that contribute to the intensity, therefore, zinc was added by immersion of the reduction layer into zinc solution (under stirring) for 1 second (to avoid the destroying the PAD). Adding zinc by this way offer advantages compare to pipetting the zinc, it reduced the dark colour of zinc accumulation in the device. The intensity of blank was reduced by around 22 %. In addition, immersion helped to deposit zinc in the two side of the device. Even though by immersion the amount of zinc added was unknown, addition of zinc by immersion introduced an easy used method which is reproducibly as well as efficient. The blank signal was reduced by total of 43% because of the reduction of zinc dark colour due to the addition of zinc by immersion (22% of reduction) and also due to the availability of the several layers (21% of reduction). The reduction in the blank signal means improvement in the sensitivity of the device. The reduction efficiency of the method was found to be 53.61 ±0.78%. Based on this reduction efficiency The time of the analysis was found to be 8 minutes of dipping the PAD into the solution/sample. The PAD was able to detect up to around 27.10±2.64 mg kg^{-1} and 34.35±2.77 mg kg^{-1} of nitrate in soil by scanner and phone respectively and this is lower than the lower level of nitrate (44 mg kg^{-1} [348,426,427]) below which fertilizer need to be applied by farmer.

The PAD was found to be robust in the presence of interferences. The heavy metals like Zn^{2+} and Mn^{2+} interfere at concentration higher than 100 mg L^{-1} and their level in soil is lower than this level (**Table** 4.9). Anions and cations like Cl$^-$, SO_4^{2-}, PO_4^{3-}, K$^+$, Na$^+$, Ca^{2+} showed also high tolerance level which most of them do not exist in soil at this high concentration (**Table** 4.9). The tolerance of the PAD to the pH change was from pH 5 to 10, within this range is the best range for plant growth [394]. The device expiry date was also important to determine to inform user about the lifetime of the device, The device was stable for 17 days (around 2 weeks) at room temperature (22 ^{0}C) in the dark and for around 53 days around 8 weeks in the freezer (-4 ^{0}C). This information is important to be mentioned with the PAD when is sale for user.

Compared to other studies (**Table** 4.11) the developed PAD focus on soil sample analysis. None of the previous studies focus on the study of soil sample, most of them concentrate in the water and food samples. The multi layers provide filtration system for the PAD which enable to filter the soil particles before reaching the detection zone. The developed PAD design allowed dipping system for sample introduction and hence easier use in the field. When same Soil samples were analysed the PAD and IEC showed no significant difference. Soil CRM was also used to validate PAD, IEC and cafetière extraction. The true value from sealer agreed with no significant difference with result from these methods. The developed work was also compared to the

existed palintest kit (commercia kit) which require the use of several chemicals and several steps work. The palintest overestimated the content of nitrate. This might happen due to several steps of the work that maybe lead to systematic error. The developed PAD offers advantages due to the use of non-toxic and user-friendly chemicals in micro amount and due to its simplicity.

This chapter demonstrated fast (13 min), easy, robust and reliable potential approach to enable farmers to monitor soil nitrates on-site in a timely manner via cafetière-based extraction (within 5mnutes, 90% extraction efficiency) combined with a PAD readout (within 8 minutes). Future work will include studying robustness of workflow with lay people towards readout at environmentally relevant levels for farmland.

Chapter 5 Nitrate workflow with volunteers

5.1 Introduction

Monitoring of the nutrients in soils is vital to achieve good crop yield [396]. Understanding the nutrient levels influences the quantities of fertilisers needed which then links to the cost of food production. Farmers in low-income countries do not always have access to cheap analytical tools that will allow them to continually monitor nutrient levels[430], hence they may not be properly informed about the levels of fertilizers needed for optimum crop yield.

 Nutrients vary geographically and over the course of the year [13,14], consequently regular monitoring is needed. Lab based monitoring requires multiple steps and logistics which may be problematic in low-income countries [19,108,116,119,122,123,370,372,414,431]. Lab based analysis can also take significant time for the information to come back to farmer. In addition, it may be prohibitively expensive especially if a large area requires monitoring.

An alternative is soil nutrient sensors deployed directly into the field. These typically use optical or electrochemical (electrodes) approaches and some of them are portable [432-435]. These sensors can be sensitive to the part per billion (ppb) level; however, they are still expensive, require maintenance and require expertise to use. There are some commercial field methods for nitrate determination as mentioned in chapter 4, however, each of these methods has its drawbacks [26,419,435]. Some of them are not quantitative and based on visual observations, such as common nitrate kits [26]. Some require the use of the chemical like palintest [419] and some are still prohibitively expensive [3] for widespread use low-income countries.

There are also some published PADs for nitrate determination [290-293,295,296,298,310,311]. However, there are no paper based sensors which are ready for soil analysis and combine simplicity, the use of non-toxic chemicals and the portability such as the sensor described in Chapter 4. Furthermore, the previously published PADs have only been tested in laboratory settings by the research team. None were tested by lay people who have zero prior laboratory experience. Consequently, these nitrate PAD are not ready to be released to the field.

This chapter aims to test the developed nitrate sensors with volunteers. This step was necessary to determine the simplicity of the workflow and variation that may occur due to different people running the same experiment. Quantitative and qualitative data were collected from volunteers. The workflow consists of two steps; extraction of nutrients from soil with a common, kitchen cafeteria, followed by detection of nitrate with the paper-based sensor described in chapter 4. Each of these steps were evaluated separately by volunteers. 30 volunteers participated in the workflow. In addition, results from volunteers were compared to results from researcher.

5.2 Work steps and soil collection

The workflow for nitrate detection in the soil was optimized as in Chapter 4. The optimization was done to suit the field conditions. Therefore, a smartphone camera was used instead of a flatbed scanner, a spoon was used instead of the balance to measure out the soil sample and deionized water was replaced with mineral water as the extraction solvent. In addition, a cafetiere was used for the extraction instead of the conventional shaker. All of these modifications were designed to make the analysis method of nitrate possible in the field by untrained lay people, such as farmers in low-income countries. In this chapter, the workflow for nitrate determination was tested with some volunteers in the lab. Feedback from volunteers will be used to improve the system which should finally be pulled to the farmers for field work. The tested workflow is summarised in **Figure** 5.1
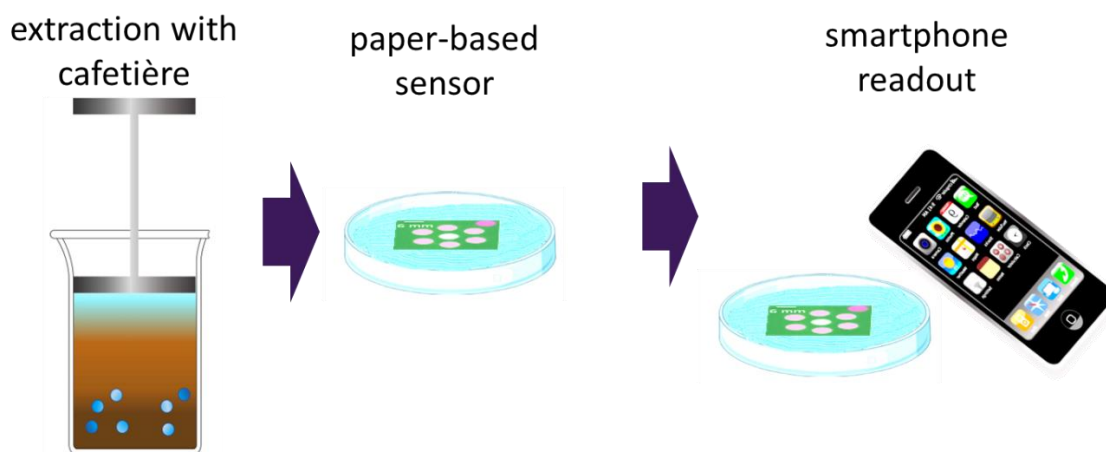
Figure 5.1 Overall workflow for nitrate analysis in soil. Step 1; extraction of nitrate from soil by cafetiere. Step 2 is the detection of nitrate with the aid of the PAD and a smart phone camera.

Instruction sheet

Initially to make the process easy instruction sheets was made to clearly show the steps of the workflow (**Figure** 5.2**).** The sheet was designed to be easy to be read and hence simple words were used to describe the steps. The sheet is divided into two boxes. The box at the top describes the extraction step and the box at the bottom describes the detection step. The volunteers were first asked to place 4 spoons of soil into the cafetiere, then add 100 mL of mineral water to the cafetiere. This is followed by mixing using the plunger for two minutes. Then the mixture is left for 3 minutes to allow the soil settle from the water. Finally, some of the solution should be poured into a separate container to be used in the detection step. For the detection, the volunteers are asked to ensure that the slits in the back of the PAD are open. Then the PAD should be dipped into the solution. After 8 minutes volunteers are asked to take two photos for the PAD, one with use of a black box and the second one without the use of the box.

The use of box helps to reduce the surrounding light effect. The use of box was clarified in **Figure** 5.3. The box contain hole on the top, this whole is used to put the phone camera and then to capture the image of PAD.

Place 4 spoons of soil in the cafetiere

Add 100 mL of mineral water up to mark

Mix for 2 min up and down slowly using plunger

Trap soil with filter for 3 minutes

Pour some liquid into the container

Open the slits on the back of the PAD

Place the PAD in the liquid

Wait for 8 min

Remove the PAD from solution

Take 2 photos (one without box and one with box) which you will upload at the end of survey

Figure 5.2 Steps for the analysis of nitrate in the field. take 4 spoons of soil into the cafetiere and then add 100 mL of mineral water to the soil. Then use the plunger to mix for two minutes. The mixture should be left for 3 minutes to allow the soil to settle from the water. Finally, some of the solution should be added into the provided container and it is ready to be used. For the detection, the farmer is asked to ensure that the back side of the PAD is opened. Then the PAD should be dipped into the solution. The dipping should be for 8 minutes. After 8 minutes take two photos for the PAD, one with use of box and the second one without the use of the box.

| Close box with hole on the top and open bottom | Pu the PAD below the box and prepare the phone | Put the phone camera on the whole, make sure no light go in through the hole |

Figure 5.3 Steps for using the box for image capture. The box is closed with hole on the top and open bottom. The PAD is put below the box. The phone camera is attached to the hole of the box and image was then captured of the PAD.

Locations for soil collection

Five soil samples were collected from 5 different locations across the University of Hull as in **Figure** 5.4 which show the location of each soil on the university map. **Table** 5.1 shows the structure of soils based on appearance. Topsoil was collected from a depth of no more than 20 cm, since the topsoil depth is usually from 13 to 25 cm deep [436]. Sampling locations were selected based on the locations moisture and conductivity sensors that have already been deployed around the University campus for an unrelated project [437]. These also provided variety in likely soil nitrate levels since these locations have different physical structures and properties. Appendix D shows some of the soil characteristic during the month of soil collection. For example, location 1 is very dry compared to other locations. Whilst location 4, in front of university main entrance, is very wet. **Figure D1** shows the moisture levels in the 5 locations at depth of 20 cm during June 2022 (the time of soil collection was 10 th June 2022). Soil location 4 and 2 are wet according with moisture levels of approximately 30% in the mid of June. Soil 1 and 5 in comparison are dry with moisture level less than 20% in the mid of June. From 5th to 10th of June the moisture level was the highest for all soils due to the high rain fall compared to the rest of the months. **Figure D2** shows the level of run during June 2022. The rain level and the moisture of the soil are crucial factors since they can dilute or wash away nutrients. Hence, the more the moisture we expect soil to have less nitrate we expect to observe [438]. Soil conductivity was also determined. **Figure D3** shows the conductivity of soil during June. The conductivity level showed small variations across the 5 sampling locations and the month of June 2022, ranging between 1200 to 1600 VIC (volumetric ion content). The level of conductivity may indicate the interfering ions that may affect the nitrate measurements. The more the conductivity the more

222

interference ions that may exist. This conductivity may help later to explain the result if any interference is observed. **Table** 5.2 summarise the level of moisture, rain, and conductivity during the collection day (10 th June 2022).

Figure 5.4 Map of University of Hull showing the locations of the five soil samples analysed by volunteers.

Table 5.1 Soil samples from sites at University of Hull from 5 different locations. The name of the soil, exact location and description based on appearance were mentioned.

Name of soil	Soil 1	Soil 2	Soil 3	Soil 4	Soil5
Description according to appearance	Dry coarse soil	Wet coarse soil	Wet soft soil	Wet soft, muddy soil	Dry soft soil

Table 5.2 Soil 1, 2, 3, 4 and 5 moisture %, rain level(mm) and conductivity (VIC) in the day of the soil collection (10th June 2022)

Measured parameter	Soil 1	Soil2	Soil 3	Soil 4	Soil 5
Moisture content (%)	17.4-18.8	28.7-29	19.2-21	31.7-32.8	14.5-16.5
Rain level (mm)	0	0	0	0	0
Conductivity (VIC)	1491-1477	1332-1337	1492-1541	1395-1404	1212-1233

Equipment given for the volunteers and survey questions.

The experiment equipment was provided to the volunteers with instruction sheet as in **Figure** 5.5. The volunteers were given the time and the space to do the experiment in a comfortable environment. A survey was prepared to determine the volunteers' level of education, and experience using the extraction system and PADs. The structure of the survey is shown in in **Figure** 5.6. The survey has four parts: information about volunteers, their experience of using the extraction, their experience of using the detection PADs and finally their overall experience of the workflow. The survey was divided into several sections to get clear feedback from volunteers that help to improve each step of the workflow. The end of the survey included a space for volunteers to suggestion ideas that might help to improve the system. In addition, informal feedback was collected during the volunteers' time using the system. The survey is shown in **Appendix E**.
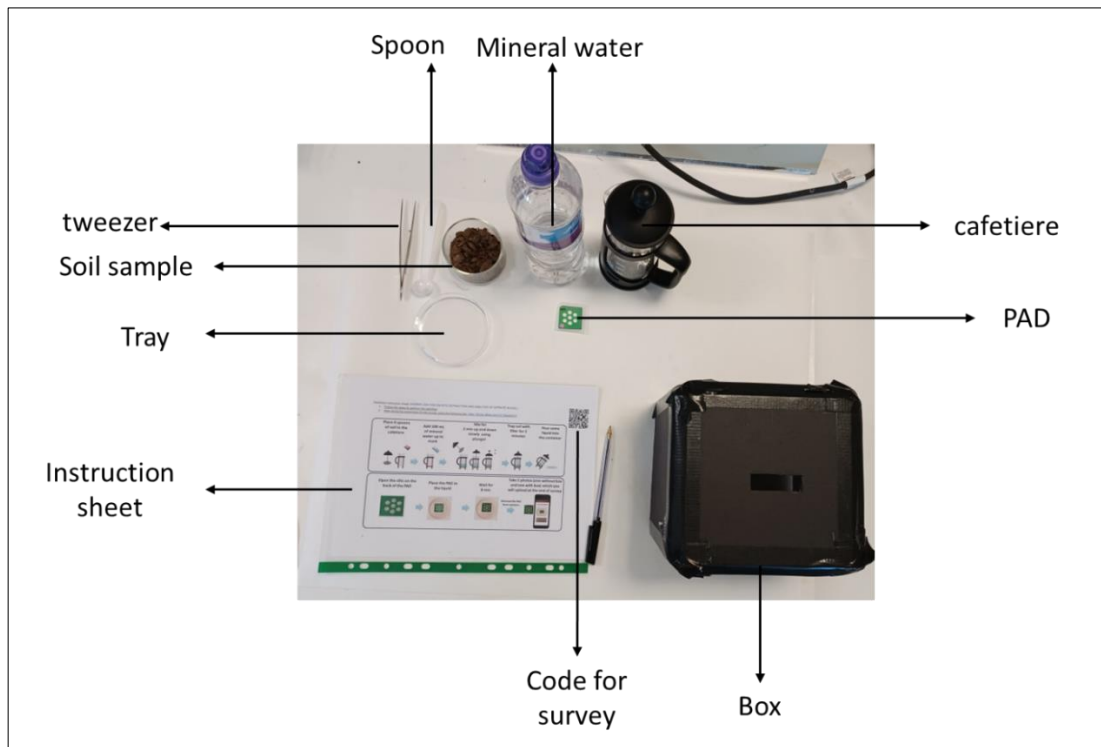
Figure 5.5 The equipment provided for volunteer to do the workflow. Cafetiere, mineral water, spoon, soil, tray, tweezer, PAD, box, instruction sheet and code for survey.
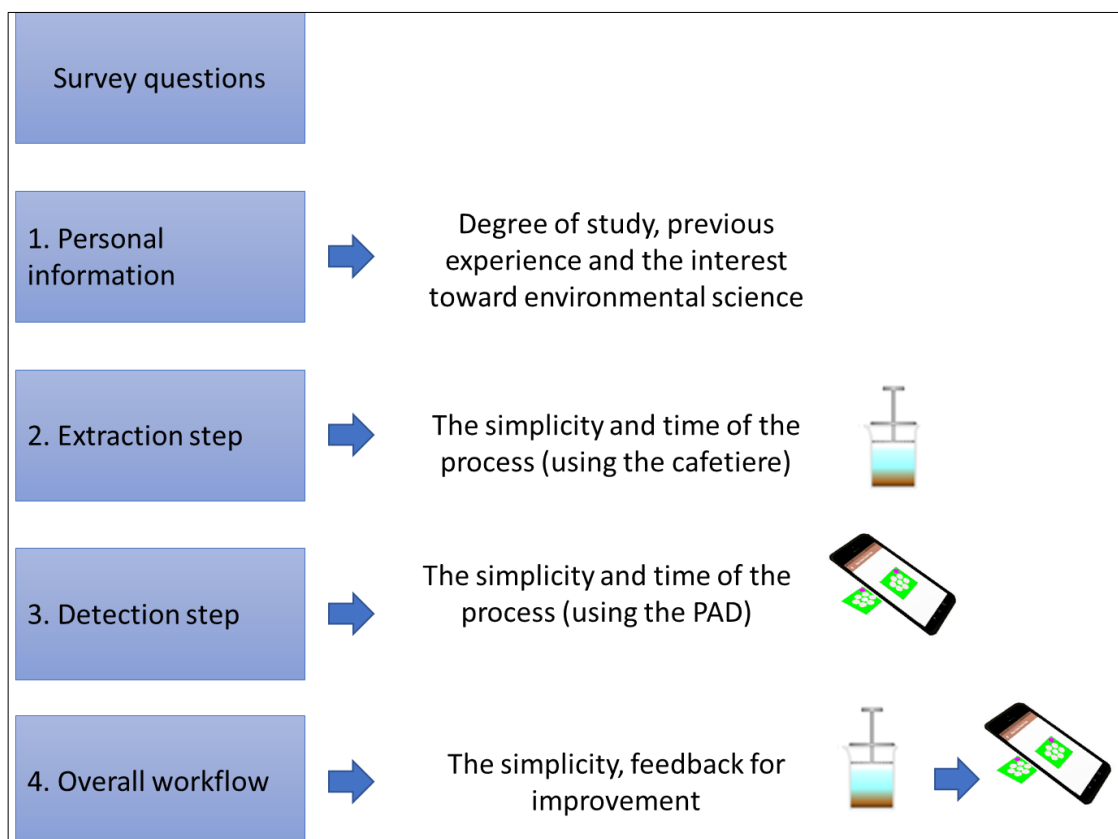
Figure 5.6 Survey structure. It consists of four parts, information about volunteers, their idea about extraction, their idea about detection and finally their overall idea about the workflow.

5.3 Information about volunteers

The volunteers were students from The University of Hull, the students had different education backgrounds and from different degrees of study. An email was sent to all the student in the university to volunteer. Random student from different major were chosen except chemistry student. The workflow was tested with 30 students. A mixture of undergraduate, Master and PhD students volunteered; 35 % undergraduate, 34% PhD, 21% taught masters and 10% research masters. 79% of the volunteers had no previous experience using PADs. In addition, the interest of the volunteers in environmental sciences were determined (**Figure** 5.7**);** 28% are extremely interested, 55 % are interested, 14 % are neutral and 3% are uninterested.
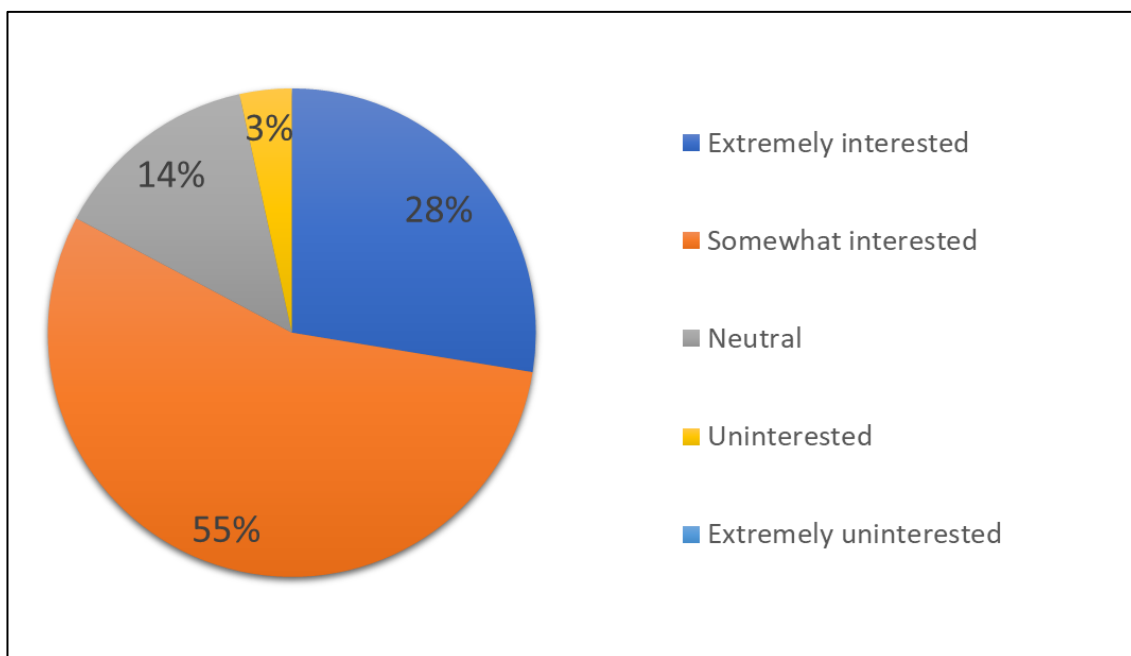
Figure 5.7 Survey question: How interested are you in environmental science? 28% are extremely interested, 55 % are interested, 14 % are neutral and 3% are uninterested.

5.4 Extraction of nitrate by volunteers

Qualitative result

The equipment provided to volunteers for extraction of nitrate from soil involves the use of a cafetiere and a plunger for mixing, a spoon (2 mL) to collect the soil sample, mineral water (HIGHLAND SPRING) as extraction solution, and a tray to add the extracted solution after extraction. Volunteers were asked about the simplicity of the extraction step; results are shown in **Figure** 5.8. Three points was evaluated; soil collection, mixing with the cafetiere and plunger and the whole extraction process. 100% of the people reported finding it easy to collect the soil

using the spoon. However, from researcher observations some of the volunteers did not fill the spoon properly with soil. Therefore, this point should be added to the instruction sheet "please take a level spoon of soil". 17 % of the volunteers reported finding the use of plunger difficult. The volunteers were given a space in the survey to add a comment about this step. Some students found it physically difficult to mix by the plunger. Another comment was "more information should be added about the strength of mixing". Mixing is a critical step to ensure efficient extraction of nitrate. Therefore, the instructions need to include a statement that gives an indication of how vigorously mixing needs to be, whilst ensuring the soil and water does not jump over the top of the cafetiere. Another comment about the quantity of the extracted solution which should be added to the container (Petri dish). From researcher observations many volunteers were asking about how much they should add into the tray. Therefore, this statement will be added to the instruction sheet "please fill the container with the extracted solution". There was also another word in the instruction sheet, which says 'trap the soil for 3 minutes'. The meaning of the word 'trap' was unclear to the volunteers, so in future this statement will be change to "please leave the mixture in the cafeteria for 3 minutes". Even though various comments were written and observed from volunteers about extraction, around 97% of the volunteers reported finding the overall extraction easy. In conclusion using the cafetiere was accepted and easy to handle by most of the volunteers.

The volunteers also evaluated the length of time it took to complete the extraction. The time of extraction in should take a total of 5 minutes; 2 minutes of mixing and 3 minute to allow the soil slurry to settle in the cafetiere. 7% of the volunteers felt this was too long, whilst 90% of them find it just right and too short. The remaining 3% are people who did not give feedback on the time. The 7% of people are mainly part of the14 % of people who are neutrally interested in environmental science as in **Figure** 5.7 and hence they found the time long. Since 90% found it as suitable time, it is expected that a farmer, or similar interested user will find the length of time needed to complete the procedure reasonable.
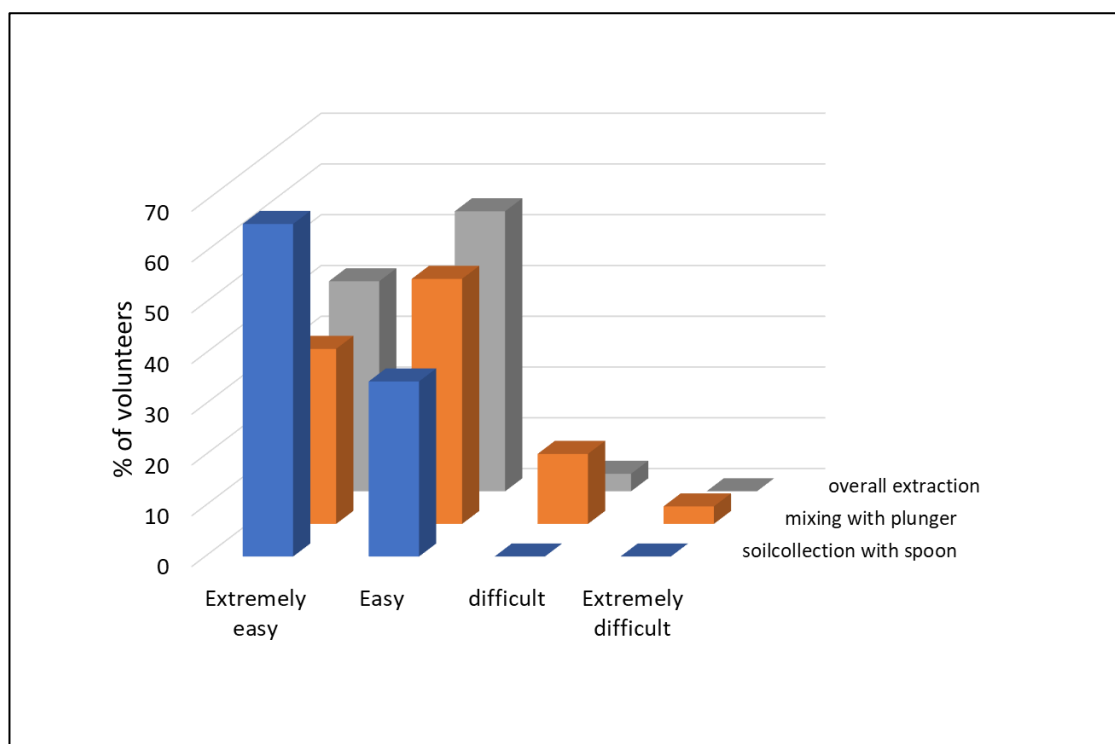
Figure 5.8 The percent of volunteers versus how easy or difficult is the exercise. Three points were evaluated, the soil collection using a spoon, the mixing with the plunger, and the overall extraction. 100% of the people find the soil collection by spoon easy. 17 % find using the plunger is difficult. However, around 97% of the volunteers find the overall extraction is easy.

Quantitative result

Quantitative data was also collected from volunteers. The extraction efficiency of the volunteers was compared with the extraction efficiency when the process was completed by a researcher. The 5 soil samples were extracted by a researcher (three times for each sample) and were analysed by ion chromatography (see chapter 4 for IEC method). The 5 soil chromatograms are shown in **Appendix F** (**Figure F1**). The nitrate peak was eluted at 3.58 minutes. The result is shown in **Figure** 5.9 which show the amount of nitrate for the 5 extracted solution of 5 soil samples. In general, the nitrate content in the five soils sample was less than 300 mg kg^{-1}. Soil 1 and 4 had the higher nitrate content compared to the other soils. However, soil 2 and 3 nitrate content are less than 45 mg kg^{-1} which is less than the lower advised limit of nitrate for a good soil [348,426,427].

The volunteer extracted solutions were also collected for further analysis. Each soil sample was measured by 6 volunteers. There were 5 soil samples and hence 30 extracted solutions were analysed by IEC. **Figure** 5.10 shows nitrate content for both extracted solution from volunteers (n=6) and researchers (n=3). The mean nitrate recoveries for Soil 1 and 4 were similar for volunteers and researcher extractions. These are soils which have high nitrate content compared to other soils. For soils 2, 3 and 5 the volunteers extracted between 40-60% of the

nitrate that was recovered by the researcher. In all samples the range of nitrate values for the volunteers was much wider than for the researchers (see error bars in **Figure** 5.10). This wide range in nitrate recoveries can be attributed to several reasons. The mixing using the plunger was done in different way by different volunteers. Also, some high results may be due to the use of high amounts of soil sample using the spoon, very full spoon can lead to increase in the amount of nitrate needed and the opposite can cause the opposite result. The feedback mentioned above in this section should be added to the instruction to avoid such variation.
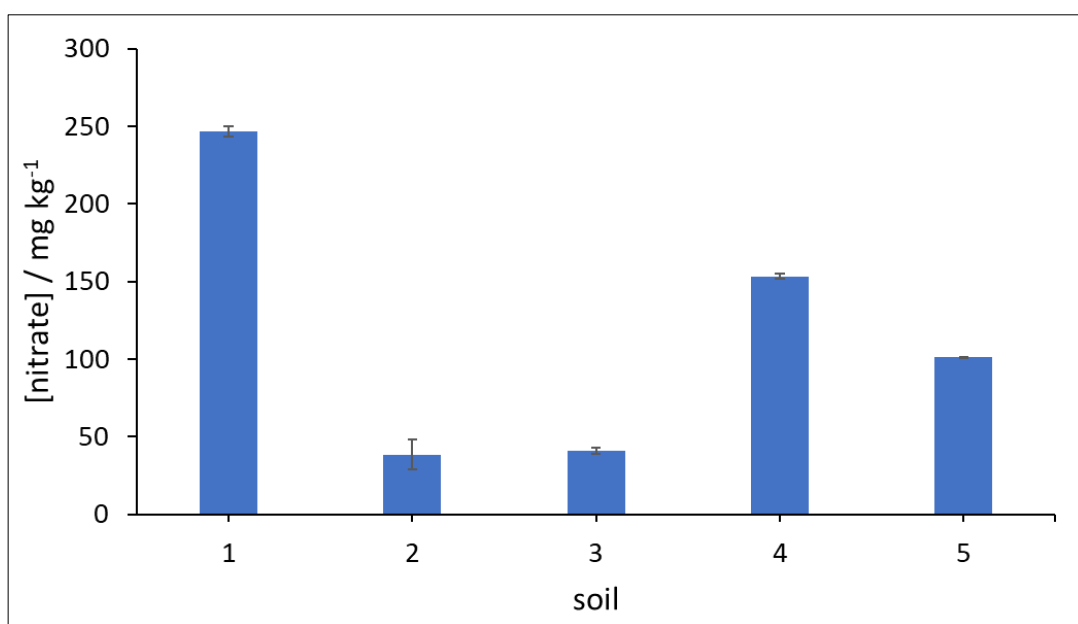
Figure 5.9 Nitrate mg kg^{-1} versus the soil type. The extraction of the samples was done by researcher using cafetiere (n=3) and analysed by IEC.

	% recovery
soil1	101.58±30.55
soil2	39.03±28.89
soil3	67.29±41.91
soil4	114.18±59.44
soil5	50.25±18.60
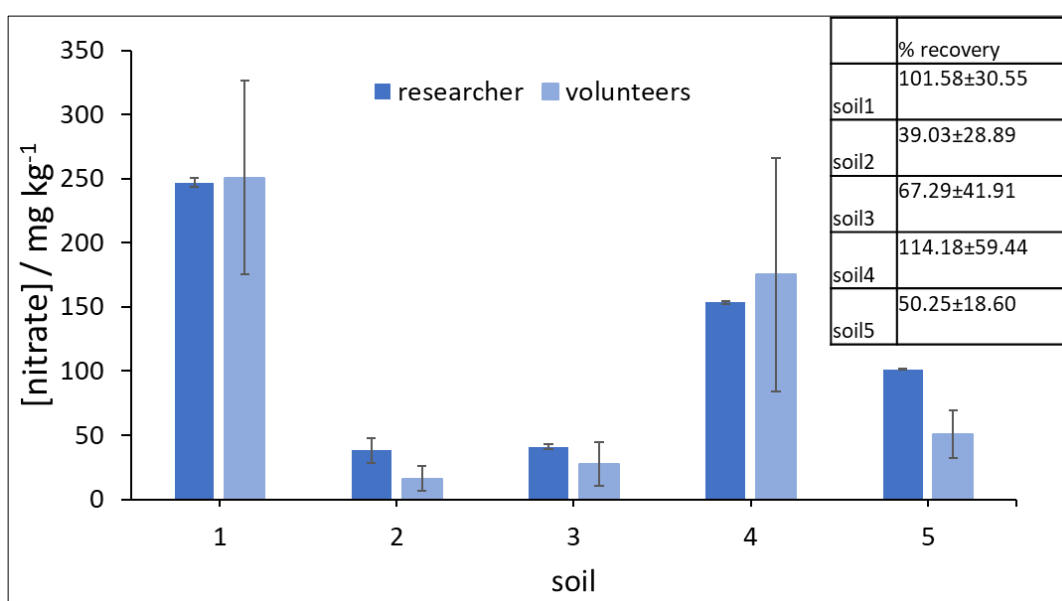
Figure 5.10 Nitrate mg kg^{-1} versus the soil type. The extraction of the samples was done by researcher (n=3) and volunteers using cafetiere (n=6) and analysed by IEC. % Recovery was determined and shown in the box for each soil sample. 5 recovery was determined using result of volunteers and result of researcher (true value).

5.5   Detection of nitrate by volunteers

Qualitative result

A nitrate PAD was used for detection of nitrate by volunteers. The instructions for detection was given in detail in the printed sheet. The volunteers were asked to take the PAD and distinguish the front and the back side. Then to dip the PAD into the detection solution for 8 minutes. Finally, to take a photo for the PAD with and without use of the provided box. **Figure** 5.11 shows the feedback of the volunteers about the use of the PAD and the phone. 3 % found the instructions on how to dip the PAD into the sample unclear. The remainder described the instructions as clear. All the volunteers reported that the instructions on how to take a photograph of the PADs was clear. Overall, the detection by the PAD was easy for 100% of volunteers. 96% found the time as suitable time to carry the work. Therefore, it is expected that the process and the time to be suitable also for end users.

Even though 100 % of volunteers described the process of taking the photos easy, many of them did not take a clear photo especially with the use of the box. **Figure** 5.12 shows some photos which were taking by volunteers when box and no box were used for image capture. Clearly the use of box was more difficult for volunteers and hence result was collected from the photos when no box was used for photo taking. Volunteers also were in doubt about the picture quality and some of them asked for more information as feedback for picture quality and the way they should to take the picture. Clear instruction sheet for picture taking will be developed.
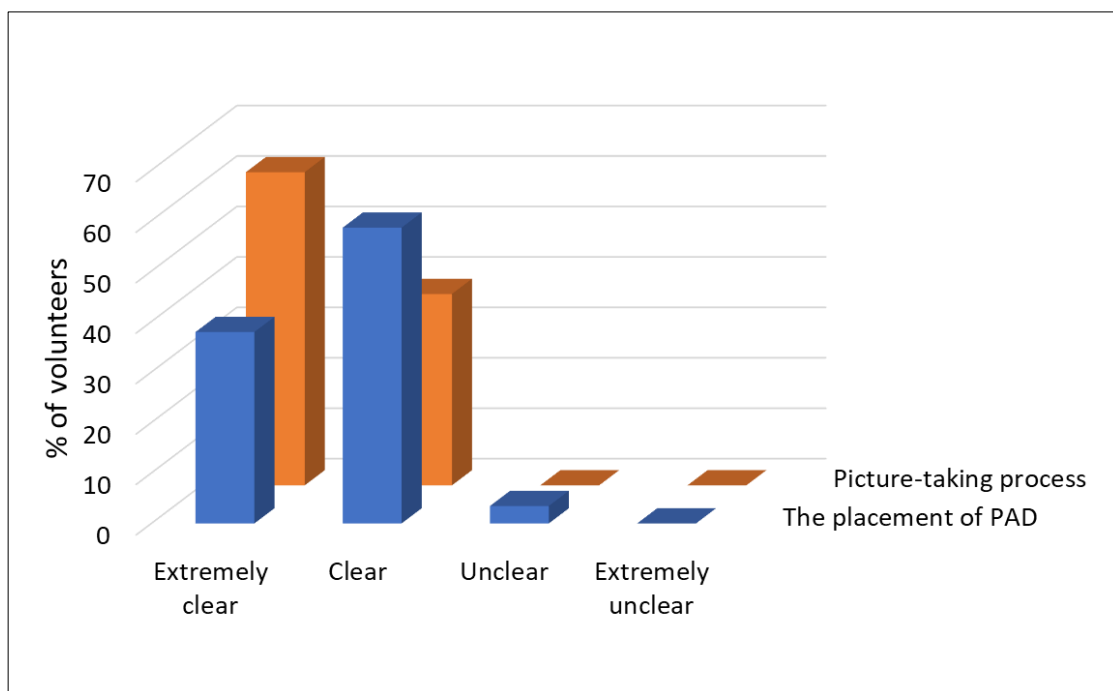
Figure 5.11 Percent of volunteers versus how clear the instruction about the detection steps is. The volunteers were asked about two things, the placement of the PAD into the sample and the picture taking process by phone. 100 % of the volunteers find picture taking clear to do. 3 % find it unclear to put the PAD in the sample, however, the rest around 96% find it clear to dip the PAD in the extracted solution.

Figure 5.12 Examples of pictures of the PAD taking by volunteers using a smart phone with a box and without a box. Result for 5 soil samples is shown.

Quantitative result

Quantitative data for the detection step was also collected using the PAD and it was also compared value derived from a researcher carrying following the same method. **Figure** 5.13 shows the result of nitrate (mg kg^{-1}) content in soil. The PADs were photographed using a flatbed scanner and a smart phone camera. The figure shows the amount of nitrate from the five soil

samples. The scanner, phone and IEC results broadly agree, when analysed using an ANOVA test (e.g., soil 1, F= 1.11, $F_{Critical}$=5.14, α=0.05, n=3, ANOVA test).

Volunteers' results for nitrate detection by the PAD were compared to the researcher's results as in **Figure** 5.14 which shows the nitrate content (mg kg^{-1}). The works of volunteers overestimates the result of nitrate content. However, the result of nitrate content in the 5 soil extracted solution (analysed by IEC) from volunteers and researchers were not extremely different (as mentioned in **Figure** 5.10) and hence results from the PAD should agree since the same solution were used by volunteers. In addition, PADs used by volunteers and PADs from researcher showed similar colour (when seen by eyes) as in **Figure** 5.15 and hence this big difference in nitrate content is impossible. Therefore, this difference may happen due to variation of the phone and the variation in the way of photo taking. Also compare to volunteers the researcher has more experience in taking photographs of PADs.
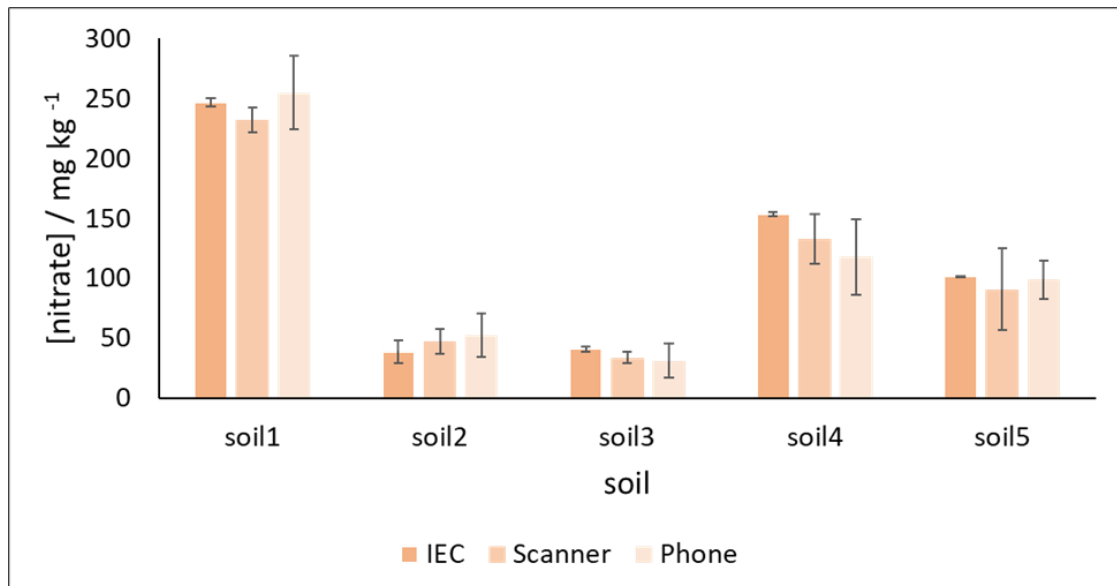
Figure 5.13 The nitrate concentration mg kg $^{-1}$ versus the type of soil when three detection method were used, IEC, scanner and phone (all by researcher).
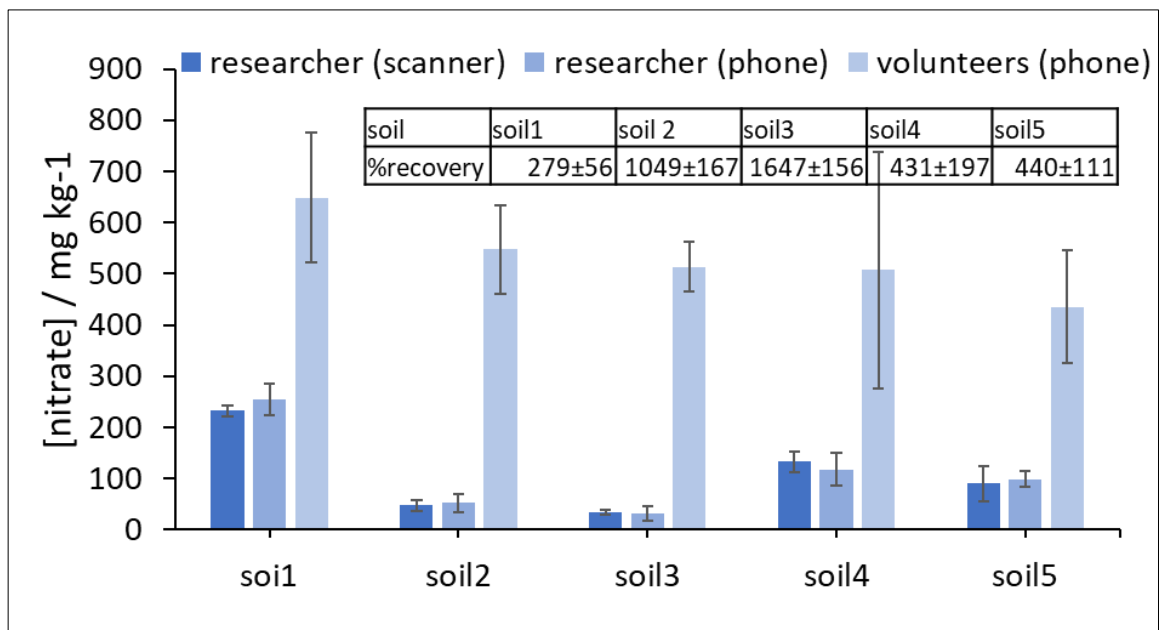
Figure 5.14 The nitrate concentration mg kg $^{-1}$ versus the type of soil when three detection method were used, scanner (by researcher), phone (by researcher)and phone by volunteers. The result from scanner and phone for researcher agree, however, they do not agree with the voluneteers' phone results.
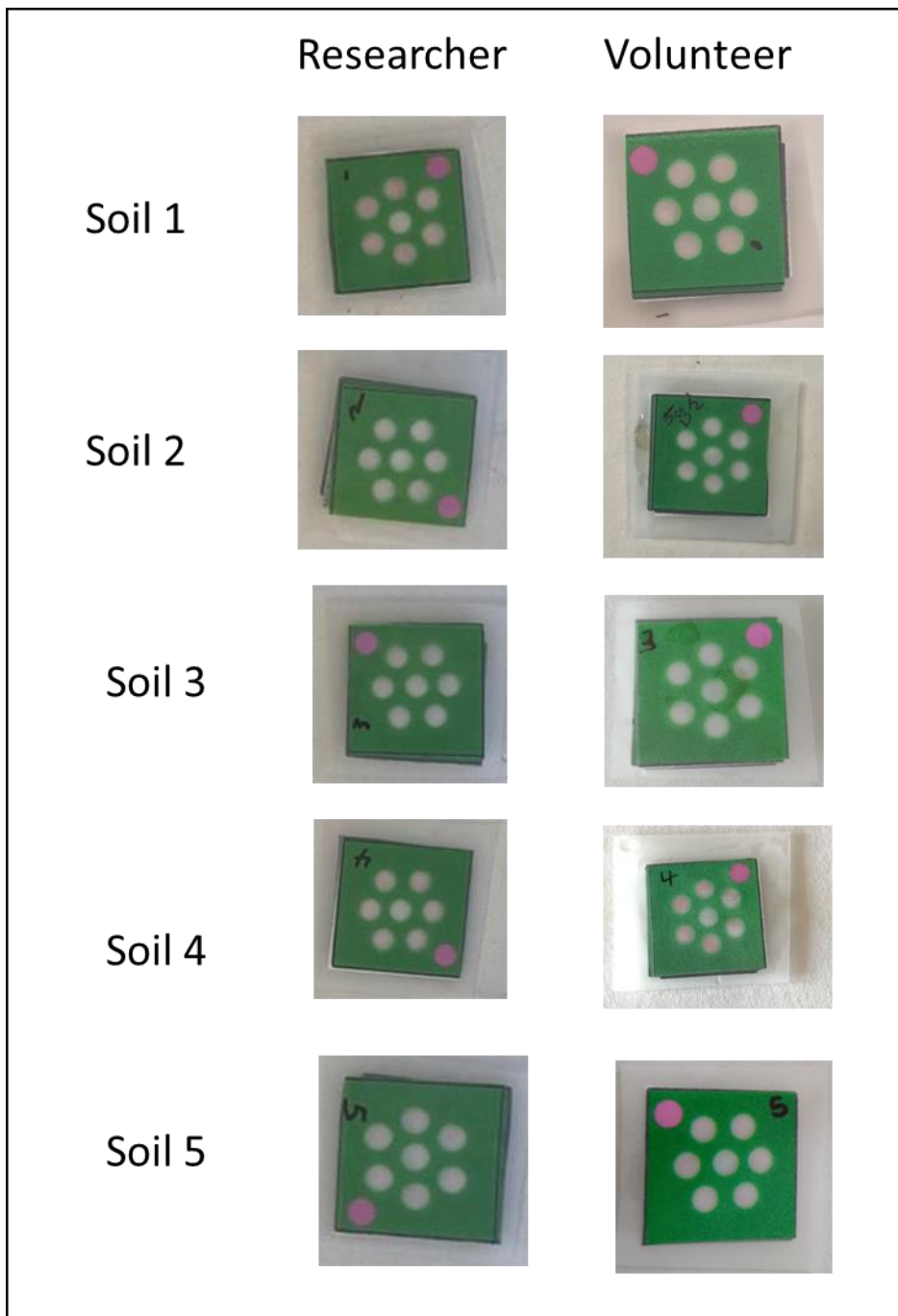
Figure 5.15 Photos taking for 5 soil samples by volunteers and researcher. Colour seen by eyes does not varies significantly.

Explanation for quantitative data variation between researcher and volunteers

Variation in image capture may happen due to differences in the phones used, variations in the way photos are taking, changes in the place where the photo is taken. Some of these problems were already discussed in literature as mentioned in **section 1.4.3**. Photos of a set of standards of nitrate were used to explain the effect of using a phone to take a photo. **Figure** 5.16 shows the printed standards which was laminated by lamination sheet to mimic the normal made PAD.

The PAD contains 6 standards each with three repeats and three internal standards to reduce the surrounded light effect.
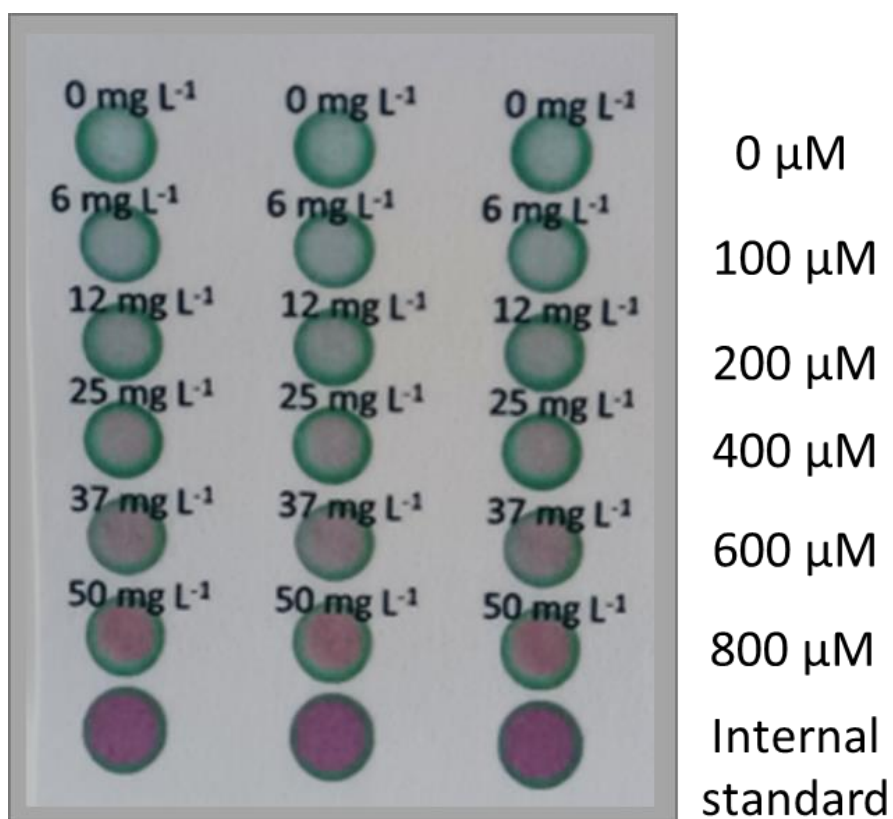
Figure 5.16 Printed photo for set of nitrate EXTERNAL standards. The paper was laminated to mimic the prepared PAD.

To study the variations in images based on the phone, three phones (Huawei, Samsung Galaxy A325G, iPhone 11) were used to take the image of the same set of external standards (mentioned in **Figure** 5.16). The result from the three phone shows similar slopes. However, the lines do not overlap even though same lighting and same distances (between phone and PAD) were used for photo taking. This meant that each phone has different image capture ability and hence obviously different quality image result. Other people in literature solve this problem by use of statistic or box to remove the surrounding light effect as mentioned in **section 1.4.3**.
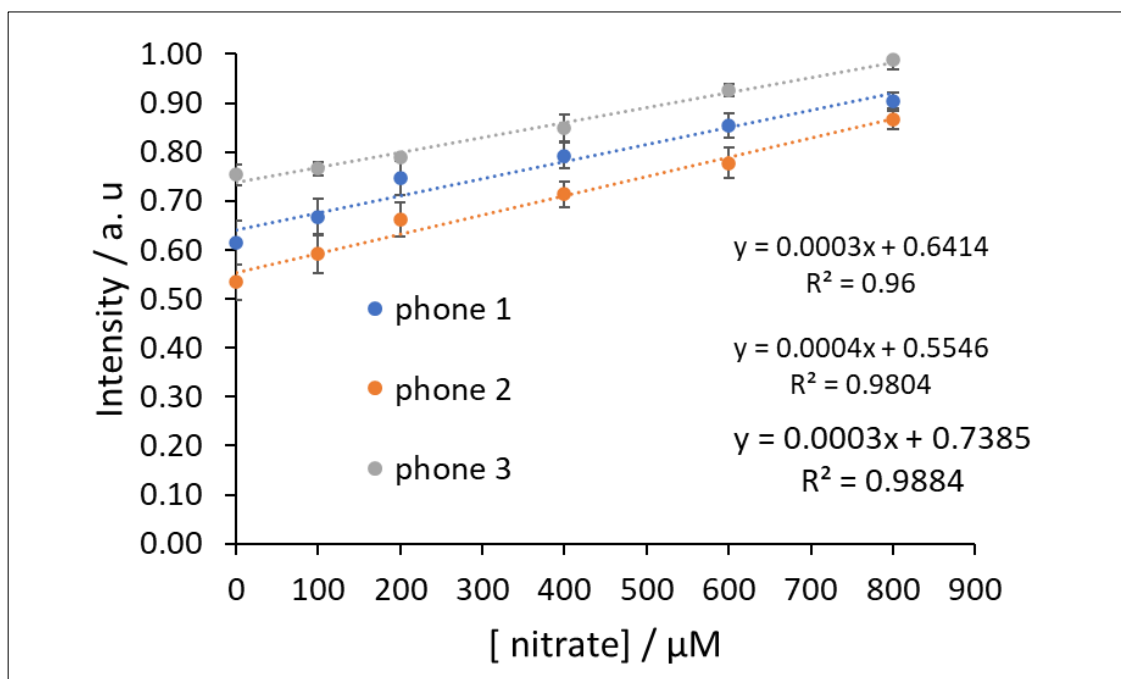
Figure 5.17 Intensity versus the nitrate concentration (µM) when three phone (Huawei, Samsung Galaxy A325G, iPhone 11) were used to take the image of the printed PAD in **Figure** 5.16. N=3.

The distance effect (between phone and PAD) was also studied. Three different distances (10, 15, 30 cm) were tested. Clearly when the distance between PAD and phone changes the calibration line also changes (**Figure** 5.18 **a**). However, when the distance was kept the same as in **Figure** 5.18 **b**. the three lines were reproducible. Consequently, the distance between phone and PAD can also has influence the image capture.
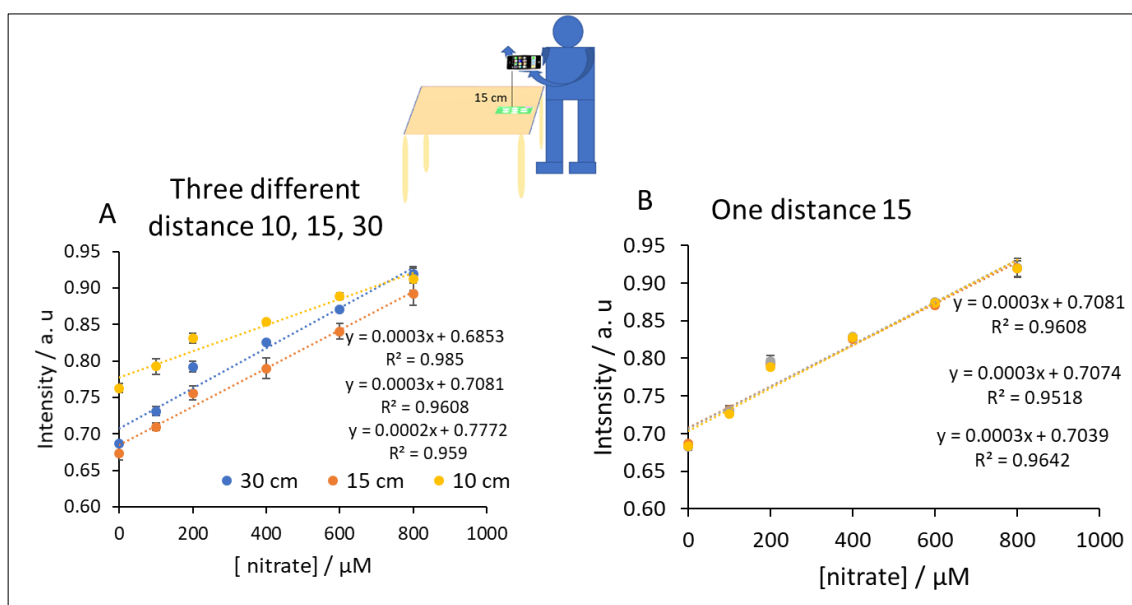
Figure 5.18 Intensity versus the nitrate concentration (µM) when different (figure A) and same (figure B) distance were used to take the image of the printed PAD in **Figure** 5.16. One phone (iPhone 11) was used, and the location was the same. N=3.

The effect of changing location was studied since different locations in the room has different lightening. **Figure** 5.19 shows the intensity versus the concentration of nitrate when photo for the same standard was taken at different locations (**a**) and at same locations (**b**). Location changes leaded to a change in the calibration line.
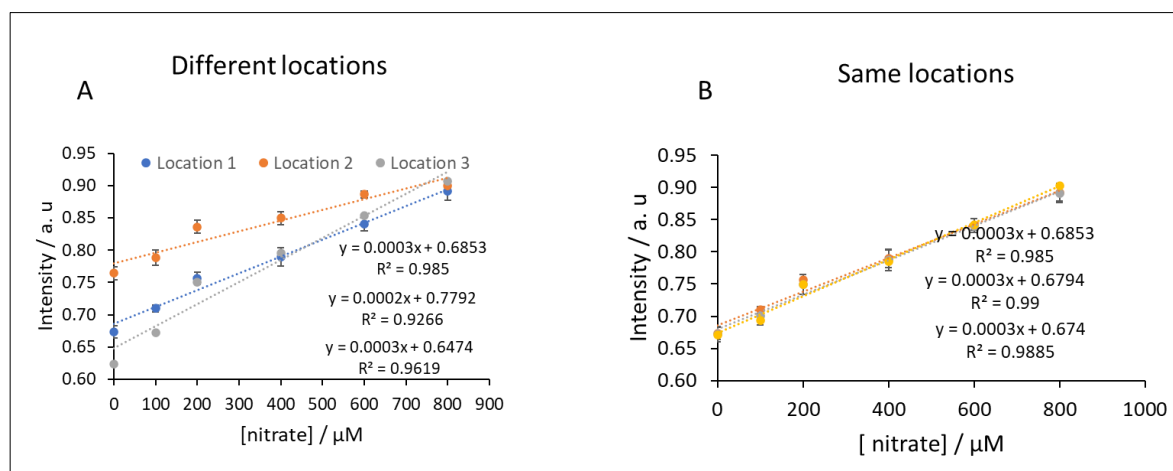
Figure 5.19 Intensity versus the nitrate concentration (μM) when different (figure A) and same (figure B) locations were used to take the image of the printed PAD in **Figure** 5.16. One phone (Huawei) was used, and distance between phone and PAD was the same. N=3.

After one year of PAD development (from the original experiment) the calibration line on real time and real standards was run again using scanner and phone as in **Figure** 5.20. The result from scanner matches the previous result which means that the method in term of reagent and PAD is reproducible. However, when the calibration line was run again by the phone the line does not overlap the previous result. Mainly this was due to the change of phone (phone was changed from Samsung to iPhone) and the change in the light of the room since it was summer, and room was brighter. Consequently, the use of the external standard to avoid such a problem is needed.

In conclusion, the model of phone, distance of photo taking (between phone and PAD) and location of photo taking can affect the image capture and consequently the result. The best way is to use the photo of the external standard with the sample analysed. Whatever effect the sample PAD image capture it affects all the standards by equal way. By using the external standard then the volunteer can take the photo using any phone and any location. A clear instruction sheet for the use of the phone and picture taking will be mentioned in **Section 5.7**.
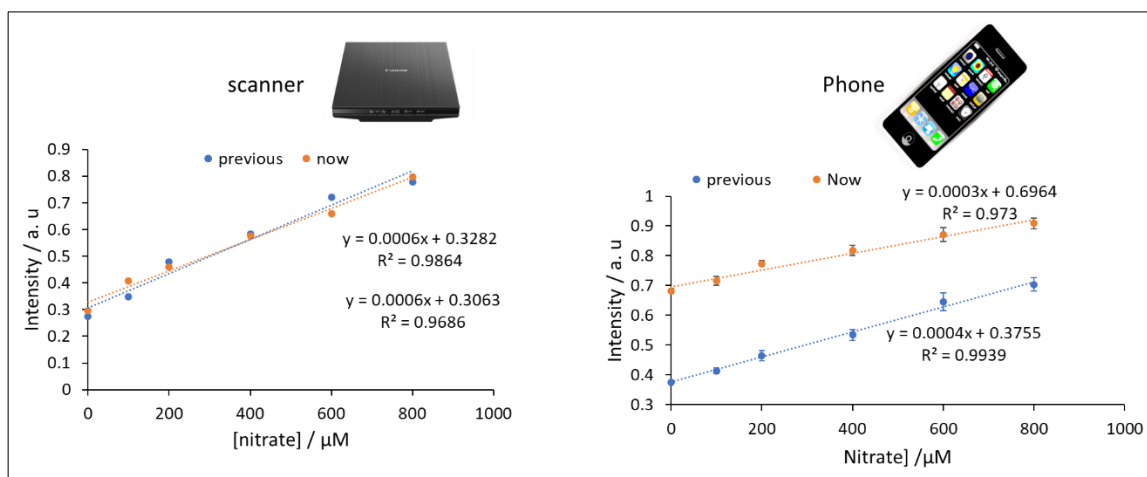
Figure 5.20 Intensity versus the nitrate concentration (µM) when different scanners and phones (iPhone 11, Samsung) were used for image capture. The previous result (before around a year) was compared to the result now (result after around a year).

5.6   Overall workflow evaluation

Qualitative result

Finally, the volunteers were asked general questions about the workflow. The first question asked about the clarity of the instruction sheet. 97% found the instructions easy to follow. While 3% find it difficult to understand. Also, the overall time of the work, 13 minutes, was not too long for 93% of the volunteers and hence it is a suitable time to perform such work. The final aim of this work is to develop a workflow that combines the accuracy, simplicity, short time and low cost. Therefore, the volunteers were asked about their opinion about this most important aspect of the workflow. This result is shown in **Figure** 5.21 and most of them chose simplicity and the accuracy as first choice compared to the price of the device and the time of work. This can reflect what the end user requires when working with such a workflow.
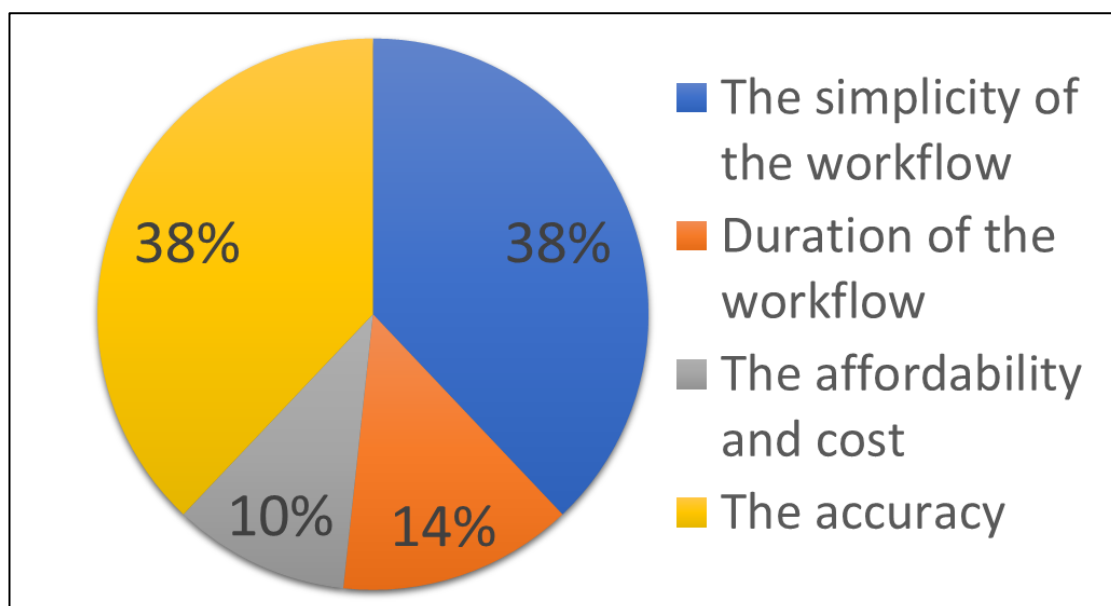
Figure 5.21 Most important aspect of the workflow based on volunteer opinion. 38% of them chose simplicity of the workflow as the first option and 38% of them chose the accuracy as first option.

5.7   improvement in the workflow based on volunteers' feedback.

qualitative improvement

Based on the volunteers' feedback and result, some improvements need to be made. The original instruction sheet is shown in **Figure** 5.2**,** the updated sheet is shown in **Figure** 5.22. The changes are made in red based on the volunteers' feedback. **Table** 5.3 shows the changes made to particular sentences. "Place 4 spoons of soil in the cafetiere" was changed to "Place 4 filled spoons of soil in the cafetiere". A photo clearly showing how this is done is now included in the instructions (as **Figure** 5.23). Volunteers were asked also to avoid collecting rocks and collect soft soil of the same texture. This helps to avoid variations of the signal that was observed in **Figure** 5.10. The statement "Mix for 2 min up and down slowly by plunger" was changed to "Vigorously and thoroughly mix the solution using the plunger for precisely 2 minutes. Caution should be exercised to prevent any water splashing during the process" since strong mixing is required to extract nitrate. Also, to make this statement easy to understand "Trap the soil in the cafetière for 3 min" it was changed to "Keep the mixture in the cafetière for 3 min". "Pour some liquid into the container" was also changed to "Fill the container with liquid". The two sides of the PAD were also clarified by the arrow in the picture in the instruction sheet to avoid users placing the PADs into the sample the wrong way up.

 The last step is photographing the PAD. Step-by-step instructions are provided in a separate sheet, as shown in **Figure** 5.24. Step 1: make sure that PAD is clean with no drops of water are

visible on the surface of the PAD. Step 2: put the phone camera at distance around 15-30 cm (distance between phone and PAD) and avoid direct light effect. Step 3: take photo of the sample with the external standards set. Step 4: photo should be with uniform light effect; examples are given for non-good photo.

Table 5.3 Changes made to the instruction sheet.

Original instructions	New instructions
Place 4 spoons of soil in the cafetière	Place 4 filled spoons of soil in the cafetière
Mix for 2 minutes up and down slowly with the plunger	Vigorously and thoroughly mix the solution using the plunger for precisely 2 minutes. Caution should be exercised to prevent any water splashing during the process
Trap the soil in the cafetière for 3 min	Keep the mixture in the cafetière for 3 min
Pour some liquid into the container	Fill the container with liquid
Sides of the PAD	clearly, the two sides of the PAD (front/back) were shown
Photo taking information	A special sheet for photo taking is added

Place 4 filled spoons of soil in the cafetiere

Add 100 mL of mineral water up to mark

Vigorously and thoroughly mix the solution using the plunger for precisely 2 minutes. Caution should be exercised to prevent any water splashing during the processof water
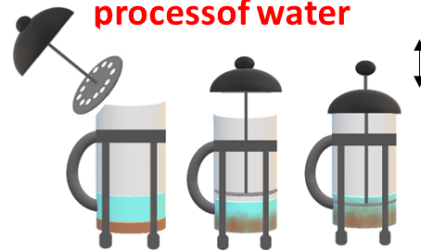
Keep the mixture in the cafetiere for 3 minutes

Fill the container with liquid

Open the slits on the back of the PAD

Back side
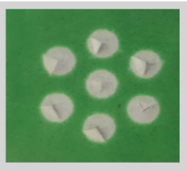
front side
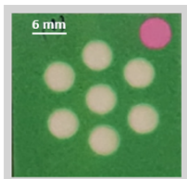
Place the PAD in the liquid
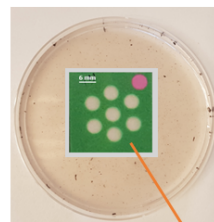
front side on the top

Wait for 8 min

Remove the PAD from solution
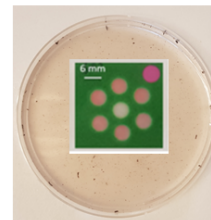
Take photo (Information in photo taking sheet) which you will upload at the end of survey

241

Figure 5.22 Improved instruction sheet based on volunteers' feedback. Place 4 spoons of soil in the cafetière was changed to Place 4 filled spoon of soil in the cafetière with photo clearly show how this is done (as Figure 5.24). They were asked also to make sure the soil is soft and of the same texture and no rocks. The statement "Mix for 2 min up and mix slowly by plunger" was changed to "Mix strongly and vigorously by the plunger within water level, avoid splash of water". "Trap the soil in the cafetière for 3 min" it was changed to "Keep the mixture in the cafetière for 3 min". "Pour some liquid into the container" was also changed to "Fill the container with liquid".

Figure 5.23 How to use the spoon to take soil. Take a 2 mL spoon and fill it with the right amount of soft soil as clarified in the photo.
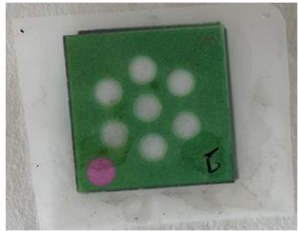
Wet with some soil ❌
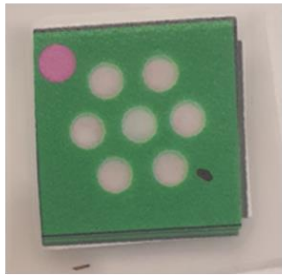
Dry and clean ✅

Avoid direct light effect ❌

15 cm

15 cm ✅

Dark light from one side

Not clear ❌

Camera is very close ❌
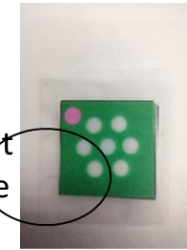
Variation in light ❌

Clear and from good distance ✅

1- make sure that PAD is clean with no drops of water are visible on the surface of the PAD.

2- put photo close to your chest and take photo from distance of around 10-30 cm from table, avoid direct light effect

3- take photo of the sample with the external standard set

4- uniform light effect, example are given for non-good photo

Figure 5.24 Photo taking instruction sheet. Step 1: make sure that PAD is clean with no drops of water are visible on the surface of the PAD. Step 2: put the phone camera at distance around 10-30 cm (distance between phone and PAD) and avoid direct light effect. Step 3: take photo of the sample with the external standards set. Step 4: photo should be with uniform light effect; examples are given for non-good photo.

Quantitative improvement

The problem of the phone was improved using the external standards as mentioned above in **section 5.5**. Two of the soil samples (1, 4) which were in Table 5.1 were studied again with volunteers (3 volunteers taken randomly from university of hull student and done the work for first time). These samples were chosen due to their high nitrate content compared to the rest. Each sample was done three times by three different volunteers and three different phones.

The detection was done with phone and with the aid of external standard. The photo of sample and the external standard were taken together by volunteers as in Figure 5.25. The concentration of nitrate in each sample (soil 1 and 4) was determined by volunteers and compared to the previous result of researcher (**Figure** 5.13) as in **Figure** 5.26. The figure shows the concentration of nitrate after the use of the external standard in two samples, 1 and 4. The result from researcher and volunteer agreed with each other using ANOVA test (e.g. soil 1, F= 1.41, $F_{Critical}$=4.07, P= 0.31, α=0.05, n=3, ANOVA test).

Even though each phone from the three volunteers shows different calibration lines (when the same set of external were used) for image captured (**Figure** 5.27), the concentration of nitrate in the same soil sample from the three volunteers is still similar after calculation and not far from the true value. Consequently, this indicates the external standard can be used to adjust for differences in smart phone cameras, as discussed in the previous **section 5.5.**

In conclusion, external standards solved the problem that may occur due to the change of people who are taking the photos by their phones.
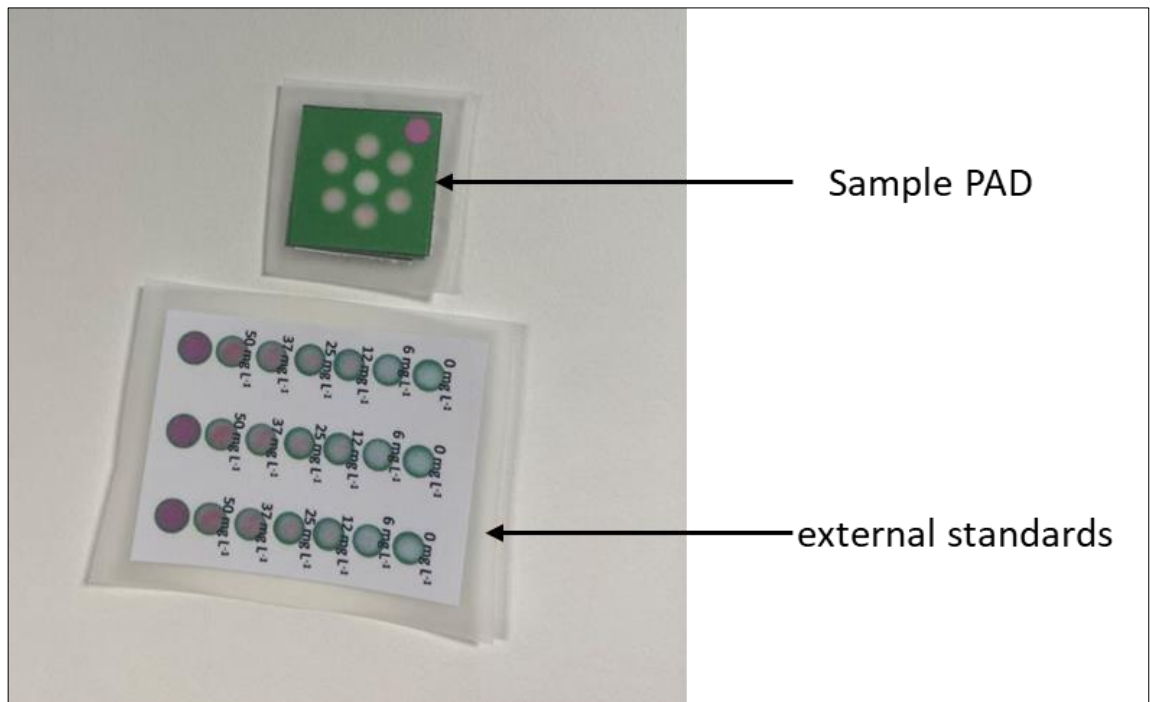
Figure 5.25 The way the photo for sample PAD and external standard were taken together for nitrate detection in soil.
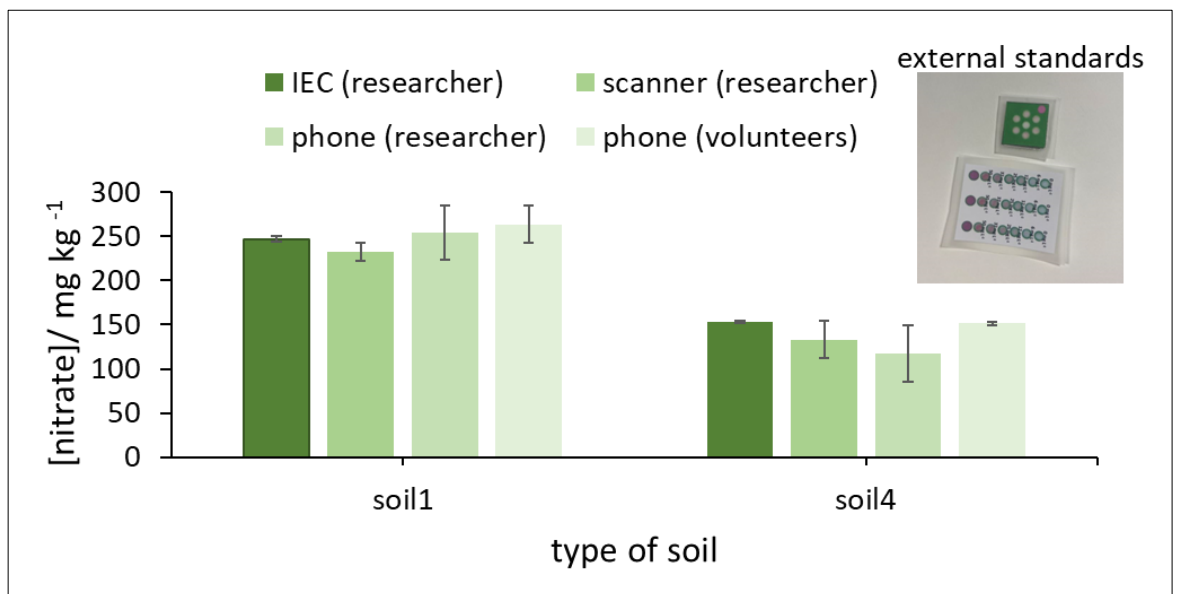
Figure 5.26 The nitrate concentration mg kg $^{-1}$ versus the type of soil when three detection method were used, IEC (researcher), scanner (researcher) and phone (researcher), phone (volunteer). The external standard was used by volunteers alone with the sample PAD. Volunteer's phones (iPhone, Samsung, Samsung). The result from researcher and volunteer agreed with each other using ANOVA test (e.g. soil 1, F= 1.41, $F_{Critical}$=4.07, α=0.05, n=3, ANOVA test).
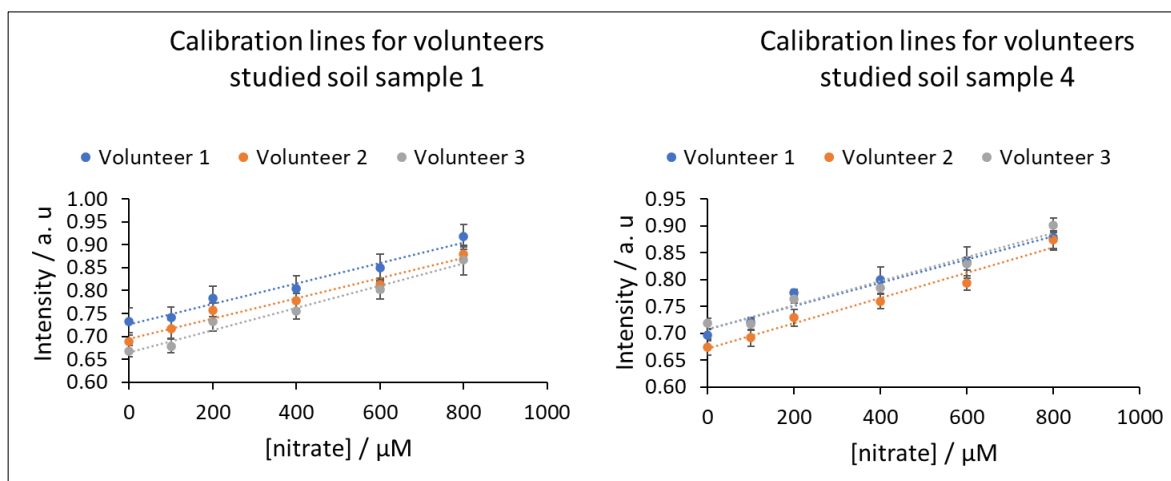
Figure 5.27 Calibration lines of the external standards image taken by volunteers who analysed for soil 1 and 4 in **Figure** 5.26**.**

5.8   Discussion and Conclusion

Nitrate paper-based sensors are commonly developed and used in the chemistry and biology laboratories. Many of these sensors are developed for laboratory testing or aiming field testing [290-293,295,296,298,310,311]. However, the published nitrate paper-based sensors were only tested by researchers who developed them detection [290-293,295,296,298,310,311]. In this work nitrate sensors, which was developed in chapter 4 was tested with volunteers. This step was necessary to determine the simplicity of the workflow and variation that may occur due to different people running the same experiment. The workflow consisted of two steps extraction with cafeteria and detection with paper-based sensor. Each of these steps were evaluated separately by 30 volunteers.

The extraction with cafetière was easy to work with according to chapter 4. The challenge is to get the same efficiency of the work when lay people are doing the same extraction. Qualitative and quantitative data about the extraction step were collected from volunteers. Even though 17% found the use of the plunger difficult, around 97% found the overall wok of extraction is easy to use. Also, the plunger of cafetiere is supposed to be used by farmers and we expect that farmers will find it easy to mix since they are stronger.

Result of soil extract from volunteers showed that the soil that has higher nitrate content above 100 mg kg^{-1} showed good recovery around 100%. The soil with low nitrate content showed low % recovery around 40-60% recovery. However, both types of soil suffered from high relative standard deviation (above 30%) of recovery. This was attributed to several reasons, the use of the spoon. Very full spoons can cause overestimation of the result and the opposite can cause the opposite result. Consequently, information was added in the instruction sheet regarding the proper use of the spoon. Another reason is the way of mixing. Therefore, more information was added in the instruction sheet regarding the strength of mixing which should be strong and vigorous to fully extract nitrate. These small changes in instruction sounds to be simple for researcher, however, they are necessary to be mentioned for lay people to get the same efficiency of work.

The detection by the PADs were also evaluated by volunteers and compared to the researcher results. 96% of volunteers found the use of the PAD clear and 100% found the use of the phone easy. However, the quantitative result from the volunteers PAD significantly vary from the researcher. When the colour (seen by eyes) from volunteers PAD was compared to the colour of the researcher PAD for the 5 soil samples, the colour does not vary significantly which means that the nitrate content should not vary significantly and that what IEC result showed. Therefore, this difference was attributed to the use of the phone to take the photo.

Use of the phone was working well in chapter 4 since it was used only by trained researcher. This chapter showed that phone use can be affected by several factors including the change in the person who is taking the photo. Type of phone, location of photo taking and the distance of photo taking (between the PAD and phone) were some factors that affect the image capture. Changing any of these parameters leaded to change in the image quality and hence change in the result. Consequently, external standards were introduced. External set of standards should be used with each photo taking for sample to avoid any of error that may occur due to change in any of the mentioned parameters. Two soil samples were run again by volunteers after the improvement in the instruction sheet and the use of the external standard. The result of PAD detection of nitrate from volunteer agreed with no significant difference with the result from researcher within the standard deviation.

In conclusion the overall work was easy to be used by most of the volunteers. Extractions step by volunteers was comparable to extraction by researcher nitrate content. Detection step showed some variation due to the used of the phone and this problem was solved using the external standards that can overcome the factors that lead to variation in image capture. Initial testing to the improved system (including instruction sheet) showed promising result with no significant difference between researcher and volunteers outcome result. In the future, the improved developed work should be tested with larger group of volunteers in the field to ensure its robustness in real testing environment.

Chapter 6 Manganese determination

6.1 Introduction

Manganese is necessary for plant growth in a healthy way. It is needed for the biosynthesis of lipid, lignin and carbohydrates in the plant [439]. Manganese has several forms Manganese with oxidation state +2, +3, +4, +5, +6 and +7 [439]. The most available forms are manganese with oxidation state +2 and +3 [1]. However, Mn^{+2} is the more soluble in soil compared to other oxidation state manganese [1]. In addition, it is the most form which is up taken by plants.

Therefore, determination of manganese (Mn^{+2}) in soil is needed to improve fertilizer application and achieve good crop. The recent available lab-based methods[23,132,133,138,139,143,144,147,148] (e.g., AAS, ICP-MS, colourimetrical, electrochemical) which are expensive and time consuming especially for low- and middle-income countries and hence regular monitoring of manganese by this method is impossible. Some of the lab developed sensor which are based in electrochemistry [440]. These methods still have its drawbacks including the complication and need of expert. There are also other available commercial field kits [24,25], however, they are still non quantitative [24], expensive, have toxic chemicals, complicated and require expert person to handle them. Colorimetric Paper base sensor [441,442] represent good alternative which is if it is made from non-toxic chemical simple, it can be used for this purpose. There are Some examples of existing paper-based sensors for manganese detection [314,315], However, most of them contain toxic chemical (e.g., chemicals contain cyanide and borate) and none of them is ready for soil sample analysis.

Prior to detection extraction of manganese is needed. Manganese extraction from the soil in the lab is challenging since manganese is strongly attached to the soil and making it not easily mobile in water and needs special reagent (e.g., EDTA, Mehlich 1, Mehlich 2, KCl, CaCl2 and others) to extract it [443-449]. The lab extraction method mainly based on the use of shaker. There is other available method for manganese extraction in the field. However, they are still requiring multi steps, equipment (e.g., filtration), and the use of chemicals. The use of cafetière was good alternative as mentioned in chapter 4. Cafetière provide a way of mixing with the use of plunger. It is easily available equipment and safe if a none-toxic and user-friendly solvent is used with it.

Here is manganese analysis in soil sample by PAD method was studied. The best colorimetric detection reagent on PAD for manganese was determined. The detection reagent was optimized for the use of user-friendly (fewer toxic options). The PAD was sealed by different ways and the best way with easiest sample introduction system was chosen. The PAD was improved to fit soil sample analysis. The PAD selectivity was determined by monitoring the effect of the interference. The developed PAD was finally combined with the cafeteria extraction system which was able

to extract specific % of manganese from soil sample when NaCl solvent was used. For validate the result from the PAD was compared with result from ICP-MS for the same soil sample.

6.2 Experimental

6.2.1 Device designs

Paper devices were fabricated using the method described in **Section 2.3.1** and **Section 2.3.2** for wax printing method and cutting method respectively. The black ink was used in the device. Black wax ink needs more heating to permeate the paper, so the devices were passed through the laminator 10 times at 125°C. Other wax ink colours can be heated at same temperature for only 3 times to penetrate the paper.

Device 13

This device (**Figure** 6.1) consisted of a detection and empty regions. On the region with the detection zones for 4 different internal standards (pink, yellow, green and red) were printed. Different colours for internal standard were utilised for the purpose of comparison. The device was made in such a way it can be fold along a central line to make a 3D device, bringing the detection and empty zones together.
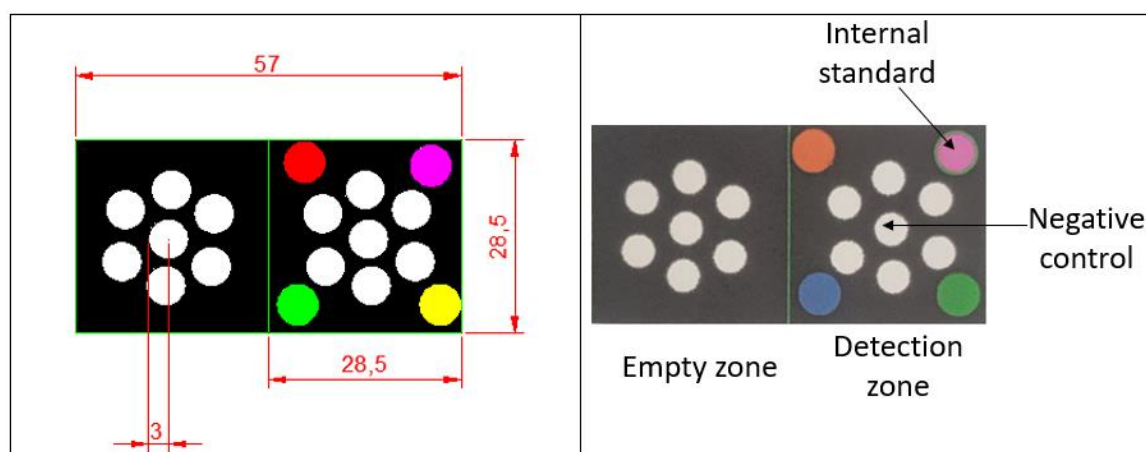
Figure 6.1 Paper device 13 (57×28.5 mm) with two zones, detection and empty zones. Each zone had 7 circles which had 6 mm diameter. The detection zone consisted of 4 internal standards, yellow, pink, green and red. The device was adopted for detection of manganese (n=6).

Device 14

Device 14 (**Figure** 6.2) was a modified form of device 13. It had similar dimensions for detection and empty zones. However, device 14 had two empty zones compare to device 13 which had one empty zone. The device was similarly folded to form three-dimension device.
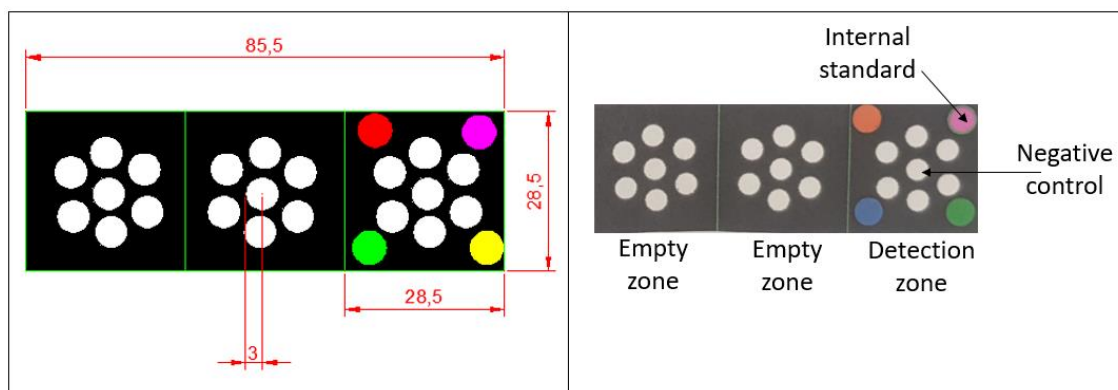
Figure 6.2 Paper device 14 (57×28.5 mm) with three zones, 2 empty and 1 detection zones. Each zone had 7 circles which had 6 mm diameter. The detection zone consisted of 4 internal standards, yellow, pink, green and red. The device was adopted for detection of manganese (n=6).

Device 15

Device 15 (**Figure** 6.3) was a modified form of device 14. It had similar dimensions for detection and empty zones. However, device 15 had three empty zones compare to device 14 which had one empty zone.
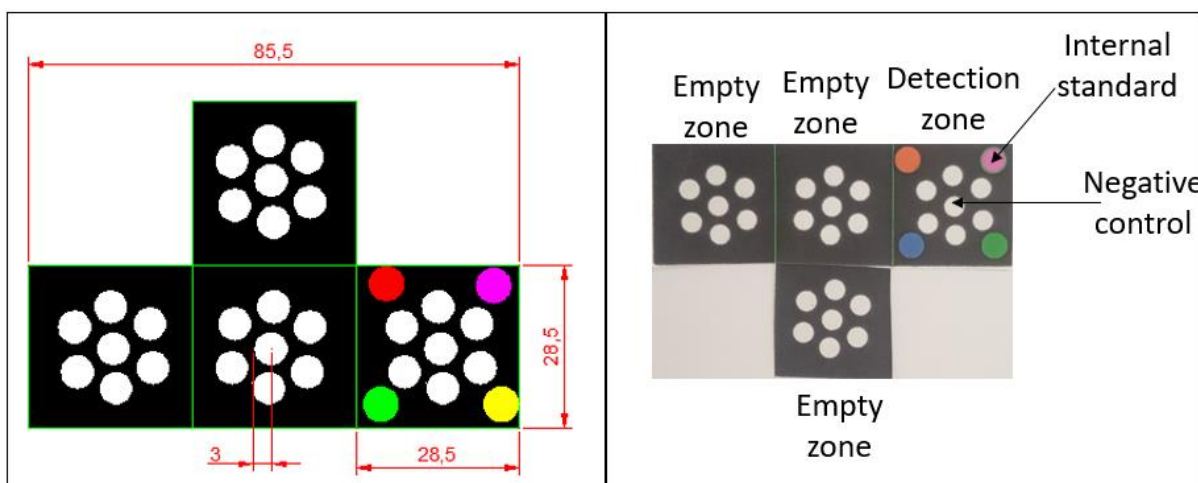
Figure 6.3 Paper device 15 (57×28.5 mm) with four zones, 3 empty and 1 detection zones. Each zone had 7 circles which had 6 mm diameter. The detection zone consisted of 4 internal standards, yellow, pink, green and red. The device was adopted for detection of manganese (n=6).

Devices 16, 17 and 18

Device 16 and 17 was fabricated with cutting; no wax barrier was used. It has circular shape with diameter of 1.5 cm. Pink internal standard (1.5 cm diameter) was used and made from wax. The circular PADs are added into two types of bases after addition of detection reagent, double side adhesive foam pad base (Aurorali, amazon) (device 16) and laminating sheet base (device 17) as in **Figure** 6.4. Device 18 was just Whiteman fitter paper no1 5×5 cm.

254
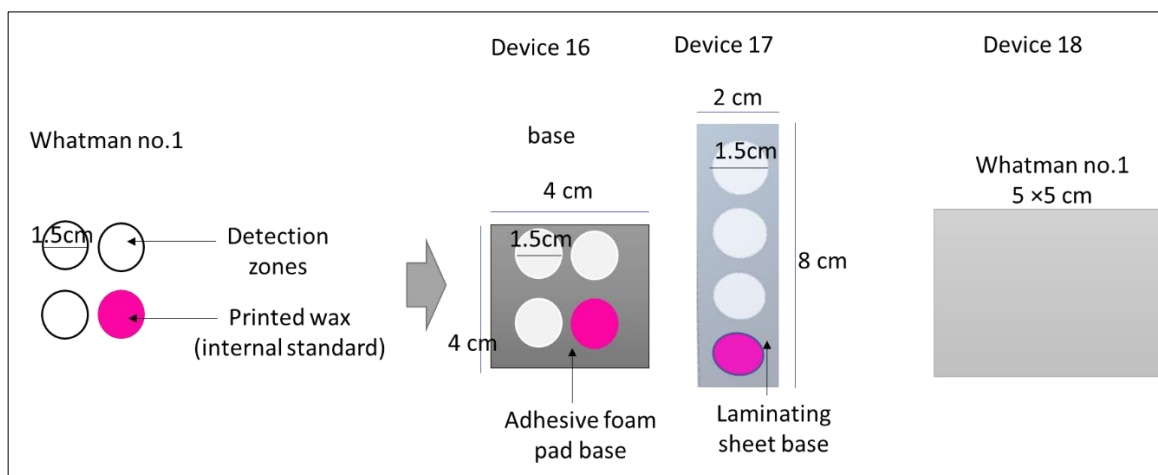
Figure 6.4 Paper device 16 and 17 (1.5 cm diameter) with three detection zones and one pink internal standard. The device was adopted for manganese detection (n=6). The circular PADs are added into two types of bases after addition of detection reagent, double side adhesive foam pad base and laminating sheet base.

6.2.2   Detection of manganese by PAR reagent

Device modification

Devices 13, 14 and 15 were modified by the same way for the manganese detection (**Figure** 6.5). Each device consisted of detection layer and empty layer. The difference between the three devices is in the number of empty layers. Device 13 has 1 empty layer, device 14 has 2 empty layers and device 15 has three empty layers. 3 µL the detection reagent solution (6mM PAR (4-(2-pyridylazo) resorcinol), 2% PDDA polymer (polyDiallydimethyl ammonium chloride), 9.9 PH glycine buffer) was added to the 6 detection circles in the detection zone. No reagent was added to the central circle in the detection zone, it was used as negative control to determine any colour which may result from the sample itself. The paper was allowed to dry in room temperature under box for 40 minutes (solution was greasy and required more time to dry). Box was used to reduce the degradation of chemicals due to light. The device was then laminated in the laminating pouch using laminator at 80 °C. Slit was made in the back side of the device by scalpel. The device was dipped into the standard/ sample for 20 minutes. photo was taken by scanner and analysed by Image-J (method 1).
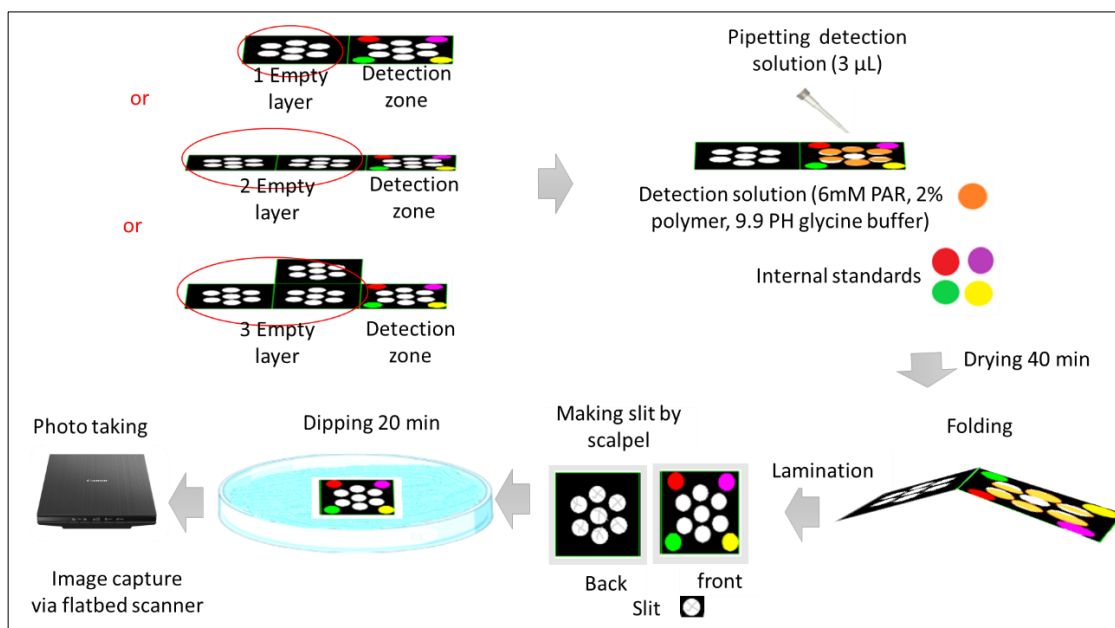
Figure 6.5 Device design 13, 14 and 15. Each device consists of detection layer and empty layer. The difference between the three devices is in the number of empty layers. 3 μL the detection reagent solution (6mM PAR, 2% polymer, 9.9 PH glycine buffer) was added to the 6 detection circles in the detection zone. The paper was allowed to dry in room temperature under box for 40 minutes. The device was then laminated in the laminating pouch using laminator at 80 °C. Slit was made in the back side of the device by scalpel. The device was dipped into the standard/ sample for 20 minutes. photo was taken by scanner and analysed by Image-J (method 1).

Optimization and calibration

Paper device design 13 was optimized for the best pH (using borate buffer). The type of buffer which was used to control the pH was optimized too by trying three buffers, borate, carbonate and glycine buffer. The amount of the detection reagent was also critical since the detection reagent itself has a yellow colour, therefore, the volume of the detection reagent which was added to the PAD was optimized too. To reduce the effect of the accumulation of the colour in the slit the number of the empty layers was optimized. **Table** 6.1 shows the optimized parameters. After optimization calibration line and its reproducibility of manganese was determined in the range and it was compared to the reproducibility of the calibration line from same detection regent by UV-Vis (The absorbance is measured in cuvette. 100 μL detection solution (2 %polymer, 6mM PAR, 9.9 Glycine buffer) was mixed with 900 μL standard were used), the absorbance was measured after 20 minutes, n=3, wavelength= 530 nm).

.

Table 6.1 Manganese device optimized parameters. pH range, Buffer type, Volume of detection reagent and Number of empty layers are the optimized parameter.

Parameter	Optimized range
pH range	8-10.5
Buffer type	Borate, carbonate, glycine
The volume of detection reagent	1-8 µL
Number of empty layers	1, 2, 3

6.2.3   Detection of manganese by PAN reagent

Device modification

Device 16 modification

Device 16 was modified as in **Figure** 6.6. Whatman filter paper 1 was cut as circle using hole punch (1.5 cm diameter). Pink wax 1.5 cm was also used as internal standard. The detection reagent (35 µL PAN(1-(2-pyridylazo)-2-naphthol) (3.8 mM) in carbonate buffer (pH 8, 8% Triton X-100) was first pipetted into the circle PADs and then dried for 30 minutes. The circular PADs were attached by adhesive foam base. The PAD then was ready to be used. Manganese solution (35 µL) was pipetted into each detection zones (n=3). Then the colour development was allowed for 7 minutes. Scanner was used for image capture. The image was analysed by Image-J (method 1).
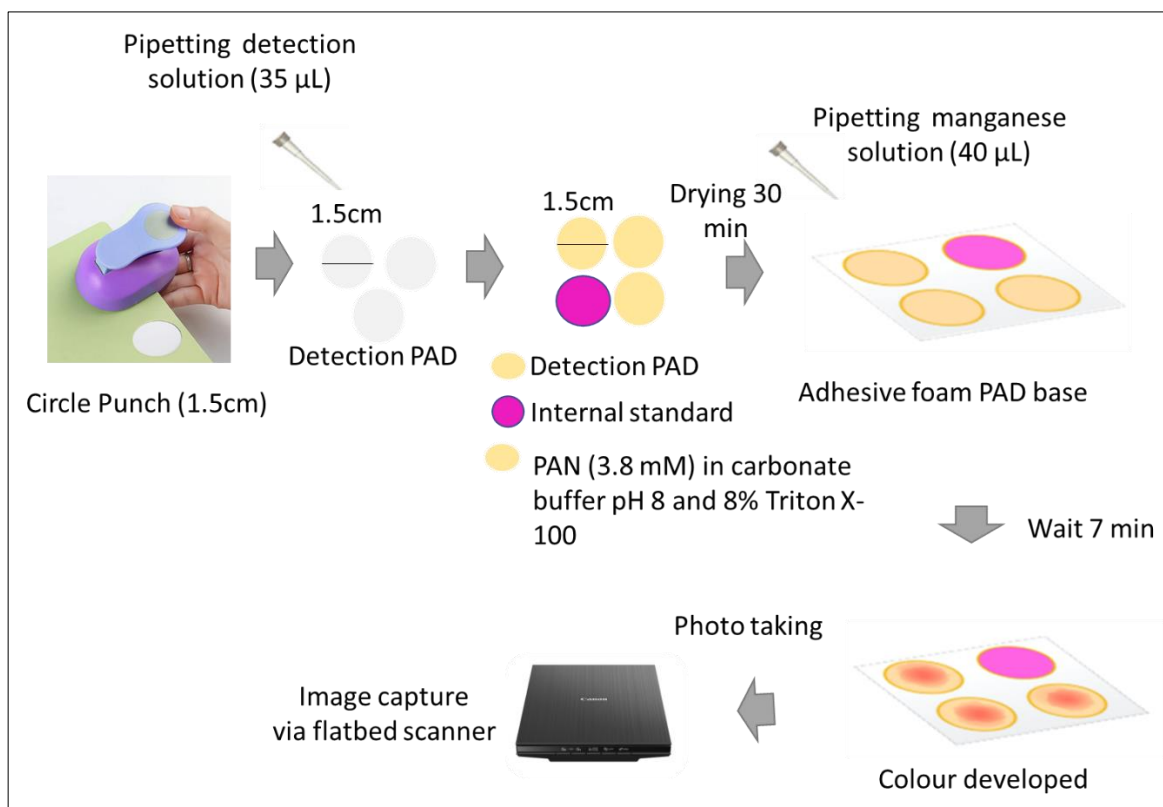
Figure 6.6 Device 16 modification. Whatman filter paper 1 was cut as circle using hole punch (1.5 cm diameter). Pink wax 1.5 cm was also used as internal standard. The detection reagent (35 µL) was first pipetted into the circlet PADs and then dried for 30 minutes. The circular PADs were attached by adhesive foam base. The PAD the is ready to be used. Manganese solution (40 µL) was pipetted into each detection zones (n=3). Then the colour development was allowed for 7 minutes. Scanner was used for image capture. The image was analysed by image J (method 1).

Device 17 modification

Device 17 was sealed device with dipping system compared to device 16. Device 17 was modified as in **Figure** 6.7. Whatman filter paper 1 was cut as circle using hole punch (1.5 cm diameter). The detection reagent (35 µL) (PAN (3.8 mM) in carbonate buffer (pH 8), 8% Triton X-100) was first pipetted into the circle PADs and then dried for 30 minutes. The circular PADs were attached to the laminating sheet which was made by Cricut explore3. The PAD was then read to be used. It was dipped for 2 second into the manganese solution and then taken away for 7 minutes colour development. Phone /scanner was used for image capture. The image was analysed by Image-J (method 2). **Figure** 6.8 shows device 17 modification with added empty layers.
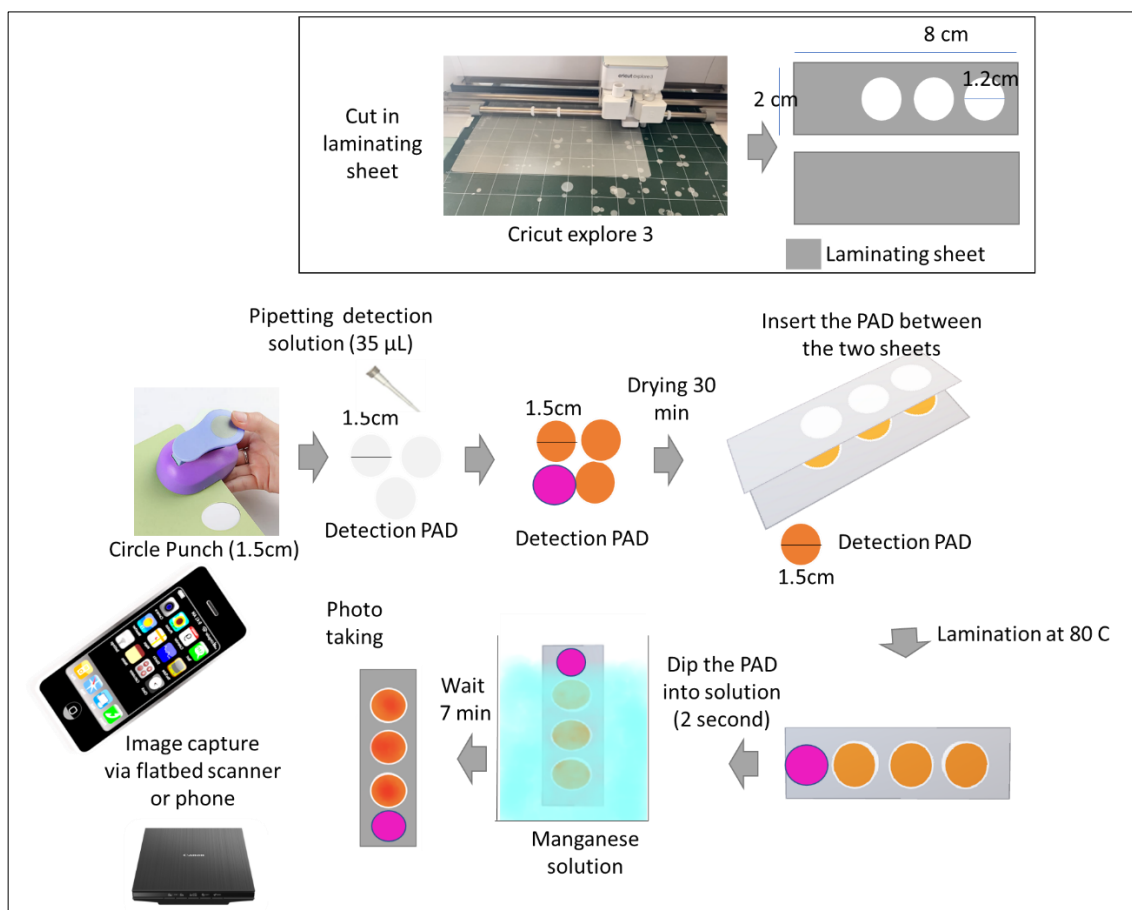
Figure 6.7 Device 17 modification. Whatman filter paper 1 was cut as circle using hole punch (1.5 cm diameter). The detection reagent (35 µL) was first pipetted into the circlet PADs and then dried for 30 minutes. The circular PADs were attached to the laminating sheet which was made by Cricut explore 3. The PAD was then read to use. It was dipped for 2 second into the solution and then taken away for 7 minutes colour development. phone (Apple iPhone 11) or scanner was used for image capture. The image was analysed by Image-J (method 2).
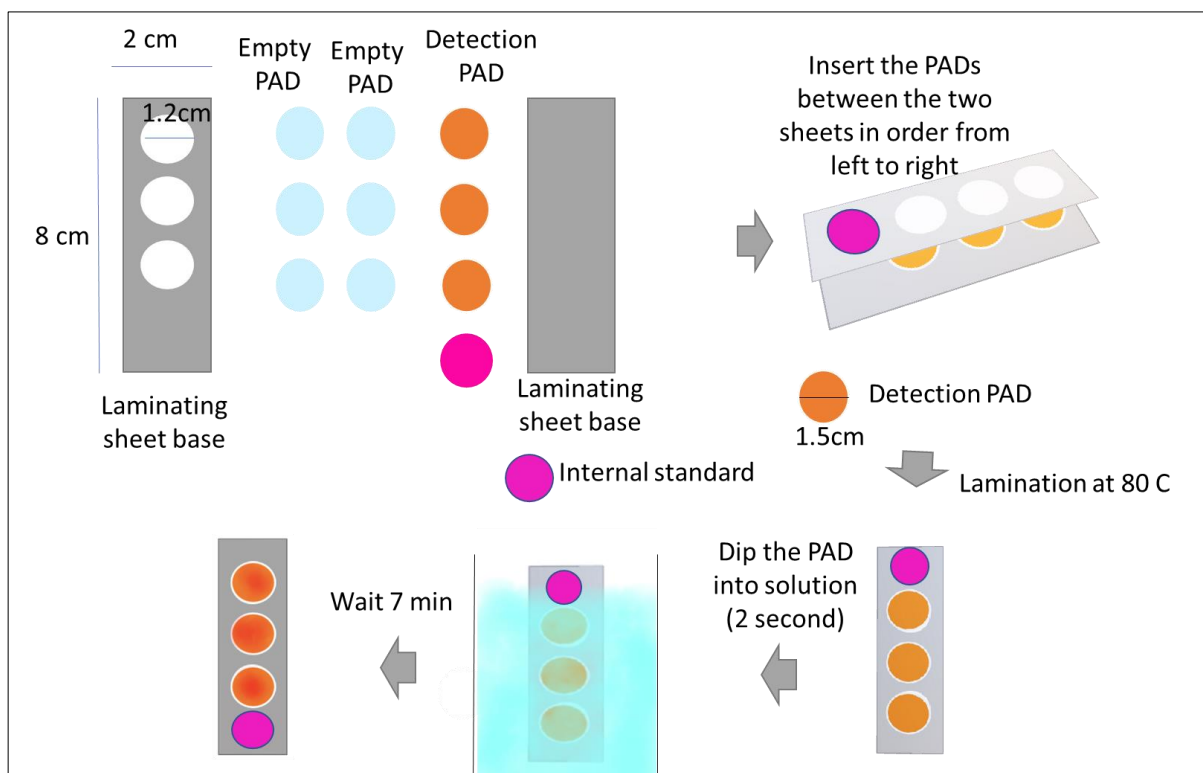
Figure 6.8 Device 17 modification. Two empty layers were added. Whatman filter paper 1 was cut as circle using hole punch (1.5 cm diameter). The detection reagent (35 µL) was first pipetted into the circlet PADs and then dried for 30 minutes. The circular PADs including empty were attached to the laminating sheet which was made by Cricut exolore3. The PAD was then read to use. It was dipped for 2 second into the solution and then taken away for 7 minutes colour development. phone (Apple iPhone 11) or scanner was used for image capture. The image was analysed by Image-J (method 2).

Device 18 modification

Device 18 (modified as in **Figure** 6.9) is barrier free device where the detection reagent was added immediately in the Whatman filter paper no 1. This device is called barrier free PAD since it has no barrier neither wax nor cut. PAD was produced from Whatman 1 paper squares (5 cm x 5 cm) attached onto adhesive tape. To detect manganese, 11 µL of PAN (3.8 mM) in carbonate buffer (pH 8, 8% Triton X-100) was added into three locations across this piece of paper and allowed to air dry for 30 min. For analysis, 10 µL of manganese solution (0 – 500 µM) was pipetted on top of the PAN zone and incubated at room temperature to allow colour development (7 min). The PAD image was then captured by a scanner and colour intensity determined using Image-J software (method 1).
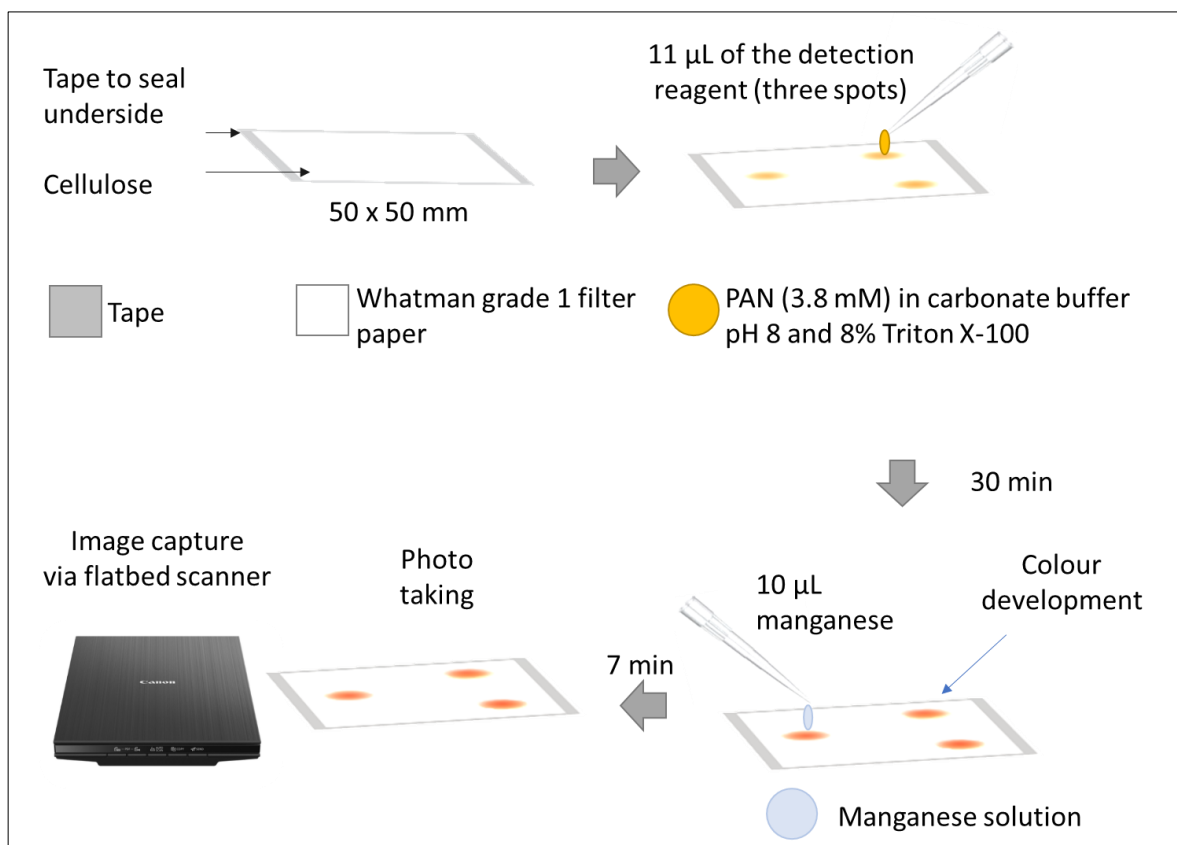
Figure 6.9 PAD 18 modification. PAD was produced from Whatman 1 paper squares (5 cm x 5 cm) attached onto adhesive tape. To detect manganese, 11 µL of PAN (3.8 mM) in carbonate buffer (pH 8, 8% Triton X-100) was added into three locations across this piece of paper and allowed to air dry for 30 min. For analysis, 10 µL of manganese solution (0 – 500 µM) was pipetted on top of the PAN zone and incubated at room temperature to allow colour development (7 min). The PAD image was then captured by a scanner and colour intensity determined using Image-J software (method 1).

Image -J analysis

Image-J analysis of devices 16 and 17 were performed as in **Figure** 6.10 where the area around the circle was kept around the same value to ensure consistently. **Figure** 6.11 show image analysis for device 18 (barrier free PAD). Same steps described in **Section 2.5** where followed.
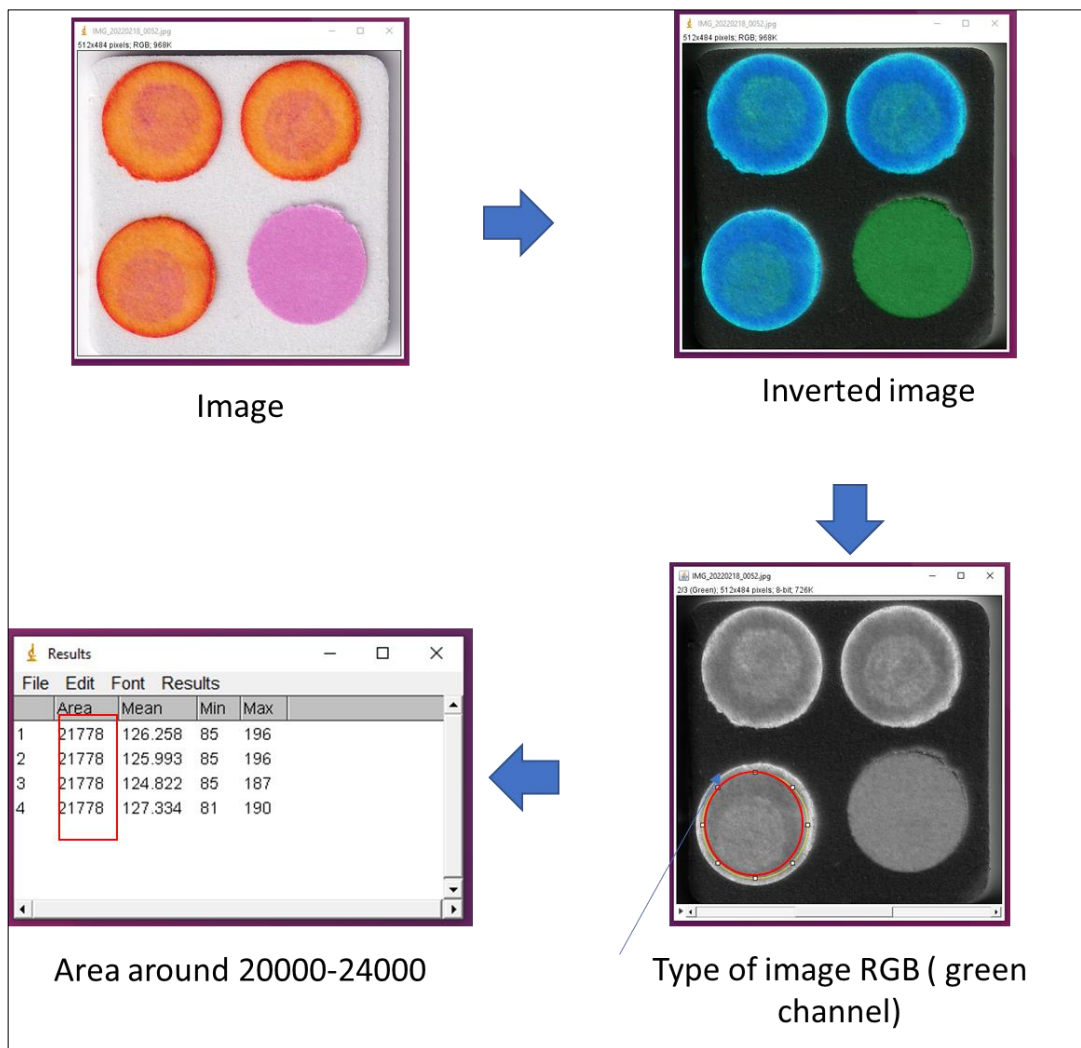
Figure 6.10 Image-J analysis for Device 16 and 17. The method is similar to method described in detail in **Section 2.5**. The area around the circle was defined for consistently.
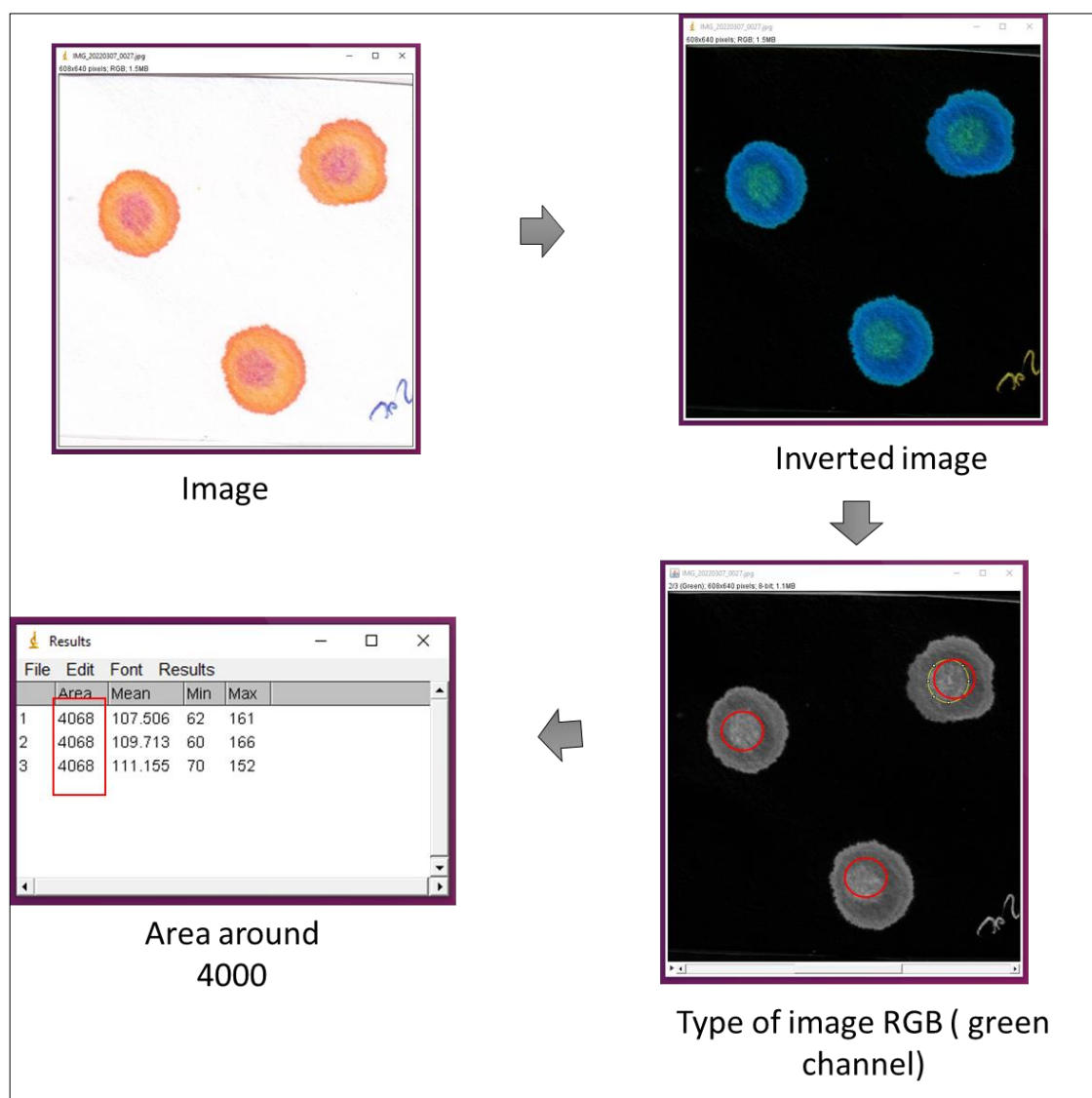
Figure 6.11 Image-J analysis for Device 18. The method is similar to method described in detail in **Section 2.5**. The area around the circle was defined for consistently.

Optimization of barrier-free bad (device 18)

The time of the reaction was optimized. The intensity was taken each minute up to 15 minutes. The volume of the detection reagent and analyte were optimized since this PAD is barrier free and the amount of the detection reagent and analyte is critical to avoid the leakage of solution outside the detection range. 5 to 13 µL of detection reagent volume were tested with constant amount of analyte 10 µL. The volume was optimized by taking the area around the detection reagent before and after the addition of the analyte (**Figure** 6.12). The area was determined by Image-J software. The area was taken before and after the reaction and it was compared.

Area of full circle measured

Before reaction   After reaction
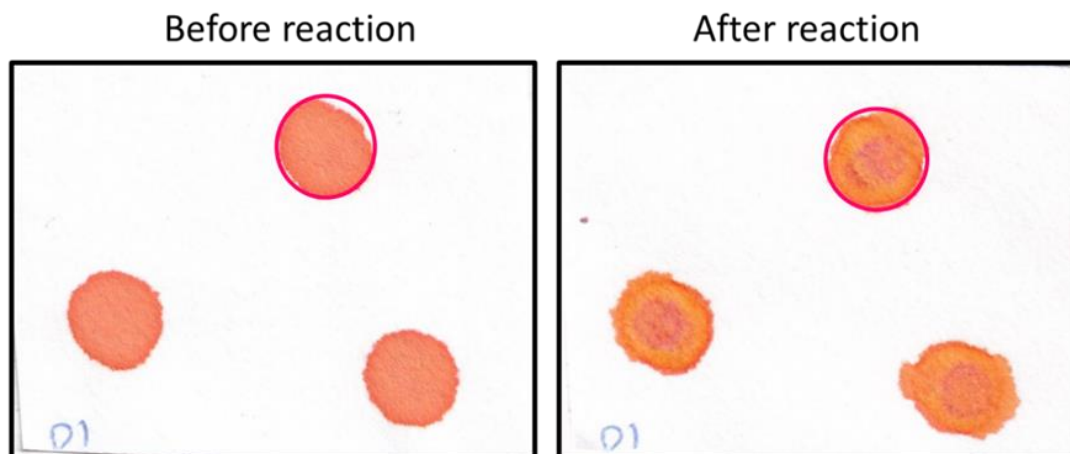
Figure 6.12 Area around the detection reagent before and after the reaction. The area was taken by image-J.

Optimization, of circular PAD (devices 16 and 17)

Optimization method 1: PAD 16 was used to optimize the detection reagent components and amount of reagent, reagent consisted of PAN, carbonate buffer and Triton X-100 surfactant. Three manganese concentrations were used in the study of optimization, 0, 100 and 200 μM. Initially the shape of the PAD (circle or square) was chosen. The dissolving reagent was tested with three types of buffers carbonate, glycine and ammonia. Amount of the detection reagent was studied in the range of 20-50 μL. Volume of the analyte was optimized in the range of 10-70 μL. The carbonate pH was studied from 6.5 to 10.5 pH. The surfactant % was also studied in the range of 0-14%. PAN concentration from 0.5 to 5 mM was optimized. Finally, the time of the reaction was studied by taking image each minute for 15 minutes. **Table** 6.2 summarized the optimized parameters.

optimization method2: origin lab was used to design experiment by the experiment design, Optimization method 2 was done to double check the close values of the detection reagent components (PAN, surfactant, pH). This was done by using box Behnken design. Three different variables with three points were chosen as the following: pH (8, 9,10), surfactant % (4, 6,8%) and PAN concentration (2.8, 3.3, 3.8 mM). The lost value was called -1, mid-point is 0 and the highest point is 1. 16 different solutions were prepared by combination of the three parameters (as suggested by the experimental design (**Table** 6.3) and deposited in the PAD which was then tested with 100 μM manganese solution. 16 PAD intensities were determined and inserted finally in the origin lab for analysis.

Sealing of the PAD

The PAD was sealed by different methods. Acrylic cover (5 cm diameter. 0.2 cm thick, two layers) with 3 circular wholes (1 cm diameter) was used and lamination (with two types of sample introduction ways, line cut or circular cut) was also used. For both pipetting and dipping sample introduction were done whenever it was possible.

Calibration and reproducibility

The calibration line of PAD 16 and 17 were determined in the range 0-500 μM and its reproducibility was determined by running the calibration line in three different days.

Table 6.2 Optimized parameters for manganese determination and the range of the study. Shape of the PAD Buffer type, Volume of detection reagent, Volume of the analyte, Carbonate pH, Triton X-100 surfactant %. PAN concentration, sealing of PAD, Sample introduction, and Calibration range were studied. Three manganese concentrations were used in the study of optimization, 0, 100 and 200 μM.

Parameter	Optimized range
Shape of the PAD	Circle/Square
Buffer type	Carbonate/ Glycine/ ammonia
The volume of detection reagent	20-50 μL
Volume of analyte	10-70 μL
Carbonate pH	6.5 to 10.5 pH
Triton X-100 surfactant %	0-14%
PAN concentration	0.5 to 5 mM
Sealing	Acrylic cover/ lamination
Sample introduction	Pipetting/ dipping
Calibration range	0-500 μM

Table 6.3 The different solutions were prepared by combination of the three parameters. Three different variables with three points were chosen as the following: pH (8, 9,10), surfactant % (4, 6,8%) and PAN concentration (2.8, 3.3, 3.8 mM). Origin lab was used to design experiment by the experiment design.

	LOW, MID, HIGH			REAL VALUES		
	pH	Surfactant%	PAN (mM)	pH	Surfactant%	PAN (mM)
solution 1	-1	0	-1	8	6	2.8
solution 2	0	1	1	9	8	3.8
solution 3	0	-1	1	9	4	3.8
solution 4	0	0	0	9	6	3.3
solution 5	1	0	-1	10	6	2.8
solution 6	-1	-1	0	8	4	3.3
solution 7	0	1	-1	9	8	2.8
solution 8	0	0	0	9	6	3.3
solution 9	0	-1	-1	9		2.8
solution 10	0	0	0	9	6	2.8
solution 11	0	0	0	9	6	2.8
solution 12	-1	1	0	8	8	2.8
solution 13	1	-1	0	10	4	2.8
solution 14	1	1	0	10	8	2.8
solution 15	1	0	1	10	6	3.8
solution 16	-1	0	1	8	6	3.8

Interferences

Interferences were studied using PAD 16. Firs the general interferences that does not need masking reagent were studied. Calcium, manganese, sodium, potassium, nitrate, phosphate, and chloride ions are some of the cations and anions that can cause interference. The general interferences were studied by preparing the PAD as usual **Figure** 6.6. This time instead of adding the manganese, a mixture of manganese and interference were added and allowed for colour development. The intensity of manganese alone was compared to the intensity of the mixture of manganese and interference.

The interferences that exist in soil and has the tendence to react directly with the PAD and compete with manganese are zinc, copper, and iron ion. Therefore, masking reagent were used to mask such interferences. DMSA (Dimercaptosuccinic acid) (0, 0.04 and 0.4 M), DFO (Deferoxamine) (0. 0.01, 0.05 M) and thiosulfate ion (o, .1, 0.5, 1M) were used for iron and cupper ion masking. EDTA (0.05 M) and EGTA (0.05 M), Citrate ion (0.05, 0.01, 0.1 and 0.5 M), Hydroxide ion (0, 0.1, 0.5 and 1 %), thiosulfate ion (o, .1, 0.5, 1M) were used for zinc ion masking. The masking reagent was added to the PAD before the detection reagent (**Figure** 6.13) and then the PAD was prepared as usual after drying of the masking reagent. The intensity of manganese alone was compared to the intensity of the mixture of manganese and interference (100 μM (5.6 mg L^{-1}) of manganese was used and 5 mg L^{-1} of interference was used each time).
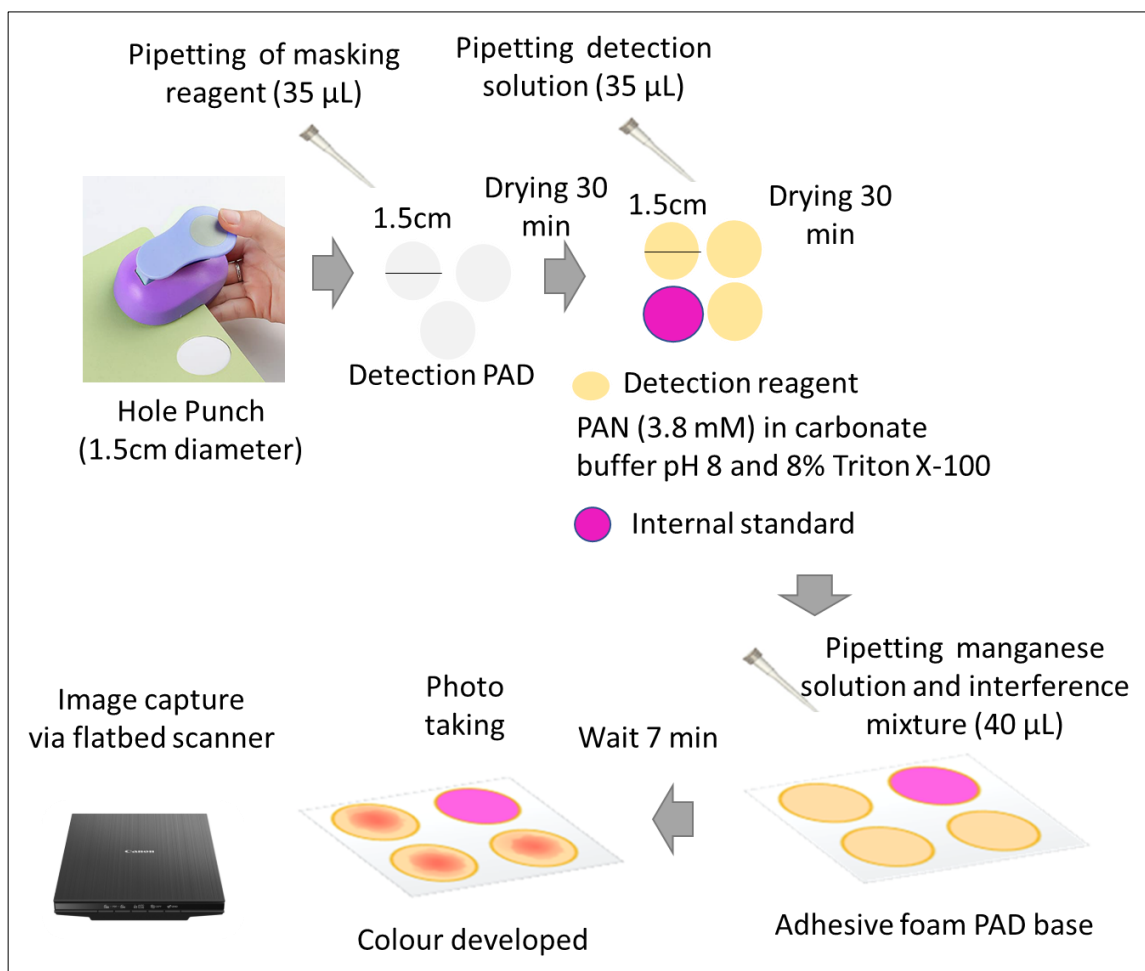
Figure 6.13 The test for interference of manganese PAD (device 16). The masking reagent was added to the PAD followed by the addition of the detection reagent. After drying the PAD is ready to be used. 40 µL of mixture of the interference and manganese was added to the PAD. This was compared to the intensity of manganese alone. 100 µM (5.6 mg L^{-1}) of manganese was used and 5 mg L^{-1} of interference was used each time.

Stability

Manganese PAD 16 was studied in three different storing conditions, out at room temperature (21 ^{0}C) in the light, out in room temperature (21 ^{0}C) in dark (47 days), and in the freezer (-4 ^{0}C) in dark (68 days). 100 µM of manganese was used for the study.

6.2.4   Soil sample treatment

Soil sample information

One soil sample was used during the manganese study, John Innes No 1 (young plants compost) from Amazon, UK.

Extraction solvent

EDTA represent the best extraction solvent that can form complex with manganese (II) ion. However, EDTA can also form complex with other heavy metals [450,451]. 0.05 M EDTA was used as extraction solvent, shaker and cafetiere was used for extraction, ICP-MS was used as detection method. cafetiere ability to extract manganese (II) ion was then compared to shaker and the efficiency of cafetiere extraction was determined. For this work EDTA was used as conventional extraction solvent when shaker and ICP-MS conventional method was used for the analysis. Other solvent like DIW, Cola (Coca cola, Original, Morrison, UK), 0.05 M HCl/0.0125 M H_2SO_4, 0.01 M $CaCl_2$, 0.01 M KCl and 0.01 M NaCl were used in this study as alternative for EDTA which interfere with PAD. Small concentrations of solvents were studied to avoid the interference that maybe caused be ions of solvent when PAD is used for analysis.

Cafetiere extraction

Extraction was as in **Figure** 6.14**.** 10 gram of soil sample was added to the cafetiere this was followed by the addition of 200 mL of the solvent (0.01M NaCl). Then the plunger was shaken up and done for 1 minutes. The soil slurry was allowed to settle for 3 minutes. The extracted solution was then added to container for analysis by PAD (**Figure** 6.14)or it was taken for analysis by ICP-MS after it was filtered by 0.22 μm filter.
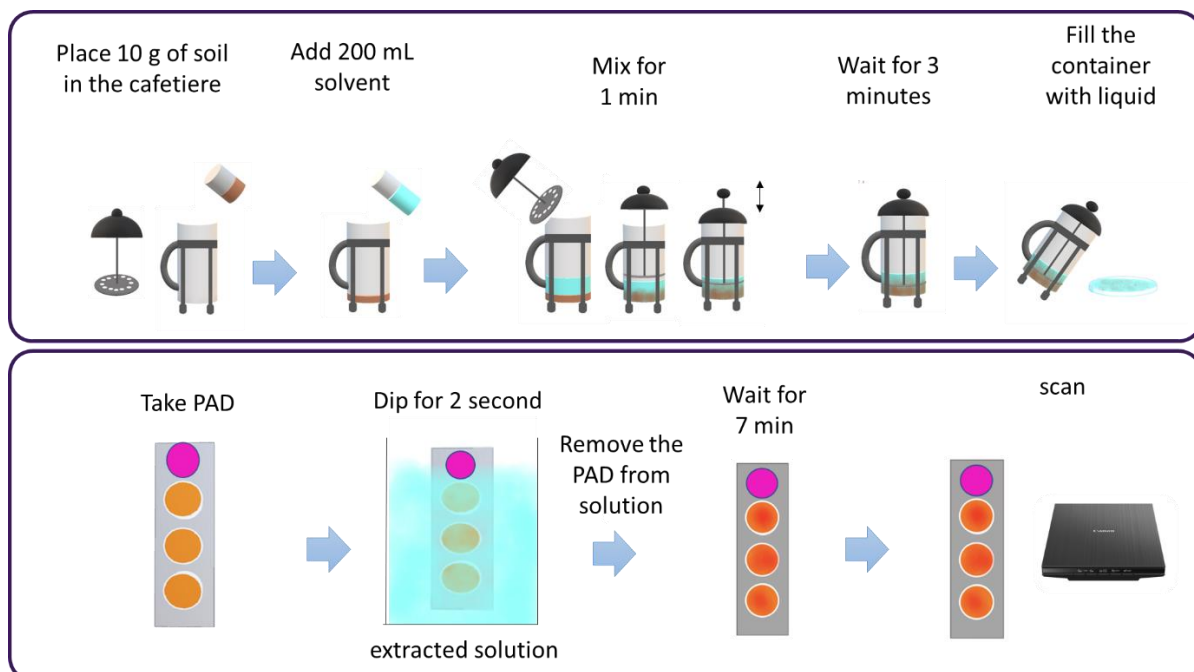
Figure 6.14 Cafetiere extraction of manganese. 10 gram of soil sample was added to the cafetiere this was followed by the addition of 200 mL of the solvent (0.01M NaCl). Then the plunger was shaken up and done for 1 minutes. The soil slurry was allowed to settle for 3 minutes. The extracted solution was then added to try for analysis by PAD. The PAD was dipped into the extracted solution for 12 second. The PAD was removed from solution and allowed for colour development for 7 minutes. Scanner was used for image capture.

Shaker extraction

10 grams of soil sample was added to the closed container, and this was followed by the addition of 200 mL of the 0.05 M EDTA solvent. The mixture was shaken in a shaker for 1h. The extracted solution was then filtered by a 0.22 µm filter and analysed by ICP-MS. Some extracted solutions may be diluted.

Time of mixing and other interferences

Time of mixing using the cafetiere was critical to extract efficient amount of manganese. The mixing was done by the plunger in cafetiere for specific minutes (1-5 minutes). Other metals (Fe, Co, Ni, Cu, Zn, Cd) that have the possibility to interfere with manganese were studied along with time of mixing in the same soil sample.

ICP-MS

ICP-MS (Thermo Scientific iCAPQc ICP-MS) was used for analysis. The samples were sent to Leeds university, Leeds, UK for analysis. They were asked to detect Mn, Fe, Co, Ni, Cu, Zn and Cd ions simultaneously.

Cafetière/PAD system

The soil (John Innes 1) sample which was studied by cafetiere/ICP-MS was studied with the developed system cafetiere/PAD and the efficiency of the PAD was determined.

6.3 Result and Discussion

6.4 Paper microfluidic for manganese detection

6.4.1 Detection of manganese by PAR reagent

Manganese reacts with PAR (4-(2-pyridylazo) resorcinol) reagent in basic condtion and existance of polymer to form a complex as in **Equation 2.3**. PAR when it is solid, it has a orange colour. However when it is dissolved in polymer and basic solution it becomes close to yellow in colur especially when it is added to the paper device. The PAD was fabricated by wax printer as in **Figure** 2.1. PAD consisted of detection zone with circles as in **Figure** 6.15 There were 6 detection circles, four internal satndards and one circle in the middle as negative control. The detection reagent is one solution (mixture of 5 mM PAR, 3% polymer PDDA (polyDiallydimethyl ammonium chloride) and borate buffer PH 9.9)[315] which was added to the detection zone only as in the **Figure** 6.15. The other layerS was empty. Parameter optimized for the developed PAD and its optimum condition was as in **Table** 6.4 and it was clarified in details in **Appendix G**, from **Figure G1** to **Figure G4**.
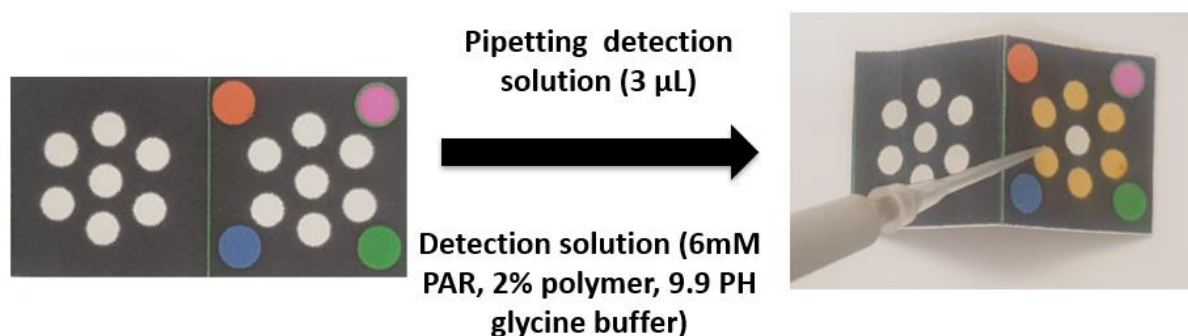
Figure 6.15 Two layers paper device before and after the addition of the detection reagent. The device consistED of the detection zone and empty zone. The detection reagent was added to the 6 circles in the detection zone.

Table 6.4 Optimum conditions for manganese determination by PAD which was based in PAR reagent as detection solution.

Parameter	Optimum
pH	9.9
Type of buffer	Glycine
The volume of detection reagent	3 µL
Number of empty layers in the device	1 layer

Calibration line

Calibration line after improving the sample entrance

The calibration line was determined using the optimum condtion in **Table** 6.4 and device 13 with one empty layers. The result still suffer from the uneven colour due to the cut in the back of the device. The sample entrance was improved by making the circular cut in the laminating sheet before the lamnation. This was done to remove avoid the secratch of the paper when the cut done after lamination. Therefore a cut in form of circle was made in the laminating sheet. The PAD with the deposited reagent was then laminated inside the lamiantion sheet, the circle in the PAD were alliend with the circle in the laminating sheet. The result as in **Figure** 6.16 which shows the intensity from PAD at different concentrations of manganese. The result were repeated three times. It was found that even though the repeats were perfprmed in the same day, the lines do not match and vary from try to try. It was found that the PAD leak with time as in **Figure** 6.17 This leakage is due to the hydrophobic polymer (PDDA) in the detection reagent. The leagkage did not happen immediately it happened after time (around 2 min) and hence the result is affected sometime. Other than the leakage the reagent itself may be another reason for the non reproducible result. The reagent may have instable behaviour on the top of the paper due to the incoptability between the hydrophilic paper and the reagents in the detection reagents Which make the reagent varied behavoiur on paper. This thoughts because the same reagent was tested with UV-Vis in cuvet and a stable reasult resulted. **Figure** 6.18 shows the the absorbance from diffrerent manganese solution after mixing with PAR detection reagent. The result from three different days were stable. This indicated that the reaction was stable when it was performed in cuvatte compare to when it is perform in paper. Therfore, another detection reagent was used in the next section.
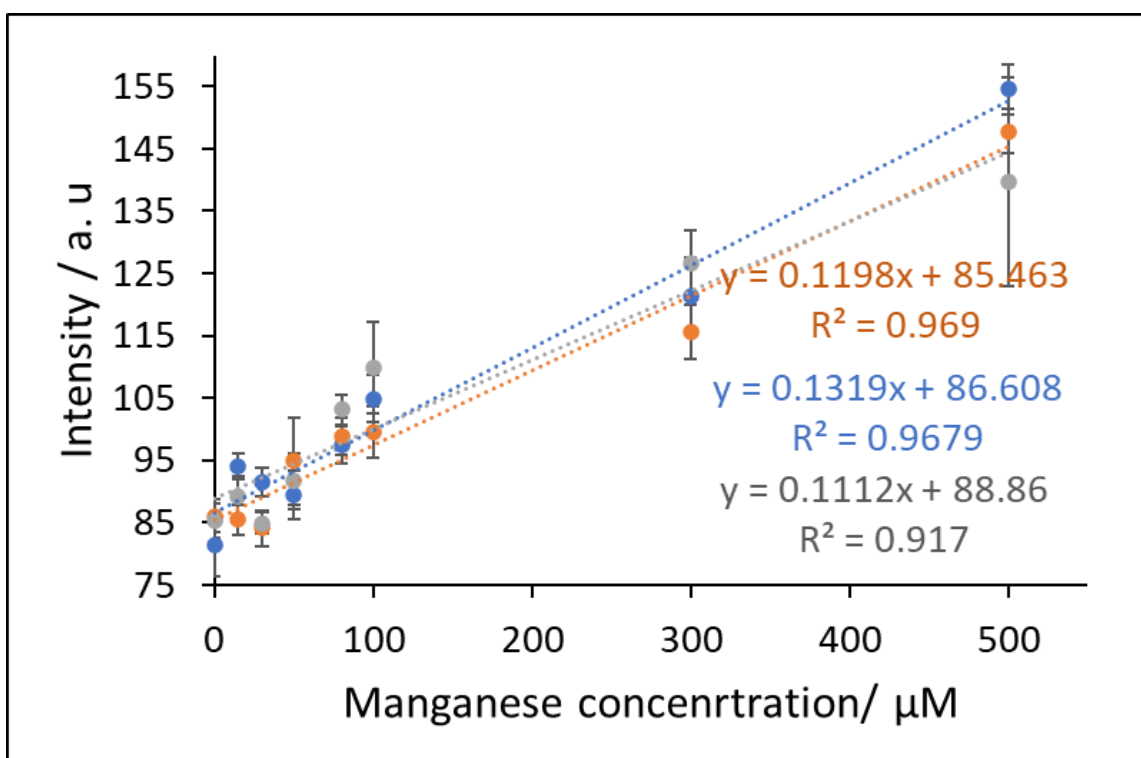
Figure 6.16 Intensity versus manganese concentration (µM). The detection reagent is 3 µLmixture of 6 mM PAR, 3% polymer PDDA (polyDiallydimethyl ammonium chloride) and glycine buffer PH 9.9. Scanner was used to take the photo. Mehtod 1 was used for the calculation of intensty. Device 13 was used.
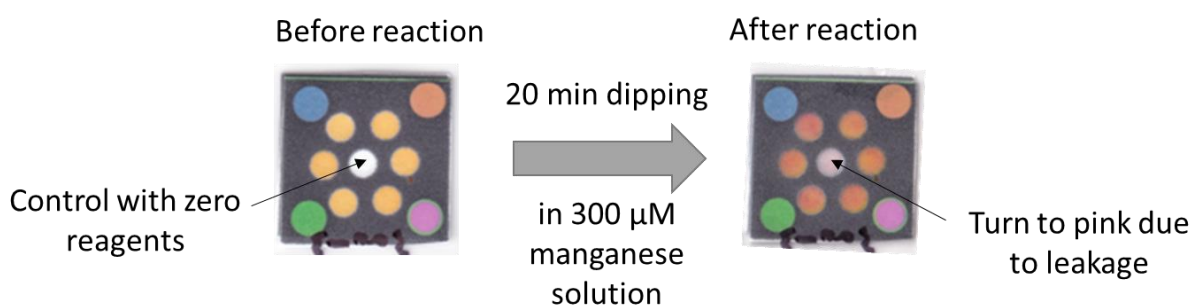
Figure 6.17 Device 13 with PAR detection reagent after dipping 20 min in 300 µM manganese solution. The control which has zero reagents should not change colour. The control change to pink colour due to the leakage. Leakage happended after 2 minutes of dipping.
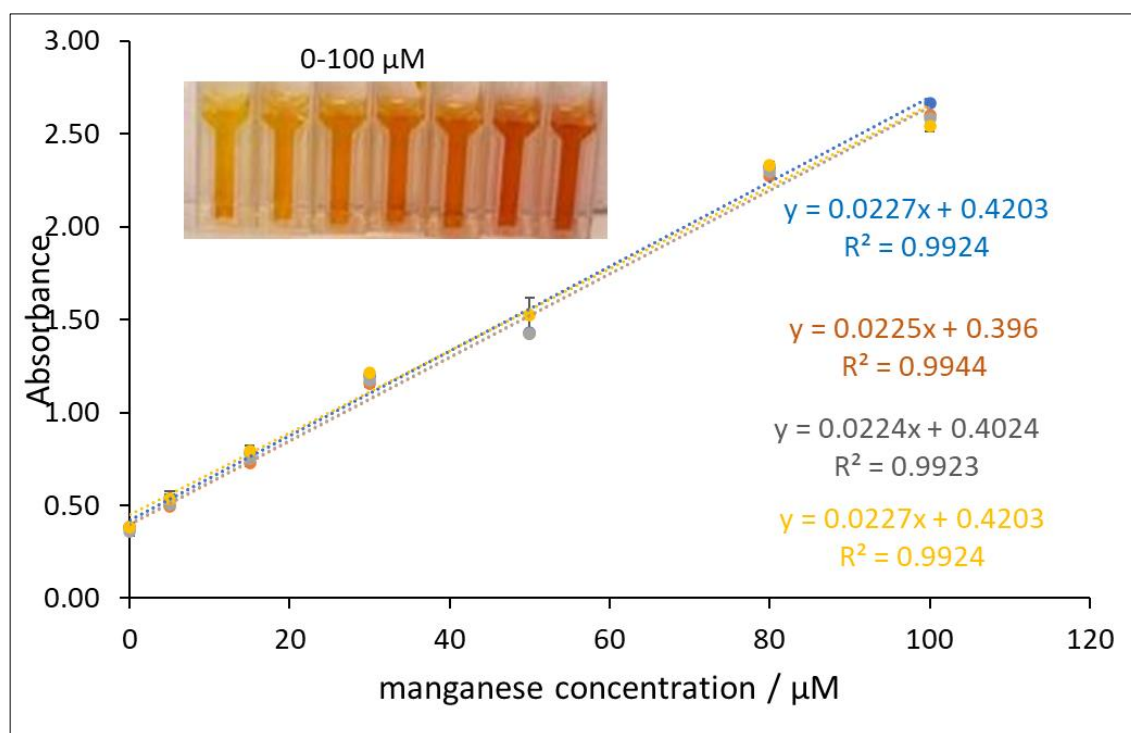
Figure 6.18 Absorbance versus manganese concentration (µM). Result from UV-Vis. The absorbalce is measured in cuvette at 20 min detectin time. 100 µL detection solution (2 %polymer, 6mM PAR, 9.9 Glycine buffer) and 900 µL standard were used, n=3, wavelength= 530 nm.

6.4.2 Detection of manganese by PAN reagent

PAN reagent was also used for colorimetric detection of manganese. PAN (1-(2-pyridylazo)-2-naphthol) form a complex with manganese in basic condition as in **Equation 2.4**. PAN does not dissolve in water, it needs solvent (methanol, ethanol) that can dissolve it or the presence of surfactant (triton X-100) with hydrophobic and hydrophilic parts. In addition, buffer is needed to control the pH and keep the stable manganese complex that form with PAN. This reaction was applied and studied on Whatman filter paper. Since the surfactant is hydrophobic it has the tendency to interact with the printed wax (**Figure** 6.19) which is hydrophobic too and hence the wax cannot be used as barrier this time. Two types of PADs were studied, PAD which was made by cutting and PAD which was barrier free.
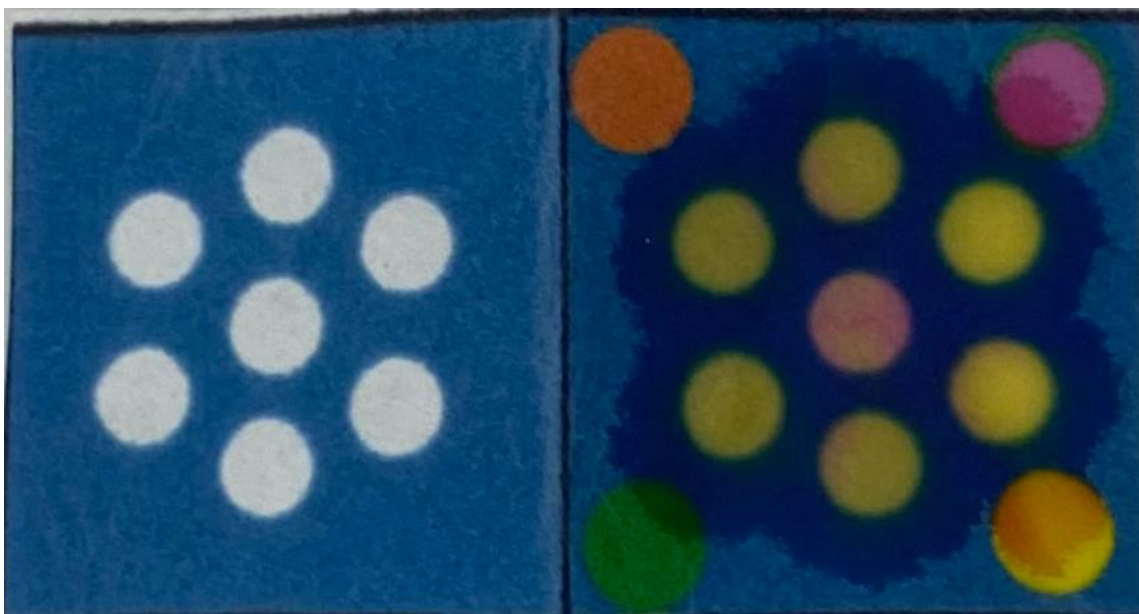
Figure 6.19 The leakage after the addition of PAN reagent in PAD made by wax.

6.4.2.1 Device made by cutting

6.4.2.1.1 Device shape

Two shapes of the device were tested, square and circular to determine the influence of the sharp edged and non-edged device in the distribution of the solution. **Figure** 6.20 shows the four devices with different dimensions (dimension were shown based on the available puncher). As it is clear from the photos above the bars the distribution was almost similar and did not show any preference in any of the PAD regardless the shape and the dimensions. The reagent distribution is non uniform. Consequently, this is maybe due to the solution itself not the edges of the PAD. The variation in the signal from PAD to PAD maybe due to the instability of the conditions and the different amount of analyte which was added each time based in the device dimension. As conclusion both square and circular PAD are good to be used as devices, of course this should be after optimization of the various conditions, including amount of analyte and detection reagent. For consistent the rest of experiment will be carried with 1.5 cm circular PAD since it is big enough to see by eyes and that what is needed for volunteers, something clear and easy to be seen. In addition, bigger diameter was chosen to avoid the dark colour that forms at the circumstance of the circle. The circumstance will be avoided when intensity is determined by Image-J.
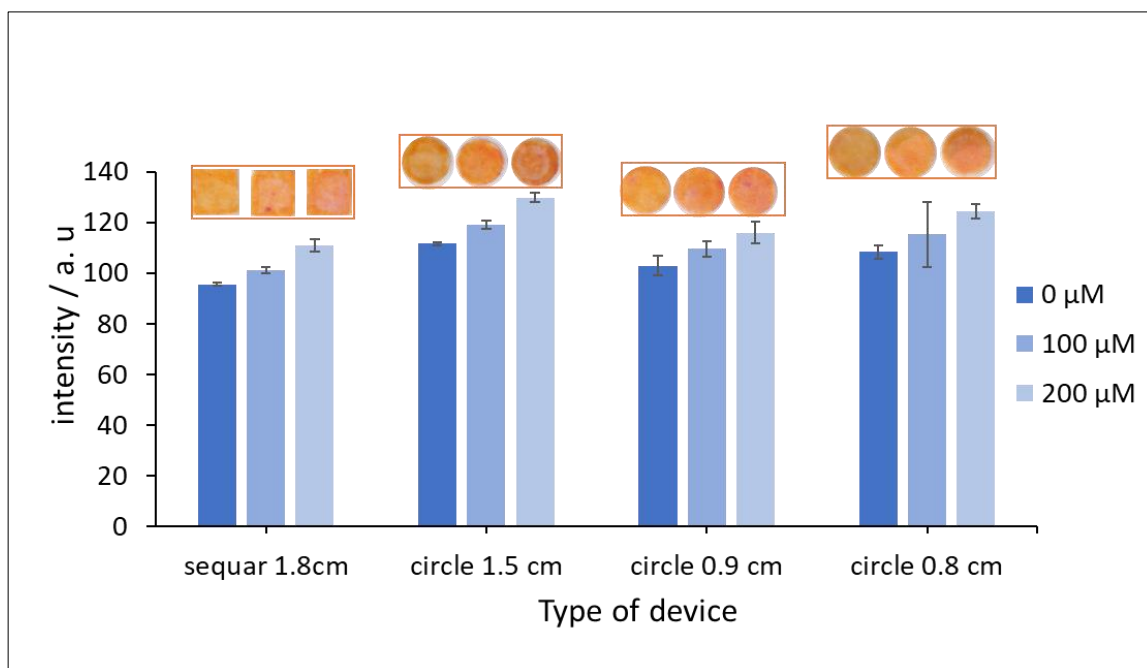
Figure 6.20 Intensity versus type of device. One square PAD (1.8 *1.8 cm) and three circular PADs (diameters, 1.5, 0.9 and 0.8 cm) were used. The PADs were cut using punches (**Figure** 2.2). Three different manganese concentration were studied 0, 100 and 200 µM. The detection reagent was added to the PAD (n=3) firs and allowed to dry, the manganese analyte was pipetted into the PAD after 3 min of waiting the PAD was scanned and image was analysed for intensity using image-J software (The intensity was measured by method 1 in **Section 2.5**).

6.4.2.1.2   Optimization Method 1

The optimization was done using two methods. The first method was by taking each parameter alone (specific range) and determine the optimum value of each parameter separately. The second method by studying all the parameter at once together to determine their effect on each other. In this section the first optimization method was discussed.

PAN dissolving reagent (Surfactant)

PAN reagent has hydrophobic characteristic and hence it needs to be dissolved in reagent with such character. Ethanol and ethanol can dissolve hydrophobic reagent and can be dissolved also in water. However, they are volatile, and this can affect PAD stability. The PAD finally should be a kind of PAD that can be stored for long time at least one month and hence it can be sold to lay people for every day normal use, not for lab use. Therefore, surfactant will be used instead of ethanol to dissolve the PAN. Surfactant has two arms, hydrophobic and hydrophilic arms in such a way it can dissolve in hydrocarbons and at the same time can be mixed in water. There are types of surfactants, ionic surfactant, and non-ionic surfactant. In this work non-ionic surfactant was used since it is the most used and since the ionic surfactant may also interact with the detected metal [314]. **Figure** 6.21 show the result of intensities from PADs when surfactant was

used to dissolve the PAN with four buffer conditions, no buffer, carbonate buffer, glycine buffer and ammonium buffer. These three buffers were chosen since they do not have the tendency to capture manganese analyte [452]. In addition, they are not as toxic as borate buffer which was commonly used in other studies with PAN reagent [314]. Both ammonia and borate are toxic. However, carbonate and glycine are not as toxic as the other options. When no buffer and ammonia buffer were used the variation between 0, 100 and 200 μM was not significant. Carbonate and glycine buffer showed clear gradient between the three concentrations of manganese. However, the detection reagent was more homogeneous on paper when carbonate buffer was used as in **Figure** 6.22. Therefore, carbonate buffer was used with the surfactant to prepare the detection solution with the surfactant.
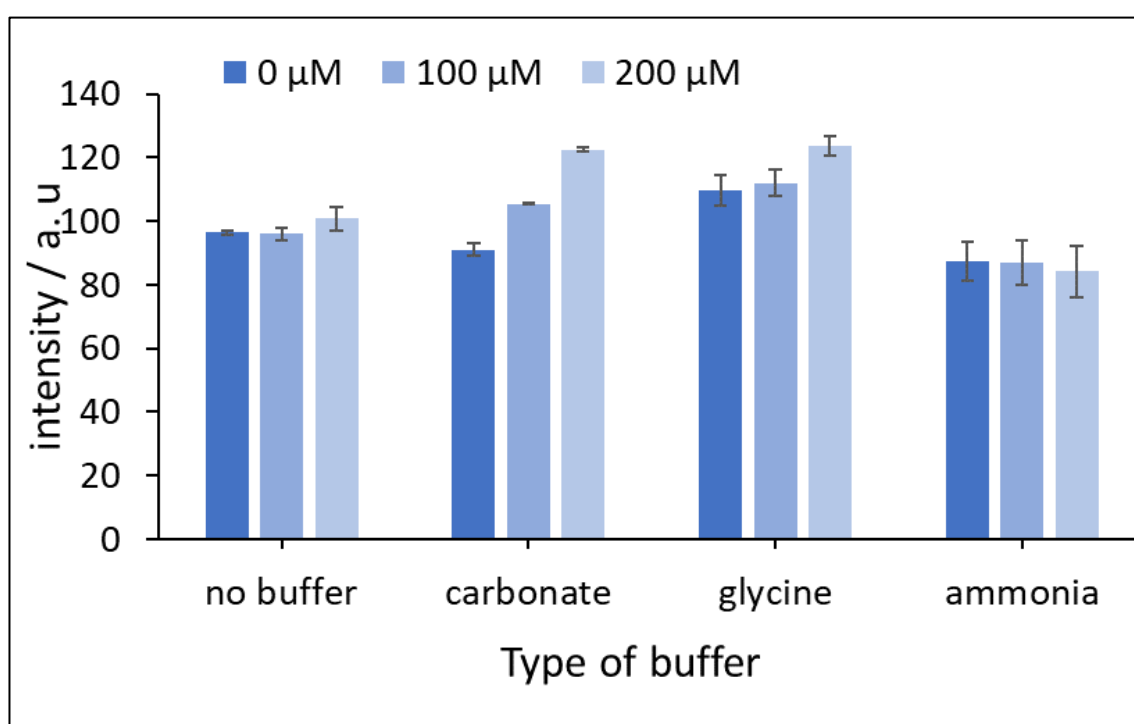
Figure 6.21 Intensity versus type of buffer. PAN reagent consisted of surfactant at four different conditions of buffer, no buffer, carbonate buffer, glycine buffer and ammonia buffer. All buffers at PH 10. Three different manganese concentration were studied 0, 100 and 200 μM. The detection reagent was added to the PAD (n=3) first and allowed to dry, the manganese analyte was pipetted into the PAD after 3 min of waiting the PAD was scanned and image was analysed for intensity using image-J software (The intensity was measured by method 1 in **Section 2.5**). Device 16 was used for the anlysis.
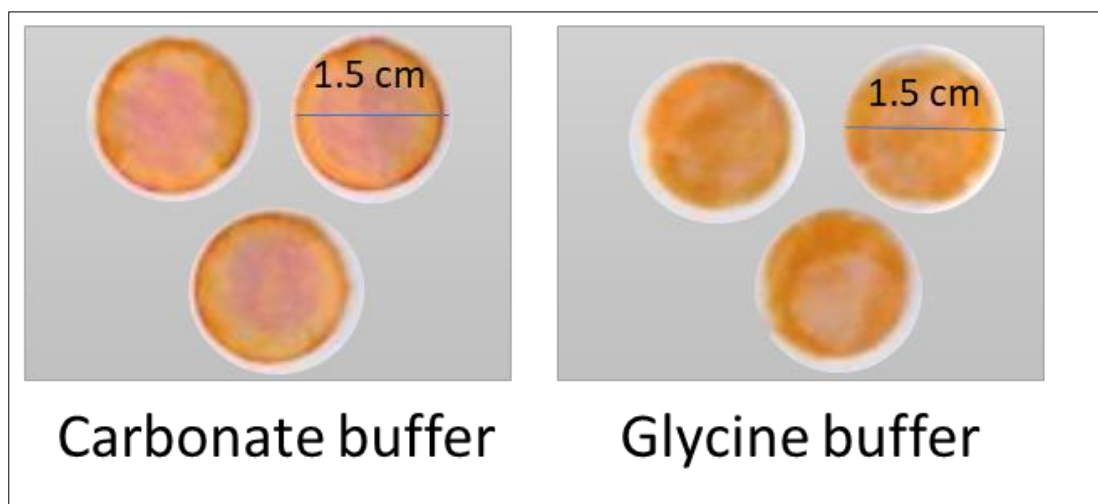
Figure 6.22 Two different conditions of buffer, carbonate buffer and glycine buffer. All buffers at PH 10. 100 µM manganese concentration were studied. The detection reagent was added to the PAD (n=3) first and allowed to dry, the manganese analyte was pipetted into the PAD after 3 min of waiting the PAD was scanned and image was analysed for intensity using image-J software. Device 16 was used for the analysis. Reagent with glycine buffer showed more nonhomogeneous distribution of the reagent in the PAD.

Amount of detection reagent

Before further optimization of the component of the detection reagent, the amount of the detection reagent added to the PAD was optimized since it significantly affects the result. The more detection reagent added the darker the colour of the PAD and the less amount added the brighter is the colour. Consequently, this can affect the reading of intensity finally after addition of the analyte. **Figure** 6.23 shows the intensity versus the amount of detection reagent added. Clearly when the amount of the reagent added increased the intensity increased for 0, 100 and 200 µM of manganese analyte. More than 45 µL was too much to be added and it needed too much time to dry. Therefore, less than 45 µL was only considered. From 30 to 40 µL of analyte intensity stable with no significant difference for 0, 100 and 200 µM using ANOVA test (e.g., at 0 µM (F= 1.42, $F_{critical}$=5.14, P=0.31, α=0.05, n=3, ANOVA test)). Therefore 35 µL the middle volume was chosen to be optimum to carry the rest of experiment.
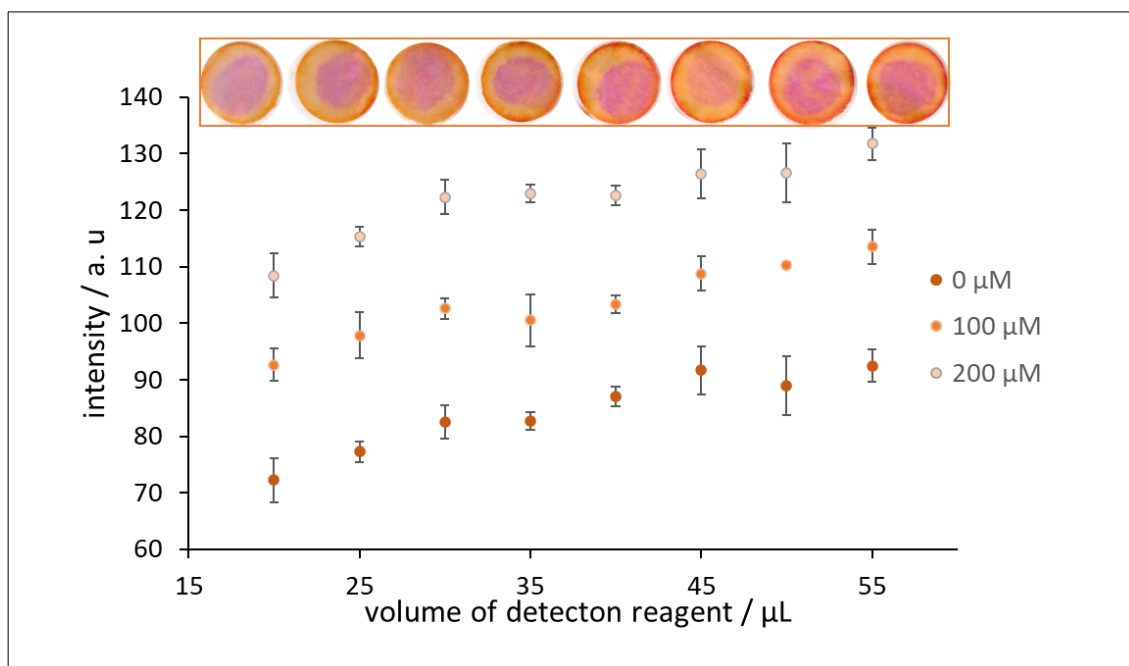
Figure 6.23 Intensity versus the volume of detection reagent. Three different manganese concentration were studied 0, 100 and 200 μM. PAN (1.3 mM) reagent consisted of 2% surfactant (Trionix-100), carbonate buffer (pH 10). The detection reagent was added to the PAD 16 (n=3) first and allowed to dry, the manganese analyte (50 μL) was pipetted into the PAD after 3 min of waiting the PAD was scanned and image was analysed for intensity using image-J software (The intensity was measured by method 1 in **Section 2.5** and **Figure** 6.10). Device 16 was used for the anlysis.

Volume of analyte

Another important factor is the volume of analyte. The more analyte added the more the intensity should be since more manganese analyte is detected. Also, the more analyte added the more time it will be needed to dry, and the less analyte added the less time needs to dry. Keeping in mind that time is critical in this study since we do not want the long experiment time because this PAD needs to be released finally to farmer. **Figure** 6.24 shows intensity versus the amount of manganese analyte added at three different concentrations 0, 100 and 200 μM. As the amount of analyte increase the intensity increase until it is stable after 50 μL of analyte with no significant difference using ANOVA test (e.g., at 100 μM (F= 0.89, $F_{critical}$=5,14, P=0.46, α=0.05, n=3, ANOVA test)). However, higher than 50 μL was too much to 1.5 cm diameter PAD and it needed longer time to dry. Therefore 50 μL was chosen as optimum amount of analyte.
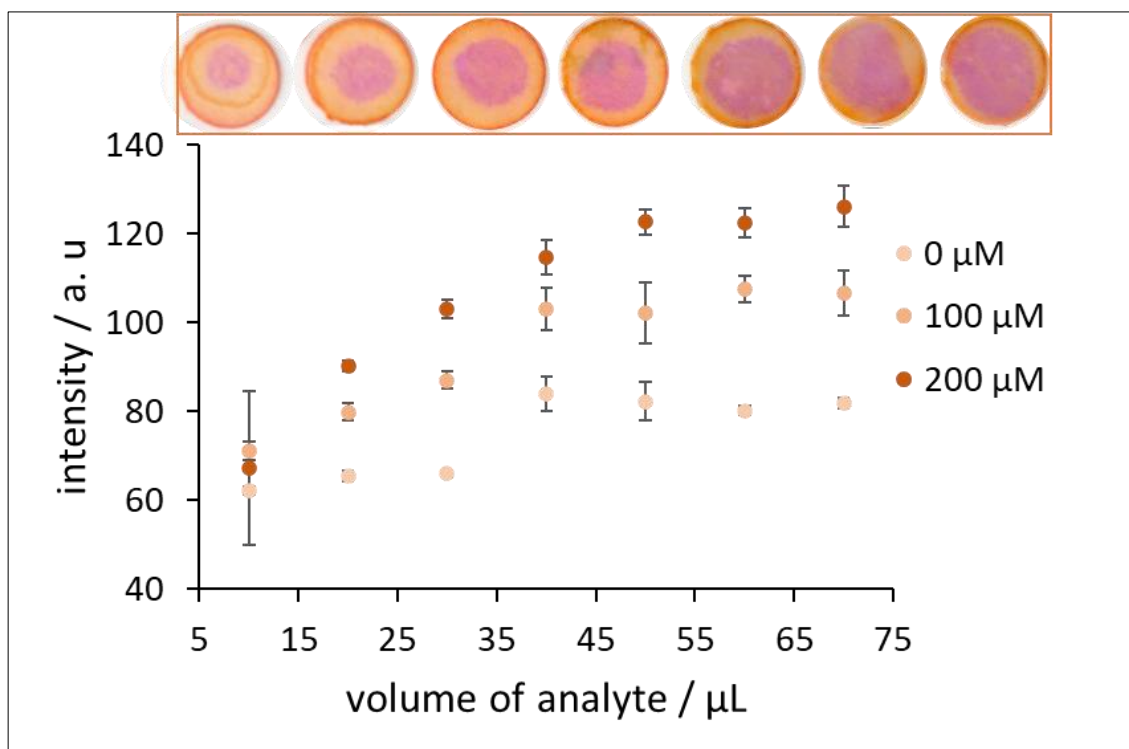
Figure 6.24 Intensity versus the volume of manganese analyte (µL). Three different manganese concentration were studied 0, 100 and 200 µM. PAN (1.3 mM) reagent consisted of 2% surfactant (Trionix-100), carbonate buffer (pH 10) The detection reagent (35µL) was added to the PAD (n=3) first and allowed to dry, the manganese analyte was pipetted into the PAD after 3 min of waiting the PAD was scanned and image was analysed for intensity using image-J software (The intensity was measured by method 1 in **Section 2.5** and **Figure** 6.10). Device 16 was used for the anlysis.

pH

Detection of manganese by PAN reagent is pH sensitive. Therefore, carbonate buffer was used to maintain the pH. The pH of the detection reagent was studied in the range 6-11.[29,30] **Figure** 6.25 shows the intensity versus the pH of carbonate buffer when 0, 100 and 200 µM of manganese analyte were used. At low pH lower than the 7.5 the PAD did show reduction in the intensity only. However, at pH 6.5 and lower the PAD showed very high standard deviation and the signal of 0, 100 and 200 µM are not any more with different intensities. At pH 8 and higher up to around 10.5 the intensity was approximately constant with no significant difference using ANOVA test (e.g., at 100 µM (F= 2.29, $F_{critical}$=3.11, P=0.11, α=0.05, n=3, ANOVA test)) . Therefore, the pH of the detection reagent was kept as 10.

281
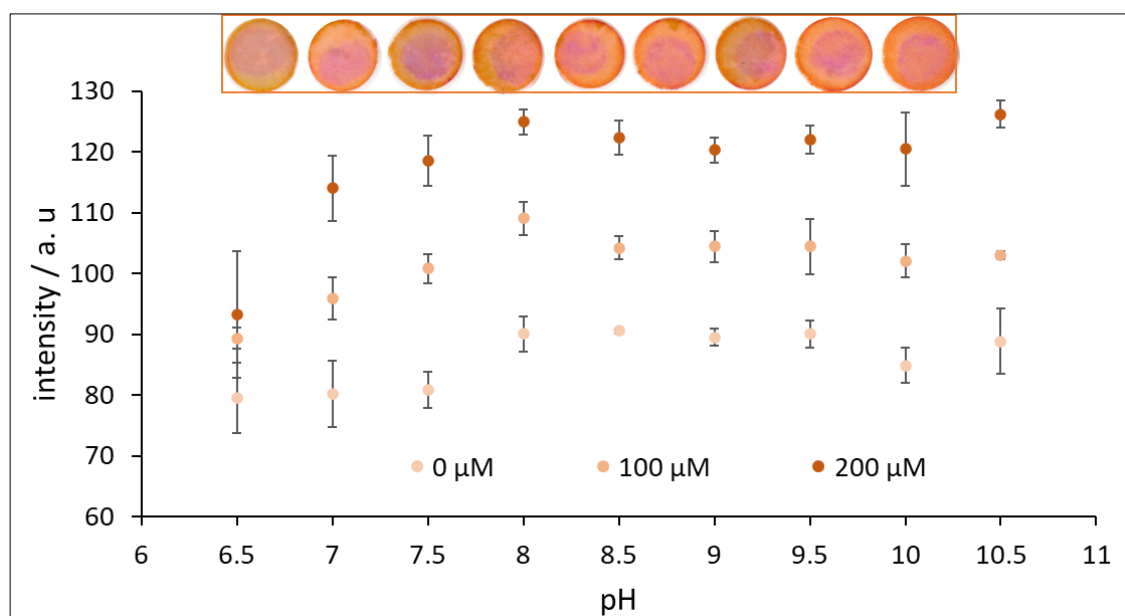
Figure 6.25 Intensity versus pH of carbonate buffer. Three different manganese concentration were studied 0, 100 and 200 µM. PAN (1.3 mM) reagent consisted of 2% surfactant (Trionix-100), carbonate buffer. 35 µL the detection reagent was added to the PAD (n=3) first and allowed to dry, 50 µL manganese analyte was pipetted into the PAD after 3 min of waiting the PAD was scanned and image was analysed for intensity using image-J software (The intensity was measured by method 1 in **Section 2.5** and **Figure** 6.10). Device 16 was used for the anlysis.

Surfactant percent

AS mentioned previously surfactant was used to dissolve the PAN reagent. Surfactant has greasy texture. Therefore, the right percent should be added. Too much surfactant can finally make the detection reagent greasy and increase the hydrophobicity of the PAD. Little of surfactant may not be enough to dissolve the PAN. Therefore, the percent of the surfactant was optimized. **Figure** 6.26 shows intensity versus the percent of the surfactant. As the percent of the surfactant increase the intensity increase and that is expected since enough surfactant dissolve the PAN reagent. At very low surfactant percent lower than 2% the PAN was not dissolved as it is clear from the PAD above in the **Figure** 6.26. At surfactant % higher than 10% the detection reagent became greasy and result in more hydrophobicity in the PAD and consequently the added analyte of manganese hardly penetrates the PAD and dry. 4 to 8 % give high intensity with no significant difference using ANOVA test (e.g., at 100 µM (F= 1.20, $F_{critical}$=5.14, P=0.37, α=0.05, n=3, ANOVA test)) which mean good dissolving of PAN and no greasy texture on paper. Therefore, 4% was chosen as optimum surfactant %.
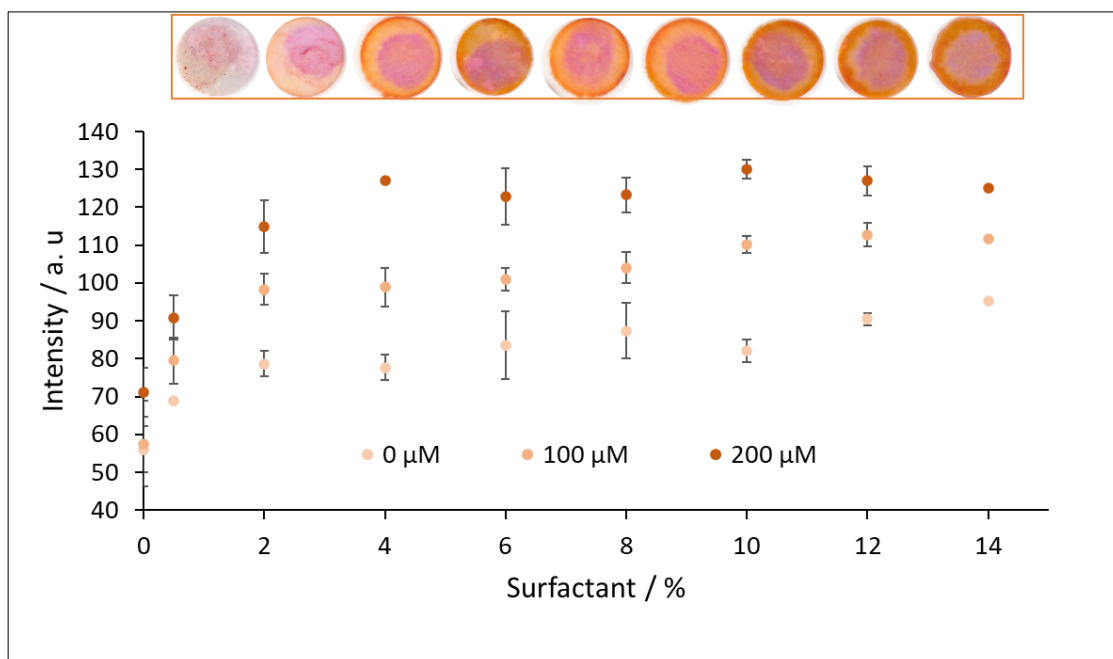
Figure 6.26 Intensity versus surfactant %. Three different manganese concentration were studied 0, 100 and 200 μM. PAN (1.3mM) reagent consisted of surfactant (Trionix-100), carbonate buffer (pH 10). 35 μL the detection reagent was added to the PAD (n=3) first and allowed to dry, 50 μL manganese analyte was pipetted into the PAD after 3 min of waiting the PAD was scanned and image was analysed for intensity using image-J software (The intensity was measured by method 1 in **Section 2.5** and **Figure** 6.10). Device 16 was used for the analysis.

PAN reagent concentration

PAN concentration was optimized in the range 0.3 to 5 mM. **Figure** 6.27 shows intensity versus PAN concentration (mM). PAN is orange in colour, consequently, the more the concentration of the PAN the more the intensity of the colour. At PAN concentration lower than 1 mM, the intensities from 0, 100, 200 mM were similar since there was not enough PAN. At PAN concentration above 4 mM the PAN was too much compared to the dissolving reagent (surfactant), and it was hardly dissolved. Therefore, PAN concentration between 1.3 and 4 mM was chosen as optimum. 3.8 mM was used for the rest of the experiments for consistency.
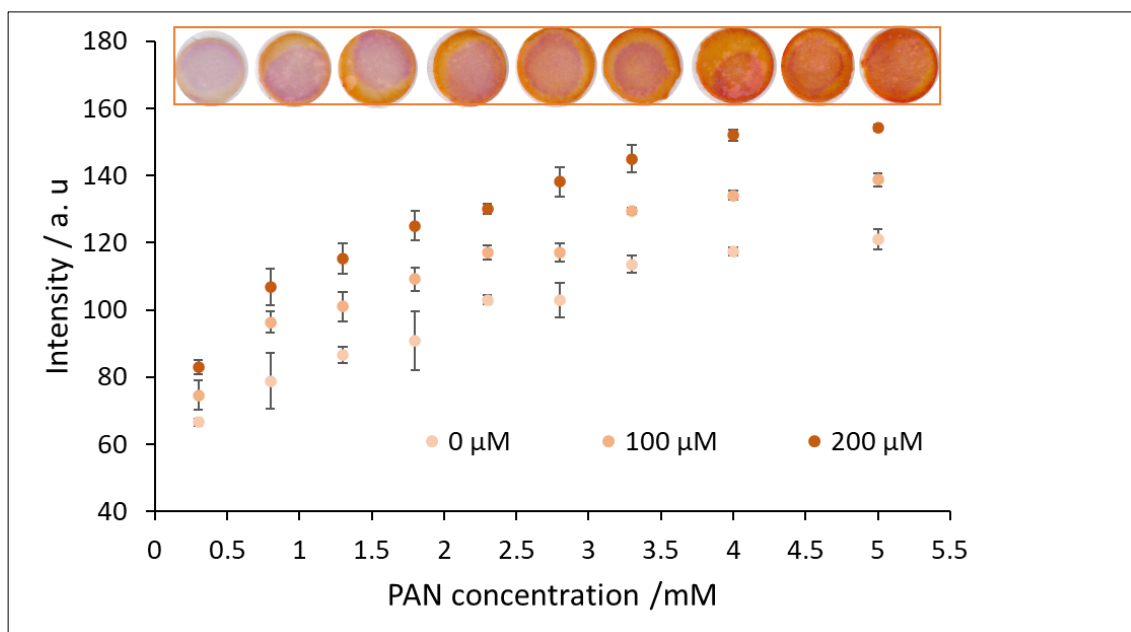
Figure 6.27 Intensity versus PAN concentration (mM). Three different manganese concentration were studied 0, 100 and 200 µM. PAN reagent consisted of 4% surfactant (Trionix-100), carbonate buffer (pH 10). 35 µL the detection reagent was added to the PAD (n=3) first and allowed to dry, 50 µL manganese analyte was pipetted into the PAD after 3 min of waiting the PAD was scanned and image was analysed for intensity using image-J software (The intensity was measured by method 1 in **Section 2.5** and **Figure** 6.10). Device 16 was used for the analysis.

Time of reaction

Time of the reaction was studied to determine at which time the intensity of the colour is stable. **Figure** 6.28 shows the intensity versus the time of the reaction (second) when three different concentrations of manganese analyte were used (0, 100, 200 µM). The intensity was taken each minute for 15 minutes. No more than 15 minutes were studied since short time PAD was required for lay people use. The intensity was maximum at zero reaction time and start to decrease gradually up to 5 minutes. This decrease maybe happened due to release in some of the complexed manganese. The intensity remained almost stable from 5 to 10 min then the intensity starts to decrease again. Previous studies when borate buffer was used the reaction time was specific exactly 1 min, after which the intensity varied [314]. In her with the use of carbonate buffer the intensity was stable for around 5 minutes, from minute 5 to minute 10 with no significant difference using ANOVA test (e.g., at 200 µM (F= 0.32, $F_{critical}$=3.13, P=0.89, α=0.05, n=3, ANOVA test)) . This provides more time for lay people (e.g., farmer) to take the image of the PAD before the change of the intensity. Therefore, 7 minutes was chosen as the optimum reaction time.
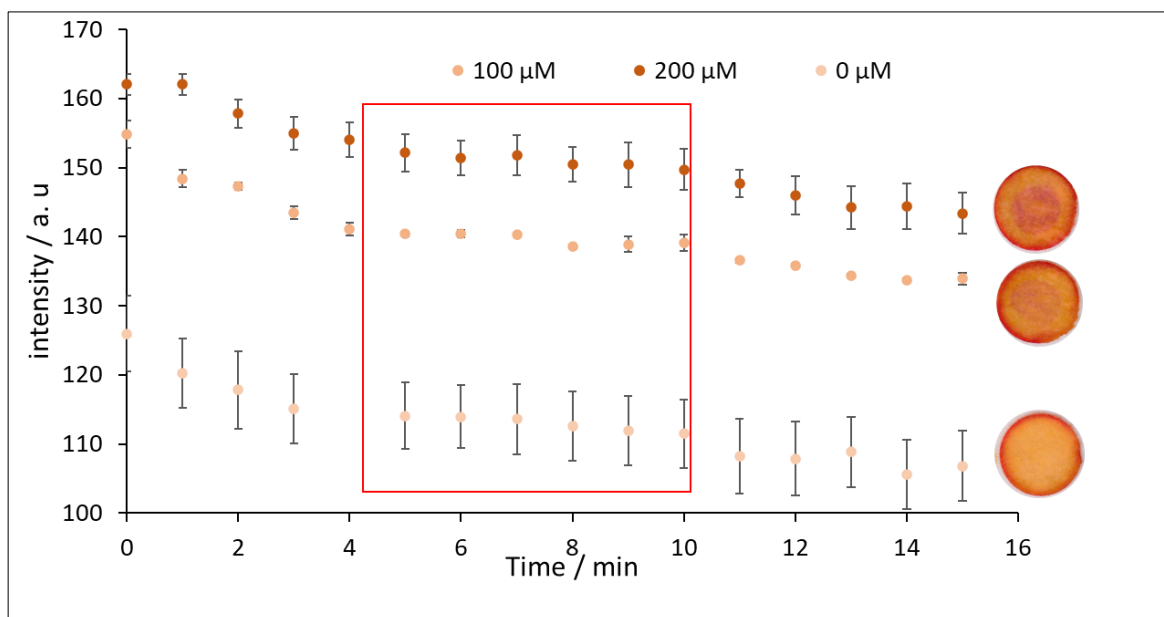
Figure 6.28 Intensity versus reaction time (s). Three different manganese concentrations were studied 0, 100 and 200 μM. PAN (3.8 mM) reagent consisted of 4% surfactant (Trionix-100), carbonate buffer (pH 10). 35 μL the detection reagent was added to the PAD (n=3) first and allowed to dry, 50 μL manganese analyte was pipetted into the PAD. the PAD was scanned each minute for 15 minutes and image was analysed for intensity using image-J software (The intensity was measured by method 1 in **Section 2.5** and **Figure** 6.10). Device 16 was used for the analysis.

Colour accumulation on PAD

Previous studies were using borate buffer to stabilize the pH. Borate buffer was effective buffer[314,315,452]. However, it is toxic and can seriously affect the reproductive system [453]. Therefore, it was replaced with carbonate buffer. The use of carbonate buffer leads to the concentration of the colour in the centre after the addition of analyte. This may happen due to the nature of the PAN reagent in the presence of the carbonate on paper compared to the borate buffer. **Figure** 6.29 shows the PAD when borate and carbonate buffer were used. Borate buffer does not cause that much concentrate of the colour compared to carbonate and that was why most of the people used borate as buffer in literature since it is the most efficient for formation of manganese complex. This PAD is to be released to lay people and hence no toxic chemicals should be used, therefore, carbonate buffer was preferred as long as it gives a stable result which is reproducible and make sense. **Figure** 6.30 shows the intensity from the 4 PADS in **Figure** 6.29. Even though borate buffer showed higher intensities, the difference between 0 and 100μ M was similar when both borate and carbonate were used.

	100 µM manganese	0 µM manganese
Borate buffer pH10		
Carbonate buffer pH 10		

Figure 6.29 Effect of type of buffer on the colour developed on the PAD. Borate (pH 10) and carbonate (pH 10) were compared when 0 and 100 µM manganese analyte were used.
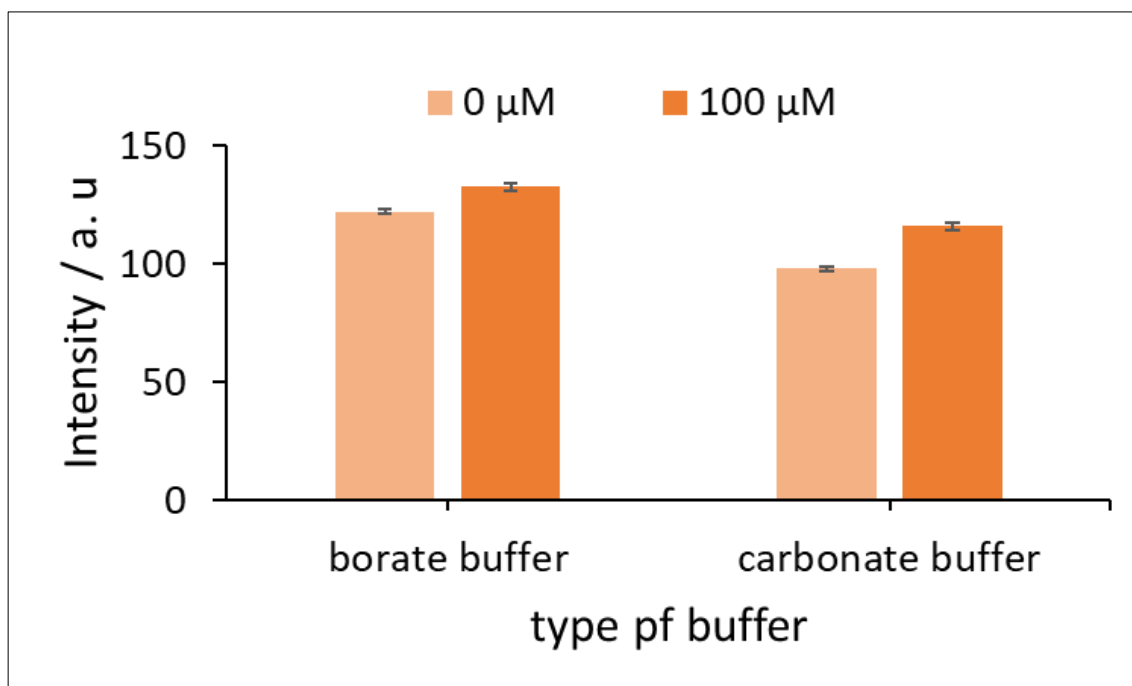
Figure 6.30 Intensity versus the type of buffer. Two buffers were compared borate (pH 10) and carbonate (pH10). The study was performed with 0 and 100 µM of manganese analyte. PAN (3.8 mM) reagent consisted of 4% surfactant (Trionix-100), carbonate buffer (pH 10). 35 µL the detection reagent was added to the PAD (n=3) first and allowed to dry, 50 µL manganese analyte was pipetted into the PAD after 7 min of waiting the PAD was scanned and image was analysed for intensity using image-J software (The intensity was measured by method 1 in **Section 2.5** and **Figure** 6.10). Device 16 was used for the analysis.

6.4.2.1.3   Optimization Method 2

Optimization method 2 was done to double check the close values of the detection reagent components (PAN, surfactant, pH) and especially pH since as in **Figure** 6.25 it was said that after pH 8, the pH start to be constant, however, there was a small rise for pH 8 compared to the higher pH. Therefore, these close values were checked. Three parameters were checked again the pH, PAN concentration and surfactant percentage. This was done by using box Behnken design [352]. box Behnken design is used to address the experiment boundaries, or to avoid the extreme points, or to check the difference between point which are close. In this study it was used to determine the difference between points which are close as it was mentioned previously about the pH. Origin lab was used to design the experiment. Three different variables with three points were chosen as the following: pH (8, 9,10), surfactant % (4, 6,8%) and PAN concentration (2.8, 3.3, 3.8 mM). The lost value was called -1, mid-point is 0 and the highest point is 1. 16 different solutions were prepared (as suggested by the experimental design **Table** 6.3) and deposited in the PAD which was then tested with 100 µM manganese solution as in **Figure** 6.31. 16 PAD intensities were determined and inserted finally in the origin lab for analysis.

Figure 6.32 shows mean of G value (G value here refer to intensity) versus the three points from each optimized parameter. The maximum intensity was at lowest pH (-1=8), however, the

difference was not significant and that what was expected from **Figure** 6.25. The increase in the surfactant % shows also increase in the intensity but this increase was not significant. In contrast, the intensity difference was significant with the increase of the PAN concentration. This was expected since PAN is the reagent which was responsible about the colour.

The effect of each parameter and combination of parameters were determined as in **Figure** 6.33 **A**. The figure shows the effect versus the parameter. Three was the optimum (value (based on ANOVA) which means if the effect above 3, it significantly influences the result. If it is less than 3, then the parameter does not have significant effect on the result. PAN alone shows very significant effect in the result. This means even small variation in the PAN concentration in the detection reagent can influence the result compared to the surfactant % and the pH. This was normal since the PAN was the one responsible about the colour.

Figure 6.33 **B** show the relationship in contour plot which show that at low pH and High PAN concentration the best result was gotten and that what was explained previously by **Figure** 6.32. Finally, the optimum conditions are pH 8, 3.8 mM PAN and 8 % surfactant and are summarized in **Table** 6.5.
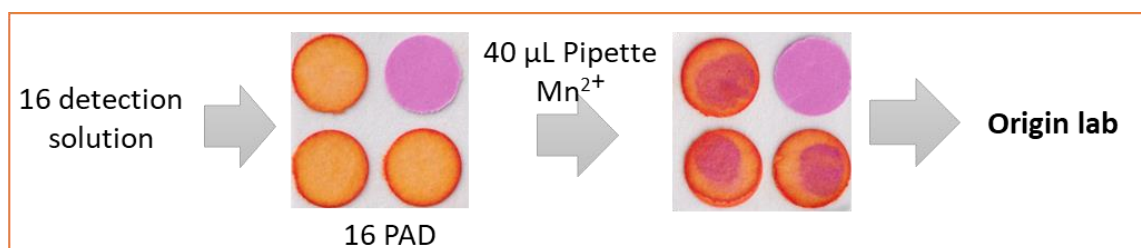
Figure 6.31 PADs treated by origin lab. 16 solution was prepared with different conditions as in Table 6.3. The solutions were then added to 16 PADs and the PADs were used to analyse manganese. The intensity was determined by image-j Software (The intensity was measured by method 1 in **Section 2.5** and **Figure** 6.10). Finally, the data was treated in origin lab. Note the analyte volume was changed from 50 μL to 40 μL to avoid the wrong intensity due to too much the liquid on PAD. Device 16 was used for the analysis, n=3.
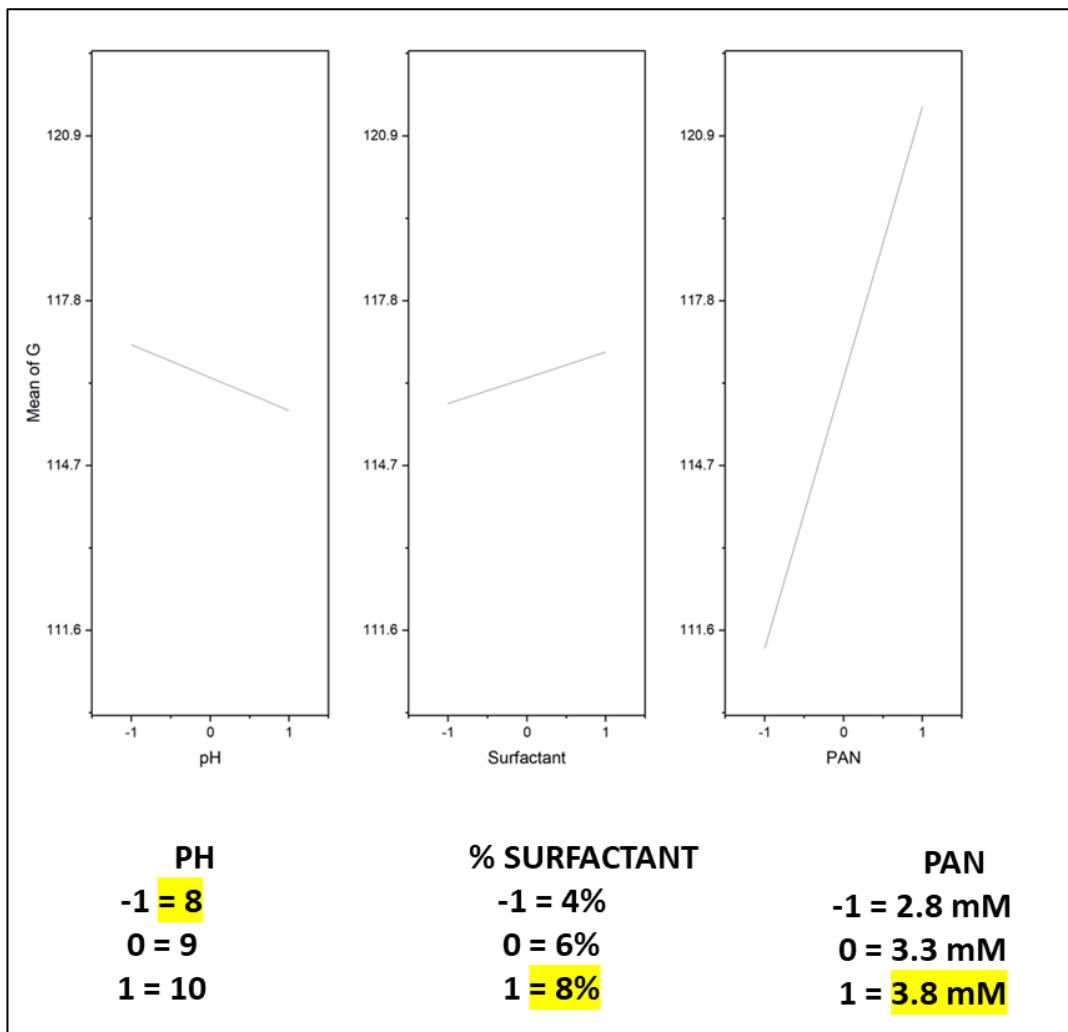
Figure 6.32 Result from origin lab. Mean of G (G is the intensity) versus the three points from each optimized parameter (pH, surfactant % and PAN concentration. -1 is lowest, 0 is mid and 1 is highest point. For pH (-1=8, 0=9, 1=10), for surfactant (-1=4%, 0=6% and 1=8%), for PAN (-1=2.8 mM, 0=3.3 mM, 1=3.8 mM). Device 16 was used for the analysis, n=3.
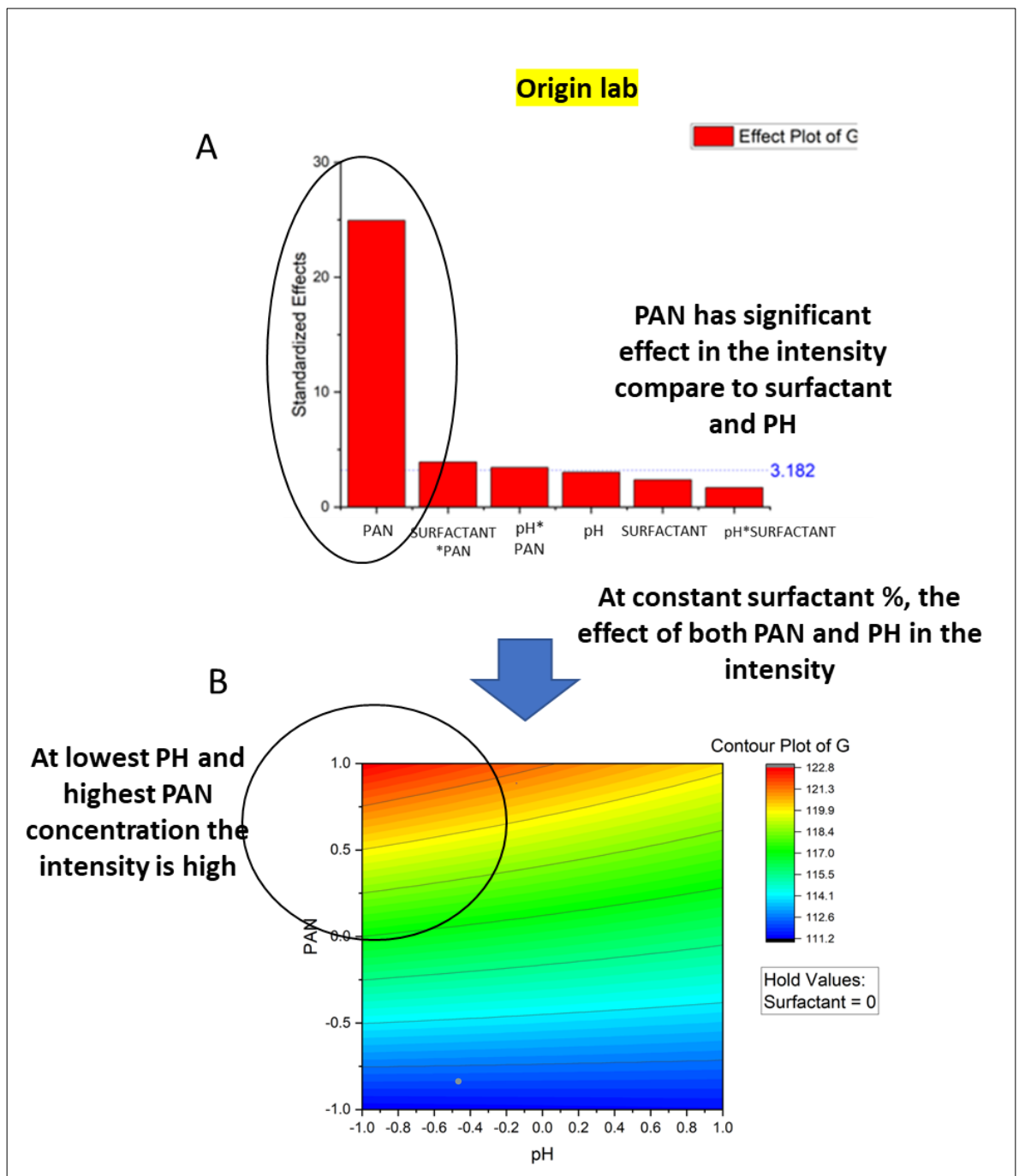
Figure 6.33 Result from origin lab. A. standardized effect versus the parameter optimized. B. contour plot of PAN concentration versus pH of the detection reagent. The optimized parameter is pH, surfactant % and PAN concentration. -1 is lowest, 0 is mid and 1 is highest point. For pH (-1=8, 0=9, 1=10), for surfactant (-1=4%, 0=6% and 1=8%), for PAN (-1=2.8 mM, 0=3.3 mM, 1=3.8 mM). Device 16 was used for the analysis, n=3.

Table 6.5 Optimum condition for manganese detection. Amount of detection reagent Amount of analyte, pH of carbonate buffer, PAN concentration, Surfactant % and Detection time were optimized.

Optimized parameter	Optimum condition
Amount of detection reagent	35 µL
Amount of analyte	40 µL
pH of carbonate buffer	8
PAN concentration	3.8 mM
Surfactant %	8%
Detection time	7 minutes

Calibration and Reproducibility

Using the optimum condition in **Table** 6.5 the calibration line for manganese was determined as in **Figure** 6.34 which shows the intensity versus the concentration of manganese (μM). As the concentration increased the intensity of the colour increased until the increase become constant After 200 μM of manganese. The linear range was from 0 to 200 μM. The reproducibility of the line in the same day was determined as in **Figure** 6.35 which shows the intensity of the colour from PAD versus the concentration of manganese (μM). The slopes were 0.1695, 0.163 and 0.159 which indicate the similar steepness of the three lines. In addition, the average LoD was 14.90±1.41 μM (0.82 mg L^{-1}). **Table** 6.6 shows summary of LoD, slope, R^2 for the three lines in μM. ANOVA test was used to compare the three lines. Each 3 points for specific concentration was compared using ANOVA (e.g., at 100 μM (F= 0.65, F$_{critical}$=5.14, P=0.56, α=0.05, n=3, ANOVA test)) and they showed no significant difference with one another within the standard deviation. Consequently, this indicates the reproducibility of the method in the same day.

The calibration line was then determined in different days ad in **Figure** 6.36. The two lines agree in slope, LoD and slope and hence the method is reproducible in different days. However, the intercept of lines was different. This maybe happen due to the variation in the detection reagent colour itself when it was prepared since the preparation of the detection solution require heating. The heating quality might be different from day to day and hence the prepared solution was affected in term of its initial colour. This can be solved by running the calibration line each time new solution is made. This means that each patch of PAD made should be made with its own calibration line.
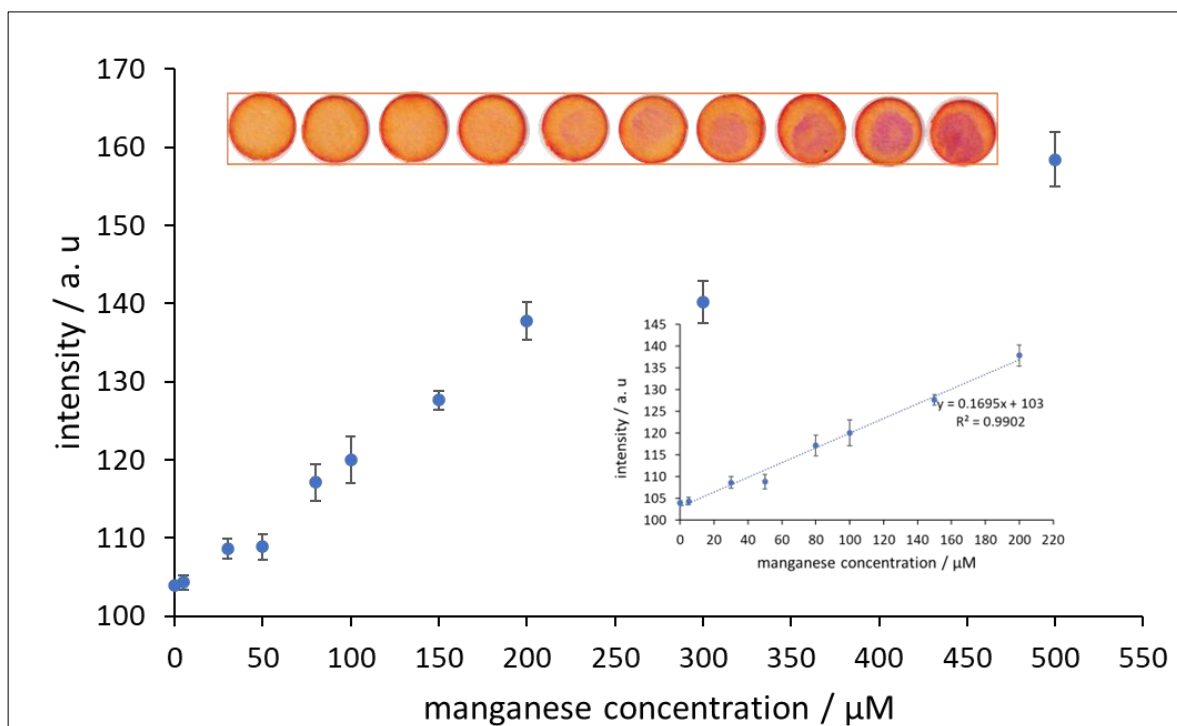
Figure 6.34 Intensity versus the concentration of manganese μM. PAN (3.8 mM) reagent consisted of 8% surfactant (Trionix-100), carbonate buffer (PH 8). 35 μL the detection reagent was added to the PAD (n=3) first and allowed to dry, 40 μL manganese analyte was pipetted into the PAD after 7min of waiting the PAD was scanned and image was analysed for intensity using image-J software (The intensity was measured by method 1 in **Section 2.5** and **Figure** 6.10). Device 16 was used for the analysis.
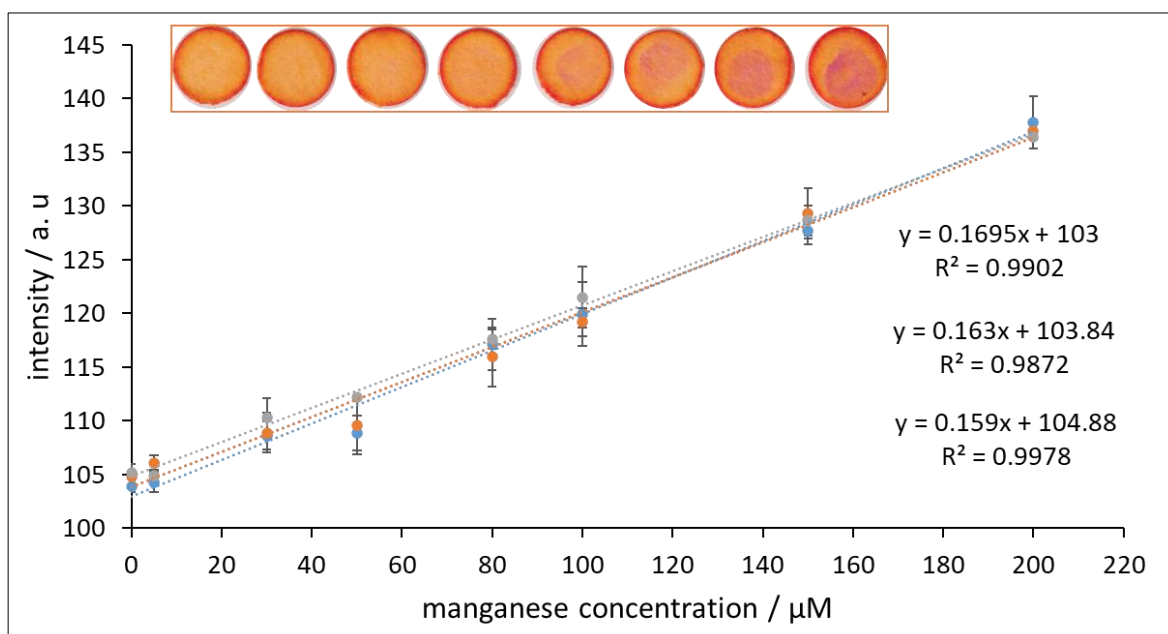
Figure 6.35 Intensity versus the concentration of manganese μM. PAN (3.8 mM) reagent consisted of 8% surfactant (Trionix-100), carbonate buffer (PH 8). 35 μL the detection reagent was added to the PAD (n=3) first and allowed to dry, 40 μL manganese analyte was pipetted into the PAD after 7min of waiting the PAD was scanned and image was analysed for intensity using image-J software (The intensity was measured by method 1 in **Section 2.5** and Figure 6.10). Lines are in the same day. Device 16 was used for the analysis.
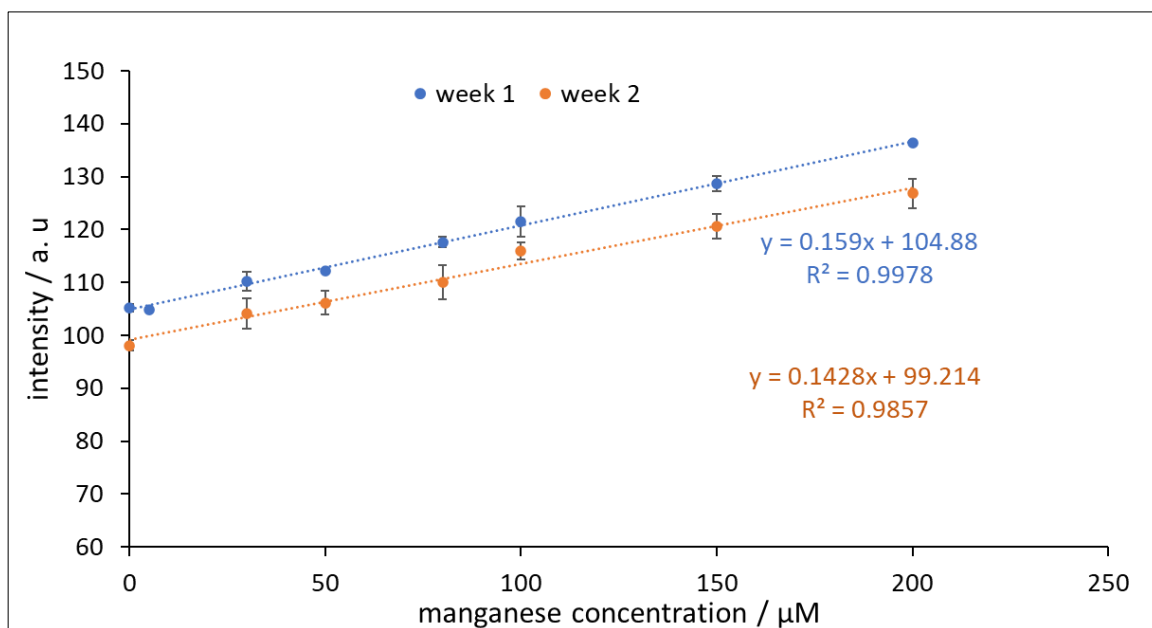
Figure 6.36 Intensity versus the concentration of manganese µM. PAN (3.8 mM) reagent consisted of 8% surfactant (Trionix-100), carbonate buffer (PH 8). 35 µL the detection reagent was added to the PAD (n=3) first and allowed to dry, 40 µL manganese analyte was pipetted into the PAD after 7min of waiting the PAD was scanned and image was analysed for intensity using image-J software (The intensity was measured by method 1 in **Section 2.5** and **Figure** 6.10). Lines are in different days. Device 16 was used for the analysis.

Table 6.6 LoD (µM), R^2 and slope of the three lines in **Figure** 6.35. LoD was calculated as in **Equations 2.5 and 2.6**.

	lne1	line 2	line 3	Average	RSD
LOD / µM	14.61	13.66	16.43	14.90±1.41	9.43
R^2	0.9902	0.9872	0.9978	0.9917±0.0055	0.55
Slope/ µM^{-1}	0.1695	0.1630	0.159	0.1638±0.0053	3.23

6.4.2.2 Barrier-free PAD

Due to the accumulation of the colour in the centre when the analyte was added (as mentioned in **Figure** 6.29), the idea of the barrier fee PAD (device 18) came, so when the analyte was added the developed colour focused on the centre and it was not leaking into the rest of the paper. Barrier-free PAD was developed. A PAD was produced from Whatman 1 paper squares (5 cm x 5 cm) attached onto adhesive tape. To detect manganese, amount of PAN in carbonate buffer (Triton X-100) was added into three locations across this piece of paper and allowed to air dry for 30 min. For analysis, a specific amount of manganese solution (0 – 500 µM) was pipetted on top of the PAN zone and incubated at room temperature to allow colour development. The PAD image was then captured by a scanner and colour intensity was determined using ImageJ software. **Figure** 6.9 describes barrier-free PAD work.

6.4.2.2.1 Optimization

Time of reaction

The time of the reaction was determined as in **Figure** 6.37 which shows the intensity versus the time of the reaction. The intensity was taken each minute up to 15 minutes. The intensity starts high and then decreases until 5 minutes then it stays stable for up to 10 minutes with no significant difference using the ANOVA test (e.g., at 100 µM (F0.029, $F_{critical}$=3.11, P=0.99, α=0.05, n=3, ANOVA test)) and then the intensity starts to decrease again.
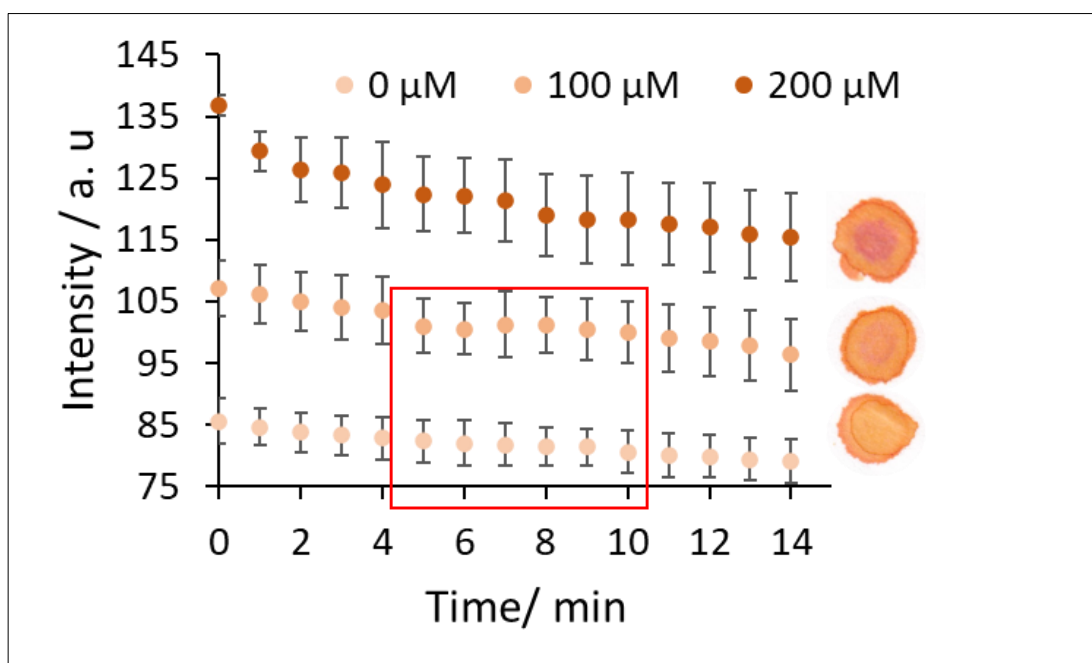
Figure 6.37 Intensity versus reaction time (min). 0, 100 and 200 µM of manganese were used. PAN (3.8 mM) reagent consisted of 8% surfactant (Trionix-100), and carbonate buffer (pH 8). 11 µL the detection reagent was added to the PAD (n=3) first and allowed to dry, 11 µL manganese analyte was pipetted into the PAD after each minute for 15 minutes the PAD was scanned, and image was analysed for intensity using image-J software. Device 18 was used for the analysis.

Volume of the detection reagent and analyte

The volume of the detection reagent and analyte were optimized since this PAD is barrier free and the amount of the detection reagent and analyte is critical to avoid the leakage of solution outside the detection range. The volume was optimized by taking the area (using Image-J) around the detection reagent before and after the addition of the analyte as in **Figure** 6.38. **Figure** 6.39 shows the area versus the volume of detection reagent added. The area was taken before and after the reaction and it was compared. When 11 µL of the detection reagent and 10 µL of analyte were added the area remain the same before and after the reaction. And hence the 11 µL of the detection reagent and 10 µL of analyte were chosen as optimum.
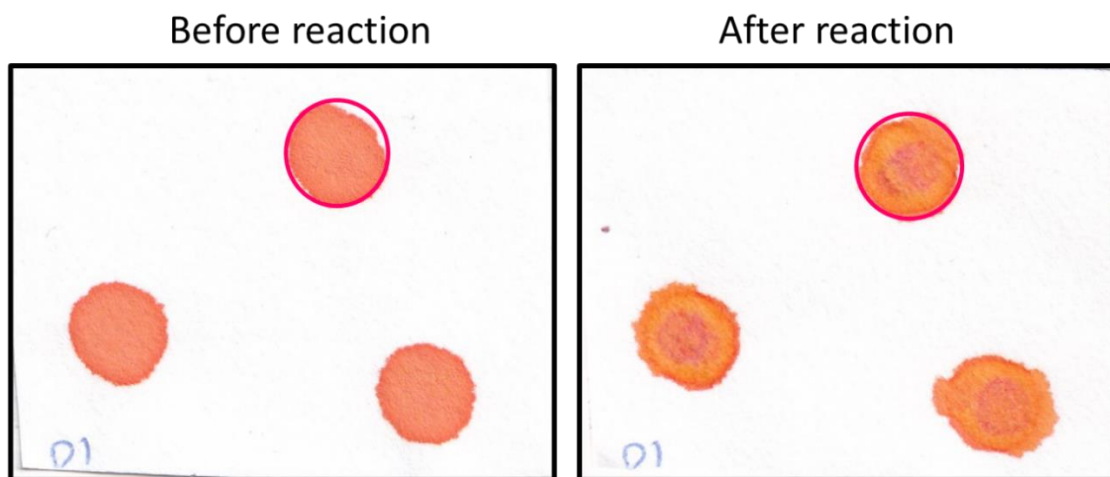
Figure 6.38 Area around the detection reagent before and after the reaction. The area was taken by image-J.
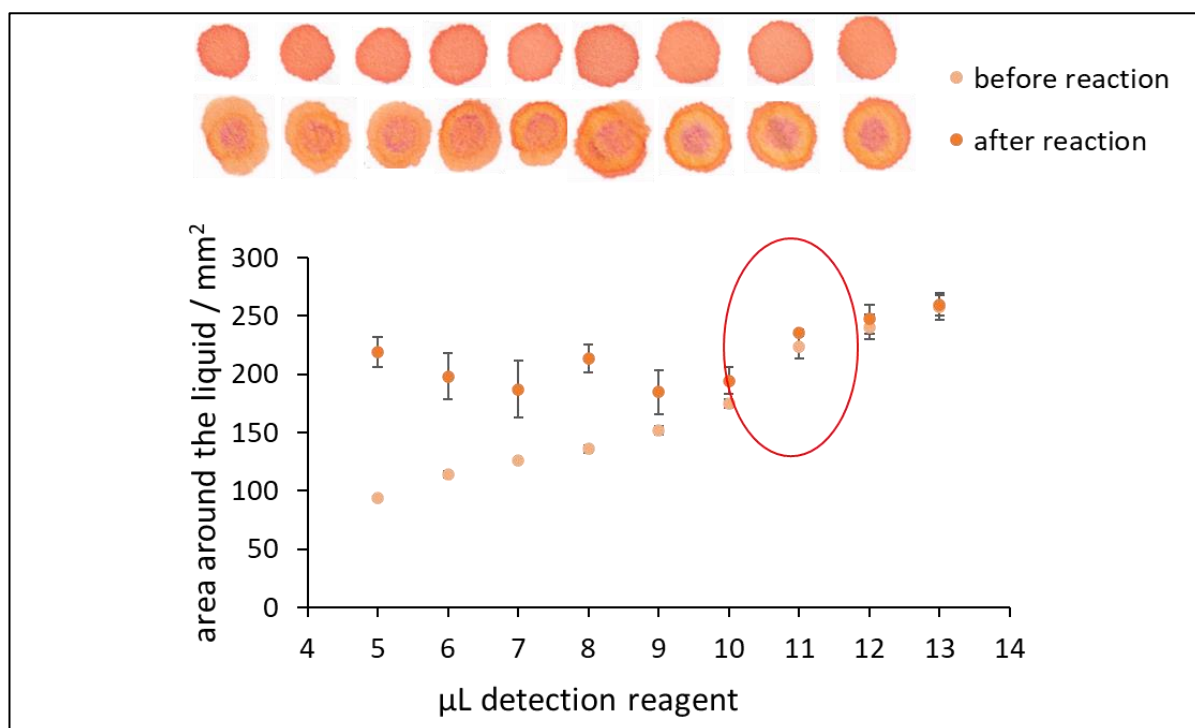
Figure 6.39 Area around the solution (mm^2) versus the volume of the detection reagent (µL). PAN (3.8 mM) reagent consisted of 8% surfactant (Trionix-100), carbonate buffer (PH 8). The detection reagent was added to the PAD (n=3) first and allowed to dry, 11 µL manganese analyte was pipetted into the PAD after 7min of waiting the PAD was scanned and image area was determined using image-J software. Device 18 was used for the analysis.

6.4.2.2.2 Calibration and reproducibility of barrier-free PAD

The calibration line for barrier-free PAD was determined in **Figure** 6.40 which shows the intensity versus the manganese concentration (µM). As the concentration increased the colour intensity increased. The linearity was up to 150 µM of manganese.

The reproducibility of the line in the same day was determined as in **Figure** 6.41 which shows the intensity of the colour from PAD versus the concentration of manganese (µM). The slopes were 0.235, 0.2431 and 0.2536 which indicate the similar steepness of the three lines. In addition, the average LoD was 10.79±1.12µM (0.59 mg L^{-1}). **Table** 6.7 shows summary of LoD, slope and R^2 for the three lines in µM. ANOVA test was used to compare the three lines. Each 3 points for specific concentration was compared using ANOVA (e.g., at 100 µM (F= 0.85, F$_{ritical}$=5.14, P=0.47, α=0.05, n=3, ANOVA test)) and they showed agreement with one another within the standard deviation except for two points. This happened maybe due to the non-uniformity of measuring the intensity since the distribution of the colour in the PAD was not uniform each time experiment was run. Therefore, it can be said the data from the barrier free PAD was more semi-quantitative rather than quantitative since it can measure the approximate result. Sealing of barrier free PAD is tested in the coming section. Sealing of the PAD decides if it can be used in the field or for lab use only.
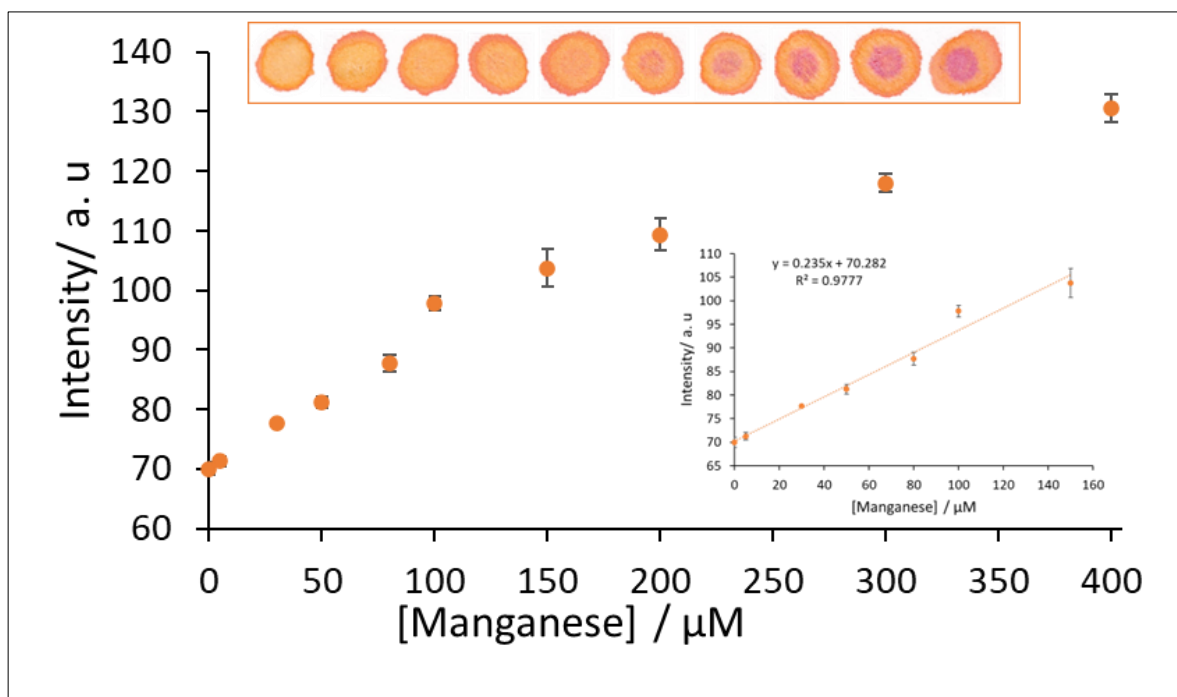
Figure 6.40 Intensity versus manganese concentration (µM). PAN (3.8 mM) reagent consisted of 8% surfactant (Trionix-100), carbonate buffer (pH 8). 11 µL the detection reagent was added to the PAD (n=3) first and allowed to dry, 11 µL manganese analyte was pipetted into the PAD after 7min of waiting the PAD was scanned and image was analysed for intensity using image-J software (The intensity was measured by method 1 in **Section 2.5** and **Figure** 6.11). Device 18 was used for the analysis.

Figure 6.41 Intensity versus manganese concentration (µM). PAN (3.8 mM) reagent consisted of 8% surfactant (Trionix-100), carbonate buffer (pH 8). 11 µL the detection reagent was added to the PAD (n=3) first and allowed to dry, 11 µL manganese analyte was pipetted into the PAD after 7min of waiting the PAD was scanned and image was analysed for intensity using image-J software (The intensity was measured by method 1 in **Section 2.5** and **Figure** 6.11). Device 18 was used for the analysis.

Table 6.7 LoD, R^2 and slope of the three lines in **Figure** 6.41. LoD was calculated as in **Equation 2.5 and 2.6**.

	line 1	line 2	line 3	Average	RSD
LoD / µM	11.91	9.67	10.78	10.79±1.12	10.39
R2	0.9777	0.9826	0.9807	0.9803±0.0024	0.25
Slope/ µM^{-1}	0.235	0.2431	0.2536	0.24±0.0093	3.82

6.4.2.3   Sealling of PAD

Sealing of barrier-free PAD

Sealing of the PAD is needed since finally it should be released for lay people use like farmer and hence it should be stored. Barrier free PAD was sealed by several methods as in **Figure** 6.42 which shows lamination of the PAD. There were two ways to introduce the sample with lamination either by making line cut or circular cut (in laminating sheet). The line cut does not work and leads to the deformation of the developed colour. The circular cut is more effective and does not cause deformation of the colour. For the circular cut the sample can be added by pipetting and dipping. The sample was added initially by pipetting the sample as in **Figure** 6.43. The intensity was taken from front (with circular holes) and the back side of the device. The back side (**Figure** 6.43**A**) showed high standard deviation compared to the front side (**Figure** 6.43 **B**). Therefore, the front side was used to take the intensity.

Barrier free PAD: sealing with lamination
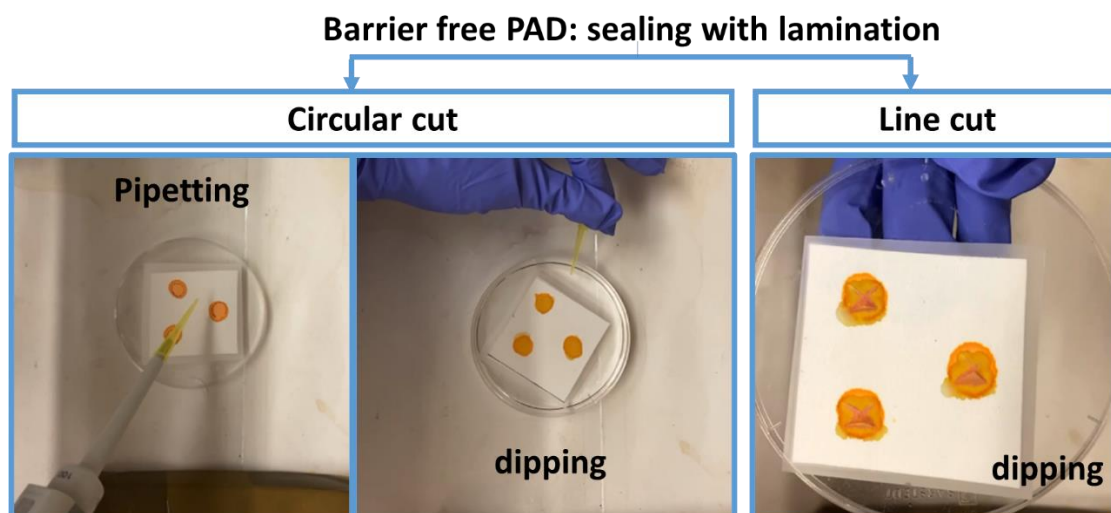
Figure 6.42 Barrier free PAD sealing with circular cut and line cut (in laminating sheet). The introduction of the sample by pipetting and dipping.
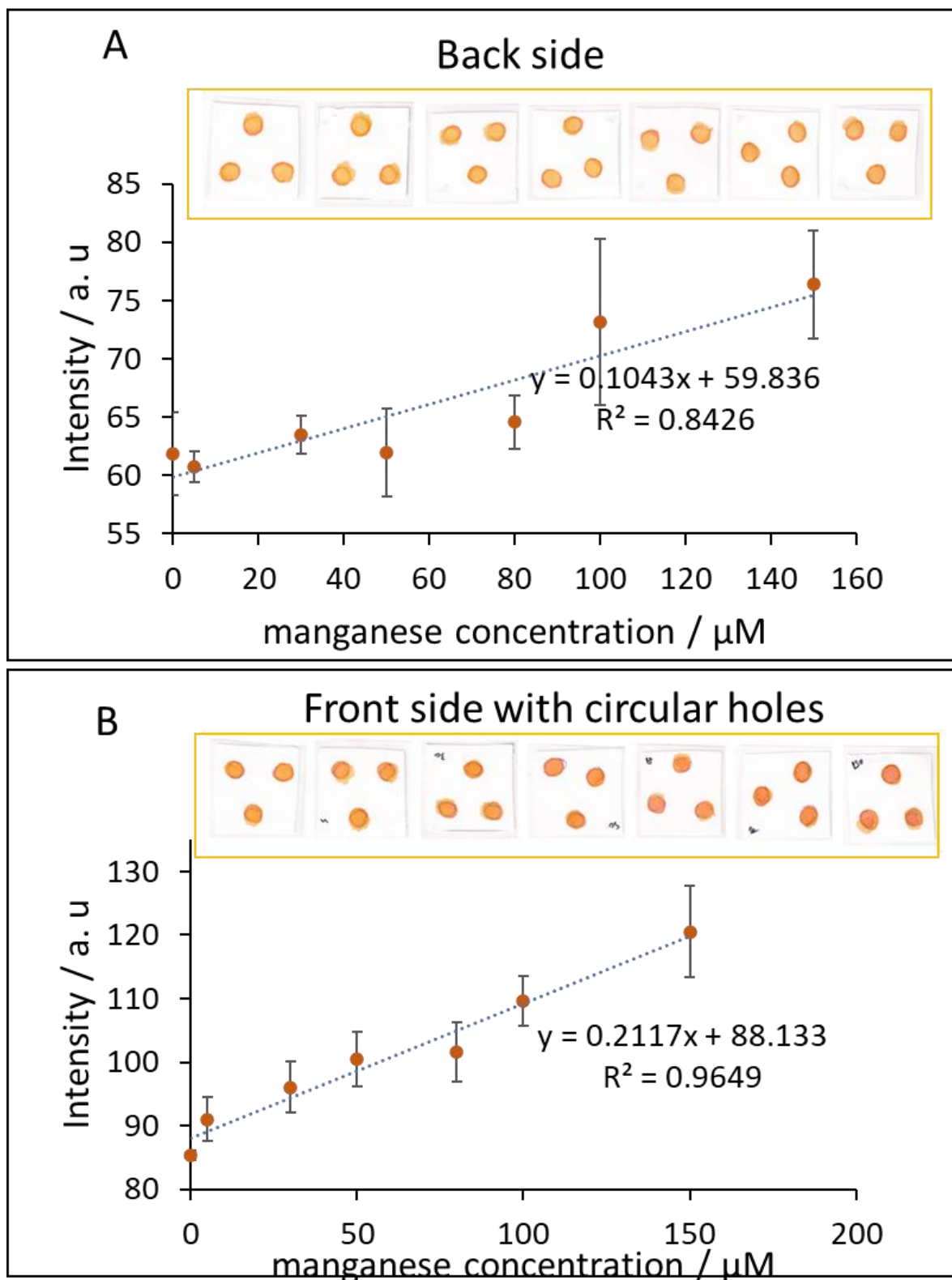
Figure 6.43 Intensity versus manganese concentration (µM). PAN (3.8 mM) reagent consisted of 8% surfactant (Trionix-100), carbonate buffer (pH 8). 11 µL the detection reagent was added to the PAD (n=3) first and allowed to dry, 11 µL manganese analyte was pipetted into the PAD after 7min of waiting the PAD was scanned and image was analysed for intensity using image-J software (The intensity was measured by method 1 in **Section 2.5** and **Figure** 6.11). (A)intensity from back side of PAD (B) intensity from the frontside of the PAD.

Dipping sample introduction was tested too since dipping is much easier way to introduce the sample by farmer compared to pipetting. The PAD was dipped for specific time into the solution as in **Figure** 6.44 **A** which shows intensity versus the time of dipping in second. 10 second was enough time of dipping to get clear intensity. Higher time may lead to destroy the PAD and increase in the standard deviation. **Figure** 6.44 **B** shows the intensity versus the concentration of manganese when the PAD was dipped for 10 second and the intensity was taken from the front side of the PAD. R^2 is low and the result still suffer from standard deviation. It is not easy to seal and dip the barrier free PAD due to the non-existence of the barrier. However, the PAD works well when the sample is pipetted, and the device was not laminated hance the barrier free PAD can be used for lab used not for in field use.
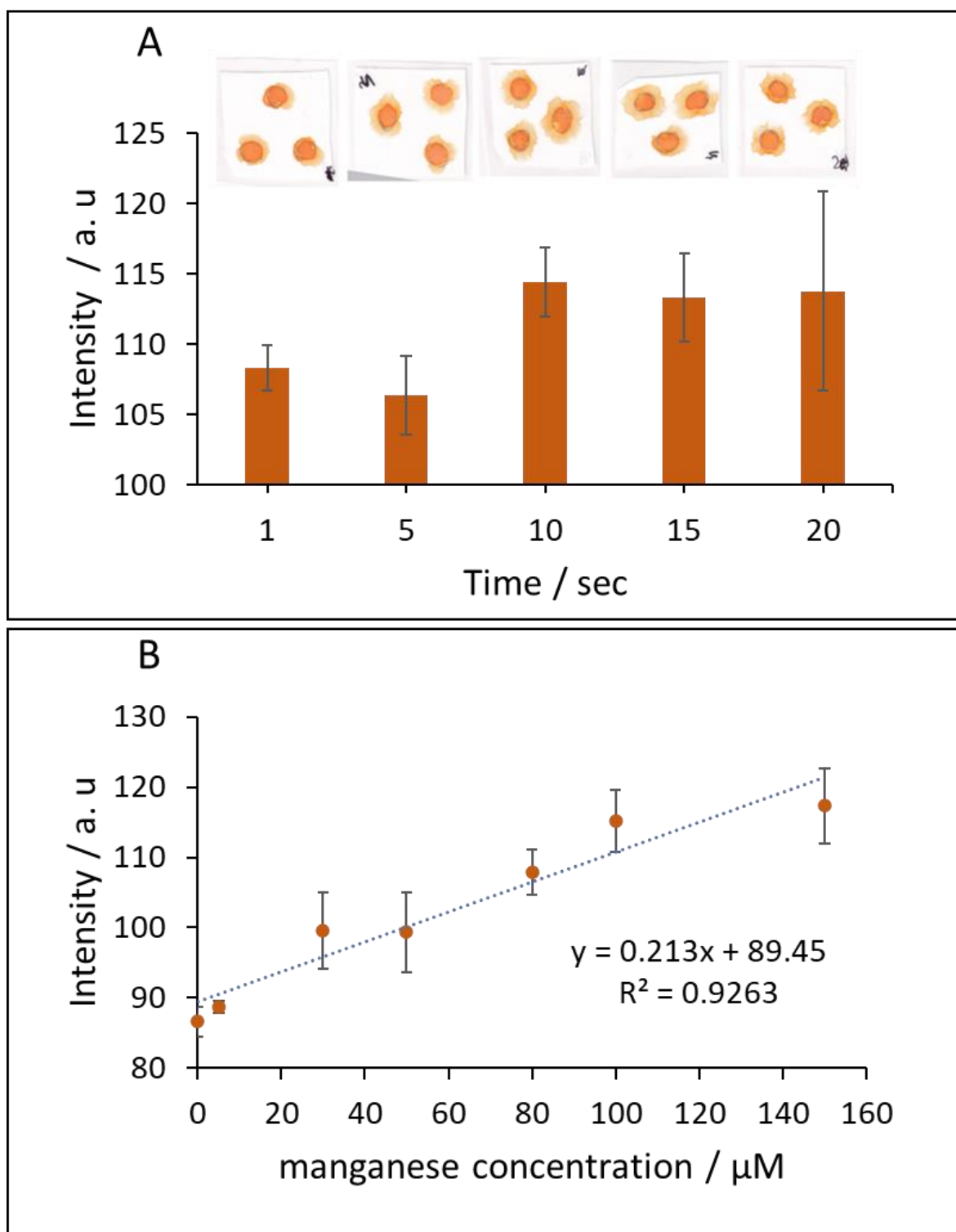
Figure 6.44 (A) Intensity versus time (s), 100 M of manganese was used. (B) intensity versus manganese concentration (µM). PAN (3.8 mM) reagent consisted of 8% surfactant (Trionix-100), and carbonate buffer (pH 8). 11 µL the detection reagent was added to the PAD (n=3) first and allowed to dry, the sample was introduced to PAD by dipping the PAD for 10second and remove it, after 7min of waiting the PAD was scanned and image was analysed for intensity using image-J software (The intensity was measured by method 1 in **Section 2.5** and **Figure** 6.11).

Sealing Circular PAD

Circular PAD was also sealed for storing purpose and to be easily released into field. The sealing was done by two ways, lamination with laminating sheet and sealing with acrylic cover (**Figure** 6.45). When acrylic sheet was used to seal the PAD three circular holes (1 cm) were made in circular acrylic sheet for sample entry. **Figure** 6.46 shows the intensity versus manganese concentration when acrylic was used for the PAD sealing. The intensity of the PAD after reaction was determined from back and front side. The back side showed high standard deviation in the result (**Figure** 6.46 **A**), The front side intensity showed a good result (**Figure** 6.46 **B**). All of these experiment with acrylic cover were done when the sample was introduced by pipetting. When the acrylic sheet was dipped, the solution did not enter the holes due to the thickness of the sheet. In conclusion the acrylic layer can be used but only when the sample is pipetted.
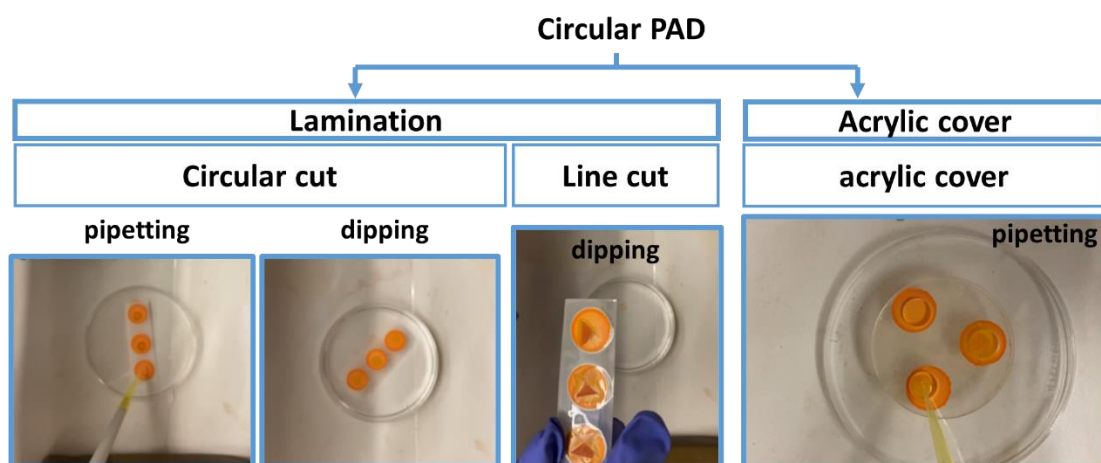
Figure 6.45 PAD sealing by acrylic sheet and lamination (circular cut and line cut). The introduction of the sample by pipetting and dipping.
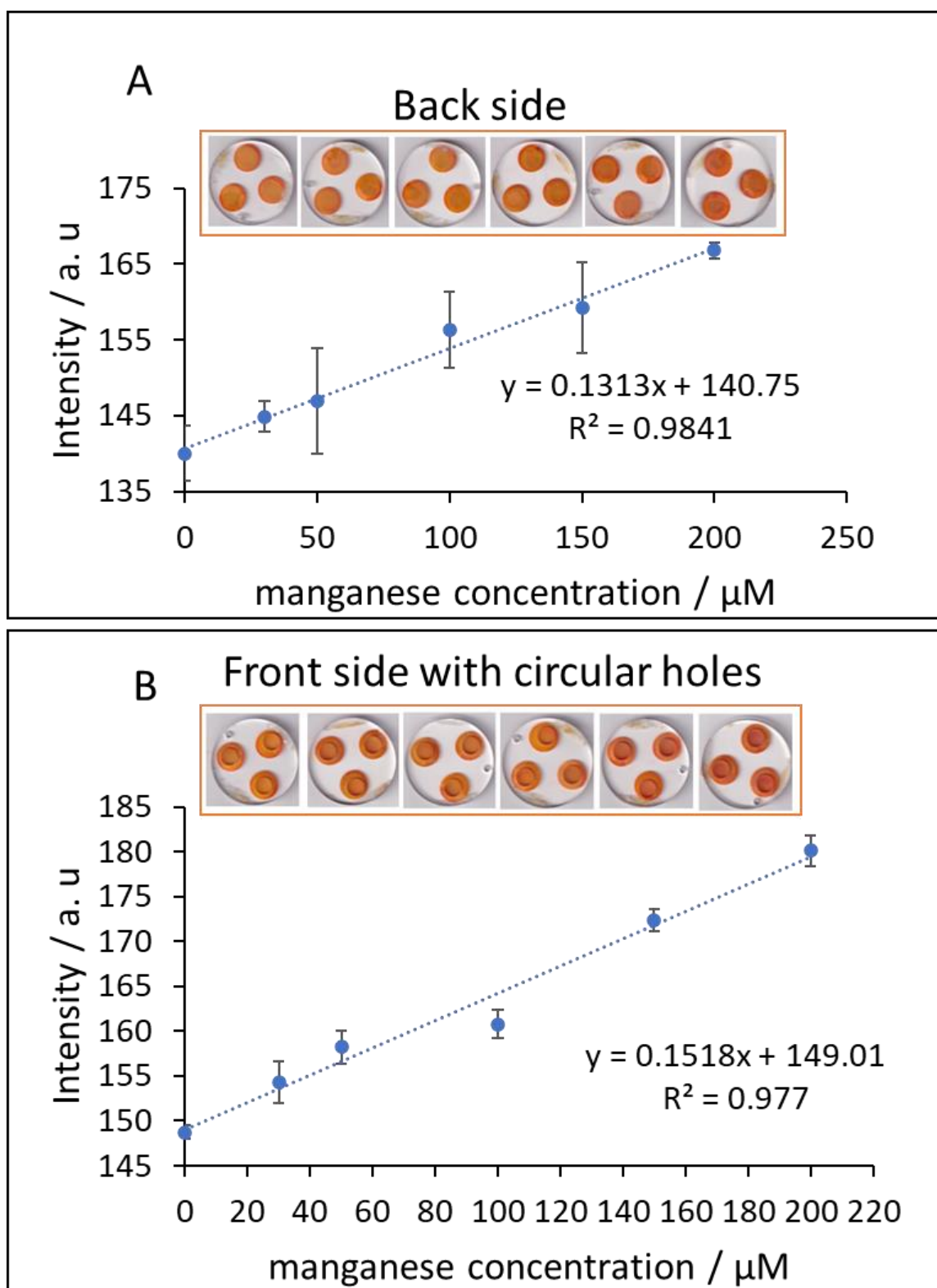
Figure 6.46 Intensity versus manganese concentration (µM). PAN (3.8 mM) reagent consisted of 8% surfactant (Trionix-100), carbonate buffer (pH 8). 35 µL the detection reagent was added to the PAD (n=3) first and allowed to dry, 40 µL manganese analyte was pipetted into the PAD after 7min of waiting the PAD was scanned and image was analysed for intensity using image-J software (The intensity was measured by method 1 in **Section 2.5**). (A)intensity from back side of PAD (B) intensity from the frontside of the PAD.

Lamination was the second method to seal the PAD. Making line cut for sample entrance was not practical since it causes disruption of the developed colour. Circular hole (by scalpel) in the laminating sheet showed promising result, however, only when the size of the hole was changed from small diameter to big diameter as in **Figure** 6.47**.** The smaller sample entrance does not allow the entrance of the solution to the rest of the PAD; therefore, bigger size diameter sample entrance (13 mm) was made. After making the sample entrance bigger the PAD was dipped into the manganese solution as in **Figure** 6.48 **A** which shows the intensity versus the time of dipping from 1 to 7 seconds. Dipping for long time leaded to the leakage of the coloured complex. 2 seconds of dipping gave good results with the highest intensity.

The calibration line was determined by dipping the PAD into the manganese solution as in **Figure** 6.48 **B**. The result was promising and still suffers from a high standard deviation.
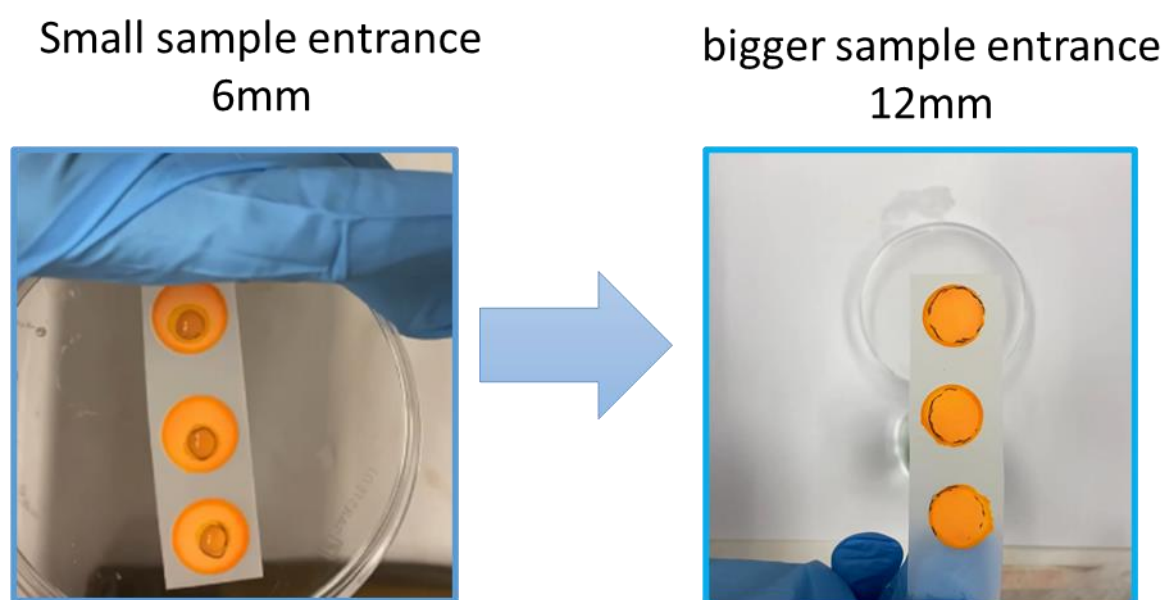
Figure 6.47 Sample entrance in the PAD as circular cut, 6 mm small cut made by punch and big cut made by scalpel around 13 mm.
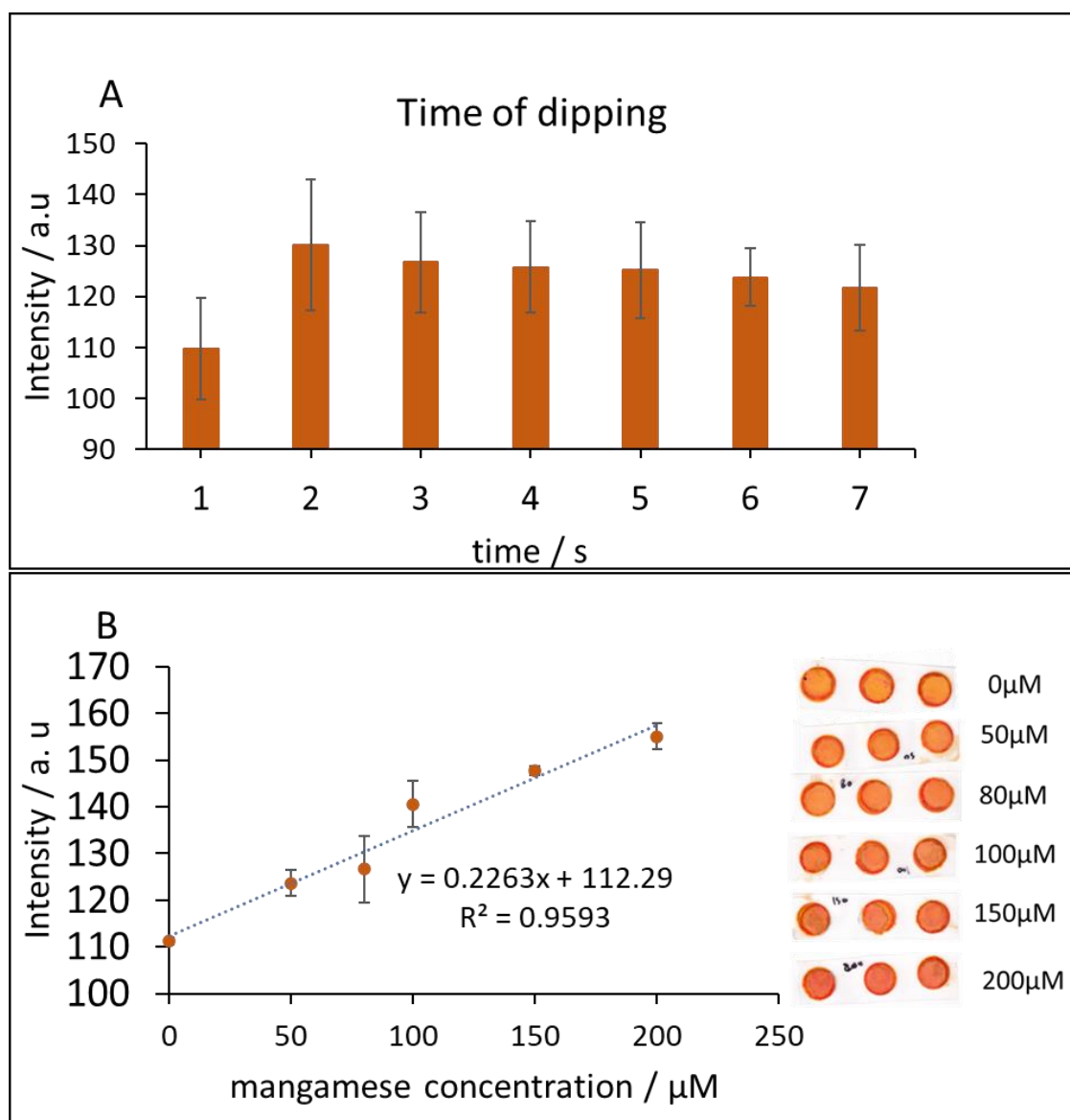
Figure 6.48 (A) Intensity versus the time of dipping (s). (B) intensity versus manganese concentration (µM). PAN (3.8 mM) reagent consisted of 8% surfactant (Trionix-100), and carbonate buffer (PH 8). 35 µL the detection reagent was added to the PAD (n=3) first and allowed to dry, the PAD was laminated with a lamination sheet with a circular sample entrance, PAD was dipped in manganese, after 7min of waiting the PAD was scanned and the image was analysed for intensity using image-J software (The intensity was measured by method 1 in **Section 2.5** and **Figure** 6.10).

Improving the cut of sample entrance and number of layers in PAD

To reduce the standard deviation in the result **Figure** 6.48 **B**, the sample entrance was made by the Cricut machine (**Figure** 6.49) instead of the scalpel since with the scalpel it was difficult to make a well-defined circular sample entrance. **Figure** 6.49 shows the instrument (Cricut explore 3) and the dimension of the uniform cuts made in the laminating sheet.

In addition, two empty layers were added to the PAD as in **Figure** 6.8. These layers aim to make the PAD suitable for soil sample analysis. Soil samples contain slurry that can interfere with the intensity determination in the detection layer. **Figure** 6.50 shows blank PAD when it

was dipped into soil extract (when one layer of PAD was used) and soil extract (when three layers of PAD were used). Intensity from one layer of PAD dipped into soil extract showed intensity higher than when three layers existed. Consequently, soil organic matter can affect the intensity if no layers exist to filter the slurry. The intensity decreased by around 40% (42.91±1.93 %) when the number of empty layers increased.
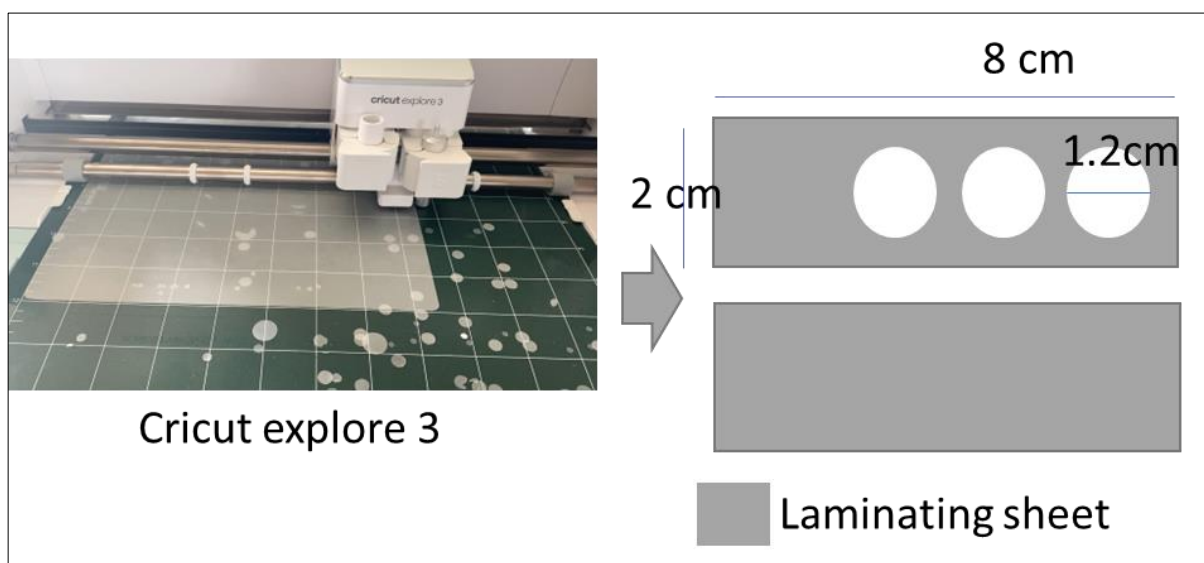
Figure 6.49 Cricut explore3 instrument which was used to cut the laminating sheet (2×8 cm) to seal the manganese detection PAD.
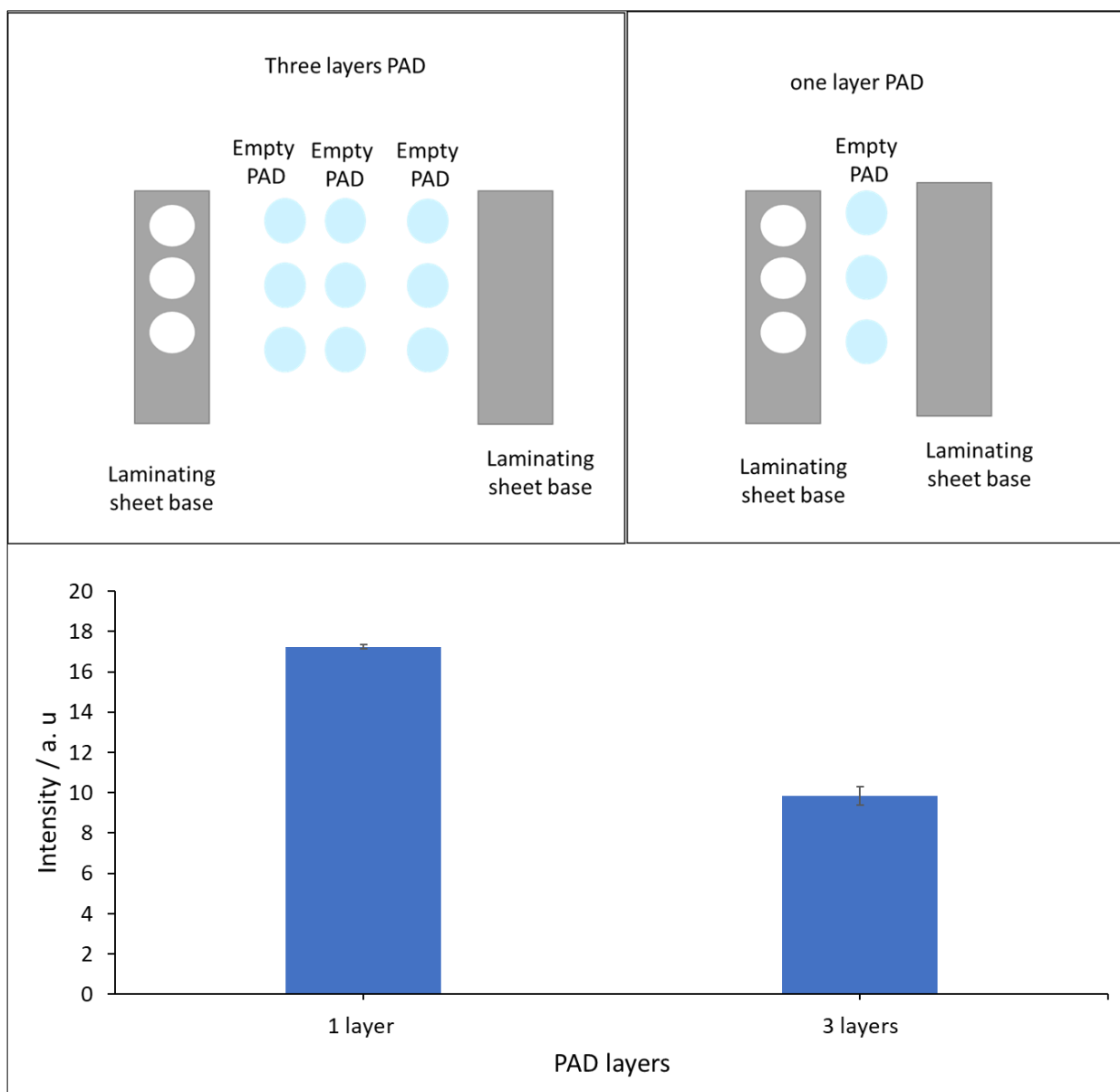
Figure 6.50 Intensity versus the number of layers when black PAD (with no reagent) was immersed for 2 seconds in soil sample extract (10 g soil, 50 mL DIW water). Increasing the number of layers causes improvement in filtration of the soil slurry that affects the PAD fibre. The intensity decreased by 40% when the number of empty layers increased.

After the improvement in sample entrance and the addition of extra layers, the calibration line was determined again as in **Figure** 6.51 which shows intensity versus the manganese concentration (μM). There was a clear improvement in the standard deviation compared to the previous result in **Figure** 6.48 **A**. In addition, the slope increases by around 20% from around 0.23 μM^{-1} to around 0.31 μM^{-1} and consequently the limit of detection decreases by around 20% from 0.29 to 0.21 mg L^{-1}**.**

Table 6.8 summarizes the slope of the calibrations line and the limit of detection for PAD sealed in different ways studied in this section.

The reproducibility of the method was also determined on three different days as in **Figure** 6.51 which shows three calibration lines with similar slop, LoD and LoQ of an average of 0.3098 ± 0.0240 μM^{-1}, 3.76 ± 0.27 μM (0.21 mg L^{-1}) and LoD of 37.25 ± 4.75 μM(2.1 mg L^{-1}) respectively and With relative standard deviation not more than 13% as in

Table 6.9. The level of manganese in the soil below which fertilizer should be applied is 10 mg kg^{-1} [130,131]. For example, if 10g of soil is used in cafetiere and 200 mL of solvent the LoD and LoQ would be 4.14 ± 0.30 mg kg^{-1} and 40.98 ± 5.23 mg kg^{-1} respectively. LoD value is lower than 10 mg kg^{-1} hence this level is visible by our PAD.
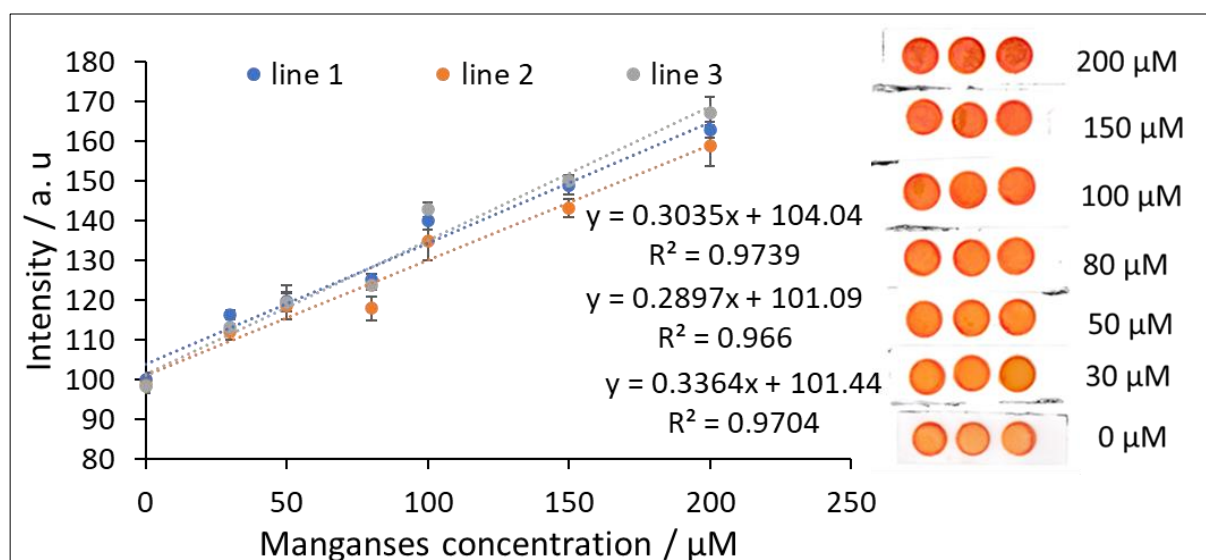
Figure 6.51 Intensity versus manganese concentration (μM). PAN (3.8 mM) reagent consisted of 8% surfactant (Trionix-100), and carbonate buffer (pH 8). 35 μL the detection reagent was added to the PAD (n=3) first and allowed to dry, the PAD was laminated with a lamination sheet with a circular sample entrance, PAD was dipped for 2 seconds in manganese, after 7 min of waiting the PAD was scanned and the image was analysed for intensity using image-J software (The intensity was measured by method 1 in **Section 2.5** and **Figure** 6.10). Device 17 was used for the analysis, modified as in **Figure** 6.8.

Table 6.8 LoD, R^2, and the slope when the PAD was sealed in different ways.

Way of sealing	LoD/ μM (mg L^{-1})	Slope μM^{-1}	R^2
No sealing /pipetting	15 (0.81)	0.17	0.9902
Acrylic sealing/pipetting	13 (0.72)	0.15	0.977
Lamination sealing/ dipping (scalpel is used for circle cut)	5 (0.29)	0.23	0.9593
Lamination sealing/ dipping (Cricut is used for circle cut)	3.80±0.26 (0.21±0.015)	0.31±0.02	0.9739

Table 6.9 LoD, LoQ, R2 and slope of the three lines in **Figure** 6.51. LoD and LoQ were calculated as in **Equations 2.5 and 2.6**.

	line 1	line 2	line 3	Average	RSD
LoD/ μM	3.47	3.99	3.81	3.76±0.27	7.116022
LoQ/ μM	42.71	34.14	34.86	37.25±4.75	12.75447
R^2	0.9739	0.9660	0.9704	0.9701±0.0040	0.408054
Slope/ μM^{-1}	0.3035	0.2897	0.3364	0.3098±0.0240	7.742734

6.4.2.4 Phone detection of manganese

An internal standard was added to the PAD for phone detection. The internal standard helps to remove the effect of the surrounding light as mentioned in chapters 3 and 4. **Figure** 6.52 shows the result when a phone was used instead of a scanner for detection. The intensity from the detection circles was divided by the intensity of the internal standard and hence the effect of the surrounding light was removed. The result from **Figure** 6.52 shows the reproducibility from three different days. The LoDs, LoQs and slopes were with average values of 4.65±1.73 µM (0.25 mg L^{-1}), 45.29±23.85 µM (2.54 mg L^{-1}), 0.0018±0.0001 µM^{-1} respectively. However, the RSD of LoD and LoQ were higher than 30% as in **Table** 6.10. This problem can be solved as in Chapter 5 using external standards which helps to remove the effect of changing phone or the way of picture taking due to changes in the angle and the place of photo taking. The addition of external standards can be future work for this PAD.
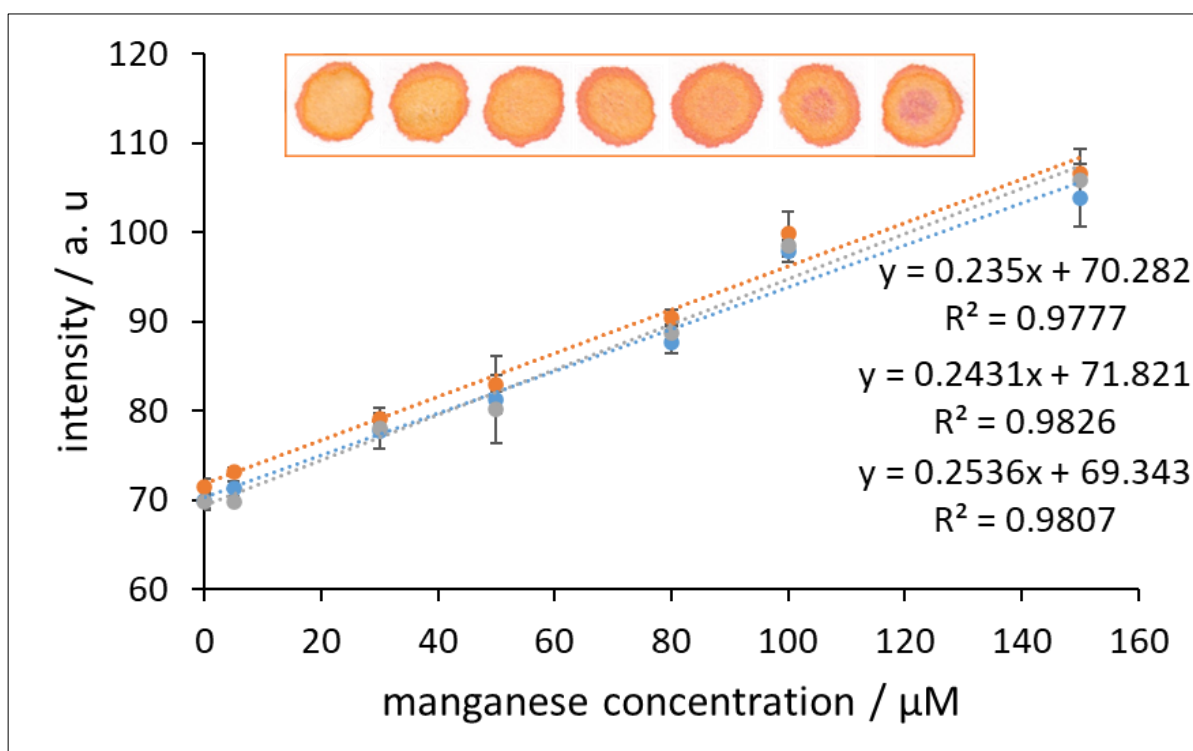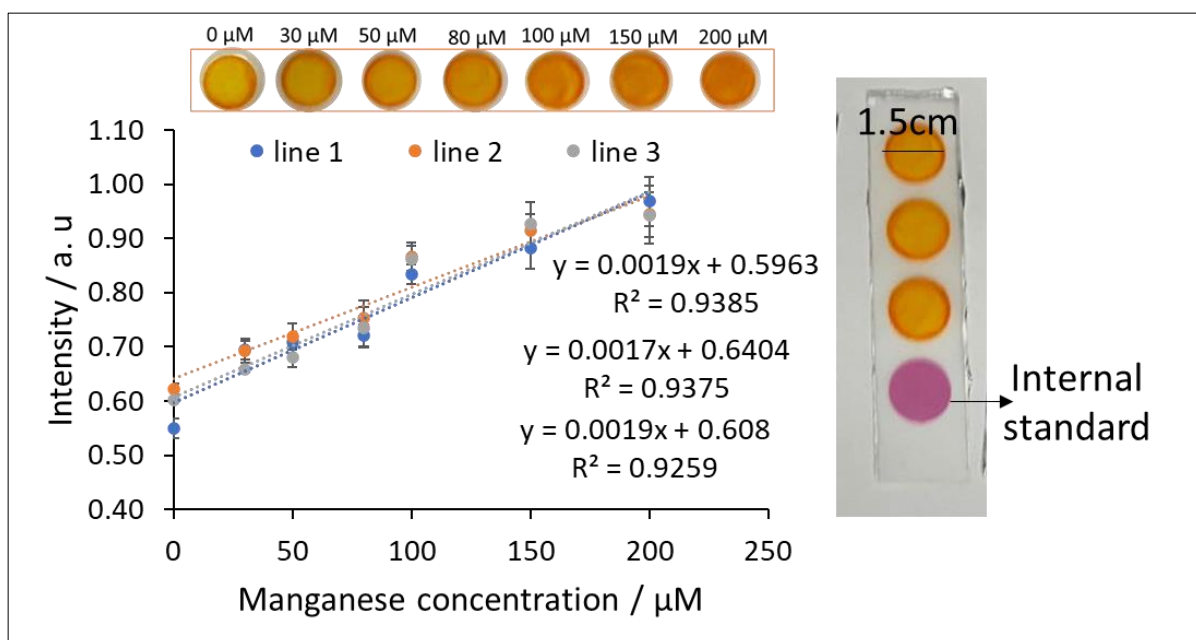

Figure 6.52 Intensity versus manganese concentration (µM). PAN (3.8 mM) reagent consisted of 8% surfactant (Trionix-100), and carbonate buffer (pH 8). 35 µL the detection reagent was added to the PAD (n=3) first and allowed to dry, empty PADs were added, the PAD was laminated with a lamination sheet with a circular sample entrance, and the PAD was dipped for 2 seconds in manganese after 7 min of waiting the PAD was phone and image was analysed for intensity using image-J software (The intensity was measured by method 2 in **Section 2.5** and **Figure** 6.10). PAD with internal standards was used due to the use of the phone. Device 17 was used for the analysis, modified as in **Figure** 6.8.

Table 6.10 LoD, LoQ, R^2 and slope of the three lines in **Figure** 6.52**.** LoD and LoQ were calculated as in **Equations 2.5 and 2.6**.

	line 1	line 2	line 3	Average	RSD
LoD / µM	3.25	6.58	4.12	4.65±1.73	37.20

LoQ/ μM	68.52	46.50	20.86	45.29±23.85	52.66
R^2	0.9385	0.9375	0.9259	0.9340±0.0070	0.75
Slope/ μM^{-1}	0.0019	0.0017	0.0019	0.0018±0.0001	6.30

6.4.2.5 Interference

Interferences require no masking reagent.

The interferences were studied based on their existence in soil and their ability to interact with the developed PAD. The main interference that exists in soil and has the tendency to react with the PAD and compete with manganese are Zinc, Copper and Iron [454]. There are also other ions (cations and anions) that can interfere, however, their tendency to interact with the masking reagent was studied. Calcium, magnesium, sodium, potassium, nitrate, phosphate and chloride are some of the cations and anions that can cause interference. The cations usually tend to compete with manganese in the PAD and hence the PAD may detect these interferences instead of the manganese. The anion can interact with the manganese itself and prevent it from reaching the detection reagent in the PAD. The general interferences were studied as in **Figure** 6.53 which shows the steps to study the interferences. The PAD was first prepared as usual. This time instead of adding the manganese, a mixture of manganese and interference were added and allowed for colour development. The intensity of manganese alone (100 μM/ 5.6 mg L^{-1}) was compared to the intensity of the mixture of manganese and interference. A mixture was used to test the interference because the interference competes with the manganese and the effect of competing is needed to be studied. The result is in **Figure** 6.54 which shows the intensities for manganese alone and manganese with each interference. At a concentration of 1000 mg L^{-1}, the interference does not interfere using a t-test (e.g., at Ca2+ 1, t_{stat}=-1.63, $t_{critical}$=2.78, P=0.1α= 0.05, n=3, two tailed test), except for phosphate which was tested again at a concentration of 500 mg L^{-1} and cause no interference at this level. Most of the time the tolerance level is higher than the level of the interference in soils as in **Table** 6.11. **Figure** 6.55 shows the interference from Ni^{2+} and Co^{2+}which does not cause interference when they are at 1 mg L^{-1} level which is around their normal level in the environmental soil [455].

Table 6.11 Interference level in the environment (soil) based on published previous studies.

Ion	mg L^{-1}	Mass: Volume	Mg kg^{-1}	reference
Mn^{2+}	27.7	0.25:10	1108	[376]
	4.225	0.25:10	169	[376]
	1.888	0.004:2.5	1180	[377]
PO$_4^{3-}$	0.148	2.5:50	2.96	[383]
	1.27-3.05	-	-	[384]
Ca^{2+}	7.54-110.15	20:80	30.16-440.6	[385]
	9.46-45.69	10:100	94.6-456.9	[386]
	9.7-18.8	10:200	194-376	[387]
SO$_4^{2-}$	2.45-3.654	20:100	12.28-18.27	[388]
	0.2-1.6	5:25	1-8	[389]
K$^+$	22.8-182	20:100	114-910	[388]
	5.7-7	2.5:25	57-70	[390]
Mg	0.85-9.85	10:200	17-197	[387]
Na$^+$	1.9-2.52	10:200	38-50.4	[387]
	1.00-1.43	10:200	20-28.6	[387]

Cl⁻	6-300	1:50	300-15000	391
	1.6	5:40	13	392
	7.8	5:40	62	392

Figure 6.53 The test for the interference of manganese PAD.35 µL of a mixture of the interference and manganese was added to the PAD. This was compared to the intensity of manganese alone. The PAD was developed as in **Figure** 6.6. The intensity was determined by image-J software (The intensity was measured by method 1 in **Section 2.5** and **Figure** 6.10).
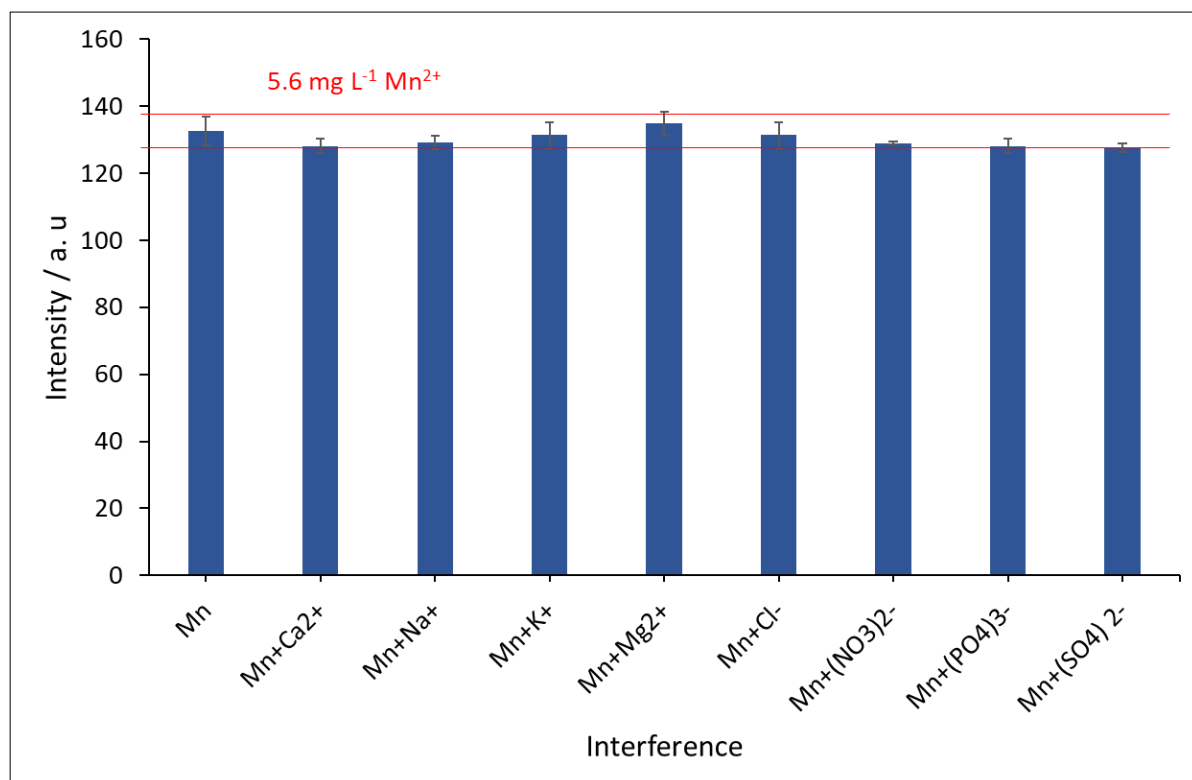
Figure 6.54 Intensity versus the interference. The interference was determined as in **Figure** 6.53. a mixture of manganese and interference was added and allowed for colour development. The intensity of manganese alone (100 µM/ 5.6 mg L^{-1}) was compared to the intensity of the mixture of manganese and one interference 1000 mg L^{-1} [NO$_3^-$, Ca^{2+}, Na$^+$, K$^+$, CO$_3^{-2}$, PO$_4^{-3}$, Cl$^-$, SO$_4^{-2}$] and5 00 mg L^{-1} [PO$_4^{-3}$].
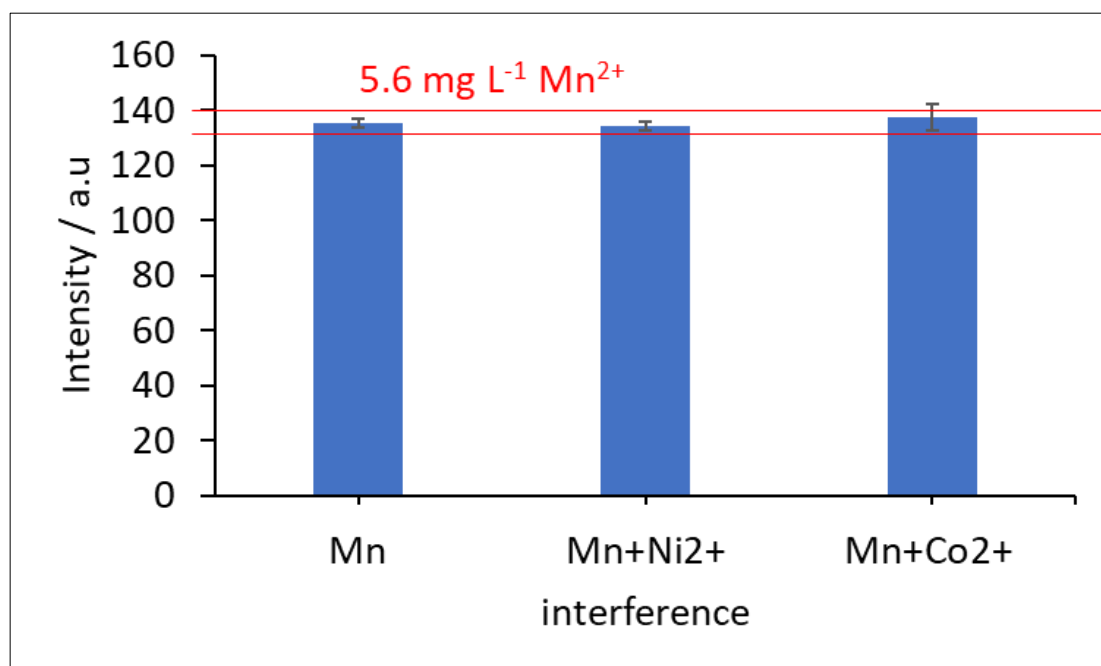
Figure 6.55 Intensity versus the interference. The interference was determined as in **Figure** 6.53. a mixture of manganese and interference was added and allowed for colour development. The intensity of manganese alone (100 µM/ 5.6 mg L^{-1}) was compared to the intensity of the mixture of manganese and one interference [Co^{2+}(1 mg L^{-1}), Ni^{2+}(1 mg L^{-1})].

Interference with masking

Iron, copper and zinc are interferences that interfere with the developed PAD at low concentrations therefore, they need to be masked. Masking reagents are used for this purpose. Masking reagents are reagents that interact with the interference and prevent them from reaching the detection reagent in the PAD.

Table 6.12 shows the level of iron, copper and zinc in environmental soil from some previous studies.

Table 6.12 Heavy metal Interference level in the environment (soil) based on some previous studies.

ion	mg L^{-1}	Mass: Volume	Mg kg^{-1}	Reference
Fe^{2+}	1.51-4.89	25:250	15.1-48.9	[378]
	65.4	2:100	3270	[379]
	0.190	1:25	4.75	[380]
Cu^{2+}	0.201, 0.133	-	-	[381]
Zn^{2+}	0.128, 0.023	-	-	[381]
	0.0067-0.1175	2:20	0.067-1.175	[382]

Iron and Copper masking

Initially, Iron was masked by DMSA (Dimercaptosuccinic acid). DMSA has two carboxylic groups and two thiol groups, and it can work as a chelating agent to catch the cations hence it was used to capture Iron [456]. **Figure** 6.56 shows the steps for the interference masking and detection. The masking reagent was added first and then allowed to dry. After that, the detection reagent was added and allowed to dry too. The PAD is then read to be used. The PAD was used to analyse blank, manganese (100 µM/ 5.6 mg L^{-1}) and mixture (manganese 100 µM (5.6 mg L^{-1}) and iron 5 mg L^{-1}). **Figure** 6.57 shows the intensities from the three PADs when three different concentrations of the masking reagent were used 0, 0.04 and 0.4 M. At zero concentration of the masking reagent the intensity from the mixture was higher than the intensity from manganese alone, this extra intensity is due to the iron interference. At 0.04M and 0.4 M of masking reagent both manganese alone and the mixture show the same intensity as blank. This means that DMSA masks manganese also. Consequently, DMSA was not the best masking reagent to use.

Another masking reagent to mask Iron is DFO (Deferoxamine). DFO is known for its tendency to mask Iron, it tends to chelate Iron [457]. Therefore, it was used as in **Figure** 6.58 which shows the intensity versus the concentration of the masking reagent (DFO). When 0.05 M of the DFO was used both iron and manganese were masked. When the concentration of the masking reagent was reduced (0.01 M DFO) the masking properties were reduced for both manganese and Iron in the same manner. Consequently, DFO masks both Iron and manganese in the same way and cannot be used for masking purposes.

Thiosulfate was another masking reagent, which was used for masking Iron and copper (II) as in **Figure** 6.59 which shows intensity versus the element masked when different concentrations of the masking reagent were used, 0, 0.1, 0.5, 1M of thiosulfate. 0.1 was enough to mask 100% of copper (II) and Iron (II). A higher concentration of the thiosulfate leads to a change in the intensity of the manganese detection PAD.
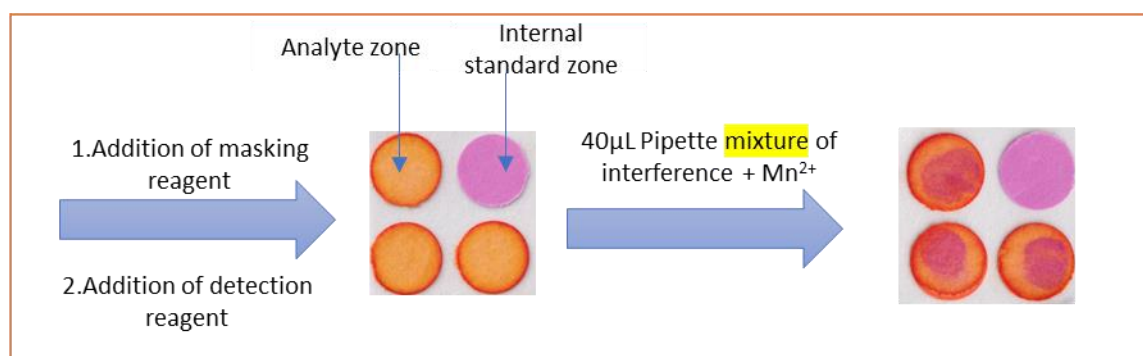
Figure 6.56 The test for interference of manganese PAD. The masking reagent was added to the PAD followed by the addition of the detection reagent. After drying the PAD is ready to be used. 40 μL of a mixture of the interference and manganese was added to the PAD. This was compared to the intensity of manganese alone. The PAD was developed as in **Figure** 6.13. The intensity was determined by image-J software (The intensity was measured by method 1 in **Section 2.5** and **Figure** 6.10).
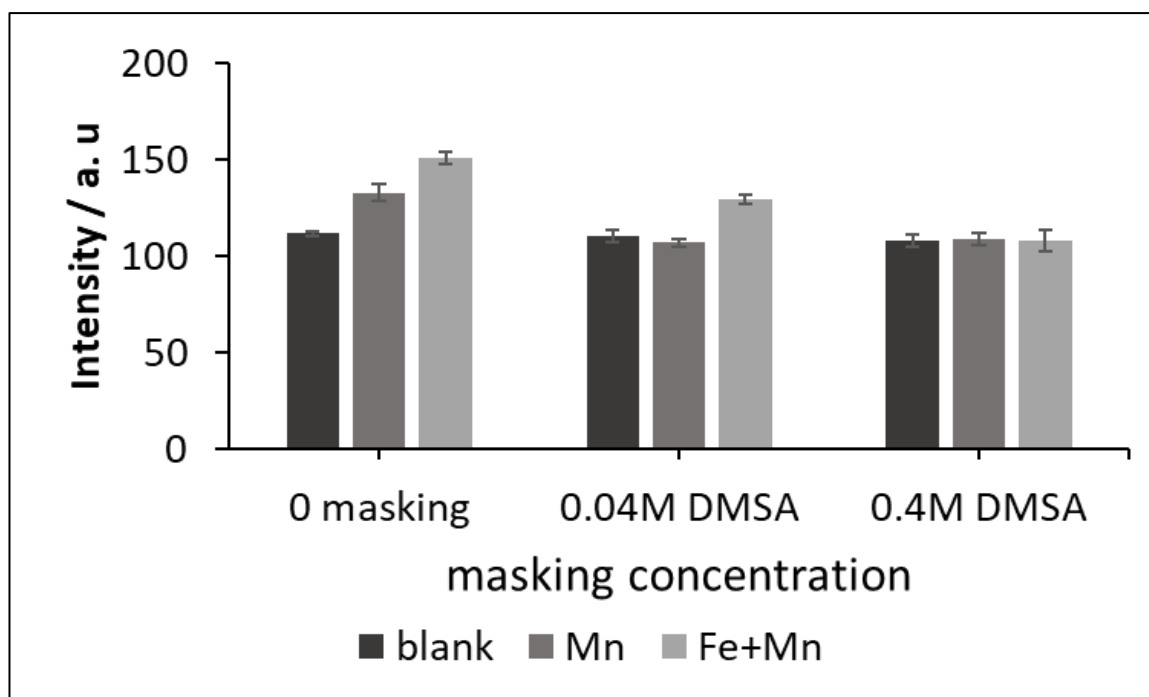
Figure 6.57 Intensity versus concentration of masking reagent when three solutions were used 0 manganese, 100 μM (5.6 mg L^{-1}) manganese alone and a mixture of (manganese 100 μM and iron 5 mg L^{-1}). The PAD was developed as in **Figure** 6.13 in experimental. The intensity was determined by image-J software (The intensity was measured by method 1 in **Section 2.5** and **Figure** 6.10).
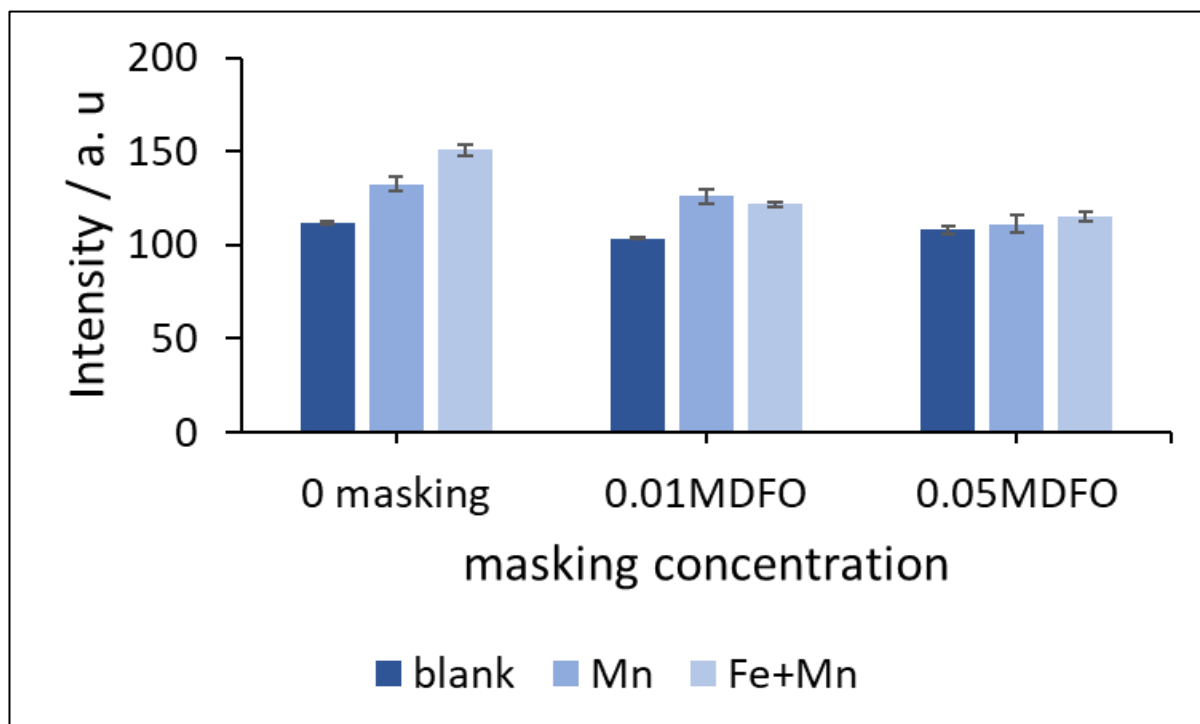
Figure 6.58 Intensity versus concentration of masking reagent (M) when three solutions were used 0manganese, 100 μM (5.6 mg L^{-1}) manganese alone and a mixture of (manganese 100 μM and iron(II) 5

mg L^{-1}). The PAD was developed as in Figure 6.13 in experimental. The intensity was determined by image-J software (The intensity was measured by method 1 in **Section 2.5** and **Figure** 6.10).
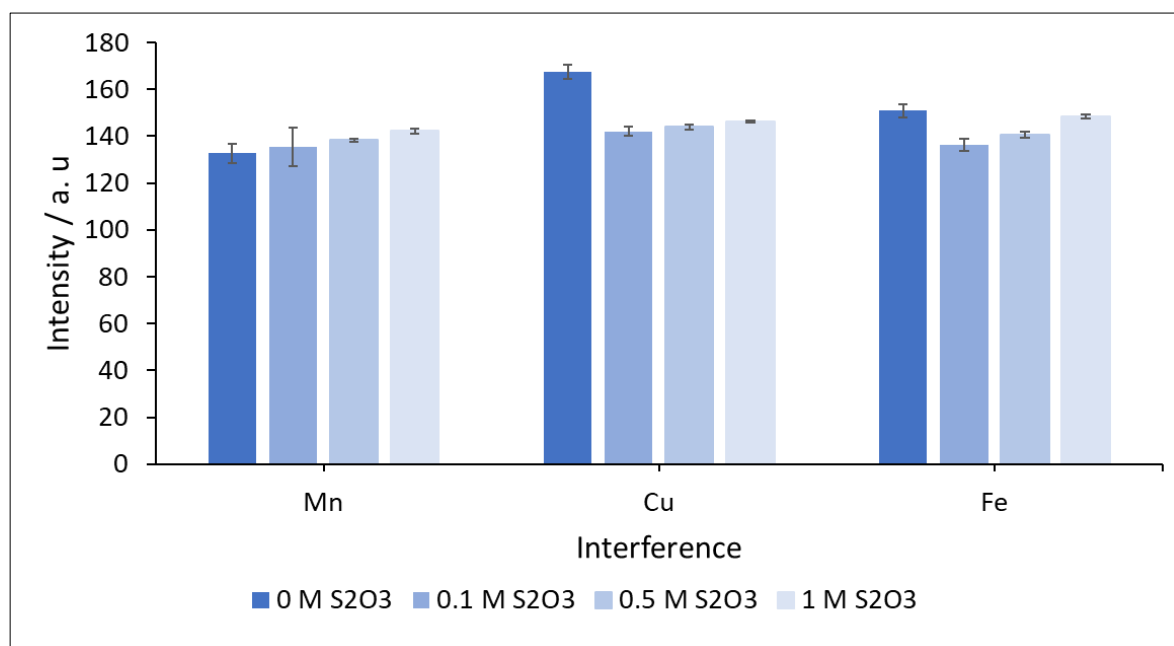
Figure 6.59 Intensity versus Interference (copper (II) and iron (II)) when four concentrations of masking reagent (0,0.1,0.5, 1M). 100 µM (5.6 mg L^{-1}) manganese alone and a mixture of (manganese 100 µM and iron 5mg L^{-1}). The PAD was developed as in **Figure** 6.13 in experimental. The intensity was determined by image-J software (The intensity was measured by method 1 in **Section 2.5** and **Figure** 6.10).

Zinc masking

Zinc also tends to interfere with manganese detection. Compared to other interference of manganese, zinc was the most sensitive to the PAD as is clear in **Figure** 6.60 which shows the intensity versus the masking reagent for zinc. When no mask was used zinc showed high intensity compared to manganese alone and hence this indicated the significant interference of zinc with the detection reagent. EDTA and EGTA were used to mask zinc since they have carboxylate and amine groups [458]. These groups can form complexes with zinc. However, according to the result in **Figure** 6.60, the groups can form also complex with manganese since the intensity of manganese detection decreased when any of the two complexes were used.

Citrate was also used to mask zinc since it can catch zinc and prevent it from reaching the detection reagent [450]. **Figure** 6.61 shows the intensity versus the concentration of citrate masking reagent when three concentrations of manganese were used. The intensity from zinc was reduce by around 20 %. Even if the concentration of the citrate increased this % remined the same. Therefore, citrate can mask only 20% of the zinc.

Another masking reagent was hydroxide ion [450]. **Figure** 6.62 shows intensity versus the % of hydroxide solution when three concentrations of manganese were used. Hydroxide was also able to mask around 20% of zinc.

In addition, thiosulfate [450] which was used to mask cupper and iron was used to mask zinc (**Figure** 6.63). Unlike iron and copper masking the zinc was masked by 20% when thiosulfate was used. Therefore, thiosulfate will be used to mask zinc too.

Figure 6.64 shows that at lower concentration of zinc the interference can be less. At 0.5, 1 and 5 mg L^{-1} of zinc the % of interference was 14, 20 and 40 respectively. Therefore, it can be said that the PAD work has only 20% of interference by zinc when the of zinc is less than 1 mg L^{-1}. And this 20 % of interference can be removed by any of the masking reagent mentioned above. In this study thiosulfate was used since it was used also to mask iron and copper.
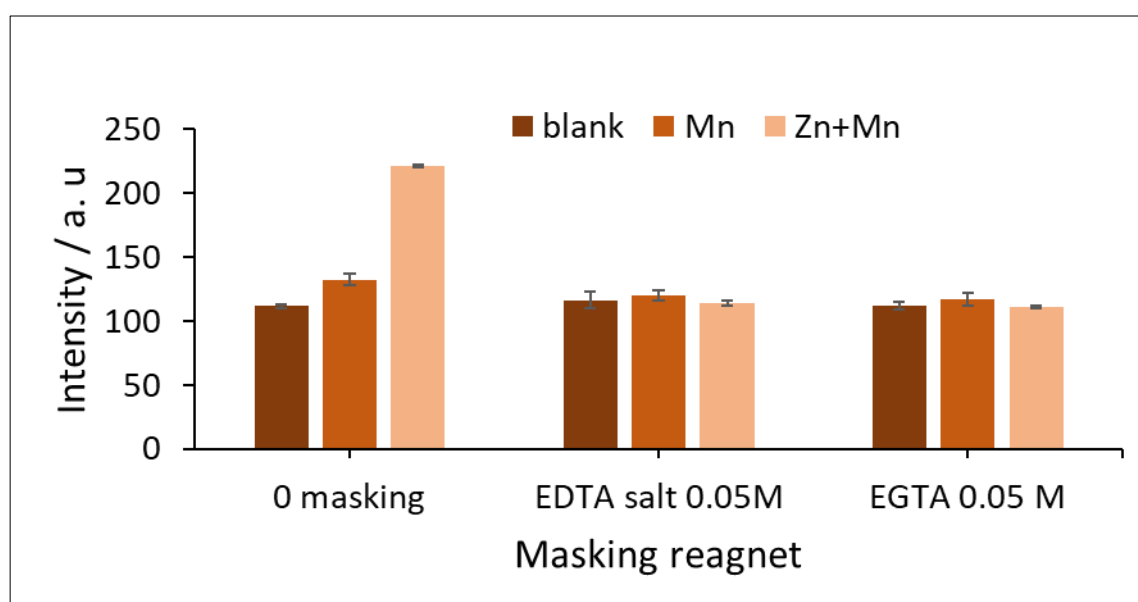
Figure 6.60 Intensity versus concentration of masking reagent (M) when three solutions were used 0manganese, 100 μM (5.6 mg L^{-1}) manganese alone and mixture of (manganese 100 μM and Zinc 5 mg L^{-1}). 0.05 of EDTA and EGTA were used as masking reagent. The PAD was developed as in **Figure** 6.13. The intensity was determined by image-J software (The intensity was measured by method 1 in **Section 2.5** and **Figure** 6.10).
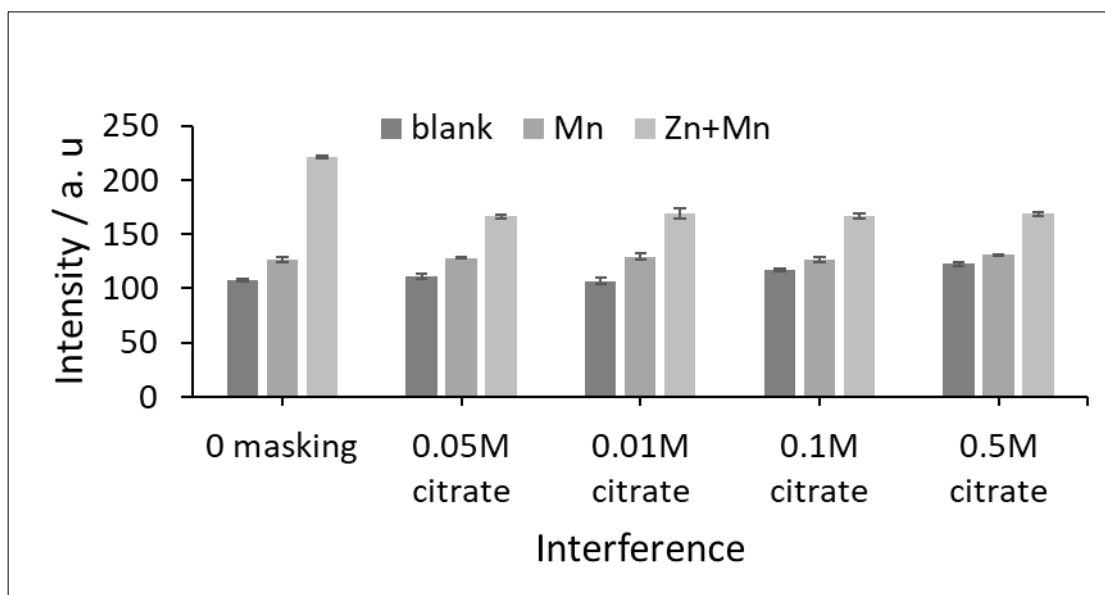
Figure 6.61 Intensity versus concentration of masking reagent (M) when three solutions were used 0manganese, 100 μM (5.6 mg L^{-1}) manganese alone and mixture of (manganese 100 μM and Zinc 5 mg L^{-1}). 0.05, 0.01, 0.1 and 0.5 M citrate were used as masking reagent. The PAD was developed as **in Figure** 6.13 in the experimental. The intensity was determined by image-J software (The intensity was measured by method 1 in **Section 2.5** and **Figure** 6.10).
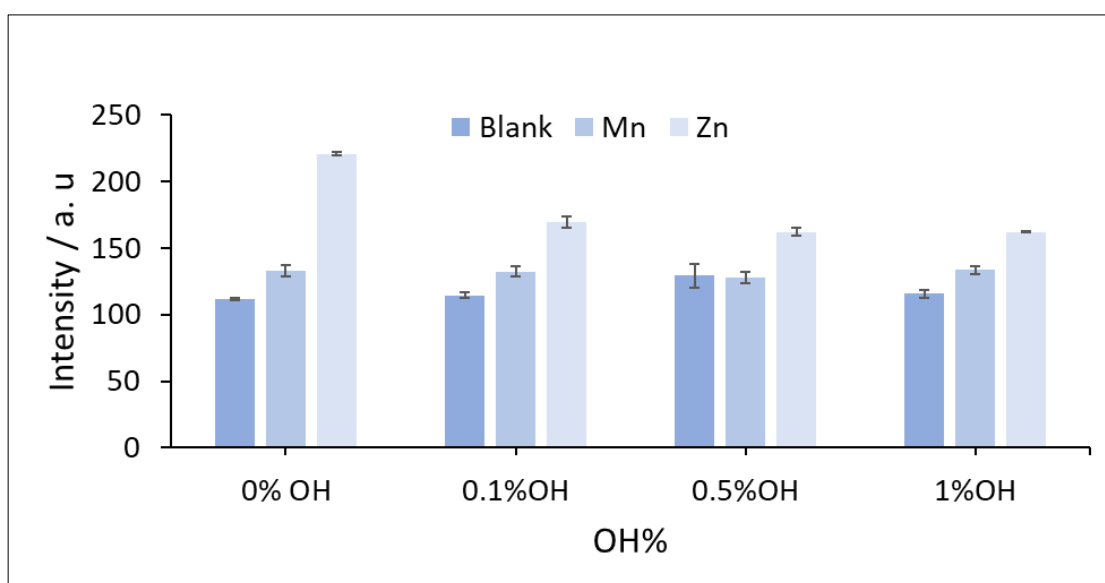
Figure 6.62 Intensity versus concentration of masking reagent (M) when three solutions were used 0manganese, 100 μM (5.6 mg L^{-1}) manganese alone and mixture of (manganese 100 μM and Zinc 5 mg L^{-1}). 0, 0.1, 0.5 and 1 % hydroxide were used as masking reagent. The PAD was developed as in **Figure** 6.13 In the experimental. The intensity was determined by image-J software (The intensity was measured by method 1 in **Section 2.5** and **Figure** 6.10).
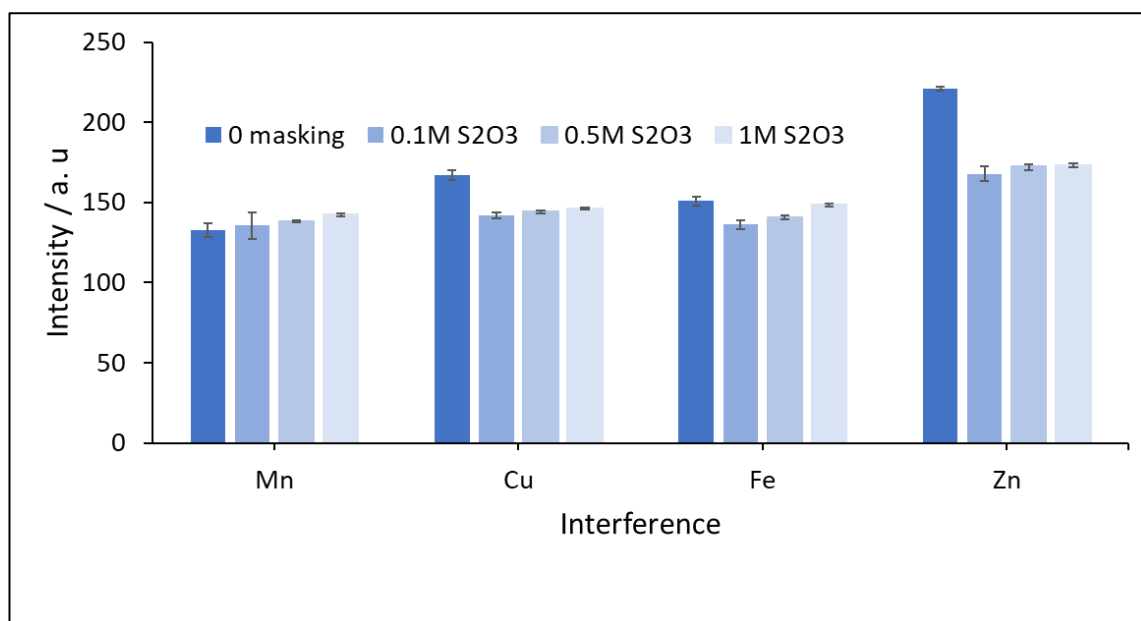
Figure 6.63 Intensity versus Interference (zinc, copper and iron) when four concentration of masking reagent (0,0.1,0.5, 1M). 100 μM (5.6 mg L^{-1}) manganese alone and mixture of (manganese 100 μM and iron/zinc/cupper 5mg L^{-1}). The PAD was developed as in **Figure** 6.13 in the experimental. The intensity was determined by image-J software (The intensity was measured by method 1 in **Section 2.5** and **Figure** 6.10).

Zinc mg L^{-1}	
	% interference
0.5	13.82±1.43
1	18.73±0.75
5	39.21±0.27
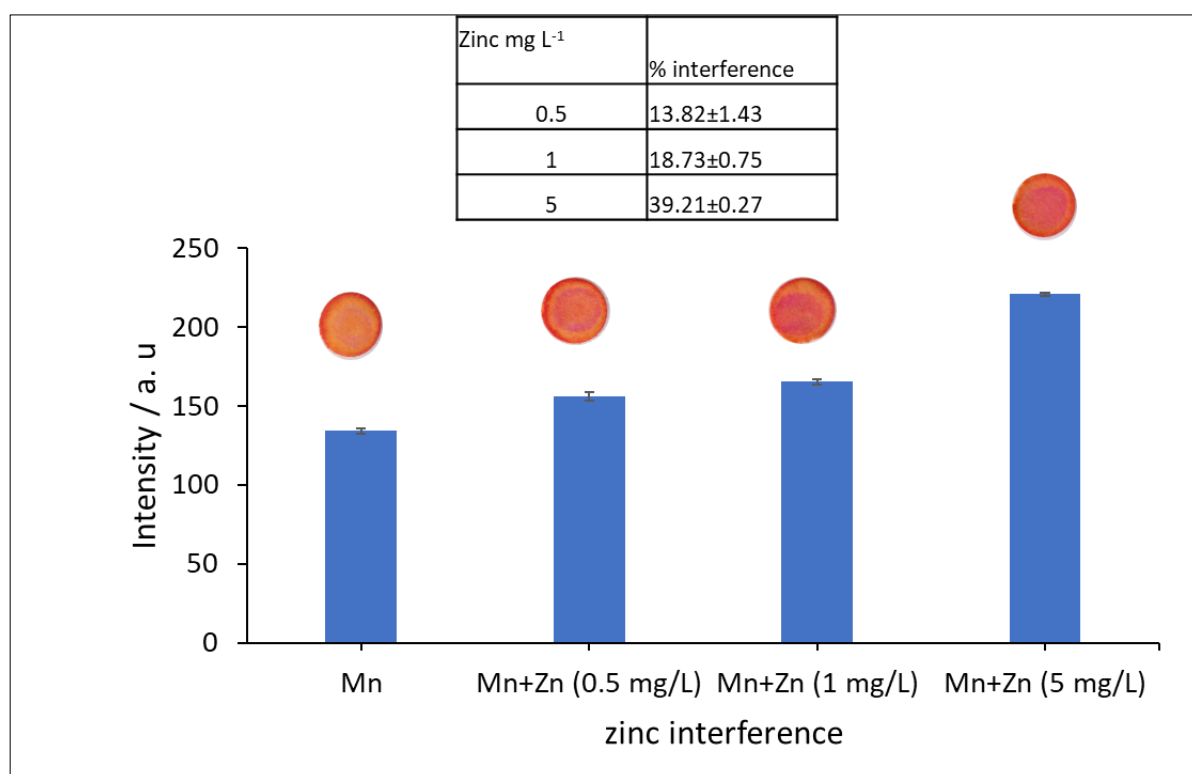
Figure 6.64 Intensity versus the zinc interference at different concentrations. 100 μM manganese alone and mixture of (manganese 100 μM and Zinc 5, 1, 0.5 mg L^{-1}). The PAD was developed as in **Figure** 6.13 in the experimental. The intensity was determined by image-J software (The intensity was measured by method 1 in **Section 2.5** and **Figure** 6.10).

6.4.2.6 Stability

The stability of the PAD is important to determine to how long the PAD can be stored before use. In another word to know the expiry date of the PAD. The stability of the PAD was studied in three different conditions. The PAD was stored in room temperature (22 ^{0}C) in dark and light conditions. These conditions were chosen to see the effect of the light in the stability of the reagent in the PAD and to determine if the PAD can be kept in the room without the use of the fridge. **Figure** 6.65 shows the intensity from the stored PAD versus the day when PAD stored in room temperature in dark and light condition. In dark condition the intensity was stable up to day 47 using ANOVA test for all day's intensities (F= 1.59, $F_{ritical}$=2.15, α=0.05, P=0.15, n=3, ANOVA test). The study was done up to 47 days the PAD maybe stable for more in room at dark condition. In room temperature and light condition, the PAD was stable for around 40 days using ANOVA test (F= 2.09, $F_{ritical}$=2.51, P=0.093, α=0.05, n=3, ANOVA test) which shows equal means for all days except for day 44 and 47.

The stability was also studied in freezer (-4 ^{0}C) as in **Figure** 6.66 which shows intensity versus the day when the PAD stored in freezer. According to ANOVA test (F= 1.73, $F_{ritical}$=1.95, P=0.089, α=0.05, n=3, ANOVA test) the PAD in the freezer was stable for around 68 days (2months). ANOVA test exclude day 51, 54 and 58 which did not show equal mean with other days. This may happen due to error in the PAD preparation since lots of PAD were prepared at once.

In conclusion, The PAD maybe survives longer than 47 days in dark room or more than 68 days in freezer. However, due to time of research the PAD was tested only for this period. More stability test needs to be done. For now, the available information about storing and expiry date will be given along with the PAD.
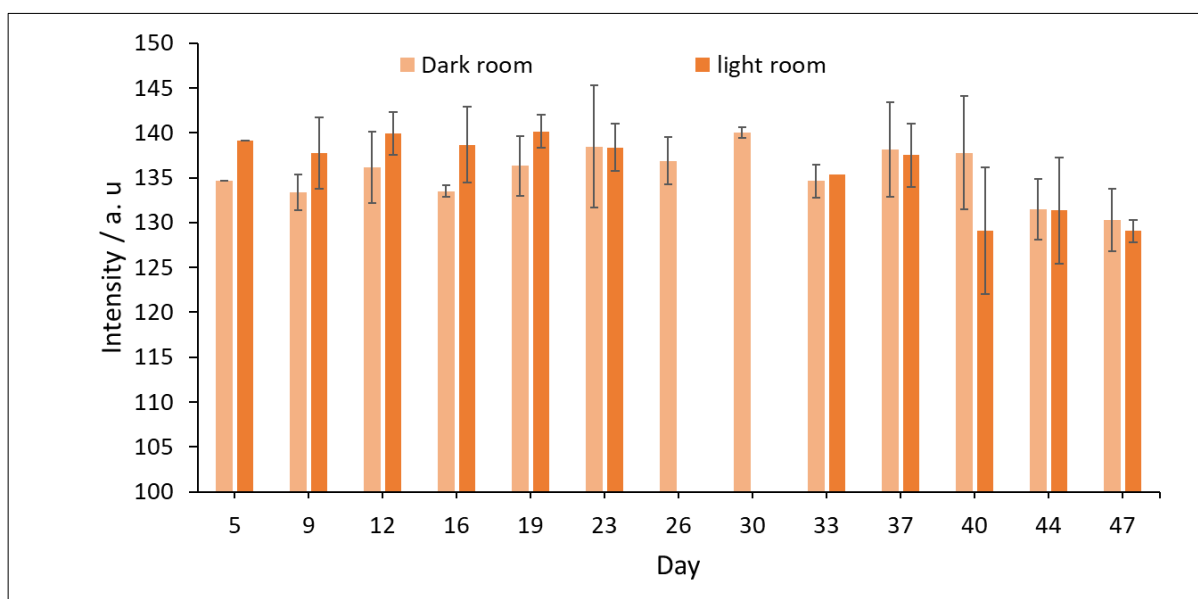
Figure 6.65 Intensity versus the day. The result was when the PAD was stored in two conditions of room temperature (22 ^{0}C) in dark condition and light condition.
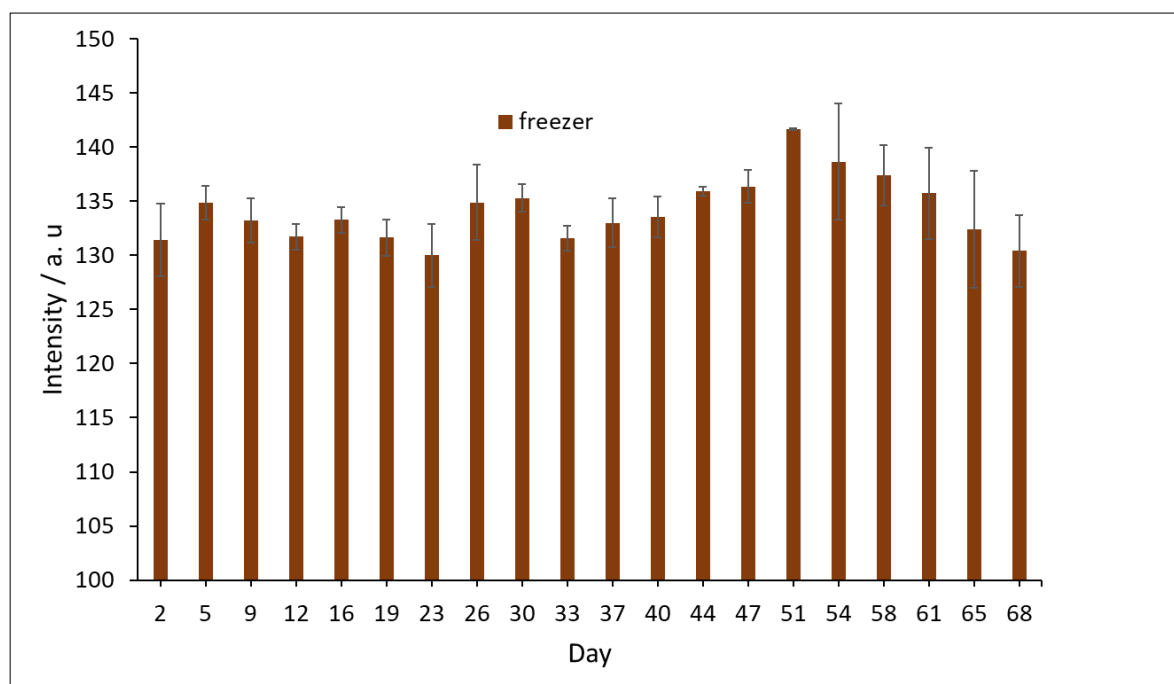
Figure 6.66 Intensity versus the day. The result when the PAD was stored in the freezer (-4 ^{0}C)
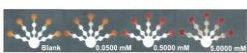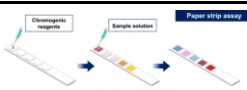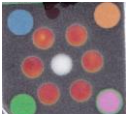
6.5   Comparison with PADs in Literature

The developed PAD was compared to the existing PAD in literature as in **Table** 6.13. The developed PAD has 0.21 mg L^{-1} limit of detection which is close to literature (**Table** 6.13). The existing manganese's detection PADs were prepared for researcher use and hence they are not ready to be used by non-expert and they were never teste with lay people [314,315]. Also, these devices [314,315] used non-user-friendly borate buffer and cyanide whereas our device use other chemicals like carbonate buffer and thiosulfate, and this make it safer for release for lay people use. Dipping was also used as sample introduction system compare other literature work which depend on pipetting of the sample. Dipping is much easier for non-researcher like farmers or lay people. In addition, all the literature PADs [314,315] for manganese were used to analyse manganese in water sample and they are not ready to be used for soil sample analysis. The developed PAD was supported with multilayers which provide the filtration of the soil extract before the detection.

In conclusion, the developed PAD combine several positive characteristics that make it usable for on-site analysis of manganese in soil sample since it were easy (based on dipping sample introduction), user friendly (use less toxic chemicals) and fast (with short time of detection 7 min), inexpensive (small amount of reagent is required, not less than 60 device can be prepared

from 1 Whatman paper (32 cm diameter)), equipment-free (no equipment and no external power is required)and attached to multilayers (provide filtration of extract prior to detection).

Table 6.13 Manganese detection PAD developed in this work compared to the existing PAD in literature.

Device shape (reference)	sample	LOD mg L-1	Colorimetric reagent	Reaction time	Sample introduction	Use of chemicals	reproducibility
315	water	0.11	PAR	120 min	Pipetting	Use of toxic chemicals like borate, thiourea and ethylenediamine	Not mentioned
314	water	0.11	PAN	1 min (specific) after which the signal decreases	Pipetting	Use of toxic chemicals like borate and cyanide	reproducible
OUR WORK		0.99	PAR	20 min	Dipping	Use glycine buffer	Not reproducible
OUR WORK	soil	0.21	PAN	7 min detection time with 5 min range of intensity stability	Dipping	Carbonate was used as a buffer instead	Reproducible different days

6.6 Soil sample treatment

The PAD was developed for the purpose of analysis of manganese in soil. before detection, manganese should be first extracted from the soil. As mentioned in chapter 4 the use of cafetiere was an option for the extraction. In addition, the use of shaker was considering as conventional method for extraction.

Cafetière Extraction efficiency

Manganese can be extracted by several solvent like phosphate, Mehlich1 (HCl/H2SO4), EDTA, Cola, $CaCl_2$, KCl, NaCl and others [451,459-462]. EDTA represent the best extraction solvent that can form complex with manganese. However, EDTA can also form complex with other heavy metals [450,451]. **Figure** 6.67 shows the concentration of heavy metals in soil sample when EDTA was used as extraction solvent, shaker and cafetiere was used for extraction, ICP-MS was used as detection method. It is clear that cafetiere was less efficient than shaker in extraction. Compare to the shaker cafetiere can extract around 30% (29.52±1.69%) of the heavy metal specifically manganese. For this work EDTA was used as conventional extraction solvent when shaker and ICP-MS conventional method were used for the analysis.
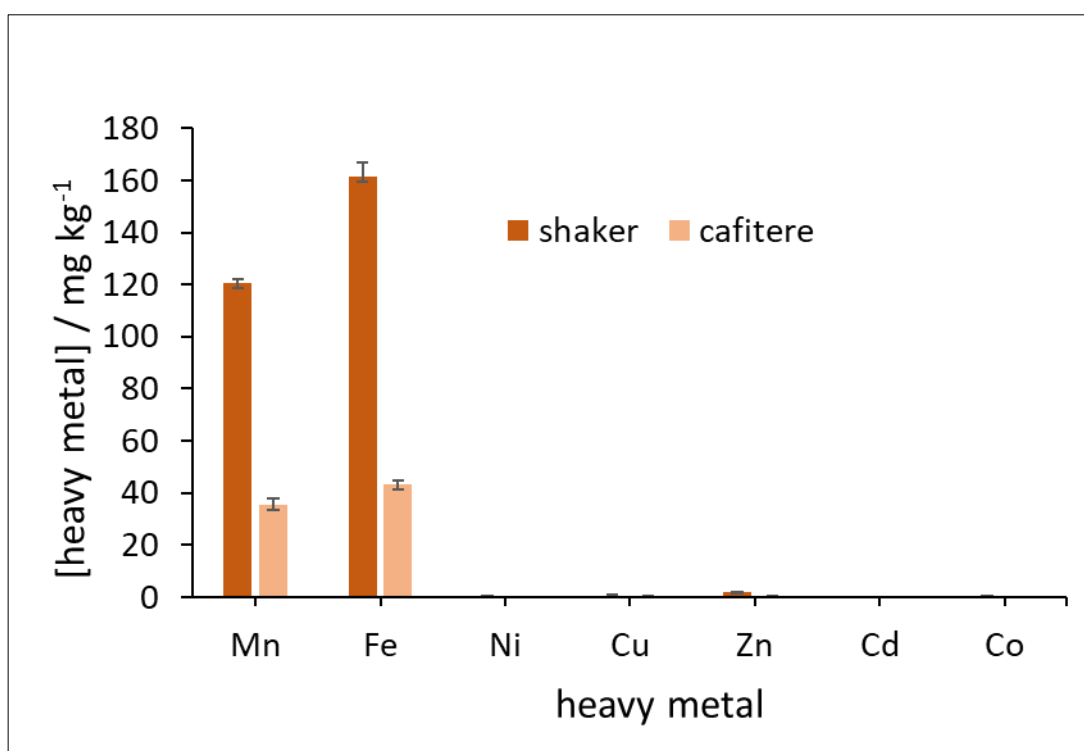
Figure 6.67 The concentration of heavy metals in soil sample(mg kg^{-1}) when 0.05 M EDTA was used as extraction solvent, shaker (1 h shaking) and cafetiere (1 min shaking) were used for extraction, ICP-MS was used as detection method. 1:5 of soil mass: solvent volume was used. Compare to the shaker cafetiere can extract around 30% of the heavy metal specifically manganese. Jhon Innes 1 was used as soil for analysis.

Extraction solvent

Other than the tendency of EDTA to form complex with other heavy metal [450] it also holds the metals (form very stable complex) and it needs releasing agent to remove the metal from the complex. Therefore, other solvents which cause no interfere, easily release the metal and not toxic were suggested. DIW, Cola, HCl/H_2SO_4, $CaCl_2$, KCl and NaCl were used in this study. **Figure** 6.68 shows manganese concentration in soil sample (Jhon Innes 1) when different solvents were used and when cafetiere was used for extraction and ICP-MS was used for detection. % of extraction was calculated based on comparison with the conventional method (EDTA was used as conventional extraction solvent, shaker extraction method and ICP-MS conventional detection method). DIW was tested first since it is the easiest available compared to the rest of the solvent. However, DIW can only extract 0.16 % of manganese which is not an efficient %. Then cola was suggested since it contains phosphate which has the tendence to extract manganese [461]. Cola can extract only 1.28 % of manganese. Acid was also an option for extraction however it can destroy the fibres of the PAD when it is in high concentration. NaCl was able to extract around 10% (11.63 ±0.30) of manganese. NaCl is salt and it is safe, non-expensive option and easily available compare acid or EDTA.

solvent	% Mn extracted
DIW	0.16
COLA	1.28
HCl/H_2SO_4	6.82
EDTA	29.52
CaCl2	8.59
KCl	3.06
NaCl	11.63
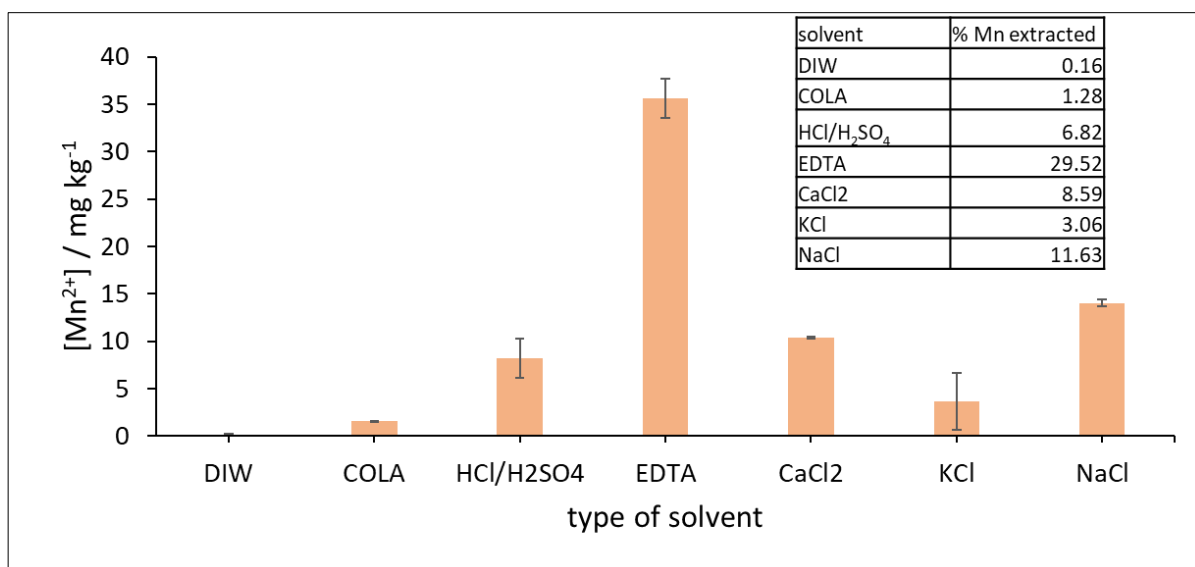
Figure 6.68 Manganese concentration in soil sample (mg kg^{-1}) versus type of solvent when cafetiere was used for extraction (1min mixing) and ICP-MS was used for detection. Jhon Innes 1 was used as soil for analysis. Concentrations of solvents are Mehlich1 (0.05M HCl/0.0125 M H_2SO_4), 0.05M EDTA, Cola, 0.01 M $CaCl_2$, 0.01 M KCl, 0.01 M NaCl. Soil mass: solvent volume (1:5) when Mehlich1, EDTA and Cola were used as solvent. Soil mass: solvent volume was 1:20 when $CaCl_2$, KCl and NaCl were used as solvent.

Extraction time

NaCl was used as extraction solvent with cafetiere extraction method. Time of mixing using the cafetiere was critical to extract efficient amount of manganese. **Figure** 6.69 shows the heavy metal concentration when the mixing was done for specific minutes. at 1 minutes the extracted amount of manganese was the maximum. The extracted amount decreases with time this decrease was not very huge and it was not expected. It is expected that the extracted amount increases with increasing shaking time. The difference was not extremely high; however, this happen maybe because at the first few minutes it takes manganese time to reach equilibrium between soil and extracted solvent. Other metals (Fe, Co, Ni, Cu, Zn, Cd) that have the possibility to interfere with manganese were studied also. The concentration of the interference extracted at 1 min shaking was lower than 10 mg Kg^{-1} (0.5 mg L^{-1}) which is lower than there interfering level studied in **Section 6.4.2.5**. Therefore, NaCl can be used for manganese extraction.
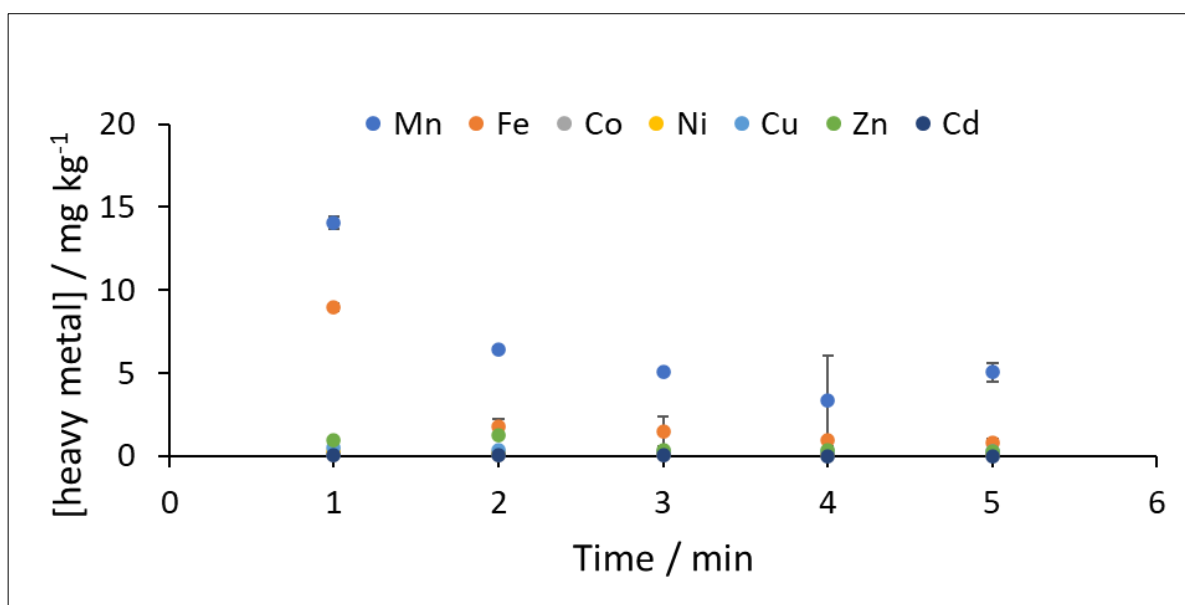
Figure 6.69 heavy metal concentration in soil sample (mg kg^{-1}) versus time of shaking (min) when cafetiere was used for extraction (0.01 M NaCl extraction solvent) and ICP-MS was used for detection. Jhon Innes 1 was used as soil for analysis. Soil mass: solvent volume was 1:20.

PAD efficiency and the whole workflow

The same soil sample which was analysed by ICP-MS for manganese content was also analysed by the developed PAD as in **Figure** 6.70. Bothe PAD and ICP-MS showed similarity in manganese content. However, the PAD showed high standard deviation compared to ICP-MS since ICP-MS is well known reliable method. More soil samples need to be analysed to compare between the two methods. This can be recommended as future work.
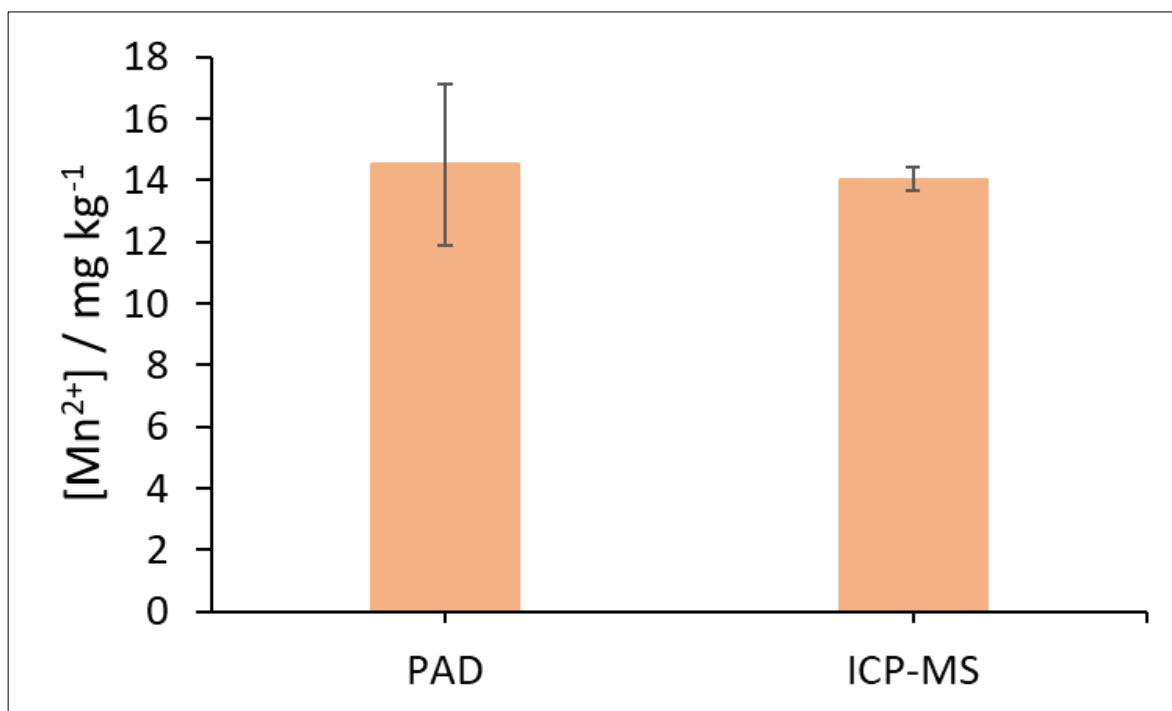
Figure 6.70 Manganese concentration in a soil sample (mg kg^{-1}) versus method of detection (ICP-MS/PAD) when cafetiere (1 min shaking) was used for extraction and 0.05 M NaCl was used as extraction solvent. John Innes 1 was used as soil for analysis. Soil mass: solvent volume was 1:20

6.7 Discussion and Conclusion

Manganese is a nutrient which is required by plant in small amount. Even though it is required in small amount it still has its influence in the growth of plant [439]. Conventional detection methods of manganese (like ICP-MS) [2] are expensive and require transfer the sample into the lab and hence time consuming. In addition, there are other field manganese detection methods which are still expensive and non-quantitative [24,25]. Regular monitoring of manganese by cheap and simple method in the field is required especially for poor countries. In this study paper-based sensor, which was inexpensive (price ≤ £1), user friendly, and with less toxic chemical and based on simple steps was developed for detection of manganese in soil calorimetrically. In addition, Initial step for PAD combination to cafetière extraction system of manganese was studied.

The choice of detection reagent was critical since detection reagent with as less as possible toxic compound and short detection time was required to fit the on-site detection requirement. PAR reagent showed non reproducible result when it was applied on the PAD compared to when it was used for manganese detection using UV-Vis. This was mainly due to the interaction between the wax and the component of the detection reagent or the manganese complex which was incompatible in the paper device. In addition, PAR reagent required longer time to react with manganese and hence the other interference that can be detected by the same reagent and form complex with detection reagent before manganese. Consequently, PAR reagent was replaced with PAN reagent. PAN reagent can capture manganese faster than PAR reagent. According to a study for Teepo et al.[314], it was able to capture manganese within 1 minutes. However, the problem with this device that the detection time was based in one minute detection after which the intensity of colour decreases and hence there was no stable range of colour to enable time for image capture. In addition, that PAD was using borate buffer and cyanide as component of the reagent detection reagent on the PAD. Consequently, the PAD is not safe for lay people use. In this study the PAD was made, and improved for lay people use. Therefore, Initially the toxic chemicals were replaced with less toxic chemicals. The borate buffer was replaced with the carbonate buffer which shows similar result to the conventional borate. The cyanide masking reagent was replaced with non-toxic thiosulfates. Most common metals that interfere with PAN reagent are iron, copper and zinc. The iron and cupper were masked totally by thiosulfate masking reagent. 20% of zinc was masked by the same masking agent. If zinc in concentration less than 1 mg L^{-1} then it causes around 23 % interference and if it is in higher concentration, it causes around 64 % interference. This information will be mentioned clearly with the PAD. In addition, Due to the change in the buffer (from borate to carbonate) the behaviour of the manganese complex was changed and the one minutes detection time which

is very specific by PAN reagent was improved by 5 minutes colour stability range and hence more time for lay people (e.g., farmer) to take the photo of the PAD before the change in the colour intensity.

Another challenge is the sample introduction into the PAD especially that the PAD was made with cutting and the studied sample is soil extract. The PAD was aimed to be use for soil sample analysis and hence the one-layer PAD obviously was influenced by the organic matter content in the soil. The two extra layers were added to the original PAD in such away the sample pass into the empty layers first (to be filtered) and then the analyte with less slurry pass into the detection zone. Around 40 % of improvement in intensity was observed when empty layers were added. Sealing of the PAD by acrylic cover and laminated sheet was studies with pipetting and dipping sample introduction system. Using acrylic cover allowed only pipetting sample introduction due to the thickness of the cover. Lamination was studied when sample introduction area was made by scalpel or by Cricut instrument. The scalpel was used to make cross line sample entrance and circular sample entrance. The crosscut sample entrance resulted in inconvenient result with high standard deviation compared to when circular entrance which was then improved by using the circuit instrument. The PAD was sealed, and dipping system was used to introduce the sample and hence this will make it easier for the farmer to introduce the sample into the PAD compared to if the sample is pipetted. Dipping system with open circular hole (made by Cricut) for sample introduction instead of pipetting with no sealing improved the limit of detection from around 15 μM to 3.8 μM of manganese (it is around 4 times increase in the sensitivity).

The sensitivity, selectivity and stability of the PAD were important to consider getting PAD which can detect manganese within the required level. The PAD was able to detect 4.14 ± 0.30 mg kg^{-1} and 5.12 ± 1.88 mg kg^{-1} of manganese when scanner and phone was used for the detection respectively. This level is lower than the lower level of manganese in soil (10 mg kg^{-1} [130,131] below which fertilizer needs to be applied). The PAD was selective for manganese in the presence of the following interference.; NO_3^- (1g L^{-1}), Ca^{2+} (1g L^{-1}), Na^+ (1g L^{-1}), K^+ (1g L^{-1}), CO_3^{-2}(1g L^{-1}), PO_4^{-3}(0.5g L^{-1}), Cl^-(1g L^{-1}), SO_4^{-2}(1g L^{-1}), Co^{2+}(1 mg L^{-1}), Ni^{2+}(1 mg L^{-1}). In addition, the PAD can be stored in the freezer for around 2 months and, in room temperature (dark condition) for around 1month.

Similarly finding simple on-site extraction system for manganese by lay people is crucial. The extraction of manganese either in field or in lab require use of equipment which followed by filtration [444,446-449]. This PAD detection system was combined with cafetiere extraction system (same as suggested in chapter 4) for simple in field extraction of manganese. The cafetiere

efficiency was compared to the conventional shaker efficiency when excellent solvent (EDTA) was used in both methods. The cafetière was able to extract around 30% of manganese from soil. EDTA can complex manganese and it is not easy to release the captured manganese unless releasing agent is available or the detection method itself like ICP-MS does such degradation to the complex. Therefore, other safe solvents options which do not cause interference with the PAD and can easily release manganese were studied. Cafetiere with the use of NaCl solvent was able to extract around 10% of manganese from the soil sample. With the 10% of NaCl cafetière extraction, the efficiency of developed PAD was determined by comparison with ICP-MS which showed similar manganese content with no significant difference as the PAD for treated soil sample (John Innes 1).

In conclusion, simple 7 min Colorimetric Paper base sensor for manganese detection was made and improved to fit the field soil sample detection and lay people use. 10 % NaCl Cafetiere extraction efficiency of manganese was combined to the PAD detection system. In the future, this extraction efficiency needs to be improved (either by change solvent concentration or by working with mixing time). External standards (which was used in chapter 5) must be added for PAD-phone detection system to avoid unrobust result due to change in person who capture the image. Finally, the whole system needs to be tested with volunteers to determine its robustness.

Chapter 7 Discussion, conclusion and future work

7.1   Discussion

Agriculture is essential source of world food. It is also main source of income for some of low- and middle-income countries [418]. Plants needs macronutrients (N, P, K) and micronutrients (Mn, Zn, Cu, Fe, etc.). Nutrients is added to soil through the use of fertilizer. To control the use of fertilizer by farmer regular soil nutrients monitoring is required. There are lab-based (ion chromatography[1], ICP-MS[2]) and commercially available monitoring methods designed for use in the field [3,24,25] . However, these methods are time consuming and expensive, meaning they are often unaffordable to farmers in developing countries. Therefore, there is a need for simple, cheap, and reliable method for *in situ* determination of soil nutrients.

In this study a simple, inexpensive, and user-friendly workflow for routine *in situ* monitoring of nitrate and manganese in soil samples was developed. It is based on colorimetric paper-based sensors and extraction of nutrient using a common kitchen cafetière.

This was achieved by initially designing a simple device that was suitable for lay people for on-site nutrient determination. Second, colourimetry nitrite PADs were developed and improved for determination of nitrite in soil. Once established, it was used for determining the existence of nitrite or not in soil. The nitrite PAD was then developed into a device that was used for nitrate detection.

The workflow was designed to include recording of the PAD colour change measurements using a smart phone camera. To make this work the PADs required not to be affected by reagents colour. Previously described PADs utilised zinc as a reducing agent, however zinc has a dark colour that contribute to the intensity associated with the intensity of detected analyte, nitrates. Therefore, zinc addition to the PAD was improved to reduce that effect to extend allow reproducible result.

 A further critical step was the development of a simple and cheap method to extract nutrients from the soil. Hence, we developed a method that utilised a common kitchen cafetière. Once developed, the whole workflow (cafetière extraction followed by use of a PAD and mobile phone-based recording of the colour changes) was validated using IEC and CRM. Finally, the developed workflow for nitrate determination was tested with group of volunteers to assess its robustness and its simplicity. Observation of the volunteers, combined with their feedback (quantitative and qualitative) was used to make improvement to the system (e.g., improvement in the instruction sheet and way of doing the work).

A similar workflow based on paper sensor and cafetière extraction was also developed for detection of the manganese. The manganese PAD was developed and improve to be easier and safer to use by lay people. This was achieved by replacing a toxic reagent typically used in published colorimetric manganese assays with user-friendly and less toxic option that provide similar sensitivity which agree to the required environmental level. The workflow was also adapted by adopting simple dipping sample introduction system that reduced steps and reduced possibility of errors.

7.1.1 Device design

For field/ point of need devices there are five processes [279] to be performed by the end user: sample collection, sample processing, device operation, detection, and readout/interpretation. Complicated designs of PADs are common in the literature. Sometimes workflows are complicated including steps that require the user to do extra step like folding the device [282], cutting the device [283], sliding paper [284], adding solution, and pressing [285] . However, for the purposes of this study it was felt that these additional steps would create an overly complicated workflow, therefore a central design principle was to develop a simple and easy to use device which requires a minimum number of steps without compromising the quality of the analyte determination.

To achieve this several device designs were compared for their simplicity and sensitivity by monitoring their calibration and RSD, and by collection of qualitative information by researcher. Device 1 and device 2 comprised two layers where folding was required. This was both difficult to use, since the extra steps of folding and holding of the two layers were required and gave a high variation in the PADs outputs since the folding step varies each time. . Devices 3,4 and 5 featured flow channels, however these were not easy to use, and the flow was not uniform within channels. In addition, sample addition must be done by pipetting the sample which adds an extra level of complexity to the workflow. Devices 6 and 7 included valves. These required careful opening and closing is at appropriate times. This additional step was deemed to add complexity without appreciable gain.

In this study device 9 was chosen as it consisted of a single reaction zone, with no flow channel or valves, and samples could be added by dipping the device directly into collected water. This decision was based on first time handling of each PAD. The aim was to find a design which is easy to use and at the same time the design with acceptable sensitivity since several step reactions (detection and reduction) should happen within the PAD to detect analyte (e.g., nitrite and nitrate). This was why the study started with complicated device that can provide several

rooms for reaction steps and hence better sensitivity. However, handling such complicated device was not as easy as expected.

In general, the more the steps the more difficult users found the workflow and the fewer the steps the easier the work to be perform by end user. For device operation and detection, the more the steps the more the possibilities of errors. Addition steps like folding, holding, pressing, and pipetting may vary from user to user and hence the reproducibility maybe affected. The collected data with volunteers and observation showed that device 9 with no valves and no channels was the easiest to use.

7.1.2   Nitrite determination (PAD detection)

Nitrite and nitrate both can be detected by Griess reagent [61,349-351]. However, nitrate needs to be reduced first into nitrite then detected by the Griess reagent. Therefore, Nitrite paper devices were initially developed in this work. Nitrite is usually present in soil in small or negligible amounts; around 0.3 mg Kg^{-1} [366,367]. Therefore, a PAD with good sensitivity to environmental level was required. The sensitivity (sensitivity to the required level) of the PAD was improved by separating the components of Griess reagent into two different layers. This is in contrast to other studies (**Table 3.14**) which keep all component in the same layer. Separation of the components reduce their possible interaction together and provide step by step reactions, since nitrite should react first with sulphanilamide in the first layer and then with NED in the second layer. The sensitivity of the PAD increased by around 40% after this separation of reactants was implemented. The LoD of the PAD was 0.39±0.06 and 0.46±0.03 mg kg^{-1} when a scanner and a phone were used for image capture, respectively. All studied soil samples showed low, or no nitrite based on the result from the developed PAD and UV-Vis. The nitrite PAD was able to detect nitrite around its environmental level in soil.

7.1.3   Nitrate determination (PAD detection and cafetiere extraction)

PAD detection

The nitrite PAD was used to develop a nitrate PAD by adding a layer for deposition of the reducing agent (zinc). The developed PAD focus on deposition of reagents at multi layers which can be aligned above each other to avoid the complexity of the device during use. Zinc addition was challenging due to it dark colour, which contribute to the measured intensity in the colorimetric assay. Most published work relied on pipetting the zinc solution into the specific zone [290,291,293,298,310], however, some of these PADs [290,291,293] had separated areas for the reduction zone which was not aligned above the detection zone, and this made it possible to add zinc with its dark colour without influencing the intensity of colour in the detection zone. In another study

another layer was added to the PAD [295], the layer was called Zinculose and it embedded zinc particles in the cotton layer. This was practical to keep the zinc embedded within the reduction area of the device. However, this still required a lot of work and preparation of the material which then was added to the PAD. In addition, still the same problem exist which is it was unknown how much zinc was added. Another group was using weighting method to add zinc [296]. Each well in the PAD was added to zinc solution and this followed by weighing of the well before and after the zinc addition [296]. This was not practical and required time. In general pipetting zinc leads to accumulation of zinc and the development of dark colour that contribute to the intensity, therefore, in this study zinc was added by immersion of the reduction layer into zinc solution (under stirring) for 1 second only (to avoid the destroying the PAD). The stirring provided homogeneous zinc solution during addition. This method was easy, practical, reproducible, and it helped to avoid the accumulation of zinc compared when it was pipetted and by immersion the zinc particles were embedded into the two sides of the paper. The intensity from blank was reduced by around 22 % due to reduction in the dark colour of zinc. The sensitivity, selectivity and stability of the PAD were studied. The PAD was able to detect as low as 27.10 ± 2.64 mg kg^{-1} and 34.35 ± 2.77 mg kg^{-1} of nitrate within 8 minutes when scanner and phone was used for the detection respectively. This level is lower than the lower level of nitrate in soil (44mg kg^{-1} [348,426,427]) below which fertilizer needs to be applied. The PAD was selective for nitrate in the presence of the following interferents.; [Ca^{2+} (0.5 g L^{-1}), Na^+ (5 g L^{-1}), K^+ (5 g L^{-1}), Fe^{2+} (1 mg L^{-1}), Cu^{2+} (1mg L^{-1}), Zn^{2+} (0.2 g L^{-1}), Mn^{2+} (2 g L^1), CO_3^{-2} (0.08 g L^{-1}), PO_4^{-3} (2 g L^{-1}), Cl^- (3 g L^{-1}), SO_4^{-2} (10 g L^{-1})]. In addition, the PAD can be stored in the freezer for around 2 months and, in room temperature (dark condition) for around 2 weeks. Expiry date of the PAD is important to issue with the PAD when it is released for lay people use. This study ends up with small PAD (28.5 mm × 28.5 mm) for nitrate determination within environmental level in soil with four layers (layers provide filtration prior of detection). The PAD is portable, fast (8 min), easy to use, disposable, user-friendly, inexpensive (price ≤ £1) and can be used in resource limited setting.

Cafetière extraction

The developed PAD for nitrate determination was combined with extraction system which meet the field requirement. There are extraction methods which have been adopted for field work; however, they generally require equipment and consumables that are not easily available, such as shakers, chemicals [443-449], filter paper [420] and syringe filters [421]. To simplify ensure the workflow can be easily used some easily acquired equipment was tested. Three devices - cafetiere, an AeroPress coffee plunger and a paper cup - were compared for their ability and simplicity to extraction nitrate. The cup has no filtration system and the AeroPress was difficult to mix and required strong pushing. The cafetière was most efficient and easiest to use for extraction since

it provides good mixing due to the availability of plunger and good filtration system due to the availability of meshes at the end of plunger. The cafetière showed around 90% extraction efficiency of nitrate within total time of 5 minutes (2 minutes of mixing and 3 minutes of settling of soil extract). The extraction method was further improved by the replacement of the weighing machine with the use of the spoon to add the soil sample. In addition, mineral water was used as solvent (as it is easy to acquire) and compared to the use of DIW. Mineral water and a spoon to measure out soil showed similar performance to extractions using DIW and a balance. Cafetière provides multi advantages including the simplicity, availability of mixing, availability filtration, user-friendly and easily available equipment. The cafetière used in this work was used for 1.5 years and it is still in a good working condition. The full workflow provided reliable estimation of nitrate content in soil based on validation by IEC and CRM.

7.1.4   Nitrate workflow with volunteers

It is not reasonable to assume that a workflow will perform well in the field without testing it with a target audience. Many published articles [290-293,295,296,298,310,311] have used phone for their developed paper-based sensors and some are claiming that this is a simple system which can be used then by lay people. However, most were never tested with group of people. The developed workflow for nitrate determination consisted of two steps extraction (5 minutes cafetière extraction) and detection (8 min phone based colorimetric paper-based sensor) with a total time of 13 minutes. Each of these steps was evaluated separately by volunteers. Around 97% found the overall extraction work easy.

The efficiency of extraction by volunteers were determined by comparing with same soil samples extracted by researcher when IEC was used as detection method. Results suffered from high relative standard deviation of recovery which went as high as around 30-70%. This was attributed to several reasons: The use of the spoon for sample collection was a source of error. Very full spoons can cause overestimation of the result and the opposite can cause the opposite result. Another source of inconsistency was the way sample were mixed. Consequently, information was added into the instruction sheet regarding the proper use of the spoon and more information was added regarding the strength of mixing, which should be strong and vigorous to fully extract nitrate.

 The detection by the PAD was also evaluated by volunteers and compared to the researcher results. 96% of volunteers found the instructions describing the use of the PAD clear and 100% found the use of the phone easy. However, the quantitative results from the volunteers' PADs varied significantly from the researcher's results. When the colour (seen by eyes) from volunteers' PADs was compared to the colour of the researcher's PAD for all soil samples, the

colour does not vary significantly which means that the nitrate content should not vary significantly and that what IEC result showed. Therefore, this difference was attributed to the use of the phone to take the photos. The type of phone, location that the photo was taken and the distance between the PAD and phone were some factors that can affect image quality. Changing any of these parameters lead to change in the image quality and hence change in the result. Other people in literature solve this problem using box or software or some logarithm and math as mentioned in **section 1.4.3**. use of box is not efficient since photo can vary from person to person and use of logarithm is difficult. In this study external standards were introduced. External standard was used to determine the calibration line at the same time of analysis. An external set of standards was used with each photo taking for sample to avoid any error that may occur due to change in any of the mentioned parameters. Two soil samples were run again by volunteers after the improvement in the instruction sheet and the use of the external standard. The result from these PADs, used to detect nitrate agreed with the results from researchers with no significant difference (**section 5.7**).

In summary, this study showed that volunteers can independently perform the workflow for nitrate determination by following simple instruction sheets. The use of the workflow was easy and reliable if detailed instructions were given to volunteers. This problem of phone use was solved using external standards.

7.1.5   Manganese determination (PAD detection and cafetiere extraction)
PAD detection

Another soil nutrient which was studied in this work is manganese. Manganese was studied since it exists in small amounts in soil, and so can be used to test if the developed system can work with micronutrients. In this study the PAD for manganese detection was developed from previously described assays and adapted to remove the toxic components, thus making the assay applicable for general use [314,315]. The borate buffer in the detection reagent was replaced with the carbonate buffer which shows a similar result to the conventional borate. The cyanide masking reagent was replaced with thiosulfates. Common metals that interfere with the manganese detection reagent (PAN) are iron, copper and zinc ions. The iron and copper ions were masked totally by the thiosulfate masking reagent. 20% of zinc was masked by the same masking agent. If zinc ion is in concentrations less than 1 mg L^{-1} then it caused around 23 % interference and if it is in higher concentration, it caused around 64 % interference. This information will be mentioned clearly in the PAD instructions[314].

 Another challenge was the sample introduction to the PAD. The PAD was aimed to be use for soil sample analysis and hence as mentioned early the one-layer PAD was influenced by the

organic matter content in the soil. Two extra layers were added to the original PAD in such a way the sample passed into the empty layers first (to be filtered) and then the analyte, with less slurry passed into the detection zone. Around 40 % improvement in intensity was observed when the empty layers were added.

Lamination was used to seal the devices and a circular cut with a dipping system was used to introduce the sample hence this will make it easier for the farmer to introduce the sample into the PAD compared to if the sample is pipetted. A dipping system with an open circular hole (made by Cricut) for sample introduction instead of pipetting with no sealing improved the limit of detection from around 15 µM to 3.8 µM of manganese (it is around 4 times increase in the LoD). The PAD was able to detect (LoD) 4.14 ± 0.30 mg kg^{-1} and 5.12 ± 1.88 mg kg^{-1} of manganese when a scanner or phone was used for the detection respectively. This level is lower than the lower level of manganese in soil (10 mg kg^{-1} [130,131] below which fertilizer needs to be applied). The PAD was selective for manganese in the presence of the following interference; NO_3^- (1g L^{-1}), Ca^{2+} (1g L^{-1}), Na^+ (1g L^{-1}), K^+ (1g L^{-1}), CO_3^{-2} (1g L^{-1}), PO_4^{-3} (0.5g L^{-1}), Cl^- (1g L^{-1}), SO_4^{-2} (1g L^{-1}), Co^{2+} (1 mg L^{-1}), Ni^{2+} (1 mg L^{-1}). According to this study the PAD can be stored in the freezer for around 2 months and, at room temperature (dark condition) for around 1 month. In summary, other than the selectivity and sensitivity the developed PAD combined several positive characteristics that make it usable for on-site analysis of manganese in soil samples. It is easy (based on dipping sample introduction as for nitrate determination), safe (less toxic chemicals) and fast (with short time of detection 7 min), inexpensive (price ≤ £1, small amount of reagent is required, at least 60 devices can be prepared from 1 Whatman paper (32 cm diameter)), instrument-free (no instrument and no external power is required) and attached to multilayers (provide filtration of extract prior to detection).

Cafetière extraction

The cafetière was tested again for manganese extraction. The cafetière with EDTA solvent was able to extract around 30% of manganese from the soil. EDTA can complex manganese and it is not easy to release the captured manganese unless the releasing agent is available or the detection method itself like ICP-MS does such degradation to the complex. Therefore, other safe solvent options which do not cause interference with the PAD and can easily release manganese were studied. Cafetiere with the use of NaCl solvent was able to extract around 10% of manganese from the soil sample. The developed extraction was combined with the paper-based sensor for manganese determination.

The developed PAD (when cafetière was used for extraction and NaCl solvent) showed efficient results with no significant difference for manganese determination when compared with ICP-

MS, for treated soil sample (John Innes 1). Changing solvent and mixing are two parameters that can be further studied in the future to improve the extraction efficiency.

7.2   Conclusion

Non-efficient application of fertilizer by farmers can lead to poor crop yield (if deficient) and environmental problems (if used in excess). To apply the fertilizer properly regular monitoring of soil nutrients is required. Novel Cafetière extraction along with a colourimetric paper-based sensor and recording using a smartphone camera was successfully developed for on-site regular monitoring of nitrate and manganese in the soil.

Nitrate determination workflow in soil was developed and tested with volunteers. The workflow with 13 minutes total time for nitrate determination, 5 minutes extraction by cafetière (DIW solvent, around 90% extraction efficiency) and 8 minutes detection by the phone-based colourimetric paper-based sensor. The developed PAD was small, portable, fast, easy to use, disposable, user-friendly, inexpensive and can be used in resource-limited settings. The workflow showed promising results in detecting nitrate in the soil without the aid of an expert. Volunteers were able to independently perform the workflow for nitrate determination by following simple instruction sheets. In the future, the improved workflow, based on volunteers' feedback, needs to be tested with a bigger group of volunteers preferably directly in the field to determine the robustness of the workflow with the end user (farmers).

The workflow for manganese determination was developed and optimised in the lab to fit the field requirement. The final workflow consists of two steps 4 min cafetière extraction (NaCl solvent, around 10% extraction efficiency) and 7 min detection (colorimetric paper-based sensor) with a total time of 11 minutes. The developed PAD was easy (based on dipping sample introduction), user-friendly and fast (with a short time of detection of 7 min), safe (user-friendly chemicals were used) inexpensive (a small amount of reagent is required, not less than 60 devices can be prepared from one Whatman paper (32 cm diameter)), instrument-free (no instrument and no external power is required) and attached to multilayers (provide filtration of the extract before detection).   Further studies are required to improve the manganese extraction efficiency using a cafetière. Extraction solvents and the time of plunging are two parameters that can be further studied for this purpose. In addition, an external standard needs to be added to the system to improve phone detection. Finally, the robustness of the workflow in the field with lay people needs to be studied too.

The availability of such simple-to-work-with systems will enable farmers in low- and middle-income countries to do soil analysis regularly. Also, it provides a means for further research into

soil change under various conditions. Consequently, this enhances the crop production. The agriculture in the world may be improved and finally, this may contribute to the economy of these countries. This work also opens the horizon for more studies of paper microfluidic in soil. in addition, it pulled the paper microfluidic research toward field and soil analysis.

7.3 Future Work

The work for infield nutrient determination still requires lots of development. The paper device is still on the top of the benchwork. There are not many studies that study the use of the paper device in the field. Future work includes three main parts. Initially the development of the PAD, second the field work with lay people, third the development of the phone app. These three main parts should be studied together. There should be communication between the people who develop the PAD and people who extend the study in the field and people who develop the app to get the result. Group work and communication are the most usable ways to pull the paper device to the field and to be able to do a lot of work in this field of science in a short time.

Reference list / Bibliography

1 H. PARK, Y. KIM, D. W. LEE, S. LEE and K. LEE, *Analytical sciences,* 2002, **18**, 343-346 (DOI:10.2116/analsci.18.343).

2 J. A. Nunes, B. L. Batista, J. L. Rodrigues, N. M. Caldas, J. A. Neto and F. Barbosa Jr, *Journal of Toxicology and Environmental Health, Part A,* 2010, **73**, 878-887.

3 *Soil NPK Sensor For Soil Nutrients in Agriculture - Renke.*

4 A. Delgado and J. A. Gómez, *The soil. Physical, chemical and biological properties*, Springer, 2016.

5 T. Keller and I. Håkansson, *Geoderma,* 2010, **154**, 398-406.

6 M. A. Altieri and C. I. Nicholls, *Soil Tillage Res.,* 2003, **72**, 203-211.

7 R. Ghorbani, S. Wilcockson, A. Koocheki and C. Leifert, *Environmental Chemistry Letters,* 2008, **6**, 149-162.

8 J. B. Jones Jr, *Plant nutrition and soil fertility manual*, CRC press, 2012.

9 A. Osvalde, *Environmental and Experimental Biology,* 2011, **9**, 1-8.

10 P. Vejan, T. Khadiran, R. Abdullah and N. Ahmad, *J. Controlled Release,* 2021, **339**, 321-334 (DOI:10.1016/j.jconrel.2021.10.003).

11 S. A. Barber, in *Agronomic Research for Food*, ed. nonymous , 1976, p. 13-29.

12 V. I. Adamchuk, A. Dobermann, M. T. Morgan and S. M. Brouder, *Feasibility of on-the-go mapping of soil nitrate and potassium using ion-selective electrodes*, American Society of Agricultural and Biological Engineers, 2002.

13 E. D. Lund, M. C. Wolcott and G. P. Hanson, *TheScientificWorldJOURNAL,* 2001, **1**, 767-776.

14 Z. Zhao, G. Liu, Q. Liu, C. Huang, H. Li and C. Wu, *International journal of environmental research and public health,* 2018, **15**, 1818.

15 A. L. Srivastav, in *Agrochemicals Detection, Treatment and Remediation*, ed. M. N. V. Prasad, Butterworth-Heinemann, 2020, p. 143-159.

16 L. Ngatia, J. M. Grace III, D. Moriasi and R. Taylor, *Monitoring of marine pollution,* 2019, **1**, 1-17.

17 G. E. Likens and F. H. Bormann, *Science,* 1974, **184**, 1176-1179.

18 S. Padua, T. Chattopadhyay, S. Bandyopadhyay, S. Ramchandran, R. K. Jena, P. Ray, P. D. Roy, U. Baruah, K. D. Sah and S. K. Singh, *Curr. Sci.,* 2018, **114**, 1241-1249.

19 J. S. Fritz, *Anal. Chem.,* 1987, **59**, 335A-344A.

20 P. E. Jackson, C. Weigert, C. A. Pohl and C. Saini, *Journal of Chromatography A,* 2000, **884**, 175-184 (DOI:10.1016/S0021-9673(99)01315-1).

21 J. A. Morales, L. S. de Graterol and J. Mesa, *Journal of Chromatography A,* 2000, **884**, 185-190.

22 Y. Miura and H. Hamada, *Journal of Chromatography A,* 1999, **850**, 153-160.

23 J. A. Nunes, B. L. Batista, J. L. Rodrigues, N. M. Caldas, J. A. Neto and F. Barbosa Jr, *Journal of Toxicology and Environmental Health, Part A,* 2010, **73**, 878-887.

24 , https://www.thomassci.com//www.thomassci.com/Laboratory-Supplies/Water-Quality-Test-Kits/_/MQuant-Manganese-Test-Method-colorimetric-with-test-strips-and-reagents, (accessed Aug 8, 2023).

25 , https://www.camlab.co.uk/manganese-lr-test-kit-mn-pan-range-0-0-7mg-l, (accessed Aug 8, 2023).

26 https://www.simplexhealth.co.uk, (accessed 13/01/ 2022).

27 E. K. Sackmann, A. L. Fulton and D. J. Beebe, *Nature,* 2014, **507**, 181-189 (DOI:10.1038/nature13118).

28 J. Credou and T. Berthelot, *J.Mater.Chem.B,* 2014, **2**, 4767-4788 (DOI:10.1039/C4TB00431K).

29 K. Abe, K. Suzuki and D. Citterio, *Anal. Chem.,* 2008, **80**, 6928-6934 (DOI:10.1021/ac800604v).

30 B. Li, L. Fu, W. Zhang, W. Feng and L. Chen, *Electrophoresis,* 2014, **35**, 1152-1159 (DOI:10.1002/elps.201300583).

31 C. Chen, W. Yeh, T. Tsai, Y. Li and C. Chen, *Lab on a chip,* 2019, **19**, 598-607 (DOI:10.1039/C8LC01255E).

32 K. Shrivas, Monisha, T. Kant, I. Karbhal, R. Kurrey, B. Sahu, D. Sinha, G. K. Patra, M. K. Deb and S. Pervez, *Analytical and bioanalytical chemistry,* 2020, **412**, 1573-1583.

33 J. Xu, X. Chen, H. Khan and L. Yang, *Sensors Actuators B: Chem.,* 2021, **335**, 129707 (DOI:10.1016/j.snb.2021.129707).

34 S. Patel, K. Shrivas, D. Sinha, Monisha, T. Kumar Patle, S. Yadav, S. S. Thakur, M. K. Deb and S. Pervez, *Food Chem.,* 2022, **383**, 132449 (DOI:10.1016/j.foodchem.2022.132449).

35 S. Richardson, A. Iles, J. M. Rotchell, T. Charlson, A. Hanson, M. Lorch and N. Pamme, *Plos one,* 2021, **16**, e0260102.

36 D. R. Keeney and D. W. Nelson, in *Methods of Soil Analysis*, ed. nonymous , 1983, p. 643-698.

37 H. Marschner, *Marschner's mineral nutrition of higher plants*, Academic press, 2011.

38 Z. Wang, Z. Zong, S. Li and B. Chen, *Huan jing ke xue= Huanjing kexue,* 2002, **23**, 79-83.

39 F. Gastal and G. Lemaire, *J. Exp. Bot.,* 2002, **53**, 789-799.

40 V. A. Sisson, T. W. Rufty and R. E. Williamson, *Crop Sci.,* 1991, **31**, 1615-1620.

41 E. G. Bollard, *Annual Review of Plant Physiology,* 1960, **11**, 141-166.

42 R. Novoa and R. S. Loomis, *Plant Soil,* 1981, **58**, 177-204.

43 S. J. Leghari, N. A. Wahocho, G. M. Laghari, A. HafeezLaghari, G. MustafaBhabhan, K. HussainTalpur, T. A. Bhutto, S. A. Wahocho and A. A. Lashari, *Advances in Environmental Biology,* 2016, **10**, 209-219.

44 A. D. Glass, *Crit. Rev. Plant Sci.,* 2003, **22**, 453-470.

45 T. Dong, J. Li, Y. Zhang, H. Korpelainen, Ü Niinemets and C. Li, *Tree Physiol.,* 2015, **35**, 632-643.

46 T. R. Gopalakrishnan, *Vegetable crops*, New india publishing, 2007.

47 N. H. Hamarashid, M. A. Othman and M. H. Hussain, *Egypt.J.Exp.Biol.(Bot.),* 2010, **6**, 59-64.

48 G. L. Terman, *Adv. Agron.,* 1980, **31**, 189-223 (DOI:10.1016/S0065-2113(08)60140-6).

49 K. W. Goulding, N. J. Bailey, N. J. Bradbury, P. Hargreaves, M. Howe, D. V. Murphy, P. R. Poulton and T. W. Willison, *The New Phytologist,* 1998, **139**, 49-58.

50 T. B. Singh, A. Ali, M. Prasad, A. Yadav, P. Shrivastav, D. Goyal and P. K. Dantu, *Contaminants in agriculture: sources, impacts and management,* 2020, , 61-77.

51 F. J. Stevenson, *Soil nitrogen,* 1965, **10**, 1-42.

52 S. F. Ledgard and K. E. Giller, *Nitrogen fertilization in the environment.Ed.PE Bacon,* 1995, , 443-486.

53 K. Mohammadi, Y. Sohrabi, G. Heidari, S. Khalesro and M. Majidi, *African Journal of Agricultural Research,* 2012, **7**, 1782-1788.

54 V. Smil, *Enriching the earth: Fritz Haber, Carl Bosch, and the transformation of world food production*, MIT press, 2004.

55 A. A. MacLean, *Am. Potato J.,* 1983, **60**, 913-918.

56 K. C. Cameron, H. J. Di and J. L. Moir, *Ann. Appl. Biol.,* 2013, **162**, 145-173 (DOI:10.1111/aab.12014).

57 K. C. Cameron, H. J. Di and J. L. Moir, *Ann. Appl. Biol.,* 2013, **162**, 145-173.

58 S. S. Mirvish, *N-nitroso compounds, nitrite, and nitrate: Possible implications for the causation of human cancer*, Elsevier, 2013.

59 P. Griess, *Berichte der deutschen chemischen Gesellschaft,* 1879, **12**, 426-428.

60 A. C. Bratton and E. K. Marshall Jr, *J. Biol. Chem.,* 1939, **128**, 537-550.

61 L. Váradi, M. Breedon, F. F. Chen, A. Trinchi, I. S. Cole and G. Wei, *RSC advances,* 2019, **9**, 3994-4000.

62 B. Narayana and K. Sunil, *Eurasian Journal of Analytical Chemistry,* 2009, **4**, 204-214.

63 E. Szekely, *Commun. Soil Sci. Plant Anal.,* 1991, **22**, 1295-1302.

64 R. Puchades, M. D. Pastor and A. Maquieira, *Commun. Soil Sci. Plant Anal.,* 1994, **25**, 3257-3280.

65 A. Henriksen and A. R. Selmer-Olsen, *Analyst,* 1970, **95**, 514-518.

66 T. A. Doane and W. R. Horwáth, *Anal. Lett.,* 2003, **36**, 2713-2722.

67 E. Murray, E. P. Nesterenko, M. McCaul, A. Morrin, D. Diamond and B. Moore, *Analytical Methods,* 2017, **9**, 680-687.

68 R. C. Dalal and R. J. Henry, *Soil Sci. Soc. Am. J.,* 1986, **50**, 120-123.

69 R. V. Rossel, D. Walvoort, A. B. McBratney, L. J. Janik and J. O. Skjemstad, *Geoderma,* 2006, **131**, 59-75.

70 S. Shibusawa, *On-line real time soil sensor*, IEEE, 2003.

71 C. D. Christy, P. Drummond and D. A. Laird, *An on-the-go spectral reflectance sensor for soil*, American Society of Agricultural and Biological Engineers, 2003.

72 M. R. Ehsani, S. K. Upadhyaya, D. Slaughter, S. Shafii and M. Pelletier, *Precision agriculture,* 1999, **1**, 219-236.

73 Y. Shao, C. Du, Y. Shen, F. Ma and J. Zhou, *Analytical Methods,* 2017, **9**, 748-755.

74 M. R. Ehsani, S. K. Upadhyaya, W. R. Fawcett, L. V. Protsailo and D. Slaughter, *Trans. ASAE,* 2001, **44**, 1931.

75 A. Shaviv, A. Kenny, I. Shmulevitch, L. Singher, Y. Raichlin and A. Katzir, *Environ. Sci. Technol.,* 2003, **37**, 2807-2812.

76 R. Linker, A. Kenny, A. Shaviv, L. Singher and I. Shmulevich, *Appl. Spectrosc.,* 2004, **58**, 516-520.

77 F. Gan, K. Wu, F. Ma, C. Wei and C. Du, *Heliyon,* 2022, **8**.

78 D. C. Harris, *Quantitative chemical analysis*, W. H. Freeman, New York, 2010.

79 P. Mikuška and Z. Večeřa, *Anal. Chim. Acta,* 2003, **495**, 225-232 (DOI:10.1016/j.aca.2003.08.013).

80 C. Garside, *Mar. Chem.,* 1982, **11**, 159-167 (DOI:10.1016/0304-4203(82)90039-1).

81 M. Yaqoob, B. Folgado Biot, A. Nabi and P. J. Worsfold, *Luminescence,* 2012, **27**, 419-425.

82 H. Gary, *Analyst,* 1983, **108**, 1274-1296.

83 R. D. Cox and C. W. Frank, *J. Anal. Toxicol.,* 1982, **6**, 148-152.

84 C. Garside, *Mar. Chem.,* 1982, **11**, 159-167.

85 E. Nagababu and J. M. Rifkind, in *Free radicals and antioxidant protocols*, ed. nonymous , Springer, 2009, p. 41-49.

86 T. Aoki, S. Fukuda, Y. Hosoi and H. Mukai, *Anal. Chim. Acta,* 1997, **349**, 11-16.

87 P. S. Francis and C. F. Hogan, in *Comprehensive Analytical Chemistry*, ed. nonymous , Elsevier, 2008, p. 343-373.

88 D. He, Z. Zhang, Y. Huang and Y. Hu, *Food Chem.,* 2007, **101**, 667-672.

89 A. Townshend, *Analyst,* 1990, **115**, 495-500.

90 E. D. Coppola, A. F. Wickroski and J. G. Hanna, *Journal of the Association of Official Analytical Chemists,* 1975, **58**, 469-473.

91 H. R. H. Ali, A. I. Hassan, Y. F. Hassan and M. M. El-Wekil, *Microchemical Journal,* 2021, **164**, 105982.

92 B. K. Afghan and J. F. Ryan, *Anal. Chem.,* 1975, **47**, 2347-2353.

93 A. K. Nussler, M. Glanemann, A. Schirmeier, L. Liu and N. C. Nüssler, *Nature protocols,* 2006, **1**, 2223-2226.

94 S. H. Lee and L. R. Field, *Anal. Chem. (Wash.),* 1984, **56**, 2647-2653 (DOI:10.1021/ac00278a007).

95 A. Lapat, L. Székelyhidi and I. Hornyák, *Biomedical chromatography,* 1997, **11**, 102-104 (DOI:10.1002/(SICI)1099-0801(199703)11:2).

96 L. Qi, R. Liang, T. Jiang and W. Qin, *TrAC Trends in Analytical Chemistry,* 2022, **150**, 116572 (DOI:10.1016/j.trac.2022.116572).

97 R. De Marco, G. Clarke and B. Pejcic, *Electroanalysis,* 2007, **19**, 1987-2001 (DOI:10.1002/elan.200703916).

98 K. J. Sibley, G. R. Brewster, T. Astatkie, J. F. Adsett and P. C. Struik, in *Advances in measurement systems*, ed. nonymous , IntechOpen, 2010.

99 R. Myers and E. A. Paul, *Can. J. Soil Sci.,* 1968, **48**, 369-371.

100 M. K. Mahendrappa, *Soil Sci.,* 1969, **108**, 132-136.

101 J. Choosang, A. Numnuam, P. Thavarungkul, P. Kanatharana, T. Radu, S. Ullah and A. Radu, *Sensors,* 2018, **18**, 3555.

102 J. F. Adsett, J. A. Thottan and K. J. Sibley, *Appl. Eng. Agric.,* 1999, **15**, 351.

103 V. I. Adamchuk, E. D. Lund, B. Sethuramasamyraja, M. T. Morgan, A. Dobermann and D. B. Marx, *Comput. Electron. Agric.,* 2005, **48**, 272-294.

104 H. Park, Y. Kim, D. W. Lee, S. LEE and K. LEE, *Analytical sciences,* 2002, **18**, 343-346.

105 S. A. Glazier, E. R. Campbell and W. H. Campbell, *Anal. Chem.,* 1998, **70**, 1511-1515.

106 L. H. Larsen, L. R. Damgaard, T. Kjær, T. Stenstrøm, A. Lynggaard-Jensen and N. P. Revsbech, *Water Res.,* 2000, **34**, 2463-2468.

107 D. Kirstein, L. Kirstein, F. Scheller, H. Borcherding, J. Ronnenberg, S. Diekmann and P. Steinrücke, *J Electroanal Chem,* 1999, **474**, 43-51.

108 L. H. Larsen, T. Kjær and N. P. Revsbech, *Anal. Chem.,* 1997, **69**, 3527-3531.

109 M. Kalbasi and M. A. Tabatabai, *Commun. Soil Sci. Plant Anal.,* 1985, **16**, 787-800.

110 M. Colina and P. Gardiner, *Journal of Chromatography A,* 1999, **847**, 285-290.

111 Y. Zhang, Y. Zhou, L. Liu and Y. Zhu, *Journal of Zhejiang University Science B,* 2007, **8**, 507-511.

112 Dionex corporation, *Sunnyvale, CA,* .

113 K. Ito, Y. Takayama, N. Makabe, R. Mitsui and T. Hirokawa, *Journal of Chromatography A,* 2005, **1083**, 63-67 (DOI:10.1016/j.chroma.2005.05.073).

114 M. I. H. Helaleh and T. Korenaga, *Journal of Chromatography B: Biomedical Sciences and Applications,* 2000, **744**, 433-437 (DOI:10.1016/S0378-4347(00)00264-4).

115 W. A. Dick and M. A. Tabatabai, *Soil Sci. Soc. Am. J.,* 1979, **43**, 899-904.

116 M. Turrión, J. Gallardo and M. González, *Commun. Soil Sci. Plant Anal.,* 1999, **30**, 1137-1152.

117 O. M. Kachurina, H. Zhang, W. R. Raun and E. G. Krenzer, *Commun. Soil Sci. Plant Anal.,* 2000, **31**, 893-903.

118 S. Cavalli, S. Polesello and S. Valsecchi, *Journal of Chromatography A,* 2005, **1085**, 42-46 (DOI:10.1016/j.chroma.2004.12.089).

119 F. Tagliaro, G. Manetto, F. Crivellente and F. P. Smith, *Forensic Sci. Int.,* 1998, **92**, 75-88.

120 M. J. Moorcroft, J. Davis and R. G. Compton, *Talanta,* 2001, **54**, 785-803.

121 E. Martínková, T. Křžek and P. Coufal, *Chemical papers,* 2014, **68**, 1008-1014.

122 A. Chattopadhyay and D. S. Hage, *J. Chem. Educ.,* 1998, **75**, 1588-1590.

123 D. Kaniansky, I. Zelensky, A. Hybenova and F. I. Onuska, *Anal. Chem.,* 1994, **66**, 4258-4264.

124 A. A. Okemgbo, H. H. Hill, W. F. Siems and S. G. Metcalf, *Anal. Chem.,* 1999, **71**, 2725-2731.

125 J. Huang, P. Liu, Q. Sun, H. Zhang, Y. Zhang and K. Wang, *Anal. Lett.,* 2017, **50**, 1620-1629.

126 *Research and Markets: Marschner's Mineral Nutrition of Higher Plants - A Third Edition Guide with Full Coverage on the Latest Molecular Advances*, Normans Media Ltd, 2011.

127 J. P. Lynch and S. B. St.Clair, *Field Crops Res.,* 2004, **90**, 101-115 (DOI:https://doi.org/10.1016/j.fcr.2004.07.008).

128 D. R. Lovley, T. Ueki, T. Zhang, N. S. Malvankar, P. M. Shrestha, K. A. Flanagan, M. Aklujkar, J. E. Butler, L. Giloteaux, A. Rotaru, D. E. Holmes, A. E. Franks, R. Orellana, C. Risso and K. P. Nevin, *Adv. Microb. Physiol.,* 2011, **59**, 1-100 (DOI:https://doi.org/10.1016/B978-0-12-387661-4.00004-5).

129 K. Geszvain, C. Butterfield, R. E. Davis, A. S. Madison, S. Lee, D. L. Parker, A. Soldatova, T. G. Spiro, G. W. Luther III and B. M. Tebo, *Biochem. Soc. Trans.,* 2012, **40**, 1244-1248.

130 S. Alejandro, S. Höller, B. Meier and E. Peiter, *Frontiers in plant science,* 2020, **11**, 300.

131 H. Marschner, *Marschner's mineral nutrition of higher plants*, Academic press, 2011.

132 A. V. Filgueiras, J. L. Capelo, I. Lavilla and C. Bendicho, *Talanta,* 2000, **53**, 433-441 (DOI:https://doi.org/10.1016/S0039-9140(00)00510-5).

133 F. Baruthio, O. Guillard, J. Arnaud, F. Pierre and R. Zawislak, *Clin. Chem.,* 1988, **34**, 227-234.

134 U. Tinggi, C. Reilly and C. Patterson, *Food Chem.,* 1997, **60**, 123-128 (DOI:https://doi.org/10.1016/S0308-8146(96)00328-7).

135 K. C. Teo and J. Chen, *Analyst,* 2001, **126**, 534-537.

136 I. Lavilla and C. Bendicho, in *Water Extraction of Bioactive Compounds*, ed. H. Dominguez González and M. J. González Muñoz, Elsevier, 2017, p. 291-316.

137 E. Wieteska, A. Zióek and A. Drzewińska, *Anal. Chim. Acta,* 1996, **330**, 251-257 (DOI:https://doi.org/10.1016/0003-2670(96)00187-0).

138 U. S. Erdemir and S. Gucer, *J. Cereal Sci.,* 2016, **69**, 199-206 (DOI:https://doi.org/10.1016/j.jcs.2016.03.009).

139 R. N. Carvalho, G. B. Brito, M. G. Korn, J. S. Teixeira, F. d. S. Dias, A. F. Dantas and L. S. Teixeira, *Analytical Methods,* 2015, **7**, 8714-8719.

140 N. Oleszczuk, J. T. Castro, M. M. da Silva, M. d. G. A. Korn, B. Welz and M. G. R. Vale, *Talanta,* 2007, **73**, 862-869 (DOI:https://doi.org/10.1016/j.talanta.2007.05.005).

141 E. Bağda, H. Altundağ and M. Soylak, *Biol. Trace Elem. Res.,* 2017, **179**, 334-339.

142 American Public Health Association, American Water Works Association, Water Pollution Control Federation and Water Environment Federation, *Standard methods for the examination of water and wastewater*, American Public Health Association., 1912.

143 E. Prasetyo, E. Purwaningsih and W. Astuti, *On the determination of manganese in the presence of iron in pregnant leach solution using derivative spectrophotometry*, IOP Publishing, 2019.

144 M. M. Hatat-Fraile and B. Barbeau, *Talanta,* 2019, **194**, 786-794 (DOI:https://doi.org/10.1016/j.talanta.2018.11.003).

145 K. B. Narayanan and H. H. Park, *Spectrochimica Acta Part A: Molecular and Biomolecular Spectroscopy,* 2014, **131**, 132-137 (DOI:https://doi.org/10.1016/j.saa.2014.04.081).

146 Y. He and X. Zhang, *Sensors Actuators B: Chem.,* 2016, **222**, 320-324 (DOI:https://doi.org/10.1016/j.snb.2015.08.089).

147 K. Goto, S. Taguchi, Y. Fukue, K. Ohta and H. Watanabe, *Talanta,* 1977, **24**, 752-753 (DOI:https://doi.org/10.1016/0039-9140(77)80206-3).

148 S. Ahrland and R. G. Herman, *Anal. Chem.,* 1975, **47**, 2422-2426.

149 F. H. Pollard, P. Hanson and W. J. Geary, *Anal. Chim. Acta,* 1959, **20**, 26-31 (DOI:https://doi.org/10.1016/0003-2670(59)80004-0).

150 W. J. Geary, G. Nickless and F. H. Polland, *Anal. Chim. Acta,* 1962, **26**, 575-582 (DOI:https://doi.org/10.1016/S0003-2670(00)88433-0).

151 R. E. Sturgeon, S. S. Berman, A. Desaulniers and D. S. Russell, *Anal. Chem.,* 1979, **51**, 2364-2369.

152 Ç Arpa Şahin, M. Efeçınar and N. Şatıroğlu, *J. Hazard. Mater.,* 2010, **176**, 672-677 (DOI:https://doi.org/10.1016/j.jhazmat.2009.11.084).

153 R. Khani and F. Shemirani, *Clean Soil Air Water,* 2010, **38**, 1177-1183 (DOI:10.1002/clen.201000244).

154 H. Górecka, K. Chojnacka and H. Górecki, *Talanta,* 2006, **70**, 950-956 (DOI:10.1016/j.talanta.2006.05.061).

155 S. K. Mehta, *Rasayan J Chem,* 2016, **9**, 603-607.

156 M. J. Ahmed, M. T. Islam and S. P. Lucky, *American Chemical Science Journal,* 2014, **4**, 357-383.

157 W. Zhou, M. Dou, S. S. Timilsina, F. Xu and X. Li, *Lab on a Chip,* 2021, **21**, 2658-2683.

158 S. Böckmann, I. Titov and M. Gerken, *AgriEngineering,* 2021, **3**, 783-796.

159 P. M. Mafla-Endara, C. Arellano-Caicedo, K. Aleklett, M. Pucetaite, P. Ohlsson and E. C. Hammer, *Communications biology,* 2021, **4**, 889.

160 M. Pucetaite, P. Ohlsson, P. Persson and E. Hammer, *Soil Biol. Biochem.,* 2021, **153**, 108078 (DOI:10.1016/j.soilbio.2020.108078).

161 X. Zhu, K. Wang, H. Yan, C. Liu, X. Zhu and B. Chen, *Environ. Sci. Technol.,* 2022, **56**, 711-731.

162 S. Dudala, S. K. Dubey and S. Goel, *IEEE Sensors Journal,* 2020, **20**, 4504-4511.

163 C. E. Stanley, G. Grossmann, X. C. i Solvas and A. J. deMello, *Lab on a Chip,* 2016, **16**, 228-241.

164 A. Pal, S. K. Dubey and S. Goel, *Comput. Electron. Agric.,* 2022, **195**, 106856 (DOI:10.1016/j.compag.2022.106856).

165 Z. Xu, X. Wang, R. J. Weber, R. Kumar and L. Dong, *IEEE Sensors Journal,* 2017, **17**, 4330-4339.

166 M. Smolka, D. Puchberger-Enengl, M. Bipoun, A. Klasa, M. Kiczkajlo, W. Śmiechowski, P. Sowiński, C. Krutzler, F. Keplinger and M. J. Vellekoop, *Precision Agriculture,* 2017, **18**, 152-168.

167 Y. Hong, Z. Xia, J. Su, R. Wang, Y. Chang, Q. Huang, L. Wei and X. Chen, *Agriculture,* 2023, **13**, 2226.

168 M. L. Braunger, F. M. Shimizu, M. J. Jimenez, L. R. Amaral, M. H. d. O. Piazzetta, Â L. Gobbi, P. S. Magalhães, V. Rodrigues, O. N. Oliveira Jr and A. Riul Jr, *Chemosensors,* 2017, **5**, 14.

169 C. Tang, D. Fu, R. Wang, X. Zhang, L. Wei, M. Li, C. Li, Q. Cao and X. Chen, *IEEE Sensors Journal,* 2024, .

170 A. Baysal, N. Ozbek and S. Akman, *Waste-Water Treatment Technologies and Recent Analytical Developments (ed.FSG Einschlag, L.Carlos),* 2013, , 145-171.

171 R. J. Moon, A. Martini, J. Nairn, J. Simonsen and J. Youngblood, *Chem. Soc. Rev.,* 2011, **4**, 3941-3994 (DOI:10.1039/c0cs00108b).

172 M. Vert, Y. Doi, K. Hellwich, M. Hess, P. Hodge, P. Kubisa, M. Rinaudo and F. Schué, *Pure and Applied Chemistry,* 2012, **84**, 377-410.

173 S. Kalia, B. S. Kaith and I. Kaur, *Cellulose fibers: bio-and nano-polymer composites: green chemistry and technology*, Springer Science & Business Media, 2011.

174 D. D. Liana, B. Raguse, J. J. Gooding and E. Chow, *Sensors,* 2012, **12**, 11505-11526.

175 E. M. Fenton, M. R. Mascarenas, G. P. López and S. S. Sibbett, *ACS applied materials & interfaces,* 2008, **1**, 124-129.

176 Y. Lu, B. Lin and J. Qin, *Anal. Chem.,* 2011, **83**, 1830-1835.

177 Y. Lu, W. Shi, L. Jiang, J. Qin and B. Lin, *Electrophoresis,* 2009, **30**, 1497-1500.

178 Anushka, A. Bandopadhyay and P. K. Das, *The European Physical Journal Special Topics,* 2023, **232**, 781-815.

179 A. Martinez, S. Phillips, M. Butte and G. Whitesides, *Angewandte Chemie International Edition,* 2007, **46**, 1318-1320 (DOI:10.1002/anie.200603817).

180 J. Ma, L. Jiang, X. Pan, H. Ma, B. Lin and J. Qin, *Microfluidics and nanofluidics,* 2010, **9**, 1247-1252.

181 W. Dungchai, O. Chailapakul and C. S. Henry, *Analyst,* 2011, **136**, 77-82.

182 J. P. Metters, S. M. Houssein, D. K. Kampouris and C. E. Banks, *Analytical Methods,* 2013, **5**, 103-110.

183 Z. Nie, F. Deiss, X. Liu, O. Akbulut and G. M. Whitesides, *Lab on a Chip,* 2010, **10**, 3163-3169.

184 A. Apilux, Y. Ukita, M. Chikae, O. Chailapakul and Y. Takamura, *Lab on a Chip,* 2013, **13**, 126-135.

185 K. Yamada, T. G. Henares, K. Suzuki and D. Citterio, *Angew. Chem. Int. Ed.,* 2015, **54**, 5294-5310 (DOI:10.1002/anie.201411508).

186 X. Li, J. Tian, G. Garnier and W. Shen, *Colloids and surfaces B: Biointerfaces,* 2010, **76**, 564-570.

187 X. Li, J. Tian, T. Nguyen and W. Shen, *Anal. Chem.,* 2008, **80**, 9131-9134.

188 J. S. Ng and M. Hashimoto, *Rsc Advances,* 2020, **10**, 29797-29807.

189 R. Ghosh, S. Gopalakrishnan, R. Savitha, T. Renganathan and S. Pushpavanam, *Scientific reports,* 2019, **9**, 7896.

190 J. Olkkonen, K. Lehtinen and T. Erho, *Anal. Chem.,* 2010, **82**, 10246-10250.

191 M. A. Mahmud, E. J. Blondeel, M. Kaddoura and B. D. MacDonald, *Analyst,* 2016, **141**, 6449-6454.

192 J. Nie, Y. Liang, Y. Zhang, S. Le, D. Li and S. Zhang, *Analyst,* 2013, **138**, 671-676.

193 Y. Lu, W. Shi, J. Qin and B. Lin, *Anal. Chem.,* 2009, **82**, 329-335.

194 L. Xiao, X. Liu, R. Zhong, K. Zhang, X. Zhang, X. Zhou, B. Lin and Y. Du, *Electrophoresis,* 2013, **34**, 3003-3007.

195 M. Younas, A. Maryam, M. Khan, A. A. Nawaz, S. H. I. Jaffery, M. N. Anwar and L. Ali, *Microfluidics and Nanofluidics,* 2019, **23**, 38.

196 D. A. Bruzewicz, M. Reches and G. M. Whitesides, *Anal. Chem.,* 2008, **80**, 3387-3392.

197 T. Songjaroen, W. Dungchai, O. Chailapakul and W. Laiwattanapaisal, *Talanta,* 2011, **85**, 2587-2593.

198 K. L. Dornelas, N. Dossi and E. Piccin, *Anal. Chim. Acta,* 2015, **858**, 82-90.

199 V. F. Curto, N. Lopez-Ruiz, L. F. Capitan-Vallvey, A. J. Palma, F. Benito-Lopez and D. Diamond, *Rsc Advances,* 2013, **3**, 18811-18816.

200 Y. Jiang, Z. Hao, Q. He and H. Chen, *RSC advances,* 2016, **6**, 2888-2894.

201 T. M. Cardoso, F. R. de Souza, P. T. Garcia, D. Rabelo, C. S. Henry and W. K. Coltro, *Anal. Chim. Acta,* 2017, **974**, 63-68.

202 N. Nuchtavorn and M. Macka, *Anal. Chim. Acta,* 2016, **919**, 70-77.

203 W. J. Paschoalino, S. Kogikoski Jr, J. T. Barragan, J. F. Giarola, L. Cantelli, T. M. Rabelo, T. M. Pessanha and L. T. Kubota, *ChemElectroChem,* 2019, **6**, 10-30.

204 E. Noviana, C. P. McCord, K. M. Clark, I. Jang and C. S. Henry, *Lab on a Chip,* 2020, **20**, 9-34.

205 J. Mettakoonpitak, K. Boehle, S. Nantaphol, P. Teengam, J. A. Adkins, M. Srisa-Art and C. S. Henry, *Electroanalysis,* 2016, **28**, 1420-1436.

206 J. A. Adkins and C. S. Henry, *Anal. Chim. Acta,* 2015, **891**, 247-254.

207 J. V. Macpherson, *Physical Chemistry Chemical Physics,* 2015, **17**, 2935-2949.

208 R. L. McCreery, *Chem. Rev.,* 2008, **108**, 2646-2687.

209 N. Dossi, R. Toniolo, A. Pizzariello, F. Impellizzieri, E. Piccin and G. Bontempelli, *Electrophoresis,* 2013, **34**, 2085-2091.

210 V. X. Oliveira, A. A. Dias, L. L. Carvalho, T. M. Cardoso, F. Colmati and W. K. Coltro, *Analytical sciences,* 2018, **34**, 91-95.

211 S. Cinti, N. Colozza, I. Cacciotti, D. Moscone, M. Polomoshnov, E. Sowade, R. R. Baumann and F. Arduini, *Sensors Actuators B: Chem.,* 2018, **265**, 155-160.

212 Q. Cao, B. Liang, T. Tu, J. Wei, L. Fang and X. Ye, *RSC advances,* 2019, **9**, 5674-5681.

213 C. Wang, J. W. Hennek, A. Ainla, A. A. Kumar, W. Lan, J. Im, B. S. Smith, M. Zhao and G. M. Whitesides, *Anal. Chem.,* 2016, **88**, 6326-6333.

214 P. Teengam, W. Siangproh, S. Tontisirin, A. Jiraseree-amornkun, N. Chuaypen, P. Tangkijvanich, C. S. Henry, N. Ngamrojanavanich and O. Chailapakul, *Sensors Actuators B: Chem.,* 2021, **326**, 128825.

215 W. Dungchai, O. Chailapakul and C. S. Henry, *Anal. Chem.,* 2009, **81**, 5821-5826.

216 Z. Nie, C. A. Nijhuis, J. Gong, X. Chen, A. Kumachev, A. W. Martinez, M. Narovlyansky and G. M. Whitesides, *Lab on a Chip,* 2010, **10**, 477-483.

217 L. Fu and Y. Wang, *TrAC Trends in Analytical Chemistry,* 2018, **107**, 196-211.

218 A. Roda and M. Guardigli, *Analytical and bioanalytical chemistry,* 2012, **402**, 69-76.

219 J. Yu, L. Ge, J. Huang, S. Wang and S. Ge, *Lab on a Chip,* 2011, **11**, 1286-1291.

220 W. Alahmad, K. Uraisin, D. Nacapricha and T. Kaneta, *Analytical Methods,* 2016, **8**, 5414-5420.

221 S. Wang, L. Ge, L. Li, M. Yan, S. Ge and J. Yu, *Biosensors and Bioelectronics,* 2013, **50**, 262-268.

222 W. Liu, J. Kou, H. Xing and B. Li, *Biosensors and Bioelectronics,* 2014, **52**, 76-81.

223 F. Liu and C. Zhang, *Sensors Actuators B: Chem.,* 2015, **209**, 399-406.

224 F. Li, L. Guo, Y. Hu, Z. Li, J. Liu, J. He and H. Cui, *Talanta,* 2020, **207**, 120346.

225 C. Gao, M. Su, Y. Wang, S. Ge and J. Yu, *Rsc Advances,* 2015, **5**, 28324-28331.

226 L. Chen, C. Zhang and D. Xing, *Sensors Actuators B: Chem.,* 2016, **237**, 308-317.

227 A. Roda, M. Guardigli, D. Calabria, M. M. Calabretta, L. Cevenini and E. Michelini, *Analyst,* 2014, **139**, 6494-6501.

228 E. Lebiga, R. E. Fernandez and A. Beskok, *Analyst,* 2015, **140**, 5006-5011.

229 M. Zangheri, L. Cevenini, L. Anfossi, C. Baggiani, P. Simoni, F. Di Nardo and A. Roda, *Biosensors and Bioelectronics,* 2015, **64**, 63-68.

230 A. W. Martinez, S. T. Phillips, M. J. Butte and G. M. Whitesides, *Angewandte Chemie International Edition,* 2007, **46**, 1318-1320.

231 L. Cai, Y. Fang, Y. Mo, Y. Huang, C. Xu, Z. Zhang and M. Wang, *AIP Advances,* 2017, **7**.

232 T. Tian, Y. An, Y. Wu, Y. Song, Z. Zhu and C. Yang, *ACS applied materials & interfaces,* 2017, **9**, 30480-30487.

233 C. W. Quinn, D. M. Cate, D. D. Miller-Lionberg, T. Reilly III, J. Volckens and C. S. Henry, *Environ. Sci. Technol.,* 2018, **52**, 3567-3573.

234 A. G. Wang, T. Dong, H. Mansour, G. Matamoros, A. L. Sanchez and F. Li, *ACS sensors,* 2018, **3**, 205-210.

235 X. Wei, T. Tian, S. Jia, Z. Zhu, Y. Ma, J. Sun, Z. Lin and C. J. Yang, *Anal. Chem.,* 2016, **88**, 2345-2352.

236 Y. Shimada and T. Kaneta, *Analytical Sciences,* 2018, **34**, 65-70.

237 D. M. Cate, S. D. Noblitt, J. Volckens and C. S. Henry, *Lab on a Chip,* 2015, **15**, 2808-2818.

238 C. Chen, L. Zhao, H. Zhang, X. Shen, Y. Zhu and H. Chen, *Anal. Chem.,* 2019, **91**, 5169-5175.

239 J. C. Hofstetter, J. B. Wydallis, G. Neymark, T. H. Reilly III, J. Harrington and C. S. Henry, *Analyst,* 2018, **143**, 3085-3090.

240 B. M. Jayawardane, I. D. McKelvie and S. D. Kolev, *Anal. Chem.,* 2015, **87**, 4621-4626.

241 Y. Chen, Y. Zilberman, P. Mostafalu and S. R. Sonkusale, *Biosensors and Bioelectronics,* 2015, **67**, 477-484.

242 F. Pena-Pereira, I. Lavilla and C. Bendicho, *Talanta,* 2016, **147**, 390-396.

243 W. Wongwilai, B. M. Jayawardane, S. D. Kolev, K. Grudpan and I. D. McKelvie, *Chiang Mai J.Sci.,* 2016, **43**, 176-182.

244 A. W. Martinez, S. T. Phillips, E. Carrilho, S. W. Thomas III, H. Sindi and G. M. Whitesides, *Anal. Chem.,* 2008, **80**, 3699-3707.

245 T. Kong, J. B. You, B. Zhang, B. Nguyen, F. Tarlan, K. Jarvi and D. Sinton, *Lab on a Chip,* 2019, **19**, 1991-1999.

246 G. Sriram, M. P. Bhat, P. Patil, U. T. Uthappa, H. Jung, T. Altalhi, T. Kumeria, T. M. Aminabhavi, R. K. Pai and M. D. Kurkuri, *TrAC Trends in Analytical Chemistry,* 2017, **93**, 212-227.

247 G. Chen, C. Fang, H. H. Chai, Y. Zhou, W. Y. Li and L. Yu, *Sensors Actuators B: Chem.,* 2019, **281**, 253-261.

248 M. O. Salles, G. N. Meloni, W. R. De Araujo and T. R. L. C. d. Paixão, *Analytical Methods,* 2014, **6**, 2047-2052.

249 A. Y. Mutlu, V. Kılıç, G. K. Özdemir, A. Bayram, N. Horzum and M. E. Solmaz, *Analyst,* 2017, **142**, 2434-2441.

250 R. Yang, W. Cheng, X. Chen, Q. Qian, Q. Zhang, Y. Pan, P. Duan and P. Miao, *Acs Omega,* 2018, **3**, 12141-12146.

251 C. Sicard, C. Glen, B. Aubie, D. Wallace, S. Jahanshahi-Anbuhi, K. Pennings, G. T. Daigger, R. Pelton, J. D. Brennan and C. D. Filipe, *Water Res.,* 2015, **70**, 360-369.

252 A. K. Ellerbee, S. T. Phillips, A. C. Siegel, K. A. Mirica, A. W. Martinez, P. Striehl, N. Jain, M. Prentiss and G. M. Whitesides, *Anal. Chem.,* 2009, **81**, 8447-8452.

253 D. C. M. Ferreira, G. F. Giordano, C. C. d. S. P. Soares, J. F. A. de Oliveira, R. K. Mendes, M. H. Piazzetta, A. L. Gobbi and M. B. Cardoso, *Talanta,* 2015, **141**, 188-194.

254 S. C. Kim, U. M. Jalal, S. B. Im, S. Ko and J. S. Shim, *Sensors Actuators B: Chem.,* 2017, **239**, 52-59.

255 A. Burklund, H. K. Saturley-Hall, F. A. Franchina, J. E. Hill and J. X. Zhang, *Biosensors and Bioelectronics,* 2019, **128**, 97-103.

256 A. Katoh, K. Maejima, Y. Hiruta and D. Citterio, *Analyst,* 2020, **145**, 6071-6078.

257 K. Mao, X. Min, H. Zhang, K. Zhang, H. Cao, Y. Guo and Z. Yang, *J. Controlled Release,* 2020, **322**, 187-199 (DOI:10.1016/j.jconrel.2020.03.010).

258 A. Nilghaz, S. M. Mousavi, M. Li, J. Tian, R. Cao and X. Wang, *Trends Food Sci. Technol.,* 2021, **118**, 273-284 (DOI:10.1016/j.tifs.2021.08.029).

259 C. Kung, C. Hou, Y. Wang and L. Fu, *Sensors Actuators B: Chem.,* 2019, **301**, 126855 (DOI:10.1016/j.snb.2019.126855).

260 M. I. G. S. Almeida, B. M. Jayawardane, S. D. Kolev and I. D. McKelvie, *Talanta,* 2018, **177**, 176-190 (DOI:10.1016/j.talanta.2017.08.072).

261 M. M. Mentele, J. Cunningham, K. Koehler, J. Volckens and C. S. Henry, *Anal. Chem.,* 2012, **84**, 4474-4480.

262 S. Comber, G. Deviller, I. Wilson, A. Peters, G. Merrington, P. Borrelli and S. Baken, *Integr Environ Assess Manag,* 2023, **19**, 1031-1047 (DOI:10.1002/ieam.4700).

263 S. Bose-O'Reilly, K. M. McCarty, N. Steckling and B. Lettmeier, *Current Problems in Pediatric and Adolescent Health Care,* 2010, **40**, 186-215 (DOI:10.1016/j.cppeds.2010.07.002).

264 G. Chen, W. Chen, Y. Yen, C. Wang, H. Chang and C. Chen, *Anal. Chem.,* 2014, **86**, 6843-6849.

265 M. Zhang, L. Ge, S. Ge, M. Yan, J. Yu, J. Huang and S. Liu, *Biosensors and Bioelectronics,* 2013, **41**, 544-550.

266 A. Apilux, W. Dungchai, W. Siangproh, N. Praphairaksit, C. S. Henry and O. Chailapakul, *Anal. Chem.,* 2010, **82**, 1727-1732.

267 A. Deep, A. L. Sharma, S. K. Tuteja and A. K. Paul, *J. Hazard. Mater.,* 2014, **278**, 559-565.

268 J. Guo, D. Huo, M. Yang, C. Hou, J. Li, H. Fa, H. Luo and P. Yang, *Talanta,* 2016, **161**, 819-825 (DOI:10.1016/j.talanta.2016.09.032).

269 M. C. Talio, M. Alesso, M. G. Acosta, M. Acosta and L. P. Fernández, *Talanta,* 2014, **127**, 244-249.

270 T. Satarpai, J. Shiowatana and A. Siripinyanond, *Talanta,* 2016, **154**, 504-510 (DOI:10.1016/j.talanta.2016.04.017).

271 B. M. Jayawardane, I. D. McKelvie and S. D. Kolev, *Talanta,* 2012, **100**, 454-460 (DOI:10.1016/j.talanta.2012.08.021).

272 R. P. Pohanish, *Sittig's handbook of toxic and hazardous chemicals and carcinogens*, William Andrew, 2017.

273 M. Santhiago, C. S. Henry and L. T. Kubota, *Electrochim. Acta,* 2014, **130**, 771-777.

274 J. Wang, L. Yang, B. Liu, H. Jiang, R. Liu, J. Yang, G. Han, Q. Mei and Z. Zhang, *Anal. Chem.,* 2014, **86**, 3338-3345.

275 L. C. Shriver-Lake, D. Zabetakis, W. J. Dressick, D. A. Stenger and S. A. Trammell, *Sensors,* 2018, **18**, 328.

276 H. Liu, W. Gao, Y. Tian, A. Liu, Z. Wang, Y. Cai and Z. Zhao, *Talanta,* 2019, **191**, 272-276.

277 B. M. Jayawardane, W. Wongwilai, K. Grudpan, S. D. Kolev, M. W. Heaven, D. M. Nash and I. D. McKelvie, *J. Environ. Qual.,* 2014, **43**, 1081-1085 (DOI:10.2134/jeq2013.08.0336).

278 H. Kettler, K. White and S. J. Hawkes, *Mapping the landscape of diagnostics for sexually transmitted infections: key findings and recommendations,* 2004, .

279 L. P. Murray and C. R. Mace, *Anal. Chim. Acta,* 2020, **1140**, 236-249.

280 J. Aveyard, M. Mehrabi, A. Cossins, H. Braven and R. Wilson, *Chemical communications,* 2007, , 4251-4253.

281 A. P. Wong, M. Gupta, S. S. Shevkoplyas and G. M. Whitesides, *Lab on a Chip,* 2008, **8**, 2032-2037.

282 E. Fu, T. Liang, P. Spicar-Mihalic, J. Houghtaling, S. Ramachandran and P. Yager, *Anal. Chem.,* 2012, **84**, 4574-4579.

283 N. Zheng, L. Yuan, Q. C. Ji, H. Mangus, Y. Song, C. Frost, J. Zeng, A. Aubry and M. E. Arnold, *Journal of Chromatography B,* 2015, **988**, 66-74.

284 H. Liu, X. Li and R. M. Crooks, *Anal. Chem.,* 2013, **85**, 4263-4267.

285 A. W. Martinez, S. T. Phillips, Z. Nie, C. Cheng, E. Carrilho, B. J. Wiley and G. M. Whitesides, *Lab on a Chip,* 2010, **10**, 2499-2504.

286 L. Shen, J. A. Hagen and I. Papautsky, *Lab on a Chip,* 2012, **12**, 4240-4243.

287 M. Jia, Q. Wu, H. Li, Y. Zhang, Y. Guan and L. Feng, *Biosensors and Bioelectronics,* 2015, **74**, 1029-1037.

288 C. Sicard, C. Glen, B. Aubie, D. Wallace, S. Jahanshahi-Anbuhi, K. Pennings, G. T. Daigger, R. Pelton, J. D. Brennan and C. D. Filipe, *Water Res.,* 2015, **70**, 360-369.

289 I. Chikowe, S. L. Bliese, S. Lucas and M. Lieberman, *Am. J. Trop. Med. Hyg.,* 2018, **99**, 233.

290 B. M. Jayawardane, S. Wei, I. D. McKelvie and S. D. Kolev, *Anal. Chem.,* 2014, **86**, 7274-7279.

291 S. Teepoo, S. Arsawiset and P. Chanayota, *Chemosensors,* 2019, **7**, 44.

292 N. Ratnarathorn and W. Dungchai, *Journal of analytical chemistry,* 2020, **75**, 487-494.

293 T. Thongkam and K. Hemavibool, *Microchemical Journal,* 2020, **159**, 105412 (DOI:https://doi.org/10.1016/j.microc.2020.105412).

294 A. Charbaji, H. Heidari-Bafroui, N. Rahmani, C. Anagnostopoulos and M. Faghri, *Chemistry Proceedings,* 2021, **5**, 9.

295 A. Charbaji, H. Heidari-Bafroui, C. Anagnostopoulos and M. Faghri, *Sensors,* 2021, **21**, 102.

296 F. T. Ferreira, R. B. Mesquita and A. O. Rangel, *Talanta,* 2020, , 121183.

297 K. G. Aukema and L. P. Wackett, *Environmental Science: Water Research & Technology,* 2019, **5**, 406-416.

298 F. T. Ferreira, R. B. Mesquita and A. O. Rangel, *Molecules,* 2021, **26**, 6355.

299 N. Lopez-Ruiz, V. F. Curto, M. M. Erenas, F. Benito-Lopez, D. Diamond, A. J. Palma and L. F. Capitan-Vallvey, *Anal. Chem.,* 2014, **86**, 9554-9562.

300 I. Ortiz-Gomez, M. Ortega-Muñoz, A. Salinas-Castillo, J. A. Álvarez-Bermejo, M. Ariza-Avidad, I. de Orbe-Payá, F. Santoyo-Gonzalez and L. F. Capitan-Vallvey, *Talanta,* 2016, **160**, 721-728 (DOI:10.1016/j.talanta.2016.08.021).

301 Y. Jiang, Z. Hao, Q. He and H. Chen, *RSC advances,* 2016, **6**, 2888-2894.

302 T. M. Cardoso, P. T. Garcia and W. K. Coltro, *Analytical Methods,* 2015, **7**, 7311-7317.

303 P. Rajasulochana, Y. Ganesan, P. S. Kumar, S. Mahalaxmi, F. Tasneem, M. Ponnuchamy and A. Kapoor, *Environ. Res.,* 2022, **208**, 112745 (DOI:10.1016/j.envres.2022.112745).

304 K. Vellingiri, V. Choudhary and L. Philip, *Journal of Environmental Chemical Engineering,* 2019, **7**, 103374 (DOI:10.1016/j.jece.2019.103374).

305 E. Vidal, A. S. Lorenzetti, A. G. Lista and C. E. Domini, *Microchemical Journal,* 2018, **143**, 467-473 (DOI:10.1016/j.microc.2018.08.042).

306 B. Wang, Z. Lin and M. Wang, *J. Chem. Educ.,* 2015, **92**, 733-736.

307 S. A. Bhakta, R. Borba, M. Taba Jr, C. D. Garcia and E. Carrilho, *Anal. Chim. Acta,* 2014, **809**, 117-122.

308 C. Hou, L. Fu, W. Ju and P. Wu, *Chem. Eng. J.,* 2020, **398**, 125573 (DOI:10.1016/j.cej.2020.125573).

309 E. Trofimchuk, Y. Hu, A. Nilghaz, M. Z. Hua, S. Sun and X. Lu, *Food Chem.,* 2020, **316**, 126396 (DOI:10.1016/j.foodchem.2020.126396).

310 T. Tesfaye and A. Hussen, *Microfluidics and Nanofluidics,* 2022, **26**, 22.

311 A. Charbaji, H. Heidari-Bafroui, N. Rahmani, C. Anagnostopoulos and M. Faghri, *Chemistry Proceedings,* 2021, **5**, 9.

312 Y. Lin, D. Gritsenko, S. Feng, Y. C. Teh, X. Lu and J. Xu, *Biosensors and Bioelectronics,* 2016, **83**, 256-266 (DOI:10.1016/j.bios.2016.04.061).

313 N. A. Meredith, J. Volckens and C. S. Henry, *Analytical Methods,* 2017, **9**, 534-540.

314 S. Muhammad-Aree and S. Teepoo, *Analytical and bioanalytical chemistry,* 2020, **412**, 1395-1405.

315 P. Kamnoet, W. Aeungmaitrepirom, R. F. Menger and C. S. Henry, *Analyst,* 2021, **146**, 2229-2239.

316 J. Miller and J. C. Miller, *Statistics and chemometrics for analytical chemistry*, Pearson education, 2018.

317 E. Carrilho, A. W. Martinez and G. M. Whitesides, *Anal. Chem.,* 2009, **81**, 7091-7095.

318 N. Lopez-Ruiz, V. F. Curto, M. M. Erenas, F. Benito-Lopez, D. Diamond, A. J. Palma and L. F. Capitan-Vallvey, *Anal. Chem.,* 2014, **86**, 9554-9562.

319 UNEP, http://www.unep.org/news-and-stories/story/three-ways-we-can-better-use-nitrogen-farming, (accessed Aug 18, 2023).

320 J. F. Tan, A. Anastasi and S. Chandra, *Current Opinion in Electrochemistry,* 2022, **32**, 100926.

321 R. Amali, H. N. Lim, I. Ibrahim, N. M. Huang, Z. Zainal and S. Ahmad, *Trends in Environmental Analytical Chemistry,* 2021, **31**, e00135.

322 M. Badea, A. Amine, G. Palleschi, D. Moscone, G. Volpe and A. Curulli, *J Electroanal Chem,* 2001, **509**, 66-72.

323 B. Narayana and K. Sunil, *EJAC,* 2009, **4**, 204-214.

324 P. Cawse, *Analyst,* 1967, **92**, 311-315.

325 R. J. Norman and J. W. Stucki, *Soil Sci. Soc. Am. J.,* 1981, **45**, 347-353.

326 M. N. Moshoeshoe and V. Obuseng, *South African Journal of Chemistry,* 2018, **71**, 79-85.

327 W. A. Dick and M. A. Tabatabai, *Soil Sci. Soc. Am. J.,* 1979, **43**, 899-904.

328 D. D. Liana, B. Raguse, J. J. Gooding and E. Chow, *sensors,* 2012, **12**, 11505-11526.

329 N. Ratnarathorn and W. Dungchai, *Journal of analytical chemistry,* 2020, **75**, 487-494.

330 F. T. Ferreira, R. B. Mesquita and A. O. Rangel, *Talanta,* 2020, **219**, 121183.

331 V. Choudhary and L. Philip, *Microchemical Journal,* 2021, **171**, 106809 (DOI:10.1016/j.microc.2021.106809).

332 Y. Lin, D. Gritsenko, S. Feng, Y. C. Teh, X. Lu and J. Xu, *Biosensors and Bioelectronics,* 2016, **83**, 256-266 (DOI:10.1016/j.bios.2016.04.061).

333 H. Kudo, K. Yamada, D. Watanabe, K. Suzuki and D. Citterio, *Micromachines,* 2017, **8**, 127.

334 X. Sun, B. Li, A. Qi, C. Tian, J. Han, Y. Shi, B. Lin and L. Chen, *Talanta,* 2018, **178**, 426-431.

335 X. Liu, C. Zong and L. Lu, *Analyst,* 2012, **137**, 2406-2414.

336 J. Dhavamani, L. H. Mujawar and M. S. El-Shahawi, *Sensors Actuators B: Chem.,* 2018, **258**, 321-330.

337 E. de Almeida, V. F. do Nascimento Filho and A. A. Menegário, *Spectrochimica Acta Part B: Atomic Spectroscopy,* 2012, **71**, 70-74.

338 J. Xu, Y. Zhang, L. Li, Q. Kong, L. Zhang, S. Ge and J. Yu, *ACS applied materials & interfaces,* 2018, **10**, 3431-3440.

339 P. Vijitvarasan, S. Oaew and W. Surareungchai, *Anal. Chim. Acta,* 2015, **896**, 152-159 (DOI:10.1016/j.aca.2015.09.011).

340 C. Kung, C. Hou, Y. Wang and L. Fu, *Sensors Actuators B: Chem.,* 2019, **301**, 126855 (DOI:10.1016/j.snb.2019.126855).

341 E. Pellegrini, M. Contin, L. Vittori Antisari, G. Vianello, C. Ferronato and M. De Nobili, *Environmental toxicology and chemistry,* 2018, **37**, 3025-3031.

342 B. M. Jayawardane, W. Wongwilai, K. Grudpan, S. D. Kolev, M. W. Heaven, D. M. Nash and I. D. McKelvie, *J. Environ. Qual.,* 2014, **43**, 1081-1085.

343 H. Arabyarmohammadi, A. K. Darban, M. Abdollahy and B. Ayati, *Journal of Environmental Health Science and Engineering,* 2018, **16**, 109-119.

344 S. S. B. Moram, C. Byram, S. N. Shibu, B. M. Chilukamarri and V. R. Soma, *ACS omega,* 2018, **3**, 8190-8201.

345 L. C. Shriver-Lake, D. Zabetakis, W. J. Dressick, D. A. Stenger and S. A. Trammell, *Sensors,* 2018, **18**, 328.

346 M. Ueland, L. Blanes, R. V. Taudte, B. H. Stuart, N. Cole, P. Willis, C. Roux and P. Doble, *Journal of Chromatography A,* 2016, **1436**, 28-33 (DOI:10.1016/j.chroma.2016.01.054).

347 P. Ryan, D. Zabetakis, D. A. Stenger and S. A. Trammell, *Sensors,* 2015, **15**, 17048-17056.

348 , https://www.horiba.com/rus/water-quality/applications/agriculture-crop-science/soil-nitrate-measurement-for-determination-of-plant-available-nitrogen/, (accessed Feb 27, 2023).

349 D. Giustarini, R. Rossi, A. Milzani and I. Dalle-Donne, *Meth. Enzymol.,* 2008, **440**, 361-380 (DOI:10.1016/S0076-6879(07)00823-3).

350 V. M. Ivanov, *Journal of Analytical chemistry,* 2004, **59**, 1002-1005.

351 D. Giustarini, I. Dalle-Donne, R. Colombo, A. Milzani and R. Rossi, *Free Radic. Res.,* 2004, **38**, 1235-1240.

352 J. S. Rao and B. Kumar, in *10th International Conference on Vibrations in Rotating Machinery*, ed. nonymous , Woodhead Publishing, 2012, p. 173-188.

353 E. Murray, E. P. Nesterenko, M. McCaul, A. Morrin, D. Diamond and B. Moore, *Analytical Methods,* 2017, **9**, 680-687.

354 L. Merino, *Food Analytical Methods,* 2009, **2**, 212-220.

355 J. Dutt and J. Davis, *Journal of Environmental Monitoring,* 2002, **4**, 465-471 (DOI:10.1039/b202670h).

356 D. He, Z. Zhang, Y. Huang and Y. Hu, *Food Chem.,* 2007, **101**, 667-672 (DOI:10.1016/j.foodchem.2006.02.024).

357 M. J. Moorcroft, J. Davis and R. G. Compton, *Talanta,* 2001, **54**, 785-803 (DOI:10.1016/S0039-9140(01)00323-X).

358 K. V. H. Sastry, R. P. Moudgal, J. Mohan, J. S. Tyagi and G. S. Rao, *Anal. Biochem.,* 2002, **306**, 79-82 (DOI:10.1006/abio.2002.5676).

359 E. Tatsch, G. V. Bochi, R. d. S. Pereira, H. Kober, V. A. Agertt, M. M. Anraku de Campos, P. Gomes, M. M. M. F. Duarte and R. N. Moresco, *Clin. Biochem.,* 2011, **44**, 348-350 (DOI:10.1016/j.clinbiochem.2010.12.011).

360 M. Miró, A. Cladera, J. M. Estela and V. Cerdà, *Analyst,* 2000, **125**, 943-948.

361 A. Aydın, Ö Ercan and S. Taşcıoğlu, *Talanta,* 2005, **66**, 1181-1186 (DOI:10.1016/j.talanta.2005.01.024).

362 R. Burakham, M. Oshima, K. Grudpan and S. Motomizu, *Talanta,* 2004, **64**, 1259-1265 (DOI:10.1016/j.talanta.2004.03.059).

363 M. J. Ahmed, C. D. Stalikas, S. M. Tzouwara-Karayanni and M. I. Karayannis, *Talanta (Oxford),* 1996, **43**, 1009-1018 (DOI:10.1016/0039-9140(95)01824-7).

364 T. TOMIYASU, Y. KONAGAYOSHI, K. ANAZAWA and H. SAKAMOTO, *Analytical sciences,* 2001, **17**, 1437-1440 (DOI:10.2116/analsci.17.1437).

365 , https://www.epa.gov/ground-water-and-drinking-water/national-primary-drinking-water-regulations, (accessed Feb 1, 2023).

366 O. Van Cleemput and A. H. Samater, *Fertilizer research,* 1995, **45**, 81-89.

367 T. M. Mc Calla, *Journal of Environmental Quality,* 1978, **7**, 158 (DOI:10.2134/jeq1978.00472425000700010035x).

368 Dionex coporation, *Sunnyvale, CA,* .

369 Y. Zuo, C. Wang and T. Van, *Talanta,* 2006, **70**, 281-285 (DOI:10.1016/j.talanta.2006.02.034).

370 E. Salhi and U. von Gunten, *Water Res.,* 1999, **33**, 3239-3244 (DOI:10.1016/S0043-1354(99)00053-6).

371 E. Murray, P. Roche, M. Briet, B. Moore, A. Morrin, D. Diamond and B. Paull, *Talanta,* 2020, **216**, 120955 (DOI:10.1016/j.talanta.2020.120955).

372 Z. Binghui, Z. Zhixiong and Y. Jing, *Journal of Chromatography A,* 2006, **1118**, 106-110 (DOI:10.1016/j.chroma.2006.01.139).

373 W.M. Johnston and E.C. Kao, *J. Dent. Res.,* 1989, **68**, 819-822 (DOI:10.1177/00220345890680051301).

374 T. M. Cardoso, P. T. Garcia and W. K. Coltro, *Analytical Methods,* 2015, **7**, 7311-7317.

375 Y. Liu, C. Hsu, B. Lu, P. Lin and M. Ho, *Dalton Transactions,* 2018, **47**, 14799-14807.

376 M. Jaafar, A. Shrivastava, S. Rai Bose, M. Felipe-Sotelo and N. I. Ward, *Journal of Food Composition and Analysis,* 2021, **96**, 103748 (DOI:https://doi.org/10.1016/j.jfca.2020.103748).

377 J. Mierzwa, Y. Sun and M. Yang, *Spectrochimica Acta Part B: Atomic Spectroscopy,* 1998, **53**, 63-69 (DOI:https://doi.org/10.1016/S0584-8547(97)00119-5).

378 D. M. C. Gomes, M. A. Segundo, J. L. F. C. Lima and A. O. S. S. Rangel, *Talanta,* 2005, **66**, 703-711 (DOI:https://doi.org/10.1016/j.talanta.2004.12.011).

379 K. Kumada and T. Asami, *Soil Sci. Plant Nutr.,* 1957, **3**, 187-193.

380 M. A. Kassem and A. S. Amin, *Food Chem.,* 2013, **141**, 1941-1946 (DOI:https://doi.org/10.1016/j.foodchem.2013.05.038).

381 J. Paluch, R. B. R. Mesquita, V. Cerdà, J. Kozak, M. Wieczorek and A. O. S. S. Rangel, *Talanta,* 2018, **185**, 316-323 (DOI:https://doi.org/10.1016/j.talanta.2018.03.091).

382 C. Mc Eleney, S. Alves and D. Mc Crudden, *Anal. Chim. Acta,* 2020, **1137**, 94-102 (DOI:https://doi.org/10.1016/j.aca.2020.08.056).

383 B. Shyla, Mahadevaiah and G. Nagendrappa, *Spectrochimica Acta Part A: Molecular and Biomolecular Spectroscopy,* 2011, **78**, 497-502 (DOI:https://doi.org/10.1016/j.saa.2010.11.017).

384 E. R. Campbell, K. Warsko, A. Davidson and W. H. (Bill) Campbell, *MethodsX,* 2015, **2**, 211-218 (DOI:https://doi.org/10.1016/j.mex.2015.04.003).

385 H. L. Barrows and E. C. Simpson, *Soil Sci. Soc. Am. J.,* 1962, **26**, 443-445.

386 A. R. A. Nogueira, S. M. Brienza, E. A. Zagatto, J. L. Lima and A. N. Araújo, *J. Agric. Food Chem.,* 1996, **44**, 165-169.

387 D. J. David, *Analyst,* 1960, **85**, 495-503.

388 H. A. Ajwa and M. A. Tabatabai, *Commun. Soil Sci. Plant Anal.,* 1993, **24**, 1817-1832.

389 A. Ghani, R. G. McLaren and R. S. Swift, *N. Z. J. Agric. Res.,* 1990, **33**, 467-472.

390 O. Kenyanya, J. M. Wachira and H. Mbuvi, 2013, .

391 I. K. Edwards, Y. P. Kalra and F. G. Radford, *Environmental Pollution Series B, Chemical and Physical,* 1981, **2**, 109-117 (DOI:https://doi.org/10.1016/0143-148X(81)90046-X).

392 T. P. Gaines, M. B. Parker and G. J. Gascho, *Agron. J.,* 1984, **76**, 371-374 (DOI:10.2134/agronj1984.00021962007600030005x).

393 , https://www.qld.gov.au/environment/land/management/soil/soil-properties/ph-levels, (accessed Feb 20, 2023).

394 , https://www.horiba.com/int/water-quality/applications/agriculture-crop-science/soil-ph-and-nutrient-availability/, (accessed Feb 20, 2023).

395 BBC Gardeners World Magazine, https://www.gardenersworld.com/how-to/grow-plants/soil-ph-level-explained/, (accessed Feb 20, 2023).

396 J. F. Herencia, J. Ruiz-Porras, S. Melero, P. Garcia-Galavis, E. Morillo and C. Maqueda, *Agron. J.,* 2007, **99**, 973-983 (DOI:10.2134/agronj2006.0168).

397 P. Singh, M. K. Singh, Y. R. Beg and G. R. Nishad, *Talanta,* 2019, **191**, 364-381 (DOI:10.1016/j.talanta.2018.08.028).

398 A. Guerrero, S. De Neve and A. M. Mouazen, *Adv. Agron.,* 2021, **168**, 1-38 (DOI:10.1016/bs.agron.2021.02.001).

399 B. Sethuramasamyraja, V. I. Adamchuk, A. Dobermann, D. B. Marx, D. D. Jones and G. E. Meyer, *Comput. Electron. Agric.,* 2008, **60**, 212-225.

400 E. M. Barnes, K. A. Sudduth, J. W. Hummel, S. M. Lesch, D. L. Corwin, C. Yang, C. S. Daughtry and W. C. Bausch, 2003, .

401 N. Rogovska, D. A. Laird, C. Chiou and L. J. Bond, *Precision agriculture,* 2019, **20**, 40-55.

402 J. Artigas, A. Beltran, C. Jimenez, A. Baldi, R. Mas, C. Domınguez and J. Alonso, *Comput. Electron. Agric.,* 2001, **31**, 281-293.

403 W. A. Dick and M. A. Tabatabai, *Soil Sci. Soc. Am. J.,* 1979, **43**, 899-904.

404 B. Narayana and K. Sunil, *Eurasian Journal of Analytical Chemistry,* 2009, **4**, 204-214.

405 E. Szekely, *Commun. Soil Sci. Plant Anal.,* 1991, **22**, 1295-1302 (DOI:10.1080/00103629109368491).

406 R. Puchades, M. D. Pastor and A. Maquieira, *Commun. Soil Sci. Plant Anal.,* 1994, **25**, 3257-3280 (DOI:10.1080/00103629409369263).

407 A. Henriksen and A. R. Selmer-Olsen, *Analyst (London),* 1970, **95**, 514 (DOI:10.1039/an9709500514).

408 T. A. Doane and W. R. Horwáth, *Anal. Lett.,* 2003, **36**, 2713-2722 (DOI:10.1081/AL-120024647).

409 D. KANIANSKY, I. ZELENSKY, A. HYBENOVA and F. I. ONUSKA, *Anal. Chem. (Wash.),* 1994, **66**, 4258-4264.

410 A. A. Okemgbo, H. H. Hill, W. F. Siems and S. G. Metcalf, *Anal. Chem. (Wash.),* 1999, **71**, 2725-2731 (DOI:10.1021/ac990198+).

411 M. K. Mahendrappa, *Soil Sci.,* 1969, **108**, 132-136.

412 J. Choosang, A. Numnuam, P. Thavarungkul, P. Kanatharana, T. Radu, S. Ullah and A. Radu, *Sensors (Basel, Switzerland),* 2018, **18**, 3555 (DOI:10.3390/s18103555).

413 S. A. Glazier, E. R. Campbell and W. H. Campbell, *Anal. Chem. (Wash.),* 1998, **70**, 1511-1515 (DOI:10.1021/ac971146s).

414 L. H. Larsen, L. R. Damgaard, T. Kjær, T. Stenstrøm, A. Lynggaard-Jensen and N. P. Revsbech, *Water Res.,* 2000, **34**, 2463-2468 (DOI:https://doi.org/10.1016/S0043-1354(99)00423-6).

415 D. Kirstein, L. Kirstein, F. Scheller, H. Borcherding, J. Ronnenberg, S. Diekmann and P. Steinrücke, *J Electroanal Chem,* 1999, **474**, 43-51 (DOI:https://doi.org/10.1016/S0022-0728(99)00302-2).

416 M. J. Moorcroft, J. Davis and R. G. Compton, *Talanta,* 2001, **54**, 785-803 (DOI:https://doi.org/10.1016/S0039-9140(01)00323-X).

417 R. N. Sah, *Commun. Soil Sci. Plant Anal.,* 1994, **25**, 2841-2869 (DOI:10.1080/00103629409369230).

418 T. Hengl, J. G. B. Leenaars, K. D. Shepherd, M. G. Walsh, G. B. M. Heuvelink, T. Mamo, H. Tilahun, E. Berkhout, M. Cooper, E. Fegraus, I. Wheeler and N. A. Kwabena, *Nutr. Cycling Agroecosyst.,* 2017, **109**, 77-102 (DOI:10.1007/s10705-017-9870-x).

419 https://www.palintest.com/, (accessed 13/01/ 2022).

420 U. Schmidhalter, *Z. Pflanzenernähr. Bodenk.,* 2005, **168**, 432-438 (DOI:https://doi.org/10.1002/jpln.200520521).

421 R. Wetselaar, G. D. Smith and J. F. Angus, *Commun. Soil Sci. Plant Anal.,* 1998, **29**, 729-739 (DOI:10.1080/00103629809369980).

422 K. J. Sibley, T. Astatkie, G. Brewster, P. C. Struik, J. F. Adsett and K. Pruski, *Precision agriculture,* 2008, **10**, 162-174 (DOI:10.1007/s11119-008-9081-1).

423 M. Turrión, J. Gallardo and M. González, *Commun. Soil Sci. Plant Anal.,* 1999, **30**, 1137-1152.

424 W. A. Dick and M. A. Tabatabai, *Soil Science Society of America Journal,* 1979, **43**, 899-904 (DOI:10.2136/sssaj1979.03615995004300050016x).

425 S. G. Lehman, M. Badruzzaman, S. Adham, D. J. Roberts and D. A. Clifford, *Water Res.,* 2008, **42**, 969-976 (DOI:10.1016/j.watres.2007.09.011).

426 L. G. Bundy and J. J. Meisinger, in *Methods of Soil Analysis*, ed. nonymous , 1994, p. 951-984.

427 G. R. Sanford, A. R. Cook, J. L. Posner, J. L. Hedtcke, J. A. Hall and J. O. Baldock, *Agron. J.,* 2009, **101**, 167-174 (DOI:10.2134/agronj2008.0126).

428 R. M. Carlson, *Anal. Chem.,* 1986, **58**, 1590-1591.

429 O. M. Kachurina, H. Zhang, W. R. Raun and E. G. Krenzer, *Commun. Soil Sci. Plant Anal.,* 2000, **31**, 893-903.

430 T. Hengl, J. G. Leenaars, K. D. Shepherd, M. G. Walsh, G. B. Heuvelink, T. Mamo, H. Tilahun, E. Berkhout, M. Cooper and E. Fegraus, *Nutr. Cycling Agroecosyst.,* 2017, **109**, 77-102.

431 H. Swerdlow and R. Gesteland, *Nucleic Acids Res.,* 1990, **18**, 1415-1419.

432 R. P. Potdar, M. M. Shirolkar, A. J. Verma, P. S. More and A. Kulkarni, *J. Plant Nutr.,* 2021, **44**, 1826-1839.

433 L. Burton, K. Jayachandran and S. Bhansali, *J. Electrochem. Soc.,* 2020, **167**, 037569.

434 A. Bah, S. K. Balasundram and M. Husni, *American Journal of Agricultural and Biological Sciences,* 2012, **7**, 43-49.

435 C. Dimkpa, P. Bindraban, J. E. McLean, L. Gatere, U. Singh and D. Hellums, *Sustainable agriculture reviews,* 2017, , 1-43.

436 Better Meets Reality, https://bettermeetsreality.com/how-much-topsoil-do-we-need-for-agriculture-how-much-is-left-will-the-world-run-out-in-the-future/, (accessed Jul 17, 2023).

437 , https://www.hull.ac.uk/research/institutes/eei/sudslab-uk.aspx, (accessed Jul 28, 2023).

438 Y. Lu, P. Li, M. Li, M. Wen, H. Wei and Z. Zhang, *Agronomy,* 2023, **13**, 1711.

439 H. Marschner, *Marschner's mineral nutrition of higher plants*, Academic press, 2011.

440 R. D. Crapnell and C. E. Banks, *Sensors and Actuators Reports,* 2022, **4**, 100110 (DOI:10.1016/j.snr.2022.100110).

441 B. Li, L. Fu, W. Zhang, W. Feng and L. Chen, *Electrophoresis,* 2014, **35**, 1152-1159.

442 K. Abe, K. Suzuki and D. Citterio, *Anal. Chem.,* 2008, **80**, 6928-6934.

443 P. B. Hoyt and M. Nyborg, *Can. J. Soil Sci.,* 1972, **52**, 163-167.

444 V. Houba, I. Novozamsky, A. Huybregts and J. J. Van der Lee, *Plant Soil,* 1986, **96**, 433-437.

445 E. Schnug, J. Fleckenstein and S. Hancklaus, *Commun. Soil Sci. Plant Anal.,* 1996, **27**, 1721-1730.

446 G. W. Randall, E. E. Schulte and R. B. Corey, *Soil Sci. Soc. Am. J.,* 1976, **40**, 282-287.

447 W. L. Lindsay and W. Norvell, *Soil Sci. Soc. Am. J.,* 1978, **42**, 421-428.

448 S. Tu, G. J. Racz and C. M. Cho, *Soil Sci. Soc. Am. J.,* 1995, **59**, 1280-1288.

449 R. S. Mylavarapu, J. F. Sanchez, J. H. Nguyen and J. M. Bartos, *Commun. Soil Sci. Plant Anal.,* 2002, **33**, 807-820.

450 J. A. Dean and N. A. Lange, *Lange's handbook of chemistry*, McGraw, New York, 1992.

451 J. Yu and D. Klarup, *Water Air Soil Pollut.,* 1994, **75**, 205-225.

452 N. A. Meredith, C. Quinn, D. M. Cate, T. H. Reilly, J. Volckens and C. S. Henry, *Analyst,* 2016, **141**, 1874-1887.

453 C. O. Yalcin and M. Abudayyak, *Journal of Trace Elements in Medicine and Biology,* 2020, **61**, 126506 (DOI:10.1016/j.jtemb.2020.126506).

454 C. S. Chin, K. S. Johnson and K. H. Coale, *Mar. Chem.,* 1992, **37**, 65-82 (DOI:10.1016/0304-4203(92)90057-H).

455 A. Kabata-Pendias, *Trace elements in soils and plants*, CRC press, 2000.

456 L. G. Egorova, I. E. Okonishnikova, V. L. Nirenburg and I. Y. Postovskii, *Pharmaceutical Chemistry Journal,* 1971, **5**, 23-26.

457 Z. Liu, T. Lin, M. Purro and M. P. Xiong, *ACS applied materials & interfaces,* 2016, **8**, 25788-25797.

458 G. Nakagawa and M. Tanaka, *Talanta,* 1972, **19**, 559-565 (DOI:10.1016/0039-9140(72)80117-6).

459 D. J. Hoff and H. J. Mederski, *Soil Science Society of America Journal,* 1958, **22**, 129-132 (DOI:10.2136/sssaj1958.03615995002200020010x).

460 V. Houba, I. Novozamsky, A. Huybregts and J. J. Van der Lee, *Plant Soil,* 1986, **96**, 433-437.

461 E. Schnug, J. Fleckenstein and S. Hancklaus, *Commun. Soil Sci. Plant Anal.,* 1996, **27**, 1721-1730.

462 L. F. Sobral, J. T. Smyth, N. K. Fageria and L. F. Stone, *Commun. Soil Sci. Plant Anal.,* 2013, **44**, 2507-2513.

Appendix A

Column and Suppressor	Sampler.AcquireExclusiveAccess (minutes)	parameter	value
Column 1		Flush	Volume = 100
		Wait	FlushState
(Dionex IonPac™ AS16 (RFIC™, 2 × 250mm) separator column, Dionex ASRS 300 (2 mm) suppressor column)		Pressure.LowerLimit =	200 [psi]
		Pressure.UpperLimit =	3000 [psi]
		%A.Equate =	%A
		CR_TC =	On
		NeedleHeight =	2 [mm]
		CutSegmentVolume =	0 [µl]
		SyringeSpeed =	3
		CycleTime =	0 [min]
		WaitForTemperature =	FALSE
		Data_Collection_Rate =	5.0 [Hz]
		CellTemperature.Nominal =	35.0 [°C]
		ColumnTemperature.Nominal =	30.0 [°C]
		Suppressor_Type =	ASRS_2mm
		; Pump_ECD.Recommended Current =	15
		; Pump_ECD.Carbonate =	0
		; Pump_ECD.Bicarbonate =	0
		; Pump_ECD.Hydroxide =	20
		; Pump_ECD.Tetraborate =	0

		; Pump_ECD.Other eluent =	0
		Suppressor_Current =	24 [mA]
		ECD_Total.Step =	0.20 [s]
		ECD_Total.Average =	Off
		Concentration =	15.00 [mM]
		Curve =	5
		Flow =	0.30 [ml/min]
		Wait	SampleReady
	0	Autozero	
		Load	
		Wait	CycleTimeState
		Inject	
		Wait	InjectState
		ECD_1.AcqOn	
		ECD_Total.AcqOn	
		Sampler.ReleaseExclusiveAccess	
	6	ECD_1.AcqOff	
		ECD_Total.AcqOff	
		End	
Column 2		Flush	Volume = 100
		Wait	FlushState

Dionex IonPac™ AS11-HC (RFIC™, 2 × 250mm) separator column, Dionex ASRS 300 (2 mm) suppressor column)		Pressure.LowerLimit =	200 [psi]
		Pressure.UpperLimit =	3000 [psi]
		%A.Equate =	%A
		CR_TC =	On
		NeedleHeight =	2 [mm]
		CutSegmentVolume =	0 [µl]
		SyringeSpeed =	3
		CycleTime =	0 [min]
		WaitForTemperature =	FALSE
		Data_Collection_Rate =	5.0 [Hz]
		CellTemperature.Nominal =	35.0 [°C]
		ColumnTemperature.Nominal =	30.0 [°C]
		Suppressor_Type =	ASRS_2mm
		; Pump_ECD.Carbonate =	0
		; Pump_ECD.Bicarbonate =	0
		; Pump_ECD.Hydroxide =	5
		; Pump_ECD.Tetraborate =	0
		; Pump_ECD.Other eluent =	0
		; Pump_ECD.Recommended Current =	6
		Suppressor_Current =	6 [mA]
		ECD_Total.Step =	0.20 [s]
		ECD_Total.Average =	Off

		Concentration =	5.00 [mM]
		Curve =	5
		Flow =	0.30 [ml/min]
		Wait	SampleReady
	0	Autozero	
		Load	
		Wait	CycleTimeState
		Inject	
		Wait	InjectState
		ECD_1.AcqOn	
		ECD_Total.AcqOn	
		Sampler.ReleaseExclusiveAccess	
	8	ECD_1.AcqOff	
		ECD_Total.AcqOff	
		End	
Column3 Dionex IonPac™ AS16 (RFIC™, 2 × 250mm) separator column, Dionex ASRS 300 (2 mm)		Flush	Volume = 100
		Wait	FlushState
		Pressure.LowerLimit =	200 [psi]
		Pressure.UpperLimit =	3000 [psi]
		%A.Equate =	%A
		CR_TC =	On

suppressor column)		NeedleHeight =	2 [mm]
		CutSegmentVolume =	0 [µl]
		SyringeSpeed =	3
		CycleTime =	0 [min]
		WaitForTemperature =	FALSE
		Data_Collection_Rate =	5.0 [Hz]
		CellTemperature.Nominal =	35.0 [°C]
		ColumnTemperature.Nominal =	30.0 [°C]
		Suppressor_Type =	ASRS_2mm
		; Pump_ECD.Recommended Current =	29
		; Pump_ECD.Carbonate =	0
		; Pump_ECD.Bicarbonate =	0
		; Pump_ECD.Hydroxide =	30
		; Pump_ECD.Tetraborate =	0
		; Pump_ECD.Other eluent =	0
		Suppressor_Current =	30 [mA]
		ECD_Total.Step =	0.20 [s]
		ECD_Total.Average =	Off
		Flow =	0.38 [ml/min]
		Wait	SampleReady
	0	Autozero	
		Load	

		Wait	CycleTimeState
		Inject	
		Wait	InjectState
		ECD_1.AcqOn	
		ECD_Total.AcqOn	
		Sampler.ReleaseExclusiveAccess	
	5	Concentration =	5.00 [mM]
	10	Concentration =	50.00 [mM]
	12	ECD_1.AcqOff	
		ECD_Total.AcqOff	
		End	

Appendix B
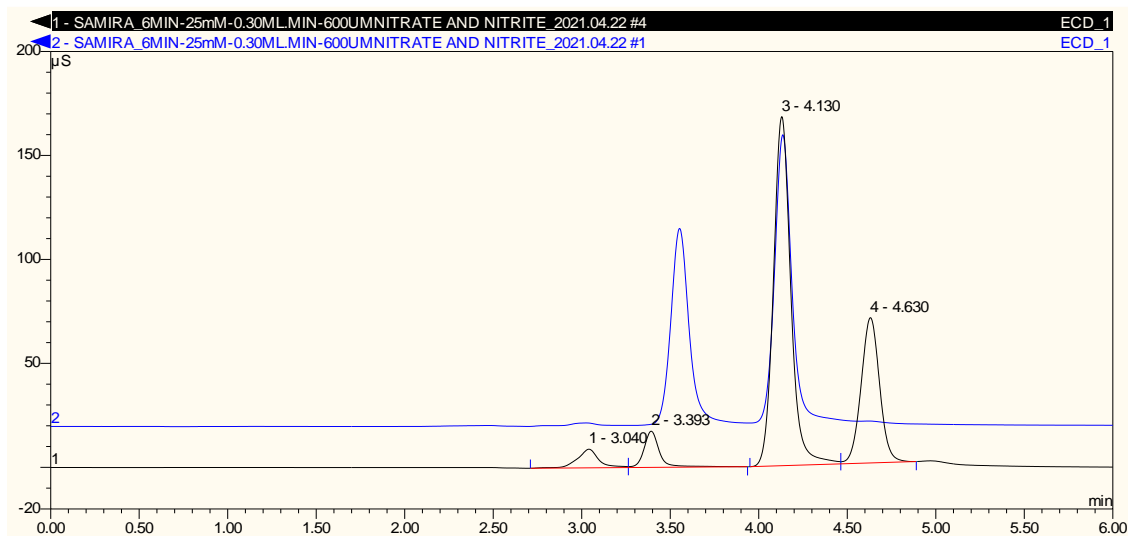
Figure B1: Peak height (µS) versus retention time (min). 600 µM nitrate and nitrite standards and soil Sample (John Innes 1) were used in the analysis. This analysis with 15 mM KOH and 0.30 mL min^{-1} flow rate.
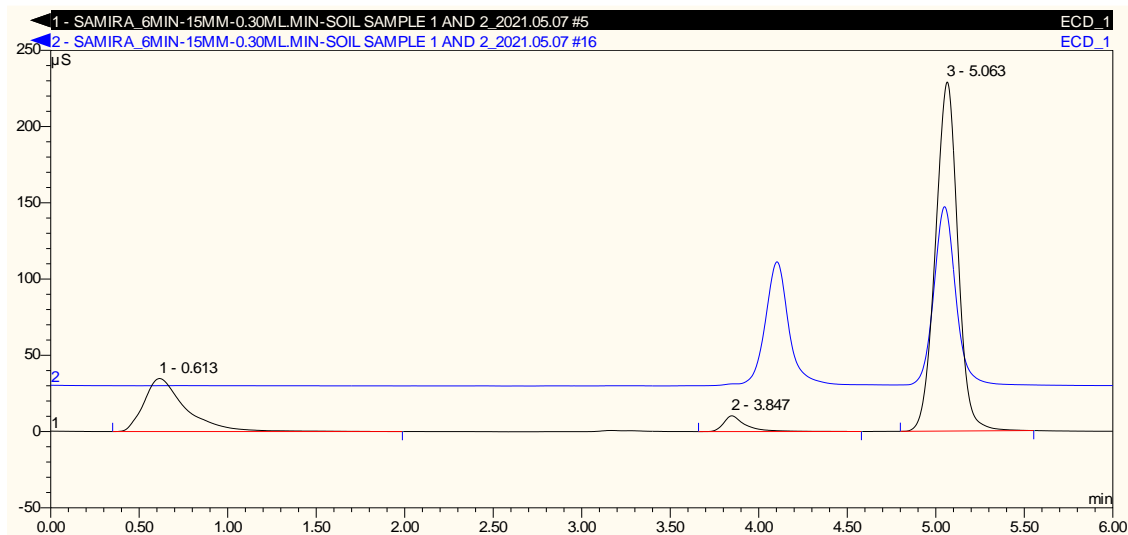
Figure B2: Peak height (µS) versus retention time (min). 600 µM nitrate and nitrite standards and soil Sample (John Innes 2) were used in the analysis.
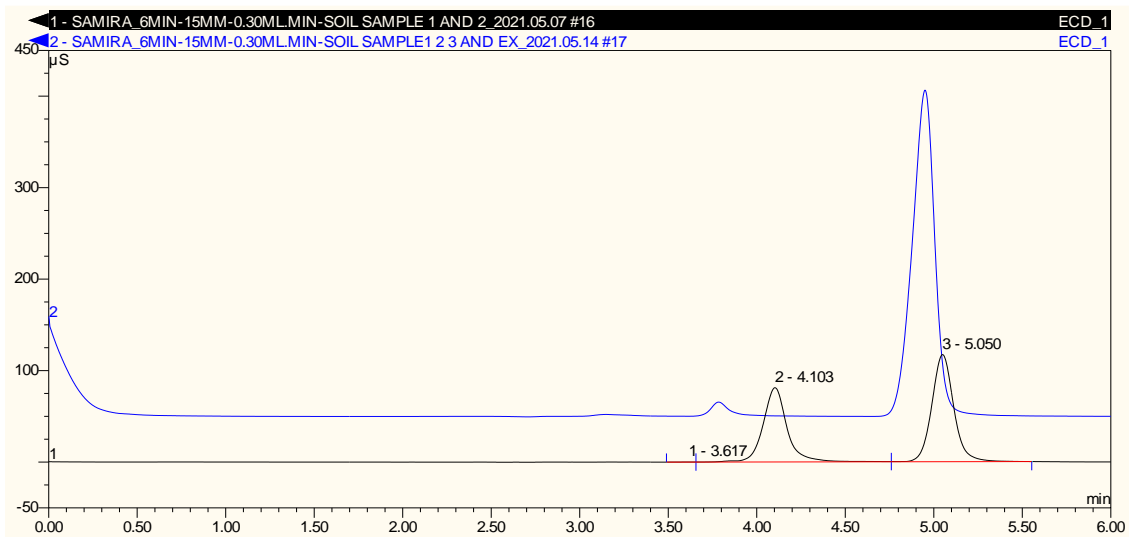
Figure B3: Peak height (μS) versus retention time (min). 600 μM nitrate and nitrite standards and soil Sample (John Innes 3) were used in the analysis.

Appendix c
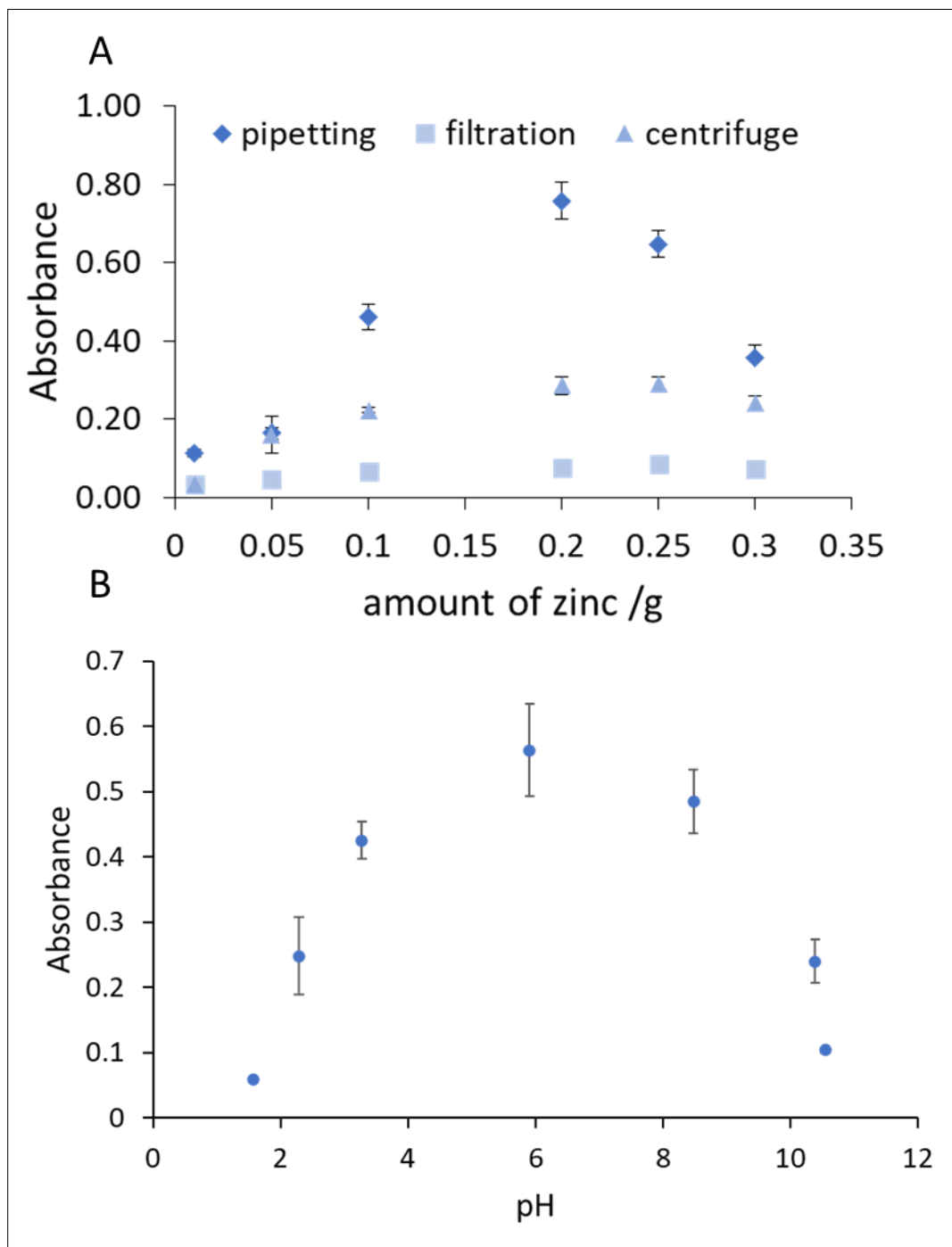
Figure C1: (A) Absorbance versus amount of zinc (g). 100 μM nitrate was mixed with zinc (≤10 μm) for 30 min and the filtered solution was then added to the Griess reagent for colour development for 14 min (10 mL nitrate mixed with 1 mL Griess reagent). Three different separation methods for zinc were used, filtration (Whatman 1), centrifuge (4500 rpm) alone and pipetting. Pipetting gave the best result. The optimum amount of zinc is 0.2g. (B) Absorbance versus pH. 100 μM nitrate and 0.2 g of zinc were mixed for 20 minutes and then the solution was allowed to stand for 1 hour. The solution then was mixed with Griess reagent for colour development for 14 minutes (10mL nitrate mixed with 1 mL Griess reagent).
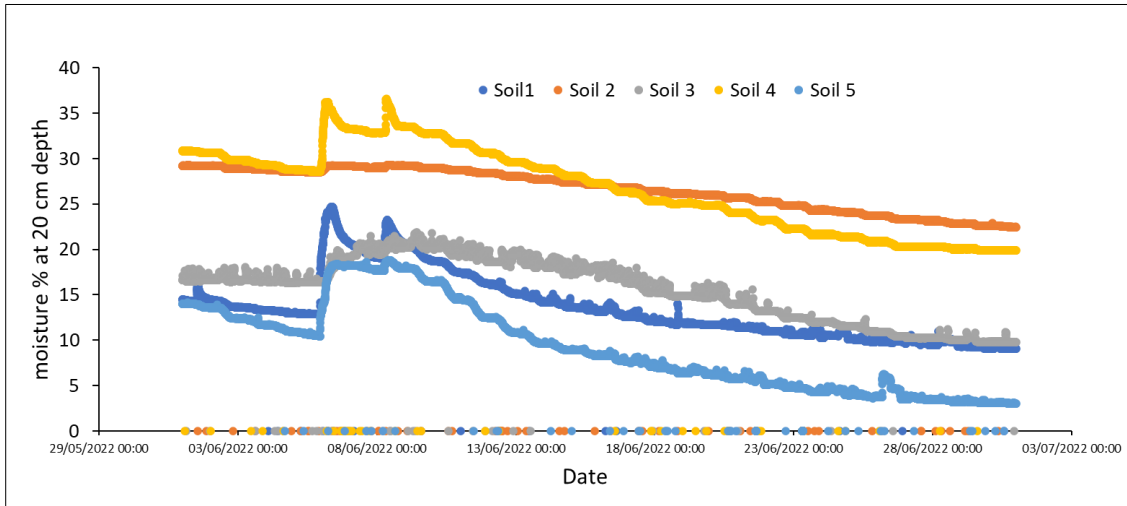
Appendix D

Figure D1: Moisture content of soil at a depth of 20 cm during June 2022. The soil samples used in this study were taken on 10th June 2022.
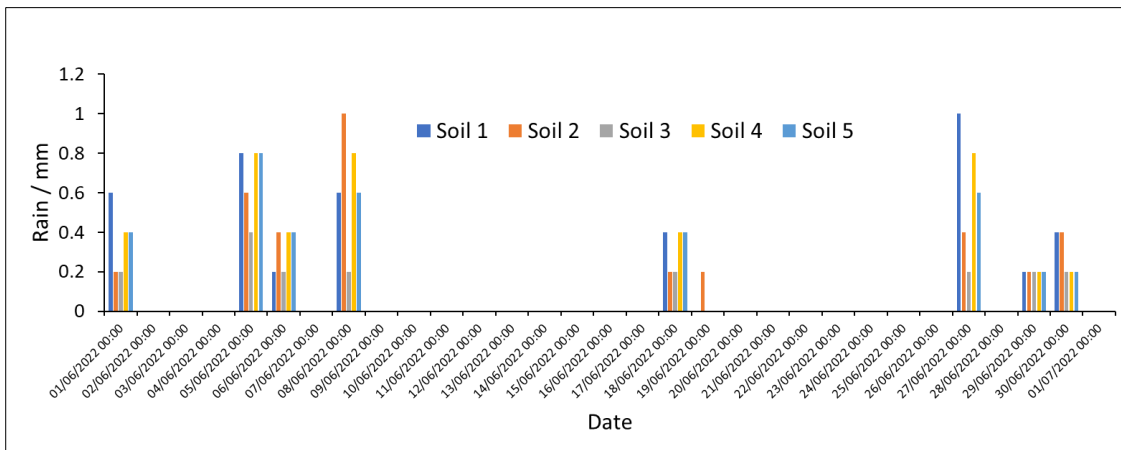

Figure D2: The level of rain (mm) in 5 soil locations across the University of Hull during June 2022. versus the date. The soil samples used in this study were taken on 10th June 2022.
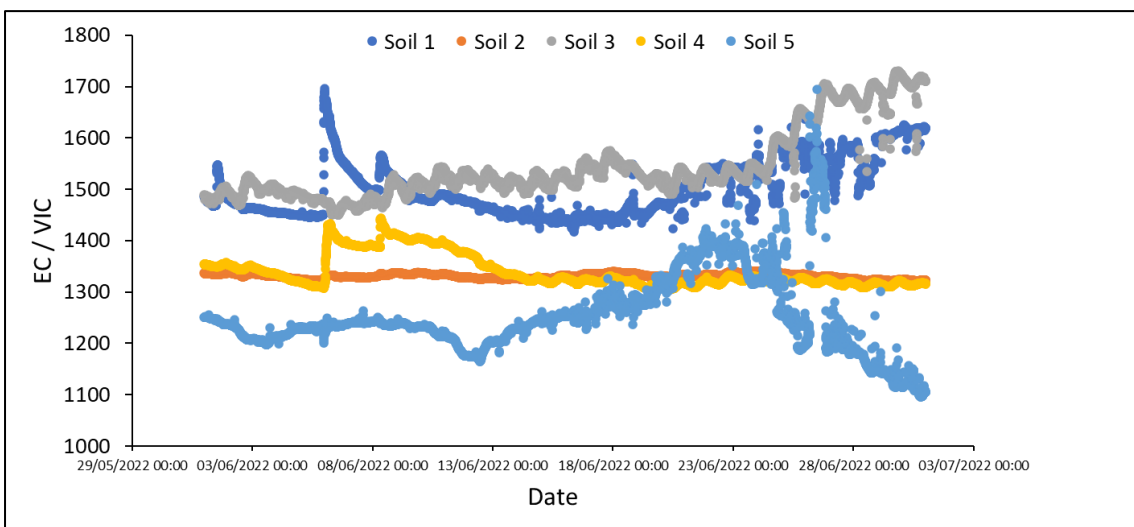

Figure D3: The electrical conductivity (VIC) of soil during June 2022. The soil samples used in this study were taken on 10th June 2022.

Appendix E

Survey questions

General information

- What are you studying *

    Undergraduate, Master(taught), Master (research), PhD(research), Postdoctoral researcher.

- Have you ever participated in similar experiments (Cafetiere/Citizen science/Soil analysis) *

    Yes, No

The use of cafietere

- Collecting the soil sample with provided tools *

    Extremely easy, Easy, Difficult, extremely difficult, N/A

- Mixing with plunger *

    Extremely easy, Easy, difficult, extremely difficult, N/A

- Overall cafetiere work *

    Extremely easy, easy, Difficult, extremely difficult, N/A

- What's your opinion on the cafetiere extraction duration (5 min)? *

    Too short, just right, too long, N/A

The work of the PAD

- The placement of PAD in the sample *

    Extremely clear, Clear, Unclear, extremely unclear N/A

- I was able to distinguish top and back sides of PAD *

    Yes, No, not sure.

- Picture-taking process *

    Extremely clear, Clear, Unclear, extremely unclear, N/A

- What's your opinion on the PAD workflow duration (8 min)? *

    Too short, just right, too long, N/A

- Overall, the use of the PAD *

    Extremely easy, Easy, Difficult, extremely difficult, N/A

Overall experience

- Instruction sheet *

  Extremely clear, Clear, Unclear, extremely unclear, N/A

- What is your opinion about the overall workflow duration (13 min)? *

  Too short, just right, too long, N/A

- How interested are you in environmental science? *

Extremely interested, somewhat interested, Neutral, Uninterested Extremely uninterested

- What is the most important aspect of the workflow? *
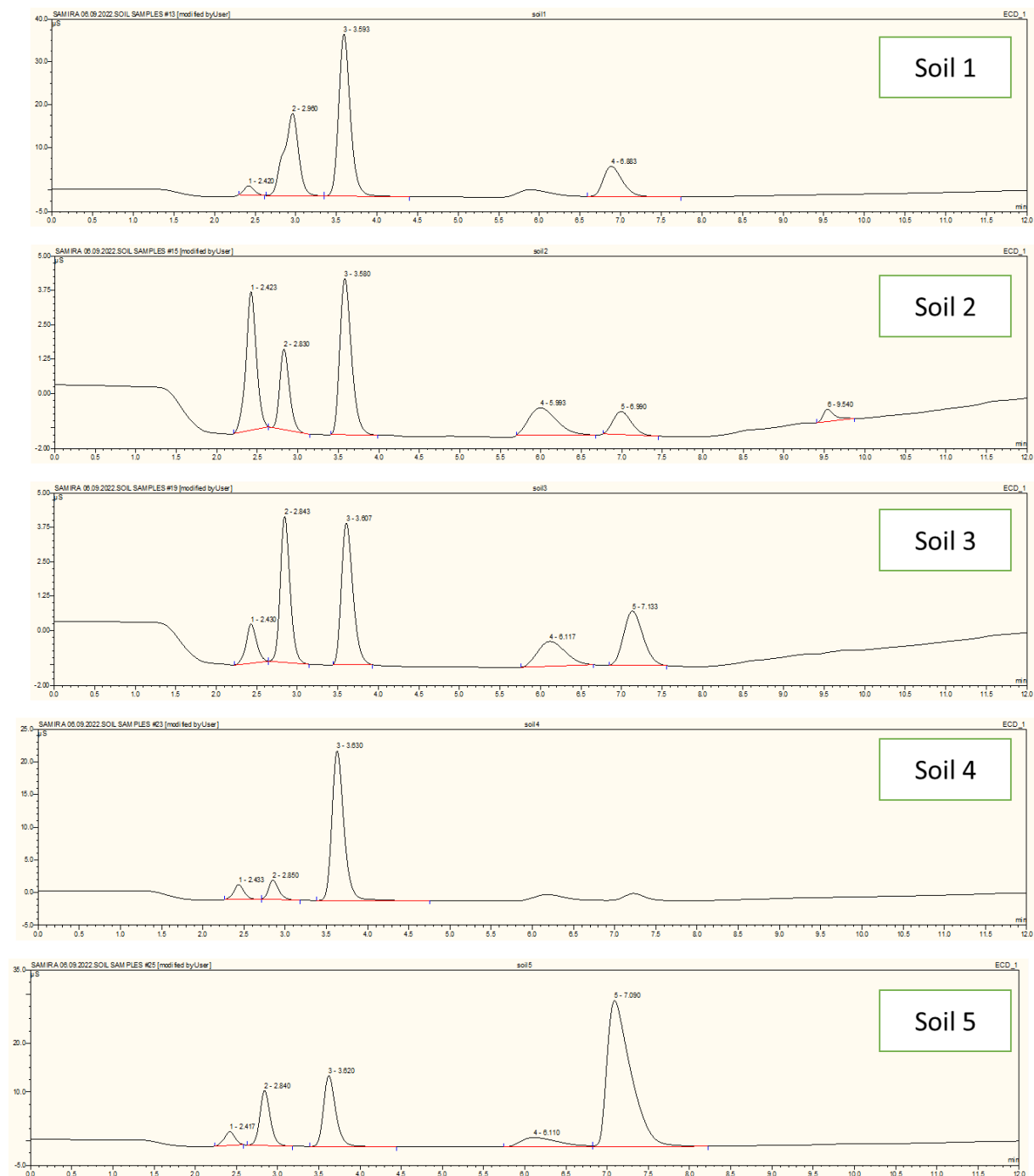- Do you have any feedback regarding the overall system?

Appendix F

Figure F1: Peak height versus time of elution in minutes. 5 soil samples for the volunteer study chapter 5. Nitrate peak was eluted at 3.58 minutes. The peak at 2.9 is the chloride peak. The peak at 2.4 minutes might be the fluoride peak since both usually are eluted first. The peaks eluted at 5.1 and 7 minutes maybe other anions like phosphate. IEC was run with 5 mM KOH for 5 minutes and then the concentration was raised to 50 mM for up to 12 minutes. 0.38 mL min^{-1} was the flow rate.
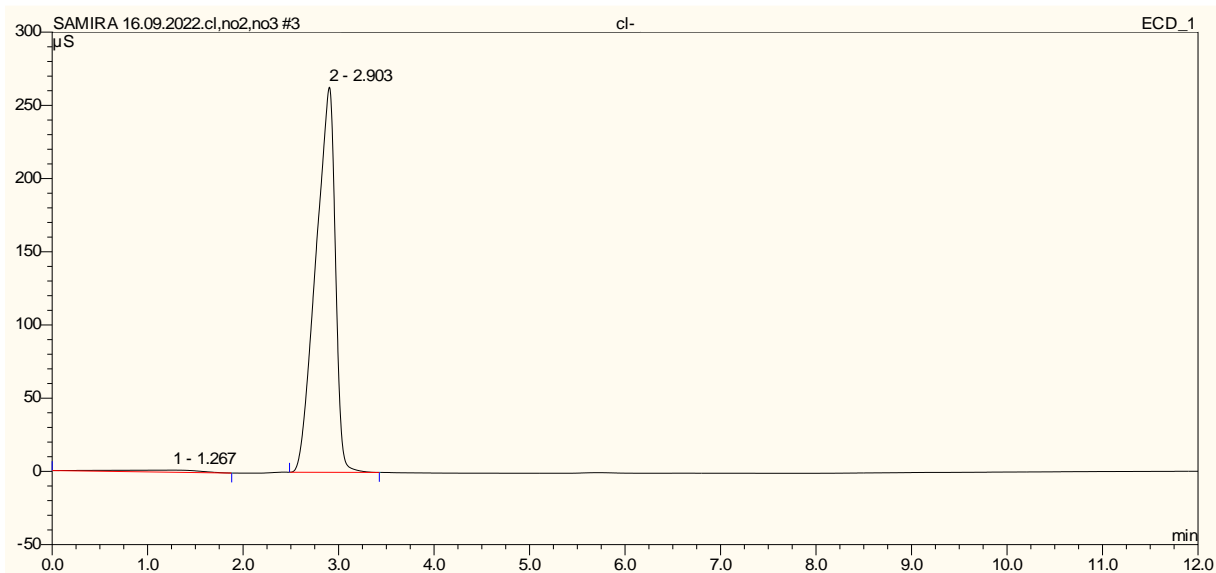
Figure F2: Peak height versus time of elution in minutes. 100 mg L^{-1} Chloride ion was analysed using the same condition as Figure F1 and it was eluted at 2.9 minutes. IEC was run with 5 mM KOH for 5 minutes and then the concentration was raised to 50 mM for up to 12 minutes. 0.38 mL min^{-1} was the flow rate.

Appendix G

pH effect
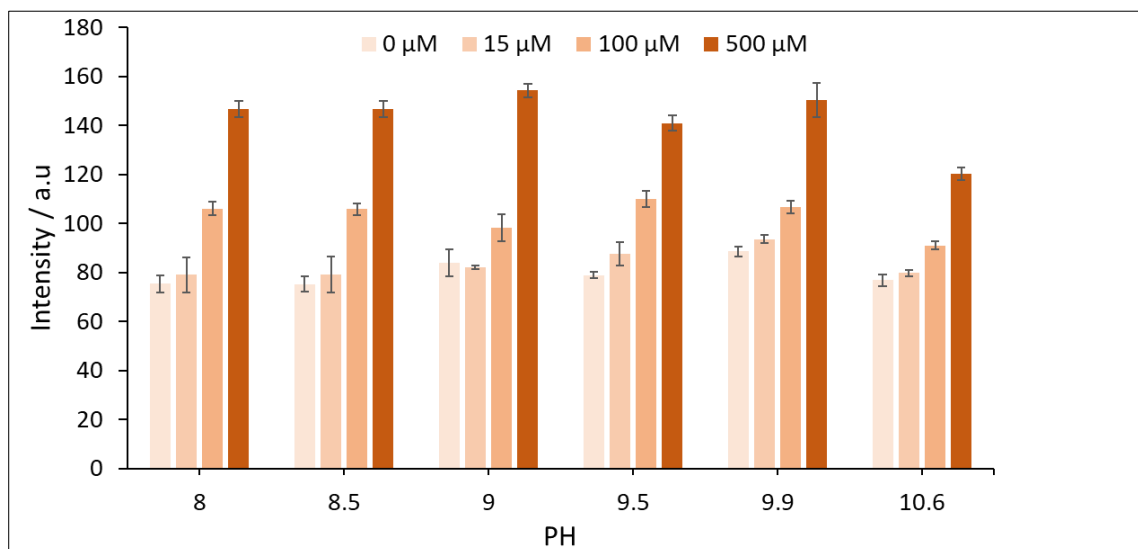

Figure G1 Intensity versus pH. The intensity was determined at four concentrations of manganese 0, 15, 100 and 500 µM. The detection reagent is a 3 µL mixture of 5 mM PAR, 3% polymer PDDA (polyDiallydimethyl ammonium chloride) and borate buffer PH varied. A scanner was used to take the photo. Method 1 was used for the calculation of intensty. Device 13 was used. The optimum PH was 9.9.
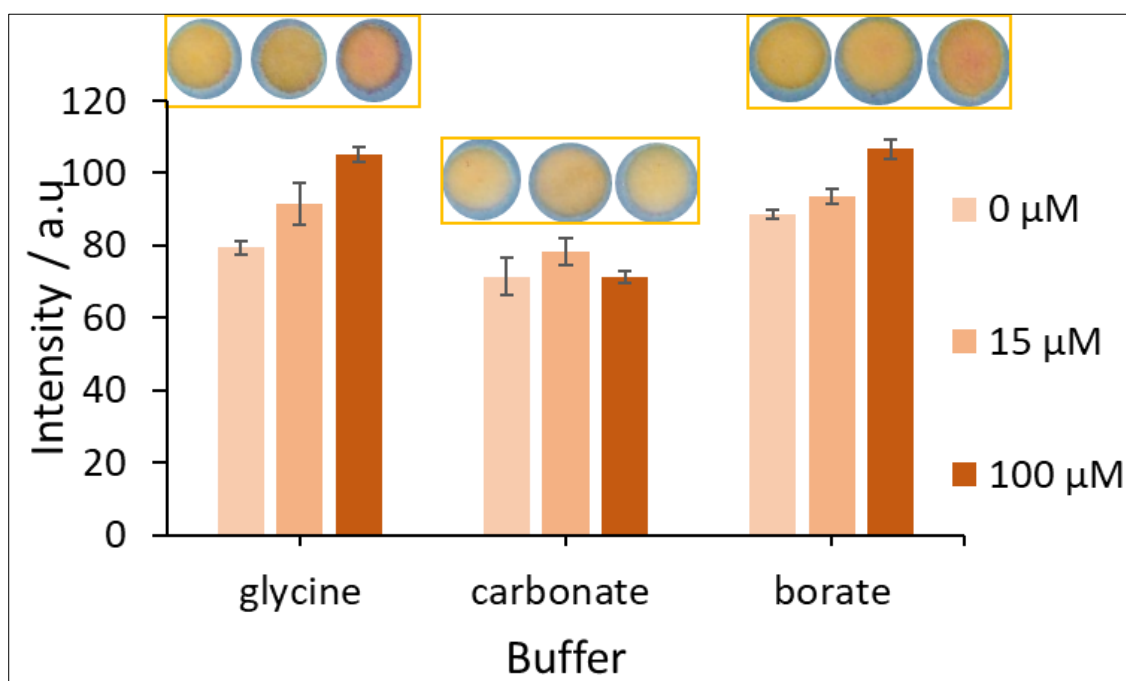
Type of buffer

Figure G2 Intensity versus type of buffer (BORATE, CARBONATE AND GLYCINE). The intensity was determined at four concentrations of manganese 0, 15, 100 and 500 µM. The detection reagent is a 3 µL mixture of 5 mM PAR, 3% polymer PDDA (polyDiallydimethyl ammonium chloride) and varies buffer PH 9.9. A scanner was used to take the photo. Method 1 was used for the calculation of intensty. Device 13 was used. The optimum buffer is glycine.
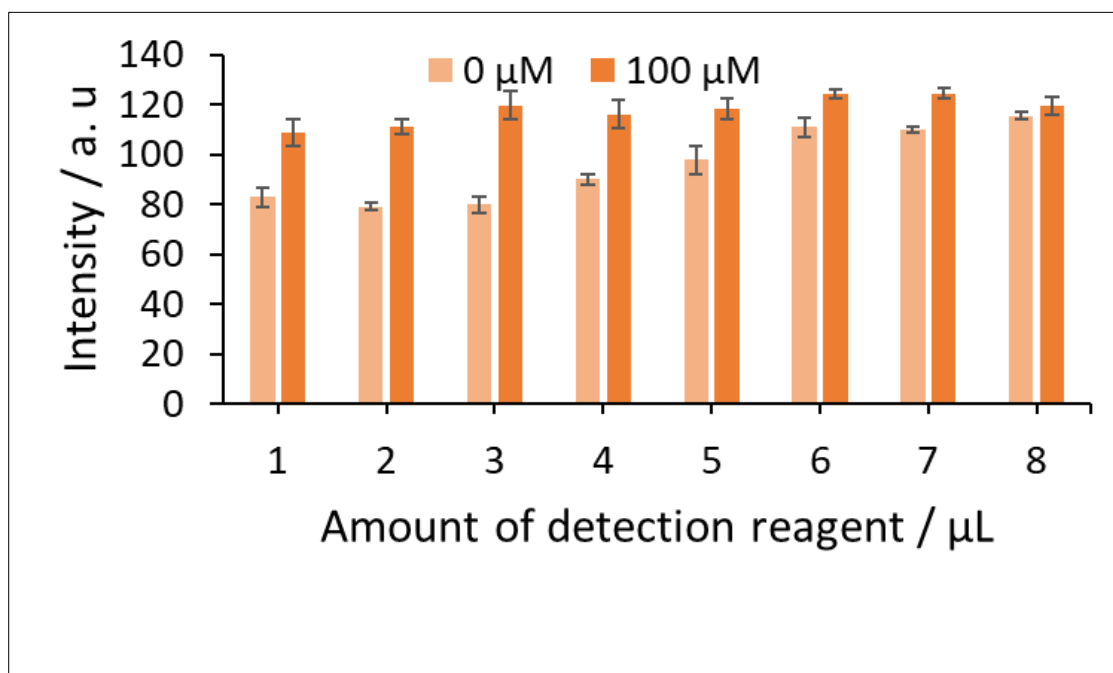
The volume of detection reagent

Figure G3 Intensity versus the amount of detection reagent µL. The intensity was determined at two concentrations of manganese 0, 100 µM. The detection reagent is various µL mixture of 6 mM PAR, 3% polymer PDDA (polyDiallydimethyl ammonium chloride) and glycine buffer PH 9.9. A scanner was used to take the photo. Method 1 was used for the calculation of intensty. Device 13 was used. 3 µL was the optimum volume.
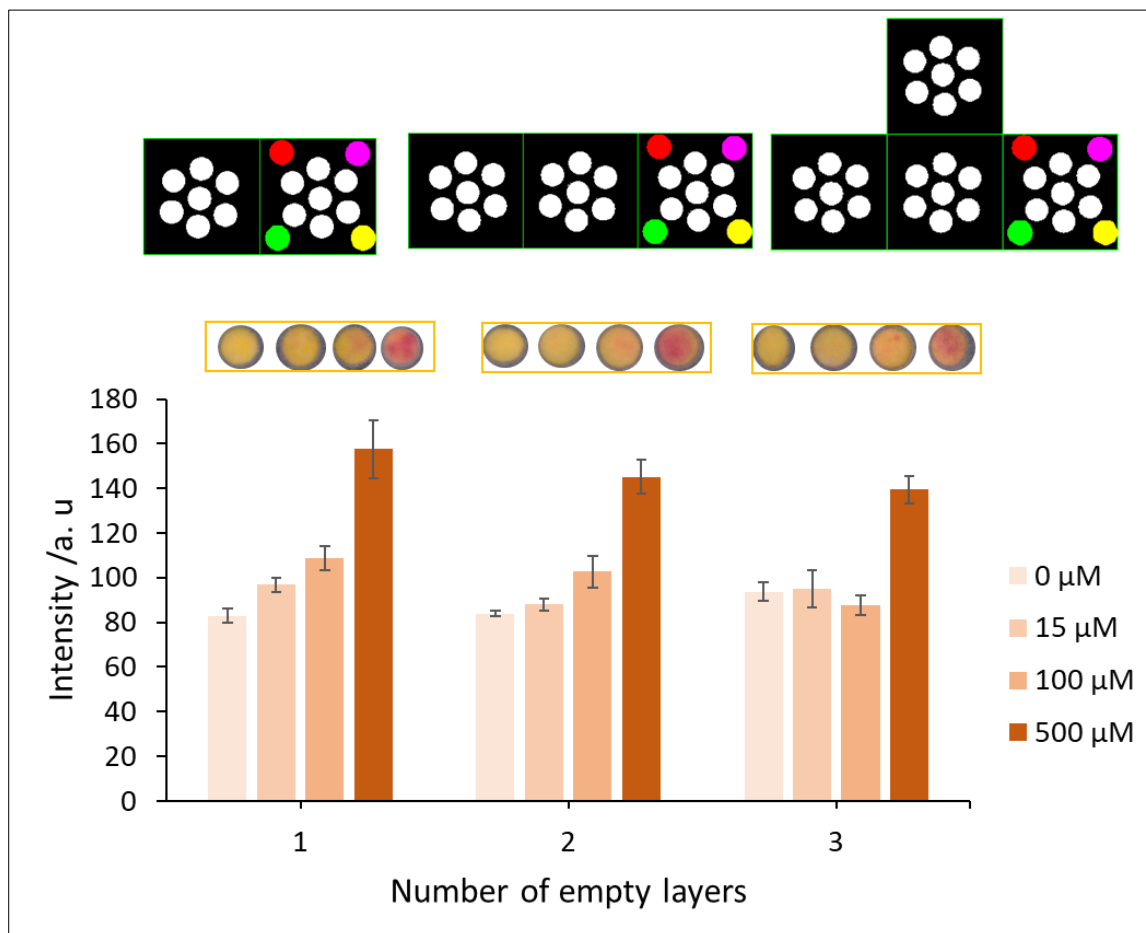
Empty layer effect

Figure G4 Intensity versus the number of empty layers. The intensity was determined at four concentrations of manganese 0, 15, 100 and 500 µM. The detection reagent was a 3 µL mixture of 6 mM PAR, 3% polymer PDDA (polyDiallydimethyl ammonium chloride) and glycine buffer PH 9.9. A scanner was used to take the photo. Method 1 was used for the calculation of intensty. Devices 13, 14, and 15 were used.

Appendix H

Table H1: The price of paper device made for nitrate determination.

material/ reagent	quantity we bought	£	price of reagent in 50 mL of solution (£)	price of reagent and material in 1 PAD (£)
WHATMAN 1	100 PAPER	59.9		0.074875
LAMINATION SHEET	25 SHEET	13		0.0325
SA	100g	74	0.296	0.00000888
NED	5g	44	0.616	0.00001848
Zn	10g	167	41.75	0.00501
			total price	0.11241236